An integrated analysis of the growth rates of southern bluefin tuna for use in estimating the catch at age matrix in the stock assessment

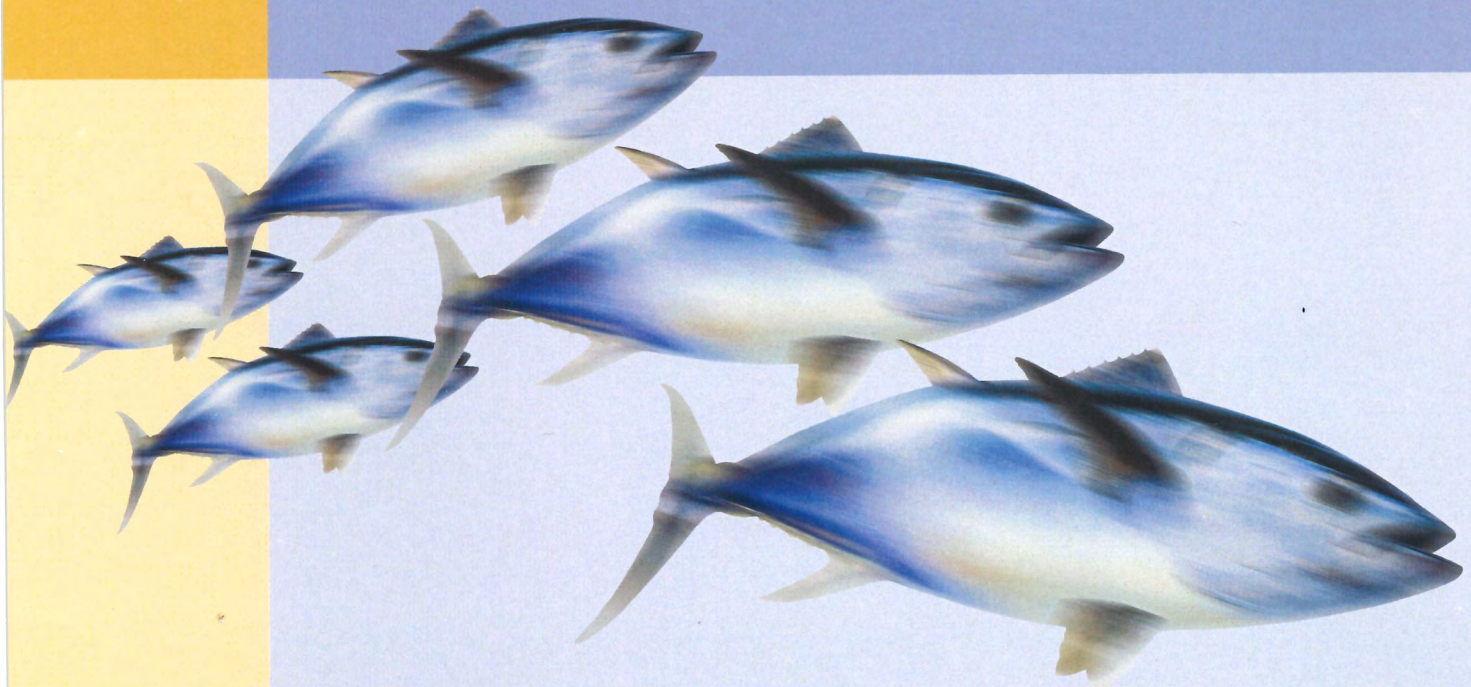

T. Polacheck

G. M. Laslett

J. P. Eveson

Project No. 99/104
August 2003

FISHERIES RESEARCH & DEVELOPMENT CORPORATION

CSIRO
MARINE RESEARCH

Polacheck, Tom.
An integrated analysis of the growth rates of southern bluefin tuna for use in estimating the catch at age matrix in the stock assessment.

Bibliography.
Includes index.
ISBN 1 876996 38 2.

1. Bluefin tuna - Australia. 2. Fish stock assessment - Australia. 3. Bluefin tuna - Age determination. 4. Bluefin tuna - Research - Australia. I. Laslett, G. M. II. Eveson, J. P. III. CSIRO. Division of Marine Research. IV. Title.

338.37277830994

Printed by CSIRO Marine Research

Table of Contents

List of Tables

List of Figures

List of Appendices

1999/104	**An integrated analysis of the growth rates of southern bluefin tuna for use in estimating the catch at age matrix in the stock assessment**

Principle Investigator: Tom Polacheck

Address: CSIRO Marine Research
P.O. Box 1538
Hobart TAS 7000
Tel: 03 6232 5312 Fax: 03 6232 5012

Objectives:

1. To develop an integrated method for modelling SBT growth that combines growth increment data from tagging experiments, length measurements and direct aging estimates from otoliths, length-frequency modal information and otolith growth increments.
2. Using this integrated method, develop models for the historical changes in SBT growth that can be used to estimate the expected length of SBT at age and the associated variance for the entire period of the commercial fishery.
3. Produce appropriate estimates of growth rate parameters for direct input into length based assessment models.
4. Develop a set of alternative hypotheses for the factors underlying changes in SBT growth that are consistent with the observed growth data.
5. Based on these alternative hypotheses, develop models for changes in the length at age that can be used in SBT stock projections.

Non-technical Summary

Outcomes Achieved

The results from this project provide comprehensive and robust estimates of average growth and variability in growth that can be used directly within the SBT stock assessment. Preliminary estimates of growth using the methods developed in this project were provided to the CCSBT Scientific Committee in 2001 and the results were adopted for use in the stock assessments conducted in 2001. It is anticipated that the results from this project will continue to be used in future SBT stock assessments and in the evaluation of management procedures that the CCSBT is currently undertaking.

The estimation of growth rates forms an essential part of the stock assessments of southern bluefin tuna (SBT). Extensive information exists that can be used for estimating SBT growth rates. These include tag-recapture data for fish released in each of the decades between 1960 and 2000, length-frequency data from the commercial catches taken by surface fisheries between 1965 and 1989, and combined direct measurements of length and age from fish collected primarily in the 1990's. However, the estimation of SBT growth rates poses a number of technical challenges. These include:

- The long lifespan of SBT requires that long time series of data be available;
- SBT growth rates are known to have changed over time, meaning that the data from different time periods cannot simply be pooled to provide a single estimate;
- None of the different sources of data provide comprehensive coverage of the years in which there were fisheries for SBT or of the full range of ages within individual cohorts (i.e. for fish born in the same year);
- Standard statistical methods for estimating overall growth rates by combining different data sources did not exist prior to this project;
- The most common growth model (the von Bertalanffy growth curve) used in fisheries' studies is not appropriate for SBT.

All of these challenges were met. A new growth model was developed and new methods of estimation were devised. All available data on SBT growth were assembled and analysed using the new methods, and estimates of the growth of SBT were produced for fish born in each of the 10-year periods between 1960 and 2000.

The results are significant — there have been marked changes in the growth of juvenile SBT born over the last 40 years. SBT from the 1980's grew considerably faster than those from the 1960's. The results also suggest that the 1970's were a period of transition and that growth of young fish in the 1990's was faster than in the 1980's, at least up to about age 4.

Various hypotheses for the changes in growth were explored. The changes appear to be consistent with a population response to reduced numbers of fish as a result of the large catches taken from the SBT stock. However, environmental factors (for example, changes in temperature) cannot be excluded. The average size of fish caught in the 1990's over 25 years of age was ~185cm while almost no fish this size were reported caught in the Japanese longline fishery until the 1970's. Thus, there may have been a substantial change in growth for fish born prior to the commencement of the SBT longline fishery.

The results from this project provide estimates of average growth and variability in growth that can be used directly within the SBT stock assessment. Preliminary estimates of growth using the methods developed in this project were provided to the CCSBT Scientific Committee in 2001 and the results were adopted for use in the stock assessments conducted in 2001. It is anticipated that the results from this project will continue to be used in future SBT stock assessments and in the evaluation of management procedures that the CCSBT is currently undertaking.

Several technical areas for further work that have the potential to improve the estimation methods developed in this project are identified. In addition, the results demonstrate the value and importance of having long time series of data available for understanding growth. In this regard, it is critical that well-designed data collection programs that are capable of providing information on growth are maintained within the SBT fisheries so that future changes in growth are detected and appropriately accounted for in the stock assessment and management of SBT.

Keywords: integrated growth modelling, southern bluefin tuna, generalized von Bertalanffy

Acknowledgements

We wish to acknowledge and thank the very large number of individuals who, over the last 40 plus years, collected the biological samples and data that underpin all of the analyses in this report. Without their commitment and dedication, the long-term data series so essential for real progress in the understanding of fisheries resources would not be possible. We also thank the SBT fishing industry for their cooperation, support and help over this same time with various aspects of the sampling, data collection and tagging programs. Without their support, the collection of the underlying data used in this report would not be possible. We would also specifically like to acknowledge the help of Naomi Clear and Jessica Farley for their assistance in the provision of and help with the interpretation of the otolith data; and Bill Hearn for his help with the location and interpretation of the historical tagging and length-frequency data. FRDC provided funding support for this project.

Background

Estimates of SBT growth rates are fundamental to the SBT stock assessment. When this project was initiated, the analytic assessment and future stock projections for the southern bluefin tuna (SBT) resource were based on virtual population analyses (VPA) (e.g. Anon 1998a,b; Polacheck et al. 1998, 1999, Tsuji and Takeuchi 1998). The concept underlying VPA is that the time series of the estimated number of fish caught by age provides sufficient information for reconstructing the history of the population (i.e. the sum of the catches from a cohort in conjunction with natural mortality must account for the individuals born in the cohort). In the application of the VPA methodology to SBT, the catch at age matrix has been estimated from length-frequency samples of the commercial catches based on growth curves estimated from tagging data (Anon. 1994, Hearn 1994).

Since the initiation of this project, alternative assessment models for SBT have been developed (e.g. Hilborn et al. 1998, Butterworth et al. 2001, Polacheck and Preece 2001, and Kolody and Polacheck 2001). These models still depend on estimating the number of fish caught by age and year (referred to as the catch at age matrix) as the primary information for reconstructing the history of the population,

but use a more statistically based approach to handle potential errors in the estimation of the catch at age. In some of the alternative models, the same estimate of the catch at age matrix used in previous VPA analyses is adopted, while in others, the estimation of the catch at age data is performed internally based on the fit to imputed estimates of the length-frequency distributions for the catch and an estimated growth curve. In all cases, an estimated growth curve for SBT is fundamental information required for performing the SBT stock assessment and providing management advice on the probabilities of stock recovery.

The SBT assessment attempts to incorporate all of the critical uncertainties in the input data and underlying population dynamics in order to ensure that the results and management advice are robust and unbiased. However, the estimate of the growth curve and the catch at age matrix has been recognized as a major uncertainty that has not been appropriately accounted for in past SBT stock assessments. Currently, a single hypothesis for growth is used in the SBT assessments, and when this project was initiated the assessment models also assumed that the catch at age matrix was known without error. These simplifications have been adopted because of the lack of an adequate range of models for SBT growth and its variability. Within the SBT assessment, a number of internal inconsistencies are recognized among the various input data (Anon. 1996, Polacheck et al. 1998). These inconsistencies have been making it increasingly difficult to provide robust and scientifically objective conclusions about the short-term change in the status of the SBT population. As such, models that provide consistent interpretation of all the input data are urgently required. Their development has been considered a very high priority by the CCSBT Scientific Committee. The SBT growth model, particularly its application in estimating the catch at age matrix, has been identified as one of the likely sources of the inconsistencies (Polacheck et al. 1998).

The SBT catch at age matrix is estimated by converting estimates of the size distribution of the catch into an age distribution based on the modelled growth rates of SBT. SBT exhibit complex growth patterns and their growth rates are known to have significantly increased over the history of the fishery based on analyses of tag return data from the 1960's and 1980's. This change of growth was first taken into account in constructing the SBT catch at age matrix in 1993 (Polacheck et al. 1993). The

change in growth had significant effects on the stock assessments and resulted in substantially reduced estimates of the probability of recovery (Anon. 1993, Polacheck et al. 1993, Klaer et al. 1993).

The question of how to incorporate changes in SBT growth rates into the construction of the catch at age matrix was reviewed in a workshop conducted under the Tri-lateral process (the precursor to the present Commission for the Conservation of Southern Bluefin Tuna). Agreed-on methods were developed at that workshop and these methods form the basis for the procedures used in constructing the SBT catch at age matrix until 2001 (Anon. 1994). However, there are a number of unresolved problems and shortcomings in these procedures, largely related to the fact that information on growth from additional sources, and statistical models for incorporating this information, were unavailable at the time of the workshop[1]. Some of the problems with the growth model include:

- Growth rates were assumed to have changed linearly between 1970 and 1980;
- Growth rates were assumed to have been constant prior to 1970 and after 1980;
- No consideration of how growth rates may change in the future is incorporated into stock projections and estimates of the probabilities of recovery for the SBT stock (this could lead to over-estimates of the probability of recovery);
- Variability in growth among individuals of the same cohort is not accounted for[2].

Since the 1994 Tri-lateral Workshop, substantial new data have been collected on SBT growth. These include:

- Estimates of the age at length of individual fish based on direct aging from otoliths
- Estimates of growth rates of fish tagged in the 1990's

[1] Preliminary results from this project which provided updated estimates of SBT growth were incorporated into the stock assessments undertaken for the 2001 CCSBT Stock Assessment Group and Scientific Committee Meetings (Eveson et al. 2001, Anon. 2001c)

[2] The length based assessment model developed in Kolody and Polacheck (2001) and presented at the 2001 CCSBT Stock Assessment Group and Scientific Committee Meetings (Anon. 2001a, b) modelled variability and overlap in lengths among age classes using preliminary estimates of the mean length at age and their variances from this project.

- Estimates of historical changes in growth rates based on otolith increment measurements.

In addition, substantial information exists on the growth of juvenile SBT from modal information contained within the length-frequency data from the surface catches. These latter data were considered by the 1994 Workshop to be broadly consistent with the tagging data. However, they were not directly used in the estimation of the SBT growth model because of insufficient time and resources to develop the appropriate statistical model. A CCSBT Peer Review in 1998 recommended that the modal data for juvenile SBT be directly incorporated into the estimation of the catch at age matrix (Anon. 1998c).

When this project was initiated, none of these additional sources of data had been incorporated directly into the estimation of SBT growth rates. An adequate framework and model for integrating these diverse sources of information did not exist. Also, the amount of data is considerable and any integrated analysis would require substantial computing resources and analytical time.

Need

The uncertainty in the SBT catch at age matrix when using cohort slicing[3] or in the SBT growth curve when fitting directly to length data has been identified as one of the main sources of unaccountable uncertainty in the SBT stock assessments. The robustness of the assessment to this uncertainty is unknown. Moreover, a critical issue in the SBT stock assessment has been the internal inconsistency that exists among the input data and the need to develop improved models that can provide consistent interpretations for all of the available data. These inconsistencies have been making it increasingly difficult to provide robust and scientifically objective conclusions about short-term changes in the status of the SBT population. The model used for estimating SBT growth rates has been identified as a likely factor

[3] Cohort slicing is a procedure for estimating the age of a fish from their length and an estimated growth curve. The procedure determines the expected mean length for each age class adjusted for the time of year based on the growth curve. A fish of a given length is assigned to the age class which has the closest mean length to it. The procedure does not take into account that the actual length distributions of age classes generally overlap.

contributing to the apparent inconsistencies in the data. The current model of SBT growth was developed in 1993/94[4] and it makes simple assumptions about how growth may have changed since 1951. In particular, it assumes that the growth rate of SBT was constant in the 1960's and then increased linearly to a higher level in the 1980's. From 1980 to present, the growth rate is assumed to have remained constant, at a level estimated using recaptures from the 1983/84 tagging program. Past changes in the growth rate of SBT are consistent with density dependent growth; the current model fails to address the question of whether growth may decrease in the future if the population recovers. Given that the incorporation of change in growth between the 1960's and 1980's had a significant effect on the stock assessment and substantially reduced estimates of the probability of recovery, it is critical for the provision of reliable assessments and management advice that changes in SBT growth are appropriately and accurately accounted for in the analyses.

Since the 1994 growth models were developed, a substantial amount of new information has been collected on SBT growth based on direct aging, otolith increment measurements and tagging experiments conducted in the 1990's. Initial analyses of some of these data suggest that the assumptions about changes in SBT growth embedded in the current models are likely to be inadequate. There is a need to incorporate these new data within a comprehensive analysis and to develop an integrated model that includes all the various sources of information on SBT growth. Such an integrated model should also provide the basis for addressing uncertainties associated with the growth curve and/or catch at age matrix within the SBT stock assessment. An improved growth model would in turn allow for the development of improved assessment models that are able to provide consistent interpretations of the available data and thus improve the reliability and robustness of the management advice based on these models.

Objectives

6. To develop an integrated method for modelling SBT growth that combines growth increment data from tagging experiments, length measurements and

[4] See footnote 1

direct aging estimates from otoliths, length-frequency modal information and otolith growth increments.

7. Using this integrated method, develop models for the historical changes in SBT growth that can be used to estimate the expected length of SBT at age and the associated variance for the entire period of the commercial fishery.
8. Produce appropriate estimates of growth rate parameters for direct input into length based assessment models.
9. Develop a set of alternative hypotheses for the factors underlying changes in SBT growth that are consistent with the observed growth data.
10. Based on these alternative hypotheses, develop models for changes in the length at age that can be used in SBT stock projections.

Methods

Data

Three primary sources of data with information relevant to SBT growth were compiled for use in the analyses conducted within this project:

1) growth increment data over a known time period from tag-recapture experiments;
2) modal progression within a year from length-frequency data from commercial catches; and
3) direct age estimates from otolith readings combined with the length of a fish at the time of capture.

These data sources provided information on SBT growth spanning the four decades from 1960 to 2000. However, for each of the data sources, the amount of data varied considerably over time, as did the coverage in terms of the age range of fish that the data spanned (see Appendix 3).

Before the compiled data were used in the estimation of growth, they were examined with respect to quality and consistency. In each of the data sets, a number of potential problems were identified and procedures were developed for data screening. The underlying principle in developing the data screening procedures was to ensure that the screening process would not introduce biases into the estimation of the growth rates (e.g. favour faster or slower growing fish) and to remove data for

which large measurement uncertainty could be identified. This latter is important to ensure precise estimation of the growth parameters and reliable estimates of the expected actual variation in growth at a given age. Details of the data screening procedures are described in Appendix 3.

In addition to the above three primary data sources, data on the growth increments between annual rings in a sample of SBT otoliths was utilized in the examination of changes in growth over time. The data used in this report are the same as those analysed by Gunn and Farley (1998). Details of the data collection and preparation can be found in this reference. A strong correlation exists between otolith length and overall fish length for SBT (Gunn and Farley 1998, Gunn et al. in prep.). As such, the distance between successive annual bands within the otolith can provide a measure of the relative growth. Comparison of growth increments within the otoliths for comparable ages from fish born at different times can indicate when and to what extent growth has changed over time. Almost all SBT otoliths have been collected from fish caught in the 1990's. Nevertheless, the increment data from these otoliths can provide retrospective information on the growth of younger fish over four decades, since SBT live up to 40 years.

Increment data are available on 489 otoliths from fish estimated to have been born between 1953 and 1994. The distances between the five first consecutive bands were recorded for each otolith (or all increments for fish with less than five bands). Otolith growth for the first year of life was not measured because the precise position of the primordium was not always distinguishable. Since only data on the increments between annual bands are available these data are not informative for estimating absolute growth rates. Even if absolute otolith sizes were available, the error in predicting fish length from otolith length and the lack of direct measurement for most of the sampled fish within the age range of the increment data would limit their use in this context.

Estimating the time of band formation

There is an important source of measurement uncertainty in the otolith data. It is associated with variation in the time of band formation. Previous studies of SBT otoliths found that SBT form annual translucent zones (bands) in their otoliths during

the austral winter (Clear et al. 2000). However, reliable information was not available to more precisely estimate when a band is likely to have formed and be detectable. Thus, there is an uncertainty of one year in the estimated age and cohort of fish for which otoliths were collected during this winter period. This in turn can translate into individuals from the same cohort being assigned to three different age groups during the period of transition (i.e. their true age group, one year older if the band has been formed but is assumed not to have been, and one year younger if the band has not been formed but is assumed to have been). In order to obtain an improved understanding of the timing of band formation and to provide a basis for estimating the probability that a band had been formed in a given month, additional otolith research was undertaken.

It should be noted that the problem of the time of band formation had not been anticipated to be a substantive complication in the use of the existing direct otolith aging data and work on developing improved estimates had not been included within the original research proposal. This additional work was undertaken and included in the current project after consultation with FRDC.

Two approaches were used to provide improved information on the time of band formation. In the first approach, we used data from a previous age-validation study (Clear et al. 2000) in which a number of SBT were caught as part of a large-scale tagging program and injected with strontium chloride at the time of tagging. Strontium chloride ($SrCl_2$) is a harmless salt that deposits in the otolith and provides a "time-stamp" of the date of tagging. When the fish are recaptured and the otoliths are removed, the number of increments formed subsequent to marking can be determined by counting the number of translucent zones deposited after the strontium mark. Because the amount of time the fish has been at liberty is known, we can determine whether or not the translucent zone for the recapture year has yet been formed (or is yet detectable). The results obtained from this investigation did not provide as fine a resolution of the time of band formation as we had anticipated. This was a significant issue for the current project because a substantial amount of direct aging data comes from fish captured during these winter months. Results of fitting growth curves to the direct aging data were found to be sensitive to assumptions about the time of band

formation. As a consequence, additional work was undertaken to see if a more precise and accurate estimate of the time of band formation could be determined.

Two methods have been developed for reading otoliths – one in which the otolith is left whole and one in which it is sectioned (Gunn et al. in press). Preliminary exploration of existing otolith data suggested that the ability to detect a translucent zone forming on the margin may differ between the two methods. For fish caught during the winter months while a marginal band is forming, it is important to know whether a true difference exists. If it does, then the age assigned to these fish could be one year different depending on the method used. A difference in age of one year for small fish can have a significant impact on the estimation of growth rates. Moreover, it was realized that if a consistent difference did exist, it could be exploited to refine the time when bands become detectable with both methods by comparing otolith readings using both methods on the same fish. For example, the first month in which a difference in the number of bands was found between the two methods would indicate the month when bands first became detectable with the method yielding the higher number of bands. This month would mark the beginning of the potential period of band formation. The subsequent month in which both methods yielded the same number of bands would indicate the month when bands were consistently detectable by both methods, and would mark the end limit of the period of band formation. In order to address the problem of whether a consistent difference did exist and whether it could be used to refine the estimates of the time of detectable band formation, we conducted a study using pairs of sagittal otoliths from the same fish. (See Appendix 11 for more detail.)

Growth curves

To allow for a range of functional forms for SBT growth to be considered, a generic growth curve was defined that could easily be formulated and parameterised to represent a variety of growth patterns. The advantage of this approach is that a single statistical estimation approach could be developed for this generic form, which could then be used to examine the suitability of a variety of different functional forms. The generic growth curve was defined to be of the form:

$$l(a) = L_\infty f(a - a_0; \theta) \quad (1)$$

where L_∞ is asymptotic length and f is a monotone increasing function with parameter set $\{a_0, \theta\}$ that approaches 1 as $a \to \infty$ and equals 0 when $a = a_0$. The parameter a_0 can be conceptualised as the theoretical age at which a fish would have had length 0 if we were to project its growth curve backwards.

Most of the growth curves commonly used in fisheries can be formulated in terms of equation 1. For example, for the von Bertalanffy curve, $\theta = \{k\}$ and $f(a - a_0; k) = 1 - \exp(-k(a - a_0))$. In the course of the project, specific formulations of this generic growth curve were used to examine the traditional von Bertalanffy and Richards growth curves (see Appendices 4 and 9). In addition, a new growth curve was developed that can accommodate a marked change in the growth pattern at some point in the life cycle, called the von Bertalanffy growth curve with a logistic k parameter (referred to here as the VB log k curve, see Appendix 4). Essentially, this growth curve is a modification of the von Bertalanffy curve that allows for the parameter k to make a smooth transition from k_1 to k_2 over time. The motivation for such a curve came from recent analyses of tag-recapture data for SBT. These suggested that a more complex curve that incorporates a two-stage growth process is required for this species (Anon. 1994, Hearn and Polacheck in press).

As would be expected in the development of an integrated growth model, a common functional form for f was used when a growth model was fitted to multiple data sources.

Fitting growth curves to tag-recapture data

A new maximum likelihood approach was developed for fitting the generic growth model (equation 1) to tag-recapture data. The details of this approach are documented in Appendix 4[5]. The method is based on modelling the joint density of tag and recapture lengths rather than the more common past approach of modelling the growth increments.

[5] A version of Appendix 4 was submitted and accepted for publication in the Canadian Journal of Fisheries and Aquatic Sciences (Laslett et al. 2002).

The following notation is used to describe the tag-recapture data in terms of the generic growth function (equation 1). Let l_1 represent the measured length of a tagged fish that was released at time t_1, and let l_2 be its measured length upon recapture at time t_2. All of these values are known. Let $A = t_1 - t_0$, where t_0 is the theoretical *time* at which a fish has length zero (analogous to the parameter a_0 on the age scale). Then A is a random variable, which we assume has density $p(\cdot)$ and whose parameters will be estimated in the model. Although the age at release is unknown, if we denote it by a_1, then A is equivalent to $a_1 - a_0$. Similarly, $A + t_2 - t_1$ is equivalent to $a_2 - a_0$, where a_2 denotes the age at recapture.

In terms of equation 1, we can specify the models for the release and recapture lengths respectively as

$$\begin{aligned} l_1 &= L_\infty f(A;\theta) + \varepsilon_1 \\ l_2 &= L_\infty f(A + t_2 - t_1;\theta) + \varepsilon_2 . \end{aligned} \qquad (2)$$

The asymptotic length is allowed to vary from fish to fish by modelling L_∞ as a random normal effect with mean μ_∞ and standard deviation σ_∞. (See below for more details on the choice of error structure used.) The terms ε_1 and ε_2 represent residual error in the release and recapture lengths respectively, which combine measurement error and residual model error (i.e. variation other than that due to variation in L_∞ among fish) since there is insufficient information with which to separate these sources of error. They are assumed independent within an individual fish and between fish, and also independent of L_∞ and A. Furthermore, they are assumed to be normally distributed with mean 0 and variance dependent on the length measurer. Two classes of measurers were distinguished in the analyses: one being scientists or trained staff and the other being fishermen or factory staff (σ_s^2 was used to represent the variance for a scientist or trained staff measured fish and σ_f^2 for the additional variation in a fisherman or factory staff measured fish). Hearn and Polacheck (in press) found significant differences in measurement error between these

two groups, with measurements made by scientists being more accurate than measurements made by fishermen. Note that the release lengths for all tagged fish were measured by scientists. Thus,

$$V(\varepsilon_1) = \sigma_s^2$$

$$V(\varepsilon_2) = \begin{cases} \sigma_s^2 & \text{if measured by a scientist} \\ \sigma_s^2 + \sigma_f^2 & \text{if measured by a fisherman.} \end{cases} \quad (3)$$

If we condition on A, then l_1 and l_2 are both the sum of random normal variables and their joint distribution, $h(l_1, l_2 \mid a)$, is bivariate normal. Their unconditional joint density can then by obtained by integrating over A. Namely,

$$h(l_1, l_2) = \int h(l_1, l_2 \mid a)\, p(a)\, da\,. \quad (4)$$

The product of the joint densities over all fish gives the likelihood function for the tag-recapture data. Thus, the negative log-likelihood function can be expressed as

$$-\ln(\lambda_1) = \sum_i \ln h(l_{1i},\, l_{2i}) \quad (5)$$

where i indexes the fish.

Methods used for performing the numerical integration were developed and are described in Appendix 4.

Fitting growth curves to length-frequency data

A two-step procedure was developed to enable efficient use of the length-frequency data in fitting growth curves. First, a mixture decomposition was performed on each half-monthly sample independently to generate a mode and an accompanying standard error for each age-class represented in the sample. Second, the summary statistics from step one were used as input into the likelihood component for the length-frequency model that was developed.

In the first step, each length-frequency sample was assumed to be a mixture of Gaussian components, where the number of components and the age-classes to which they corresponded were specified. Since the length-frequency data are dominated by juvenile fish with small numbers of fish greater than age 4, and since the modes become less distinct after age 4, no attempt was made to separate out modes beyond age 5. The modes were usually quite distinct and the corresponding age-classes were generally clear based on the lengths near the mode. There were, however, several exceptions in which our best judgement had to be used. The estimation of the mixture decomposition parameters was unconstrained except for simple bound constraints. This differs from previous modal decomposition approaches (e.g. Leigh and Hearn (2000), who constrained mean growth over a season to be linear, and Schnute and Fournier (1980), who constrained the means to follow a von Bertalanffy growth curve). The standard deviation of the components was assumed to be common within a sample, but was allowed to differ between samples. A standard error associated with each mode was calculated by inverting the observed information matrix. The estimation procedure took into account the fact that the data were scaled up from the actual sample size to the size of the catch. A detailed description of the first step is given in Appendix 7.

In the second step, a growth model was fitted to the estimated modes (denoted by $\hat{\mu}$) and standard errors (denote by s) from step one. In terms of the generic growth function (equation 1), the model can be expressed as

$$\hat{\mu}_{ijk} = \mu_{\infty} f(a_{ijk} - a_0; \theta) + e_{ijk} + \varepsilon_{ijk} \qquad (6)$$

where a_{ijk} is the mean age assigned to the mode from year i, half-month j, and age group k, and e_{ijk} and ε_{ijk} are independent random effects representing sampling error and residual model error respectively. We assume $e_{ijk} \sim N(0, s_{ijk}^2)$, where the s_{ijk} are the estimated standard errors from step one, and $\varepsilon_{ijk} \sim N(0, \sigma_{\varepsilon}^2)$. The mean age assigned to a sample is based on assuming a mean birth date of January 1 (see Appendix 7 for details on the assignment of mean age). The parameter μ_{∞} represents the average asymptotic length for a group of fish, and is modelled as a fixed effect. It

could be modelled as a random effect; however, there is almost no information from the length-frequency data alone on the mean asymptotic length of fish, let alone its variance. In practice the estimate for μ_∞ is determined by the tagging and the direct aging data in the integrated analyses. The negative log-likelihood for the length-frequency data is given by

$$-\ln(\lambda_2) = \frac{1}{2}\sum_i\sum_j\sum_k\left[\ln\left(2\pi V(\hat{\mu}_{ijk})\right)+\frac{\left(\hat{\mu}_{ijk}-E(\hat{\mu}_{ijk})\right)^2}{V(\hat{\mu}_{ijk})}\right] \quad (7)$$

where

$$E(\hat{\mu}_{ijk}) = \mu_\infty f(a_{ijk}-a_0;\theta)$$

and

$$V(\hat{\mu}_{ijk}) = s_{ijk}^2+\sigma_\varepsilon^2.$$

More complicated models for the length-frequency data were explored (e.g. random fishing season effect, within-season random half-month effect, and a within-season random age effect). However, such models did not provide improved fits (see Appendix 7 for more detail) and as such only the above model was used in the integrated modelling.

Fitting growth curves to direct aging data

In the fitting of growth curves to the direct aging data, it was assumed that the age of a fish was known without error. There are three principal potential sources of error in the estimates of age from otoliths:

1. Whether a band has formed during the year in which the fish was captured;
2. Mistakes in counting in the number of bands; and
3. The date of "birth".

Note that the last of these is primarily important for accounting for within season growth for fish past age 1. Thus, whether a fish was spawned early or late during the spawning seasons appears not to be reflected in the size at age for a fish beyond the first year (e.g. the multiple modes sometimes evident for new recruits in the size composition data does not persist past age 1). The amount of error as the result of counting errors is thought to be small (e.g. independent age readings have errors of less than 4%; Gunn et al. in press).

The possible errors associated with the time of band formation are discussed above and in Appendices 3 and 12. Although substantial work was undertaken to refine estimates of the time of band formation, the available data did not prove sufficiently informative to provide reliable estimates of the probability of a band being formed during the period from June through September, while there is a high degree of certainty outside of these months (see below and Appendix 11). Results for estimated curves were found to be sensitive to assumptions made about the timing of band formation within this June to September period. As such, otoliths collected during these months were excluded in the fitting process. While this reduced the amount of direct aging data, it ensured that no biases were introduced into the fitting process as a result of assumptions about the time of band formation.

The age of a fish was estimated based on the number of bands which were counted and the date of capture assuming a January 1 "birth" date. A decimal age was assigned to each fish as follows:

$$\text{age} = \begin{cases} n + r/365 & \text{if } r < d \\ n - 1 + r/365 & \text{if } r \geq d \end{cases} \tag{8}$$

where n = the number of bands counted,

r = the capture date, and

d = the date of band formation.

Both r and d are expressed in Julian days since January 1 of the year of capture. Note that d was assumed to be July 1, but its exact date has no effect on the results since otoliths collected between June-September were excluded. See Appendices 3 and 9 for more detail.

Assuming there is no error in the age estimate, the model for fitting the direct aging data is

$$l_i = L_\infty f(a_i - a_0; \theta) + \gamma_i \tag{9}$$

where l = a fish's length

a = its age,

i = the index for an individual fish, and

γ = measurement and residual model error.

We assume that γ is normally distributed with mean 0 and standard deviation σ_γ. As with the tag-recapture data, L_∞ is modelled as a random normal effect with mean μ_∞ and standard deviation σ_∞. We assume that L_∞ and γ are independent. It follows that the negative log likelihood for the direct aging data is

$$-\ln(\lambda_3) = \frac{1}{2}\sum_i \left[\ln(2\pi V(l_i)) + \frac{(l_i - E(l_i))^2}{V(l_i)} \right], \tag{10}$$

where

$$E(l_i) = \mu_\infty f(a_i - a_0; \theta)$$

and

$$V(l_i) = \sigma_\infty^2 f(a_i - a_0; \theta)^2 + \sigma_\gamma^2.$$

The integrated estimation model

Given the likelihood equations developed above for the different sources of data, the overall negative likelihood function when fitting to multiple data sources is simply the sum of the relevant negative log-likelihood functions given above. Namely,

$$\Lambda = -(\ln(\lambda_1) + \ln(\lambda_2) + \ln(\lambda_3)). \tag{11}$$

The parameters common to all three components are θ (the parameters of the growth function f) and μ_∞ (the mean asymptotic length). The asymptotic variance parameter σ_∞ is common to the tag-recapture and direct aging components. For the length-frequency component, we are not modelling lengths of individual fish but rather we are modelling mean lengths (see equation 6). As such, the asymptotic length parameter should have the same mean but not the same variance as the asymptotic

length parameter in the tag-recapture and direct aging models. There is no information on fish older than age 4 in the length-frequency data alone to estimate the relevant asymptotic variance parameter, so we modelled the asymptotic length as a fixed effect for this component. Whether the asymptotic length is assumed to be random or fixed will have virtually no effect for fish aged 1 to 4. The parameter a_0 is common to the direct aging and length-frequency components; this parameter is not present in the tag-recapture model because it is encompassed in the random variable A. The parameters defining the lognormal distribution of A, namely $\mu_{\log A}$ and $\sigma_{\log A}$, are unique to the tag-recapture component. The various error parameters are unique to their corresponding components, namely σ_s and σ_f for the tag-recapture component, σ_ε for the length-frequency component, and σ_γ for the direct aging component.

Simulating growth curves

Extensive simulation testing of the statistical models and estimation procedures were conducted to ensure that the models were robust and provided adequate performance in terms of their statistical properties. The simulation studies were also conducted to provide insight into the selection of an appropriate error structure to use in modelling SBT growth.

The simulation methods consisted of generating monte-carlo simulated data sets under a variety of model structures with different levels of underlying variability and for differing levels of sampling intensity and age coverage. The growth parameters were then estimated using the maximum likelihood methods described above under a variety of model assumptions. The results of these fits were then compared in terms of how well the estimated growth curves captured the "true" or underlying growth curve in the simulated data sets. Appendix 6 contains further details on the simulation methods and their evaluation. Results of these simulations are summarized below and more detail results are contained in Appendices 4 and 6.

Changes in growth

Two primary approaches were used to examine changes in SBT growth over time. The first approach was to apply the above integrated model to data from

different periods and compare the resulting estimates. This first approach is straightforward and required no additional methodological development (see Appendix 10).

The second approach was to develop a model that would allow for changes in growth to be estimated and described by time varying parameters within a single overall model of growth. There has been little previous work on this problem. The approach we adopted was to model the growth rate parameters as a function of time. We focussed on modelling changes in growth rates over time since the mean asymptotic length appears to change by at most a few centimetres over the 40 year period of the study (see Appendix 10). We examined various ways in which the growth rate parameters may be modelled in a flexible but parsimonious manner (Appendix 8).

We developed a model in which the growth rate $k(t)$ varies according to a series of superimposed logistic curves. It is clear intuitively that such a model has the capacity to follow changes in growth. The basic model is aimed at situations in which a von Bertalanffy growth curve applies, then a change in environment dictates that growth changes until a new von Bertalanffy growth phase is achieved. Extensions of the model to the VB log k model were also explored (Appendix 8). The model allows for several such transitions, often in concert. An expression for k(t) is

$$k(t) = n\xi_0 + \sum_{i=1}^{n}(\xi_i - \xi_0)\frac{1}{1+\exp(-\beta(t-\alpha_i))} \qquad (12)$$

where $\alpha_1 < \ldots < \alpha_n$ and $\beta > 0$. Note that t is time, and hence spans the whole real line. As $t \to -\infty$, $k(t) \to n\xi_0$, and as $t \to \infty$, $k(t) \to \sum_{i=1}^{n}\xi_i$. The ξ_i values can be any number, positive or negative subject to $k(t) > 0$. β could also be made dependent on i but this would likely make the model over-parameterised. Although the above equation encapsulates the reasoning for this model, it is not a suitable form for computation. We developed two alternative parameterisations of the model (see Appendix 8 for details). We also extended this logistic k model to allow for seasonal differences in growth.

In Appendix 8, we also considered and developed two alternatives approaches to the above logistic set of curves for modelling trends in k over time (polynomial and hyperbolic splines). We concluded that the logistic curve approach appeared more suitable and used it for estimating trends in k over time for SBT.

In addition, we compared results from the otolith increment data in relationship to the results we obtained from the above two approaches.

Results

The time of band formation

The results indicate that otolith bands are generally formed between May and September. There is substantial variability in time of formation among individual fish, with July 1 being an approximate average. In the study of sister otoliths read whole and sectioned, no consistent difference was found between the number of bands counted and the time of year for the two methods. This means that comparison of number of bands from the same fish using the two methods cannot be used to provide further information on the timing of band formation (see Appendix 11 for more detail).

With the available data, it was not possible to further refine the time period when bands are formed or to reliably assign relative probabilities that a band had formed by a certain date. As such, uncertainty of a year (plus or minus) exists about the age of a fish caught during the period of band formation. As noted above, this uncertainty can induce substantial uncertainty and potential bias into the estimation of growth curves if fish caught during this transition period are included without appropriate consideration. Some preliminary results suggested that estimates would be sensitive if a fixed date were used as the time when a band was formed. We developed some initial statistical approaches for dealing with this problem (see Appendix 12). However, their application turned out to be highly complex and required substantially more data than were available. As such, the application of this approach was beyond the scope of the current project. An alternative solution was simply to exclude direct aging data from those months when bands are being formed.

It is important to note that this solution does not bias the estimation of growth, while their inclusion with some assumption about the time of band formation could. Moreover, given the sample sizes, this solution does not have a substantial effect on the resulting precision of the estimates. Thus, only direct aging data from fish caught outside the proposed months of band formation (i.e. from October through April) were included in growth analyses for the current project. In doing this, we believe that we should have excluded almost all, if not all, fish for which the time of band formation could potentially confound the estimation of its age.

Although the main purpose of comparing whole and sectioned otolith readings was to see if the results could be used to refine the time of band formation, the work produced important results for future direct aging studies. Thus, while the two methods show quite good agreement (64%), there appears to be a tendency for the sectioned count to have one more band than the whole count. The discrepancy between the whole read and the sectioned read does not appear to be related to the size of the fish (see Appendix 11), although the sample sizes in the smaller length-classes are too small to be certain. As discussed in Appendix 11, examination of the length of the smaller fish in relationship to age estimates from the otoliths suggests that the whole count is more reliable for young (small) fish. However, the whole method cannot be used for larger fish (fork length >135 cm). Thus, with respect to using direct aging, it is preferable to use the whole otoliths technique for smaller sizes, and sectioned method subsequently.

Model fitting – introduction

Given the multiple sources of information and years over which the data were collected, a stepwise approach was used to arrive at a final integrated model. This ensured that each of the methods for each of the sub-components of the integrated likelihood constituted an appropriate and robust estimator for a particular data source. It also allowed for development and exploration of the "best" statistical approach for a given set of data without simultaneously having to deal with the complexities arising from the other sources. This stepwise approach resulted in substantial methodological developments and results in terms of estimating growth curves from tag-recapture data and length-frequency data separately. As such, results are presented first in terms

of fitting these two data sources, before results from the integrated fitting are provided.

Choice of error structure

Substantial variability exists in the size of fish at any given age. This variability stems from a combination of genetic (e.g. individual propensity to grow faster and/or larger) and environmental factors that can vary throughout the life of a fish (e.g. food availability, water temperatures, density of con-specifics, etc). In addition, measurement error will exist both in the determination of age and in the measurement of lengths. As such, defining appropriate errors structures to represent how variability in growth translates into variability in length is an important component of the statistical modelling of growth and the evaluation of the adequacy of the fit of any model to observed data. Moreover previous work on the estimation of growth from tag-recapture data has found that the choice of the error structure used in the estimation of the growth curve is important and that selection of the wrong error structure can induce substantial bias into the estimates of the parameters (e.g. (Sainsbury 1980, Maller and deBoer 1988).

The effects of different sources of variability will tend to be confounded, which can complicate selection of the most appropriate model. There is no *a priori* way to determine what sources of variability are the primary contributors to the observed variation in any particular data set. Different sources of variability will lead to different patterns in how the amount of observed variability varies with age (see Appendix 6). These differences can be used to provide guidance in selecting the most appropriate model. We considered four basic alternatives:

1. that the variability is constant across all ages;
2. that there is individual variability among fish in their asymptotic length (L_∞);
3. that there is individual variability among fish in their intrinsic growth rates (e.g. the k parameter in a VB growth model);
4. that there is individual variability among fish in their asymptotic length and in their intrinsic growth rates.

In all of the latter three alternatives, we also allowed for an element of constant variability that reflects a combination of both model error (i.e. random variation due to environmental variation for example) and measurement error.

Inspection of the length at age distribution from direct otolith data for older fish approaching their asymptotic length (e.g. fish over 25 years of age) indicated that there was substantial variability, and that the variability is rather constant and does not decrease with age (see Figures in Appendix 10). Such a pattern is not consistent with one in which the dominant source of variability is individual variation in intrinsic growth rates. In addition, in all cases where we fit growth curves using either the tagging or direct aging data, inclusion of a term for individual variability in L_∞ resulted in a significantly better fit than simply assuming a constant variance[6] (e.g. see results in Appendices 4, 9 and 10). As such, the above suggests that either the second or fourth alternative would be the most appropriate.

The simulation study reported in Appendix 6 indicates that only including a term for individual variability in L_∞ when there is both individual variability in L_∞ and in the intrinsic rate of growth has only minimal effects on the estimation of the growth curve. In addition, results of fitting tagging data with the above four alternative error structures to a standard VB growth curve indicated that the most appropriate error structure to use was one that only included individual variability in L_∞ (Table 1). For these reasons, we chose an error structure in our modelling of SBT growth that included individual variability in L_∞ plus an additional random component. This does not necessarily mean that there is not individual variability in the intrinsic growth rates, but only that it appears not to be distinguishable from the residual variance. As such, inclusion of a term for this adds little or nothing to the estimation of SBT growth within the resolution of the existing data.

At the beginning of this section we noted that previous studies found that selection of the wrong error structure can induce substantial bias into the parameter estimates. In these studies, the estimation of growth curves was based on the fitting of

[6] The length-frequency data are not informative about the appropriateness of including a term for variability in L_∞ because the data only provide information on fish up to age 4 (see Appendix 9).

tag increment data (initially using the Fabens (1965) method). In the simulation analyses that we conducted, we found that the parameter estimates were generally highly robust to the choice of the error structure even for tag-recapture data (see Appendix 6). The difference appears to be due to the estimation method that we developed in this project for tag-recapture data that jointly models both the release and recapture lengths, instead of simply the increment data (see Appendix 4). This is an important property as it suggests that robust and unbiased estimates can be obtained even in situations where the data may not be informative for discriminating what is the most appropriate error structure (e.g. because of small sample size or incomplete age coverage).

Choice of growth curves – fitting the 1980's tagging data

Previous studies of SBT growth have suggested there is a change in the growth process for SBT during the transition from juveniles to adults that cannot be adequately captured by a standard von Bertalanffy growth curve (Anon. 1994, Hearn and Polacheck, in press). Anon. (1994) and Hearn and Polacheck (in press) model SBT growth as a two-stage process in which the growth in each stage follows a different VB curve, such that there is a discontinuity in the growth rate at the transition between the two stages. In this project, we have developed an alternate growth curve that can accommodate a change in the growth pattern at some point in the life cycle but allows for a gradual, smooth transition between stages (for details Appendix 4). We call this new curve the von Bertalanffy growth curve with a logistic growth rate (abbreviated VB log k) to reflect the fact that the change in growth rate is modelled using a logistic function. The growth function for the VB log k model is given by

$$f(a-a_0;\{k_1,k_2,\alpha,\beta\}) = 1-e^{-k_2(a-a_0)}\left\{\frac{1+e^{-\beta(a-a_0-\alpha)}}{1+e^{\alpha\beta}}\right\}^{-(k_2-k_1)/\beta} \qquad (13)$$

As a increases, this function makes a smooth transition from a VB curve with growth rate parameter k_1 to a VB curve with parameter k_2. β governs the rate of the transition (being sharper for larger values), and α governs the age at which the midpoint of the transition occurs. As discussed in Appendix 4, this new growth

function provides an improved formulation for modelling growth with a transition phase than the two stage von Bertalanffy model used previously and overcomes some the statistical problems that Hearn and Polacheck (in press) encountered in fitting the stage von Bertalanffy to SBT tag-recapture data.

In Appendix 4 results of applying this VB log k model to 1980's tag-recapture data are presented using the new estimation method developed in this project. The results indicate that the VB log k model results in a substantially better fit to the 1980's SBT tag data than a standard VB curve. Thus, the results confirmed the importance of allowing for a transition phase when modelling SBT growth. The results also indicate that the VB log k model can provide an appropriate function for modelling growth with tag-recapture data when a transition exists and that the estimation procedure produces unbiased results. As such, in the subsequent modelling of SBT we used the VB log k function, but also compared the results with those from fitting a standard VB curve.

Fitting the length-frequency data

The results from fitting length-frequency data independently suggest that growth patterns within these data do not conform tightly to a particular growth curve (see Appendix 7 for detail). There appear to be significant additional sources of variation operating between years (i.e. fishing seasons), between age groups within years, between half-months within years and between age groups and half-months within years (interactive effects). We are unable to offer explanations for all of these effects in terms of covariates, and suggest that initially they should be modelled as independent hierarchical and crossed random effects. Otherwise standard errors of growth parameters derived from length-frequency data are likely to be optimistically small. We suspect that a substantial portion of the variability may be due to the clustered sampling of the population that occurs in the surface fishery (e.g. the schooling nature of SBT involves apparent size/age segregation overlaid with spatial clustering of schools and large within and between year variability in location, migration and residence time within the area of the fishery).

Despite this complexity, the results indicate that southern bluefin tuna consistently exhibit a seasonal pattern in which growth is fastest over the summer but

flattens off in autumn. A sine curve with amplitude and phase parameters estimated from the data appears to provide an adequate model for capturing this within-year seasonal effect. The results also indicate that broad changes in growth from year to year occurred based on the estimated between-year random effects (Appendix 7). Furthermore, these year effects change rather smoothly over time, and indicate that they should be modelled as systematic effects rather than random effects.

The results from fitting the length-frequency data indicate that at a qualitative level, the mean length of one-year-old fish has changed only in minor ways between 1960 and 1989, but age 4 fish in the 1980's are considerably longer than those in the 1960's. This question is explored further in the context of the integrated and time varying k models in Appendices 8 and 10.

The results from modelling the length-frequency data clearly demonstrate that these data provide unique and valuable information for modelling growth. However, these data generally do not contain information on older individuals and thus are not adequate by themselves. The modelling approach we used required an assumed value for the mean asymptotic length when fitting the length-frequency data alone (this is not necessary in the integrated model). We chose a value of 185 cm based on results in Appendix 4 and mean length of older directly measured fish. The results over the age range represented by the length-frequency data are not sensitive to the value chosen. Thus, the methods we developed for estimating growth from length-frequency data provide a robust method for estimating growth of younger fish from length-frequency data as long as a reasonable estimate of the asymptotic length is available.

We also note that the approach developed in Appendix 7 could be used to provide direct estimates of the age distribution of the catches from these length-frequency distributions. This approach would be preferable to the current practice of estimating the age distribution using cohort slicing as it takes into account the overlap in size among age classes.

An integrated model for the 1980's

The general integrated likelihood approach that we developed in this project was first applied to combined data sets for the 1980's in order to ensure that the method provided consistent estimates and to determine the appropriate level of model complexity that needed to be considered when applying the modelling approach to the full data sets. The results of the model development and evaluation process are described in detail in Appendix 9.

The results of this fitting process indicated that an integrated model using a common growth function could be fitted to each of the data sources and that each of the data sources provided a generally consistent and complementary fit. The only indication of any substantive inconsistency was in estimates for age 1 fish from the direct aging and length-frequency data. As discussed in detail in Appendices 3 and 9, this stems from the fact that within the age 1 fish there is spatial segregation by size that appears to be related to the actual age (i.e. age in terms of a when fish were spawned). However, in both of these data sources we are not able to resolve age to a finer level than individual year-class. SBT are also growing quite rapidly at this young age. Thus, any estimate for size of one year old fish will be highly sensitive to both the timing of the sampling and the proportion of fish in the overall sample that come from different locations. It should be noted that SBT growth during their first six to nine months is extremely rapid and would be expected to be functionally different than subsequent growth. Further, in terms of this project's primary objective for modelling SBT growth (i.e. for estimation of the age structure of the catch in an assessment context), precise estimation of the size of fish aged 1 and younger is not critical.

In developing the integrated model, we considered the addition of a seasonal component to the basic VB log k model. SBT growth, particularly as juveniles, appears to be substantially greater during the austral summer months than during the winter. Seasonality in growth was modelled by replacing $a - a_0$ with $a - a_0 + S(t)$ in equation 1, where t is the fractional time of year since January 1. Within year growth was modelled as a sinusoidal function:

$$S(t) = \frac{u}{2\pi}\sin(2\pi(t-w)) \tag{14}$$

where u is the amplitude and w is the phase. The amplitude was constrained to be between 0 and 1 to prevent negative growth and the phase was constrained to be between –0.5 and 0.5. (Note any bounds for the latter with a span of one could have been chosen due to the periodicity of the function.) In this formulation, the rate of growth is maximal at $t = w$ and diminishes symmetrically about w to a minimum at $t = w - 0.5$ and $t = w + 0.5$.

Comparison of results for the complete data sets for the 1980's with and without this seasonal component indicated that inclusion of the seasonal component yielded a substantial and statistically significant improvement in the overall fit, although it had little effect on the parameter estimates for describing the longer-term growth (e.g. μ_∞, k_1 and k_2). The inclusion of the seasonal component resulted in a noticeable improvement to the residuals for the length-frequency data (see figures in Appendix 9). It was also important in that it allowed information on growth from tag-recaptures with short time at liberty to be included in the analyses. Previous studies had excluded tag returns with less than 270 days at liberty because the strong seasonal signal in growth was seen as problematic if these shorter term recaptures were included (Anon. 1994, Hearn and Polacheck in press). There are substantial numbers of tag returns with times of liberty less than 270 days. Such tags can provide valuable additional information on the growth at younger ages (since these were the ages that were tagged) as long as seasonal effects are appropriately accounted for.

It is worth noting that previous questions have been raised about the validity of estimating mutual growth parameters in an integrated framework using more than one data source (Francis 1988). The results in Appendix 9 (and additionally in Appendix 10) demonstrate not only that consistent estimates can be achieved, but also that there is considerable advantage in combining data from more than one source, particularly when there is poor or incomplete coverage of the full age range of fish within any one data source. However, in doing this, it is essential that appropriate models and likelihood functions be developed that reflect the information on growth and appropriate error structures for each data source. It is also important that the data

are comparable in terms of the group of fish (e.g. cohorts) for which growth is being estimated.

Comparison of growth curves over four decades

The integrated estimation method was applied to the data from cohorts from the 1960's through the 1990's. We separated the data by decade in order to obtain estimates of the average realized growth by cohorts from each of these decades[7]. We applied the VB log k model with a seasonal component to each data set and obtained estimates for the parameter values (Table 2). Comparison of the parameter values suggests that there has been little or no change in the mean asymptotic length (μ_∞) but that there has been an increasing trend in growth rates at younger ages as reflected in estimates of the k_1 parameters. Comparison of the estimated average growth curves from the maximum likelihood fit indicates that the predicted length of juvenile fish increased between the 1960's and 1970's, continued to increase between the 1970's and 1980's, and changed little between the 1980's and 1990's (Figure 1). The overall increase between the 1960's and 1980's is quite substantial. Thus, the estimated average size of a two year old in the 1980's is nearly equal to that of a three year old in the 1960's. Although Figure 1 suggests that there may not be much difference in growth between the 1980's and 1990's, a closer examination of the two curves suggests that a difference of about 4 cm existed at age 2 and about 2 cm at age 3 (see Appendix 10). After this age, the estimated differences were generally less than 1 cm.

The results for the data from the 1970's suggest that the 1970's were a period of transition with quite variable growth. The results from the integrated analyses from this decade suggest that growth rates at younger ages were slightly greater than those in the 1960's. Examination of residual plots for the length-frequency data either by year or cohort (Appendix 10) suggests that growth in the early part of the decade was substantially slower than in the latter half and even lower in the 1960's. Similar

[7] For the tag-recapture data, we separated the data by decade of release because of the technical problem that estimates of the age and thus cohort for any individual tag release are only obtainable in the context of fitting the growth model. (Even in this context, the estimated age/cohort is considered as a random variable.) Additionally, the length-frequency data (which covered fish up to age 4) were separated by decade of capture since we did not want to split up data collected within the same year in our analyses (for reasons given in Appendix 10). This means that in each decadal data set there will be a small percentage of fish that were actually born in the last few years of the previous decade. This does not have any substantive effect on the results.

results were also found in the analyses in Appendix 8. The pooled results for this decade will thus provide intermediate values. Attempts to further resolve the growth in the 1970's using this integrated framework were not successful. The data for the 1970's are relatively sparse and would not, for example, support half-decadal estimates. The limitations in the 1970's data are important to recognize in any interpretation of the results. In particular, there is little information on growth for intermediate ages (i.e. between 6 and 15 years of age).

Examination of the residuals revealed no systematic deviations from the fitted curves for any of the different data sources. Thus, the change in growth was consistently seen in three independently derived data sources, indicating that the observed difference was not an artefact of differences in the data collection or processing procedures over time. The estimated difference in the growth curves between the 1960's and 1980's decades is somewhat less than that estimated previously in either Hearn and Polacheck (1993, in press) and Anon. (1994). These previous studies were based only on tag-recapture data and used Fabens' estimation method (Fabens 1965) without any allowance for individual variability in growth. Fabens' approach has been shown to be biased if in fact there is individual variability in L_∞ (Maller and deBoer 1998). The results in this and previous appendices strongly suggest such variability exists, and explicitly taking it into account in the model is the primary source of the difference.

We examined in detail various aspects of the model fits to the data from each decade, including variance estimates for the estimated parameters (see Appendix 10). The results suggest that μ_∞ was approximately 3 cm larger for the 1960's data than for subsequent decades. They also suggest that for the 1960's data there is no significant difference between the standard VB and VB log k model, while a significantly better fit was obtained for the other decades with the VB log k model. Interpretations of these results are discussed in detail in Appendix 10. However, in terms of prediction of lengths within a stock assessment context, issues such as whether to use a VB or a VB log k model for the 1960's or whether there is a common μ_∞ for all decades will have at most minor effects.

Changes in SBT growth rates over time – time varying k

Estimates of $k(t)$ from fitting a time varying VB model to the length-frequency data are illustrated in the upper panel of Figure 2. The estimates of $k(t)$ are relatively constant in the 1960's, decline sharply in the late 1960's and early 1970's, increase to a peak in 1973 and decline again before increasing in the 1980's to a level higher than that in the 1960's. The temporal pattern broadly follows the shape of the seasonal effect estimated in the length-frequency analyses in Appendix 7 (see Figure 6 in Appendix 7). However, there is a noticeable difference, namely that the level of the peak in 1973 is about the same as that in 1985.

It is important in interpreting the upper panel of Figure 2 to keep in mind that what is depicted is the estimated growth rate parameter (adjusted to one point in the year) and not an estimate of the actual change in size. The predicted size at age a from this model is the integration of the estimated $k(t)$ from $t-a$ to t. As such, the temporal trend in the predicted size over time for any age can be substantially different from the temporal pattern of $k(t)$. This is illustrated in the lower panel of Figure 2, which shows how the predicted mean lengths for age groups 1 to 4 vary over time. There are important differences from the pattern in the upper panel. Thus, the 1973 and 1985 peaks are the same height for the one-year-old fish, but the 1985 peak is clearly higher for the four-year-old fish. The two-year-old and three-year-old fish show intermediate effects. These results are consistent with the decade by decade results presented above and in Appendix 10. These show that the differences in the mean length at age of SBT between the 1980's and previous decades were small for the one-year-olds, but were progressively larger for older age groups.

In Appendix 7, when comparing half-month Gaussian mixture fits to the 1970's length-frequency data, we experienced difficulty in following the age group changes. The fact that the growth rates during the 1970's appears to have been following a "sine"-shaped curve through that decade may explain the difficulty. Inspection of the residuals to the fit of this $k(t)$ suggests that the four-year-old fits are too low in the 1980's. This would suggest that the actual change in size is being underestimated by this model. This in turn indicates that the von Bertalanffy model is incapable of fully capturing the fast early growth of 1980's juvenile fish and is yet

another indicator that a more complex growth model (e.g. VB log k) is more appropriate.

We encountered technical difficulty in applying the changing $k(t)$ model to the tag-recapture data. The optimisation method was too slow to use with the full data set. In order to be able to produce estimates for the tag-recapture data, preliminary results from a sub-sample of size 1000 was used. We restricted the tagging data to releases from the 1960's to the 1980's to have comparable results with those for the length-frequency data and to ensure that there was sufficient data to support the analysis. The estimates of $k(t)$ and the mean lengths for age groups 1 to 4 are qualitatively similar to those estimated from the length-frequency data (see Appendix 8), even though the data sets in the two analyses were independent. There are some differences in the results but taken together the results support the conclusion that the rate of growth of SBT was faster in the 1980's than in the 1960's. The 1970's saw a period of change followed by a rise to the 1980's level starting in the late 1970's. It should be stressed that the tag-recapture data set is deficient in the 1970's. As such, the estimation of $k(t)$ from these data is likely to be relatively poor during this time.

Changes in SBT growth – otolith increment data

The mean otolith increments by decades indicate a similar pattern of change to that seen in the decadal estimates of SBT growth from the integrated analyses in Appendix 10 and discussed above. Thus, on a decadal scale, the mean growth increment in the otoliths between bands 1 to 2 and between bands 2 to 3 were similar for the 1960's and 1970's and were significantly smaller than for the 1980's and 1990's (Table 3). The mean increments in the 1990's were also greater than those for the 1980's. The same tendency is seen in the mean increments for bands 3 to 4, although the magnitude is much smaller. There is little difference in the mean increments for bands 4-5. (Note there are few increment data for the 1990's in this case.) These results are similar to those presented in Gunn and Farley (1998) and Gunn et al. (in prep). Interpretation of the increments for these older ages is more problematic as the absolute magnitude of the increment declines with age and thus the relative precision of the estimates decreases because measurement errors become proportionally greater. Moreover, the expected absolute growth increment of a fish

declines with its size. As such, even if fish were growing faster post 1970's (e.g. a greater k), the differences in the absolute growth increment would decrease with age.

It should be noted that the comparisons for growth increments between different ages in Table 3 are not independent since they are all based on increments measured from the same set of fish. As can be seen in Table 4, within any cohort, there tends to be a positive correlation between the growth increments between successive ages. In other words, a fish with a larger than average growth increment in its otolith for band 1-2 also tends to have a larger increment for band 2-3, etc. This positive correlation is consistent with substantive individual variability in growth (i.e. it supports the importance of considering L_∞ as a random variate). If substantive individual variability did not exist, then successive growth increments from the same fish would be expected to be negatively correlated (as a result of growth being a function of size and also as a result of measurement error, since consecutive increment measurements share a common middle band measurement). As such, comparisons of the increments for different ages are confounded. The overall cumulative increment for bands 1-4 or bands 1-5 would appear to be the most relevant measurement in terms of comparing overall trends in juvenile growth rates and for minimizing the relative contribution of any measurement error. These values are given in Table 3.

In addition to the decadal comparisons in Table 3, the otolith increment data can be used to provide an indication of finer temporal resolution in changes in growth. Figure 3 shows the mean otolith increment between bands 1 to 5 by cohort for cohorts born between 1960 and 1989. Also shown are the estimated 95% confidence limits. The increments have been scaled to the overall mean for this period to facilitate interpretation. The precision of the estimates for any given year is relatively low in that for all but a few cohorts the confidence intervals for the deviation from the overall mean overlap zero. Nevertheless, there is a general trend in the mean for cohorts born in the 1980's to be greater than the overall mean and those born in the early 1960's to be less. The 1977 and 1978 cohorts stand out as the two cohorts with significantly smaller increments. Overall, this figure suggests a relatively similar growth for cohorts born prior to 1978 and an increase (and perhaps an increasing

trend) for the 1980's cohorts. The transition between these two periods depends in part on the interpretation given to the 1977 and 1978 cohorts.

The correlation in the increments for an individual otolith (Table 4) means year and cohort effects tend to be confounded in this data set. For example, the correlation between the mean growth increments for bands 1 to 2 and bands 2 to 3 among cohorts is 0.73, while the mean correlation between the same band increments within a year is 0.35. This might suggests that cohort effects are stronger than year effects. However, if the otolith samples are randomly divided within a year into two groups in order to obtain two independent samples, the correlation with cohort and year are both reduced and are of similar magnitude (0.28 and 0.22 respectively). Overall, this confounding between year and cohort means that distinguishing the specific temporal signals in these data is problematic.

Comparison of the temporal pattern in the otolith increment data (Figure 3) with the pattern estimated in the time varying k analyses (e.g. Figure 2 and Appendix 8, Figure 5) suggest that there is consistency in all of them in terms of predicting that there was a decline in growth rates just prior to the increase in the 1980's. However, within the otolith increment data, there is no indication of the large decline in growth rates at the beginning of the 1970's, a feature seen in both of the analyses in Appendix 8. As such, it is not clear whether the apparent decline in the late 1970's is merely a coincidence. The coefficient of variation in the mean otolith increments between ages 1 to 5 for a cohort is on the order of 5%. The difference in the estimated decadal mean lengths for juvenile SBT is of the order of 10% or less. As such, the power of the otolith increment data to detect fine scale temporal differences would be small, particularly given that the otoliths provide an indirect measure of actual growth.

Discussion

The estimation of fish growth is challenging and complex, particularly for long-lived species such as SBT in which growth processes can be expected to vary in different components of the life cycle and can change over time, potentially differentially with age. This necessitates that extensive data be collected over considerable time periods if reliable estimates are to be obtained. Moreover, given the long lifespan of SBT, commonly used sources of information on growth (e.g.

length-frequency and tagging data) are likely only to be informative for portions of the age range. As such, it is important to have methods that can incorporate and integrate a variety of data.

The integrated methods developed and applied to the SBT data sources have been able to provide a comprehensive set of estimates for the growth of SBT over four decades. In particular, the combining of length-frequency, tag-recapture and direct aging data has been a powerful mechanism for obtaining estimates for the 1960's and 1970's periods, where there are substantive deficiencies in coverage in the historical data from any particular source. The inclusion of the direct aging data has been particularly informative with respect to the asymptotic length. None of the individual data sources, by themselves, were sufficient to provide estimates of growth for the 1970's. By being able to combine the different data sets, the overall data sets for SBT constitute one of the most comprehensive, long-term data sets for a large pelagic fish stock. Nevertheless, as discussed below and in the appendices, there are still substantive limitations in the coverage provided by this integrated data set that need to be taken into account in interpreting the results. The direct ageing data provided the best information on asymptotic length, the length-frequency data the best information on within-season growth and the tag-recapture data the best information on intermediate ages and on between-fish variability (σ_∞). Thus all three types of data were essential in developing a comprehensive growth model for SBT.

Another advantage of an integrated approach is that it allows for the consistency of the data from different sources to be evaluated. Because of the high correlation among parameter estimates in standard growth models (e.g. k and L_∞ in the VB model) comparison of results from independently fitting to separate data sources can be problematic. In addition, examination of the residuals from an integrated source provides an indication of the overall robustness of the resulting estimates and can be a powerful means of gaining insight into the underlying processes.

It is important to consider what the estimates of the growth parameters represent when interpreting them. At the most fundamental level, the estimates in

conjunction with the underlying growth model provide a mathematical description of the realized average length at age along with associated variances in the distribution of length at age for the group of fish (i.e. cohorts) over which the data have been aggregated. To the extent that growth rates vary over time the results do not provide a direct description of the growth at any particular instant in time. Different components/ages within the population at any given instance may have been following very different growth trajectories depending on the cumulative past and current factors that have affected and are affecting their growth.

At another level, examination of the estimated growth parameters can provide insight into the underlying growth processes, how they have changed and the factors responsible for them (see discussion below). However, in doing this, caution is warranted because of the problem of inferring process from pattern, the large correlation among some of the estimated parameters, and the potential problems with the lack of separability in the observed realization of multiple and cumulative effects. A further complication is that observed growth comes from the individual that survived to that age. To the extent that there is size specific mortality within an age group (either natural or fishery induced) the resulting observed growth curves represent a combination of the underlying growth and mortality processes. Finally all the observed data on growth comes from fish that were captured in a fishery (in most cases commercial but "scientific" in the case of tagging). If there is large size selectivity within an age class, then the resulting growth curves do not provide a fully unbiased estimate for the underlying population. As discussed above, there appears to be significant size selectivity due to spatial segregation within the one-year-old age class and also within ages 8-14 on the spawning grounds during the spawning season. These have been taken into account in the analyses. Other potential sources of size selectivity within an age class, particularly ones that may have changed over time, would appear to be small (e.g. hook selectivity in the longline fishery). However, this inherent limitation of fishery-collected data on growth should be kept in mind when interpreting results.

Hypotheses for the changes in growth

The size of a fish at a point in time represents the integration of a complex mixture of factors that have determined its growth up until that age. At the population

level, changes in the average size at age indicate that there has been a change in one or more of the dominant factors that affect growth. Four general categories of factors at the population level are likely to effect observed changes in growth:

1. the genetic structure of the population with respect to factors controlling individual growth;
2. the physical environment (e.g. temperature) experienced by the population;
3. the productivity and available resources within the utilized habitat;
4. the size of the population.

More than one of these factors can change over time and be an influential contributor to changes in growth. Moreover, these factors are not independent and changes in one factor can induce changes in the other. For example, changes in the density of the population can affect the availability of food resources and result in tropic interactions on the productivity of the ecosystem. Alternatively, increases in the size of the population can result in more marginal habitats being used and thus change the average physical environment that is experienced. Changes in population size can also change the selection pressures with respect to growth within a population.

Nevertheless, when substantive changes in growth have been observed, as has been the case with SBT, it is important to consider possible alternative hypotheses with respect to the likely dominant factor in terms of their implication for stock assessments and the provision of management advice. In particular, the potential effects of changes in the size of the population on growth as the result of fishing are important to consider.

In Appendix 10, possible hypotheses for the observed decadal changes in growth are discussed. In that appendix, it is suggested that a hypothesis entailing a density dependent response in juvenile growth rates should be considered as one alternative for the changes in decadal growth observed in the estimates of growth. It is also suggested that a hypothesis of density dependent growth in the post adult phase that entails at least a change in μ_∞ should be considered as an explanation of the lack of fish greater than 184 cm in the early longline catches. As noted in this appendix, these two density dependent hypotheses are clearly speculative, but they are at least

broadly consistent and plausible given the set of estimated growth rate parameters from this integrated analysis, the history of the fishery and the general trends in the SBT stock.

The other general alternative to a density dependent hypothesis is that the changes in SBT growth have been driven primarily by changes in the physical nature and productivity of SBT habitats. In terms of the decadal growth estimates, a large-scale climatic "regime shift" in the mid 1970's has been linked to major ocean basin productivity changes and flow-on effects for fish populations (Polovina et al. 1995, Mantua et al. 1997, Beamish et al. 1999). While the best information on these linkages comes from the North Pacific, the climatic shifts have been linked to other areas including the Indian Ocean (e.g. Minobe 1997). As such, the changes in SBT growth could be considered to be broadly consistent with this observed decadal climatic change. It is less clear what environmental signal could be considered consistent with a large change in μ_∞, if this is in fact the cause of the absence of fish in the larger size classes (e.g. >184 cm) in the early longline catches (see Appendix 10).

Unfortunately, the decadal estimates of growth are not very informative in terms of rejecting or accepting hypotheses about the underlying factors affecting growth. Thus, they provide estimated growth curves that broadly represent the average "growth" experienced by cohorts from each of these decades. There is no information in the estimates to resolve at a finer time scale whether broadly coherent hypotheses are consistent with the finer scale dynamics of the hypothesised causative factors (i.e. environmental or abundance changes).

The methods developed and the analyses conducted in Appendix 8 were undertaken to provide finer scale estimates of how SBT growth has changed over time. While the methods developed in Appendix 8 appear promising, they expose general limitations to the modelling and estimation of how growth rates change. It is now clear that extensive data are required, particularly in the case of tagging data[8].

[8] Problems inherent in tagging data for this purpose are that the age of the fish needs to be estimated as part of the analysis and for longer-term recaptures the observed change in lengths represent an

Given the limitations in the temporal coverage within the various data sources (see below and Appendix 3), the methods in Appendix 8 were only able to provide an indication of how growth rates may have changed and then only for the juvenile age classes.

Ideally, for analysing how growth has changed over time, the data should allow for reasonably precise separation of estimates of growth by age and time period. Although the data for estimating SBT growth rates are extensive, there are real limitations in terms of the comparability of the age range within any single source and the ability to provide a time series of growth rates by age and year. There are inherent problems in tagging data for being able to do this and substantial gaps exist within the 1960-2000 timeframe because few or no tags were released (e.g. during the 1970's and in the mid to late 1980's). There are also sampling limitations in the direct aging data. In particular, because the otolith samples were almost all collected in the 1990's, the direct aging data provide little information for comparing or modelling growth rates over time for similar size/age range of fish (e.g. there is no information on juvenile growth in the direct aging data for the 1960's and 1970's). However, it is worth noting if otolith sampling continues on a routine basis that the resulting direct aging data would provide a very powerful data set for tracking how growth rates change in the future and for developing an understanding of the underlying mechanisms. The length-frequency data provide for a complete time series of growth rate estimates over a consistent age range. However, the age range in this case is only for ages 1-4 and no useable data exist for the 1990's.

Despite the limitations just noted, the results from Appendix 8 provide a set of finer resolution estimates of both the change in growth rates and the resulting change in mean size at age (particularly for the transition between the 1960's and 1980's). Given the limitations of the data and model fitting problems, the results should be considered more as a relative indication of how growth rates may have changed – particularly since the fits to the length-frequency and tagging data yielded qualitatively similar temporal patterns but somewhat different quantitative estimates. The results indicate that the transition between the 1960's and 1980's was not a

integration of the growth rates experienced by that fish. Thus, there is no direct observation on how growth rates may have varied within the interval between release and recapture.

smooth continuous increase. Instead they suggest that growth rates in fact decreased in the early 1970's and that a large fraction of the increase in the average size of juveniles between the 1960's and 1980's occurred rapidly near the end of the 1970's. The decrease in the growth rate in the early 1970's is also consistent with the residual pattern by year or cohort for the length-frequency data seen in the integrated fits to the decadal data (Appendix 10). Although the length-frequency data are included in both cases and thus the two analyses are not independent, the consistency between the two different statistical models and approaches lends some additional support to the early 1970's being a period of depressed growth. However, it should be noted that such a signal is not apparent in the back-calculated otolith increment data (see above). In contrast these otolith increment data also suggest that the increase in size between the 1960's and 1980's occurred relatively rapidly near the end of the 1970's (Figure 3).

If the early 1970's was a period with lower growth rates followed by a period of rapid growth subsequently, environmental or density dependent effects could be hypothesized for the underlying factor. Given the imprecision in being able to estimate the timing and magnitude of the change combined with the shortness of the time series, attempting to correlate it with a range of specific environmental signals would probably result in at least one positive, but potentially spurious, result, especially if lags were also considered. Information on changes in juvenile density during this period suggests that a density dependent effect would also be broadly consistent with such a pattern of growth during the 1970's. Thus, Japanese longline CPUE trends for juveniles (ages 4 and 5) suggest that the early 1970's was a period of high density (Figure 4). This is in spite of the large catches of younger fish being caught by the Australian surface fishery. The stock assessment models integrate these CPUE trends and catch data to provide estimates of recruitment. In this regard, the resulting estimates of the recruitment trends also suggest that the late 1960's and the first year of the 1970's was a period of somewhat elevated recruitment relative to an overall declining trend and that this was followed by a short period of lower recruitment in 1971 and 1972 (Figure 5). Allowing for these recruits to age suggests that the pattern of recruitment is broadly consistent with the estimates of change in growth rates in Appendix 8.

Growth rate parameters for use in SBT stock assessment models

As discussed above estimates of the growth rates of SBT are critical for the SBT stock assessments. Both the traditional VPA assessments and the more recently developed statistical time series approach require estimates of the expected mean length of a fish by year and age. In addition, the catch at length based models require estimates of the variance in length of fish in a given year and age class. The results from the integrated analyses of SBT growth conducted in this project provide a basis for generating estimates of the mean lengths at age and their variances that can be used as input into these stock assessments. However, this is not a straightforward task because SBT growth rates have varied substantially over time. Thus, the distributions of lengths at age have changed, while the available data are incomplete for robustly estimating these changes.

In considering what estimates should be used it is important to bear in mind what data actually underpin the estimates, particularly in terms of the age ranges and years covered. The stock assessments need to take into account the uncertainty in the available growth data and consider plausible alternatives, particularly where data are sparse or unavailable. The available data provide information on cohorts born between 1960 and 2000. However, the data provide no direct information on the growth of fish or length at age for fish existing at the time when the fishery began in the early 1950's or for the large catches from the spawning stock that occurred in the early 1960's (e.g. these spawning catches would have been greater than 8-12 years of age based on current estimates of maturity). Whatever values are used for these early cohorts must be based on hypotheses about SBT growth dynamics. As such, the question of what growth relationships to use in the SBT stock assessments is most appropriately addressed in two parts: (1) for those cohorts born since 1960 for which data on growth actually exists and (2) for those cohorts caught in the fishery for which no direct observations are available (i.e. born before 1960).

The expected length at age for the post-1960 cohorts

For the post 1960 cohorts, ideally, separate estimates for each cohort could be derived. However, the data are not comprehensive enough to permit this (see Appendices 3, 8 and 10). Appendix 10 provides estimates of the growth rates by decades. The results in this appendix can be used to provide one alternative set of

growth rate parameters. Within this alternative, each set of decadal growth rate parameters would be used to provide estimates of the expected length at age for cohorts that were born in that decade. Table 5 provides an example of such estimates based on the parameters from the best fit to the VB log k model (Table 2). The parameter values from constraining all cohorts to have the same μ_∞, as well as the parameter estimates for the 1960's fit to the VB model, could also be considered as an alternative hypothesis. However, the differences in the expected lengths at age are small. Given the other elements of uncertainty within the stock assessment, the differences between these different growth rate estimates would seem rather inconsequential. As such, it would not seem necessary to consider each as a separate alternative within the stock assessment. Whatever set of parameters are used, it may be worth considering smoothing over time the change in mean size at age, instead of having a discontinuity every 10 years. Whether such a refinement is necessary is best determined by those actually conducting the assessment.

It should be noted that the estimates in Table 5 represent a different treatment of the growth estimates for the 1960's cohort data than is currently utilized in the SBT stock assessments (e.g. Hearn 1994). Within the SBT stock assessments, the 1960's growth curve is used to estimate the mean length at age within a year for catches up to 1969. After this year, the mean length at age is assumed to increase; i.e. the transition between the growth curves for the 1960's and 1980's is assumed to occur across years and not across cohorts. However, this is logically inconsistent with the data that were actually used for estimating these growth curves. It was sensible to adopt this convention at the time. The estimates of the 1960's and 1980's growth curves implied that the mean length at age for some ages and in some years overlapped (i.e. younger fish were estimated to be larger than older ones). The cohort slicing method being used for estimating the age structure of the catch could not handle such overlaps. Given the growth curves estimated here, overlaps no longer occur (Table 5). Moreover, within the SCALIA catch at length model (Kolody and Polacheck 2001), such overlaps would not be a problem. As such, it would seem more appropriate to use estimates for the length at age that are consistent with the time period from which the data used in the estimation of the underlying growth curves were collected.

An alternative to simply using the decadal estimates from Appendix 10 would be to incorporate the year specific changes in k from Appendix 8. However, these estimates are not sufficient in themselves as they are primarily applicable to juvenile fish and we were not able to get satisfactory estimates of $k(t)$ for the 1990's because of the lack of length-frequency data and difficulties in applying this to tag-recapture data. Also, the estimates of $k(t)$ were estimated based on fitting a VB growth model, and we know that a more complex model such as the VB log k is more appropriate. One possibility would be to use these estimates of changing k in conjunction with the decadal VB log k estimates for the k_1 parameters in Table 2 or Appendix 10. This alternative would be based on the recognition that the changes in growth since the 1960's appear to be primarily associated with juvenile fish (see Appendix 10).

Variance estimates for the expected length at age

Catch at length based assessment models generate predicted catch at length distributions for comparison with observed distributions (e.g. Kolody and Polacheck 2001). The predicted catch at length distributions are generated from modelled estimates of the catch at age distributions which are transformed into length distributions based on estimates of the mean length at age and the variances around this mean. The time step in the assessment models is one year. Thus, the predicted catch at length distributions generated by these models represent aggregated annual distributions. The question of an appropriate error structure for modelling growth was discussed above. In terms of predicting catch at length distributions, there are four principal components of the variance that need to be considered within a specific set of parameter values for a growth model:

1. Individual variability in the basic growth process;
2. Temporal variability in the underlying growth process (e.g. environmental effects);
3. Measurement errors;
4. Growth within a time period (usually annual) as a result of aggregating catches.

Individual variability in growth within this project has been modelled by treating L_∞ as a normal random variable. As such, the estimates for σ_∞ provide a

basis for estimating the first of these components. The estimates of σ_∞ in Appendix 10 range from 3.5 to 4.7 percent of the estimates of μ_∞. The estimates tend to increase over time. The σ_∞'s for the 1980's and 1990's would be expected to be less well determined since in both cases no actual observations are possible for fish at ages where they would be expected to have approached their asymptotic length (i.e. the oldest observation possible is for age 20). Thus, the estimates of σ_∞ for the 1960's and 1970's could be considered more reliable. The average of these two yields an estimate of 7.46 for σ_∞.

The second and third components of variance are not completely separable and each of the different data sources provide a separate estimate which should reflect a combination of specific measurement errors associated with each data source plus the temporal variability component that is common to all sources (see Appendix 9 for further discussion on this). In terms of predicting the distributions of catch at length, the variance associated with the length-frequency data superficially might appear to be the most appropriate since these were derived from sampling the commercial catches. However, these are based on a limited age range and have confounded within them the σ_∞ variance component. As such, the estimates from the tag-recapture data would appear to provide the most reasonable estimate for this component of the variance. Taking the average of the variance estimates for scientist measured fish (i.e. the σ_s^2's) from the results in Appendix 10 (also in Table 2) would suggest that a value of ~4.4 might be reasonable for those catch length-frequency distributions in which scientific staff actually performed the measurements.

The estimates from the tag-recapture component also provide estimates of the additional measurement variance as a result of fishermen making the measurements (σ_f^2). Since, in some years, the length-frequency distributions from the Japanese longline fleet were made on board vessels by fishermen, the σ_f^2's (as given in Table 2 and Appendix 10) could be used to provide an estimate of this additional variance. Taking the average of the σ_f^2's across decades results in an estimate of 7.4 for this additional variance component.

It should be noted that in the actual length-frequency data from the catch, there is an additional measurement variance component in some years for the Japanese longline data. This stems from the use of weight measurements that were converted into lengths. Estimation of this variance component is outside the scope of the current project, as the data on growth in most cases did not contain associated weight information. However, the variance in weight at age is likely to increase with age. As such, those performing the stock assessment would need to develop an appropriate model if the additional variance due to the conversion of weights into lengths is judged important to incorporate.

Finally, within the observed length-frequency of the catches used in the stock assessments, there is an additional component of variance resulting from aggregation of the length-frequency distributions into an annual distribution. This additional variation results from within year growth. Thus, even if there was no variation in the length of a fish at a given age and all fish had the same birth date, there would be variation in the length of fish caught within a year-class throughout a year because fish at the beginning of the year would be smaller than later in the year. The additional variance is related to the amount of within year growth and the temporal distribution of catches within a year. It is straightforward to show that an expression for the overall variance that includes this aggregation component is:

$$V(l_{a,y}) = \sum_{j=1}^{p} \frac{n_{j,a,y}(\sigma^2_{j,a,y} + I^2_{j,a,y})}{N_{a,y}} \qquad (15)$$

where

$l_{a,y}$ = length of a fish of age a caught in year y

$n_{j,a,y}$ = the number of fish caught in year y of age a during time period j

$\sigma^2_{j,a,y}$ = the variance in length of fish caught in year y of age a during time period j

$I_{j,a,y}$ = the difference in the expected size for a fish of age a caught in y and time period j from the overall expected size of a fish[9]

$N_{a,y}$ = the total number of fish caught in year y of age a

The variance in length for an age class at any particular time within a year will be approximately constant and this dependency changes relatively slowly (see Appendix 8). As such, the above expression can be approximated by:

$$V(l_{a,y}) \approx \bar{\sigma}^2_{j,a,y} + \sum\left(\frac{n_{j,a,y} I^2_{j,y,a}}{N_{a,y}}\right) \qquad (16)$$

Thus, the additional component of variance due to within-year growth will be a weighted average of the square of the growth increments (relative to their mean), where the weights are proportional to the distribution of catches taken within a year. Clearly, the importance of this additional variance component will vary with age. Figure 6 provides an example of the estimated variance component that would be expected for SBT as a function of age for a fishery in which catches were evenly distributed throughout the year. This additional component is relatively small except for younger ages (i.e. <5) in which there is substantial growth within a year. The contribution of this component to the variance will depend upon the distribution of fishing within a year. The effect, even for younger ages, will be relatively small for highly seasonal fisheries.

The above four sources of variance for the distribution of lengths at age are independent. Thus, they can be added together to provide an overall estimate of the variance. Figure 7 illustrates estimates of the total variance and the relative contribution of each component for the parameter estimates from the best fit to the 1980's data. Results for the parameter estimates from the other decades are similar. The total variance is dominated by the estimated variability in individual growth (σ^2_∞). However, for younger ages, particularly ages 1 and 2, within-year growth

[9] Note that $I_{j,a,y} = E(l_{j,a,y}) - \frac{\sum_{j=1}^{p} n_{j,a,y} E(l_{j,a,y})}{N_{a,y}}$ where $E(l_{j,a,y})$ is the expected length of a fish of age a in year y caught in time period j (derived from the appropriate growth curve).

would be the largest source of variance under the assumption of equal distribution of catches throughout the year. Thus, for fisheries in which there are substantial catches of juveniles, it will be important to account for the within-year growth and distribution of fishing effort. Since these fisheries are often seasonal (e.g. the South Australian surface fishery), the contribution from within-year growth would be expected to be smaller than that shown in Figure 7. As such, appropriately accounting for the seasonal aspects of the catches would be important in appropriately reducing the magnitude of this variance component. Judicious aggregations and appropriate time steps within the assessment model would all reduce this source of variance.

The estimated coefficient of variation for the distribution of ages at lengths is estimated to be around 10% for most age classes (Figure 8). The approximate 95% confidence intervals for the distributions indicate that a large amount of overlap in length among age is to be expected, particularly for older ages (Figure 9). Interestingly, these estimated confidence intervals are almost identical for the situations where scientists and fishermen measure the lengths. However, the estimate of the additional variance contributed by fishermen doing the measurements is based on their measurement of recaptured tagged fish. The extrapolation to length measurement of the catch by fishermen assumes that the level of measurement error would be the same. There may be a tendency for recaptured tagged fish to be measured more carefully than measurements taken during routine monitoring of the catch. In addition, there may be a large amount of difference between different fishermen, as well as potential biases.

Growth parameter values for the pre-1960 cohorts

Since no data exist with which to estimate growth rates for cohorts born prior to 1960, any values used will be based on assumptions about the underlying factors controlling the changes in the growth. This issue is discussed in Appendix 10. Three basic hypotheses that could be considered are:

1. that growth for cohorts born prior to 1960 was similar to that observed for cohorts born in the 1960's;
2. that SBT growth has a substantial indeterminate component related to adult density which resulted in a substantial increase in the average asymptotic length associated with the large declines in the spawning stock in the 1960's;

3. that post juvenile growth rates (i.e. k_2), as well as the asymptotic lengths, have a density dependent component which increased in response to the large declines in the spawning stock in the 1960's.

The first of these is perhaps the least plausible given the lack of very large fish (e.g. > 184 cm) in the initial catches from spawning grounds and the increases in the proportion of very large fish over time in the longline catches (see Appendix 10). An alternative to the second and third hypotheses would be that there were large long-term environmentally driven changes in growth (see above). There is no information available to distinguish these hypotheses. However, in terms of the stock assessment, they would tend to have a similar effect.

Figure 10 provides examples of possible growth curves for pre 1960's cohorts that would be consistent with the latter two hypotheses. In constructing these, we have used a value of 165cm for μ_∞ based on the observed length distributions on the spawning ground in the initial longline catches (see Appendix 10) and have considered a range of values for the k_2 parameter (namely 0.1, 0.125 and 0.15). In constructing these curves, we have kept the other parameter values equal to those estimated from the best fit to the VB log k model for the 1960's data except for the value of a_0. We have adjusted the value of a_0 so that the expected size of an age 2 fish remained the same as that estimated in the 1960's. This was necessary because, in the VB log k model, changing the value of μ_∞ also affects growth during the first stage. It is not clear what is the most reasonable parameterisation for juvenile growth in a situation where μ_∞ changes. We could have, alternatively, kept a_0 fixed at the value estimated for the 1960's data, which would have implied an associated decrease in the size of juvenile fish (Figure 11). It should be noted that the curves in Figure 11 clearly do not represent an exhaustive set of plausible hypotheses. However, they do provide a useful range for discussion and consideration within the SBT stock assessment.

Growth models for projections

The alternative hypotheses discussed above and in Appendix 10 for the changes in growth observed historically provide the most appropriate basis for

possible alternative models for future changes in growth to use in stock projection. The hypothesis that the changes in SBT growth represent a density dependent response is broadly consistent with the large reductions in both spawning biomass and juveniles resulting from the high rates of exploitation. As such, a density dependent response represents one alternative for future stock projections. Under this general alternative, juvenile growth should be linked to the projected size of the juvenile stocks in the future[10]. The growth rates in the projections would need to be set so that when the future juvenile stock sizes in the projections were similar to the historical stock sizes estimated in a stock assessment then the corresponding growth curve would be used.

To implement this hypothesis would require specification of which component(s) in the population (e.g. number at age) is the actual density dependent driver and the underlying functional relationship. A range of alternatives could be considered. Given the current stock status, the primary focus for considering such a density dependent hypothesis within projections would be to evaluate the potential consequences for obtaining management's recovery objective (i.e. recovery to the 1980 spawning biomass). The main consequence of including a density dependent response in this context is that it would tend to slow the rate of any projected recovery (i.e. as the projected stock begins to recover, cohorts will contribute less per capita to the spawning stock at any given age and would need to be harvested in greater numbers to obtain the same yield). In this context, it may be sufficient to use recruitment as the density dependent driver and an "empirically" based relationship based on the average recruitment in each decade. Any such density dependent response would not be expected to have a substantial effect on the projections until there was some substantive rebuilding (i.e. recruitment or juvenile stock sizes approaching the 1980 level). As such, the consideration of density dependent growth responses is probably a secondary effect in terms of shorter-term projections.

[10] Potentially, consideration could also be given to density dependent hypotheses linking the mean asymptotic length to the spawning stock (see above and Appendix 10). However, if the asymptotic length has changed and if the change is linked to the early reductions in the spawning stock, the changes would appear to have occurred over the range experienced in the 1950's and 1960's and perhaps early 1970's. Given that the focus of current management is recovery to the 1980 spawning stock levels, consideration of density dependent hypotheses for asymptotic lengths would be of little relevance in the projection context.

Nevertheless, it is a possibility that should be considered in longer-term projection simulations for evaluating management strategies.

The other general category of hypotheses for the historical change in growth is that the changes in SBT growth have been driven primarily by changes in the physical environment and productivity of SBT habitats (i.e. large regime shifts). As discussed above, the historical estimates of growth are not very informative in terms of identifying the underlying mechanisms or for providing prediction about the likely frequency and duration of regime shifts if they are in fact the underlying source of the historically observed changed. If it is considered that regime shifts hypotheses should be incorporated into the projections, then a range of magnitudes and durations consistent with past changes should be allowed for. Thus, consideration would need to be given to allowing for changes in the asymptotic lengths consistent both with the relatively minor estimated change between the 1960's and 1970's and the more substantial hypothesized change for fish born prior to 1960 and afterwards. Consideration would also need to be given to changes in juvenile growth rates that are at least consistent with those that have been observed in the past.

Benefits

One of the primary direct benefits of this research will be an improved and more robust basis for the estimation of growth rates that are an essential component of the SBT stock assessments. The results of this research provided improved methods for predicting the mean length at age and also provided estimates of variances based on all available data. The results provide the basis for generating alternative hypotheses for SBT growth and how it has changed over time. This should ensure that this source of uncertainty is adequately addressed within the SBT stock assessments and reflected in the subsequent management advice.

The estimation of growth is integral component of fishery biology and the assessment of fish stocks. The growth models, the statistical procedures and integrated methods developed in this project are applicable to a large number of fisheries. The methods have the potential to provide an improved basis for modelling and understanding growth in other fisheries. In particular, the ability to combine data

from disparate data sources has been shown to be a powerful mechanism to improve the overall estimation of growth curves, especially where there are substantive deficiencies in the coverage in the historical data from any particular source.

Further Development

A number of areas where there is scope for improvements in the analytical and statistical methods are identified in the appendices of this report. Particular problems that would warrant further investigation include:

1. Further development of modelling approaches for taking into account the sources of variation in length-frequency data (Appendix 7). Is it possible to fit a growth model with hierarchical error structure to the raw data rather than the summary statistics?
2. Further work on modelling time variation into growth models and the development of efficient methods for fitting such models to tag-recapture data as well as to multiple data sources simultaneously (see Appendix 8).
3. Further development and application of appropriate statistical models for the analysis of direct aging data that take into account variability in the time of band formation, size segregation in space, errors in age readings and differences in spawning dates (see Appendix 12);
4. Further development of methods for estimating the standard errors of the growth curve parameter estimates (Appendix 10).
5. Further development of the analysis of tag-recapture data. Key issues are computational efficiency; Bayesian analysis (which was attempted, but the algorithm stalled on the VB log k growth curve for unknown reasons); explicit inclusion of spatial effects (location of capture and recapture); estimation equations for general growth curves; non-parametric estimation of the growth curve for comparison with parametric models; non-parametric estimation of the age at capture and its consequences for standard errors of growth curve parameters; the effect of imposing constraints on various parameters to prevent over-fitting.

In addition, the results from this report identify the importance of obtaining improved understanding and estimates of the timing of annual band formation within SBT

otoliths for the interpretation of growth and age data based on the counts of annual bands (See Appendices 3, 11 and 12).

Finally, this report highlights the importance and value of having long time series of data available in order to understand and obtain robust estimates of growth. Such time series are also essential for modelling the way growth rates change over time and the underlying growth processes. SBT growth has been shown to vary over time and these changes in growth have important implications for stock assessments and the management of the SBT resource. In this regard, it is critical that well-designed data collection programs that are capable of providing information on growth are maintained within the SBT fisheries so that future changes in growth are detected and appropriately accounted for in the stock assessment and management of SBT.

Planned Outcomes

The primary planned outcome for this project was the production of growth rate parameters for use in the SBT stock assessments. The results in Appendix 4 were completed in the first year of this project and presented as work in progress to the CCSBT Scientific Committee (Eveson et al. 2001, Anon. 2002c). Although the results were only preliminary in that they were only based on tag release and recapture data, they were considered to constitute an improvement over previous estimates being used in the CCSBT stock assessments. The results were incorporated into the growth curves used in the SBT stock assessment preformed in 2001 (e.g. Anon. 2002b). It is anticipated the results from this project will be incorporated into future SBT stock assessments.

The other primary planned outcome was the development of an integrated method for the analysis of growth from different data sources. The project produced an integrated method for combining tagging, length-frequency and direct aging data. In the process, the project also developed a new growth curve and statistical estimation approaches, as these were required components in the overall integrated analysis. These methodological developments are generally applicable to other species and should have relevance to the estimation of growth beyond the specific

SBT application. One paper documenting these methodological developments has already been published (Laslett et al. 2002, which is essentially Appendix 4). We anticipate preparing at least four additional manuscripts (i.e. one based on Appendices 5, 7, 8 and 9 respectively) for publication in the primary scientific literature to ensure a wider dissemination of the results.

Conclusion

All of the primary objectives of this project have been completed. An integrated method for modelling SBT growth that uses growth increment data from tagging experiments, length measurements and direct aging estimates from otoliths, and length-frequency modal information was developed. These methods were applied to the available historical data from SBT to produce estimates of SBT growth curves over four decades. As demonstrated in the report, the parameter estimates from fitting these curves can be used to estimate the expected length of SBT at age and associated variances for the cohorts represented in these data. A set of growth curves was developed for possible use for cohorts caught in the early years of the SBT fishery for which no direct data exist for estimating their growth rates. The estimates of growth rate parameters can be used as direct input into length based assessments. Alternative hypotheses have been developed for the factors underlying changes in SBT growth that are consistent with the observed growth data and suggestions have been proposed for how these might be used in future stock projections. However, the scale of resolution in these hypotheses was limited by the resolution and coverage within the available data. In addition, a number of new statistical methods and methods for modelling growth were developed, in particular the VB log k growth curve (Appendix 4), new maximum likelihood approaches for fitting tag-recapture data and length-frequency data (Appendix 4 and 7), and statistical methods for estimating temporal changes in growth rates parameters (Appendix 8).

In summary, the results from this project suggest the following conclusions:

1. Length-frequency, tag-recapture and direct aging data can be integrated to provide a consistent estimate for SBT growth;
2. On a decadal scale, there have been significant changes in the growth of juvenile SBT born over the last 40 years. SBT from the 1980's grew

significantly faster than those from the 1960's. The results suggest that the 1970's were a period of transition and that growth of young fish in the 1990's was faster than in the 1980's up to about age 4.

3. Estimates of the mean asymptotic length of SBT born since the 1960's indicate at most small changes in the asymptotic length. However, the mean asymptotic lengths from these cohorts is significantly greater than would be expected for earlier cohorts based on the length-frequency distribution of spawning fish captured in the 1950's and 1960's. This suggests that the mean asymptotic length may have increased.
4. The time of year at which SBT deposit a translucent zone in their otoliths can vary from May to September, with July 1 being an approximate average date, and there is considerable variability among individual fish.
5. Combining length-frequency, tag-recapture and direct aging data provides a powerful mechanism for obtaining growth curve estimates where there are substantive deficiencies in coverage in the available data from any particular source.

References

Anon. 1993. Report of the twelfth meeting of Australian, Japanese and New Zealand scientists on southern bluefin tuna, Hobart, Australia, 13-19 October 1993.

Anon.1994. Report of the southern bluefin tuna trilateral workshop. Hobart, Tasmania. 17 January - 4 February 1994.

Anon. 1996a. Report of the CCSBT workshop on VPA and CPUE modelling. 4-15 March 1996. Hobart, Tasmania.

Anon. 1998a. Report of the 1998 Scientific Committee meeting. 3-6 August 1998. Tokyo, Japan.

Anon. 1998b. Report of the 1998 Stock Assessment Group meeting. 23-31 July 1998. Shimizu, Japan.

Anon. 1998c. Southern bluefin tuna 1998 peer review panel. Report produced for the CCSBT.

Anon. 2001a. CCSBT. Report of the sixth meeting of the Scientific Committee. Tokyo, Japan, 28 - 31 August 2001

Anon. 2001b. CCSBT. Report of the Second Stock Assessment Group meeting 19-28 August 2001. Tokyo, Japan.

Anon. 2001c. Report of the sixth meeting of the Scientific Committee. 19-24 March. Tokyo, Japan.

Beamish, R.J., Noakes, D.J., McFarlane, G.A., Klyashtorin, L., Ivanov, V.V., and Kurashov, V. 1999. The regime concept and natural trends in the production of Pacific salmon. Can. J. Fish. Aquat. Sci. **56**: 516-523.

Butterworth, D.S., Ianelli, J.N., and Hilborn, R. 2000. A statistical time-series model for stock assessment of southern bluefin tuna. CCSBT Stock Assessment Procedures Workshop, Tokyo, May 2000. Document 9.

Clear, N.P., Gunn, J.S., and Rees, A.J. 2000. Direct validation of annual increments in

the otoliths of juvenile southern bluefin tuna, *Thunnus maccoyii*, by means of a large-scale mark-recapture experiment with strontium chloride. Fish. Bull. **98**: 25-40.

Eveson, J.P., Polacheck, T., and Laslett, G.M. 2001. Preliminary results from combined analyses of direct aging and tag-recapture data for estimating SBT growth curves. CCBST-SC/0103/18.

Fabens, A.J. 1965. Properties and fitting of the von Bertalanffy growth curve. Growth **29**: 265-289.

Francis, R.I.C.C. 1988a. Are growth parameters estimated from tagging and age-length data comparable? Can. J. Fish. Aquat. Sci. **45**: 936-942.

Gunn, J.S. and Farley, J.H. 1998. Otolith analyses suggest that the growth rate of juvenile SBT began to increase in the late 1970's and that growth rates have continued to increase through the 1980's and 1990's. CCSBT-SC/9807/9.

Gunn, J., Polacheck, T., Davis, T., Klaer, N., Cowling, A., Farley, J., Caton, A., Williams, K., Hearn, W., Preece, A., Clear, N. 1998. Fishery Indicators for the SBT Stock: An update of 12 indicators first used in 1988 plus additional indicators from the 1990's. CCSBT/9807/40.

Gunn, J.S., Farley, J.H., and Hearn, W.S. In prep. Catch-at-age; age at first spawning; historical changes in growth and natural mortality of SBT: An integrated study of key uncertainties in the population biology and dynamics of SBT based on direct age estimates from otoliths. FRDC Report 97/111.

Hearn, W.S. 1994. Models for estimating SBT age at length during the transition period. SBFWS/94/13.

Hearn, W.S. and Polacheck, T.W. 1993. Estimating age-at-length relations for the 1960's and 1980/90's. SBFWS/93/4.

Hearn, W.S. and Polacheck, T.W. In press. Estimating long-term growth rate changes of southern bluefin tuna from tag-return data. Fishery Bulletin.

Hilborn, R., Butterworth, D.S., and Ianelli, J.N. 1998. A statistical time-series model for stock assessment of southern bluefin tuna. CCSBT/9807/31.

Klaer, N., Polacheck, T., and Sainsbury, K. 1993. Southern bluefin tuna stock projections. SBFWS/93/18.

Kolody, D. and Polacheck, T. 2001. Application of a statistical catch-at-age and length integrated analysis model for the assessment of southern bluefin tuna stock dynamics 1951-2000. CCSBT-SC/0108/13.

Laslett, G.M., Eveson, J.P., and Polacheck, T.W. 2002. A flexible maximum likelihood approach for fitting growth curves to tag-recapture data. Can. J. Fish. Aquat. Sci. **59**: 976-986.

Leigh, G.M. and Hearn, W.S. 2000. Changes in growth of juvenile southern bluefin tuna (*Thunnus maccoyii*): an analysis of length-frequency data from the Australian fishery. Mar. Freshwater Res. **51**: 143-154.

Maller, R.A. and deBoer, E.S. 1988. An analysis of two methods of fitting the von Bertalanffy curve to capture-recapture data. Aust. J. Freshwater Res. **39**: 459-466.

Mantua, N.J., Hare, S.R., Zhang, Y., Wallace, J.M., and Francis, R.C. 1997. A Pacific interdecadal climate oscillation with impacts on salmon production. Bulletin of the American Meteorological Society **78**: 1069-1079.

Minobe. S. 1997. A 50-70 year climatic oscillation over the North Pacific and North America. Geophys. Res. Lett. **24**: 683-686.

Polacheck, T., Sainsbury, K. and Klaer, N. 1993. Assessment of the status of the southern bluefin tuna stock using virtual population analysis - 1993. 12th Trilateral Scientific Meeting on SBT. SBFWS/93/16.

Polacheck, T., Preece, A., and Klaer, N. 1998a. Assessment of the status of the southern bluefin tuna stock using virtual population analyses – 1998. CCSBT/9807/17.

Polacheck T., Preece, A., Klaer, N., and Betlehem, A. 1999. "Treatment of data and model uncertainties in the assessment of southern bluefin tuna stocks." In: F. Funk, T.J. Quinn II, J. Heifetz, J.N. Ianellis, J.E. Powers, J.F. Schweigert, P.J. Sullivan, and

C.-I. Zhang (eds.), *Fishery stock assessment models*. University of Alaska Sea Grant, AK-SG-98-01.

Polacheck, T. and Preece, A. 2001. An integrated statistical time series assessment of the southern bluefin tuna stock based on catch at age data. CCSBT-SC/0108/19.

Polvina, J.J., Mitchum, G.T., and Evans, C.T. 1995. Decadal and basin-scale variation in the mixed layer depth and the impact on biological production in the central and North Pacific, 1960-88. Deep-Sea Res. **42**:1701-1716.

Ricard, D. and Polacheck, T. 2002. Trends in catch, effort and nominal catch rates in the Japanese longline fishery for SBT. CCSBT-SC/0209/26.

Sainsbury, K.J. 1980. Effect of individual variability on the von Bertalanffy growth equation. Can. J. Fish. Aquat. Sci. **37**: 241-247.

Schnute, J. and Fournier, D.A. 1980. A new approach to length-frequency analysis: growth structure. Can. J. Fish. Aquat. Sci. **37**: 1337-1351.

Tsuji, S. and Takeuchi, Y. 1998. Stock Assessment and future projection of southern bluefin tuna - 1998-07-22. CCSBT/9807/27.

Table 1: Comparison of the negative log-likelihood value for the best fit of the 1980's tagging data to the VB growth curve for four different error models (see text for more detail).

Error model	Number of error parameters	Neg. log-likelihood
Constant	1	14695.59
Random L_∞ plus a constant	2	14622.95
Random k plus a constant	2	14663.52
Random L_∞ and k plus a constant	3	14622.98

Table 2: Parameter estimates for the VB log k model with a seasonal growth component based on the integrated best fit to the complete data set from each decade.

Decade	L_∞	σ_∞	k_1	k_2	α	β	u	w	$\mu_{\log A}$	$\sigma_{\log A}$	σ_s	σ_f	a_0	σ_γ	σ_ε
1960s	187.8	7.00	0.14	0.15	5.53	30.00	0.53	-0.069	1.19	0.16	2.40	1.49	-1.57	5.87	2.01
1970s	184.3	7.92	0.15	0.19	5.66	30.00	0.92	0.061	0.77	0.12	2.05	3.06	-1.28	0.00	3.54
1980s	184.7	8.06	0.22	0.17	2.83	18.33	0.34	0.129	0.58	0.17	2.08	2.61	-0.43	4.57	4.30
1990s	184.9	8.69	0.25	0.16	2.46	12.40	0.41	0.255	0.72	0.32	1.81	3.36	-0.31	5.57	-

Table 3: Comparison of the decadal mean otolith increments for different band increments.

		1960's	1970's	1980's	1990's
	Mean	0.32	0.30	0.36	0.39
Band 1-2	SE	0.008	0.006	0.006	0.009
	N	104	157	163	63
	Mean	0.24	0.23	0.26	0.27
Band 2-3	SE	0.006	0.005	0.005	0.006
	N	104	157	163	63
	Mean	0.19	0.19	0.20	0.21
Band 3-4	SE	0.004	0.003	0.004	0.008
	N	104	157	163	63
	Mean	0.16	0.16	0.17	0.19
Band 4-5	SE	0.003	0.003	0.003	0.011
	N	104	157	157	6
	Mean	0.74	0.72	0.82	0.88
Band 1-4	SE	0.014	0.011	0.01	0.018
	N	104	157	163	39
	mean	0.91	0.88	0.98	1.04
Band 1-5	SE	0.015	0.012	0.012	0.037
	N	104	157	157	6

Table 4: The correlation by cohort among the growth increments between different bands within individual otoliths. For each cohort and band increment, the mean increment was calculated. The deviations from these means were then calculated for each otolith and the correlation coefficient for these deviations was then determined.

Cohort	N	Bands1-2 & 2-3	Bands1-2 & 3-4	Bands1-2 & 4-5	Bands 2-3 & 3-4	Bands 2-3 & 4-5	Bands 3-4 & 4-5
1960	3	0.92	0.19	0.56	-0.22	0.19	0.92
1961	4	1.00	0.08	-0.29	0.05	-0.28	0.51
1962	6	0.73	0.97	0.72	0.82	0.59	0.82
1963	7	0.41	0.76	0.53	0.49	-0.01	0.62
1964	13	0.70	0.15	-0.16	0.62	-0.04	-0.13
1965	11	0.40	-0.06	-0.46	0.79	0.08	0.44
1966	21	0.44	-0.03	-0.12	0.32	0.12	0.27
1967	11	0.66	0.62	-0.30	0.65	-0.22	0.35
1968	16	0.22	0.30	0.45	0.44	-0.13	-0.36
1969	12	0.53	0.20	0.14	0.44	0.74	0.26
1970	18	0.36	0.08	-0.14	0.59	-0.34	0.10
1971	15	0.34	0.06	0.63	0.54	0.58	0.20
1972	17	0.71	0.75	0.38	0.80	0.20	0.38
1973	15	0.31	0.03	-0.45	0.21	0.06	0.36
1974	15	0.72	-0.08	0.34	-0.01	0.37	0.38
1975	14	0.73	0.09	0.09	0.28	0.36	0.74
1976	19	0.84	0.50	-0.06	0.67	-0.17	-0.03
1977	16	0.63	0.12	-0.08	0.33	0.36	0.53
1978	14	0.12	-0.05	-0.33	0.70	-0.02	0.39
1979	14	0.52	0.27	-0.08	0.43	-0.08	0.35
1980	17	0.09	0.15	-0.14	0.64	0.21	0.38
1981	10	0.61	0.38	0.26	0.36	0.53	0.19
1982	14	0.45	0.17	-0.54	0.45	-0.03	0.40
1983	16	0.59	0.33	0.12	0.39	0.25	0.58
1984	15	0.29	0.15	-0.36	0.71	-0.07	0.02
1985	18	0.49	0.24	-0.03	0.56	0.29	0.43
1986	12	-0.18	0.24	0.22	0.41	0.35	0.27
1987	27	0.26	-0.31	-0.31	0.29	0.13	0.62
1988	25	0.35	0.08	-0.13	0.54	0.31	0.79
1989	9	0.55	0.01	0.73	0.33	0.62	0.63
1990	35	0.23	-0.14	-0.43	0.40	-0.37	0.68

Table 5: The expected average length at age by year based on the application of the parameters from the best fit to the VB log k model to the decadal data from Table 2. The mean lengths at age have been applied to cohorts corresponding to data used in estimating the decadal growth curves. The values represent one alternative hypothesis for the expected length at age that could be used in the SBT stock assessments.

	Age														
Year	1	2	3	4	5	6	7	8	9	10	11	12	13	14	15
1960	58	75	-	-	-	-	-	-	-	-	-	-	-	-	-
1961	58	75	90	-	-	-	-	-	-	-	-	-	-	-	-
1962	58	75	90	103	-	-	-	-	-	-	-	-	-	-	-
1963	58	75	90	103	115	-	-	-	-	-	-	-	-	-	-
1964	58	75	90	103	115	125	-	-	-	-	-	-	-	-	-
1965	58	75	90	103	115	125	134	-	-	-	-	-	-	-	-
1966	58	75	90	103	115	125	134	141	-	-	-	-	-	-	-
1967	58	75	90	103	115	125	134	141	148	-	-	-	-	-	-
1968	58	75	90	103	115	125	134	141	148	153	-	-	-	-	-
1969	56	75	90	103	115	125	134	141	148	153	158	-	-	-	-
1970	56	74	90	103	115	125	134	141	148	153	158	162	-	-	-
1971	56	74	90	103	115	125	134	141	148	153	158	162	166	-	-
1972	56	74	90	103	115	125	134	141	148	153	158	162	166	169	-
1973	56	74	90	103	117	125	134	141	148	153	158	162	166	169	171
1974	56	74	90	103	117	129	134	141	148	153	158	162	166	169	171
1975	56	74	90	103	117	129	138	141	148	153	158	162	166	169	171
1976	56	74	90	103	117	129	138	146	148	153	158	162	166	169	171
1977	56	74	90	103	117	129	138	146	153	153	158	162	166	169	171
1978	56	74	90	103	117	129	138	146	153	159	158	162	166	169	171
1979	48	74	90	103	117	129	138	146	153	159	163	162	166	169	171
1980	48	75	90	103	117	129	138	146	153	159	163	167	166	169	171
1981	48	75	94	103	117	129	138	146	153	159	163	167	170	169	171
1982	48	75	94	109	117	129	138	146	153	159	163	167	170	173	171
1983	48	75	94	109	120	129	138	146	153	159	163	167	170	173	175
1984	48	75	94	109	120	131	138	146	153	159	163	167	170	173	175
1985	48	75	94	109	120	131	139	146	153	159	163	167	170	173	175

Table 5 (continued):

	Age														
Year	1	2	3	4	5	6	7	8	9	10	11	12	13	14	15
1986	48	75	94	109	120	131	139	146	153	159	163	167	170	173	175
1987	48	75	94	109	120	131	139	146	152	159	163	167	170	173	175
1988	48	75	94	109	120	131	139	146	152	157	163	167	170	173	175
1989	52	75	94	109	120	131	139	146	152	157	162	167	170	173	175
1990	52	81	94	109	120	131	139	146	152	157	162	165	170	173	175
1991	52	81	98	109	120	131	139	146	152	157	162	165	168	173	175
1992	52	81	98	111	120	131	139	146	152	157	162	165	168	171	175
1993	52	81	98	111	122	131	139	146	152	157	162	165	168	171	173
1994	52	81	98	111	122	131	139	146	152	157	162	165	168	171	173
1995	52	81	98	111	122	131	139	146	152	157	162	165	168	171	173
1996	52	81	98	111	122	131	139	146	152	157	162	165	168	171	173
1997	52	81	98	111	122	131	139	146	152	157	162	165	168	171	173
1998	52	81	98	111	122	131	139	146	152	156	162	165	168	171	173
1999	-	81	98	111	122	131	139	146	152	156	161	165	168	171	173
2000	-	-	98	111	122	131	139	146	152	156	161	164	168	171	173

Table 5 (continued):

	Age														
Year	16	17	18	19	20	21	22	23	24	25	26	27	28	29	30
1974	174	-	-	-	-	-	-	-	-	-	-	-	-	-	-
1975	174	176	-	-	-	-	-	-	-	-	-	-	-	-	-
1976	174	176	177	-	-	-	-	-	-	-	-	-	-	-	-
1977	174	176	177	179	-	-	-	-	-	-	-	-	-	-	-
1978	174	176	177	179	180	-	-	-	-	-	-	-	-	-	-
1979	174	176	177	179	180	181	-	-	-	-	-	-	-	-	-
1980	174	176	177	179	180	181	182	-	-	-	-	-	-	-	-
1981	174	176	177	179	180	181	182	183	-	-	-	-	-	-	-
1982	174	176	177	179	180	181	182	183	184	-	-	-	-	-	-
1983	174	176	177	179	180	181	182	183	184	184	-	-	-	-	-
1984	177	176	177	179	180	181	182	183	184	184	185	-	-	-	-
1985	177	178	177	179	180	181	182	183	184	184	185	185	-	-	-
1986	177	178	179	179	180	181	182	183	184	184	185	185	185	-	-
1987	177	178	179	180	180	181	182	183	184	184	185	185	185	186	-
1988	177	178	179	180	181	181	182	183	184	184	185	185	185	186	186
1989	177	178	179	180	181	182	182	183	184	184	185	185	185	186	186
1990	177	178	179	180	181	182	183	183	184	184	185	185	185	186	186
1991	177	178	179	180	181	182	183	183	184	184	185	185	185	186	186
1992	177	178	179	180	181	182	183	183	183	184	185	185	185	186	186
1993	177	178	179	180	181	182	183	183	183	184	185	185	185	186	186
1994	175	178	179	180	181	182	183	183	183	184	184	185	185	186	186
1995	175	176	179	180	181	182	183	183	183	184	184	184	185	186	186
1996	175	176	178	180	181	182	183	183	183	184	184	184	184	186	186
1997	175	176	178	179	181	182	183	183	183	184	184	184	184	185	186
1998	175	176	178	179	180	182	183	183	183	184	184	184	184	185	185
1999	175	176	178	179	180	180	183	183	183	184	184	184	184	185	185
2000	175	176	178	179	180	180	181	183	183	184	184	184	184	185	185

Figure 1: (*top*) The optimal integrated seasonal VB log k growth curve for each decade. (*bottom*) The same curves plotted relative to the 1960's curve for better comparison.

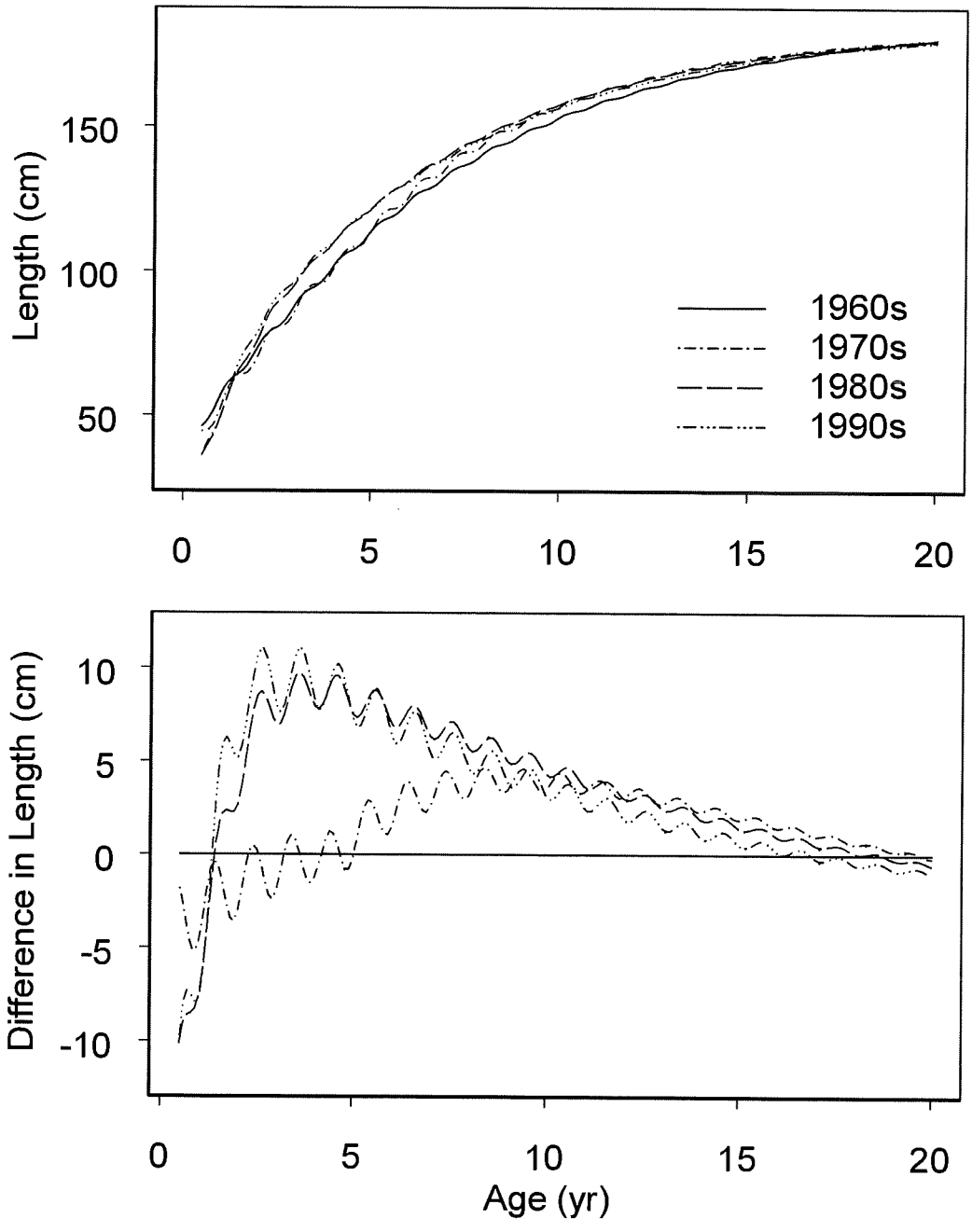

Figure 2: Results from fitting a time-varying von Bertalanffy growth model to South Australian length-frequency data. a) The fitted von Bertalanffy growth rate $\hat{k}(t)$ versus time t. b) The mean lengths for age groups 1 to 4 versus time t. Note that the curves exhibit subtle differences, in that the early 1970s peak moves to the right as age increases, and the relative heights of the 1973 and 1985 peaks change with age group. See Appendix 8 for more detail.

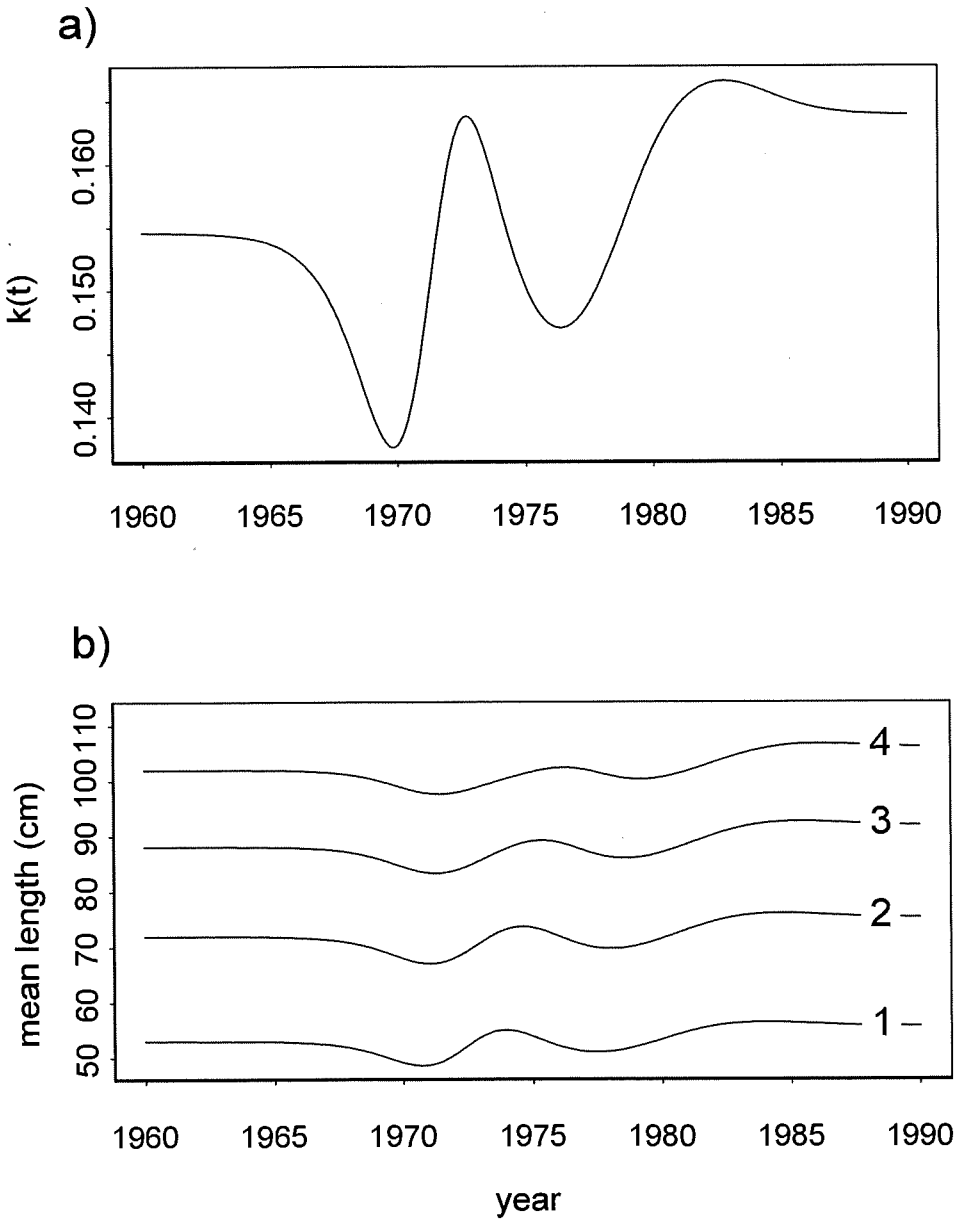

Figure 3: Average deviation for a cohort from the overall mean and 95% confidence intervals for the band 1-5 increment in SBT otoliths.

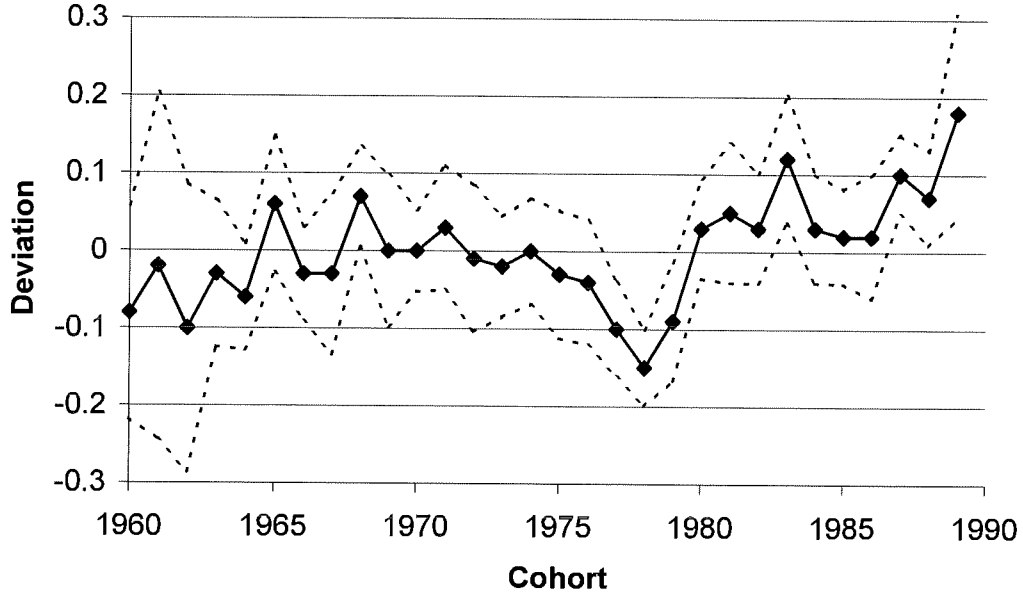

Figure 4: Nominal CPUE (number of SBT per 1000 hooks) trends for ages 4 and 5 for Japanese longline vessels fishing on their feeding grounds (Statistical Areas 4-9) during the second and third quarters (adapted from Ricard and Polacheck, 2002).

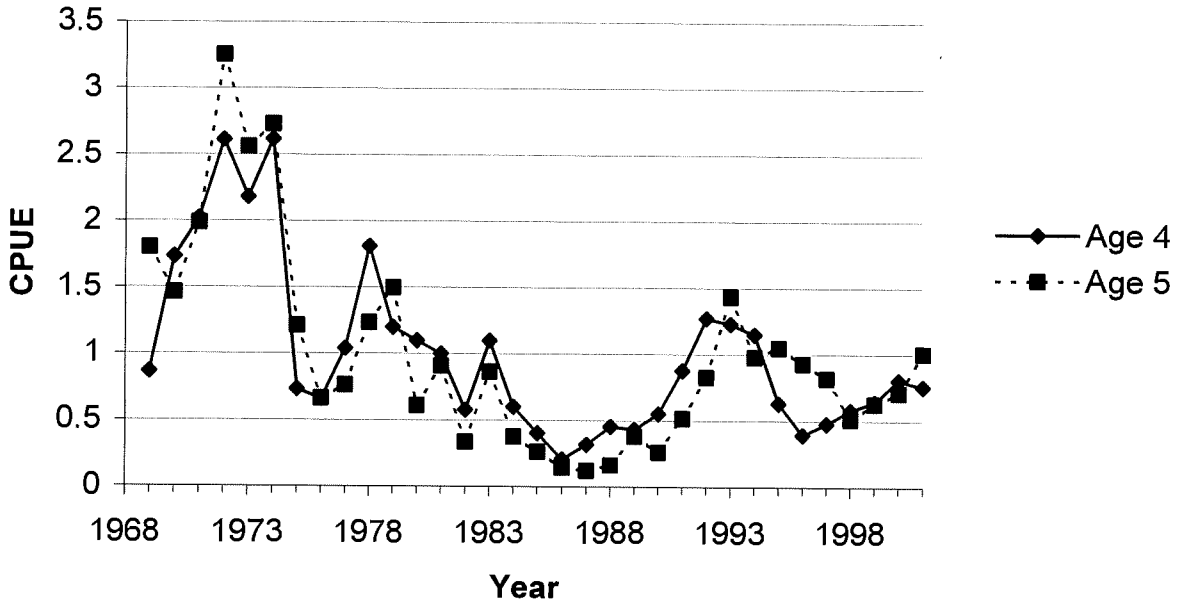

Figure 5: Examples of estimates of recruitment trends from SBT stock assessments. These estimates are taken from Polacheck and Preece (2001), but similar trends are seen in other stock assessment results. Shown are a set of different estimates derived from alternative hypotheses for interpretation of input data and parameters. The three rather distinct bands represent three different options considered for natural mortality rates.

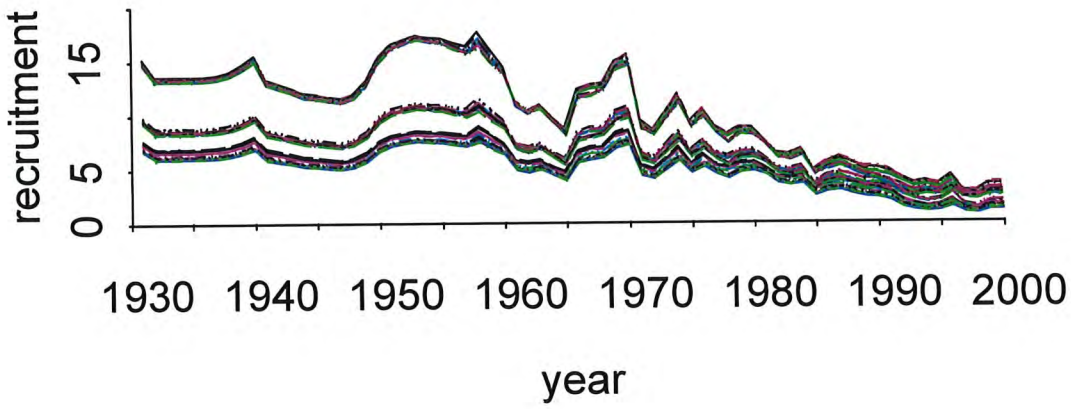

Figure 6: An example of the coefficient of variation as a function of age for the variance component resulting from aggregating length-frequency data over a year in the situation in which catches were evenly distributed throughout the year (see text for details).

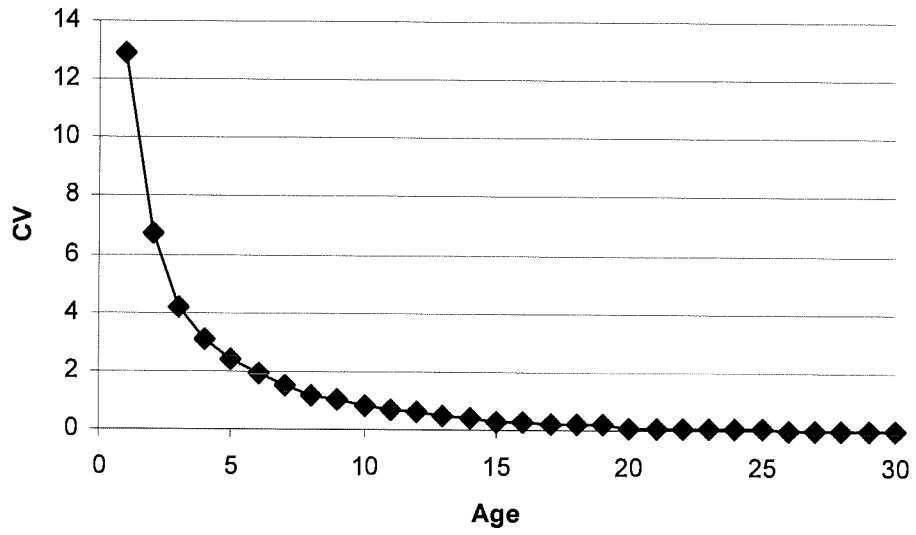

Figure 7: Estimates for the various variance components as a function of age that would contribute variance in the observed length-frequency of SBT commercial catches (see text for details).

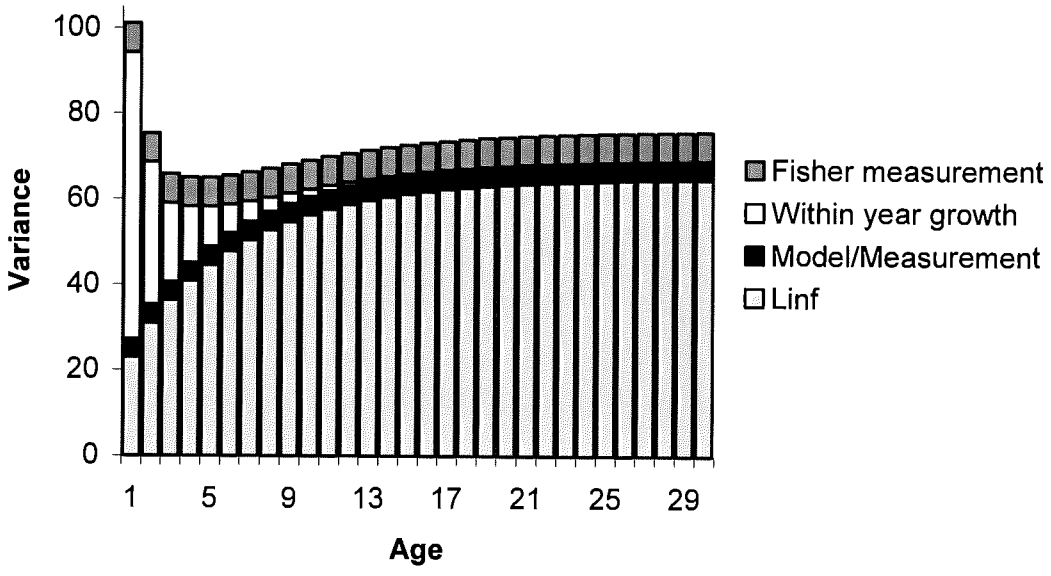

Figure 8: Estimates of the coefficient of variation expected in observed length at age distributions for SBT. The upper curve represents the situation in which all the length measurements are made by fishermen and the lower curve represents the situation where all measurement are made by scientists or trained technicians. The estimates assume that catches were aggregated and uniformly taken throughout a year.

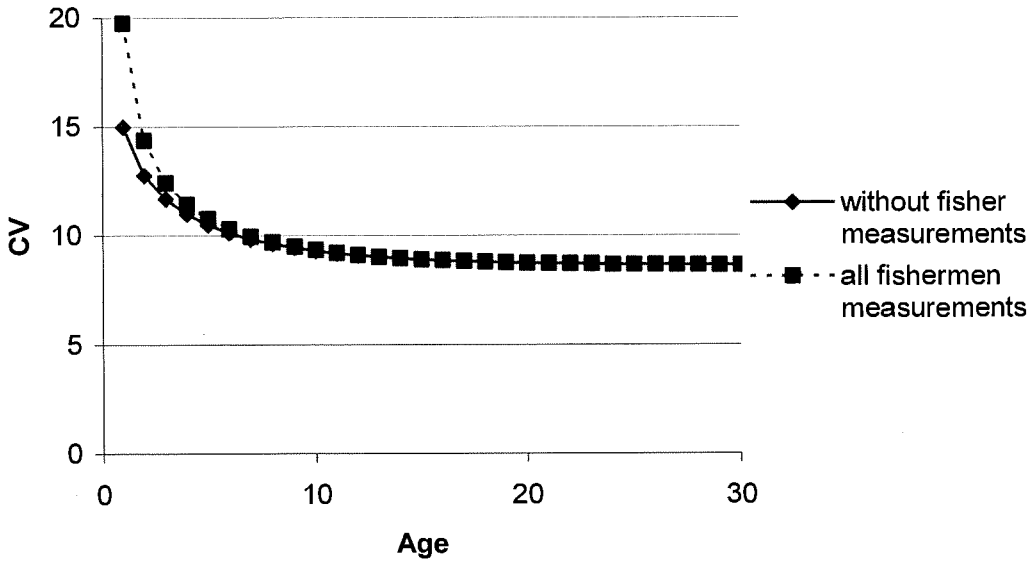

Figure 9: Estimates of the expected length and 95% confidence interval for the observed distribution of lengths at age based on the best fit to the 1980's data and using the variance model developed in the discussion (including the additional component for fishermen-measured lengths).

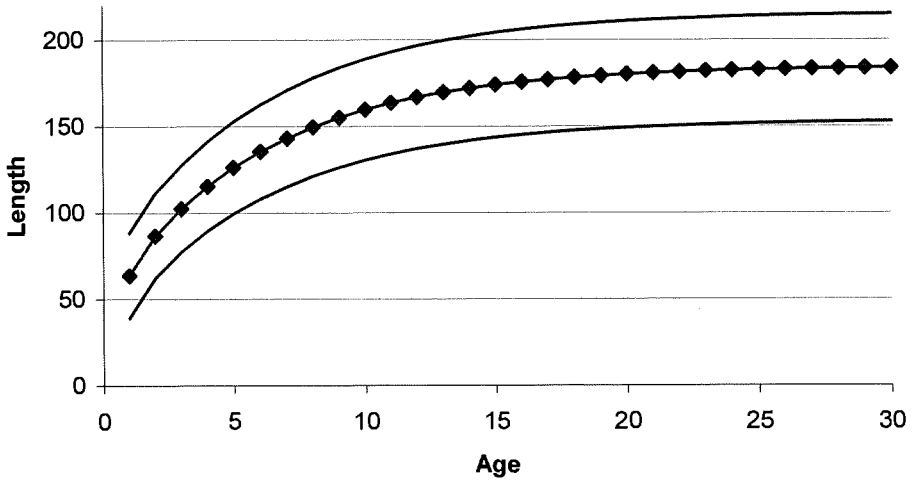

Figure 10: Possible growth curves (the three lower lines) for cohorts born prior to 1960 to use as alternative hypotheses in estimating the expected length-frequency distribution of SBT catches from these cohorts. All curves were calculated assuming a value of 165 cm for μ_∞. The lower curve uses a value of 0.100 for k_2, 0.125 for the middle curve and 0.150 for the upper one. The parameter a_0 has been adjusted so that each curve yields the same size of an age 2 fish as that estimated for the 1960's. Also shown is the curve estimated for the 1960's (uppermost line).

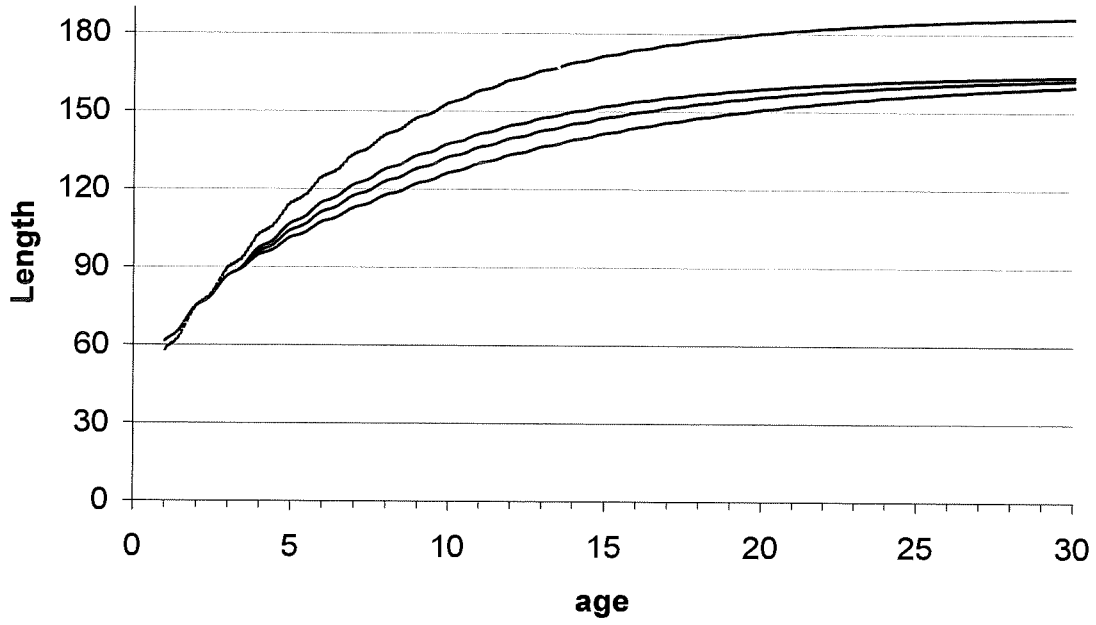

Figure 11: The three possible growth curves for cohorts born prior to 1960 shown in Figure 10 (upper broken lines) compared with the same three growth curves when the value of a_0 has been left unadjusted at the value estimated for the 1960's (lower solid lines). Only estimates up to age 8 have been shown so the differences in the curves can be clearly seen.

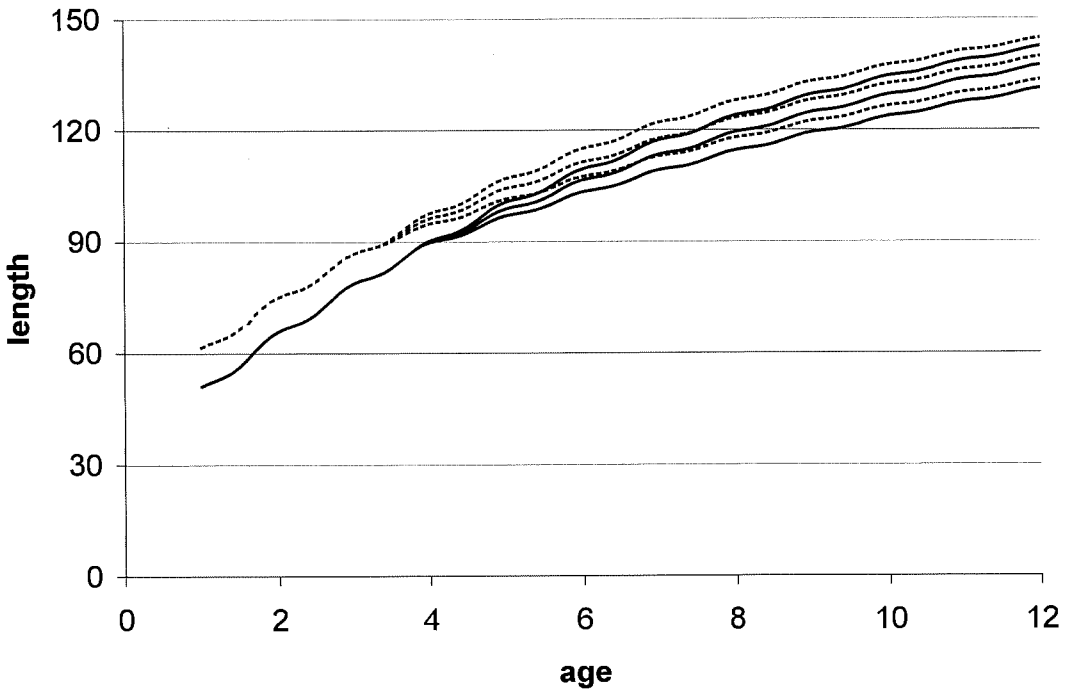

Appendix 1: Intellectual Property

No commercial intellectual property arose from this work.

Appendix 2: Staff

Tom Polacheck

Geoff M. Laslett

J. Paige Eveson

Naomi P. Clear

Appendix 3:

The data: details of the tag-recapture, length-frequency and direct aging data used for studying growth of southern bluefin tuna (*Thunnus maccoyii*)

J. Paige Eveson, Tom Polacheck and Geoff M. Laslett

FRDC Project 1999/104

Introduction

Three types of data that contain information on the growth of SBT were used in the analyses conducted within this project:

1) tag-recapture data;
2) length-frequency data from commercial catches; and
3) direct aging data from otoliths.

This Appendix provides a description of each of these and documents the data selection procedures used to obtain the final data sets that were used in the analyses presented in this report.

In all data sources, we find that one-year old SBT caught off the coast of Western Australia are smaller on average than one-year olds caught off the coast of South Australia at the same time. This is consistent with current beliefs about SBT spawning and migration. SBT are spawned in the northeast Indian Ocean between Indonesia and the northwest coast of Australia, generally between the months of September and April. Catches indicate that there tends to be two peak spawning times, one around September/October and one around January/February, although there is a high degree of variability between years (Davis and Nurhakim 2001). Juveniles migrate southward along the west coast of Australia, and then a large percentage of them turn and travel eastward along the south coast of Australia to the Great Australian Bight. If SBT are spawned at two peak times, then we might expect to find the larger, earlier spawned fish off of South Australia at the same time we find the smaller, later spawned fish off of Western Australia. There is no indication of this size segregation persisting past age one.

In our analysis of the length-frequency and the direct aging data, we make the assumption that SBT have a birth date of January 1. This date is chosen since it represents a midpoint of the spawning season, and thus the mean of the assigned ages should be close to the true mean.

Tag-Recapture Data

Extensive tagging experiments were conducted by CSIRO from the 1960's through the 1990's in which juvenile SBT were caught, tagged, and released in the

coastal waters off southern Western Australia, South Australia and southeastern Tasmania. Most of the tagged fish were initially caught using pole and line gear with a barbless hook, although a small number were caught with troll lines. After a fish had been hooked, it was hauled aboard the vessel. In the 1960's and 1970's, it was placed on a measuring board and its nose to caudal fork length was measured; in the 1980's and 1990's, it was placed on a vinyl cradle and the same length measurement was taken. The fish was then tagged with either one or two 12 cm plastic spaghetti dart tags (generally referred to as "conventional" tags). Tags were inserted into a fish about 4 cm to the rear of the second dorsal fin on either side of the fish. Tagging operations were designed to minimize handling time, and fish were re-released to the water within about 30 seconds of being brought on board. After 1963, almost all fish were double-tagged. The tag numbers and length of each fish were recorded, together with the location and date of release. Additional information about the release was also recorded, such as the quality of tagging, the health of the fish, and the name of the tagger and the vessel. This information was later transferred to a computer database.

In addition to the tagging conducted directly by CSIRO, a large number of fish were tagged and measured by contract fishermen in the 1960's and 1970's. Fishermen were paid according to the number and size of the fish released. This would have created an incentive to exaggerate the length measurement. Examination of the data suggests this may have been the case since a high proportion of fish tagged by fishermen had a release length larger than their recapture length, even after several months at liberty. Return rates from fishermen-tagged fish were also low relative to those for scientist-tagged fish, which suggests that there may have been problems of substantial stress and tag-induced mortality among these fish. In order to ensure that negative biases were not introduced into the growth analyses, we excluded any data where the tagger was a fisherman, a crewmember, or unknown.

Excluding the fishermen-tagged fish, a total of 26740 fish were tagged with conventional tags and released into the wild[1] during the 1960's (including 1959), 6668 during the 1970's, 10741 during the 1980's, and 68034 during the 1990's. Of these fish, the total number of returns to date (January 2002) by decade has been 1392, 612, 4256 and 7779, respectively. Recaptures occurred throughout the geographical distribution of SBT, ranging in longitude from 0 to 180°E and in latitude from 30 to 50°S. In a few cases, recaptured fish were re-released into the wild. The above release and recapture numbers only include original releases and terminal recaptures (i.e. recaptures for which the fish was not re-released), and only growth information from terminal recaptures was used in our analyses. Not all tagged fish that were recaptured will have been reported, and for some fisheries non-reporting rates have been estimated to be substantial (Polacheck et al. 1998). However, there is no reason to believe that a fisherman's choice to report a tag is related to fish size or growth, so growth analyses based on information from reported tags should be unbiased.

Upon recapture, the finder measured the caudal fork length of the fish and recorded this length along with the tag number, the date and location of recapture, and sometimes the weight of the fish. This information was sent to CSIRO and entered into the computer database, along with the name of the finder and the vessel and a judgment about the quality of the recapture information.

The change in length of a fish over the time it was at liberty gives information about individual growth, and this data can be used collectively to model the growth of the population. Unfortunately, some of the tag-recapture data is either unreliable or unsuitable for studying growth due to various reasons. Using the subsidiary information recorded on release and recapture, we applied a rigorous screening process as follows.

In cases where for some reason either the release length or recapture length was not measured, we excluded the entry. For example, the finder did not always record the length of the fish. Plus, a few of the returns were tags found without a fish on the beach

[1] CSIRO has also conducted tagging experiments with caged tuna in tuna farming operations and with archival tags in the 1990's. Data from these tagging experiments were not included in the analyses presented in this project.

for which a fish recapture length was clearly not possible. Entries for which both length measurements exist were only included if both were reported as being measured accurately.

In cases where the whole weight or dressed weight of the fish was measured and recorded on recapture, the relationship between length and weight could be used to identify questionable data. Specifically, we calculated the expected weight of a fish using the relationship of Robins (1963),

$$W = 3.131 \cdot L^{2.9058} \cdot 10^{-5}$$

for fish with length less than 130 cm, and the relationship of Warashina and Hisada (1970),

$$W = 1.15 \cdot 2.178 \cdot L^{3.4229} \cdot 10^{-6}$$

for fish with length greater than 130 cm. W is whole weight in kg and L is caudal fork length in cm. When only a dressed weight was measured for a fish, a factor of 1.15 was used to convert it to a whole weight (Caton 1991). Note this factor also appears in the equation of Warashina and Hisada to convert it from dressed weight to whole weight. We chose to use this composite weight-length relationship based on the 1994 SBT Trilateral Workshop Report (Anon. 1994). As a check, we fitted a power relationship to the weight and length data available from the tag-recapture database and the resulting curve was almost identical to the composite curve used (Figure 1).

If the expected weight was either less than 0.64 or greater than 1.27 of the reported weight, then the entry was considered an outlier and excluded from our analysis. These limits were chosen because they are the 2.5% and 97.5% percentiles of the empirical distribution of expected to observed weight ratios. Unfortunately, the recapture weight was not measured for a large percentage of fish, especially in the 1960's, and therefore this screening criterion often could not be applied. In the absence of weight information, we assumed the recapture length to be accurate and included the data.

A few vessels were noted to have a very high proportion of weight-length outliers and therefore all data from these vessels were considered unreliable and omitted from the analysis. The criterion used to omit a vessel was as follows. For each vessel, we calculated a 95% confidence interval on the percentage of recaptures that were outliers

(using the binomial distribution). If the lower limit of the confidence interval exceeded 20%, then all recapture records from that vessel were omitted. Using the confidence interval rather than the point estimate takes into account the number of recaptures actually made by the vessel, so that 1 outlier out of 3 recaptures is not considered too high but 30 outliers out of 90 is.

The date of recapture was not always known precisely. Uncertainties in the day of recapture were allowed, but if the month or year was uncertain, then the entry was excluded.

If the tagger judged the injury to the tuna upon tagging to be anything more than slight, then the record was excluded since the injury could affect the fish's growth. Even well inserted tags may have an initial effect on fish growth. We assumed that, in terms of length, this initial effect would be unappreciable after 30 days; thus, only fish at liberty for 30 days or more were included in the analysis.

In the 1990's, tuna farming commenced and many of the fish that had been tagged were caught and put into farms. The date of entry into the farm was recorded but the length of the fish was not measured until it was harvested. We would expect the growth rate of fish in farms to differ from than that of wild fish, in which case including farm recaptures in our analysis would bias the results. The length data does not actually seem to support this hypothesis. It is likely that farmed fish increase more quickly in weight than wild fish but not in length. Although we do not have initial weights at tagging to confirm this, the fact that farm fish weigh more at recapture than wild fish of the same length lends support. In any event, we have opted to err on the side of caution and exclude the farm fish from our growth analyses. Note that the sample size in the 1990's was large so the exclusion of farm fish should not affect the precision of the growth parameter estimates.

As mentioned earlier, a few fish were recaptured and subsequently re-released, some of which were recaptured again. We only included information from the terminal recapture (when there was one) in our growth analyses because usually no length measurement was taken on the first recapture before the fish was re-released. The number of re-released tagged fish was very small.

After applying the above screening criteria, the number of recaptures remaining for analysis was 791 in the 1960's, 202 in the 1970's, 2181 in the 1980's and 2980 in the 1990's. The release lengths ranged from 38 to 125 cm with a mean of 68 cm, and the recapture lengths ranged from 38 to 186 cm with a mean of 97 cm. Although the times at liberty ranged from 30 days (a minimum imposed by the screening process) to 5115 days (≈14 years), the average was 598 days and most fish were at liberty less than three years.

The average growth rate, calculated as centimeters growth per day at liberty, for fish of similar lengths and relatively similar times at liberty suggest that growth rates have increased from the 1960's to the 1980's, with perhaps a transitional period in the 1970's and a stabilization in the 1990's (Figure 2). Subsequently, any long-term growth analysis should take temporal changes into consideration.

Having two data points for each fish, and thus information about the growth of individuals, is a valuable feature of tag-recapture data that the other data sources lack. However, not knowing the age of the fish at release is a drawback. Another limitation is that the majority of fish have relatively short times at liberty so that growth information for older fish tends to be lacking.

Length-Frequency Data

We only consider data from the Australian surface fishery in this report. We did not include length-frequency data from the Japanese longline fishery for several reasons: the procedure used to collect length samples was not consistent; the data is pooled quarterly within a year; and fish caught in the longline fishery are generally older fish for which the length distributions overlap considerably and are not suitable for modal analysis.

Length-frequency data from commercial catches of SBT caught in the Australian surface fishery has been gathered from the 1963-64 fishing season (the fishery was relatively small prior to this) to the present. Not all fish caught were measured for length. Instead, individual landings were sampled at the place of processing. Sampling protocols were designed to avoid introducing biases into the selection of fish to be measured. For details, refer to Majkowski (1982), Majkowski and Morris (1986), and Deriso and Bayliff (1991). Caudal fork lengths were measured and recorded to the nearest centimeter and

pooled into one-centimeter bins. The bin counts were scaled up by the total weight of the landing to give a length-frequency distribution for the landing. The length-frequencies from individual landings were then pooled across half-months and fishing areas (South Australia, Western Australia, and New South Wales). Usually not all landings in a half-month and area were sampled, so the length-frequency distributions were scaled up again by the total weight of the catch from all landings in that period and area. This was possible since the bulk catch from every landing was weighed, regardless of whether the landing was sampled for length.

When using the length-frequency data to study the growth of the population, we assume that the catch provides a reasonably unbiased sample of the lengths of fish within an age class. Size-selectivity in the fishery would invalidate this assumption. Prior to 1990, most fish were caught for the canning market using purse seine vessels, which use nets that catch the majority of a school and do not have the ability to select by size within a school. However, in the 1990's, major changes occurred in the fishery to make size-selectivity a concern. In particular, the focus of the fishery switched to catching tuna for the sashimi market using pole and line vessels that targeted larger fish within a school. In order to avoid introducing biases from size-selective fishing into our analyses, we only include data up to and including 1989.

The length-frequency distributions derived from SBT caught over a short time interval (in this case, half-monthly) generally exhibit modes that correspond to different age classes. The progression of these modes over time can be tracked to give an estimate of population growth. In particular, seasonal growth patterns can often be identified. Ages are assigned to the modes based on knowledge of the relationship between age and length, along with some common sense. Because the Australian fishery catches mainly juvenile SBT aged 5 or less, there is usually a maximum of five modes, and even if older fish are present, the lengths tend to overlap too much for the modes to be distinguished. Examples of the length-frequency data from South Australia in 1981 and 1983 are given in Figure 3.

Although the length-frequencies have been aggregated into three fishing areas, we only include the data from South Australia in our study since it is most abundant and also appears to be most consistent with respect to the progression of modes. The New South

Wales data are somewhat sporadic, and, from the mid-1970's onward, consist predominantly of fish aged 3 and older. Furthermore, the New South Wales fishery collapsed in the mid-1980's. The Western Australia catches are dominated by one-year-old fish (based on direct aging estimates). As such, there is little information in these data on growth of fish older than age one. In addition, for a number of years and periods, there appears to be two one-year old modes, probably due to two peaks in the time of spawning. This double mode does not follow through to the two-year olds, which suggests that the smaller fish catch up in size by the age of two, nor does it appear in the South Australia data, perhaps because the early and late spawned fish have different migration routes or perhaps because the late spawned fish have not yet reached South Australian waters by the end of the fishing season. For these reasons, we chose not to include the Western Australia data in our current analysis.

A complete list of the available South Australian length-frequency data by half-months for years 1964 to 1989 is given in the Annex at the end of this Appendix. The catch figures are in numbers of fish, estimated from the weight of the catch using year and area specific weight-length relationships (hence the non-integer numbers). As discussed already, the length-frequency data in the database are scaled up to represent the total catch for a given half-month and area. Using these data as the raw data in our analyses would not be correct from a statistical viewpoint since the actual samples sizes are much smaller than the catch sizes and varied among years. To correct for this scaling up, we adopted the scale factors proposed by Leigh and Hearn (2000), which take into account the two-stage nature of the scaling-up procedure. The catch size divided by the scaling factor gives an estimate of the "effective sample size" had a simple random sample from the total catch been taken.

Although length-frequency data are subject to biases, and growth information is limited to the first few years of life, the amount of data is considerable with the advantage that it exists over the history of the fishery. Furthermore, length-frequency data provides valuable information about the growth of young fish and about seasonal patterns of growth, which can be used in conjunction with the other sources of data to model the entire growth curve.

Direct Aging Data

Since the late 1980's, thousands of SBT otoliths have been collected by CSIRO scientists on tagging expeditions as well as by trained observers on commercial fishing vessels. The majority of tagging expeditions occurred off the coasts of Western Australia and South Australia, whereas observers were placed on fishing vessels that operated throughout the geographical range of SBT. The sampling protocol involved removing both otoliths whenever possible. The caudal fork length of the fish was measured and recorded, in addition to other information such as the date and location of recapture. The fish chosen for sampling were, to the greatest extent possible, a random sample of the catch.

In recent years, a large number of otoliths have also been collected from tuna on the spawning grounds. SBT are sampled at the export processing sites at Benoa, Bali as part of a large-scale catch-monitoring program (Davis et al. 1998). SBT graded as not suitable for export are available for length measurement and otolith sampling, whereas export grade SBT are immediately plunged into ice and are unavailable for sampling. The lengths of most reject SBT are measured, and otoliths are taken from as many reject SBT as is practical at the time. For example, reject fish will be sampled in the order that they were handled until the sampler runs out of time. Their order is not based on size. Between 500 and 600 sets of otoliths are sampled each season. SBT are graded for export based on flesh quality, which is dependent on handling and/or condition. There is no selection based on length (Davis and Farley 2001); however, fish of poor condition will be lighter for a given length.

The otolith samples are stored in the CSIRO Hardparts Archives, and the data are stored in the CSIRO Hardparts Database. A summary of the number of otoliths collected by year and area is presented in Table 1.

Increments are formed annually in the otoliths of SBT (Clear et al. 2000). Each increment is comprised of an opaque zone corresponding to a period of fast summer growth and a narrower, translucent zone corresponding to slower winter growth (Gunn et al. In press). This translucent zone appears as a dark band when placed on a black background under a dissecting microscope, so that the number of bands can, theoretically, be counted to determine the age of the fish. We refer to this procedure as

"reading" an otolith. In practice, identification of the bands can be difficult, especially in older SBT for which grow is very slow and annuli are very closely spaced.

An otolith can be read using two methods, one in which the otolith is left whole and one in which it is sectioned. Details of the methods are given in Gunn et al. (In press). The whole otolith method can generally only be used for fish less than six years old (~135 cm fork length). Sectioned otoliths can be used for all ages, however the first four or five increments can be difficult to distinguish. With both methods, if the start of a translucent zone can be detected on the outer margin of the otolith, it is counted as one year.

Approximately 4500 of the archived otoliths have been aged to date. In the selection of otoliths for age determination, some were selected based on size stratification (10-cm length categories). This was done to ensure that the youngest and oldest age classes were represented in the direct aging database. Although it is possible for such a procedure to introduce bias into the mean length at age, especially at the very young ages, we do not anticipate the bias to be significant, and if it was, it should be evident through inconsistencies with the other data sources.

Two trained and experienced CSIRO staff made almost all of the otolith readings. Over 80% of the otoliths have had multiple independent readings, ranging from two to seven, made by one or both readers. Each read is assigned a confidence level based on a discrete scale ranging from very uncertain to very confident. A final band count is then assigned based on all of the available information. For each sample, the final count as well as the individual reads and their corresponding reader, confidence level, and method are recorded in the CSIRO Hardparts Database.

From all otoliths aged to data, the final band counts range from 0 to 41 years, and the fork lengths of corresponding SBT range from 26 to 216 cm. Such a wide span of age-length information is desirable for defining a complete growth curve; however, we must use caution. Because the otoliths were collected from fish caught in recent years, all growth information on older fish comes from fish born in the 1950's to 1970's, whereas all information on younger fish comes from fish born in the 1980's and 1990's (Figure 4). This issue will need to be addressed if size-selective mortality exists for SBT

so that Lee's phenomenon (Ricker 1969) is present, or if growth rates have changed over time as the tagging data suggest.

Determining ages from otolith readings is not as straightforward as it may first appear. Firstly, there is uncertainty in the number of bands counted. Information from the multiple readings could potentially be used to estimate the variability in the number of bands counted. Even if we assume the final band count to be accurate, we need to know the time of band formation (namely whether or not the last band was formed in the year of catch) in order to assign an age to the fish. For example, if we assume fish are born on January 1, then a fish caught in September with n bands in its otolith would have an integer age of n if it had already deposited a band in the year of catch; however, it would have an integer age of $n-1$ if it had not yet deposited a band. Information suggests that for SBT the date of formation can vary from the beginning of May to the end of August (Appendix 11). Thus, for a fish caught during this time period, we cannot know whether or not it has yet formed a band in that year, which leads to an uncertainty in its age of one year. We have chosen to omit any fish for which this uncertainty applies and only include direct aging data from fish caught between October 1 and April 30 (see Appendix 11 for more details on why this was done).

Further complications arise from using the direct aging data collected from the spawning grounds to model growth. Comparing lengths of fish of the same age on and off the spawning grounds shows that the fish on the spawning grounds are larger, with the difference in mean length at age being significant for ages 8 (the youngest age on the spawning grounds to date) to 14 inclusively (Farley et al. 2001). This is consistent with maturity having a size-dependent component so that larger fish mature earlier and show up on the spawning grounds before smaller fish of the same age. Since a large number of otoliths were collected from the spawning grounds, including these data in our growth analysis could bias the results. Thus, we have chosen to omit the direct aging data for fish aged 8 through 14 caught on the spawning grounds. In doing so, we could possibly bias the results towards smaller fish if fish of ages 8 to 14 off the spawning grounds are smaller than the population average. This does not appear to be the case; direct age-length data from the period May to September when fish are not spawning and are not

found on the spawning grounds look consistent with age-length data of fish caught off the spawning grounds during the time of spawning from October to April (Figure 5).

As with the length-frequency data, the one-year old direct aging data from Western Australia poses some problems. A small number of otoliths have been collected off the west coast of Western Australia around the latitude of Perth. Fish with one band in their otolith that were caught off the west coast were very small compared to fish with one band caught off of the south coast of either Western Australia or South Australia around the same time. We believe that these small fish were spawned very late in the season, such that they were younger and not as far in their migration route as those spawned earlier. We are not attempting to model the very early stage of growth (birth to, say, 9 months) in our analysis because growth is very rapid during this time and highly seasonal, and there is insufficient information with which to adequately model it. Thus, we omit the data from fish caught off the west coast of Western Australia with one otolith band because we believe that the growth information from these fish is primarily relevant to growth within the first 9 months. For the same reason, we also omit any data from fish with no bands in their otoliths.

After excluding data due to the above reasons, the numbers of otoliths left for analysis is 2530. A breakdown by year and area is presented in Table 1 (in parentheses underneath the total number in the archives).

The length of each annual increment (i.e. the distance between translucent bands) has also been measured for a number of fish (approximately 490). If fish length and otolith length are highly correlated, as evidence suggests (Gunn and Farley 1998), then the incremental otolith data contains useful information for studying growth. However, a practical shortcoming of the data is that increments are only measured for the first five years, after which the bands become too close together to get an accurate measurement. There are a number of complications in attempting to incorporate these data into the integrated growth model developed here. In particular, there is no information on the actual length of a fish at ages corresponding to each measured otolith increment. While there is a correlation between otolith size and fish length, there is still considerable variability around this relationship. Moreover, there is no data to assess how this relationship may have varied over time when substantial changes in growth have

occurred. Thus, these data provide only limited additional information to estimate absolute growth rates relative to the large amount of growth data available from other sources. Consequently, we have not used the incremental data in our estimation of the integrated growth model. The main information content of the incremental data is on possible changes in growth rates over time, and we have considered the data within this context.

References

Anon. 1994. Report of the southern bluefin tuna trilateral workshop. Hobart, Australia, January/February 1994. 161 pp.

Caton, A.E. 1991. Review of aspects of southern bluefin tuna: biology, population and fisheries. Inter-Amer. Trop. Tuna Comm., Spec. Rep., 7: 181-357.

Clear, N.P., Gunn, J.S., and Rees, A.J. 2000. Direct validation of annual increments in the otoliths of juvenile southern bluefin tuna, *Thunnus maccoyii*, by means of a large-scale mark-recapture experiment with strontium chloride. Fish. Bull. **98**: 25-40.

Davis, T.L.O. and Nurhakim, S. 2001. Catch monitoring of the fresh tuna caught by the Bali-based longline fishery. CCSBT-SC/0108/11.

Davis, T.L.O., Bahar, S., Naamin, N., and Le, D. 1998. Catch monitoring of the fresh tuna caught by the Bali-based longline fishery. CCSBT-SC/9807/6.

Davis, T.L.O. and Farley, J.H. 2001. Size partitioning by depth of southern bluefin tuna (*Thunnus maccoyii*) on the spawning ground. Fish. Bull. **99**: 381-386.

Deriso, Richard B. and Bayliff, William H. (*Editors*). 1991. Inter-American Tropical Tuna Commission, Special Report No. 7.

Farley, J.H., Davis, T.L.O., and Eveson, J.P. 2001. Length and age distribution of SBT in the Indonesian longline catch on the spawning ground. CCSBT-SC/0108/12.

Gunn, J.S., Clear, N.P., Carter, T.I., Rees, A.J., Stanley, C.J., and Farley, J.H. In press. The direct estimation of age and growth in southern bluefin tuna, *Thunnus maccoyii* (Castelnau), using otoliths, scales and vertebrae. Fish. Bull.

Gunn, J.S. and Farley, J.H. 1998. Otolith analyses suggest that the growth rate of juvenile SBT began to increase in the late 1970's and that growth rates have continued to increase through the 1980's and 1990's. CCSBT-SC/9807/9.

Leigh, G.M. and Hearn, W.S. 2000. Changes in growth of juvenile southern bluefin tuna (*Thunnus maccoyii*): an analysis of length-frequency data from the Australian fishery. Mar. Freshwater Res. **51**: 143-154.

Majkowski, J. (*Editor*). 1982. CSIRO database for southern bluefin tuna (*Thunnus maccoyii* (Castlenau)). CSIRO Marine Laboratories Report No. 142.

Majkowski, J. and Morris, G. (*Editors*). 1986. Data on southern bluefin tuna (*Thunnus maccoyii* (Castelnau)): Australian, Japanese and New Zealand systems for collecting, processing and accessing catch, fishing effort, aircraft observation and tag release/recapture data. CSIRO Marine Laboratories Report No. 179.

Polacheck, T.W., Hearn, W.S., Miller, C., and Stanley, C.J. 1998. Updated estimates of mortality rates for juvenile SBT from multi-year tagging cohorts. CCSBT-SC/9807/20.

Ricker, W.E. 1969. Effects of size-selective mortality and sampling bias on estimates of growth, mortality, production, and yield. J. Fish. Res. Board Canada **26**: 479-541.

Robins, J.P. 1963. Synopsis of biological data on bluefin tuna, *Thunnus thynnus maccoyii* (Castlenau) 1872. FAO Fisheries Report **6**: 562-587.

Warashina, I. and Hisada, K. 1970. Spawning activity and discoloration of meat and loss of weight in the southern bluefin tuna. Bull. Far Seas Fish. Res. Lab. **3**: 147-165.

Table 1. Number of otoliths in the CSIRO Hardparts Archives by catch year and area. The numbers underneath in parentheses are the corresponding numbers of otoliths that have been aged to date and are remaining for growth analysis after data screening.

Catch Year	South Australia	Western Australia	New South Wales	Tas-mania	New Zealand	Indo-nesia	SE Indian Ocean	South Africa	Other	Total
1983	0	20	0	0	0	0	0	0	0	20
1984	24	45	0	0	0	0	0	0	0	69
1985	277 (4)	475 (10)	0	0	0	0	0	0	0	752 (14)
1986	5	42 (6)	0	0	0	0	0	0	0	47 (6)
1987	1	0	0	0	0	0	0	0	0	1
1988	59 (10)	98 (20)	0	36 (3)	0	0	0	0	5	198 (33)
1989	151 (14)	10	0	308 (8)	0	0	0	0	18	487 (22)
1990	42 (28)	89	12	465 (15)	0	0	0	5	7	620 (43)
1991	54 (39)	21 (4)	0	375 (22)	0	0	109 (15)	0	0	559 (80)
1992	71 (16)	88 (21)	0	350 (65)	84 (1)	2	413 (62)	52 (35)	30	1090 (200)
1993	64 (45)	299 (57)	0	684 (36)	0	10	0	105	31 (3)	1193 (141)
1994	73 (71)	93	0	563 (8)	0	357 (212)	156 (3)	74	1	1317 (294)
1995	26 (23)	71 (8)	17	378 (8)	0	500 (325)	157 (21)	144	3	1296 (385)
1996	5	0	89	329	0	514 (205)	0	0	5	942 (205)
1997	209	0	0	302	0	472 (307)	0	0	1	984 (307)
1998	460	0	88	1	547 (9)	412 (244)	0	0	2	1510 (253)
1999	134	0	0	0	0	873 (505)	0	0	0	1007 (505)
2000	360	0	0	0	0	502 (42)	6	0	0	868 (42)
2001	254	132	6	0	0	470	0	0	0	862
Unknown	32	35	1	10	0	1	0	52	468	599
Total	2446 (250)	1521 (126)	273	3801 (165)	631 (10)	4113 (1840)	841 (101)	432 (35)	571 (3)	14629 (2530)

Figure 1. Caudal fork length versus whole weight for southern bluefin tuna (SBT). The points are measurements taken from recaptures of tagged fish. The dashed line is the curve obtained from fitting a power relationship to the data shown. The solid line shows the weight-length curve taken from the 1994 Report of the SBT Trilateral Workshop.

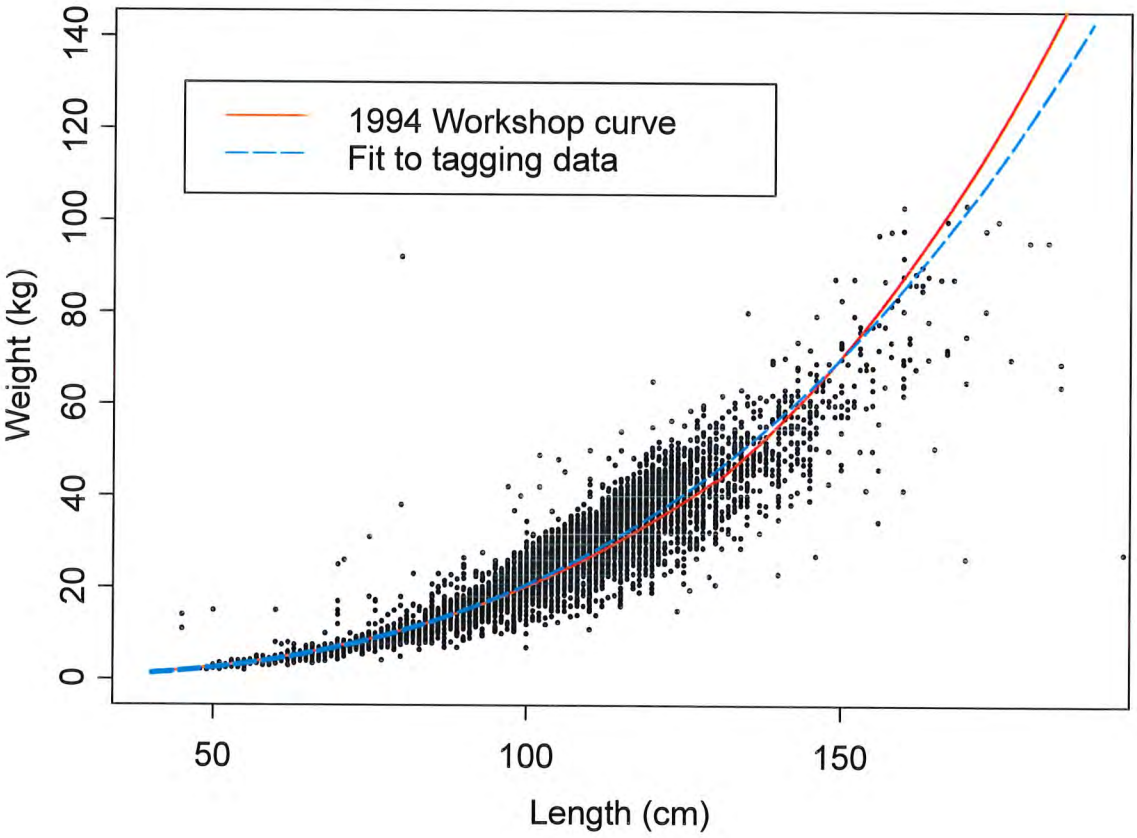

Figure 2. Mean growth rate of recaptured fish (calculated as centimeters growth per day at liberty) versus release length. To make growth rates comparable, fish at liberty for similar number of days are grouped together. Each plotting symbol represents a different decade (solid square = 1990's; solid circle = 1980's; x = 1970's; open circle = 1960's). For readability we did not include standard error bars, but note that there is very little data in the 1970's.

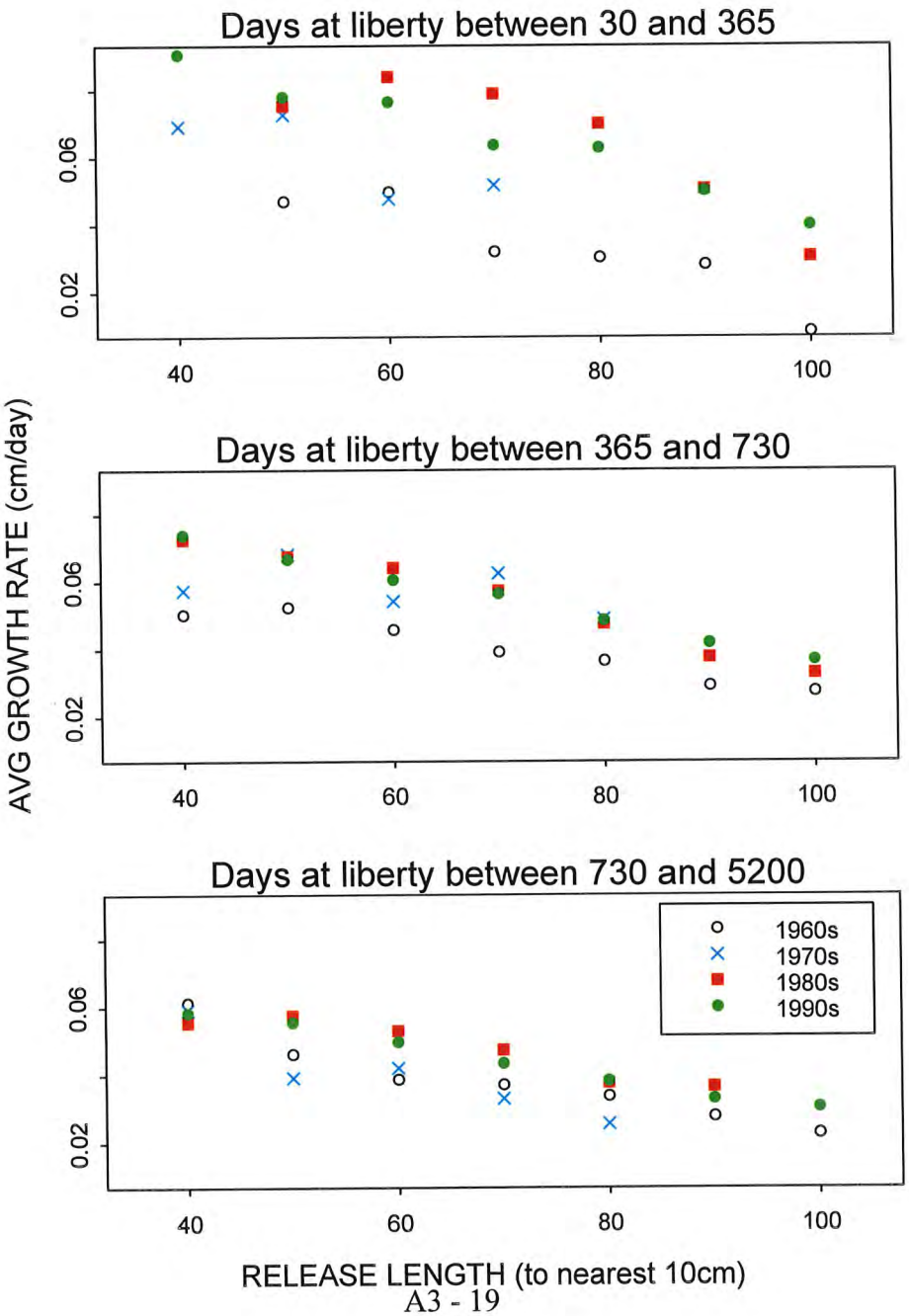

Figure 3. Examples of the length-frequency data available from the commercial catch. Periods 1 to 6 correspond to the first half of January through the last half of March.

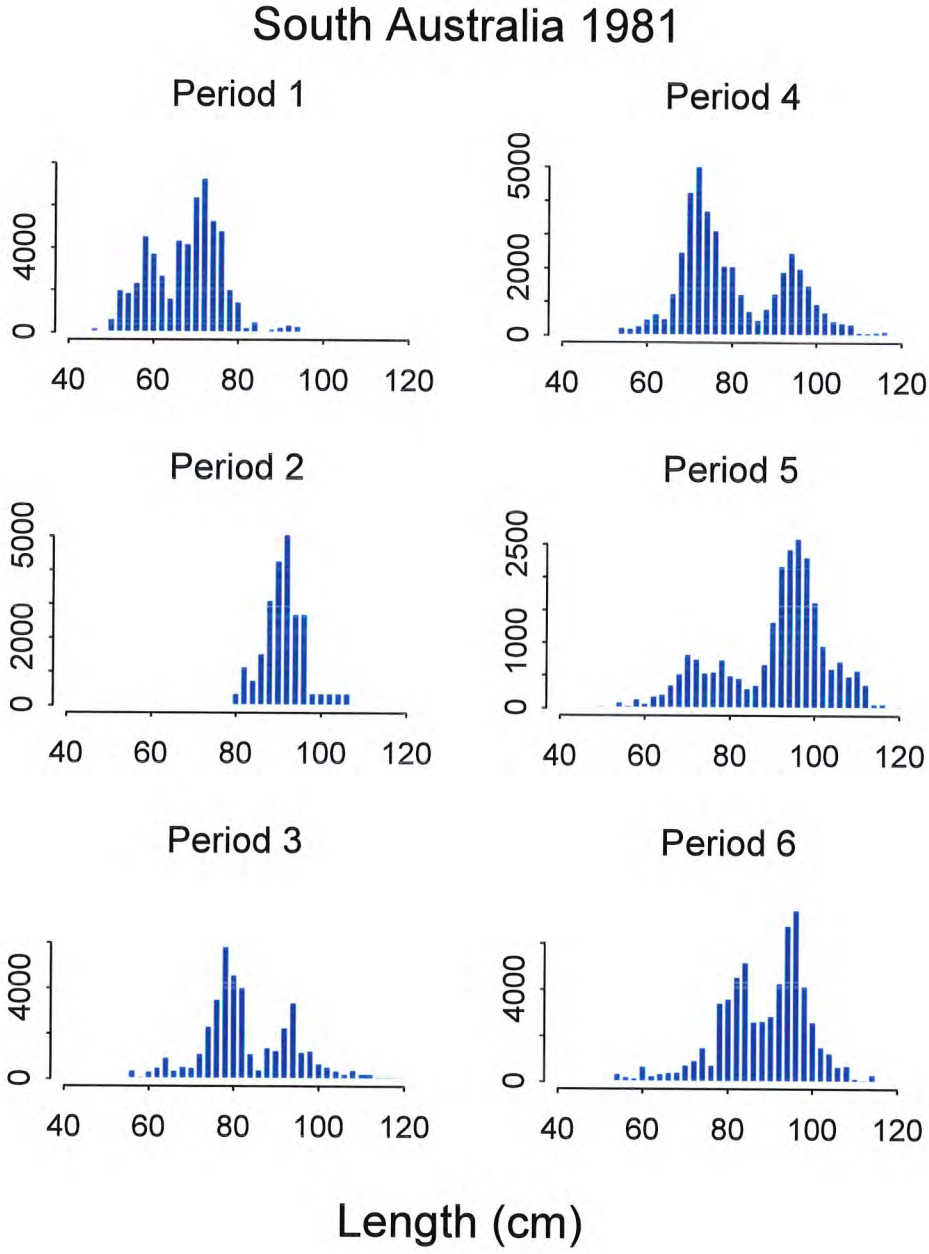

Figure 3 (cont).

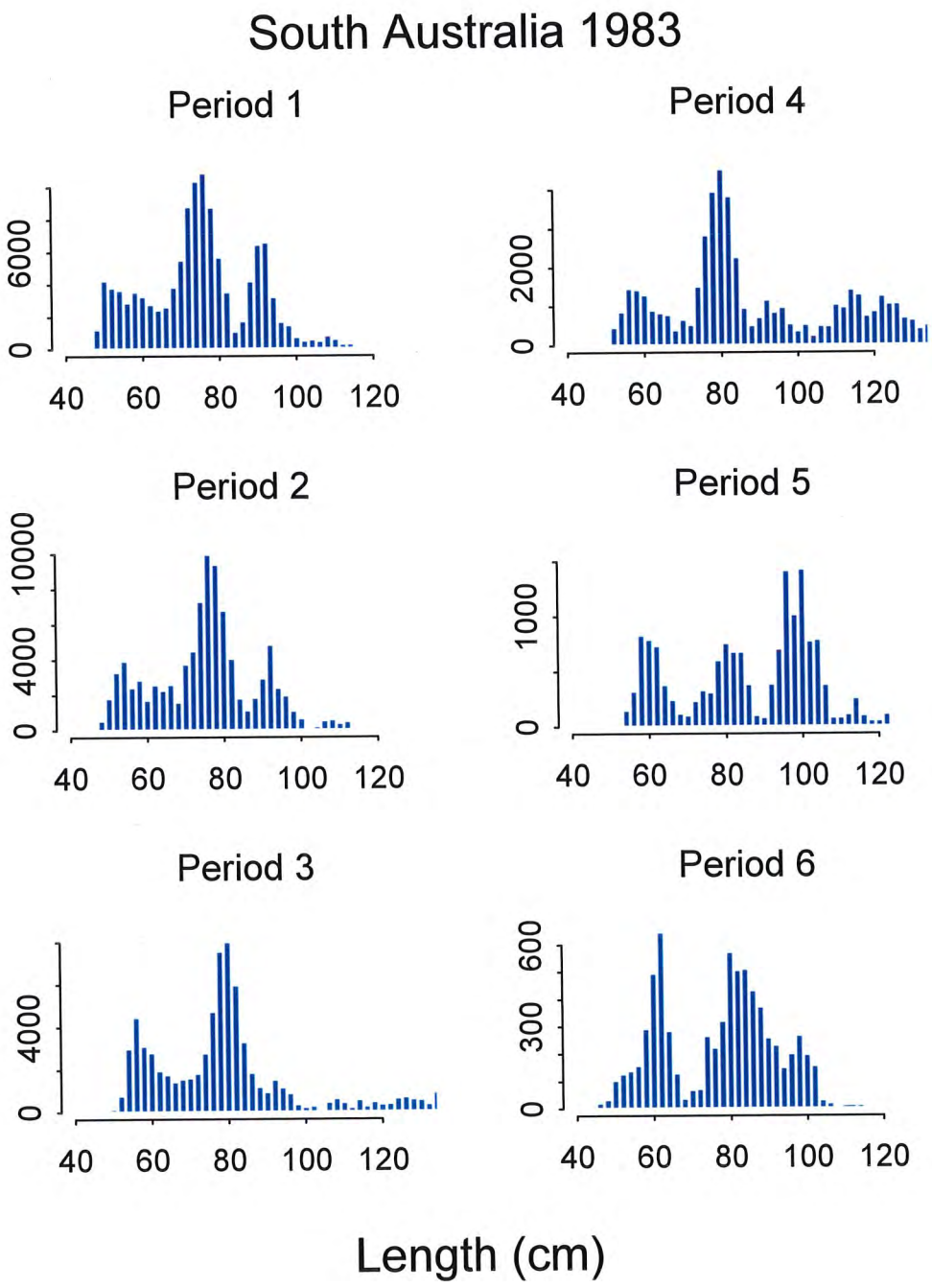

Figure 4. Caudal fork length versus number of otolith bands. Different plotting symbols are used to indicate the decade in which the fish was born.

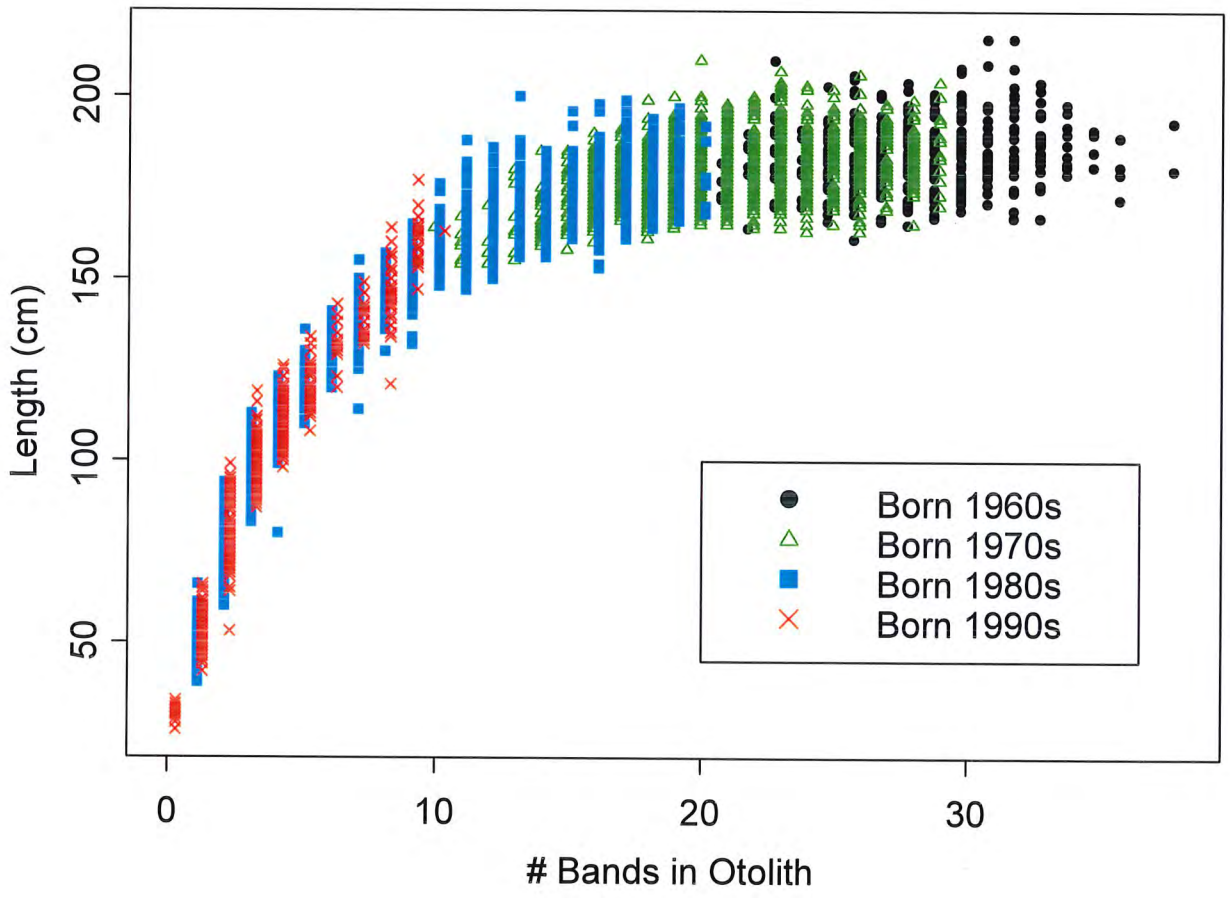

Figure 5. Close-up of direct age-length data to compare the lengths of fish on and off the spawning grounds (SG). Fish of ages 8 to 14 caught on the spawning grounds are larger on average than fish of the same age caught off the spawning grounds at the same time.

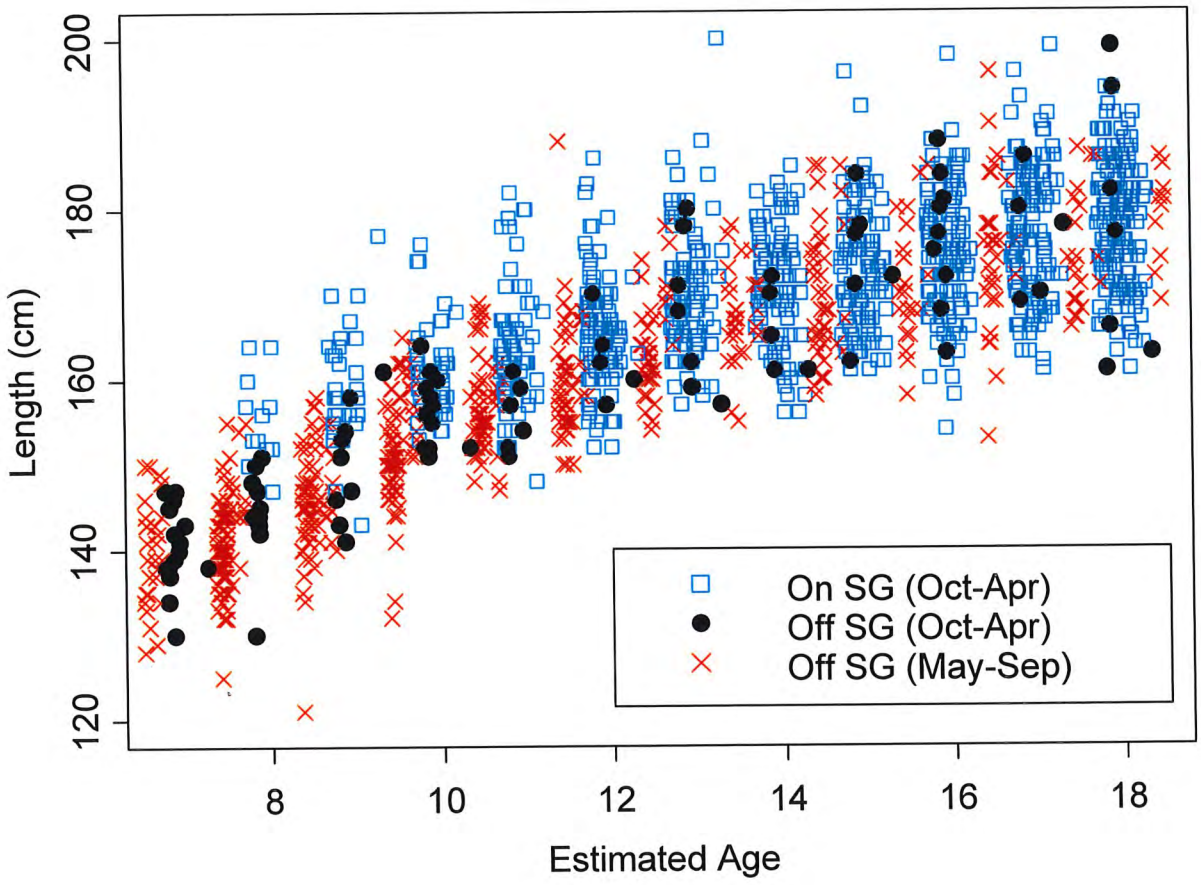

ANNEX:

A summary of the length-frequency data available from the Australian surface fishery, 1964-1989. Refer to the text for an explanation of the scale factors and effective sample sizes.

Year	Period	Catch	Scale Factor	Effective Sample Size
1964	2	39066.8	22.78	1715.0
1964	3	40376.7	33.53	1204.2
1964	4	60828.8	17.29	3518.1
1964	5	41511.9	12.43	3339.7
1964	6	65960.7	27.73	2378.7
1964	7	42242.4	14.69	2875.6
1964	8	60269.5	18.39	3277.3
1964	9	28625.8	17.17	1667.2
1965	2	9070.8	4.3	2109.5
1965	3	27863.4	4.3	6479.9
1965	4	53407.4	28.15	1897.2
1965	5	41604.8	10.81	3848.7
1965	6	62788	18.9	3322.1
1965	7	52801.2	23.85	2213.9
1965	8	37408.7	12.19	3068.8
1965	9	3714.3	n/a	n/a
1966	2	8480	n/a	n/a
1966	3	63785.7	10.29	6198.8
1966	4	104452.6	13.16	7937.1
1966	5	85043.7	10.36	8208.9
1966	6	72328.2	19.11	3784.8
1966	7	43536.3	14.67	2967.7
1966	8	39186.8	14.53	2697.0
1967	1	14225.5	13.66	1041.4
1967	2	10657.3	7.28	1463.9
1967	3	45327.6	10.09	4492.3
1967	4	51425.7	6.8	7562.6
1967	5	56905.3	7.1	8014.8
1967	6	11778	5.2	2265.0
1967	7	14939.8	7.2	2075.0
1967	8	5771.1	15.34	376.2
1967	9	8421.6	10.99	766.3
1967	10	2147.9	5.45	394.1
1967	11	15742.9	13.74	1145.8
1967	12	7910	4.69	1686.6
1968	1	5269.2	26.35	200.0

Year	Period	Catch	Scale Factor	Effective Sample Size
1968	2	29155.4	18.9	1542.6
1968	3	41175.9	32.66	1260.7
1968	4	54340.9	22.9	2373.0
1968	5	31668.5	14.34	2208.4
1968	6	19210.7	14.63	1313.1
1968	7	38281.3	15.36	2492.3
1968	8	32203.8	9.55	3372.1
1968	9	8019.2	7.98	1004.9
1968	10	4051.6	9.93	408.0
1969	1	22064.4	152.89	144.3
1969	2	91893.7	31.32	2934.0
1969	3	50102	22.23	2253.8
1969	4	64666.2	17.56	3682.6
1969	5	79212	20.21	3919.4
1969	6	56819.9	31.85	1784.0
1969	7	16105.7	8.75	1840.7
1969	8	38296.4	24.23	1580.5
1969	9	8556.1	6.75	1267.6
1969	24	10306	28.83	357.5
1970	1	3785	7.42	510.1
1970	2	42734.6	14.14	3022.2
1970	3	59458.2	49.12	1210.5
1970	4	32011.3	27.04	1183.8
1970	5	39262.3	14.02	2800.4
1970	6	71803.9	15.79	4547.4
1970	7	50039.8	12.35	4051.8
1970	8	18045.8	13.38	1348.7
1970	9	3682.2	11.12	331.1
1970	10	2576.1	6.61	389.7
1971	1	42400.5	35	1211.4
1971	2	38629	10.46	3693.0
1971	3	62297.8	28.83	2160.9
1971	4	48421.1	19.51	2481.9
1971	5	26285.7	10.61	2477.4
1971	6	20246.1	11.89	1702.8
1971	7	47925.3	20.89	2294.2
1971	8	7004.3	7.03	996.3
1971	9	15855.8	12.3	1289.1
1971	10	12654.8	6.64	1905.8
1971	11	13123.1	10.73	1223.0
1971	12	887.7	6.94	127.9
1971	13	7818.4	10.09	774.9
1972	1	10630	23.82	446.3
1972	2	64954.2	33.73	1925.7

Year	Period	Catch	Scale Factor	Effective Sample Size
1972	3	77707.2	39.41	1971.8
1972	4	82433.5	35.97	2291.7
1972	5	81564	44.26	1842.8
1972	6	46640.4	67.54	690.6
1972	7	17416.5	17.03	1022.7
1972	8	13594.3	66.28	205.1
1972	9	22931.4	27.91	821.6
1972	10	17799.1	8.5	2094.0
1972	11	13984.4	17.12	816.8
1972	12	4360.4	9.98	436.9
1972	24	29769.7	32.08	928.0
1973	1	16173.9	8	2021.7
1973	2	81753	54.17	1509.2
1973	3	80269.2	18.72	4287.9
1973	4	72143.2	18.85	3827.2
1973	5	68896.4	17.68	3896.9
1973	6	87018.9	20.97	4149.7
1973	7	21606.5	5.39	4008.6
1973	8	16530.5	6.19	2670.5
1973	10	28587.3	19.33	1478.9
1973	12	3423.5	17.17	199.4
1974	1	190231.4	n/a	n/a
1974	2	105335.3	111.8	942.2
1974	3	59393.5	23.84	2491.3
1974	4	135935.7	50.33	2700.9
1974	5	89873.8	26.28	3419.9
1974	6	28862.8	12.13	2379.5
1974	7	21606.3	15.73	1373.6
1974	8	53015.2	30.77	1723.0
1974	9	39068.3	11.64	3356.4
1974	10	30102.8	11.1	2712.0
1974	11	2701	3.39	796.8
1974	23	43660.1	n/a	n/a
1974	24	48244.5	21.05	2291.9
1975	1	48933.7	14.21	3443.6
1975	2	107140.7	53.73	1994.1
1975	3	94083.7	43.93	2141.7
1975	4	66255.4	12.46	5317.4
1975	5	80574.4	13.85	5817.6
1975	6	22220.3	5.28	4208.4
1975	7	18995.7	6.79	2797.6
1975	8	52164.8	17.41	2996.3
1975	9	9865.9	10.02	984.6
1975	10	6905.7	5.07	1362.1

Year	Period	Catch	Scale Factor	Effective Sample Size
1975	23	189799.5	60.13	3156.5
1976	1	140522	33.06	4250.5
1976	2	93513.1	39.99	2338.4
1976	3	71541.5	32.68	2189.2
1976	4	90475.1	24.78	3651.1
1976	5	92784.5	15.69	5913.6
1976	6	120908.1	23.21	5209.3
1976	7	30034.6	7.62	3941.5
1976	8	10086.5	2.92	3454.3
1976	9	17016.2	8.82	1929.3
1976	10	8773.7	4.4	1994.0
1976	23	33384.4	21.84	1528.6
1976	24	226382	290.43	779.5
1977	1	248989	75.86	3282.2
1977	2	219755	63.93	3437.4
1977	3	137406.1	61.57	2231.7
1977	4	43826	49.74	881.1
1977	5	77668.3	33.44	2322.6
1977	6	64589.3	59.11	1092.7
1977	7	21936.7	19.48	1126.1
1977	8	62378.7	36.75	1697.4
1977	9	15170.1	17.21	881.5
1977	10	8207.1	23.51	349.1
1977	23	133841.8	113.83	1175.8
1978	1	102331	97.43	1050.3
1978	2	58363.2	41.26	1414.5
1978	3	94733	49.68	1906.9
1978	4	84485.4	39.15	2158.0
1978	5	49657.4	36.33	1366.8
1978	6	10907.9	8.26	1320.6
1978	7	11015.2	27.17	405.4
1978	9	2685.2	12.51	214.6
1978	24	109806.5	591.26	185.7
1979	1	55838.3	46.19	1208.9
1979	2	119911.8	84.54	1418.4
1979	3	135040.6	41.9	3222.9
1979	4	98281.7	18.23	5391.2
1979	5	30775.8	31.64	972.7
1979	6	18622.8	75.34	247.2
1979	8	37791.2	191.31	197.5
1979	10	25713.4	60.44	425.4
1979	22	80502.4	205.27	392.2
1979	24	161497.1	323.42	499.3
1980	1	162294	109.96	1475.9

Year	Period	Catch	Scale Factor	Effective Sample Size
1980	2	185941	128.64	1445.4
1980	3	159338.7	202.18	788.1
1980	4	61118.6	122.85	497.5
1980	5	88531.5	109.21	810.7
1980	7	73045.9	137.14	532.6
1980	8	39075.8	143.99	271.4
1980	9	33870.3	49.92	678.5
1980	10	30649.4	49.65	617.3
1980	11	6711.6	45.63	147.1
1980	22	640.8	n/a	n/a
1980	23	61533.3	n/a	n/a
1980	24	114055.8	n/a	n/a
1981	1	114037.8	159.78	713.7
1981	2	43124	392.04	110.0
1981	3	86564.9	87.04	994.5
1981	4	83599.2	58.44	1430.5
1981	5	47464.2	33.03	1437.0
1981	6	128252.7	53.22	2409.9
1981	7	69314.7	43.13	1607.1
1981	8	33990	18.07	1881.0
1981	9	23487.9	39.34	597.0
1981	10	8715.2	18.06	482.6
1981	11	2508.9	3.06	819.9
1981	12	2110.5	10.55	200.0
1981	23	17487.9	44.25	395.2
1981	24	140031.4	138.22	1013.1
1982	1	170500.4	74.54	2287.4
1982	2	204331.6	63.35	3225.4
1982	3	196890.2	80.58	2443.4
1982	4	64955.5	27.39	2371.5
1982	5	127111.8	85.45	1487.6
1982	6	78629.7	60.77	1293.9
1982	7	118154.4	89.86	1314.9
1982	8	53963.5	136.32	395.9
1982	9	3110.3	n/a	n/a
1982	11	3986.7	8.19	486.8
1982	13	5281.9	9.83	537.3
1982	22	3695.8	34.05	108.5
1982	23	112087.5	179.48	624.5
1982	24	369328.5	2894.34	127.6
1983	1	243447.8	514.52	473.2
1983	2	191300.9	70.53	2712.3
1983	3	166018.2	156.58	1060.3
1983	4	101179.6	41.22	2454.6

Year	Period	Catch	Scale Factor	Effective Sample Size
1983	5	32555.9	108.33	300.5
1983	6	15213.4	41.11	370.1
1983	11	4730.1	n/a	n/a
1983	13	4581.9	n/a	n/a
1983	24	285578.1	507.7	562.5
1984	1	101117.1	n/a	n/a
1984	2	183673	177.92	1032.3
1984	3	144167.5	730.52	197.3
1984	4	60020	52.25	1148.7
1984	5	6770.8	20.24	334.5
1984	6	1360.7	85.24	16.0
1984	7	166.2	n/a	n/a
1984	8	4516.9	n/a	n/a
1984	9	4093.4	n/a	n/a
1984	10	27513	n/a	n/a
1984	11	11267.6	n/a	n/a
1984	12	1550.1	n/a	n/a
1984	23	37754.7	58.69	643.3
1984	24	153186.9	24.6	6227.1
1985	1	155835.2	23.22	6711.2
1985	2	102531.5	18.34	5590.6
1985	3	76452	18.27	4184.6
1985	4	24594.7	15.94	1543.0
1985	5	28859.1	9.28	3109.8
1985	6	46413.7	14.3	3245.7
1985	7	33903.2	20.07	1689.2
1985	8	27536	28.24	975.1
1985	9	29165.3	17.07	1708.6
1985	10	8798.4	n/a	n/a
1985	11	2199	n/a	n/a
1985	23	57567.2	17.88	3219.6
1985	24	70811.9	15.09	4692.6
1986	1	146647.5	26.97	5437.4
1986	2	123718.1	28.78	4298.8
1986	3	123578.9	28.49	4337.6
1986	4	83000.1	28.89	2873.0
1986	5	96871.7	27.61	3508.6
1986	6	92355.6	24.01	3846.5
1986	7	51194.8	28.16	1818.0
1986	8	31243.8	50.73	615.9
1986	9	6663.4	39.22	169.9
1986	10	942	n/a	n/a
1986	11	2216.3	n/a	n/a
1986	12	242.6	n/a	n/a

Year	Period	Catch	Scale Factor	Effective Sample Size
1986	23	1605.2	4.6	349.0
1986	24	63505.4	16.57	3832.6
1987	1	73247.7	25.53	2869.1
1987	2	99417.9	23.13	4298.2
1987	3	164043.9	28.69	5717.8
1987	4	94007.5	27.92	3367.0
1987	5	61121.9	22.25	2747.1
1987	6	44380.4	26.04	1704.3
1987	7	33797.5	19.77	1709.5
1987	8	4302	n/a	n/a
1987	9	1038	n/a	n/a
1987	10	118.9	n/a	n/a
1987	11	49	n/a	n/a
1987	12	29.7	n/a	n/a
1987	23	7543.7	11.75	642.0
1987	24	21005.7	29.46	713.0
1988	1	68502.1	23.28	2942.5
1988	2	191509.7	30.13	6356.1
1988	3	109463.4	32.93	3324.1
1988	4	69194.5	27.86	2483.7
1988	5	60131.5	32.99	1822.7
1988	6	179547.5	40.13	4474.1
1988	7	41463.4	54.64	758.8
1988	8	92070.4	78.34	1175.3
1988	9	17812.5	n/a	n/a
1988	10	13102.9	n/a	n/a
1988	11	167.1	n/a	n/a
1988	23	9	n/a	n/a
1988	24	21653.6	34.14	634.3
1989	1	92509.3	37.23	2484.8
1989	2	78710.6	20.12	3912.1
1989	3	65978.1	28.59	2307.7
1989	4	75930.1	44.46	1707.8
1989	5	37010.4	19.87	1862.6
1989	6	36536.8	42.1	867.9
1989	7	1404	n/a	n/a
1989	8	1919.1	n/a	n/a
1989	9	1144.5	n/a	n/a
1989	23	9435.2	n/a	n/a
1989	24	13893.6	16.29	852.9

Appendix 4:
A flexible maximum likelihood approach for fitting growth curves to tag-recapture data

Geoff M. Laslett, J. Paige Eveson and Tom Polacheck

FRDC Project 1999/104

Introduction

Understanding how fish grow is a fundamental component of fish biology, and quantitative information on growth is critical to the stock assessment process. However, it is not only mean growth that is important to characterise, but also the variability among individuals. One of the primary sources of information used for estimating the growth rates of fish comes from tagging studies. In these studies, the length of a fish is measured and recorded when the fish is released and recaptured. The times of release and recapture are also recorded so that the time at liberty is known. The estimation of growth rates from these data presents a difficult challenge for several reasons: there are only two measurements per fish, the age at first release is not precisely known, and fish vary in their growth from individual to individual.

Despite these obvious difficulties, several efficient methods of estimating growth curves from tag-recapture data have been developed (e.g., Fabens 1965; Francis 1988; Palmer et al. 1991). The estimation process involves both determining an appropriate parametric form for the growth curve and a reliable statistical procedure for fitting the data to the growth curve. The determination of the appropriate curve is often an iterative process using standard statistical model selection criteria. Non-parametric estimation of growth from tag-recapture data is generally not feasible because of the paucity and structure of the data. In any case, parametric models can provide insights into the underlying functional processes and allow for direct comparison of growth curves across time and space or between different populations or species. Moreover, differences among individuals can be captured by modelling some of the growth parameters as random variables.

A wide variety of parametric models has been used to model fish growth, with the von Bertalanffy (VB) growth model being the most ubiquitous. However, the generalized von Bertalanffy, the Richards, the Gompertz and the logistic models have all been advocated (see Schnute 1981). In fact, any cumulative statistical distribution scaled by an asymptotic length could be used, although the growth curve preferably should have a biological motivation. Almost all modelling of fish growth

has been based on modelling the growth rate as a continuous, smooth, monotonically decreasing function of age. However, recent analyses of growth in southern bluefin tuna (SBT) suggest that there is a marked change in the growth process somewhere during the transition from the juvenile to sub-adult part of the life cycle (Anon. 1994; Hearn and Polacheck 2002). Hearn and Polacheck (2002) suggest this might also be a feature in other tuna species. In the SBT case, growth has been modelled as a two stage process in which growth in each stage follows a different VB curve, with a discontinuity in the growth rates at the transition point between the two. However, Hearn and Polacheck (2002) identify problems both with the biological interpretation of this model and in statistically fitting it. Thus there is a need, at least in the case of SBT, for alternative growth models that can adequately represent the complex pattern of growth.

A large scientific literature exists on the statistical estimation of growth curves from tag-recapture data. The most widely used approach in fisheries' research has been the one developed by Fabens (1965). However, this approach does not take into account variability among individuals in their growth curves, cannot be applied to the full range of potential growth models, and is not asymptotically consistent (Maller and de Boer 1988). Extensions to the Fabens approach that can accommodate individual variability in growth within a VB model framework have been developed by Sainsbury (1980) and Hampton (1991), but these methods still bear some limitations of a Fabens-type approach. James (1991) and Wang (1998) have developed fitting procedures based on estimating equations as a statistically rigorous alternative to Fabens' method, but again there are problems in applying the estimating equations approach to more complicated growth models. As such, there remains a need for a flexible estimation method that can be adopted to a wide range of alternative growth models, that can accommodate individual variability in the growth parameters, and that can provide a statistical basis for selecting the most appropriate and parsimonious model.

In the current paper, we develop an alternative maximum likelihood approach

for estimating growth curves from tag-recapture data which is based on estimating the joint density of tag and recapture lengths rather than modelling growth increments. The method allows for individual variability in growth by having selected parameters considered as random effects. Standard statistical tests based on likelihood theory and Akaike's information criteria (Akaike 1974) may be used to compare and select among alternative models. Although Wang et al. (1995) have proposed a similar approach, ours requires less restrictive assumptions and can easily be applied to a wide range of growth curves. Furthermore, we have developed a new growth curve that can accommodate a marked change in the growth pattern at some point in the life cycle. We apply our estimation method along with the proposed new growth curve to tag-recapture data for SBT.

Methods

The joint density of tag and recapture lengths for a general growth model

In this section, we derive the joint density of tag and recapture lengths for a single fish. This is formulated in terms of a general model for fish growth in which the asymptotic length varies from fish to fish. Other parameters are fixed. The joint density is needed for maximum likelihood fitting of the growth model and inference about its relative fit.

In tag-recapture studies, a fish is tagged at time t_1 with length l_1 and is recaptured at time t_2 with length l_2. We know that fish growth during the very early stages of life (e.g., during the egg and larval stages) follows a different process from subsequent growth. However, we do not have data with which to model this initial growth. We define t_0 to be the time at which a fish would have had length 0 if we were to project its post-larval growth trajectory backwards. We acknowledge that t_0 is a theoretical value with no real biological interpretation.

Let $A = t_1 - t_0$, then A varies from fish to fish, partly because the fish are spawned at different times (which results in t_0 varying between fish), and partly because there may be several tagging expeditions (so that t_1 varies). For convenience, we will refer to A simply as the age at tagging, keeping in mind that it is age relative to t_0, not relative to birth.

We assume that a generic growth function $f(t)$ is available, where $f(t)$ is a monotone increasing function of time, t. It approaches 1 as $t \to \infty$, and is 0 when t is t_0. The growth of each fish follows the form of $f(t)$, although with individual variations.

The assumed growth curve for the fish is

$$l(t) \;=\; L_\infty \, f(t; A, \theta)\,, \tag{1}$$

where L_∞ (the asymptotic length) is random from fish to fish with mean μ_∞ and variance σ^2_∞, A is random from fish to fish with density $p(.)$, θ is a vector of fixed unknown parameters, and t is real time. For example, for the von Bertalanffy model,

$$f(t; A, \theta) \;=\; \begin{cases} 1 - \exp(-k(A + t - t_1)) & \text{if } t > t_1 - A; \\ 0 & \text{otherwise,} \end{cases}$$

so $\theta = \{k\}$ has only one component. Let $\delta t = t_2 - t_1$ be the time increment between tagging and recapture. To analyse tag-recapture data, we need the familiar equations

$$\begin{aligned} f(t_1; A, \{k\}) &= 1 - \exp(-kA) \\ f(t_2; A, \{k\}) &= 1 - \exp(-k(A + \delta t))\,. \end{aligned}$$

James (1991), Palmer et al.(1991) and Wang et al. (1995) have all discussed the estimation of von Bertalanffy parameters from tag-recapture data using this style of model. Our aim is to show that parameter estimation is still feasible for more complex and realistic growth models $f(.)$ in (1).

In this article we assume that L_∞ and A are both random variables. Models in which either L_∞ or A are the same unknown constants for all fish are implausible, and models for which L_∞ and A are different constants are over-parameterised, so ours is the simplest realistic assumption. We denote random variables by capital letters. We follow James (1991), Palmer et al. (1991) and Wang et al. (1995) in assuming that L_∞ and A are independent. We have no evidence to the contrary.

We assume for convenience that L_∞ has a normal distribution. Intuitively this seems reasonable, and we have no data to refute it. We also assume that measurements are taken at times t_1 and t_2 (with $t_1 < t_2$), so that

$$l_1 = l(t_1) + \epsilon_1 \tag{2}$$

$$l_2 = l(t_2) + \epsilon_2 \tag{3}$$

where ϵ_1 and ϵ_2 represent measurement error. They are also normally distributed with mean 0 and variance σ^2, and independent from fish to fish. We assume also that ϵ_1 and ϵ_2 are independent of L_∞ and A.

We are now in a position to derive the joint distribution of l_1 and l_2. For the moment, we argue conditional upon a known value of A, say $A = a$. Then l_1 and l_2 are both the sum of normal random variables, and hence are themselves normal. Their first and second moments are

$$\mu_1(a) = \mathrm{E}(l_1|a) = \mu_\infty f_1$$

$$\mu_2(a) = \mathrm{E}(l_2|a) = \mu_\infty f_2$$

$$\begin{aligned}
\sigma_1^2(a) &= \mathrm{Var}(l_1|a) = \sigma_\infty^2 f_1^2 + \sigma^2 \\
\sigma_2^2(a) &= \mathrm{Var}(l_2|a) = \sigma_\infty^2 f_2^2 + \sigma^2 \\
\mathrm{Cov}(l_1, l_2|a) &= \sigma_\infty^2 f_1 f_2 \\
\rho(a) &= \mathrm{Corr}(l_1, l_2|a) = \frac{\sigma_\infty^2 f_1 f_2}{\sigma_1(a)\,\sigma_2(a)} .
\end{aligned}$$

where $f_1 = f(t_1; a, \theta)$ and $f_2 = f(t_2; a, \theta)$. Clearly, l_1 and l_2 are joint normal with conditional density

$$h(l_1, l_2|a) = \frac{1}{2\pi\sigma_1(a)\sigma_2(a)\sqrt{1-\rho(a)^2}} \exp\left\{-\frac{q_{12}(a)}{2(1-\rho(a)^2)}\right\} \qquad (4)$$

where

$$q_{12}(a) = \frac{(l_1-\mu_1(a))^2}{\sigma_1(a)^2} - 2\rho(a)\frac{(l_1-\mu_1(a))(l_2-\mu_2(a))}{\sigma_1(a)\sigma_2(a)} + \frac{(l_2-\mu_2(a))^2}{\sigma_2(a)^2} .$$

If A is random, the unconditional joint density of l_1, l_2 is

$$h(l_1, l_2) = \int_0^\infty h(l_1, l_2|a)\, p(a)\, da . \qquad (5)$$

There are several points to note. First, the joint density (5) involves a single integral, whereas Wang et al. (1995) have a double integral. Second, $l_2 < l_1$ is allowed, whereas Wang et al. (1995) do not allow it. Third, a more complex model for the measurement error may be desirable, and can easily be incorporated. For example, in the case of SBT, recapture lengths are measured by fishermen and scientists, but tag lengths are measured by scientists only. The fishermen are believed

to be less precise. Hence it may be desirable to structure the measurement errors so that $\mathrm{Var}(\epsilon_2) > \mathrm{Var}(\epsilon_1)$ when l_2 is measured by fishermen. Fourth, correlation between ϵ_1 and ϵ_2 may also be allowed for very easily, although it is likely to be poorly identified. Finally, conditioning on non-linear components to simplify the analysis of partially non-linear models has a long history in statistics. A seminal paper is Halperin (1963).

The joint density for zero measurement error

It is useful to have a special formula for $h(l_1, l_2)$ when $\sigma^2 = 0$, since it is not immediately clear what (5) reduces to. We first look at the von Bertalanffy model. It is possible then to calculate exactly what A must be if l_1, l_2 and k are known: it is

$$a^* = -\frac{1}{k}\log\left(\frac{l_2 - l_1}{l_2 - dl_1}\right) \tag{6}$$

where $d = \exp(-k(t_2 - t_1))$. Arguing from first principles, we obtain

$$h_0(l_1, l_2) = \frac{1}{\sigma_\infty f_2^*}\,\phi\left(\frac{l_2/f_2^* - \mu_\infty}{\sigma_\infty}\right) p(a^*)\,\frac{1}{k}\left\{\frac{1}{l_2 - l_1} - \frac{d}{l_2 - dl_1}\right\} \tag{7}$$

where $f_2^* = f(t_2; a^*, \theta)$ and $\phi(.)$ is the standard normal density. If $l_2 \leq l_1$, then $h_0(l_1, l_2)$ is set to 0.

For general log-concave growth curves, the formula is

$$h_0(l_1, l_2) = \frac{1}{\sigma_\infty f_2^*}\,\phi\left(\frac{l_2/f_2^* - \mu_\infty}{\sigma_\infty}\right) p(a^*)\,\frac{\partial a^*}{\partial l_1} \tag{8}$$

suggesting that an explicit formula for a^* in terms of l_1 and l_2 is needed for each model. However, it is easy to prove that

$$\frac{1}{f_2^*}\frac{\partial a^*}{\partial l_1} = \left(l_2 \frac{\partial f_1^*}{\partial a^*} - l_1 \frac{\partial f_2^*}{\partial a^*}\right)^{-1}$$

so we really only need to differentiate $f(t; a, \theta)$ with respect to a and evaluate it at (t_1, a^*) and (t_2, a^*). Note that a^* is the solution to $f_1/l_1 = f_2/l_2$, which may need to be solved numerically. A growth curve $f(t)$ is log-concave if $\log f(t)$ is concave: that is, any straight line joining two points on the curve $\log f(t)$ lies on or beneath the curve. Many of the commonly used simple growth curves are log-concave. For several examples, we confirmed numerically that $h(l_1, l_2)$ converges to $h_0(l_1, l_2)$ as $\sigma^2 \to 0$.

Numerical computation of the integral

Computation of the integral in (5) is not straightforward. When maximising a likelihood, the integral needs to be computed separately for each fish at each step of the likelihood maximisation. If there are 1000 fish in the study, and the likelihood optimisation routine takes 500 steps to find the optimal parameters, the integral will need to be computed 500 000 times. For large-scale applications, a fast and accurate quadrature method is required. We used Gauss-Hermite integration, after using a robust search method to locate the approximate maximum of the integrand. For details, refer to the Appendix.

A new growth curve: the von Bertalanffy with logistic growth rate parameter

Extensive tagging studies of southern bluefin tuna were undertaken during the 1960s and 1980s. This large data base has enabled researchers to examine the

adequacy of the von Bertalanffy growth curve, which has traditionally been the standard for this species. As noted in the introduction, recent analyses suggest that a more complex model which incorporates a two stage growth process is required (Hearn and Polacheck 2002).

Wang (1998) has proposed the following generalization of the von Bertalanffy growth curve. Suppose a fish has length 0 at time t_0. Then the growth rate at time t is given by

$$l'(t) = (L_\infty - l(t))\, k(t)\,,$$

where $k(t)$, the function that controls the growth rate, may depend on time. The solution is

$$l(t) = L_\infty[1 - \exp(-K(t_0, t))]$$

where $K(t_0, t) = \int_{t_0}^{t} k(u)\, du$. Hearn and Polacheck (2002) argue that for SBT $k(t)$ should be a constant value, k_1 say, for juvenile tuna and a lower value, k_2, for adult tuna. Thus $k(t)$ is a step function

$$k(t) = \begin{cases} k_1 & \text{for } t < t_0 + \alpha; \\ k_2 & \text{otherwise.} \end{cases} \tag{9}$$

In this model, α is the age at which juveniles become adults — it is denoted by t^* in Hearn and Polacheck (2002). The Hearn and Polacheck model is slightly more general than this, but the extra generality is only mildly supported by the data.

The step-function (9) seems harsh from a biological viewpoint. We would at least like to allow for the possibility of a slower transition between juvenile and adult

growth. In addition, the step function may cause problems for statistical analysis. For example, the likelihood in Hearn and Polacheck's (2002) analysis has two modes, which might be caused by the step function.

We propose instead modelling $k(t)$ by a logistic curve:

$$k(t) = k_1 + (k_2 - k_1)\frac{1}{1+\exp(-\beta(t-t_0-\alpha))}. \tag{10}$$

For $t \ll t_0 + \alpha$, $k(t) \approx k_1$, and for $t \gg t_0 + \alpha$, $k(t) \approx k_2$. As t increases, $k(t)$ makes a smooth transition from k_1 to k_2. The rate of transition is governed by β, being sharper for larger β. As $\beta \to \infty$, (10) reduces to the step function given in (9). An advantage of the logistic form is that it can be explicitly integrated, yielding the growth curve

$$l(t) = L_\infty \left[1 - e^{-k_2(t-t_0)} \left\{\frac{1+e^{-\beta(t-t_0-\alpha)}}{1+e^{\beta\,\alpha}}\right\}^{-(k_2-k_1)/\beta}\right]$$

if $t \geq t_0$. Of course, $l(t) = 0$ if $t < t_0$. In the notation of equation (1), $\theta = \{k_1, k_2, \alpha, \beta\}$ has four components, in contrast to the ordinary von Bertalanffy curve which has one. We propose calling this the von Bertalanffy growth curve with logistic growth rate, and abbreviating it as the 'VB $\log k$' model. The traditional von Bertalanffy curve is recouped if $k_1 = k_2 = k$. Note that the VB $\log k$ model is not a member of the Schnute (1981) class.

The 'VB $\log k$' model could be further generalized to three or more phases in growth, reflecting different growth conditions for multiple life-stages. It is also possible to generalize the von Bertalanffy by using a logistic rate $k(t)$ on the length scale: $l(t) = L_\infty\,(1-e^{-k(t)(t-t_0)})$. However, this model does not have a simple growth rate interpretation, so we leave it for future investigation.

Estimation

Wang et al. (1995) suggest that a gamma distribution be used for $p(.)$, the distribution of A, although we shall prefer the lognormal. In fact, an advantage of our approach is that any well-behaved parametric model for A can be adopted. Once the models for A and for growth $f(t)$ have been decided upon, the unknown parameters can be estimated by maximising the log-likelihood

$$\sum_{i=1}^{n} \log h(l_{1i}, l_{2i}) ,$$

where n is the number of fish, and (l_{1i}, l_{2i}) are the two measurements for fish i. A numerical optimisation algorithm with bound constraints is needed to fit the model.

After successfully maximising the log-likelihood, the user may wish to estimate the realised values of A and L_∞ for each fish. One way to do this is to calculate the estimated posterior distribution using Bayes' Theorem.

Thus, for a given fish, we can calculate

$$p(A = a|l_1, l_2) \quad = \quad \frac{h(l_1, l_2|a)\, p(a)}{h(l_1, l_2)}$$

by plugging in the maximum likelihood estimates of the unknown parameters. This distribution gives the plausible range of values of A compatible with the data l_1 and l_2. Of course, calculating this conditional distribution might be practical if there are only a few fish, but often there are hundreds. The user really requires a single summary statistic for each fish. The mean would probably be chosen, although other summary statistics, such as the median, mode, trimmed mean and so on, could be used if desired. The mean requires a one-dimensional integration. It is worth noting that the mode of A given l_1 and l_2 is already determined for each fish if the method

outlined in the Appendix for calculating the likelihood is followed. Typically, we find little difference between the mean and the mode.

Similarly, we can calculate $q(L_\infty|l_1, l_2)$, the density of the the asymptotic length given the data. In practice, we would probably use the mean of $q(L_\infty|l_1, l_2)$ as a point estimate of the asymptotic length for a particular fish. The direct approach yields a double integral, but this can be avoided by exploiting the joint normality of L_∞, l_1 and l_2 when a is known. The formula is

$$\mathrm{E}(L_\infty|l_1, l_2) = \frac{\int_0^\infty \mathrm{E}(L_\infty|l_1, l_2, a)\, h(l_1, l_2|a)\, p(a)\, da}{h(l_1, l_2)} \tag{11}$$

where

$$\mathrm{E}(L_\infty|l_1, l_2, a) = \mu_\infty + \frac{\sigma_\infty^2}{\sigma^2 + \sigma_\infty^2(f_1^2 + f_2^2)}(f_1(l_1 - \mu_\infty f_1) + f_2(l_2 - \mu_\infty f_2)) \tag{12}$$

Thus, the conditional means $\mathrm{E}(L_\infty|l_1, l_2)$ can be calculated by substituting (12) into (11) and using one-dimensional integration. It is reassuring to note that this yields the correct result when $\sigma^2 = 0$, in which case $l_1 = L_\infty f_1$ and $l_2 = L_\infty f_2$, and it is readily checked that $\mathrm{E}(L_\infty|l_1, l_2, a) = L_\infty$. Of course, the bivariate conditional distribution $p(A, L_\infty|l_1, l_2)$ could also be calculated, although there seems little point.

Results

Simulated data

In order to test our proposed model fitting procedure and its generality, we carried out a number of simulations. We generated growth data according to various models, looking at the effect of different growth curves, different distributions on the age at tagging, and different amounts of measurement error.

Initially we considered the traditional von Bertalanffy (VB) curve. In all model runs, L_∞ was taken to be normally distributed with mean 100 and standard deviation 5, and k was taken to be 0.5, such that 95% of the average maximum length was achieved by age six. The times at liberty were generated according to a $\Gamma(1,1)$ distribution, which was chosen to be representative of tagging studies in which the majority of recaptures occur quickly and subsequently decrease (in this case, 63% within the first year and 95% within three years).

At first, ages at tagging, A, were generated according to a lognormal distribution with mean and standard deviation on the log scale of 0.5 and 0.5 respectively (which we will denote by $A \sim \text{LogN}(0.5, 0.5)$). This gives a positively skewed distribution with a mode around 1.5 years of age. The effect of varying the amount of measurement error was investigated by setting σ equal to 0, 2, and 4 in different simulations. For each situation, a total of 100 simulations using a sample size of 100 recaptures per simulation were carried out.

We now summarize the results from the above simulations. The parameter estimates obtained using the new estimation method were all unbiased, except for a slight underestimation of the variability in L_∞ as the measurement error increased (Table 1, rows 1 to 4). Otherwise, the effect of increasing the measurement error was only to increase the standard deviation of the parameter estimates. Note that in the case of zero measurement error we ran simulations using both the likelihood based on the joint density developed for measurement error (equation (5)) and the likelihood based on the joint density for no measurement error (equation (8)). The two methods gave comparable estimates (Table 1, rows 1 and 2).

With such a small sample size and relatively short times at liberty, there is not much information on older fish with which to discern the distribution of L_∞. Hence, it is not too surprising that the variability in L_∞ is slightly biased; perhaps more surprising is that the mean value is estimated correctly. Increasing the sample size from 100 to 500 or, alternatively, changing the distribution on the times at liberty to be uniform on [1,7] eliminated the slight bias in the standard deviation of

L_∞ when σ was equal to 4.

For many studies, the ages at tagging may not follow a simple distributional form. For example, in the case of SBT, fish spawn from October to April, and tagging is performed most commonly during January. This results in a multi-modal distribution for the release ages. Thus, it is important that our estimation method works for a variety of distributions for A. We generated values for A that we believe are representative of the real ages at tagging for SBT using the following steps. Firstly, from the true tagging data for SBT, we took a random sample of 100 fish and retained their release date and integer age (an integer age had been assigned to each fish based on its release length, and this age is likely to be accurate for young fish). Next, we generated a 'birth date' for each fish from a normal distribution with a mean of zero (representative of January 1) and a standard deviation of 1.5 months (so that roughly 95% of the birth dates fell between October 1 and April 1). Lastly, we calculated a release age for each fish by taking its integer age (in years) and adding the difference between its release date and birth date (expressed in decimal years).

The distribution of release ages generated in the above manner has distinct modes at ages 1 and 2, and is clearly not lognormal (Figure 1). A Gaussian mixture model appears to be an appropriate choice. Thus, we applied our estimation method to simulated data that included such ages at tagging assuming that they follow a two-component Gaussian mixture distribution with means u and v, a common standard deviation σ_c, and a proportion p belonging to the first component. We again generated times at liberty according to a $\Gamma(1,1)$ distribution, and tag and recapture lengths according to a VB curve with $k = 0.5$ and L_∞ random normal with mean 100 and standard deviation 5. The standard deviation of the measurement error was taken to be 2. The mean parameter estimates for L_∞, k and σ were unbiased (Table 1, second last row), which shows that the method works even for fairly complex distributions for A.

To investigate the robustness of our method to the distribution assumed for

A, we reran the above simulations assuming a lognormal distribution for A. Again, the growth parameter estimates were unbiased (Table 1, last row). In this case, the lognormal distribution gave a fair approximation to the true distribution of A, as shown in Figure 1 where the fitted lognormal curve is overlaid on the histogram of release ages. In most situations, the researcher will have some information about the release ages, and the method appears to be quite robust provided a reasonable distribution for A is chosen. For example, in the above simulations, we could have chosen the gamma distribution instead of the lognormal and achieved equally good results.

One of the advantages of our estimation method is its ability to generalize to a wide range of growth curves. To illustrate this, we ran simulations on growth data generated from a logistic curve, a generalized von Bertalanffy (GVB) curve, as well as a von Bertalanffy curve with a logistic growth rate (VB $\log k$, as described in the Methods section). The logistic curve can be expressed as

$$l(t) = L_\infty \left(2(1+\exp(-k(t-t_0)))^{-1} - 1\right), \tag{13}$$

parameterized such that $l(t) = 0$ when $t = t_0$ and $l(t)$ approaches L_∞ as $t \to \infty$. The equation for a GVB curve is

$$l(t) = L_\infty \left(1-\exp(-k(t-t_0))\right)^r, \tag{14}$$

for $r > 0$. Note that the logistic and GVB curves are both special cases of the Richards growth curve. In our simulations for all models, we took L_∞ to be normally distributed with mean 100 and standard deviation 5, A to be LogN(0.5, 0.5), the times at liberty to be Γ(1,1), and σ to be 2.

For the logistic curve we set k equal to 0.5, and for the GVB curve we set k equal to 0.5 and r equal to 2. These two curves have a slower rate of growth than

the VB curve, and the GVB curve has an inflection point at age $\log(2)/0.5 \approx 1.4$ (Figure 2(a)). For the logistic and GVB models, we ran 100 simulations with 100 recaptures per simulation. For both models, all parameter estimates were accurate with the exception of σ_∞, which shows a small negative bias and larger variability (Table 2). As with our simulations for the VB model, this is not surprising since we are generating data that has very little information on older fish. We illustrate a typical simulated data set for the logistic model along with the true curve (Figure 2(b)). The asymptotic length is not reached until approximately age ten but there is little data exceeding age six. Still, μ_∞ is estimated very accurately, and with more extensive data coverage, σ_∞ would be estimated with greater accuracy and precision as well.

For the VB $\log k$ model, we set k_1 equal to 0.8, k_2 to 0.3, α to 1.5, and β to 4, giving a fairly rapid reduction in growth rate from about age 0.5 to age 2.5 (Figure 3). In order to avoid identifiability problems, we did not optimize over β since β appears to be highly correlated with k_1 and k_2. Furthermore, we increased the sample size to 500 recaptures in each of the 100 model runs since the data are otherwise insufficient to discriminate between likelihoods for many sets of parameter values. Even for this more complex growth model, the parameter estimates were accurate and unbiased (Table 3, row 1).

The necessity to fix β can be relaxed if the data are more comprehensive such that there is sufficient information before and after the transitional stage in the growth rate; however care must still be used. We increased α to 2.5 so there was more data before the transition and also changed the times at liberty to be uniform over the interval [1,7], then ran simulations in which β was allowed to vary. In several data sets, either β, k_1 or k_2 converged to one of its set bounds. Nevertheless, for the 82 of the 100 model runs in which this did not occur, the mean estimates for the parameters were good (Table 3, row 2). Note that the coefficient of variation in β is much larger than in any of the other parameters.

SBT tag-recapture data

To illustrate the method on real data, we used tag-recapture data from SBT that were released in the 1980s. A total of 1412 recaptures were included in the analysis. The times at liberty ranged from 270 days (an imposed minimum to remove the effects of seasonal growth) to 4356 days (12 years), with 95% of the returns occurring in the first three years.

We began by using our method to fit the standard von Bertalanffy growth curve. We assumed that the ages at tagging followed a lognormal distribution, since our simulations in the previous section using release ages generated from the SBT tagging data indicated this was a reasonable assumption. Furthermore, we assumed the measurement errors in release and recapture lengths, ϵ_1 and ϵ_2, were normally distributed with mean 0 and common variance, σ^2. We proceeded to make the model more complex by fitting the VB $\log k$ growth curve, leaving all other assumptions the same. Finally, we fit both the VB and the VB $\log k$ growth curves incorporating a more complicated error structure in which the error variance in recapture lengths differed according to the measurer, scientific staff or fishermen. Scientists measured all release lengths so there was no need to make this distinction for ϵ_1. In particular,

$$\begin{aligned} \mathrm{Var}(\epsilon_1) &= \sigma^2 \\ \mathrm{Var}(\epsilon_2) &= \begin{cases} \sigma^2 & \text{if measured by a scientist} \\ \sigma^2 + \sigma_f^2 & \text{if measured by a fisherman} \end{cases} \end{aligned}$$

For a given growth curve (either the VB or VB $\log k$), the estimates of the growth parameters were very similar regardless of the error structure assumed (Table 4). However, the fits were significantly better when the measurer-dependent error structure was included, as indicated by the smaller Akaike information criteria (AIC) values (Table 4). This suggests that the more complex error structure is a worthwhile addition as it explains a significant amount of the residual variation.

Both of the VB log k models gave a significantly improved fit compared to the VB model with an equivalent error structure. Again this is indicated by the smaller AIC values. The mean fitted curves for the VB and VB log k models with measurer-dependent error variance are very similar up until an age of about seven, at which point the VB log k curve becomes progressively higher than the VB curve (Figure 4). To further compare and evaluate these models, we calculated residuals for the fitted recapture lengths (Figure 5). To calculate these fitted values requires a realised value of A and L_∞ for each fish, which we estimated using the procedures described in the Methods section (under Estimation). Briefly, for each fish we calculated the mean of the posterior distribution for A and for L_∞ given the fish's release length and recapture length. Two features of the residual plots are worth noting. First, the improved fit of the VB log k model over the VB model is apparent in the residuals for large fish. We see that the mean asymptotic length is being underestimated in the VB model. Secondly, the reason for incorporating a measurer-dependent error structure seems clear since the residuals are markedly smaller for lengths measured by scientists than for those measured by fishermen.

Approximate errors for the parameter estimates can be obtained by inverting the observed information matrix $\{\partial^2 l/\partial p_i \partial p_j\}$, where l is the maximum log-likelihood and p is the vector of parameters. Parameters on the boundary of the parameter space must be regarded as fixed. We used this method for the VB log k model with simple error structure (Table 4, row 3). The estimates 0.220 of k_1 and 0.163 of k_2 have standard errors of 0.011 and 0.013 respectively, with correlation 0.918. Thus the estimate of $k_1 - k_2$ is 0.057 with standard error 0.017, confirming that k_1 and k_2 are significantly different, and that a simple VB model is inadequate. Similarly, for the VB log k model with measurer-dependent error variance (Table 4, row 4), the estimate of $k_1 - k_2$ is 0.053 with standard error 0.019, leading to the same conclusion.

For the VB log k models, β, the parameter that governs the rate at which the growth rate changes in the VB log k model, was optimised at a set upper bound of

30. This means an almost instantaneous switch in growth rate from k_1 to k_2 at age α. However, in the previous section we saw that the estimate of β can be high even if the true value of β is low when the data coverage is inadequate. To check this, we ran a number of simulations of 1400 fish with parameters close to those for the fitted VB $\log k$ model with simple error structure (Table 4, row 3), but with $\beta = 3$. The times at liberty were sampled from the observed times. We found that β was estimated correctly more than half the time, but converged to 30 (the upper bound) in the remaining runs. The other parameters were all estimated with minimal bias and good precision regardless of the estimate of β. Hence we cannot be certain of the rate of transition between the phases, but we expect the other parameter estimates to be unaffected.

Discussion

The results from this paper show that the maximum likelihood method we propose for fitting growth models to tag-recapture data is a viable alternative to the methods already in existence. By modelling the joint density of l_1 and l_2, we avoid the inconsistency problems that result from applying Fabens' method. However, in return, we must model the distribution of A.

Wang (1998) has recommended fitting growth models using first-order estimating equations. This appears attractive because it also is statistically rigorous, yet it avoids the need to model A. We therefore consider this method more closely for our own situation. James (1991) has described the method for the von Bertalanffy model, but it may be extended to other more realistic models following the principles outlined by Wang (1998). For the VB $\log k$ model, let

$$S(t_1, t_2) = k_2(t_2 - t_1) + \frac{k_2 - k_1}{\beta}[\log(1 + e^{-\beta(t_2 - t_1 - \alpha)}) - \log(1 + e^{\alpha\beta})].$$

and

$$\eta(t_1, t_2, l_1, l_2) \;=\; l_2 - l_1 - (\mu_\infty - l_1)(1 - e^{-S(t_1,t_2)})\,.$$

For fish i, let $S_i = S(t_{1i}, t_{2i})$ and $\eta_i = \eta(t_{1i}, t_{2i}, l_{1i}, l_{2i})$. The five unknown parameters $\{\mu_\infty, k_1, k_2, \alpha, \beta\}$ may be estimated by solving the five non-linear equations

$$\sum_{i=1}^{n} \eta_i = 0; \quad \sum_{i=1}^{n} \frac{\partial S_i}{\partial k_1}\,\eta_i = 0; \quad \sum_{i=1}^{n} \frac{\partial S_i}{\partial k_2}\,\eta_i = 0; \quad \sum_{i=1}^{n} \frac{\partial S_i}{\partial \alpha}\,\eta_i = 0; \quad \sum_{i=1}^{n} \frac{\partial S_i}{\partial \beta}\,\eta_i = 0\,.$$

We attempted to solve these equations for the 1980s tagging data using commercial routines, with starting values near the maximum likelihood estimates for the VB $\log k$ model with simple error structure. We obtained $\hat{\mu}_\infty = 164.5$, $\hat{k}_1 = 0.265$, $\hat{k}_2 = 0.263$, $\hat{\alpha} = -0.606$ and $\hat{\beta} = 12.5$. These are suspiciously close to a simple VB solution. Suppose that $\tilde{k}$ and $\tilde{\mu}_\infty$ are the solutions of the simple VB estimating equations. It is then easy to show that setting $k_1 = k_2 = \tilde{k}$, $\alpha = 0$, $\beta \to \infty$ and $\mu_\infty = \tilde{\mu}_\infty$ will solve the VB $\log k$ estimating equations — in fact, α and β merely need to satisfy $\sum_{i=1}^{n} \zeta_i \eta_i = 0$, where $\zeta_i = \log(1+e^{-\beta(t_{2i}-t_{1i}-\alpha)})$, so other combinations of α and β may suffice. Hence a simple VB model always provides one solution. It is possible that the equations have other solution classes, but the existence of a simple VB solution is already an unsatisfactory feature.

There are other problems with these estimating equations: they do not yield estimates of σ_∞ and the residual variance parameters, and there is no way of estimating and testing for structure in the residual variation. These problems might be solved by moving to second-order estimating equations. However, we recommend staying with maximum likelihood, at least until the estimating equations approach is better understood.

Although the literature on fitting growth models to tag-recapture data is vast, most methods in existence bear some limitation. Either they do not allow for individual variability in growth, are restrictive in the way in which individual variability can be incorporated, give inconsistent parameter estimates, are inflexible in the error structures that can be assumed, or are not easily generalized to growth functions other than the von Bertalanffy. Our proposed maximum likelihood method appears to overcome these weaknesses.

In the case of a random L_∞, the method can easily be generalized to any growth function. This was suggested in the derivation of the likelihood, which used a generic growth function, $f(t)$, and illustrated in our simulations using a range of growth functions.

Although we only allowed for individual variability in growth through a random asymptotic length, the likelihood equations can be derived for other random effects. For example, in the von Bertalanffy model, we might want to assume a random k parameter instead. We can adapt the argument presented in the Methods section and condition on both A and k, but a double integration is now required and would be time-consuming computationally. Alternatively, we can use modified Sheiner-Beal linearisation to make the model linear in its random effects (Jones 1993, Chapter 7). If these are Gaussian, we avoid any integration problems, even where L_∞ and k are both random. However, we concur with the arguments summarized in the discussion of Wang et al. (1995) that reject the need for letting both k and L_∞ vary.

As a final point, the VB log k growth curve that we proposed shows potential as a growth curve for modelling SBT and other large pelagic species. The improved fit from applying this model compared to the simple von Bertalanffy lends support to the idea of a two-stage growth process for SBT.

References

Akaike, H. 1974. A new look at the statistical model identification. Institute of Electrical and Electronic Engineers Transactions on Automated Control **AC-19:** 265-289.

Anon. 1994. Report of the southern bluefin tuna trilateral workshop. Hobart, Australia, January/February 1994. 161 pp.

Brent, R.P. 1973. Algorithms for minimization without derivatives. Prentice-Hall, Englewood-Cliffs, New Jersey.

Fabens, A.J. 1965. Properties and fitting of the von Bertalanffy growth curve. Growth, **29:** 265-289.

Francis, R.I.C.C. 1988. Maximum likelihood estimation of growth and growth variability from tagging data. N.Z. J. Mar. Freshwater Res. **22:** 42-51.

Halperin, M. 1963. Confidence interval estimation in non-linear regression. J. Roy. Statist. Soc. B, **25:** 330-333.

Hampton, J. 1991. Estimation of southern bluefin tuna *Thunnus maccoyii* growth parameters from tagging data, using von Bertalanffy models incorporating individual variation. Fish. Bull. U.S. **89:** 577-590.

Hearn, W.S., and Polacheck, T. 2002. Estimating growth rate changes of southern bluefin tuna from tag-return data. Fish. Bull., in press.

James, I.R. 1991. Estimation of von Bertalanffy growth curve parameters from recapture data. Biometrics, **47:** 1519-1530.

Jones, R.H. 1993. Longitudinal data with serial correlation: a state-space approach. Chapman and Hall, London.

Maller, R.A., and de Boer, E.S. 1988. An analysis of two methods of fitting the von Bertalanffy curve to capture-recapture data. Aust. J. Mar. Freshwater Res. **39:** 459-466.

Palmer, M.J., Phillips, B.F., and Smith, G.T. 1991. Application of nonlinear models with random coefficients to growth data. Biometrics, **47:** 623-635.

Sainsbury, K.J. 1980. Effect of individual variability on the von Bertalanffy growth equation. Can. J. Fish. Aquat. Sci. **37:** 241-247.

Schnute, J. 1981. A versatile growth model with statistically stable parameters. Can. J. Fish. Aquat. Sci. **38:** 1128-1140.

Wang, Y-G. 1998. Growth curves with explanatory variables and estimation of the effect of tagging. Aust. N.Z. J. Stat. **40:** 299-304.

Wang, Y-G., Thomas, M.R., and Somers, I.F. 1995. A maximum likelihood approach for estimating growth from tag-recapture data. Can. J. Fish. Aquat. Sci. **52:** 252-259.

Appendix

We discuss the efficient and accurate numerical computation of the integral in equation (5). Denote the integrand by

$$g(a) \;=\; h(l_1, l_2|a)\, p(a)$$

for given l_1 and l_2. Note that $g(a)$ is proportional to the conditional distribution of A given l_1 and l_2. Consideration of several examples with A lognormal suggests that $g(a)$ is often unimodal, and nearly Gaussian in appearance. We can exploit this observation to integrate $g(a)$ efficiently. We first need to find the mode and spread of $g(a)$. After considerable experimentation, we decided on the following scheme:

1. Use an efficient and robust search method (e.g., Brent's method) to locate the maximum of $g(a)$ (Brent, 1973, Chapter 5). This is best done on the log scale, since $g(a)$ is approximately Gaussian near its maximum, and hence approximately quadratic on the log scale. Denote the location of the maximum by μ_g.

2. Estimate the standard deviation of $g(a)$ by

$$\sigma_g \;=\; \sqrt{-1/z''(\mu_g)}\,,$$

where $z(a) = \log g(a)$. A simple way of calculating $z''(\mu_g)$ is to fit a quadratic to $\log g(a)$ in the neighbourhood of μ_g.

Once we have good estimates of μ_g and σ_g, we can use any accurate quadrature method to calculate (5). We preferred to use Gauss-Hermite integration because it

does not require many function evaluations. Define $g(a) = 0$ for $a < 0$. Thus

$$\begin{aligned} h(l_1, l_2) &= \int_0^\infty g(a)\, da \\ &= \int_{-\infty}^\infty g(a)\, da \\ &= \sqrt{2}\,\sigma_g \int_{-\infty}^\infty g(\sqrt{2}\,x\,\sigma_g + \mu_g)\, dx \\ &\approx \sqrt{2}\,\sigma_g \sum_{k=1}^m w_k\, e^{x_k^2}\, g(\sqrt{2}\,x_k\,\sigma_g + \mu_g)\,, \end{aligned}$$

where x_k $(k = 1, 2, \ldots, m)$ and w_k $(k = 1, 2, \ldots, m)$ are the abscissae and weights of m-point Gauss-Hermite quadrature. Note that $\sum_{k=1}^m w_k = \sqrt{\pi}$ for any m, so that the above version of Gauss-Hermite quadrature is exact if $g(a)$ is proportional to a Gaussian density with mean μ_g and standard deviation σ_g. For 20-point quadrature, the composite factors $w_k\, e^{x_k^2}$ range from 0.491 to 0.899, whereas the weights w_k range from 0.462 down to 2.23×10^{-13}. Hence it is best to use the composite factors $w_k\, e^{x_k^2}$ directly. Experimentation with this integration scheme confirmed that it is very accurate provided good values of μ_g and σ_g have been found.

For maximum likelihood estimation, $\log h(l_1, l_2)$ is required rather than $h(l_1, l_2)$. A stable method of computing this is

$$\begin{aligned} \log h(l_1, l_2) &= \log g(\mu_g) + \log \int_0^\infty \exp(\log g(a) - \log g(\mu_g))\, da\,, \\ &= \log g(\mu_g) + \log \int_{-\infty}^\infty z_0(a)\, da\,, \\ &\approx \log g(\mu_g) + \log \sigma_g + \log \sum_{k=1}^m w_k e^{x_k^2} \{\sqrt{2}\, z_0(\sqrt{2} x_k \sigma_g + \mu_g)\} \quad (15) \end{aligned}$$

where $z_0(a) = \exp(\log g(a) - \log g(\mu_g))$ if $a \geq 0$ and is 0 otherwise. In $z_0(a)$, $\log g(a)$ is computed directly, not by taking logs of exponentials. Thus $\log g(a) = \log h(l_1, l_2|a) + \log p(a)$, where

$$\log h(l_1, l_2|a) \;=\; -\log(2\pi) - \log\sigma_1(a) - \log\sigma_2(a) - 0.5\log(1-\rho(a)^2) - \frac{q_{12}(a)}{2(1-\rho(a)^2)}\,,$$

and, if $p(a)$ is log normal with parameters $\mu_{\log A}$ and $\sigma_{\log A}$,

$$\log p(a) \;=\; -0.5\log(2\pi) - \log\sigma_{\log A} - \log a - 0.5(\log a - \mu_{\log A})^2/\sigma^2_{\log A}\,.$$

Computation of $\log g(a)$ rather than $g(a)$ avoids overflow problems: a value of $g(a)$ of e^{-1000} may be truncated to 0 on a computer, but $\log g(a) = -1000$ is computed very accurately. In $z_0(a)$, $\log g(a) - \log g(\mu_g)$ is computed before exponentiating. Also, $z_0(\mu_g) = 1$ at μ_g and $0 \le z_0(a) \le 1$ for all a, so that the sum in (15) and its log may be computed accurately for any set of parameters. If $g(a)$ is proportional to a Gaussian curve with mean μ_g and standard deviation σ_g ($\sigma_g \ll \mu_g$), then $\sum_{k=1}^{m} w_k e^{x_k^2}\{\sqrt{2}\, z_0(\sqrt{2}x_k\sigma_g + \mu_g)\} = \sqrt{2\pi} \approx 2.5066$. However, when fitting the model in row 1 of Table 4, for example, we found that this quantity varied between about 1.8 and 3.5, so that approximating $g(a)$ by a Gaussian curve (a common statistical procedure, sometimes called Laplace's approximation) is not accurate.

When the measurement error is small, $g(a)$ can exhibit a very small spread. In this case, Gauss-Hermite integration is particularly useful since it makes use of the mode and spread of the distribution. However, precise values of these parameters are required in order to achieve accurate integration. Occasionally we have encountered situations in which A given l_1 and l_2 is not unimodal. This seems to occur when A has a complicated distribution, or when the growth curve is complex, and when the measurement error is substantial. We have found that Simpson's rule or the extended trapezoidal rule is satisfactory under such circumstances, although it tends to be slower than Gauss-Hermite integration.

Table 1. Mean parameter estimates (and standard deviations) from applying our new estimation method to simulated von Bertalanffy growth data. For each model we ran 100 simulations with 100 recaptures per simulation. Data were generated with $L_\infty \sim N(100, 25)$ and $k = 0.5$. Times at liberty were taken to be $\Gamma(1,1)$ distributed. The standard deviation of the measurement error, σ, was varied, as was the distribution on the true and assumed age at tagging, A. LogN(u, v) denotes a lognormal distribution with mean u and standard deviation v on the log scale; Gaus.Mixt.(u,v,σ_c, p) denotes a Gaussian 2-component mixture with means u and v, common standard deviation , σ_c, and proportion p belonging to the first component.

Distribution of A			Mean growth parameter estimates (standard deviation)				Mean parameter estimates for A (standard deviation)			
True	Assumed	σ	μ_∞	σ_∞	k	σ	u	v	σ_c	p
LogN(0.5, 0.5)	LogN(u, v)	0	100.3 (1.8)	5.0 (0.4)	0.50 (0.02)	0.01(0.02)[a]	0.50 (0.06)	0.50 (0.04)	–	–
		0	99.9 (0.8)	5.0 (0.2)	0.50 (0.01)	– [b]	0.50 (0.03)	0.50 (0.03)		
LogN(0.5, 0.5)	LogN(u, v)	2	100.1 (2.2)	4.7 (1.0)	0.50 (0.04)	2.0 (0.2)	0.50 (0.06)	0.50 (0.04)	–	–
LogN(0.5, 0.5)	LogN(u, v)	4	99.7 (3.0)	4.3 (2.2)	0.51 (0.05)	3.9 (0.4)	0.49 (0.08)	0.50 (0.04)	–	–
Multi-modal	Gaus.Mixt.(u,v,σ_c, p)	2	100.0 (3.3)	5.1 (1.1)	0.50 (0.05)	2.1 (0.5)	1.1 (0.06)	2.1 (0.14)	0.20 (0.03)	0.80 (0.05)
Multi-modal	LogN(u, v)	2	100.6 (2.9)	4.8 (1.1)	0.49 (0.04)	2.0 (0.2)	0.21 (0.05)	0.31 (0.03)	–	–

[a] Parameters were estimated using likelihood for measurement error and setting lower bound on σ at 0.001.
[b] Parameters were estimated using likelihood for no measurement error.

Table 2. Mean parameter estimates (and standard deviations) from applying our new estimation method to simulated logistic and generalized von Bertalanffy (GVB) growth data. For each model we ran 100 simulations with 100 recaptures per simulation. Data were generated assuming $L_\infty \sim$ N(100, 25), k = 0.5, age at tagging $A \sim$ LogN(0.5, 0.5) and σ = 2. Times at liberty were taken to be $\Gamma(1,1)$ distributed.

	Mean growth parameter estimates (standard deviation)					Mean parameter estimates for A (standard deviation)	
Growth curve	μ_∞	σ_∞	k	r	σ	$\mu_{\log A}$	$\sigma_{\log A}$
Logistic	100.0 (2.9)	4.2 (1.5)	0.50 (0.03)	–	2.0 (0.2)	0.51 (0.07)	0.49 (0.03)
GVB (r = 2)	100.2 (3.3)	4.4 (1.3)	0.50 (0.05)	2.1 (0.6)	2.0 (0.2)	0.49 (0.15)	0.50 (0.07)

Table 3. Mean parameter estimates (and standard deviations) from applying our new estimation method to simulated von Bertalanffy logistic k growth data. We ran n =100 simulations with 500 recaptures per simulation. Data were generated with $L_\infty \sim$ N(100, 25), $k_1 = 0.8$, $k_2 = 0.3$, α = 1.5 or 2.5 (as specified in the table), β = 4, age at tagging $A \sim$ LogN(0.5, 0.5), and $\sigma = 2$. The distribution on the times at liberty, dt, was varied from a gamma distribution ($\Gamma(1,1)$) to a uniform distribution (Unif(1,7)).

			Mean growth parameter estimates (standard deviation)							Mean parameter estimates for A (standard deviation)	
$dt \sim$	n	α	μ_∞	σ_∞	k_1	k_2	α	β	σ	$\mu_{\log A}$	$\sigma_{\log A}$
$\Gamma(1,1)$	100	1.5	99.7 (2.2)	5.0 (0.4)	0.81 (0.06)	0.31 (0.04)	1.5 (1.1)	4 [a]	2.0 (0.1)	0.50 (0.05)	0.50 (0.02)
Unif(1,7)	82[b]	2.5	100.4 (2.1)	5.0 (0.3)	0.83 (0.08)	0.30 (0.09)	2.4 (0.3)	4.3 (1.8)	1.9 (0.4)	0.48 (0.08)	0.51 (0.02)

[a] Fixed at 4 to avoid identifiability problems.

[b] Of the 100 simulations, 18 had identifiability problems in which β, k_1 or k_2 converged to a set bound.

Table 4. Parameter estimates from applying our estimation method to 1980s southern bluefin tuna tag-recapture data (n = 1412). Negative log-likelihood values and Akaike's information criteria (AIC) are also given. Results are for the von Bertalanffy (VB) and von Bertalanffy logistic k (VB log k) growth curves with both simple and measurer-dependent error structures.

Growth curve	Error structure	Parameter estimates										– log likelihood	AIC
		μ_∞	σ_∞	k_1	k_2	α	β [c]	$\mu_{\log A}$	$\sigma_{\log A}$	σ	σ_f		
VB	Simple	160.6	8.8	0.28	–	–	–	0.55	0.17	3.9	–	9633.1	19278.2
VB	Sci./Fish.	162.0	7.1	0.27	–	–	–	0.56	0.18	2.9	4.2	9611.3	19236.6
VB log k	Simple	188.2	10.9	0.22	0.16	3.0	30	0.58	0.16	3.7	–	9609.7	19237.4
VB log k	Sci./Fish.	186.6	9.3	0.22	0.17	2.9	30	0.58	0.18	2.6	4.1	9585.7	19191.4

[c] β constrained to be ≤ 30

Figure 1. Histogram of simulated realistic ages at tagging for southern bluefin tuna, scaled such that the total area of the bars is one. The line shows the fitted probability density function (pdf) assuming a lognormal distribution.

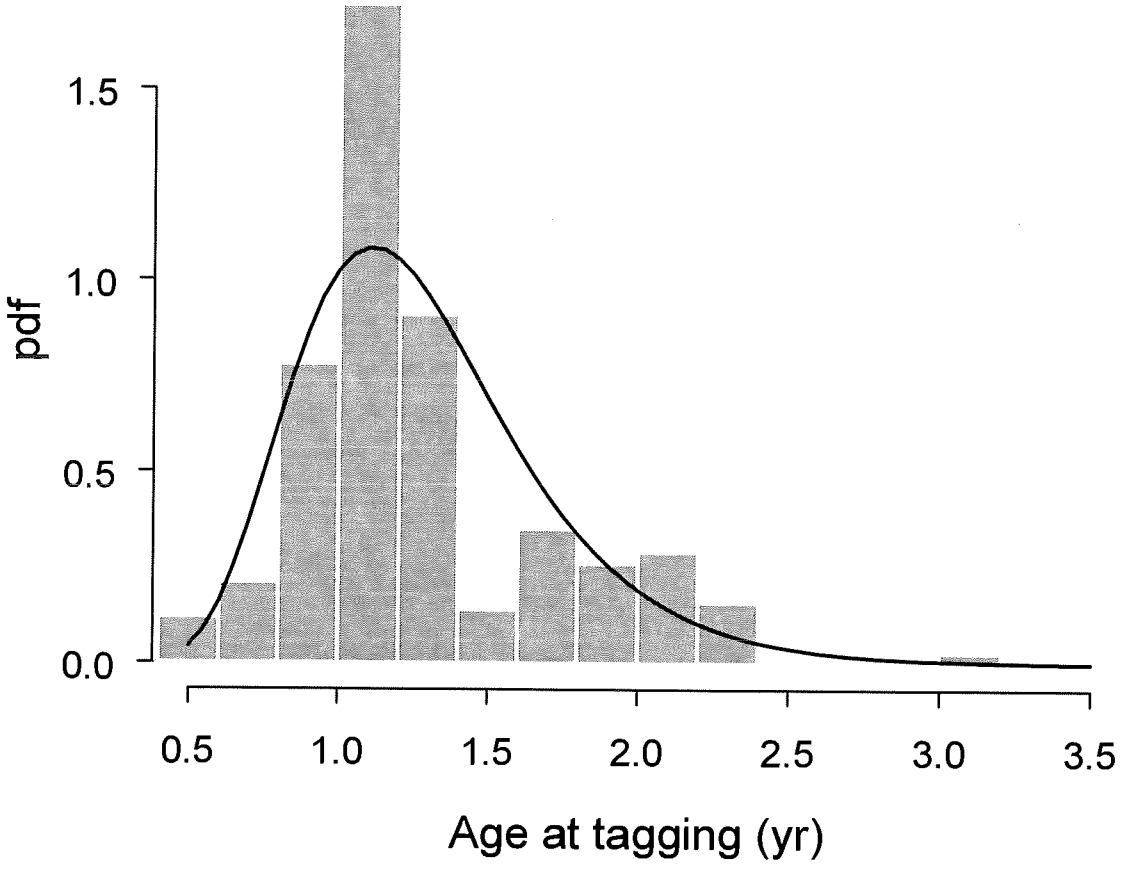

Figure 2. (a) Comparison between the von Bertalanffy (VB), logistic, and generalized von Bertalanffy (GVB) growth curves with $L_\infty = 100$ and $k = 0.5$ for all curves and r=2 for the GVB curve. (b) A typical simulated data set to which we are fitting the logistic growth curve.

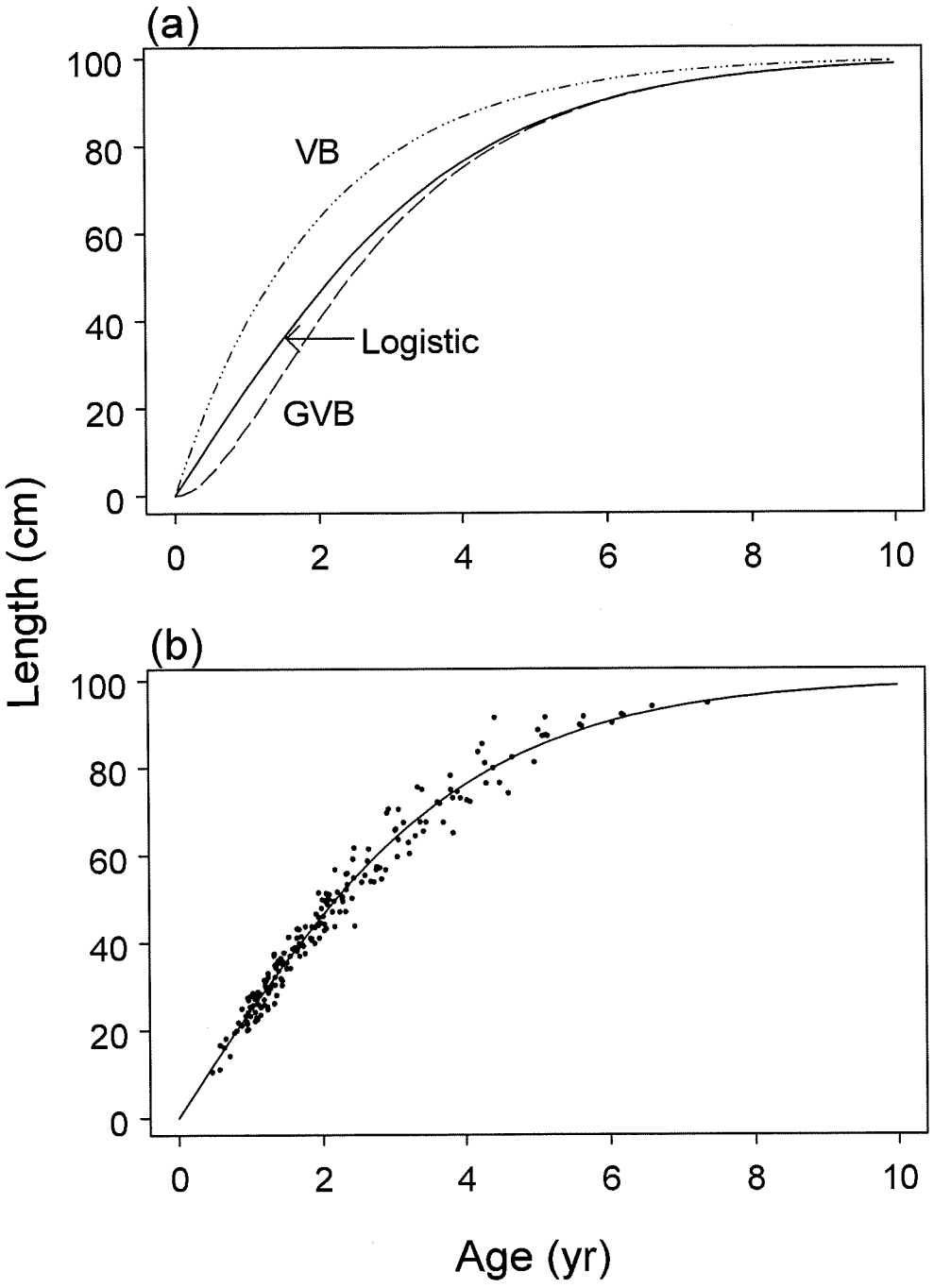

Figure 3. (a) Logistic growth rate with $k_1 = 0.8$, $k_2 = 0.3$, $\alpha = 1.5$ and $\beta = 4$. (b) von Bertalanffy curve with logistic growth rate (parameters as above) and $L_\infty = 100$.

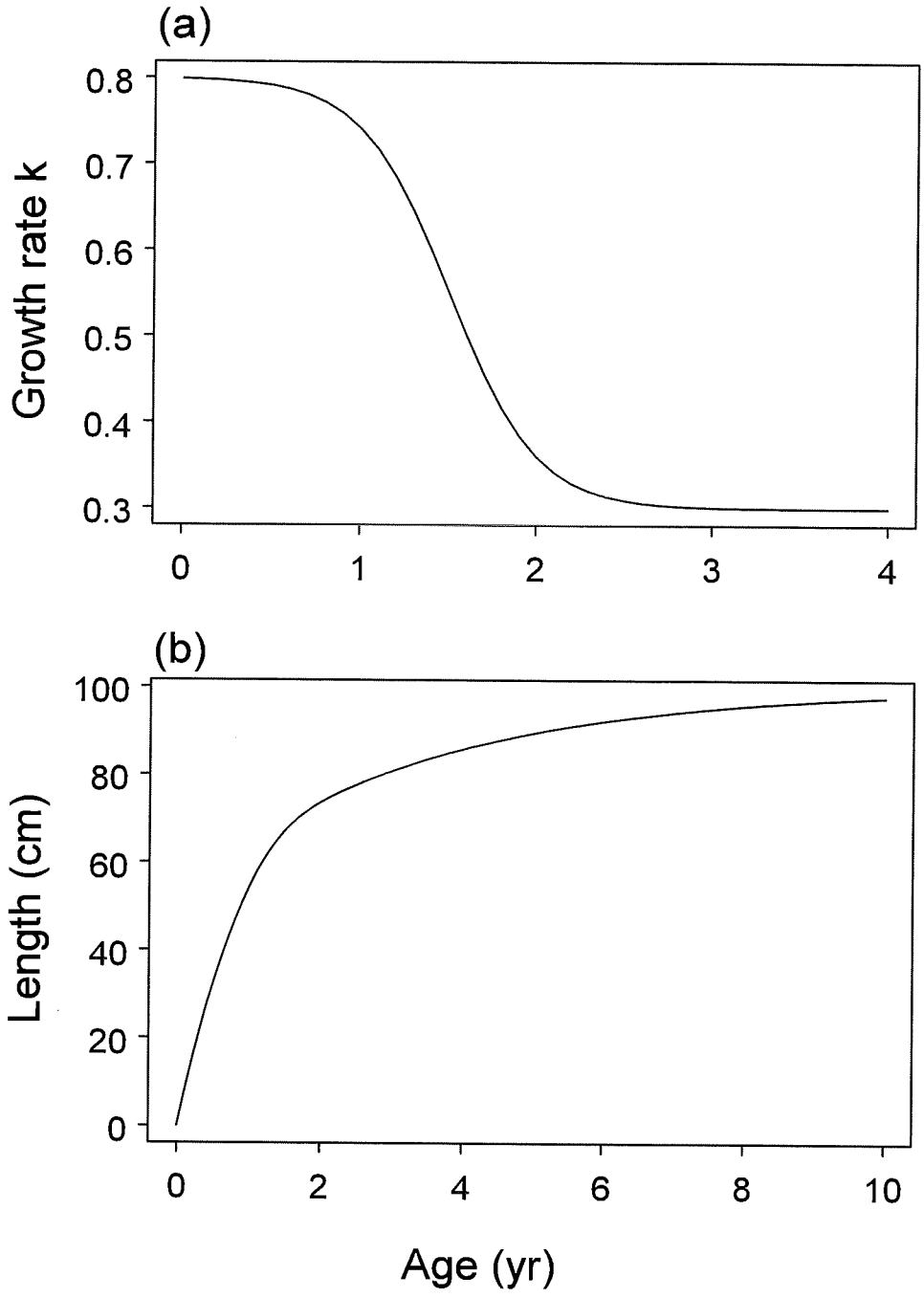

Figure 4. Mean growth curves for the 1980s southern bluefin tuna tag-recapture data. The solid line is the von Bertalanffy fit and the broken line is the von Bertalanffy logistic k fit, both from models incorporating a measurer-dependent error structure. The dotted vertical line shows the estimated transition point, α, for the von Bertalanffy logistic k model.

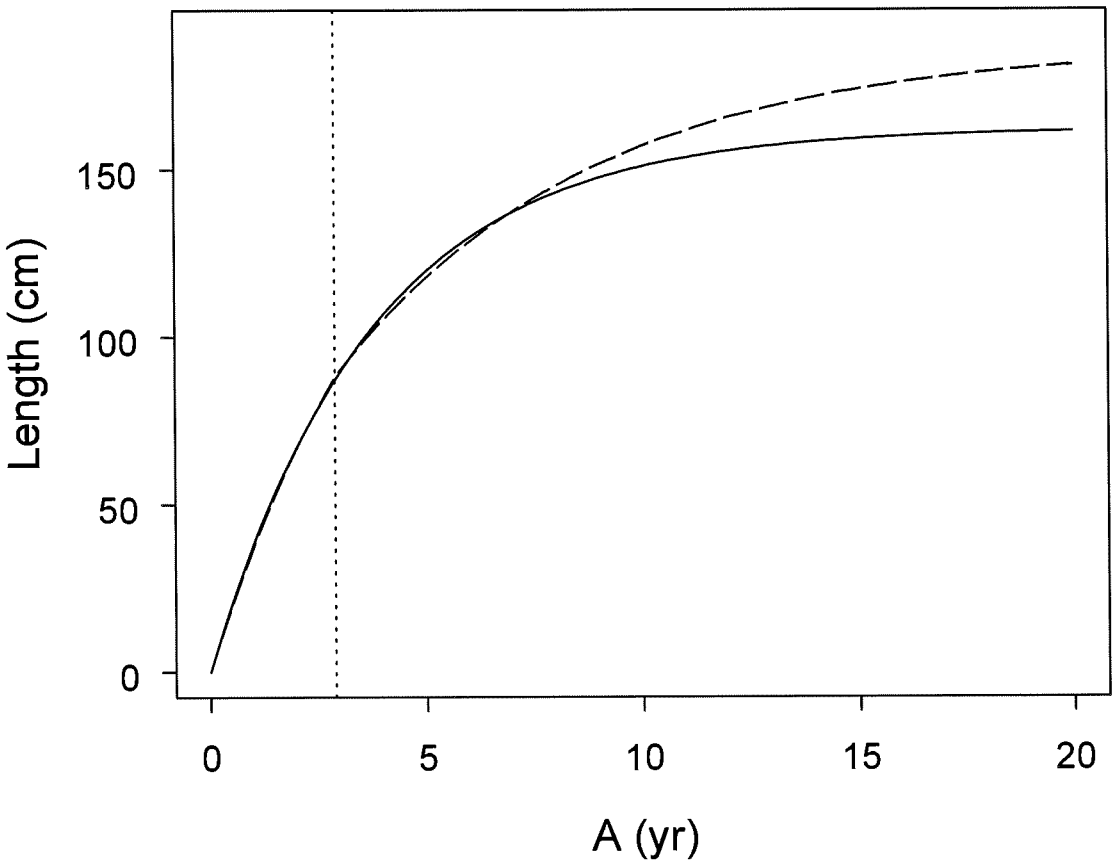

Figure 5. Residuals between the actual and fitted recapture lengths for (a) the von Bertalanffy model and (b) the von Bertalanffy logistic k model fit to the 1980s southern bluefin tuna tag-recapture data. Both models incorporate a measurer-dependent error structure; the pluses indicate length measurements made by fishermen, whereas the open circles indicate length measurements made by scientists.

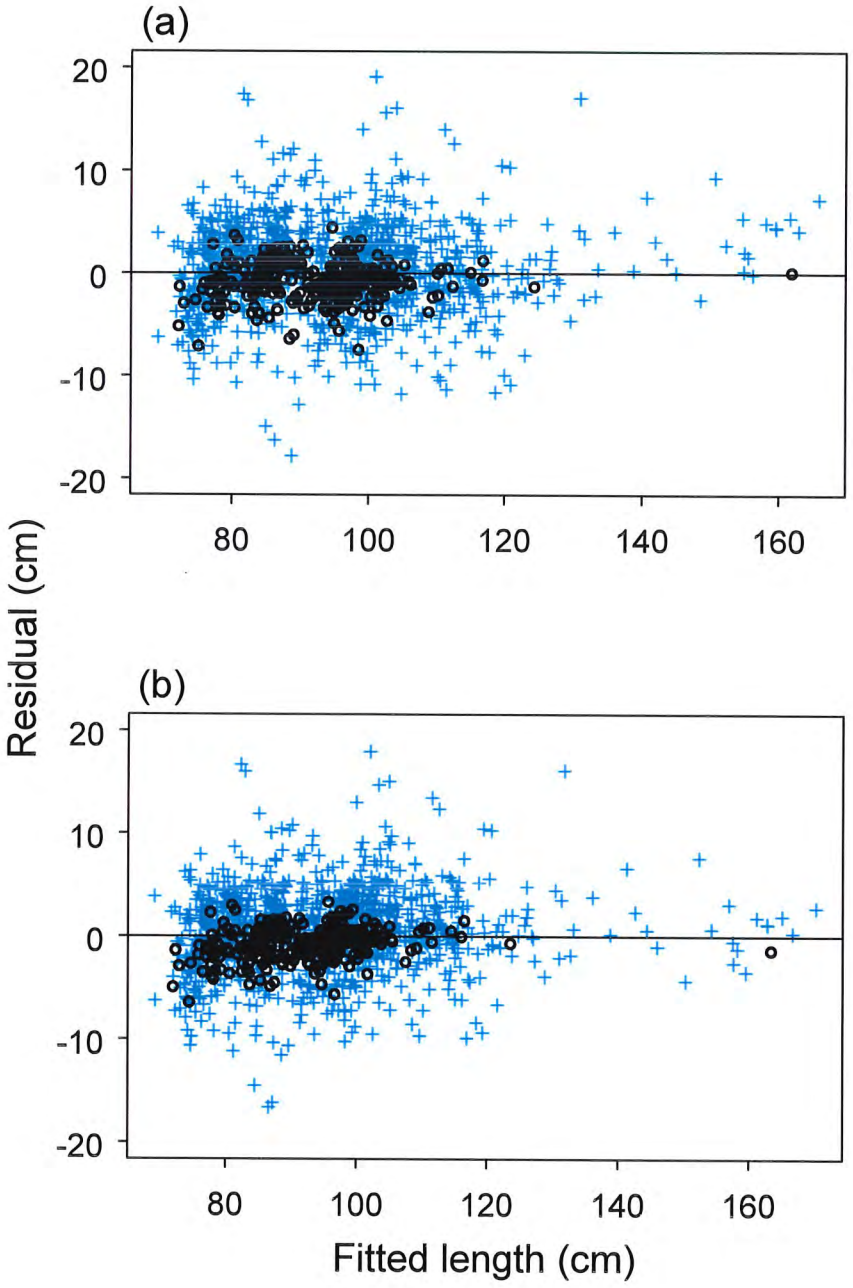

Appendix 5:
Estimating the release age in capture-recapture studies of fish growth

Geoff M. Laslett, J. Paige Eveson and Tom Polacheck

FRDC Project 1999/104

Introduction

Growth curves are an essential component of stock assessments in fisheries. These assessments govern the management of the fishery, including the assessment of long-term sustainability and, ultimately, quota setting. For southern bluefin tuna (SBT) and other species, tag-recapture studies are the main source of information for determining growth. A capture-recapture study has two stages: in the first, the fish are caught, tagged, measured and released; in the second, the fish are caught and measured. In the case of SBT, the first stage is usually undertaken on specially commissioned scientific voyages, but the second is a byproduct of commercial activity. Incentives (t-shirts, cash rewards, et cetera) are often provided for each tag returned to the tagging laboratories.

The resulting data consist of two lengths and times (l_1, t_1, l_2, t_2) for those fish tagged and recaptured. The statistical model for a tagged and recaptured fish is

$$l_1 = l(t_1) + \epsilon_1 \tag{1a}$$

$$l_2 = l(t_2) + \epsilon_2 \tag{1b}$$

where $l(t)$ is the true length of the fish at time t, and ϵ_1 and ϵ_2 represent measurement error. It is usually assumed that the errors are Gaussian distributed with mean 0 and variance σ^2, and independent from fish to fish.

It is standard practice in fisheries to assume a parametric form for the growth curve $l(t)$. For example, for the von Bertalanffy model, the length of a fish at time t is

$$l(t) = \begin{cases} L_\infty(1 - \exp(-k(A + t - t_1))) & \text{if } t > t_1 - A; \\ 0 & \text{otherwise,} \end{cases} \tag{2}$$

where L_∞ is the asymptotic length, A is the time from spawning to tagging and k is a growth rate parameter. The age of the fish is $a = A + t - t_1$. Typically, L_∞ and A are regarded as random from fish to fish, and k is an unknown fixed effect, although more complex models may be considered if the data seem to warrant them. In

addition, L_∞ is usually taken as Gaussian ($L_\infty \sim N(\mu_\infty, \sigma^2_\infty)$), A might be Gamma, lognormal or a mixture of Gaussians truncated at 0, and L_∞ and A are statistically independent. In addition, ϵ_1 and ϵ_2 are independent of L_∞ and A. The model might be fitted using likelihood methods, estimating equations or Bayesian analysis. The random effects A and L_∞ are usually estimated using the minimum variance predictors $\hat{A} = \mathrm{E}[A|l_1, l_2]$ and $\hat{L}_\infty = \mathrm{E}[L_\infty|l_1, l_2]$. The fitted growth curve is, in the von Bertalanffy example, $\hat{\mu}_\infty(1 - \exp(-\hat{k}a))$, where μ_∞ is the mean of L_∞ and $\hat{k}$ is the fitted value of k, and a is the age of the fish in years. Maller and de Boer (1988), James (1991), Palmer *et al.* (1991) and Wang *et al.* (1995) have all discussed this style of model for capture-recapture data.

Once the model has been fitted, it is natural to plot the fitted growth curve, and to superimpose l_1 versus $\hat{A}$ and l_2 versus $\hat{A} + t_2 - t_1$, to see if the model fits. Figure 1 gives an example for 1412 southern bluefin tuna caught in South Australian waters in the 1980s. The von Bertalanffy growth curve has been fitted to the capture-recapture data by maximum likelihood ($\hat{k} = 0.276$, $\hat{\mu}_\infty = 160.65$ cm, $\hat{\sigma}_\infty = 8.76$ cm, $\hat{\sigma} = 3.912$ cm), where $A \sim$ lognormal with the mean of $\log A$ estimated as 0.547 and the standard deviation of $\log A$ as 0.172. Only the estimated release ages and lengths $(\hat{A}, l_1)$ have been plotted for clarity.

Two features stand out. First, there is a disparity between the data and the fitted model. Second, the degree of variation of the lengths l_1 for a given value of $\hat{A}$ is much less than we might have anticipated from the parameter estimates $\hat{\sigma}_\infty$ and $\hat{\sigma}$. This article explains these phenomena using classical statistical methods.

Alternative growth model formulations

It is natural to ask why we have chosen L_∞ and A to be random variables in (2). That the asymptotic length and the age at tagging vary from fish to fish is indisputable, but we could let them be different unknown constants for each fish. However, this implies more unknown parameters than data values. The next possibility is to let L_∞ be a random variable but A be a fixed effect — we would

choose this rather than the reverse because L_∞ is likely to have a simple distribution (e.g. Gaussian) whereas A might be quite complex. However, this formulation causes trouble.

To illustrate the problem, consider the growth model

$$l(t) = \mu_\infty \left[1 - e^{-k_2(t-t_0)} \left\{ \frac{1 + e^{-\beta(t-t_0-\alpha)}}{1 + e^{\beta\alpha}} \right\}^{-(k_2-k_1)/\beta} \right] \tag{3}$$

where t_0 is the theoretical time at which the fish has 0 length. Thus $A = t_1 - t_0$, and t_0 is assumed to be a different constant for each fish. This model, introduced in Appendix 4, captures the separate juvenile and adult growth phases in southern bluefin tuna. When this model is fitted by maximum likelihood to the data set of the Introduction, different solutions are obtained depending on the starting values. Two such solutions are presented in Table 1.

Table 1: Two solutions to fitting a growth model with a separate spawning time for each fish.

$\hat{\mu}_\infty$	$\hat{k}_1$	$\hat{k}_2$	$\hat{\alpha}$	$\hat{\beta}$	residual sum-of-squares
170.64	0.210	0.245	2.049	10	31650.5
186.77	0.207	0.165	3.988	10	32112.9

In both fits, β has hit a preset upper bound of 10. There are 2824 data values and 1418 parameters. It appears that the large number of parameters combined with the flexible growth model has created a multimodal likelihood surface. A plot of the profile log-likelihood versus α is distinctly bimodal (Figure 2). Neither the number of modes in the likelihood surface nor the location of the global maximum is known. Other growth data from direct ageing studies suggest that $\mu_\infty = 170.6$ is too low, so the mode with the lower log-likelihood (higher residual sum-of-squares) has more biological credibility.

To reduce these problems, we let the age at tagging A be a random variable. While this does not guarantee that the likelihood surface will be unimodal, the num-

ber of parameters is now relatively small (< 10), and we expect that the likelihood will be better behaved.

The linear model

A simple linear growth model

We first look at the problem illustrated in the Introduction for a very simple linear growth model. The data are generated by

$$l_1 = bA + \epsilon_1 \tag{4a}$$

$$l_2 = b(A + \delta t) + \epsilon_2 \tag{4b}$$

where $\delta t = t_2 - t_1$, b is a known constant, $A \sim N(\mu_a, \sigma_a^2)$ and $\epsilon_i \sim N(0, \sigma^2)$. There are two measurements per fish, and A varies randomly from fish to fish. The ϵ_i represent independent measurement errors. Thus (A, l_1, l_2) are trivariate normal, and hence the best linear unbiased predictor (BLUP) of A is

$$\hat{A} = \mathrm{E}(A|l_1, l_2) = \mu_a + \frac{b\sigma_a^2}{\sigma^2 + 2b^2\sigma_a^2}(l_1 - b\mu_a + l_2 - b(\mu_a + \delta t)) .$$

Note in passing that if $\sigma^2 > 0$, $\hat{A}$ is conditionally biased for A, because

$$\mathrm{E}[\hat{A}|A] = \mu_a + \frac{2b^2\sigma_a^2}{\sigma^2 + 2b^2\sigma_a^2}(A - \mu_a) .$$

Thus $\mathrm{E}[\hat{A}|A] < A$ if $A > \mu_a$ and $\mathrm{E}[\hat{A}|A] > A$ if $A < \mu_a$.

Set $d = (l_1 - l_2 + b\,\delta t)/2$, noting that $\mathrm{E}[d] = 0$. Then it is readily proved that

$$l_1 = b\,(\mu_a + \frac{(2b^2\sigma_a^2 + \sigma^2)}{2b^2\sigma_a^2}(\hat{A} - \mu_a)) + d$$

and that $\mathrm{Cov}[\hat{A}, d] = 0$. Because l_1 and $\hat{A}$ are bivariate Gaussian, $\mathrm{E}[d|\hat{A}] = 0$, and so $\mathrm{E}[l_1|\hat{A}] = b(1 + r)\hat{A} - r\mu_a$, where $r = \sigma^2/(2b^2\sigma_a^2)$. The plot of l_1 versus $\hat{A}$ tends to have slope bigger than b, the value expected for l_1 versus A. However, the slope $\to b$ as $\sigma^2 \to 0$. Further, the intercept should be 0, but in fact is $-r\mu_a$. Each

fish supplies an independent realisation of $(l_1, l_2, \hat{A}, d)$ according to this model. This explains, in a linear context, the biases seen in Figure 1.

The parameters b, μ_a and σ_a^2 are confounded in this example, although we are treating them as known. This example is a lead-in to non-linear growth models, where the confounding disappears.

A more general linear growth model

Explaining and correcting the bias in growth model plots

For a given fish, generalise (4a) and (4b) to

$$l_i = a_i + b_i A + \epsilon_i \tag{5}$$

for $i = 1, \ldots, n$, where a_i and b_i are known constants, the vector of errors $\epsilon \sim N(0, \Sigma)$, $A \sim N(\mu_a, \sigma_a^2)$ and A and ϵ are independent. Of course, a_i could be absorbed into l_i and b_i into A, but the generalisation to non-linear models is easier if we keep them explicit. In growth models, $a_i = b_i \delta t_i$, where $\delta t_1 = 0$ and δt_i is the time increment from the first capture to the $(i-1)$th recapture. Hence $l_i = b_i(A + \delta t_i) + \epsilon_i$. The BLUP of A is

$$\hat{A} = \mu_a + \frac{\sigma_a^2}{1 + \sigma_a^2 b' \Sigma^{-1} b} b' \Sigma^{-1} (l - a - b\mu_a) \tag{6}$$

where l, a and b are the vectors of observed lengths, intercepts and slopes respectively.

We assert that

$$l_i = a_i + b_i(\mu_a + \frac{1 + \sigma_a^2 b' \Sigma^{-1} b}{\sigma_a^2 b' \Sigma^{-1} b}(\hat{A} - \mu_a)) + d_i \,. \tag{7}$$

where d_i, defined later, and $\hat{A}$ are independent Gaussian random variables and $\mathrm{E}[d_i] = 0$. In the growth model context, a plot of l_1 versus $\hat{A}$ will have slope larger than b_1 on average.

Given that the plot of l_1 versus the BLUP $\hat{A}$ of A does not reproduce the model correctly, it is natural to ask if there is an estimator of A that does. Now

(5) looks like a regression model with A as an unknown parameter. The regression estimate of the realised value of A, treated as a fixed effect, should reproduce the linear model (5) in an unbiased way. Define

$$\tilde{A} \;=\; \mu_a + \frac{1}{b'\Sigma^{-1}b}\, b'\Sigma^{-1}(l - a - b\mu_a) = \frac{b'\Sigma^{-1}(l-a)}{b'\Sigma^{-1}b}\,. \tag{8}$$

Note that $\tilde{A} = A + \eta$, where $\eta = b'\Sigma^{-1}\epsilon / b'\Sigma^{-1}b$ and ϵ is the vector of errors. Set $d_i = l_i - a_i - b_i\tilde{A}$. Then, using standard regression calculations,

$$\begin{aligned}
\mathrm{Cov}[\tilde{A}, d_i] &= \mathrm{Cov}[A + \eta, -b_i\,\eta + \epsilon_i] \\
&= \mathrm{Cov}[\eta, -b_i\,\eta + \epsilon_i] \\
&= \frac{-b_i + b'\Sigma^{-1}\mathrm{Cov}[\epsilon, \epsilon_i]}{b'\Sigma^{-1}b} \\
&= \frac{-b_i + b'e_i}{b'\Sigma^{-1}b} \\
&= 0\,,
\end{aligned}$$

where e_i is the vector of length n with ith entry 1 and the rest 0. Hence

$$l_i \;=\; a_i + b_i\tilde{A} + d_i\,. \tag{9}$$

This equation mimics the true relationship (5), because $\tilde{A}$ and d_i are conditionally independent. In regression, it is usual to plot l_i versus b_i for a given fish, but in growth models, it is more natural to plot l_i versus $\hat{A} + \delta t_i$.

How may $\tilde{A}$ be formally interpreted in the random effects context, to contrast it with the BLUP estimator? Since $\mathrm{E}[\tilde{A}|A] = A$, $\tilde{A}$ is a linear conditionally unbiased estimator of A. We assert also that $\tilde{A}$ minimises the conditional variance $\mathrm{Var}[A^*|A]$ amongst all linear conditionally unbiased estimators A^*.

Explaining the reduced scatter in growth model plots

We now explain, in the linear model context, why the scatter about the curve in Figure 1 is much less than we might anticipate from the fitted parameters. We do this for l_1 versus $\tilde{A}$ rather than l_1 versus $\hat{A}$, but the arguments are essentially identical.

The correlated error effect: The variance of d_i may be considerably smaller than the variance of ϵ_i. Let $n = 2$, $b_1 = b_2 = b$ and ϵ_1 and ϵ_2 have common variance σ^2 and correlation ρ. Then $d_1 = -d_2 = (\epsilon_1 - \epsilon_2)/2$, so that $\text{Var}[d_i] = \sigma^2(1-\rho)/2$. If ρ is near 1, $\text{Var}[d_i] \ll \text{Var}[\epsilon_i]$. Hence a scatterplot of l_i versus $\tilde{A}$ will follow the true line $a_i + bA$, but the scatter around the line will be considerably less than for the true line.

In model (5) it is customary to think of the ϵ_i as measurement errors, but they could represent more than that. The growth model (2) in the Introduction has two latent random variables L_∞ and A that could be estimated from the data l_1 and l_2. By analogy, consider the linear model

$$l_i = c_i + b_i A + m_i L + \delta_i \tag{10}$$

for $i = 1, \ldots, n$, where $A \sim N(\mu_a, \sigma_a^2)$, $L \sim N(\mu_l, \sigma_l^2)$, the vector of errors $\delta \sim N(0, \Sigma_\delta)$, A, L and δ are mutually independent and all fixed effects are known. Then

$$l_i = a_i + b_i A + \epsilon_i$$

where $a_i = c_i + m_i\mu_l$ and $\epsilon_i = m_i(L - \mu_l) + \delta_i$. Hence $\text{Var}[\epsilon] = \Sigma = \Sigma_\delta + \sigma_l^2 mm'$, where m is the vector of m_i values. The theory for the linear model carries through without change, except that the scatterplot l_i versus $\tilde{A}$ clearly follows the mean line $c_i + m_i\mu_l + b_i A$ rather than the individual lines $c_i + b_i A + m_i L$. Further, the term $\sigma_l^2 mm'$ is likely to induce a strong positive correlation in the residuals ϵ_i, so that the estimated residuals d_i will exhibit very small scatter.

The changing slope effect: In capture-recapture studies of growth curves, the slope of the growth curve at capture is usually much larger than the slope at recapture. Consider a linear example in which the capture length l_1 and recapture length l_2 are modelled as

$$\begin{aligned} l_1 &= b_1 A + \epsilon_1 \\ l_2 &= b_2(A + \delta t) + \epsilon_2 \end{aligned}$$

where $b_2 < b_1$, $\epsilon_i \sim N(0, \sigma^2)$ and ϵ_1 and ϵ_2 are independent. Then $d_1 = b_2 d$ and $d_2 = -b_1 d$ where $d = (\epsilon_1 b_2 - \epsilon_2 b_1)/b'b$. It follows that $\mathrm{Var}[d_1] < \mathrm{Var}[d_2]$. In real studies, it is common that $b_2 \ll b_1$, so that the scatterplot of l_1 versus $\tilde{A}$ will exhibit considerably less scatter around the growth curve than the scatterplot of l_2 versus $\tilde{A} + \delta t$. We shall see this effect in Figure 5.

The reduced scatter seen in Figure 1 is caused by a combination of the correlation and changing slope effects.

Linear growth models with non-Gaussian random effects

We finish with a final comment about non-Gaussianity, because in practice A is usually not Gaussian. We drop the assumption that A and ϵ are Gaussian in (5), but retain all other assumptions. We ignore $\hat{A}$ given by (6) and commence with the formula for $\tilde{A}$ given by (8). Then $\tilde{A}$ is still conditionally unbiased for A, and $\tilde{A}$ and d_i are uncorrelated. This does not immediately imply that l_1 plotted against $\tilde{A}$ will follow the linear growth model, in the sense that $\mathrm{E}[l_i|\tilde{A}] = a_i + b_i\tilde{A}$, but there are two reasons for believing that this will be nearly true. Firstly, under the usual regularity conditions, the central limit theorem applies to both $\tilde{A}$ and d_i; for example, $\eta = b'\Sigma^{-1}\epsilon/b'\Sigma^{-1}b$ is closer to normality than any individual ϵ_i. Secondly, we proved that $\mathrm{Cov}[\tilde{A}, d_i] = 0$, which implies that $\tilde{A}$ and d_i are globally uncorrelated. But it is just as easy to demonstrate a stronger result, $\mathrm{Cov}[\tilde{A}, d_i|A] = 0$, which implies that $\tilde{A}$ and d_i are locally uncorrelated as well.

Nonlinear growth models

In fisheries' research, growth models are typically non-linear. We focus on the problem of correcting the bias in the plot of l_1 versus $\hat{A}$ seen in Figure 1. A common generic growth model in fisheries' research is

$$l_i = L_\infty f(A + \delta t_i) + \epsilon_i\,, \tag{11}$$

where $i = 1$ for capture, and $i = 2, 3 \ldots$ for subsequent recaptures, $f(.)$ is a monotonically increasing curve with asymptote 1, the asymptotic length $L_\infty \sim N(\mu_\infty, \sigma^2_\infty)$, the errors $\epsilon_i \sim N(0, \sigma^2)$ and A, L_∞ and $\epsilon_1, \epsilon_2, \ldots$ are independent. An obvious approach is to produce an estimator $\tilde{A}_m$ of A that is conditionally median unbiased. Then, since f is monotone increasing, $\mu_\infty f(\tilde{A}_m + \delta t)$ will be conditionally median unbiased for $\mu_\infty f(A + \delta t)$. However, we do not know how to construct A_m, except by correcting the median bias in a nearly conditionally unbiased estimator, so we discuss three alternatives for doing so: linearising the growth model about an initial estimate of A; treating the realised value of the random effect A as a fixed effect; and estimating A by a conditionally unbiased estimator. In linear growth models, these approaches are equivalent. The linear estimators are Gaussian under certain conditions, and we expect that the non-linear estimators will be approximately Gaussian under the same conditions, so that they will be approximately conditionally median unbiased. If desired, they could be used as a starting point for a conditionally median unbiased estimator.

Linearising the non-linear growth model

Consider the generic growth model (11). Let A_0, a known constant, be an initial guess at the realised value of A; $A_0 = \mathrm{E}[A|l_1, \ldots, l_n]$ is often a good choice. We can use the method of Vonesh and Carter (1992) to linearise the model with respect to the random effects:

$$\begin{aligned} l_i &\approx \mu_\infty f(A_0 + \delta t_i) + \mu_\infty f'(A_0 + \delta t_i)(A - A_0) + f(A_0 + \delta t_i)(L_\infty - \mu_\infty) + \epsilon_i \\ &= a_i + b_i A + \delta_i \,, \end{aligned} \tag{12}$$

where $a_i = \mu_\infty \left(f(A_0 + \delta t_i) - f'(A_0 + \delta t_i) A_0\right)$, $b_i = \mu_\infty f'(A_0 + \delta t_i)$ and $\delta_i = f(A_0 + \delta t_i)\,(L_\infty - \mu_\infty) + \epsilon_i$. It is usual to assume that A and L_∞ are independent. The theory of the general linear growth model then applies. We denote the estimator by $\tilde{A}_l$.

Treating the realised value of A as a fixed effect

The second option is to treat the realised value of A as an unknown fixed effect. For simplicity, we consider only the case of a single recapture. The data are

$$l_1 = L_\infty f_1 + \epsilon_1 \quad (13)$$

$$l_2 = L_\infty f_2 + \epsilon_2 \quad (14)$$

where $f_1 = f(A)$, $f_2 = f(A + \delta t)$, $L_\infty \sim N(\mu_\infty, \sigma_\infty^2)$ and $\epsilon_i \sim N(0, \sigma_i^2)$. Here the errors and L_∞ are all mutually independent. We assume that all parameters, apart from A, are known, or have been estimated from all fish assuming that A is distributed according to a parametric model. The problem then is to estimate the realised value of A for a given fish, treating it as an unknown fixed effect. Let $r_i = l_i - \mu_\infty f_i$. The log-likelihood is

$$-\frac{1}{2}\log|V| - \frac{\sigma_1^2 r_2^2 + \sigma_2^2 r_1^2 + \sigma_\infty^2 (r_1 f_2 - r_2 f_1)^2}{2|V|}$$

where $|V| = \sigma_\infty^2 (\sigma_1^2 f_2^2 + \sigma_2^2 f_1^2) + \sigma_1^2 \sigma_2^2$.

The likelihoods for all fish may be maximised simultaneously by using a vectorised version of Brent's method (Brent, 1973, Chapter 5). We denote the estimate by $\tilde{A}_f$. The conditional mean and variance of $\tilde{A}_f$ may be calculated by numerical integration. The variance of $\tilde{A}_f$ may also be approximated using likelihood theory.

We emphasise that we are only treating A as a fixed effect at this stage, and only for the purpose of graphical model checking. If we were to treat A as a fixed effect when fitting the parameters of the model, then $\hat{k}$, $\hat{\mu}_\infty$ and the other parameter estimates would be different from those used above.

A conditionally unbiased non-linear random effects estimator

As a lead-in, we examine a general situation in which we wish to predict a random variable X from a random vector Y. We set $\hat{X} = \mathrm{E}[X|Y]$ as the standard minimum variance estimator of the random effect X given Y, but we wish to modify $\hat{X}$ to a conditionally unbiased estimator $\tilde{X}$.

Let $h(X) = \mathrm{E}[\hat{X}|X]$. We argue that the estimator $\tilde{X}$, obtained by solving

$$h(\tilde{X}) = \hat{X},$$

is, under mild conditions, much closer to being conditionally unbiased than $\hat{X}$. There is a simple geometrical interpretation of $\tilde{X}$, shown in Figure 3. It is the inverse estimator, obtained by plotting the curve $\mathrm{E}[\hat{X}|X]$ versus X, drawing a horizontal line from $\hat{X}$ on the y-axis until it hits the curve, and then dropping down to $\tilde{X}$ on the x-axis. In this sense, $\tilde{X}$ is a natural estimator.

It is immediately obvious that we can refine $\tilde{X}$ to $\tilde{X}^{(2)}$, obtained by solving

$$\tilde{X} = \mathrm{E}[\tilde{X}|\tilde{X}^{(2)}].$$

Since $\tilde{X}$ has a much smaller conditional bias than $\hat{X}$ in general, we expect that $\tilde{X}^{(2)}$ will have a smaller conditional bias than $\tilde{X}$.

In principle, a sequence of estimators $\tilde{X}^{(j)}$ could be computed, starting from $\tilde{X}^{(0)} = \hat{X}$ and $\tilde{X}^{(1)} = \tilde{X}$. Each would satisfy

$$\tilde{X}^{(j)} = \mathrm{E}[\tilde{X}^{(j)}|\tilde{X}^{(j+1)}].$$

However, for practical purposes computation of $\tilde{X}^{(2)}$ should be adequate. We could start with a different estimator from $\hat{X}$ to derive $\tilde{X}^{(j)}$, but $\hat{X}$ is a stable starting estimator.

We briefly indicate why $\tilde{X}$ is almost conditionally unbiased. Suppose that

$$h(X^*) \approx h(X) + h'(X)(X^* - X)$$

for X^* in the neighbourhood of X. For example, for bivariate Gaussian random variables (X, Y) with means 0, unit variances and correlation ρ, $h(X) = \rho^2 X$. The iterative scheme $\tilde{X}_0 = \hat{X}$ and

$$\tilde{X}_j = \hat{X} + \tilde{X}_{j-1} - \mathrm{E}[\hat{X}|\tilde{X}_{j-1}] \tag{15}$$

for $j = 1, 2, \ldots$ yields

$$\tilde{X}_j \approx \hat{X} + \tilde{X}_{j-1} - h(X) - h'(X)(\tilde{X}_{j-1} - X).$$

Take conditional expectations on X, and set $\beta_j = \mathrm{E}[\tilde{X}_j|X]$. Then

$$\begin{aligned}\beta_j &\approx h(X) + \beta_{j-1} - h(X) - h'(X)(\beta_{j-1} - X) \\ &= \beta_{j-1} - h'(X)(\beta_{j-1} - X)\,.\end{aligned}$$

If $\beta_j \to \beta$, then clearly $\beta = X$, so that $\mathrm{E}[\tilde{X}_j|X]$ is asymptotically unbiased for X. Further, if $\gamma_j = \beta_j - X$, then $\gamma_j \approx (1 - h'(X))^j$, so that β_j converges geometrically to X if $0 < h'(X) < 2$.

In fact, this argument depends on local linearity of $h(X)$, and non-linearity may imply some conditional bias in $\tilde{X}$. For this reason, we recommend calculating $\tilde{X}^{(2)}$ to reduce this conditional bias.

When applied to capture-recapture growth data, we suggest that l_1 should be plotted against $\tilde{A}$ or, even better, $\tilde{A}^{(2)}$ rather than $\hat{A}$. Similarly, l_2 should be plotted against $\tilde{A}^{(2)} + t_2 - t_1$.

Southern bluefin tuna

We illustrate some of these ideas on the southern bluefin tuna study that motivated this article.

Linearising the von Bertalanffy growth model

We first calculated $\tilde{A}_l$ for the von Bertalanffy growth curve by setting $A_0 = \mu_a$, but the resulting estimate of A using (8) was very poor. So we set $A_0 = \hat{A}$. We computed $r_l(A) = \mathrm{E}[\tilde{A}_l|A] - A$ on a fine grid of $\log \delta t$ and A values (each combination of $\log \delta t = -0.5, -0.4, \ldots, 2.5$ and $A = 1.0, 1.1, \ldots, 3.0$). The average value of $|r_l(A)|$ was 0.004 ($\sim 0.2\%$), equivalent to about 1.5 days. This conditional bias is probably small enough for exploratory work, since capture and recapture times are recorded to the nearest day, and the conditional standard error of A_l is about 10%.

Although the linearisation method worked on this data set, we have found data sets for which it fails, even when $A_0 = \hat{A}$. We cannot recommend it in general, even though it has superficial appeal.

Treating the realised value of A as a fixed effect

The computation of $\tilde{A}_f$ was straightforward, but the conditional moments were not. In theory

$$\mathrm{E}[\tilde{A}_f^k|A,\delta t] = \int_0^\infty \int_0^\infty \tilde{A}_f^k\, h(l_1,l_2|A,\delta t)\, dl_2\, dl_1$$

for any integer k, where $h(l_1,l_2|A,\delta t)$ is the density of l_1, l_2 for release age A and recapture age $A+\delta t$. However, $\tilde{A}_f$ could not be computed for extreme combinations of l_1, l_2 not found in real data. Consider $l_1 = 100$ cm at age $A = 3$ years and $l_2 = 50$ cm at age 6 years. This is unrealistic for two reasons: $l_1 \gg l_2$ and 6 year-old-fish are much longer than 50 cm. To overcome these problems, we simulated 50,000 lengths for fish of a given age a and fitted a lower envelope curve $\lambda(a)$ and an upper envelope curve $\nu(a)$ so that all the lengths fell between $\lambda(a) + 3$ cm and $\nu(a) - 3$ cm. That is, $\lambda(a)$ and $\nu(a)$ were slightly expanded beyond the range of the data. We then evaluated the moments by

$$\mathrm{E}[\tilde{A}_f^k|A,\delta t] = \int_{\lambda(A)}^{\nu(A)} \int_{\lambda(A+\delta t)}^{\nu(A+\delta t)} \tilde{A}_f^k\, h(l_1,l_2|A,\delta t)\, dl_2\, dl_1\,.$$

The average value of $|r_f(A)|$, where $r_f(A) = \mathrm{E}[\tilde{A}_f|A] - A$, on the test grid of A and δt values was 0.002, smaller than for A_l. Because it is easy to calculate and is nearly conditionally unbiased, we recommend A_f as an estimator of A for graphical model checking.

A conditionally unbiased non-linear random effects estimator

Finally we computed $\tilde{A}^{(2)}$, which was non-trivial: both $\tilde{A}_l$ and $\tilde{A}_f$ are much quicker to calculate than $\tilde{A}^{(2)}$. The average value of $|r(A)|$, where $r(A) = \mathrm{E}[\tilde{A}^{(2)}|A] - A$, on the test grid of A and δt values was 0.0001, smaller than for $\tilde{A}_l$ and $\tilde{A}_f$, and confirming that $\tilde{A}^{(2)}$ is, for practical purposes, conditionally unbiased.

The first panel in Figure 4 shows the resulting estimates $\tilde{A}_l$ of A plotted against $\tilde{A}^{(2)}$. The estimates agree closely, although they are not identical. The second panel shows $\tilde{A}_l - \tilde{A}^{(2)}$ plotted against $\tilde{A}^{(2)}$. There is a small but obvious bias.

Further, although we do not show the plot, the agreement between $\mathrm{Var}[\tilde{A}^{(2)}|A]$ and $\mathrm{Var}[\tilde{A}_l|A]$ was excellent. Similar plots with $\tilde{A}_f$ replacing $\tilde{A}_l$, not shown here, were even more impressive. The agreement between $\tilde{A}^{(2)}$ and $\tilde{A}_f$ is better, in that the small bias disappears.

We briefly return to the problem outlined in the Introduction, and analyse it using the tools developed here. The upper panel of Figure 5 shows l_1 versus $\tilde{A}^{(2)}$ and the fitted von Bertalanffy growth curve. The fit is much better than in Figure 1. The lower panel of Figure 5 displays l_2 versus $\tilde{A}^{(2)} + \delta t$, which shows clearly that the model underpredicts longer lengths. To emphasise this, we have simulated 20 data sets from the fitted model using the same δt values as in the tuna study. A cubic smoothing spline curve fitted to the 28240 simulated $(\tilde{A}^{(2)} + \delta t, l_2)$ is so close to the growth curve we have decided to omit it. We have shown the running 5% and 95% quantiles fitted to the simulated data as short broken lines. They confirm that the data should fall symmetrically about the curve if the model is correct. The simulations are very quick, and are an essential aid to interpreting the plot. If we used $\hat{A}$ instead of $\tilde{A}^{(2)}$ in the lower panel of Figure 5, we could not necessarily be confident that the pattern in this panel indicated model failure. The mismatch between model and data seen in Figure 1 may carry over to some extent to the plot of l_2 and $\hat{A}+\delta t$ — whether it does depends on the link between l_1 and l_2 and between A and $A+\delta t$. The lack of fit can be established more traditionally by embedding the von Bertalanffy growth model in a larger parametric family, and formally testing for the adequacy of the embedded model. However, it is useful to see this conclusion supported in a plot of the data.

Computation of $\mathrm{E}[\hat{A}|A]$, $\mathrm{E}[\tilde{A}|A]$, $\mathrm{E}[\tilde{A}^{(2)}|A]$ and $\mathrm{Var}[\tilde{A}^{(2)}|A]$ in this example presented a mild challenge. Each fish had its own time interval δt between capture and recapture, which meant that $\mathrm{E}[\hat{A}|A]$ differed for each fish. Precise computation of $\mathrm{E}[\hat{A}|\tilde{A}_j]$ at each step of (15) separately for each of the 1412 fish would be very slow: 20 iterations of (15) would require 28240 computations of $\mathrm{E}[\hat{A}|A]$ by numerical integration, which would take about 50 hours of computing time using the excellent

routines of Berntsen *et al.* (1991a,b) on a 500 MHz Pentium PC. Instead we computed $\mathrm{E}[\hat{A}|A]$ and $\mathrm{E}[\tilde{A}|A]$ for $0.5 \leq A \leq 8$ and $-0.5 \leq \log \delta t \leq 2.5$ on a fine 76×31 grid, which took less than 5 hours of computing time, and estimated the required values by bicubic spline interpolation when solving $\hat{A} = \mathrm{E}[\hat{A}|\tilde{A}]$ and $\tilde{A} = \mathrm{E}[\tilde{A}|\tilde{A}^{(2)}]$ by iteration. The number of iterations of (15) is then not limited by time considerations. Additional covariates could be handled the same way in principle, but this could cause problems if there are too many covariates.

Estimating the distribution of A

A final disadvantage of $\hat{A}$ is that a density plot of its values does not match the true density of A. Figure 6(a) shows the fitted lognormal density of A. The mean of the lognormal is 1.754, almost identical to 1.757, the mean of $\tilde{A}^{(2)}$. However, the estimates $\tilde{A}^{(2)}$ are overdispersed with respect to the true distribution of A, so we rescale them around their mean to have the same standard deviation as the fitted lognormal:

$$\tilde{A}_s^{(2)} = \hat{\mu}_{a2} + \frac{\hat{\sigma}_{ln}}{\hat{\sigma}_{a2}}(\tilde{A}^{(2)} - \hat{\mu}_{a2}) \,,$$

where $\hat{\mu}_{a2}$ and $\hat{\sigma}_{a2}$ are the mean and standard deviation of the $\tilde{A}^{(2)}$ values and $\hat{\sigma}_{ln}$ is the standard deviation of the fitted lognormal distribution. A histogram of the $\tilde{A}_s^{(2)}$ values is also plotted on Figure 6(a). It is immediately evident that a more skewed and longer-tailed distribution needs to be fitted. There is a suggestion that A may be a mixture. Of course, if a new model for A is chosen, the estimates $\tilde{A}^{(2)}$ will change.

A more sophisticated method involves estimating the density of A from $\tilde{A}^{(j)}$ ($j \geq 1$) by modelling $\tilde{A}^{(j)}$ as

$$\tilde{A}^{(j)} = A + e \,,$$

where e is an error with 0 mean and variance $\mathrm{Var}[\tilde{A}^{(j)}|A]$. Such a model is consistent with $\tilde{A}^{(j)}$ being conditionally unbiased for A. The variance may be computed explicitly as a function of A using the maximum likelihood parameter estimates,

and then estimated by $\mathrm{Var}[\tilde{A}^{(j)}|A]|_{A=\tilde{A}^{(j)}}$ for each fish. Nonparametric estimation of the distribution of A when it is observed with error has been researched intensively, and there are dozens of papers on this topic in the mainstream statistical literature, although many assume that e has constant variance. Notable exceptions are Goutis (1997), Cordy and Thomas (1997) and various papers in the empirical Bayes literature (e.g. Maritz and Lwin 1989). For our data, the standard deviation of e ranges from about 0.1 to 0.5 when $j = 2$, and increases with $\tilde{A}^{(2)}$. For the purposes of exploratory analysis, we assume that the errors e are independent, which is true if the population parameters are known, and Gaussian, which is a convenient approximation. Figure 6(b) shows the density of A estimated using the method of Cordy and Thomas (1997). This confirms that the lognormal is inadequate. The distribution of A appears complex, and its estimation may warrant the nonparametric method of Palmer *et al.* (1991).

It should be evident that conditionally unbiased estimates of random effects can play a diagnostic role in capture-recapture studies for growth.

Concluding remarks

Conditionally unbiased estimators of random effects are an important didactic tool in capture-recapture studies used to estimate growth curves. When the capture lengths are plotted against the traditional minimum variance estimates $\hat{A} = \mathrm{E}[A|\mathrm{data}]$ of the times to first capture, the points do not fit the growth model even when it is correct. This causes alarm amongst those unfamiliar with the regression-to-the-mean property of random effects estimators. Because of this, the estimates $\hat{A}$ do not match the statistical properties of the quantities A they estimate, and this causes the apparent lack of fit. The problem can be crystallised by calculating conditionally unbiased estimators, and contrasting their behaviour with the traditional ones. In particular, they can be shown to

- largely correct the misfit in the plot of l_1 versus $\hat{A}$;

- have a higher mean squared error than $\hat{A}$;
- be over-dispersed with respect to the distribution of A.

This, hopefully, will lead to better appreciation of the relative merits of $\hat{A}$ and of conditionally unbiased estimators of random effects.

Conditionally unbiased estimators of random effects can play a diagnostic role in growth curve modelling from capture-recapture data. A plot of l_2 versus $\tilde{A}^{(j)} + \delta t$ may exhibit lack of fit in a parametric growth model. The histogram of $\tilde{A}^{(j)}$ for $j = 2$, say, can, after rescaling, be compared with the fitted distribution of A to see if the chosen form is reasonable. Alternatively, $\tilde{A}^{(2)}$ can be deconvoluted nonparametrically to yield an estimate of the density of A. The minimum variance estimator $\hat{A}$ can be misleading in these roles.

In the growth curves we have studied, approximate conditionally unbiased random effects estimators $\tilde{A}_l$ and $\tilde{A}_f$ of the time to capture A may be calculated, although we have experienced data sets for which $\tilde{A}_l$ fails. Thus $\tilde{A}_f$ in particular may be used as a practical alternative to $\tilde{A}^{(2)}$. Conditional moments, and hence the variance, may be calculated by two-dimensional integration over the space of possible l_1 and l_2 values.

We have mainly discussed the case of a single recapture, by far the most common case in pelagic fisheries. With other species, such as lobsters and terrestrial animals in a local habitat, multiple recaptures are possible. The two-dimensional integration needed to calculate E[A|data] will need to be replaced by high-dimensional integration. It is possible that simulation techniques may be needed to estimate E[A|data] in those circumstances.

References

BERNTSEN, J., ESPELID, T.O. AND GENZ, A. (1991a) An adaptive algorithm for the approximate calculation of multiple integrals. *ACM Trans. Math. Software,* **17,** 437-451.

BERNTSEN, J., ESPELID, T.O. AND GENZ, A. (1991b) An adaptive multidimensional integration routine for a vector of integrals. *ACM Trans. Math. Software,* **17,** 452-456.

BRENT, R.P. (1973) Algorithms for minimization without derivatives. Prentice-Hall: Englewood-Cliffs, New Jersey.

CORDY, J.B. AND THOMAS, D.R. (1997) Deconvolution of a distribution function. *Journal of the American Statistical Association,* **92,** 1459-1465.

GOUTIS, C (1997) Nonparametric estimation of a mixing density via the kernel method. *Journal of the American Statistical Association,* **92,** 1445-1450.

GRAYBILL, F.A. (1976) *Theory and application of the linear model.* Duxbury Press: North Scituate, Massachusetts.

JAMES, I.R. (1991) Estimation of von Bertalanffy growth curve parameters from recapture data. *Biometrics,* **47,** 1519-1530.

MALLER, R.A. AND DE BOER, E.S. (1988) An analysis of two methods of fitting the von Bertalanffy curve to capture-recapture data. *Australian Journal of Marine and Freshwater Research,* **39,** 459-466.

MARITZ, J.S. AND LWIN, T. (1989) *Empirical Bayes Methods.* Chapman and Hall: New York.

PALMER, M.J., PHILLIPS, B.F. AND SMITH, G.T. (1991) Application of nonlinear models with random coefficients to growth data. *Biometrics,* **47,** 623-635.

VONESH, E.F. AND CARTER, R.L. (1992) Mixed-effects nonlinear regression for unbalanced repeated measures. *Biometrics,* **48,** 1-17.

WANG, Y-G, THOMAS, M.R. & SOMERS, I.F. (1995) A maximum likelihood approach for estimating growth from tag-recapture data. *Can. J. Fish. Aquat. Sci.,* **52,** 252-259.

Figure 1. Plot of capture length l_1 against $\hat{A}$. A von Bertalanffy growth curve with random asymptotic length has been fitted to capture-recapture data for 1412 southern bluefin tuna tagged and released in Australian waters in the 1980s. The time A from spawning to capture is assumed to be lognormally distributed. The mean growth curve, fitted by maximum likelihood, is shown as a solid line. The capture length l_1 is plotted against $\hat{A}$, but does not follow the growth curve.

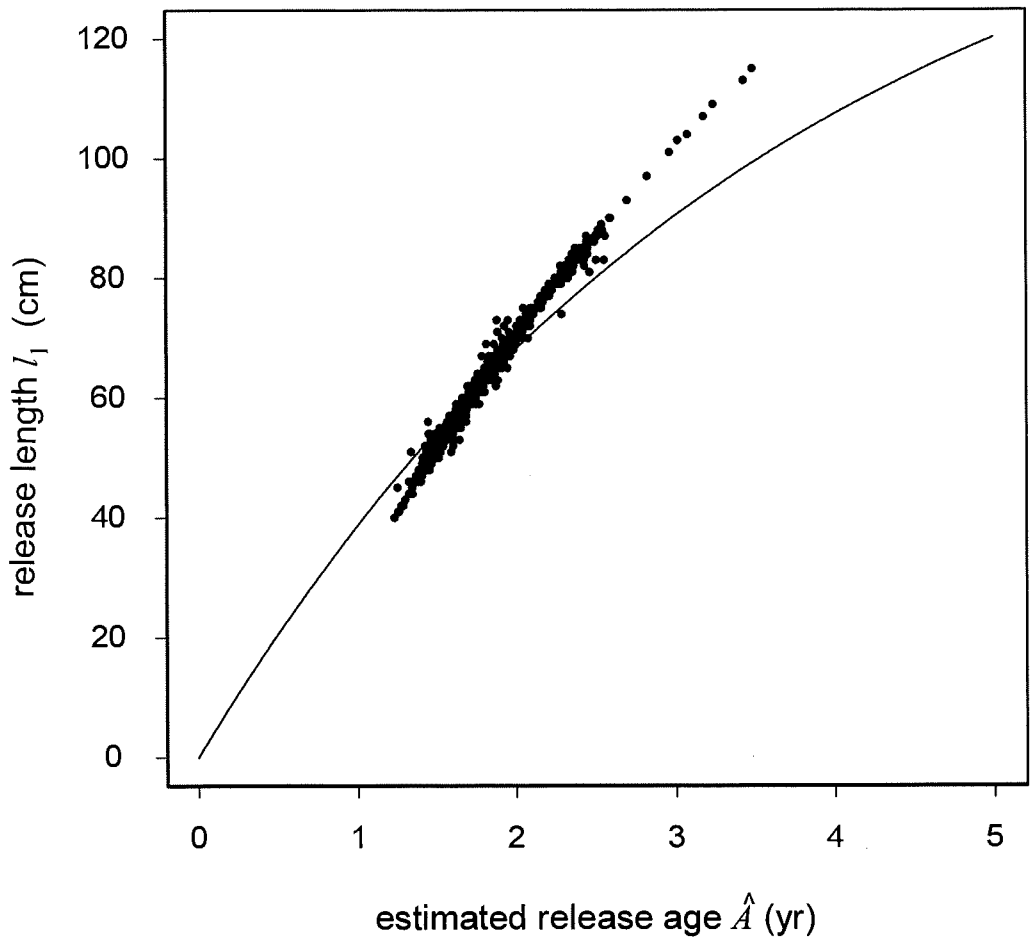

Figure 2. Profile log-likelihood for a two-phase growth model versus α. The parameter α is the age of transition between juvenile and adult growth phases in the new growth model (3). The profile log-likelihood is clearly bimodal, and its complex shape suggests that the log-likelihood surface may possess additional modes.

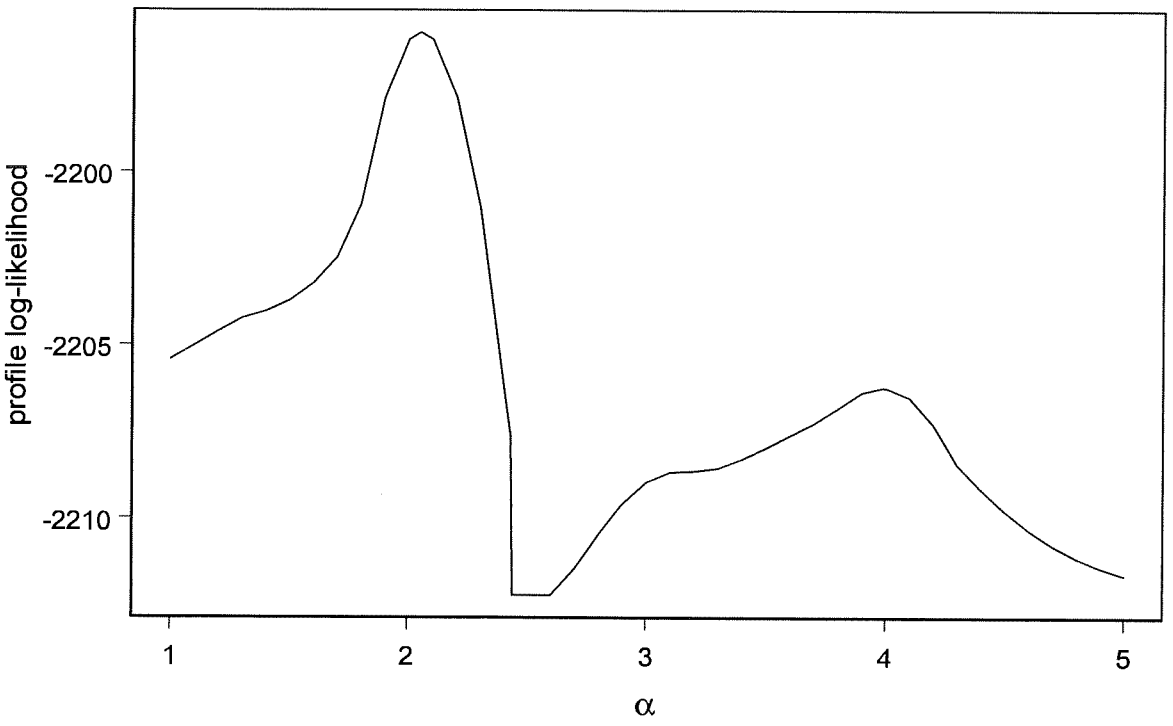

Figure 3. A graphical interpretation of $\tilde{A}$. We assume that A, the time between spawning and capture, is a two-component Gaussian mixture, and let $\hat{A} = \mathrm{E}[A \mid l_1, l_2]$ be the traditional random effects estimator of A. The solid curve is $\mathrm{E}[\hat{A} \mid A = a]$ versus a. To obtain $\tilde{A}$, plot $\hat{A}$ on the y-axis, draw a horizontal line from $\hat{A}$ to the curve, and then read off $\tilde{A}$ as the corresponding ordinate.

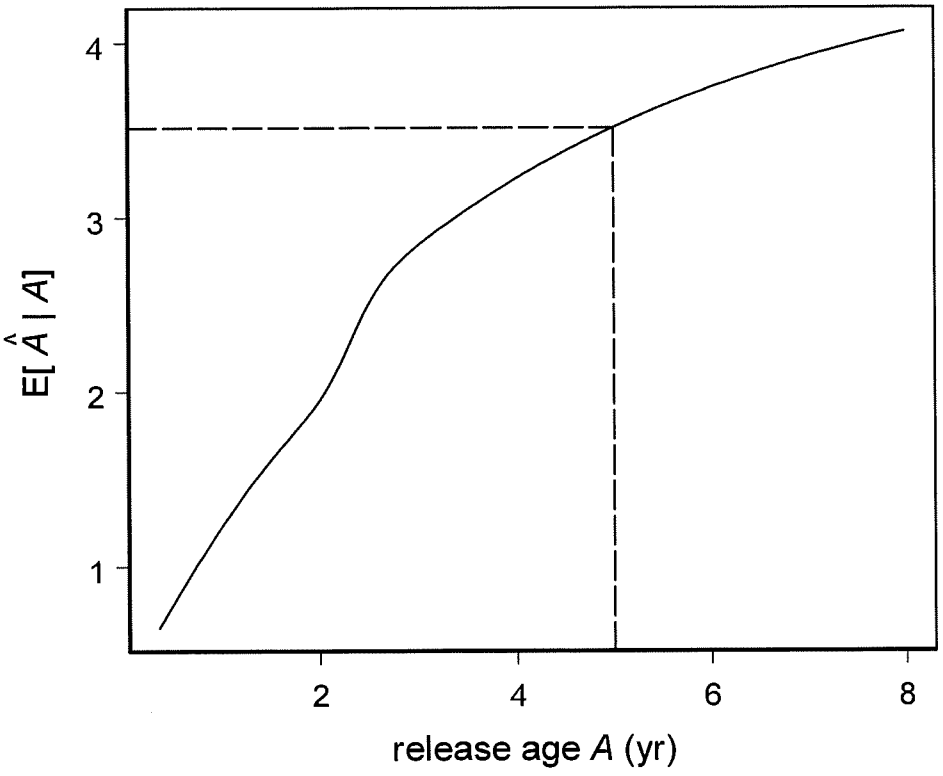

Figure 4. An approximate conditionally unbiased estimator of A. In panel (a), an approximate estimator $\tilde{A}_1$ of A obtained from (12) and (8) is plotted against $\tilde{A}^{(2)}$, and in panel (b) the difference $\tilde{A}_1 - \tilde{A}^{(2)}$ is plotted against $\tilde{A}^{(2)}$. These plots indicate that the approximate estimator is slightly biased, but suggest that it is possibly adequate for exploratory work.

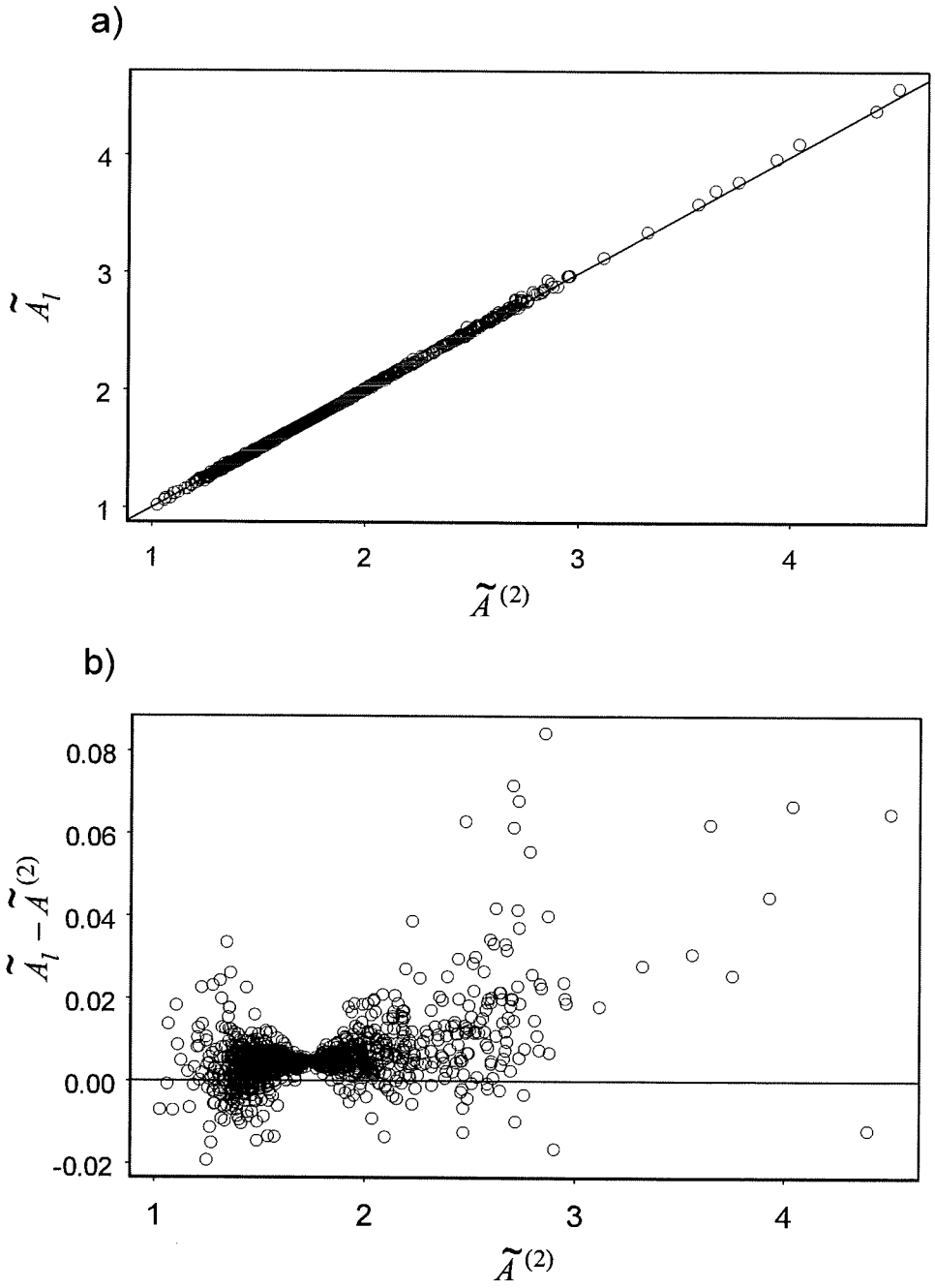

Figure 5. Growth curve for the southern bluefin tuna data. Panel (a) shows the capture length l_1 versus the estimated age at capture $\widetilde{A}^{(2)}$ and panel (b) shows the recapture length l_2 versus the estimated age at recapture $\widetilde{A}^{(2)} + t_2 - t_1$ with the fitted von Bertalanffy growth curve. The bias in Figure 1 is largely corrected in (a), but (b) suggests that the model is still inadequate. Running 5% and 95% quantiles of l_2 versus $\widetilde{A}^{(2)} + t_2 - t_1$, estimated from simulated data, are shown as short broken lines.

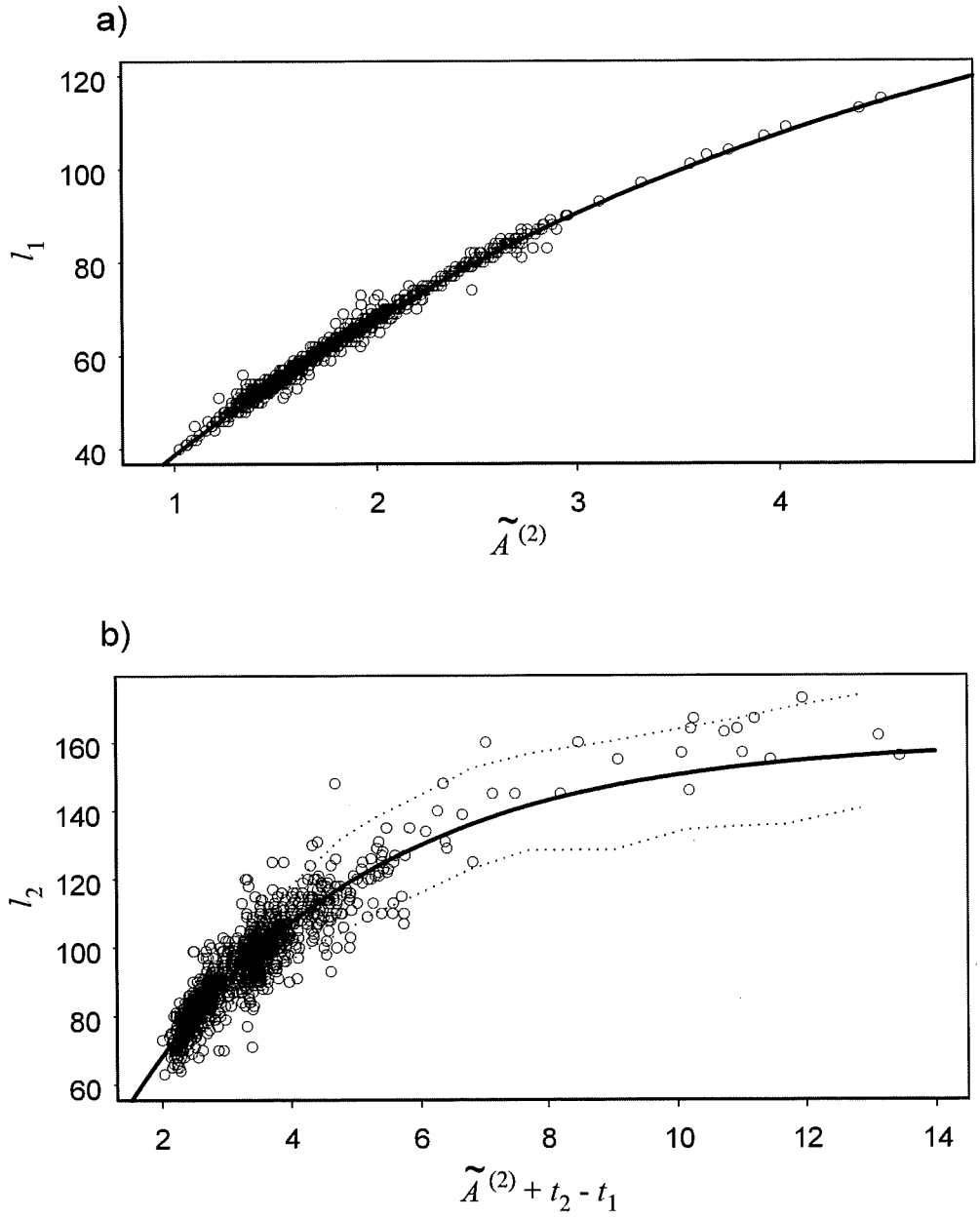

Figure 6. The distribution of the time to capture for the southern bluefin tuna data. In panel (a), the solid line is the fitted lognormal model, and the histogram represents values of $\widetilde{A}^{(2)}$ scaled around their mean to have the same standard deviation as the lognormal. The plot suggests that the time to capture is much more complicated than lognormal. In panel (b), $\widetilde{A}^{(2)}$ has been deconvoluted nonparametrically using the method of Cordy and Thomas (1997). The comparison between the fitted lognormal (solid line) and the nonparametric density estimate (broken line) confirms that the lognormal is inadequate.

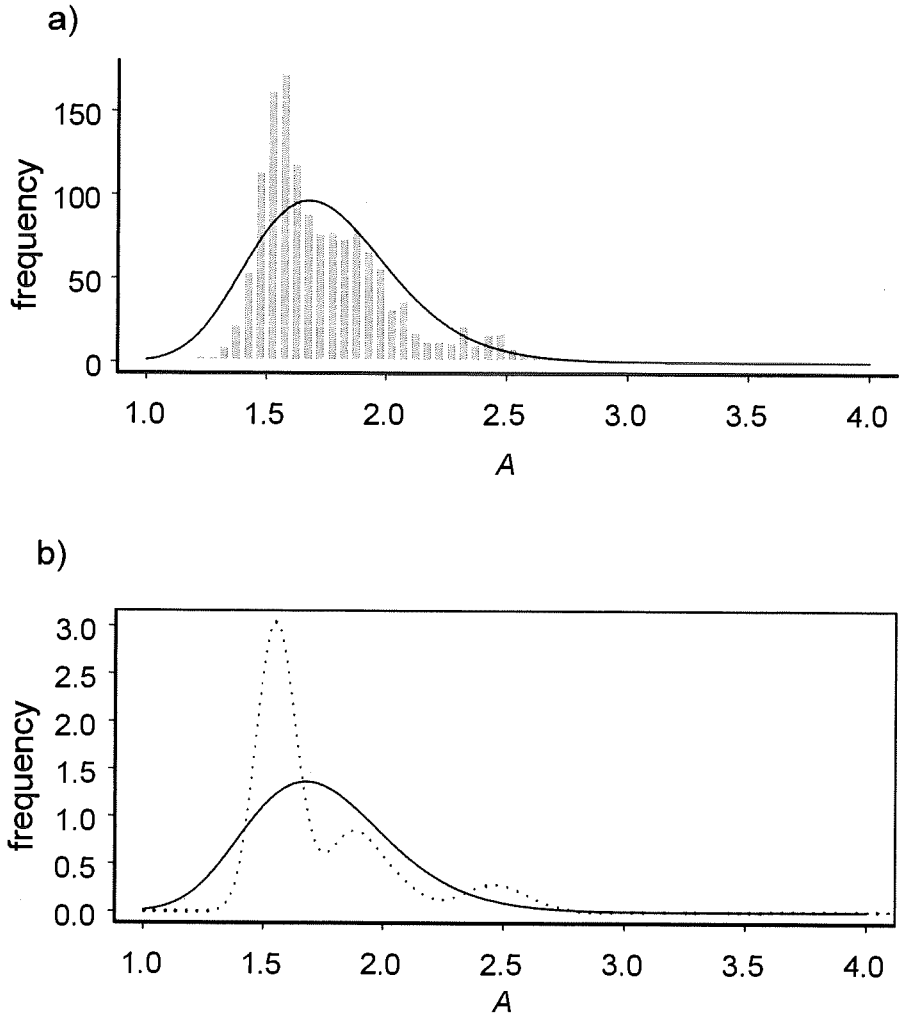

Appendix 6:

Investigating sources of individual variability in von Bertalanffy growth models – a simulation study

J. Paige Eveson, Tom Polacheck and Geoff M. Laslett

FRDC Project 1999/104

Introduction

Modelling the growth of a species is a widely studied topic. A key step is to determine a functional form that describes the growth process. In fisheries literature, it is most often assumed that the mean growth of the population follows a von Bertalanffy (VB) curve, namely

$$l(a) = L_\infty(1-\exp(-k(a-a_0))) \tag{1}$$

where a and l are the age and length of a fish respectively. The parameter L_∞ represents asymptotic length, k governs the growth rate, and a_0 is the theoretical age of length zero. It is generally accepted that the growth of individuals will vary from the mean, however the sources of variation are usually unknown.

Individual variation from the mean population growth curve can occur through variability in one or more of the growth parameters (L_∞ and k for the VB curve) and/or through a random process error, due perhaps to environmental influences. Hampton (1991) discusses these sources of variation, in addition to measurement error, and he analyses a set of southern bluefin tuna tag-recapture data assuming various combinations of them. Measurement error can undoubtedly be a source of variability, but without any external information with which to estimate it, it is confounded with any constant term in the process error. Thus, we do not include measurement error as a separate source of variability in our investigation. It is also possible that variability from the mean growth curve occurs because the underlying growth process (i.e. the functional form) varies between individuals. For example, individuals may not grow according to a VB relationship even though the mean growth of the population follows a VB curve. Wang et al. (1995) examine this situation, however we will not consider it here.

Our goal is to investigate, through simulations, the effect of assuming different sources of variation given some truth, and to do so for various truths. The motivation for such a study is that in practice we cannot know without uncertainty what is the true cause of variability in growth. We must use our best discretion to choose a model based on the data and our knowledge of the species' biology. Thus, it is important to know the consequences of choosing an incorrect model formulation in practical terms, such as the

effect on prediction. Does it really matter if we assume that variability is due to a random asymptotic length L_∞ when it is actually due to a random k? Or if we assume a constant process error term when in fact L_∞ varies between individuals? What if we make the random process error an increasing function of length, such that a fish strays further from the mean curve as it grows? This is plausible, for example, if a fish lives for a prolonged period in an environment of poor or favourable feeding conditions.

Of course, the phrase "does it matter" depends on the researcher's purpose and also on the method chosen to evaluate the adequacy of the model. In simulation studies, we can compare the estimated parameter values with the true values to look for evidence of bias. However, with a model such as the von Bertalanffy where the parameters are highly correlated, two different parameter sets can lead to very similar length predictions over a restricted range of ages. Thus, we consider alternative methods of evaluation as well. For example, plots of the difference in length between the fitted curve and the true curve across ages are very useful.

The results will presumably depend on the type of growth data being modelled and the method used to fit the model. In the case of direct age and length data, a straightforward maximum likelihood method can be applied. However, in the case of tag-recapture data, where the ages of the fish at release and recapture are not known, there are several possible approaches. The traditional approach has been to analyse the length increments and times at liberty assuming a VB growth model and using the fitting method proposed by Fabens (1965). It is well documented that using Fabens' method when individual variability in the growth parameters exists results in biased parameter estimates (Sainsbury 1980, Maller and deBoer 1988). In particular, Sainsbury (1980) shows that the mean value of k is underestimated when variability in k exists but is not accounted for; this is true for both age-length data and length-increment data but the bias is much greater in the latter case. More recent approaches to analysing tag-recapture data model the joint density of the release and recapture lengths as opposed to modelling length increments (Wang et al. 1995, Laslett et al. 2002). Such approaches require the age at release to be modelled.

Other factors that will affect the results are the variability and comprehensiveness of the data. In this Appendix, we concentrate on direct age and length data, considering situations with low and high variability and complete and incomplete coverage. It would be too lengthy to include the full suite of situations for tag-recapture data as well; however, we realize that for many marine species, tag-recapture data is the most abundant source of growth information. Thus, we include an abbreviated set of results for tag-recapture data as well.

Methods

Direct age and length data

When we have direct age and length observations, we can formulate a growth model based on the von Bertalanffy curve given in (1) as

$$l(a) = L_\infty(1-\exp(-k(a-a_0))) + \varepsilon(a) \qquad (2)$$

for $a > a_0$. The component $\varepsilon(a)$ represents process error and it is assumed to be independent random normal with mean 0 and variance $\sigma^2(a)$. In our simulations, we considered the following five model variations:

a) fixed L_∞, fixed k, and constant error variance, namely $\sigma(a) = \sigma$

b) fixed L_∞, fixed k, and error variance that increases with mean length, namely $\sigma(a) = (1-\exp(-k(a-a_0)))^\theta \sigma \quad (\theta > 0)$

c) random L_∞ (normally distributed with mean μ_∞ and variance σ_∞^2), fixed k, and constant error variance

d) fixed L_∞, random k (gamma distributed with mean μ_k and variance σ_k^2), and constant error variance

e) random L_∞ (normally distributed with mean μ_∞ and variance σ_∞^2), random k (gamma distributed with mean μ_k and variance σ_k^2), and constant process error.

In models where either L_∞ or k are random effects we assume that they are independent of the process error, and in the model where they both are random we assume they are also independent of each other.

Maximum likelihood methods were used to fit all of the models. Assuming L_∞ and k are fixed effects, the density of l is normal. This is also true when L_∞ is a random normal variable. When k has a gamma distribution, the exact expectations and variances for l can be calculated (see Sainsbury (1980) for the exact formulation). The distribution of l is now unknown, but using the approximation that it is normal should be reasonable, as our simulation results confirm.

There are a couple of points worth noting. First, the assumption that k is gamma distributed seems quite realistic for most species, including southern bluefin tuna. However, if there is reason to doubt this assumption, the exact expectation and variance of l can be calculated for a number of distributions (those with explicit moment-generating functions). Second, the exact distribution of l can be calculated for any distributions of L_∞ and/or k by conditioning. Suppose both L_∞ and k are random with densities $p(L_\infty)$ and $q(k)$ respectively. Then the conditional distribution of l given L_∞ and k, $h(l \mid L_\infty, k)$, is normal. To determine the unconditional distribution of l requires a double integration, namely

$$\iint h(l \mid L_\infty, k)\, p(L_\infty)\, q(k)\, dL_\infty\, dk \qquad (3)$$

This reduces to a single integration if either L_∞ or k is fixed (or if L_∞ has a normal distribution). Even for a single integration, computing (3) for every fish can be very time-consuming.

In generating age-length data, two sets of model parameter values were chosen – one that corresponds to fairly low variability (a coefficient of variation[1] of approximately 0.2), and one that corresponds to much higher variability (a coefficient of variation of approximately 0.4). In all cases, we kept the mean value of L_∞ at 200, the mean value of k at 0.2, and the value of a_0 at 0. For the low-variability case, the parameter values we chose for the five models were as follows:

---

[1] The coefficient of variation for a data set was calculated as $\sqrt{\sum_{r=1}^{2}\sum_{i=1}^{n}\left(\frac{l_{ri}-E(l_{ri})}{E(l_{ri})}\right)^2}$, where r indexes release or recapture and i indexes the fish.

a) $L_\infty = 200$, $k = 0.2$, $\sigma = 10$

b) $L_\infty = 200$, $k = 0.2$, $\sigma = 20$, $\theta = 0.6$

c) $\mu_\infty = 200, \sigma_\infty = 15$, $k = 0.2$, $\sigma = 8$

d) $L_\infty = 200$, $\mu_k = 0.2$, $\sigma_k = 0.03$, $\sigma = 7$

e) $\mu_\infty = 200$, $\sigma_\infty = 15$, $\mu_k = 0.2$, $\sigma_k = 0.03$, $\sigma = 5$

For the high-variability case, the parameter values we used were:

a) $L_\infty = 200$, $k = 0.2$, $\sigma = 20$

b) $L_\infty = 200$, $k = 0.2$, $\sigma = 40$, $\theta = 0.6$

c) $\mu_\infty = 200, \sigma_\infty = 35$, $k = 0.2$, $\sigma = 15$

d) $L_\infty = 200$, $\mu_k = 0.2$, $\sigma_k = 0.05$, $\sigma = 15$

e) $\mu_\infty = 200$, $\sigma_\infty = 35$, $\mu_k = 0.2$, $\sigma_k = 0.05$, $\sigma = 9$

Figure 1 shows how the error structures of model a) through e) differ in their patterns across ages. Although we have displayed the results for the low-variability parameter values, the general pattern is the same for the high-variability case as well.

To carry out the simulations, we first generated age data as described below. We then generated corresponding length data according to model a) initially, using the low-variability parameter values. We fitted the data five times, assuming each of models a) to e) to be true. This was repeated for models b) to e). Finally, the whole procedure was repeated using the high-variability parameter values. In all cases, 100 simulated data sets consisting of 1000 age-length points were fitted.

We initially generated ages according to a uniform distribution over the interval 0.1 to 20 years. For a VB curve with $L_\infty = 200$, $k = 0.2$, and $a_0 = 0$, the asymptotic length is achieved around age 20, so this choice for an age distribution gives rather comprehensive growth information. In order to see how much the age distribution affects the results, we also generated ages according to a lognormal distribution with mean and standard deviation on the log scale of 1 and 0.7 respectively. This gives a highly right-skewed distribution with a median of 2.7 years and a 95th percentile of 8.6 years. The actual age distribution expected in a field study will depend on the species and the sampling procedures used; almost any distribution seems possible. For southern bluefin

tuna, the assumption of a uniform distribution that spans the range of common ages is fairly realistic.

Evaluation methods

In order to evaluate how well a model performed, we calculated the mean of the parameter estimates over all 100 runs and compared these to the true parameter values. We also calculated the average difference in length between the 100 fitted mean curves and the true mean curve as a function of age, a, namely

$$g(a) = \frac{1}{100}\sum_{i=1}^{100}\left(\hat{L}_{\infty,i}(1-\exp(-\hat{k}_i(a-\hat{a}_{0,i})))-200(1-\exp(-0.2a))\right). \qquad (4)$$

A plot of $g(a)$ versus a is a useful tool to evaluate how well a model fits. From this plot, we can determine the maximum error in the fitted length at age. More generally, we can visualize the fit across a range of ages. The latter is important in cases where a model has a very large error at a particular age, or range of ages, but fits well elsewhere.

The above methods assess how well the mean growth curve is being fitted. Another evaluation method, which indicates the overall goodness of fit of the models to the data, is to compare likelihood values. For each of the five assumed models, we calculated the average negative log-likelihood over the 100 runs. We expect that the true model will have the smallest average negative log-likelihood value; however, this is not necessarily the case when the true model is nested within another model. For example, if the true model has a random k, then when we fit the data assuming a random L_∞ and k, we can get an equally good fit. In these cases, taking the number of parameters into account will most often result in the true model coming out the winner. Thus, we also calculated the average Akaike's information criterion (AIC) value for the purpose of comparison (Akaike 1974).

Tag-recapture data

In tag-recapture studies, the length of a fish on release and recapture (l_1 and l_2) are measured and recorded, as are the times of release and recapture (t_1 and t_2). Because age is unknown, the way to model the data is not as clear-cut now. We chose to use the maximum likelihood method of Laslett et al. (2002), which models the joint density of l_1

and l_2, since it can accommodate a wide range of error structures. Briefly, this method models the age at release relative to the time of theoretical length zero, $t_1 - t_0$, as a random variable denoted by A. For the von Bertalanffy growth curve, the model is formulated as

$$l(t) = L_\infty(1-\exp(-k(A+t-t_1))) + \varepsilon(A+t-t_1) \quad (5)$$

for $t > t_1 - A$. Then the release and recapture lengths can be expressed as

$$l_1 = L_\infty(1-\exp(-kA)) + \varepsilon(A)$$

and

$$l_2 = L_\infty(1-\exp(-k(A+t_2-t_1))) + \varepsilon(A+t_2-t_1).$$

Again, $\varepsilon(A+t-t_1)$ represents process error and is assumed to be independent random normal with mean 0 and variance $\sigma^2(A+t-t_1)$. In models where L_∞ and/or k are random, we assume L_∞, k, and A are all independent of each other as well as independent of the process error.

To derive the likelihood function, we need to know the joint density of l_1 and l_2. First consider the joint likelihood conditional on A. When L_∞ and k are fixed effects, the joint density of l_1 and l_2 given A is bivariate normal. This is true even if L_∞ is a random normal variable. If k is random, we take the same approach as we did with the direct age-length simulations and assume that it has a gamma distribution. As such, we can calculate the exact expectations and variances of l_1 and l_2 given A, then make the assumption that the joint density of l_1 and l_2 given A is approximately bivariate normal. Once we have the conditional density, the derivation of the (unconditional) likelihood is straightforward, involving a single integration over A. See Laslett et al. (2002) for the exact formulation.

The exact joint density of l_1 and l_2 can be calculated for any distributions of L_∞ and k by conditioning on the random parameters and then integrating (analogously to the direct age-length case). However, calculation of the likelihood is already slow since it involves a single integration for each fish; further integrations would be very expensive (and perhaps unfeasible) time-wise to perform.

We carried out simulations on tag-recapture data using the same five model variations as we did for the direct age-length simulations. For every combination of true and assumed models, 100 simulated data sets consisting of 500 pairs of release and recapture information were fitted.

We generated release ages, A, using a lognormal distribution with mean and standard deviation on the log scale of 0.5 and 0.3 respectively. This translates to a mean age of release of 1.7 years and a standard deviation of 0.5 years. The times at liberty were generated according to a gamma distribution with shape parameter 3.0 and rate parameter 0.5, giving an average time at liberty of 6 years and 95% of the recaptures occurring within 12 years. Corresponding release and recapture lengths were generated according to each of the models using the high-variability parameter values. For conciseness, we only present the results for one set of parameters; we chose the high-variability case because it accentuates the problems in the model fits where they exist.

The same evaluation methods were used, with a slight modification to the average error in length formula, $g(a)$, given in equation (4). In tag-recapture simulations we do not get an estimate of a_0; instead we get an estimate of the parameters for the lognormal distribution of A. Thus, we calculate the average difference in length between the fitted and true growth curve as a function of age relative to a_0, say α, in which case the function is

$$g^*(\alpha) = \frac{1}{100}\sum_{i=1}^{100}\left(\hat{L}_{\infty,i}(1-\exp(-\hat{k}_i\,\alpha)) - 200(1-\exp(-0.2\alpha))\right).$$

Results

Direct age and length data using a uniform age distribution

Before discussing the results, it may be of interest to look at a typical data set for each of the model variations a) to e), generated assuming a uniform age distribution over 0.1 to 20 years. Figure 2 shows data corresponding to the low-variability parameter values, and Figure 3 shows data corresponding to the high-variability parameter values. The data are very comprehensive, giving good information about both the asymptotic length and the rate of growth. We can see how the different patterns in the error

structures, as illustrated in Figure 1, carry through to the data. The difference in variability between the data generated using the low-variability parameter values and the high-variability parameter values is apparent. The low-variability data is more representative of the age-length data seen for southern bluefin tuna. We imagine it is more likely to represent the variability in length-at-age for other species as well; however, for completeness, we consider a more extreme situation as well.

We first present the results for the low-variability case. To see how well each of the assumed models estimates the true mean growth curve, we plotted the average error in the fitted mean length, $g(a)$, versus age, a (Figure 4). As we expect, the true model estimates the mean growth curve accurately in all cases, even for models d) and e) where an approximation was used for the likelihood. More interestingly, we see that in almost all cases the incorrect models estimate the mean growth curve equally well. In the few cases where the fitted model shows an error – this occurs when the true model has increasing process error and when the true model involves a random k – the error is less than 2 cm across all ages shown. The estimates of the growth curve parameters (namely μ_∞, μ_k, and a_0) reinforce the observation that the mean curve is estimated well regardless of the true model and the model being assumed (Table 1).

Of course, this does not mean that all models describe the data equally well. With respect to the AIC values, the true model gave the best fit in all cases (Table 1). This reflects the fact that the incorrect models are generally not capable of capturing the error structure; that is, they do not explain the variability in the data very well. There are a few exceptions. Clearly when the true model is nested within another, the other model always comes a close runner-up. For example, when the true model has constant process error, all other models have similar AIC values. Likewise, when the true model is the random L_∞ model or the random k model, then the model with both a random L_∞ and k fits the data just as well. The more interesting exceptions are that the random L_∞ and k model captures the error structure of the increasing process error model fairly well, and vice versa. Also, the random L_∞ model provides a reasonable fit to the increasing process error model, and vice versa. For all other models, the AIC value is considerably larger than the best fit. Nevertheless, the researcher's primary interest may be the mean growth

of the population, and this is being estimated without bias regardless of which model is assumed.

We now turn to the results for the high-variability simulations (Table 2; Figure 5). We have kept the y-axis scale the same in the plots of the low- and high-variability results for easy comparison. For the most part, the observations made for the low-variability case remain true. A notable exception is that the random k model shows a significant bias when being fitted to the model with increasing process error. Furthermore, models that showed a small bias in the low-variability simulations now show a larger bias and the nature of the bias, while still the same, is more obvious. In particular, the random L_∞ and k model being fitted to the increasing process error model slightly overestimates μ_∞, whereas the random L_∞ model slightly underestimates it. Also, any of the incorrect models being fitted to the random k model (with the exception of the random L_∞ and k model within which it is nested) underestimate both μ_∞ and μ_k. Similarly, all of the incorrect models show biases when being fitted to the random L_∞ and k model; however, the nature of the biases differs between them.

Again, a model that estimates the mean growth curve accurately does not necessarily provide a good overall fit to the data. In fact, if we use the AIC value as our measure of goodness-of-fit, then many of the models that show a bias in their estimate of the mean growth curve actually describe the data better than some of the models that get the mean curve right (Table 2). For example, consider the case when the true model has increasing process error. Then the model with constant process error is the only other model that estimates the mean growth curve without a noticeable error. However, the AIC value for the constant error model is much larger than the AIC value for either the random L_∞ model or the random L_∞ and k model.

Direct age and length data using a lognormal age distribution

Our next step is to see how the results differ when we use age and length data with less extensive coverage. We again start by plotting typical age-length data sets for each of the five model variations, this time with ages generated according to a lognormal distribution with mean and standard deviation on the log scale of 1 and 0.7 respectively.

Figure 6 shows data corresponding to the low-variability parameter values, and Figure 7 shows data corresponding to the high-variability parameter values. The data is far less comprehensive than when a uniform distribution was used to generate the ages. In particular, growth information for older fish is lacking, which not only makes the mean curve (in particular the asymptotic length) more difficult to estimate, but also obscures the error structure.

The low-variability and high-variability simulation results show almost identical patterns, with the magnitude of the errors being significantly larger for the high-variability case. This observation is true with respect to the mean growth curve, and is apparent if we compare plots of the errors in the fitted mean length for the low- and high-variability simulations (see Figures 8 and 9 – note that y-axis scales are different this time since the magnitude of the errors is very different). It is also true for the overall fits of the models to the data, as indicated by the fact that the ranking of the AIC values for the five models fitted to any true model is the same between the low- and high-variability results (Tables 3 and 4). Thus, we will discuss the errors for both cases collectively, keeping in mind that the size of the errors for the low-variability case are generally less than 4 cm and not likely to be of real concern whereas the errors for the high-variability case are in the order of three times larger.

The random k model does not fit very well when the true model is the increasing process error model, the random L_∞ model, or the random L_∞ and k model. In all three cases, the mean curve is estimated poorly (μ_∞ is overestimated and μ_k is underestimated), and the overall fit to the data as measured by the AIC value is also poor. In terms of estimating the mean growth curve, the random k model produces the most notable errors; however several other models also show some biases. We will not specify all cases here, as they can be ascertained from the tables and figures.

In comparison to the simulation results for uniformly distributed ages, the errors are of much greater magnitude. In fact, the magnitude of the errors for the low-variability simulations using lognormal ages is in line with the magnitude of the errors for the high-variability simulations using uniform ages. Not only are the sizes of the errors similar in these two situations, but the patterns of the errors are also very similar in

general. One noticeable difference is that the bias in the fit of the random k model to the random L_∞ model and to the random L_∞ and k model is quite a bit larger. A more subtle difference is the shape of the error across ages when the true model involves a random k parameter – the error curves tend to be more rounded and have larger errors at young ages when the ages are uniformly distributed compared to when the ages are lognormally distributed. This shape difference results from the fact that both μ_∞ and μ_k are underestimated when the ages are uniform, but only μ_∞ is underestimated when the ages are lognormal.

Tag-recapture data

So far we have only considered the consequences of assuming various error models when fitting direct age and length data. Because tag-recapture data is a common source of growth information for many species, we take an abridged look at how the results change when tag-recapture data is used.

A typical data set generated according to each of the five model variations using the high-variability parameter values is shown in Figure 10. The amount of growth information available diminishes with age – a feature we would expect in most tag-recapture studies.

The mean parameter estimates are presented in Table 5, and plots of the mean error in length at age (i.e. $g^*(\alpha)$ versus α) are shown in Figure 11. The results are somewhat similar to those obtained from the direct age and length data in the case of high-variability and lognormal ages (for which growth information also diminishes with age). In both cases, incorrectly assuming a random k model produced the largest biases in the estimated mean growth curve, and the errors in length at age were around the same magnitude. The differences include:

- With tag-recapture data, all models except the random k model estimated the mean curve accurately when the true model had increasing process error; this was not true with direct age-length data for which the random L_∞ model and the random L_∞ and k model also showed biases (of much smaller magnitude than the random k model).

- With tag-recapture data, the models with constant process error and increasing process error showed fairly large biases when fitted to the model with both a random L_∞ and k, and to a lesser extent so did the increasing process error model fitted to the model with a random L_∞. None of these biases existed with the direct age-length data.
- The nature of the biases differs somewhat. For tag-recapture data, the tendency is for L_∞ to be overestimated and k to be underestimated; this leads to S-shaped error-in-length plots that transition from a negative error to a positive error with age. For the direct age-length data, this pattern is only present when incorrectly fitting the random k model. Otherwise k tends to be estimated well, and the biases are the result of L_∞ being underestimated.

Discussion

The consequences of assuming an incorrect error structure for a growth model are dependent on the type of data being modelled; for this reason we considered both direct age and length data and tag-recapture data in our simulations. The results will also depend on the variability and completeness of the data. With direct age and length data, it is feasible to have comprehensive growth information covering all ages and lengths; this is less likely for tag-recapture data because it would require fish of all ages to be tagged or else long times at liberty to be common. The amount of variability in length-at-age between individuals will depend on the species.

For the direct age and length data, we carried out simulations for four cases, using two levels of data variability (low and high) and two levels of data coverage (complete and incomplete). While there is obviously a continuum of situations between those considered, results for these situations can be inferred from the results presented. For the sake of brevity, we only considered one case for tag-recapture data, that of high variability and fairly comprehensive data coverage. We simulated tag-recapture data that diminished with age, since this is an expected feature of most tag-recapture studies, however the times at liberty that we generated gave more complete data coverage than might be expected in many studies. We ran some simulations with much shorter times at

liberty (maximum ages of approximately 10 years) and, not surprisingly, the errors in the mean length-at-age increased where present. However, the errors within the range of the data were generally of the same magnitude as the errors obtained using long times at liberty; it was beyond the range of the data that large errors sometimes occurred.

It is difficult to concisely summarize all of the results obtained, however a few observations stand out. When considering direct age and length data, most of the biases occurred when incorrectly assuming a random k model, and these biases were probably only large enough to be of concern in the case of high-variability data and incomplete data coverage. Otherwise, assuming any of the models that we presented gave a reasonable estimate of the mean growth curve, regardless of the true model. A similar observation can be made regarding the tag-recapture simulations – the largest errors occurred when incorrectly fitting a random k model. The only other errors of a similar magnitude occurred when fitting the constant process error model and the increasing process error model to the model with both a random L_∞ and k. On the other hand, the errors in the mean growth curve obtained from fitting any of the incorrect models to the random k model were not severe, regardless of the type of data or the case being considered. This would suggest that in the absence of knowledge about the true error structure, it is generally wise not to assume a random k model.

For the tag-recapture simulations, an interesting outcome resulted from modelling the release age as a random variable. The fitting routine is able to manipulate the distribution of the release ages to make the data better agree with the error structure of the model being assumed. There were many cases where the parameter estimates for the distribution of A were highly biased, and this occurred even in cases where the mean growth curve was estimated well. Realistic bound constraints could be put on the parameters of A based on prior knowledge about the size of the fish that were released.

Our investigation of model selection using Akaike's information criterion proved to be fairly predictable in qualitative terms. Histograms of the best fitting models for the direct age and length simulations using the low-variability parameter values and lognormal ages are presented in Figure 12. The same results for the high-variability parameters are shown in Figure 13. In the vast majority of cases, AIC chose the correct style of model, the only exception being the case when the true model was e), in which

L_∞ and k are both random. In this case, AIC confused models b) and e). According to Figure 1, the curves of standard deviation versus the mean are somewhat similar for these models. Hence the patterns in Figures 12 and 13 can be interpreted as a tendency for AIC to choose the most parsimonious model that fits the data. In particular, L_∞ and k are both random only if necessary. When a less complex model is chosen, it has a similar mean-variance relationship to the true model. Very similar remarks apply when considering the results from the direct age and length simulations using uniform ages (not shown). The results in Figure 14 for the tag-recapture data are harder to explain. The AIC often chooses a more complex model than the truth. The reason for this is unknown, but it almost certainly reflects the flexibility of the tag-recapture model, which includes parameters modelling the time to capture in addition to the growth model and error structure parameters. The results suggest that more hard information should be included in the tag-recapture model, such as realistic constraints on the release ages and prior distributions on the growth parameters. Bayesian methods of model fitting might be required.

References

Fabens, A.J. 1965. Properties and fitting of the von Bertalanffy growth curve. Growth **29**: 265-289.

Hampton, J. 1991. Estimation of southern bluefin tuna *Thunnus maccoyii* growth parameters from tagging data, using von Bertalanffy models incorporating individual variation. Fish. Bull. U.S. **89**: 577-590.

Laslett, G.M., Eveson, J.P., and Polacheck, T. 2002. A flexible maximum likelihood approach for fitting growth curves to tag-recapture data. Can. J. Fish. Aquat. Sci. **59**: 976-986.

Maller, R.A. and deBoer, E.S. 1988. An analysis of two methods of fitting the von Bertalanffy curve to capture-recapture data. Aust. J. Freshwater Res. **39**: 459-466.

Sainsbury, K.J. 1980. Effect of individual variability on the von Bertalanffy growth equation. Can. J. Fish. Aquat. Sci. **37**: 241-247.

Wang, Y.-G., Thomas, M.R., and Somers, I.F. 1995. A maximum likelihood approach for estimating growth from tag-recapture data. Can. J. Fish. Aquat. Sci. **52**: 252-259.

Table 1. Mean parameter estimates for the direct age and length simulations using the low-variability parameter values and assuming a uniform age distribution over the interval 0.1 to 20 years. The average negative log likelihood and Akaike's information criterion (AIC) are also given. All values are averaged over the 100 simulation runs.

True model	Assumed model	μ_∞	σ_∞	μ_k	σ_k	a_0	σ	θ	-log likelihood	AIC
a)	a)	200.0	0.0	0.200	0.000	0.00	10.0	0.00	3717.4	7442.7
a)	b)	200.0	0.0	0.200	0.000	0.00	10.0	0.02	3717.1	7444.2
a)	c)	200.0	1.6	0.200	0.000	0.00	9.8	0.00	3717.1	7444.2
a)	d)	200.1	0.0	0.200	0.004	0.00	9.9	0.00	3717.2	7444.4
a)	e)	200.1	1.9	0.200	0.005	0.00	9.6	0.00	3716.9	7445.7
b)	a)	200.1	0.0	0.200	0.000	0.00	17.0	0.00	4253.2	8514.5
b)	b)	200.0	0.0	0.200	0.000	0.00	20.0	0.60	4180.9	8371.8
b)	c)	199.7	20.4	0.201	0.000	0.00	5.8	0.00	4189.6	8389.2
b)	d)	200.1	0.0	0.200	0.001	0.00	17.0	0.00	4253.3	8516.5
b)	e)	200.7	19.4	0.200	0.025	0.00	3.4	0.00	4182.2	8376.5
c)	a)	200.2	0.0	0.199	0.000	-0.01	14.4	0.00	4083.8	8175.6
c)	b)	200.5	0.0	0.197	0.000	-0.03	15.8	0.34	4051.0	8112.1
c)	c)	200.2	15.0	0.199	0.000	-0.01	7.9	0.00	4044.4	8098.8
c)	d)	200.2	0.0	0.199	0.001	-0.01	14.4	0.00	4083.8	8177.7
c)	e)	200.3	15.0	0.199	0.006	-0.01	7.7	0.00	4044.2	8100.4
d)	a)	199.3	0.0	0.198	0.000	-0.01	10.3	0.00	3749.5	7506.9
d)	b)	199.3	0.0	0.198	0.000	-0.01	10.3	0.01	3749.4	7508.8
d)	c)	199.3	0.0	0.198	0.000	-0.01	10.3	0.00	3749.5	7508.9
d)	d)	200.1	0.0	0.200	0.030	0.00	6.9	0.00	3712.2	7434.3
d)	e)	200.1	1.3	0.200	0.030	0.00	6.6	0.00	3711.9	7435.8
e)	a)	199.3	0.0	0.198	0.000	-0.01	15.0	0.00	4124.2	8256.5
e)	b)	199.1	0.0	0.199	0.000	0.00	16.8	0.39	4090.9	8191.8
e)	c)	198.8	15.3	0.200	0.000	0.00	8.9	0.00	4101.9	8213.8
e)	d)	199.5	0.0	0.198	0.011	-0.01	14.6	0.00	4123.6	8257.3
e)	e)	200.1	14.9	0.200	0.030	0.00	5.0	0.00	4087.2	8186.5

Table 2. Mean parameter estimates for the direct age and length simulations using the high-variability parameter values and assuming a uniform age distribution over the interval 0.1 to 20 years. The average negative log likelihood and Akaike's information criterion (AIC) are also given. All values are averaged over the 100 simulation runs.

True model	Assumed model	μ_∞	σ_∞	μ_k	σ_k	a_0	σ	θ	-log likelihood	AIC
a)	a)	200.1	0.0	0.200	0.000	0.00	19.9	0.00	4410.5	8829.0
a)	b)	200.1	0.0	0.200	0.000	0.00	20.0	0.02	4410.3	8830.5
a)	c)	200.1	3.2	0.200	0.000	0.00	19.5	0.00	4410.3	8830.5
a)	d)	200.2	0.0	0.200	0.008	0.01	19.7	0.00	4410.4	8830.7
a)	e)	200.3	3.8	0.200	0.009	0.01	19.1	0.00	4410.0	8832.0
b)	a)	200.3	0.0	0.199	0.000	0.00	34.0	0.00	4946.4	9900.8
b)	b)	200.1	0.0	0.200	0.000	0.01	39.9	0.60	4874.0	9758.0
b)	c)	198.4	39.7	0.205	0.000	0.02	12.1	0.00	4883.1	9776.2
b)	d)	209.4	0.0	0.183	0.052	-0.05	28.1	0.00	4951.9	9913.7
b)	e)	203.0	38.8	0.201	0.050	0.01	6.7	0.00	4875.4	9762.8
c)	a)	200.4	0.0	0.198	0.000	-0.02	31.6	0.00	4873.4	9754.8
c)	b)	202.2	0.0	0.190	0.000	-0.09	35.7	0.43	4827.0	9664.0
c)	c)	200.5	35.1	0.198	0.000	-0.02	14.7	0.00	4819.6	9649.1
c)	d)	201.0	0.0	0.197	0.007	-0.03	30.0	0.00	4876.6	9763.3
c)	e)	200.9	35.0	0.197	0.011	-0.02	14.3	0.00	4819.3	9650.7
d)	a)	197.9	0.0	0.195	0.000	-0.04	19.7	0.00	4397.9	8803.7
d)	b)	197.9	0.0	0.196	0.000	-0.04	19.8	0.02	4397.6	8805.1
d)	c)	197.9	0.0	0.195	0.000	-0.04	19.7	0.00	4397.9	8805.7
d)	d)	200.2	0.0	0.199	0.049	-0.01	15.0	0.00	4380.2	8770.5
d)	e)	200.1	3.4	0.200	0.049	-0.01	14.4	0.00	4379.9	8771.9
e)	a)	197.9	0.0	0.195	0.000	-0.05	30.0	0.00	4878.6	9765.2
e)	b)	197.6	0.0	0.196	0.000	-0.03	36.5	0.51	4820.5	9650.9
e)	c)	195.7	36.7	0.203	0.000	-0.01	13.0	0.00	4826.5	9662.9
e)	d)	200.5	0.0	0.191	0.027	-0.05	29.3	0.00	4876.2	9762.4
e)	e)	200.1	34.9	0.200	0.050	-0.01	8.6	0.00	4818.1	9648.2

Table 3. Mean parameter estimates for the direct age and length simulations using the low-variability parameter values and assuming a lognormal age distribution with mean and standard deviation on the log scale of 1 and 0.7 respectively. The average negative log likelihood and Akaike's information criterion (AIC) are also given. All values are averaged over the 100 simulation runs.

True model	Assumed model	μ_∞	σ_∞	μ_k	σ_k	a_0	σ	θ	-log likelihood	AIC
a)	a)	200.0	0.0	0.200	0.000	0.00	10.0	0.00	3716.2	7440.5
a)	b)	200.0	0.0	0.200	0.000	0.00	10.1	0.02	3716.0	7442.0
a)	c)	200.0	1.7	0.200	0.000	0.00	9.9	0.00	3716.0	7442.0
a)	d)	200.0	0.0	0.201	0.005	0.01	9.8	0.00	3716.0	7442.0
a)	e)	200.0	1.4	0.201	0.004	0.01	9.7	0.00	3715.9	7443.7
b)	a)	200.0	0.0	0.201	0.000	0.01	12.4	0.00	3933.1	7874.2
b)	b)	200.2	0.0	0.200	0.000	0.00	19.9	0.60	3853.1	7716.3
b)	c)	199.0	22.5	0.202	0.000	0.01	6.1	0.00	3858.0	7726.0
b)	d)	207.9	0.0	0.188	0.034	-0.03	5.6	0.00	3893.2	7796.3
b)	e)	201.3	17.8	0.200	0.025	0.00	4.4	0.00	3853.4	7718.9
c)	a)	199.9	0.0	0.201	0.000	0.00	10.8	0.00	3796.8	7601.7
c)	b)	200.6	0.0	0.199	0.000	-0.01	14.1	0.32	3768.4	7546.8
c)	c)	200.1	14.8	0.200	0.000	0.00	8.0	0.00	3765.0	7540.0
c)	d)	202.9	0.0	0.196	0.023	-0.01	8.2	0.00	3786.8	7583.7
c)	e)	200.3	14.2	0.200	0.006	0.00	7.8	0.00	3764.7	7541.4
d)	a)	198.7	0.0	0.200	0.000	-0.01	11.2	0.00	3837.3	7682.6
d)	b)	198.2	0.0	0.201	0.000	0.00	14.2	0.27	3821.4	7652.9
d)	c)	197.7	12.6	0.202	0.000	0.00	9.4	0.00	3828.6	7667.2
d)	d)	200.0	0.0	0.200	0.031	0.00	6.8	0.00	3814.5	7638.9
d)	e)	199.8	1.8	0.201	0.030	0.00	6.8	0.00	3814.3	7640.6
e)	a)	198.8	0.0	0.200	0.000	-0.01	12.4	0.00	3937.4	7882.8
e)	b)	198.3	0.0	0.201	0.000	0.00	19.0	0.52	3878.1	7766.3
e)	c)	196.9	21.6	0.203	0.000	0.00	7.0	0.00	3884.3	7778.6
e)	d)	204.5	0.0	0.192	0.036	-0.02	5.5	0.00	3894.6	7799.2
e)	e)	200.2	14.4	0.200	0.030	0.00	4.9	0.00	3876.2	7764.4

Table 4. Mean parameter estimates for the direct age and length simulations using the high-variability parameter values and assuming a lognormal age distribution with mean and standard deviation on the log scale of 1 and 0.7 respectively. The average negative log likelihood and Akaike's information criterion (AIC) are also given. All values are averaged over the 100 simulation runs.

True model	Assumed model	μ_∞	σ_∞	μ_k	σ_k	a_0	σ	θ	-log likelihood	AIC
a)	a)	200.0	0.0	0.201	0.000	0.01	19.9	0.00	4409.4	8826.8
a)	b)	200.0	0.0	0.201	0.000	0.01	20.2	0.02	4409.2	8828.3
a)	c)	200.0	3.4	0.201	0.000	0.01	19.7	0.00	4409.2	8828.3
a)	d)	200.2	0.0	0.201	0.009	0.01	19.5	0.00	4409.2	8828.3
a)	e)	200.2	2.8	0.201	0.008	0.01	19.4	0.00	4409.0	8830.0
b)	a)	200.3	0.0	0.202	0.000	0.01	24.7	0.00	4626.3	9260.5
b)	b)	200.5	0.0	0.200	0.000	0.00	39.8	0.60	4546.3	9102.5
b)	c)	189.8	39.9	0.223	0.000	0.06	13.4	0.00	4552.9	9115.8
b)	d)	229.4	0.0	0.164	0.064	-0.08	6.1	0.00	4567.0	9144.0
b)	e)	205.0	35.3	0.199	0.051	0.01	8.8	0.00	4546.6	9105.2
c)	a)	200.1	0.0	0.201	0.000	0.01	22.6	0.00	4536.4	9080.8
c)	b)	203.5	0.0	0.193	0.000	-0.03	31.8	0.41	4491.6	8993.1
c)	c)	200.5	34.7	0.200	0.000	0.00	15.0	0.00	4487.4	8984.8
c)	d)	222.1	0.0	0.169	0.050	-0.09	13.3	0.00	4512.2	9034.3
c)	e)	201.6	33.5	0.199	0.012	0.00	14.6	0.00	4487.1	8986.1
d)	a)	197.2	0.0	0.198	0.000	-0.03	20.8	0.00	4452.3	8912.5
d)	b)	196.4	0.0	0.200	0.000	-0.02	24.5	0.19	4443.9	8897.7
d)	c)	195.6	18.4	0.202	0.000	-0.01	18.6	0.00	4447.5	8905.0
d)	d)	200.3	0.0	0.199	0.048	-0.01	15.2	0.00	4440.5	8891.0
d)	e)	199.9	3.3	0.200	0.047	0.00	15.2	0.00	4440.3	8892.6
e)	a)	196.8	0.0	0.200	0.000	-0.02	23.9	0.00	4593.7	9195.4
e)	b)	196.4	0.0	0.201	0.000	-0.02	38.2	0.59	4516.4	9042.9
e)	c)	191.1	42.7	0.212	0.000	0.01	11.7	0.00	4519.7	9049.4
e)	d)	223.9	0.0	0.166	0.063	-0.09	6.8	0.00	4533.6	9077.2
e)	e)	200.6	33.8	0.200	0.050	0.00	8.7	0.00	4515.3	9042.7

Table 5. Mean parameter estimates for the tag-recapture simulations using the high-variability parameter values. The average negative log likelihood and Akaike's information criterion (AIC) are also given. All values are averaged over the 100 simulation runs.

True model	Assumed model	μ_∞	σ_∞	μ_k	σ_k	$\mu_{\log A}$	$\sigma_{\log A}$	σ	θ	-log likelihood	AIC
a)	a)	199.6	0.0	0.201	0.000	0.50	0.29	19.9	0.00	4525.1	9060.2
a)	b)	199.5	0.0	0.202	0.000	0.50	0.30	20.1	0.02	4524.9	9061.8
a)	c)	199.4	3.0	0.202	0.000	0.50	0.30	19.7	0.00	4524.9	9061.7
a)	d)	200.2	0.0	0.202	0.009	0.49	0.30	19.6	0.00	4524.5	9060.9
a)	e)	200.1	2.2	0.202	0.007	0.49	0.30	19.5	0.00	4524.4	9062.7
b)	a)	200.9	0.0	0.201	0.000	0.52	0.01	29.2	0.00	4791.6	9593.1
b)	b)	200.7	0.0	0.201	0.000	0.49	0.31	39.7	0.60	4742.6	9497.2
b)	c)	201.0	29.0	0.202	0.000	0.51	0.02	24.0	0.00	4761.2	9534.4
b)	d)	213.1	0.0	0.178	0.037	0.58	0.01	26.3	0.00	4783.9	9579.8
b)	e)	201.0	29.0	0.202	0.001	0.51	0.02	24.0	0.00	4761.2	9536.4
c)	a)	203.0	0.0	0.192	0.000	0.55	0.19	26.2	0.00	4724.0	9458.1
c)	b)	210.8	0.0	0.172	0.000	0.58	0.37	34.3	0.58	4666.0	9344.1
c)	c)	198.8	34.7	0.204	0.000	0.49	0.30	15.0	0.00	4629.4	9270.7
c)	d)	222.0	0.0	0.163	0.054	0.62	0.05	18.5	0.00	4654.1	9320.2
c)	e)	200.5	34.3	0.200	0.011	0.50	0.29	15.0	0.00	4625.9	9265.8
d)	a)	204.1	0.0	0.177	0.000	0.58	0.38	18.3	0.00	4518.4	9046.9
d)	b)	203.4	0.0	0.179	0.000	0.56	0.41	21.0	0.25	4508.3	9028.5
d)	c)	198.1	20.4	0.194	0.000	0.52	0.38	14.3	0.00	4498.3	9008.7
d)	d)	199.7	0.0	0.201	0.051	0.50	0.30	14.8	0.00	4483.9	8979.8
d)	e)	199.3	3.6	0.202	0.050	0.49	0.30	14.6	0.00	4483.9	8981.8
e)	a)	218.9	0.0	0.149	0.000	0.69	0.37	24.2	0.00	4737.3	9484.6
e)	b)	224.2	0.0	0.140	0.000	0.70	0.47	39.9	1.00	4620.1	9252.1
e)	c)	196.8	40.9	0.198	0.000	0.51	0.35	8.2	0.00	4531.1	9074.1
e)	d)	221.4	0.0	0.162	0.069	0.59	0.21	11.8	0.00	4561.3	9134.5
e)	e)	199.0	36.4	0.200	0.043	0.50	0.31	8.6	0.00	4527.1	9068.2

Figure 1. Comparison of the error structures for models a) through e). The lines show the standard deviation in length at age for the five model variations, calculated using the parameter values for the low variability case.

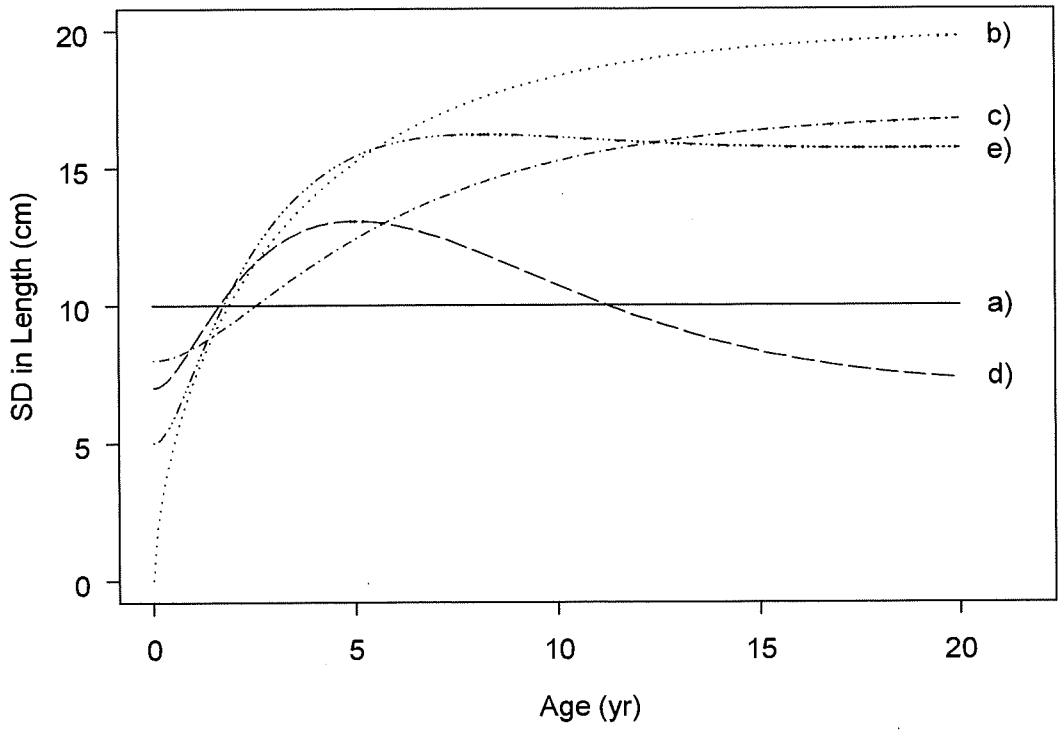

Figure 2. Examples of simulated direct age and length data sets for models a) through e), using the low-variability parameter values and assuming a uniform age distribution over the interval 0.1 to 20 years.

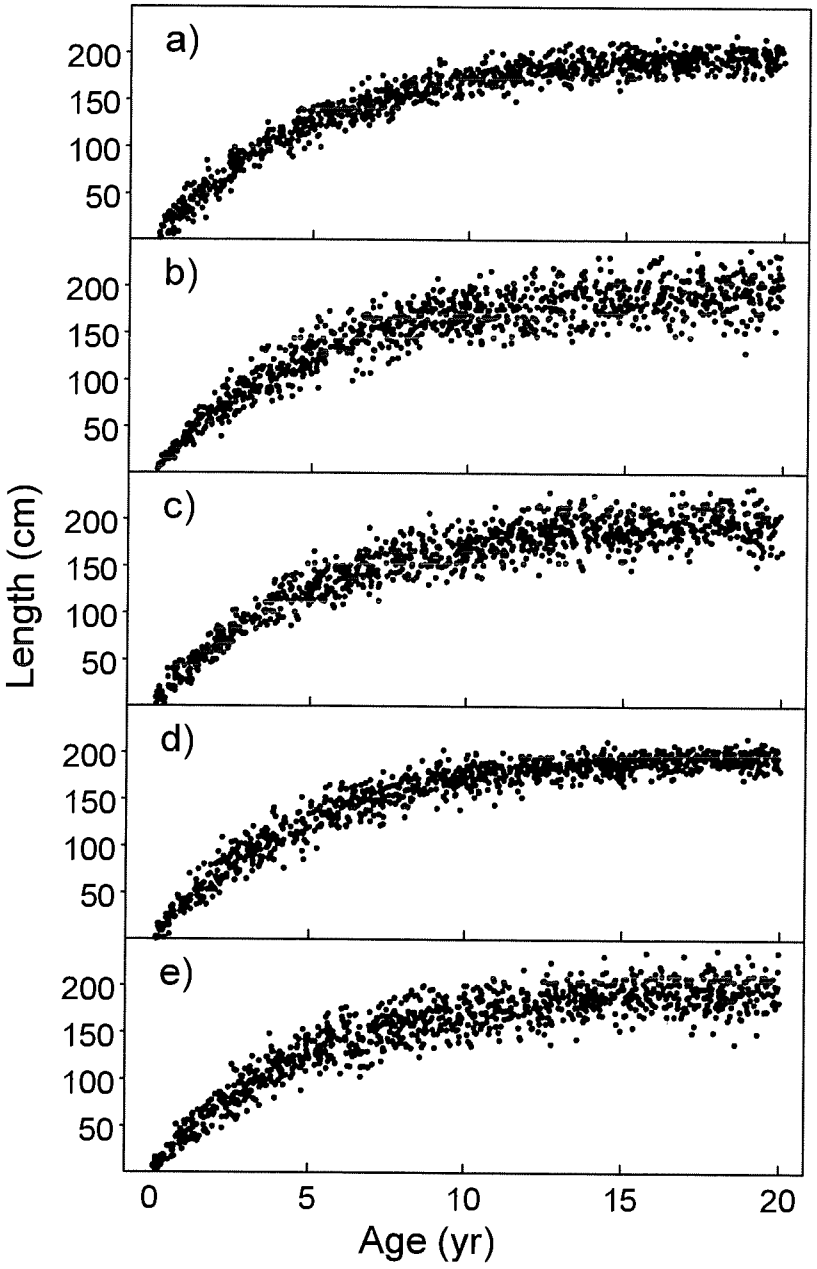

Figure 3. Examples of simulated direct age and length data sets for models a) through e), using the high-variability parameter values and assuming a uniform age distribution over the interval 0.1 to 20 years.

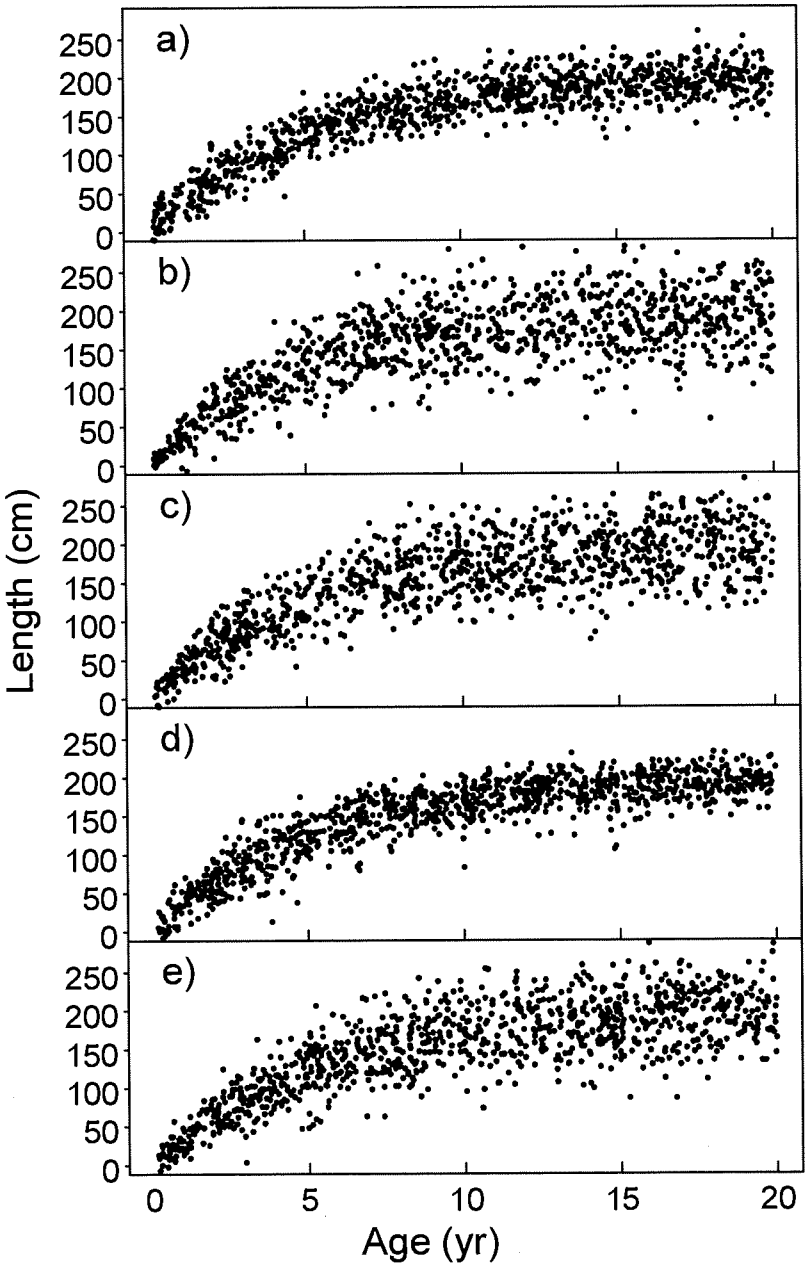

Figure 4. Results from the direct age and length simulations using the low-variability parameter values and assuming a uniform age distribution over 0.1 to 20 years. The figure shows the difference between the fitted and true mean length (averaged over 100 runs) versus age, i.e. $g(a)$ versus a. Panels a) to e) correspond to the results when the true models are models a) to e) respectively. The lines correspond to the models being assumed: — for model a); ··· for model b); –·– for model c); – – – for model d); and –···– for model e).

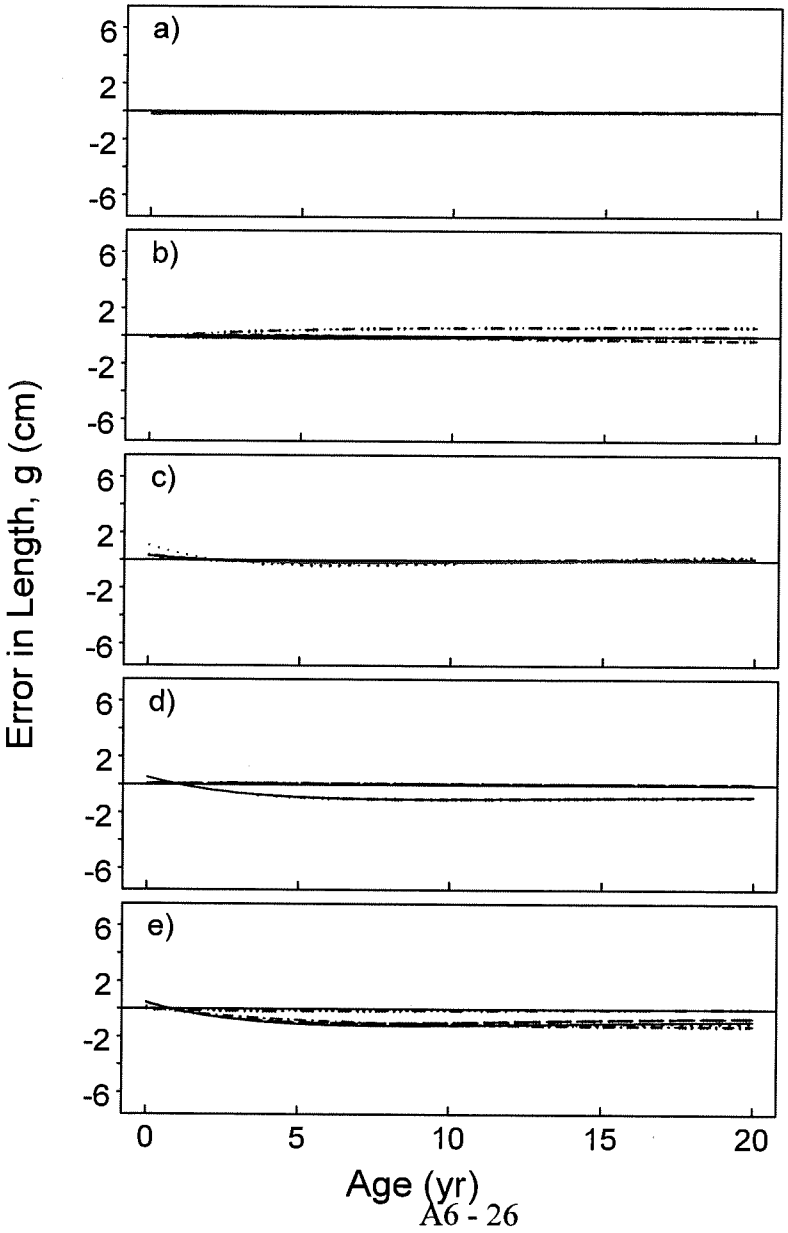

Figure 5. Results from the direct age and length simulations using the high-variability parameter values and assuming a uniform age distribution over 0.1 to 20 years. See Figure 4 for a complete description.

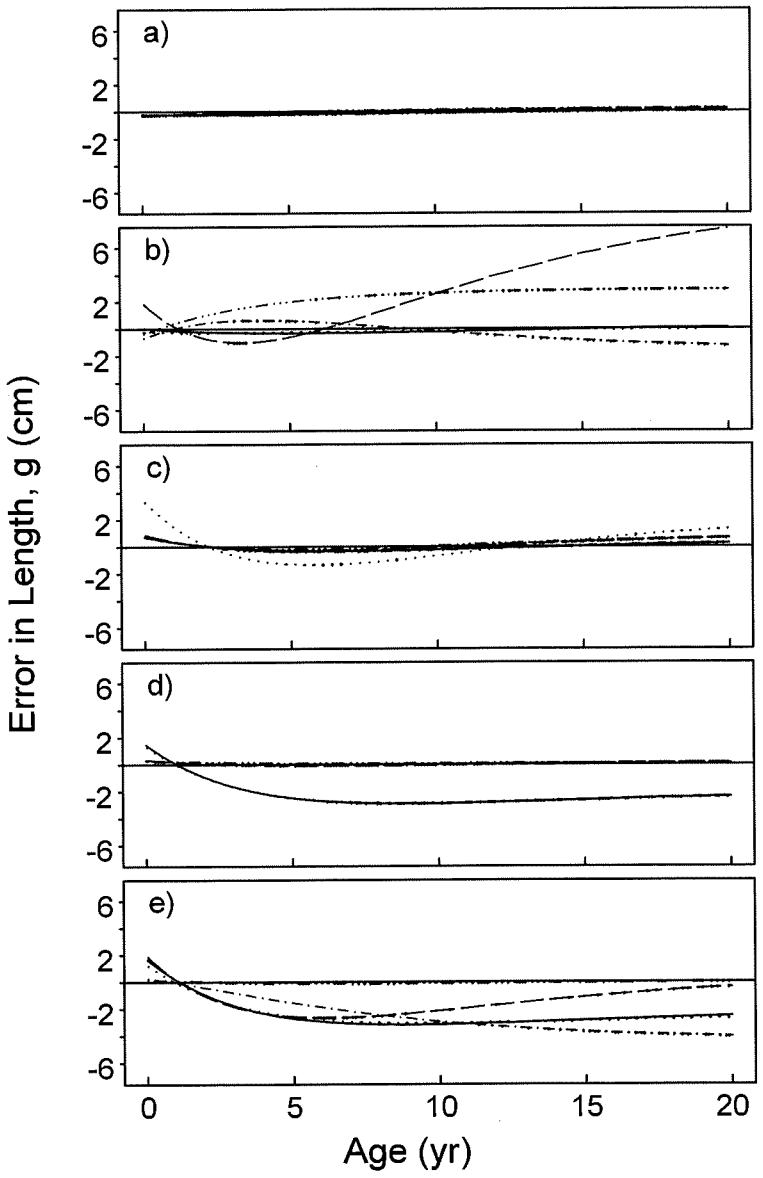

Figure 6. Examples of simulated direct age and length data sets for models a) through e), using the low-variability parameter values and assuming a lognormal age distribution with mean and standard deviation on the log scale of 1 and 0.7 respectively.

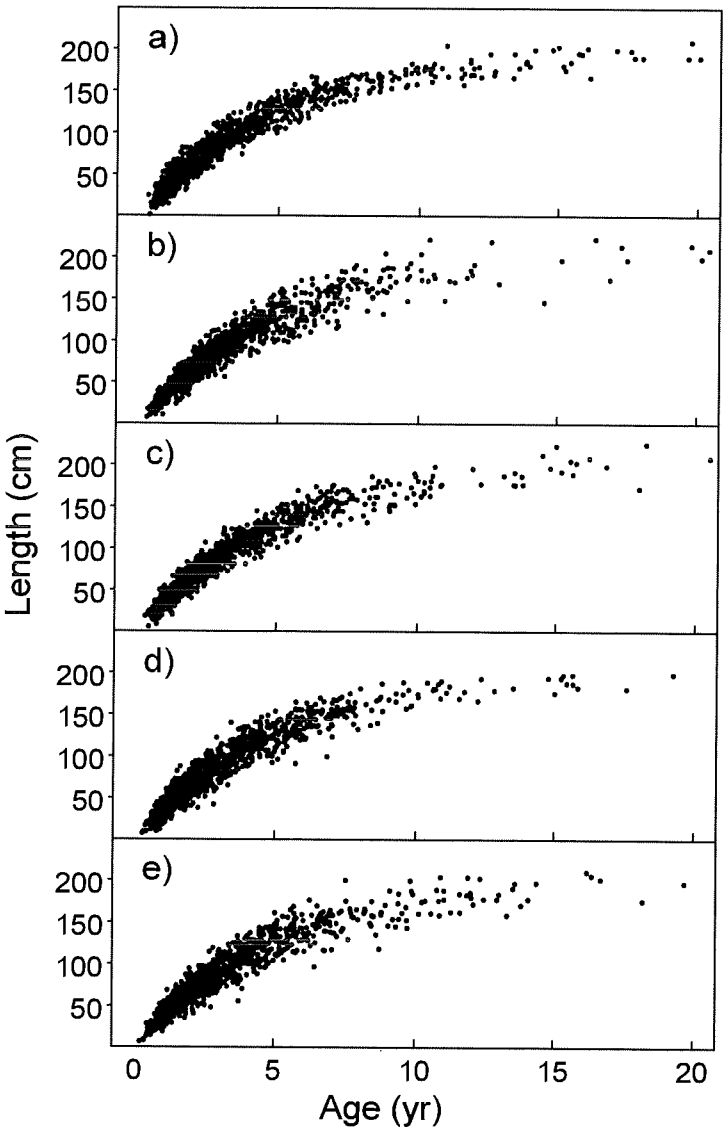

Figure 7. Examples of simulated direct age and length data sets for models a) through e), using the high-variability parameter values and assuming a lognormal age distribution with mean and standard deviation on the log scale of 1 and 0.7 respectively.

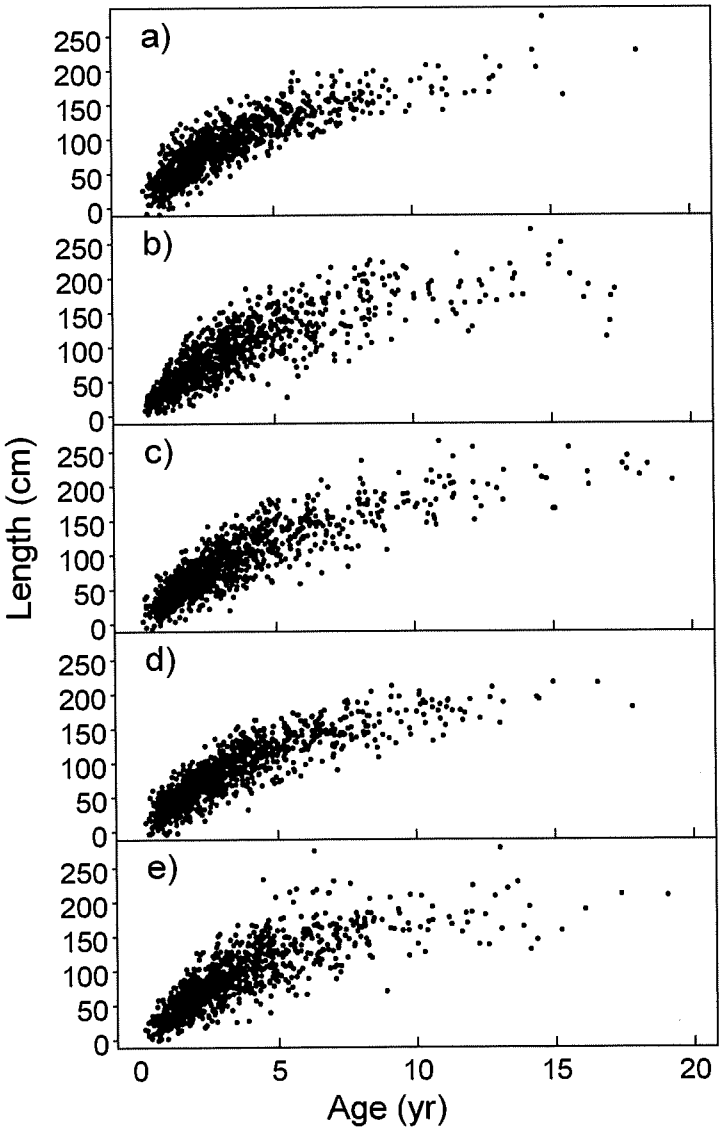

Figure 8. Results from the direct age and length simulations using the low-variability parameter values and assuming a lognormal age distribution with mean and standard deviation on the log scale of 1 and 0.7 respectively. See Figure 4 for a complete description.

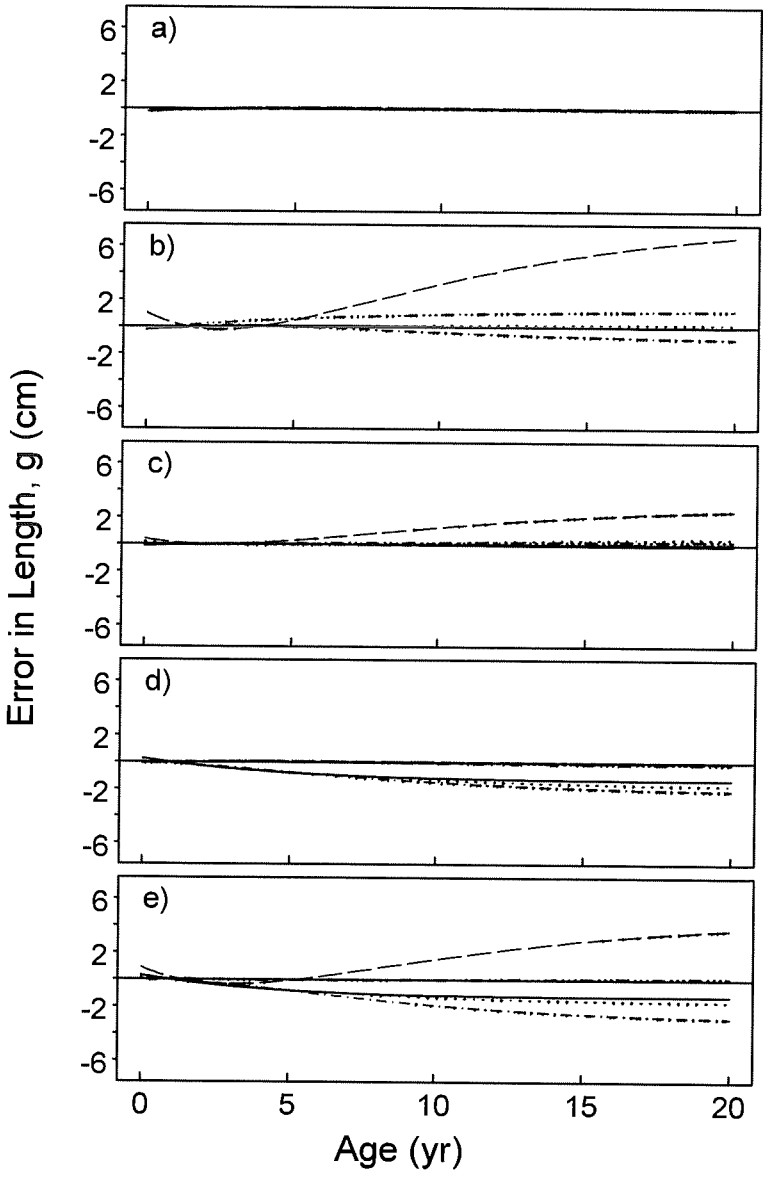

Figure 9. Results from the direct age and length simulations using the high-variability parameter values and assuming a lognormal age distribution with mean and standard deviation on the log scale of 1 and 0.7 respectively. See Figure 4 for a complete description.

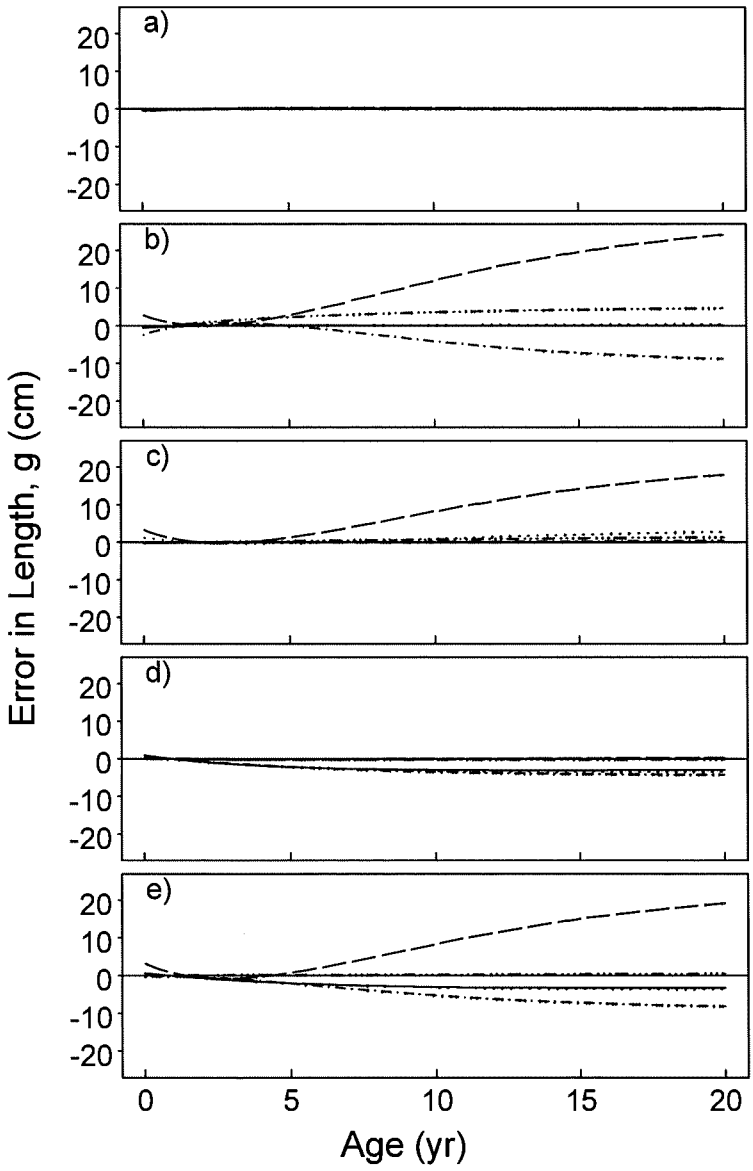

Figure 10. Examples of simulated tag-recapture growth data for models a) through e) using the high variability parameter values. The x's represent release information; the dots represent recapture information.

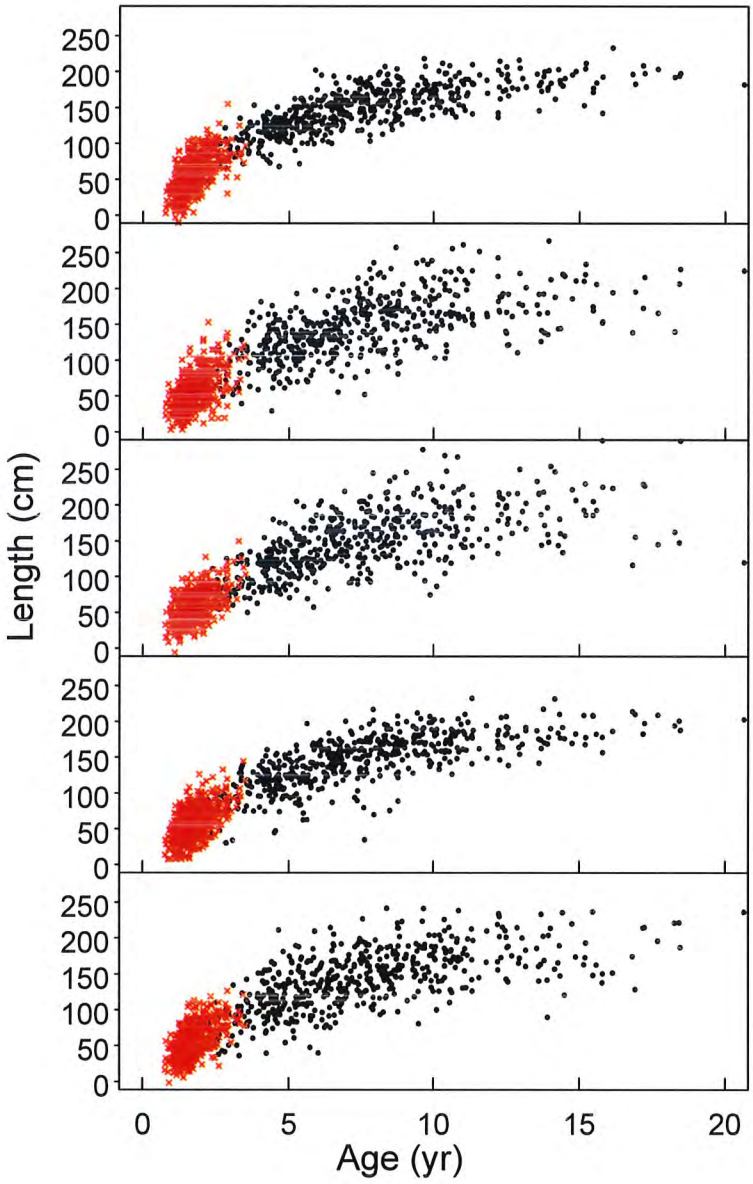

Figure 11. Results from the tag-recapture simulations using the high-variability parameter values. The details are the same as in Figure 4 except the ages are now relative to a_0, such that we are plotting $g^*(\alpha)$ versus α.

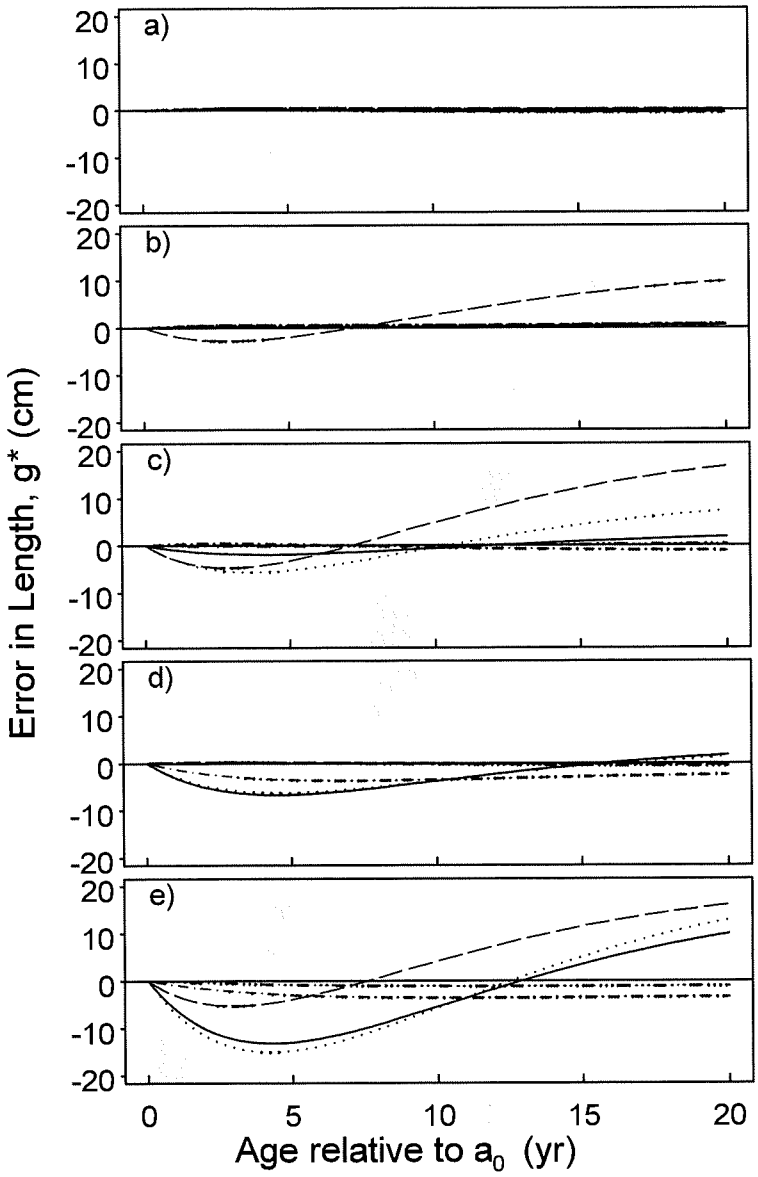

Figure 12. Histograms showing the best fitting models for the direct age and length simulations using the low-variability parameter values and lognormal ages. Moving from top to bottom, the 5 panels show the results when the true model is model a to e respectively. In panel *x*, the bars show the number of times (out of 100 simulations) that each of models a to e had the minimum AIC value when fitted to data from true model *x*.

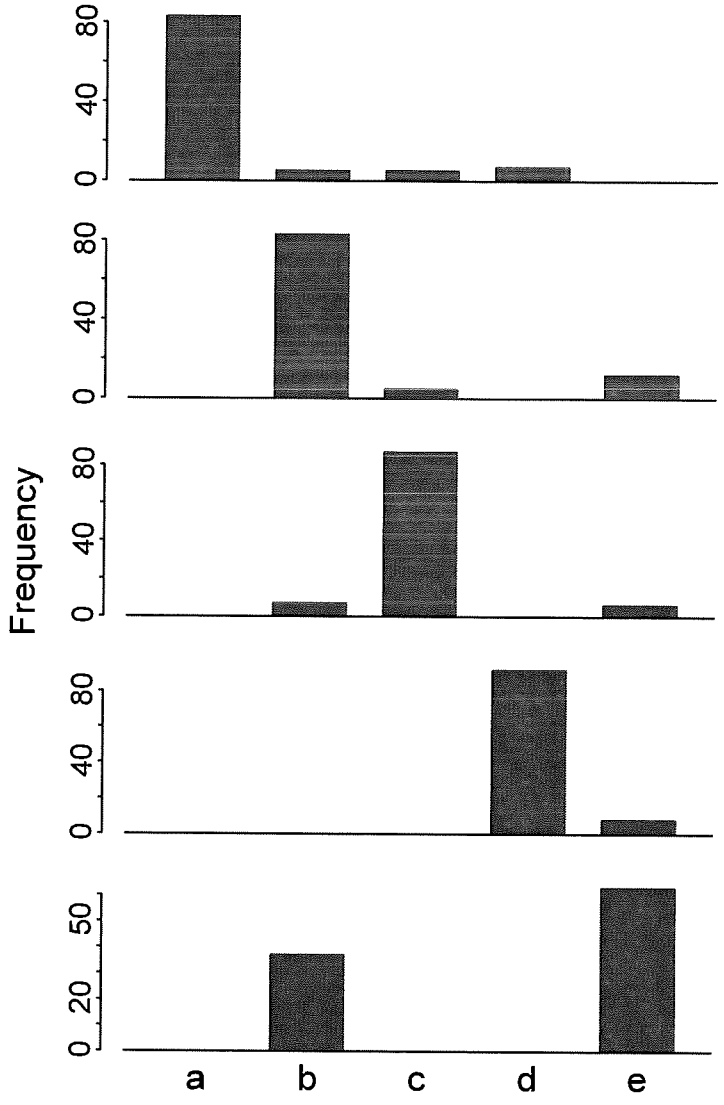

Figure 13. Histograms showing the best fitting models for the direct age and length simulations using the high-variability parameter values and lognormal ages. Moving from top to bottom, the 5 panels show the results when the true model is model a to e respectively. In panel *x*, the bars show the number of times (out of 100 simulations) that each of models a to e had the minimum AIC value when fitted to data from true model *x*.

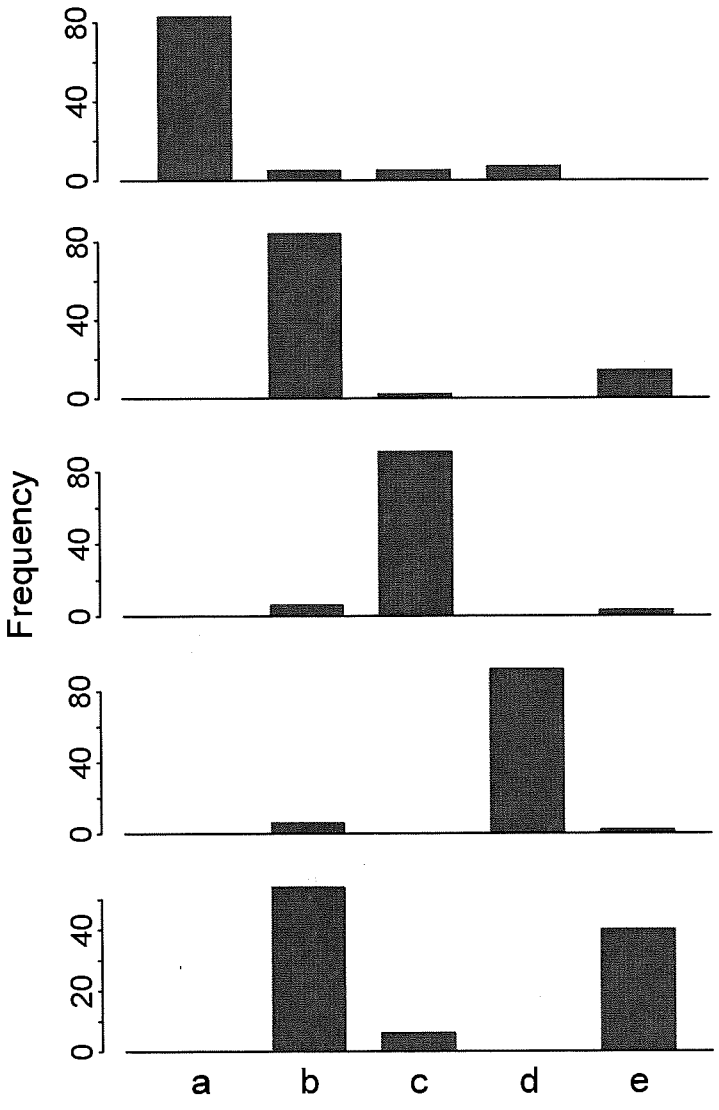

Figure 14. Histograms showing the best fitting models for the tag-recapture simulations using the high-variability parameter values. Moving from top to bottom, the 5 panels show the results when the true model was model a to e respectively. In panel *x*, the bars show the number of times (out of 100 simulations) that each of models a to e had the minimum AIC value when fitted to data from true model *x*.

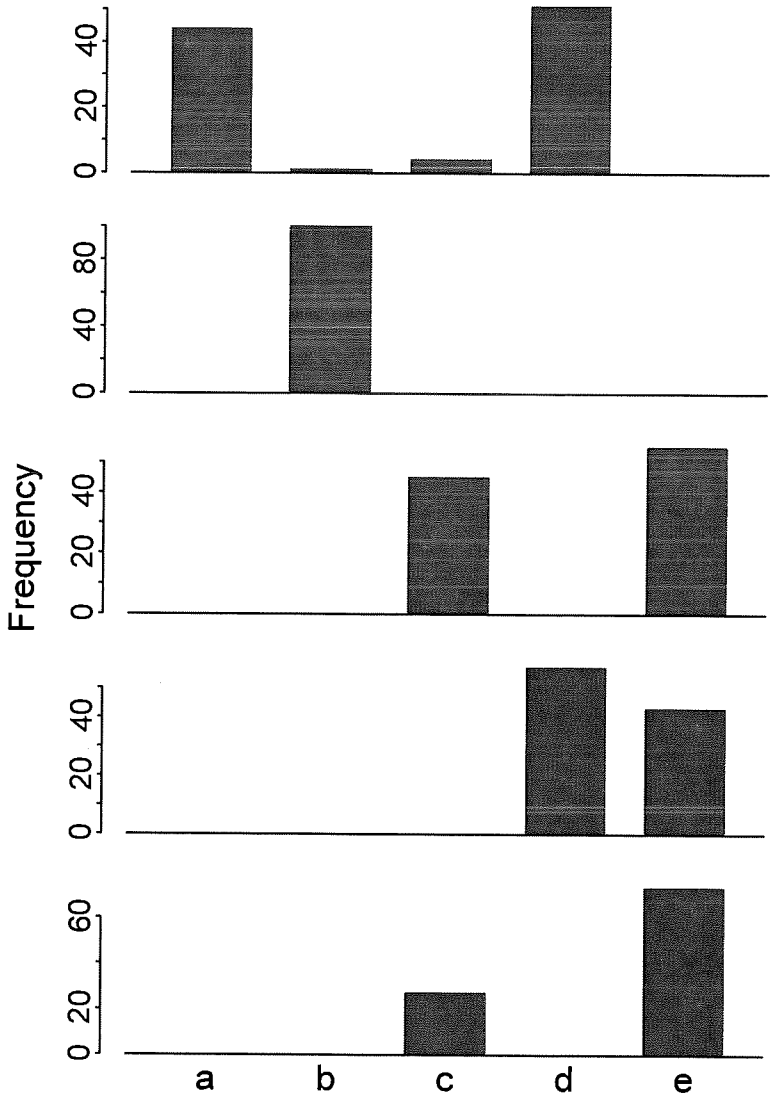

Appendix 7:

Fitting growth models to length-frequency data

Geoff M. Laslett, J. Paige Eveson and Tom Polacheck

FRDC Project 1999/104

Introduction

Commercial catch data contain important information on the growth of southern bluefin tuna. In one sense they are more informative than any other data source because commercial fishing data are more abundant and more consistent over time than data from scientific research programs. In principle, fish can be sampled for measurement every time that a boat comes in to port. This provides a regular time series of length-frequency data for the researcher to work with.

Extracting the information on growth from commercial data is not straightforward. First, a large number of age groups are potentially represented in the commercial catch. There is no quick way to calculate the age of a tuna, so length-frequency data do not come with any age attribution. For growth work the researcher has to assign the fish to age groups, either explicitly or statistically. Second, tuna are spawned over a period of several months, and nothing is known about the relative growth patterns of fish that were spawned early versus those spawned late in the season. Third, commercial fishing is not a random sampling exercise, and in one week boats can return with almost no one-year-olds, for example, but in an adjacent week the one-year-olds can be plentiful. Finally, measurement error exists and may be dependent on the measurer. There appear to be minor irregular inconsistencies in growth patterns from year to year, week to week and age-group to age-group. It is important to build methods that capture these sources of variation.

The biggest southern bluefin tuna fishery in Australia operates out of Port Lincoln in South Australia. The length-frequency data from this fishery provide information on two aspects of southern bluefin tuna growth. First, yearly growth can be estimated by comparing the average length of one-year-olds, two-year-olds, three-year-olds and so on caught at the same time. Second, the Port Lincoln fishery operates during the Southern summer, when tuna are growing fastest. Seasonal growth can be inferred by comparing the growth of a particular age-group from week to week and month to month. Other data sources, such as those derived from tag-recapture surveys and otolith studies, are usually too coarse to provide detailed

information on seasonal growth. Length-frequency data are vital for this reason alone.

This Appendix presents our method for extracting growth information from length-frequency data. Ours has some features in common with other methods presented in the quantitative fisheries' literature, but we depart from them in significant ways. In particular, we develop a two-phase approach to the analysis. In the first phase each half-month of length-frequency data is decomposed into age-groups using a Gaussian mixture model, and relevant summary statistics are extracted. In the second phase, the summary statistics are used as raw data for growth modelling. This approach allows us to explore and visualise the sources of variation in the data prior to final modelling. More direct methods are likely to overlook the many possible complications in real length-frequency data.

In this Appendix we first discuss the form of the length-frequency data to which we have access, and some of its features. Next is a critical review of the Leigh and Hearn (2000) analysis of length-frequency data, summarising our reasons for rejecting a combined analysis of the data for each season using a separate linear growth model for each age group. We outline our alternative method, in which we fit a growth model to summary statistics derived from fitting mixture models to each half-month of length-frequency data. The final section is more speculative. It discusses how we might model or understand some of the additional sources of variation in length-frequency data.

The data

Length frequency data are measurements of lengths of fish caught in a particular season at a particular location, usually from commercial fishing. For southern bluefin tuna, the data look like

Table 1: Typical length-frequency data.

catch year	period type	period #	period start	statistical area	class width	class centre	catch count
1960	H	2	01/16/1960	SA	1	57	5.8
1960	H	2	01/16/1960	SA	1	58	8.2
1960	H	2	01/16/1960	SA	1	59	11.0
1960	H	2	01/16/1960	SA	1	60	8.2
1960	H	2	01/16/1960	SA	1	61	2.8
⋮	⋮	⋮	⋮	⋮	⋮	⋮	⋮

Most columns are self-explanatory. The period type H means half-monthly: Australian data are generally recorded twice a month, but Japanese data only once, and is then listed as M. These tuna have been caught in South Australia (SA), but New South Wales and Western Australia also have tuna fisheries. The catch is divided into one centimetre classes, so that the first line says that 5.8 fish are between 56.5 and 57.5 cm in length. The reader will immediately ask: why 5.8, rather than a whole number? The number of fish is scaled up from a sample, as explained below.

We specify more exactly the definition of the half-monthly periods. The half-months start on day 1 or 16 of each month:

Table 2: Half-month indices

Period #	Period start
1	1/1
2	16/1
3	1/2
4	16/2
5	1/3

Table 2: continued

6	16/3
⋮	⋮
24	16/12

Note that February has only 28 or 29 days, so period 4 is relatively short. These period numbers are used in the output from the mixture fitting programs. In South Australia the fishing season extends from the first half of October to the second half of September the following year. For example, the 1964-65 season covers period 19 in 1964 to period 18 in 1965. Thus when analysing a season of South Australian data, period 24 $\rightarrow$ 0, 23 $\rightarrow$ -1 and so on.

There are a two major issues that arise in the analysis of length frequency data, and a number of minor issues. We discuss the major issues immediately.

Mixture of ages

The length data from a given year and area come from fish of all ages, although the fish belonging to a particular age group have been spawned over a relatively short period, and hence exhibit a limited range of lengths. In addition, the younger fish are growing fast, so the histogram of lengths will often show obvious modes for the 1, 2, 3 and 4 year-olds, but for older fish the modes cannot be distinguished. Leigh and Hearn (2000) have published a mixture decomposition method that attempts to decompose the length data into their constituent age groups. Their method is somewhat different from a widely-used industry method, MULTIFAN (Fournier *et al.*, 1990).

Scaling up of catches

Not all fish caught in a given period are measured for length, and the frequencies are scaled up so that the total catch reflects that of the whole fishery. The

scaling up is in two phases: firstly the measured sample from a landing is scaled up by the weight of fish in that landing; and secondly the catches from sampled landings are scaled by the weight of the entire catch from all landings in the fishery, to allow for landings that were not sampled.

This scaling-up means that a conventional statistical analysis is not appropriate, because the recorded catch is larger than the sampled catch. Standard error estimates from treating the recorded data as raw data would be too small, in general.

We need to correct for this scaling in the analysis if we are to obtain meaningful results. Leigh and Hearn (2000) argue for a rather complicated scaling factor, based on the variance of the mean. They assume that k landings have been sampled, and that landing i contains n_i fish of which q_i are measured. They then propose the scaling factor $\alpha = (n_r/n_s^2)\sum_{i=1}^{k} n_i^2/q_i$, where n_r is the scaled-up estimate of the total number of fish caught and $n_s = \sum_{i=1}^{k} n_i$ is the number of fish caught in the k landings. We have no information on which to base any alternative scaling factor, so we continue to use the Leigh and Hearn scaling factors in this study.

The Leigh and Hearn method

Leigh and Hearn (2000) assumed that the data were generated from a simple Gaussian mixture. For a given sample, suppose there are m_j fish of length l_j for $j = 1, \ldots, n$. Here and elsewhere m_j is the recorded catch count divided by the Leigh and Hearn scaling factor, so that m_j is effectively the number of fish in class j if a random sample of fish had been collected. The lengths are assumed to be generated from a K component mixture in which the probability density of component k is $g_k(y)$. The likelihood is

$$\prod_{j=1}^{n} \left\{ \sum_{k=1}^{K} \pi_k g_k(l_j) \right\}^{m_j} .$$

The log-likelihood is

$$h = \sum_{j=1}^{n} m_j \log \left(\sum_{k=1}^{K} \pi_k \, g_k(l_j) \right) . \qquad (1)$$

To estimate parameters, we would like to maximise the log-likelihood of the data from several samples. After considerable experimentation, it transpires that we need an optimisation method that uses first and second derivatives. Derivative-free optimisation methods for this problem may be slow and do not necessarily converge to the maximum likelihood estimates.

First derivatives of the log-likelihood

We calculate the first derivatives of the log-likelihood h with respect to the various parameters. We assume that $g_k(l_j)$ is a Gaussian density

$$g_k(l_j) = \frac{1}{\sqrt{2\pi}\sigma} \exp\left(-\frac{(l_j - \mu_k)^2}{2\sigma^2}\right).$$

Some basic tools we shall use are

$$\frac{\partial g_k(l_j)}{\partial \mu_k} = g_k(l_j)\frac{(l_j - \mu_k)}{\sigma^2} \equiv g_k(l_j)\,\eta_{jk}$$

and

$$\frac{\partial g_k(l_j)}{\partial \log \sigma} = g_k(l_j)\left(\frac{(l_j - \mu_k)^2}{\sigma^2} - 1\right) \equiv g_k(l_j)\,\theta_{jk}\,.$$

Also for convenience we define

$$S_j = \sum_{k=1}^{K} \pi_k g_k(l_j)\,.$$

Thus

$$\frac{\partial h}{\partial \mu_k} = \pi_k \sum_{j=1}^{n} m_j \frac{g_k(l_j)}{S_j}\,\eta_{jk}$$

To compute this robustly, we should use the form

$$\frac{\partial h}{\partial \mu_k} = \pi_k \sum_{j=1}^{n} m_j \frac{g_k(l_j)/g_{k(j)}(l_j)}{S_j^*}\,\eta_{jk}\,,$$

where $S_j^* = \sum_{k=1}^{K} \pi_k g_k(l_j)/g_{k(j)}(l_j)$ and $k(j)$ is the index of the maximum value of $g_k(l_j)$ for a given l_j. We shall take the robust computational forms as understood in this section.

The derivative with respect to $\log\sigma$ is

$$\frac{\partial h}{\partial \log\sigma} = \sigma\frac{\partial h}{\partial \sigma} = \sum_{j=1}^{n} m_j \frac{\sum_{k=1}^{K} \pi_k g_k(l_j)\,\theta_{jk}}{S_j}\,.$$

We have parameterised the proportions so that there are $K-1$ free parameters $x_1, \ldots, x_{K-1}$, and

$$\pi_k = \frac{e^{x_k}}{1+\sum_{l=1}^{K-1} e^{x_l}}$$

for $k = 1, \ldots, K-1$ and

$$\pi_K = \frac{1}{1+\sum_{l=1}^{K-1} e^{x_l}}\,.$$

Thus, for $k \le K-1$,

$$\begin{aligned}
\frac{\partial h}{\partial x_k} &= \sum_{r=1}^{K} \frac{\partial h}{\partial \pi_r}\frac{\partial \pi_r}{\partial x_k} \\
&= \sum_{r=1}^{K}\sum_{j=1}^{n} m_j \frac{g_r(l_j)}{S_j}\left(\pi_r I(r=k) - \pi_r\pi_k\right) \\
&= \pi_k \sum_{j=1}^{n} m_j \frac{g_k(l_j)}{S_j} - \pi_k \sum_{j=1}^{n} m_j\,.
\end{aligned}$$

Second derivatives of the log-likelihood

We now calculate the second derivatives of h with respect to the various parameters. Thus

$$\frac{\partial^2 h}{\partial \mu_k^2} = -\frac{\pi_k}{\sigma^2}\sum_{j=1}^{n} m_j \frac{g_k(l_j)}{S_j} + \pi_k \sum_{j=1}^{n} m_j \frac{g_k(l_j)}{S_j}\eta_{jk}^2 - \pi_k^2 \sum_{j=1}^{n} m_j \frac{g_k(l_j)^2}{S_j^2}\eta_{jk}^2$$

where $S_j = \sum_{l=1}^{K} \pi_l g_l(l_j)$. Also

$$\frac{\partial^2 h}{\partial \mu_k \partial \mu_s} = -\pi_k\pi_s \sum_{j=1}^{n} m_j \frac{g_k(l_j) g_s(l_j)}{S_j^2}\,\eta_{jk}\,\eta_{js}\,.$$

The second derivative with respect to $\log\sigma$ is

$$\begin{aligned}
\frac{\partial^2 h}{\partial (\log\sigma)^2} &= \sum_{j=1}^{n} m_j \frac{\sum_{k=1}^{K} \pi_k\, g_k(l_j)\,\theta_{jk}^2}{S_j} + \sum_{j=1}^{n} m_j \frac{\sum_{k=1}^{K} \pi_k\, g_k(l_j)\,(-2\theta_{jk}-2)}{S_j} \\
&\quad - \sum_{j=1}^{n} m_j \frac{\left(\sum_{k=1}^{K} \pi_k\, g_k(l_j)\,\theta_{jk}\right)^2}{S_j^2}\,.
\end{aligned}$$

The partial derivative with respect to $\log\sigma$ and μ_s is

$$\begin{aligned}\frac{\partial^2 h}{\partial \log\sigma \partial \mu_k} &= -2\pi_k \sum_{j=1}^{n} m_j \frac{g_k(l_j)\eta_{jk}}{S_j} + \pi_k \sum_{j=1}^{n} m_j \frac{g_k(l_j)\,\theta_{jk}\,\eta_{jk}}{S_j} \\ &\quad -\pi_k \sum_{j=1}^{n} m_j\, g_k(l_j)\eta_{jk} \frac{\sum_{l=1}^{K} \pi_l\, g_l(l_j)\,\theta_{jl}}{S_j^2}.\end{aligned}$$

The partial derivative with respect to $\log\sigma$ and π_k is

$$\frac{\partial^2 h}{\partial \log\sigma \partial \pi_k} = \sum_{j=1}^{n} m_j \frac{g_k(l_j)\theta_{jk}}{S_j} - \sum_{j=1}^{n} m_j\, g_k(l_j) \frac{\sum_{l=1}^{K} \pi_l\, g_l(l_j)\,\theta_{jl}}{S_j^2}.$$

We need this quantity in terms of the dummy variable x_k. Then

$$\begin{aligned}\frac{\partial^2 h}{\partial \log\sigma \partial x_k} &= \sum_{r=1}^{K} \frac{\partial^2 h}{\partial \log\sigma \partial \pi_r} \frac{\partial \pi_r}{\partial x_k} \\ &= \sum_{r=1}^{K} \frac{\partial^2 h}{\partial \log\sigma \partial \pi_r} (\pi_r I(r=k) - \pi_r \pi_k) \\ &= \pi_k \frac{\partial^2 h}{\partial \log\sigma \partial \pi_k} - \pi_k \sum_{r=1}^{K} \pi_r \frac{\partial^2 h}{\partial \log\sigma \partial \pi_r} \\ &= \pi_k \frac{\partial^2 h}{\partial \log\sigma \partial \pi_k},\end{aligned}$$

since $\sum_{r=1}^{K} \pi_r \frac{\partial^2 h}{\partial \log\sigma \partial \pi_r} = 0$.

The partial derivative with respect to μ_k and π_s is

$$\frac{\partial^2 h}{\partial \mu_k \partial \pi_s} = -\pi_k \sum_{j=1}^{n} m_j \frac{g_k(l_j)\eta_{jk} g_s(l_j)}{S_j^2}$$

when $s \neq k$. Otherwise

$$\frac{\partial^2 h}{\partial \mu_k \partial \pi_k} = \sum_{j=1}^{n} m_j \frac{g_k(l_j)\eta_{jk}}{S_j} - \pi_k \sum_{j=1}^{n} m_j \frac{g_k^2(l_j)\eta_{jk}}{S_j^2}$$

We need this quantity in terms of the dummy variable x_s. Then

$$\begin{aligned}\frac{\partial^2 h}{\partial \mu_k \partial x_s} &= \sum_{r=1}^{K} \frac{\partial^2 h}{\partial \mu_k \partial \pi_r} \frac{\partial \pi_r}{\partial x_s} \\ &= \sum_{r=1}^{K} \frac{\partial^2 h}{\partial \mu_k \partial \pi_r} (\pi_r I(r=s) - \pi_r \pi_s) \\ &= \pi_s \frac{\partial^2 h}{\partial \mu_k \partial \pi_s} - \pi_s \sum_{r=1}^{K} \pi_r \frac{\partial^2 h}{\partial \mu_k \partial \pi_s} \\ &= \pi_s \frac{\partial^2 h}{\partial \mu_k \partial \pi_s},\end{aligned}$$

since $\sum_{r=1}^{K} \pi_r \frac{\partial^2 h}{\partial \mu_k \partial \pi_r} = 0$.

The partial derivative with respect to x_k and π_s is

$$\frac{\partial^2 h}{\partial x_k \partial \pi_s} = -\pi_k \sum_{j=1}^{n} m_j \frac{g_k(l_j) g_s(l_j)}{S_j^2}$$

when $s \neq k$. Otherwise

$$\frac{\partial^2 h}{\partial x_k \partial \pi_k} = \sum_{j=1}^{n} m_j \frac{g_k(l_j)}{S_j} - \sum_{j=1}^{n} m_j - \pi_k \sum_{j=1}^{n} m_j \frac{g_k^2(l_j)}{S_j^2}.$$

We need this quantity in terms of the dummy variable x_s. Then

$$\begin{aligned}
\frac{\partial^2 h}{\partial x_k \partial x_s} &= \sum_{r=1}^{K} \frac{\partial^2 h}{\partial x_k \partial \pi_r} \frac{\partial \pi_r}{\partial x_s} \\
&= \sum_{r=1}^{K} \frac{\partial^2 h}{\partial x_k \partial \pi_r} (\pi_r I(r = s) - \pi_r \pi_s) \\
&= \pi_s \frac{\partial^2 h}{\partial x_k \partial \pi_s} - \pi_s \sum_{r=1}^{K} \pi_r \frac{\partial^2 h}{\partial x_k \partial \pi_s} \\
&= \pi_s \frac{\partial^2 h}{\partial x_k \partial \pi_s} + \pi_s \pi_k \sum_{j=1}^{n} m_j ,
\end{aligned}$$

since $\sum_{r=1}^{K} \pi_r \frac{\partial^2 h}{\partial x_k \partial \pi_r} = -\pi_k \sum_{j=1}^{n} m_j$.

Individual samples

We can apply this method of analysis to each half-month of data separately, so we choose a particular half-month to illustrate the issues. The first period for which reliable data were collected was period 2 in the 1964/5 season. Before we can analyse the data, we need to make some decisions as follows.

Number of groups: We have to choose K. Hunt and Jorgensen (1999) discuss this issue for fisheries length-frequency data, highlighting the point that some older groups may have no fish or very few fish in the sample. Hence K is impossible to choose from sample data alone. They conclude, and we concur, that K should be chosen by the modeller. Our strategy was to eliminate data greater than 130 cm, and to start with $K = 5$. If one or more parameters

was on the boundary of the parameter space, K was reduced by 1, and the model refitted. It was quite common to end up with $K = 3$ or $K = 4$, but occasionally $K = 2$ or even $K = 1$.

Starting values: The starting values for μ_k were derived from a growth model fitted to corresponding tag-recapture data. For this, the k-year-old group was assigned the age $k + (j - 0.5)/24$ years, where j is the half-month index and 24 is the number of half-months. Thus, the five groups for period 2 in 1965 would be assigned the ages 1.0625, 2.0625, 3.0625, 4.0625 and 5.0625 years, where 0.0625=1.5/24. From a seasonal VB $\log k$ growth model fitted to tag-recapture data (Appendix Tag-Recapture), the estimated mean lengths are $\hat{\mu}_1 = 55.0$, $\hat{\mu}_2 = 72.8$, $\hat{\mu}_3 = 87.8$, $\hat{\mu}_4 = 100.9$ and $\hat{\mu}_5 = 112.2$ cm. These are taken as starting values for μ_k. So that the optimisation routine could not switch groups, the μ_k were assumed to lie between the bounds l_k and u_k, where $l_1 = \hat{\mu}_1 - 30$, $l_k = (\hat{\mu}_{k-1} + \hat{\mu}_k)/2$ for $k \geq 2$, $u_k = l_{k+1}$ for $1 \leq k \leq K - 1$ and $u_K = \hat{\mu}_K + 30$ cm. The initial values of $\hat{\mu}_k$ and the bounds for the South Australian 1964/5 data are thus

Table 3: Initial estimates of μ_k and bounds.

age group	initial value	lower bound	upper bound
k	$\hat{\mu}_k$	l_k	u_k
1	55.0359	25.0359	63.9349
2	72.8338	63.9349	80.3305
3	87.8271	80.3305	94.3443
4	100.8616	94.3443	106.5274
5	112.1933	106.5274	142.1933

The starting value for σ was generally $\sigma = 4$, and the proportions were assumed to be equal.

Proceeding in this way, we fitted a Gaussian mixture model to each half-month of South Australian length-frequency data from 1964/5 to 1998/89. The results for odd half months in the 1981/2 season are shown in Figure 1. The patterns seen there are typical: the data display a number of modes, although the number of components of the fitted mixture does not necessarily equal the number of modes; the fit is sometimes excellent, and sometimes problematic; when the half-month has only a few fish, the fit can appear very bad, and the fitted modes are little more than mathematical artefacts. In most half-months, the allocation of fitted components to age groups was easy and unequivocal. However, in a few cases an extra age group (usually a young one-year-old group in the latter part of the season) appeared. This mainly happened in the 1970s (1974 was the worst case). In such cases we usually fitted a single age component to the bimodal group, although in 1974 half-months 8 to 11 we omitted the one-year-old modes from the summary statistics. The retained data for the next phase of analysis were the fitted modes and their standard errors, estimated by inverting the observed information matrix. We also kept the estimated number of fish in each group. For example, for the most complex panel in Figure 1, half month 7 of 1982, the summary statistics are set out in Table 4 .

Table 4: Fitted modes, half-month 7 in 1982.

age group	fitted mode	s.e.	estimated
k	$\hat{\mu}_k$		# in group
1	63.0032	0.5611	225
2	81.1072	0.3419	648
3	102.5016	0.9188	259
4	113.9566	0.8886	182

The fitted modes for the 1960s, 1970s and 1980s are shown in Figures 2, 3 and 4 respectively. Here the estimated means $\hat{\mu}_k$ from the maximum likelihood fitting program are plotted against half-month, and means for different age-groups are distinguished by a different plotting symbol. We estimate the number of fish

in each age-group by multiplying the effective sample size ($\sum m_j$) by the estimated proportions in each age-group. Groups with less than 50 fish are not included in the next phase of analysis, because we doubt their accuracy in general. The three figures show a consistent pattern. Although there are inconsistencies between years, on average the means for a particular age group tend to increase up to about half-month 6 and then flatten off. This is consistent with a seasonal growth pattern in which growth is most pronounced over summer, but is quite minimal over winter. Figure 5 overplots the summary data for all three decades. This suggests that growth in the 1960s and 1970s was similar, but that fish grew faster in the 1980s.

Multiple samples: the Leigh and Hearn approach

Leigh and Hearn (2000) proposed a method for the combined analysis of multiple half-month data, which we now discuss. When there are S independent samples, the combined log-likelihood is

$$h = \sum_{i=1}^{S} \sum_{j=1}^{n} m_{ij} \log \left(\sum_{k=1}^{K} \pi_{ik} g_{ik}(l_{ij}) \right) .$$

Leigh and Hearn (2000) assume that the components are Gaussian, with

$$g_{ik}(l_{ij}) = \frac{1}{\sqrt{2\pi}\sigma} \exp \left(-\frac{(l_{ij} - \mu_{ik})^2}{2\sigma^2} \right) .$$

They could quite easily assume that σ^2 varies with time, with component or with the mean, but they assume it is constant for simplicity.

We shall be applying this model to the half-monthly length-frequency data from Australian tuna fisheries. A season usually consists of three to six months of fishing, so we typically have data from 6 to 12 half-months. Leigh and Hearn (2000) assumed that the mean growth curve over a season is linear, so that

$$\mu_{ik} = \alpha_k + \beta_k (t_i - \bar{t})$$

where t_i is the time of the mid-point of the ith half-month, and $\bar{t}$ is the mean of the t_i. The proportions π_{ik} satisfy the usual constraints $0 \leq \pi_{ik} \leq 1$ and $\sum_{k=1}^{K} \pi_{ik} = 1$ but are otherwise completely unconstrained.

If there are K components and S half-months, there are $(K-1)S$ proportions to estimate, $2K$ trend parameters and σ. This is $(K-1)S+2K+1$ parameters in total. For South Australia in 1966-67, for example, there were $S=12$ half-months, $K=4$ components so that 45 parameters required estimation.

Maximisation of the likelihood was not straightforward. Initially we chose a derivative-free optimisation algorithm, but it took several hours to converge. We switched to a routine in which the user supplied first and second derivatives, which converged in seconds.

Let

$$I = -\left\{\frac{\partial^2 h}{\partial\theta_k \partial\theta_l}\right\}$$

be the observed information matrix, where θ is the vector of parameters, and θ_k is a generic component. The asymptotic variance-covariance matrix is I^{-1}. We actually want the submatrix corresponding to α_k, β_k and $\log\sigma$. In all trials, I^{-1} could be calculated directly without problem, and the relevant submatrix extracted.

We illustrate the method on the South Australian 1964/5 length-frequency data. When we fitted the Leigh and Hearn mixture model with 4 age groups to the 1964/5 data, we obtained the results in Table 5.

Table 5: Leigh and Hearn (2000) estimates of linear growth parameters: 1964/5 season.

age group	growth parameters	
k	$\hat{\alpha}_k$	$\hat{\beta}_k$
1	59.69	1.81
2	77.84	1.28
3	92.76	0.60
4	109.01	0.99

The estimates are derived from data from half-months 2 to 9, so that 59.69

cms is the estimated mean length of one-year-olds at 5.5 half-months (mid-March) and 1.81 cms is the expected increase in growth per half-month. We immediately see a potential weakness of this method: if we extrapolate the one-year-old linear growth model for 24 half-months, we predict that two-year-olds in mid-March will be $59.69 + 24 \times 1.81 = 103.13$ cms, whereas the direct estimate is 77.84 cms.

It transpires that this is a bigger problem than might be anticipated. The within-season growth for a particular age-group is being reduced to two summary statistics (mean growth and slope), and this is simply insufficient to capture the more complex growth patterns evident in Figures 2, 3 and 4. For this reason we preferred to carry out the individual half-month analyses first, and to use the summary statistics from these as raw data for fitting growth models. This approach does not come without some cost: first, the Leigh and Hearn (2000) approach is unambiguous with respect to allocation of fitted means to age-groups, whereas the individual analyses can be more problematic; second, the number of groups for a Leigh and Hearn (2000) analysis is easier to determine.

It may be possible to compromise, and to fit a non-linear growth model using the Leigh and Hearn approach. The most common parametric models (such as quadratics or exponentials) are not well-tailored to the data. However, a suitable model for initial analysis might be a monotonically increasing hyperbolic spline growth model with an asymptote, somewhat similar to the models fitted by Griffiths and Miller (1973). However, this is then quite complicated, and for simplicity we prefer the two-phase approach of fitting the mixture model to each half-month separately, generating suitable summary statistics, and then fitting a global growth model from the summary statistics.

Fitting a growth model to half-month summary statistics

We assume that we have performed a mixture decomposition on the data for each half-month, and we have generated a mode and an accompanying standard error for each age group. Denote these by $\hat{\mu}$ and s respectively. The standard error s is obtained by inverting the observed information matrix. Let i index the season, j the half-month and k the age-group. We assume that we can allocate a mean age a to the fish at half-month j and age-group k. Then our initial model is

$$\hat{\mu}_{ijk} = \mu(a_{ijk}) + \tau_i + \nu_{ij} + \omega_{ik} + e_{ijk} + \epsilon_{ijk}$$

where $\mu(a)$ is the mean growth of fish of age a, and τ, ν, ω, e and ϵ are all independent random effects. We assume that $\tau \sim N(0, \sigma_\tau^2)$, $\nu \sim N(0, \sigma_\nu^2)$, $\omega \sim N(0, \sigma_\omega^2)$, $e \sim N(0, \sigma_e^2)$ and $\epsilon \sim N(0, s^2)$. Thus τ represents a random seasonal effect, ν a within-season random half-month effect, ω a within-season random age effect and e is a within-season half-month age interaction. Finally, ϵ represents sampling error, and its variance is assumed known. Strictly speaking, ϵ_{ijk} and $\epsilon_{ijk'}$ for $k \neq k'$ and a given i and j should be correlated, because $\hat{\mu}_{ijk}$ and $\hat{\mu}_{ijk'}$ have been derived from the same mixture decomposition. In our experience such correlations are usually weak, and they should be absorbed in the ν_{ij} random effects. Note that ν_{ij} and ω_{ik} are crossed within seasons — this is an occasion in which crossed random effects make sense.

The mean growth curve can depend on several (at least three) parameters. A minimal model is the von Bertalanffy growth curve:

$$\mu(a) = \mu_\infty \left(1 - \exp(-\kappa(a - a_0))\right)$$

where μ_∞, κ and a_0 are parameters to be estimated. It would be possible to add the random effects to μ_∞, to make κ depend on cohort and to make a_0 vary with age-group, for example, but we prefer to fit the most parsimonious model we can to the data. However, one complication cannot be ignored. We have already seen

that growth within seasons is faster in summer than winter, and any model fitted to length-frequency data must capture this effect. The seasonal von Bertalanffy growth curve is

$$l(t) \quad = \quad L_\infty[1 - \exp(-\kappa(t - t_0 + (u_s/2\pi)\,\sin(2\pi(t - w_s)))]$$

where u_s is the amplitude of the seasonal growth pattern and w_s is the phase. The condition $-1 \leq u_s \leq 1$ guarantees that growth is monotone, and it is customary for length frequency data to impose the constraint $-0.5 < w_s \leq 0.5$ on the phase.

We assume that we estimate the parameters by maximising the likelihood of the data. The data for each season are assumed independent, so we can add up the log-likelihoods for each season. We can write the model in vector form as

$$\hat{\mu}_i = \mu + 1\tau_i + X_\nu \nu_i + X_\omega \omega_i + e_i + \epsilon_i$$

where $\hat{\mu}_i$ is vector of data and μ is the vector of mean growths. Also, X_ν and X_ω are design matrices: thus, $X_{\nu,mj} = 1$ if element m belongs to half-month j and is zero otherwise.

We need to compute the likelihood within a season. The log-likelihood is

$$\log \lambda = -0.5 \log |V| - 0.5(\hat{\mu} - \mu)' V^{-1} (\hat{\mu} - \mu)\,,$$

and V is the variance-covariance matrix of the data. Now

$$V = \sigma_e^2\, I + D_\epsilon + \sigma_\tau^2 11' + \sigma_\nu^2 X_\nu X_\nu' + \sigma_\omega^2 X_\omega X_\omega'$$

where D_ϵ is the diagonal matrix with diagonal elements $d_{mm} = s_m^2$. We can write V as

$$V = D + XX'$$

where $D = \sigma_e^2\, I + D_\epsilon$ is a diagonal matrix and $X = (\sigma_\tau 1 \;\; \sigma_\nu X_\nu \;\; \sigma_\omega X_\omega)$ is a design matrix. Most software packages are unable to solve the likelihood equations for this model, because the user cannot specify in advance the value of any variance component. We now indicate how to maximise the likelihood from first principles.

We assume that we are in an iteration trial of an optimisation routine, so that all parameter values are known, and we need to compute the likelihood.

When calculating the likelihood we need to compute $|D + XX'|$, where X is an $n \times p$ matrix, where n is the number of data values in the season, and p is the number of design levels. Generally, $n > p$ and sometimes $n \gg p$. For example, for the 1980s length-frequency data from South Australia, we have

Table 6: Dimension of X by season.

season	n	p
1979/80	26	17
1980/81	30	17
1981/82	31	17
1982/83	24	14
1983/84	11	10
1984/85	34	16
1985/86	36	16
1986/87	30	14
1987/88	29	15
1988/89	18	12
Total	269	148

Computations involving matrices of order n are generally proportional to n^3, so if we can make the computations of order p rather than n, we should increase speed by about $(269/148)^3 \approx 6$ times. It turns out that this means about 2 or 3 minutes instead of 15 minutes, which is substantial.

We can use the following well-known identity to reduce the amount of computation in this way: $|I_n + XX'| = |I_p + X'X|$, where $|A|$ denotes the determinant of the square matrix A, and I_r is the $r \times r$ identity matrix. Now $|I_n + XX'|$ is the

determinant of an $n \times n$ matrix and $|I_p + X'X|$ is that of a $p \times p$, so the latter requires much less computer time to calculate. In fact, we need $|D + XX'|$. Set $Y = D^{-1/2}X$, and note that

$$D + XX' = D^{1/2}(I + YY')D^{1/2}\,.$$

Thus $|D + XX'| = |D||I + YY'| = |D||I + Y'Y|$.

We also need to be able to compute $(I + XX')^{-1}$. We simply note that

$$(I + XX')^{-1} = I - X(I + X'X)^{-1}X'\,.$$

This result is easily checked. In fact, we need $(D + XX')^{-1}$. Note again that

$$D + XX' = D^{1/2}(I + YY')D^{1/2}\,.$$

Hence

$$(D + XX')^{-1} = D^{-1/2}(I + YY')^{-1}D^{-1/2}\,.$$

We need to compute $(\hat{\mu} - \mu)'(D + XX')^{-1}(\hat{\mu} - \mu)$. Set $\alpha = D^{-1/2}(\hat{\mu} - \mu)$. Then

$$\begin{aligned}(\hat{\mu} - \mu)'(D + XX')^{-1}(\hat{\mu} - \mu) &= \alpha'(I + YY')^{-1}\alpha \\ &= \alpha'(I - Y(I + Y'Y)^{-1}Y')\alpha \\ &= \alpha'\alpha - \beta'(I + Y'Y)^{-1}\beta \\ &= \alpha'\alpha - \beta'\gamma\end{aligned}$$

where γ is the solution of the equations $(I + Y'Y)\gamma = \beta$ and $\beta = Y'\alpha$.

Finally, we compute the log-likelihood as

$$\log\lambda = -0.5d_t - 0.5r\,.$$

Using this methodology we can explicitly include the sampling error with *known* variance. It appears to be impossible to do this in any of the major statistical packages using the inbuilt commands for mixed modelling.

It is sometimes helpful to calculate the gradient of the likelihood as well as the likelihood itself. This can speed up optimisation routines. For a growth parameter θ_j, we have

$$\frac{\partial \log \lambda}{\partial \theta_j} = (\hat{\mu} - \mu)' V^{-1} \frac{\partial \mu}{\partial \theta_j}.$$

For a given suite of parameters, we first compute $v_\mu = V^{-1}(\hat{\mu} - \mu)$ efficiently, using the dimension-reductions techniques described above. The vector of partial derivatives $\partial\mu/\partial\theta$ is then computed — sometimes there are specific features of the growth curve that can be exploited to help calculate these quickly.

The variance parameters are slightly more problematic. For a generic additive error structure,

$$V = \sum_{j=1}^{q} \sigma_j^2 V_j$$

the general rule is that

$$\frac{\partial \log \lambda}{\partial \sigma_j} = \sigma_j \left[-\mathrm{tr}(V^{-1} V_j) + (\hat{\mu} - \mu)' V^{-1} V_j V^{-1} (\hat{\mu} - \mu) \right],$$

where tr(.) stands for the trace of a matrix. Usually V_j is either diagonal or of the form $X_j X_j'$, where the number of columns in X_j is small. The second term on the right is just $v_\mu' V_j v_\mu$, and we have already computed v_μ, so this term is readily computed for either form of V_j. If $V_j = D_j$ is diagonal, then

$$\mathrm{tr}(V^{-1} D_j) = \sum_{i=1}^{n} D_{j,ii}/D_{ii} - \mathrm{tr}(D_j^{-1/2} D^{-1/2} Y (I + Y'Y)^{-1} Y' D^{-1/2} D_j^{-1/2}).$$

If $V_j = X_j X_j'$, then

$$\mathrm{tr}(V^{-1} X_j X_j') = \mathrm{tr}(X_j' D^{-1} X_j) - \mathrm{tr}(X_j' D^{-1/2} Y (I + Y'Y)^{-1} Y' D^{-1/2} X_j).$$

The trace of a matrix M is the sum of its diagonal elements, but it is not always necessary to compute all elements of M and then sum the diagonals. Thus for $n \times p$ matrices A and B it is readily verified that $\mathrm{tr}(A'B) = \sum_{i=1}^{n} \sum_{j=1}^{p} A_{ij} B_{ij}$. This can be used to reduce the computational burden in most cases.

Once the likelihood has been maximised, we need to calculate the random effects. It is usual to use the BLUPs:

$$\begin{aligned}
\hat{\tau}_i &= \hat{\sigma}_\tau^2 \, 1' V^{-1} (\hat{\mu} - \mu) \\
\hat{\nu}_i &= \hat{\sigma}_\nu^2 \, X_\nu' V^{-1} (\hat{\mu} - \mu) \\
\hat{\omega}_i &= \hat{\sigma}_\omega^2 \, X_\omega' V^{-1} (\hat{\mu} - \mu) \\
\hat{e}_i &= \hat{\sigma}_e^2 \, V^{-1} (\hat{\mu} - \mu)
\end{aligned}$$

Using our usual notation,

$$V^{-1}(\hat{\mu} - \mu) = D^{-1/2}(\alpha - Y\gamma) \, .$$

The standardised BLUPs are obtained by dividing through by the relevant standard deviation:

$$\begin{aligned}
\hat{\tau}_i / \hat{\sigma}_\tau &= \hat{\sigma}_\tau \, 1' V^{-1} (\hat{\mu} - \mu) \\
\hat{\nu}_i / \hat{\sigma}_\nu &= \hat{\sigma}_\nu \, X_\nu' V^{-1} (\hat{\mu} - \mu) \\
\hat{\omega}_i / \hat{\sigma}_\omega &= \hat{\sigma}_\omega \, X_\omega' V^{-1} (\hat{\mu} - \mu) \\
\hat{e}_i / \hat{\sigma}_e &= \hat{\sigma}_e \, V^{-1} (\hat{\mu} - \mu)
\end{aligned}$$

These are scale invariant. The corresponding true standardised random effects (e.g. τ_i / σ_τ) have mean 0 and variance 1. If $\hat{\sigma}_r = 0$ for any random effect r, then the BLUPs and standardised BLUPs are obviously 0.

Trials of this method proved reasonably satisfactory when analysing length-frequency data alone. The parameter estimates when fitting a seasonal von Bertalanffy growth model to the 1960s, 1970s and 1980s summary statistics are set out in Table 7. We fixed μ_∞ at 185 cm, because there were no data bearing on this parameter.

Table 7: Fitted VB growth model parameters, South Australian Length-Frequency data

decade	μ_∞	$\hat{\kappa}$	$\hat{a}_0$	$\hat{u}_s$	$\hat{w}_s$	$\hat{\sigma}_\tau$	$\hat{\sigma}_\nu$	$\hat{\sigma}_\omega$	$\hat{\sigma}_e$
1960s	185	0.146	-1.46	0.878	0.088	0.557	0.620	1.182	0.997
1970s	185	0.141	-1.51	0.902	0.108	1.551	1.171	2.306	1.780
1980s	185	0.170	-1.16	0.720	0.185	1.428	0.010	1.461	1.911
combined	185	0.154	-1.32	0.753	0.130	2.454	0.831	2.152	1.738

The fits for the separate decades were not perfect: for example, the one-year-olds in the 1980s did not quite fit the growth model. However, the fits were adequate for preliminary interpretation. The growth parameters for the 1960s and 1970s are almost identical, but growth appears to be faster in the 1980s. The seasonal parameters u_s and w_s appear to be quite sensible. The random effects standard deviations do not show much consistency: about the only real pattern is that σ_ω and σ_e tend to be larger than σ_τ and σ_ν. This inconsistency may simply reflect the lack of fit of the growth model.

A rather interesting pattern of random effects emerged from a combined analysis of all the length-frequency data. The estimated seasonal effects $\hat{\tau}_i$ are shown in Figure 6. These are supposed to be estimated realisations of independent random effects, but they follow a reasonably smooth trend. It seems likely that growth has been changing systematically over these three decades, and that this should be incorporated into a time-dependent growth model. We attempt this in Appendix 8.

The method was not robust when used in an integrated analysis of tag-recapture, otolith and length-frequency data: for example, either $\hat{\sigma}_\tau = 0$ or $\hat{\sigma}_\tau$ was very large. Partly for this reason, and partly because of the inconsistency in the estimates of σ_τ, σ_ν, σ_ω and σ_e, we decided to employ a simpler model

$$\hat{\mu}_{ijk} = \mu(a_{ijk}) + e_{ijk} + \epsilon_{ijk}$$

when doing an integrated analysis.

Other approaches

The approach adopted by Leigh and Hearn (2000) and the two-phase method recommended in this paper are convenient, but more general approaches are theoretically possible. Here we outline two possible directions for future work.

Mixtures with multiple components of variation

A Gaussian mixture model with K components may be written as

$$L = \sum_{k=1}^{K} I_k Z_k \quad .$$

where $Z_k \sim N(\mu_k, \sigma_k^2)$, $Z_1, Z_2, \ldots, Z_K$ are independent and the I_k are indicator random variables such that $I_k = 0$ or 1 and $\sum_{k=1}^{K} I_k = 1$. There are various ways of generating I_k, but a sequential method is appealing:

1. $I_1 = J_1$;
2. $I_2 = (1 - J_1)J_2$;
3. $I_3 = (1 - J_1)(1 - J_2)J_3$;

and so on, where J_k are independent Bernoulli random variables with $\Pr\{J_k = 1\} = p_k$, so that $\Pr\{I_k = 1\} = \pi_k$, where $\pi_k = \prod_{j=1}^{k-1}(1 - p_j)p_k$. It is convenient to define the vectors $I = (I_1, \ldots, I_K)'$ and $Z = (Z_1, \ldots, Z_K)'$.

When we have a sample of size n, the model becomes

$$L_i = \sum_{k=1}^{K} I_{ik} Z_{ik}$$

where $I_{(i)} \equiv (I_{i1}, \ldots, I_{iK})' \sim I$ and $Z_{(i)} \equiv (Z_{i1}, \ldots, Z_{iK})' \sim Z$ are independent from fish to fish. This model generates the likelihood (1) that we maximise for a single sample.

If there are multiple sources of variation, then we can generalise the mixture model by setting

$$Z_{ik} = T + V_i + W_k + E_{ik}$$

where $T \sim N(0, \sigma_\tau^2)$, $V_i \sim N(0, \sigma_\nu^2)$ $(i = 1, \ldots, n)$, $W_k \sim N(0, \sigma_\omega^2)$ $(k = 1, \ldots, K)$ and $E_{ik} \sim N(\mu_k, \sigma_k^2)$ $(i = 1, \ldots, n; k = 1, \ldots, K)$ are all independent. Then

$$L_i = T + V_i + \sum_{k=1}^{K} I_{ik}(W_k + E_{ik}) .$$

Note that the marginal distribution of $W_i^* = \sum_{k=1}^{K} I_{ik} W_k$ is $N(0, \sigma_w^2)$, but that the correlation between W_i^* and $W_{i'}^*$ is $\sum \pi_k^2$ when $i \neq i'$. Hence W^* represents covariation between L_i and $L_{i'}$ intermediate between that caused by T (correlation 1) and V_i (correlation 0). For this reason, it is probably more realistic than either T or V_i.

We first look at the effect of V_i. Consider a single observation, so that the model is

$$L = V + \sum_{k=1}^{K} I_k E_k .$$

where $V \sim N(0, \sigma_\nu^2)$, $E_k \sim N(\mu_k, \sigma_k^2)$ and V and $(E_1, \ldots, E_K)$ are independent. We write the density of V as $g(\nu)$ and of E_k as $g_k(e)$. Then

$$\begin{aligned}
\Pr\{L = l\} &= \int_{-\infty}^{\infty} \Pr\{V = v\} \Pr\{L = l | V = \nu\} \, d\nu \\
&= \int_{-\infty}^{\infty} \Pr\{V = \nu\} \Pr\{\sum_{k=1}^{K} I_k E_k = l - \nu | V = \nu\} \, d\nu \\
&= \int_{-\infty}^{\infty} g(\nu) \left\{ \sum_{k=1}^{K} \pi_k g_k(l - \nu) \right\} d\nu \\
&= \sum_{k=1}^{K} \pi_k \int_{-\infty}^{\infty} g(\nu) \, g_k(l - \nu) \, d\nu .
\end{aligned}$$

Now $\int_{-\infty}^{\infty} g(\nu) \, g_k(l - \nu) \, d\nu$ is the density of $V + E_k$, which is $N(\mu_k, \sigma_v^2 + \sigma_k^2)$. Hence

$$\Pr\{L = l\} = \sum_{k=1}^{K} \pi_k \phi_k(l)$$

where ϕ_k is the density of a $N(\mu_k, \sigma_v^2 + \sigma_k^2)$ variate. Thus L is a K-component Gaussian mixture, in which component k has mean μ_k and variance $\sigma_\nu^2 + \sigma_k^2$. At first sight this result seems rather curious, because $(V + E_1, \ldots, V + E_K)$ are correlated through the common V. However, $(I_1 V, \ldots, I_K V)$ are uncorrelated. In words, only one E_k of $(E_1, \ldots, E_K)$ is chosen, and the realised value is $V + E_k$. If component

k is chosen, the value of the other components is effectively 0, so their dependence on V is irrelevant. From an inferential viewpoint, we can forget V in the model, because its effect is to simply inflate the variance of component k.

Hence, without loss of generality, the mixture model with multiple components of variation can be reduced to a hierarchical model

$$Z_{ik} = T + W_k + E_{ik}$$

where $T \sim N(0, \sigma_\tau^2)$, $W_k \sim N(0, \sigma_\omega^2)$ $(k = 1, \ldots, K)$ and $E_{ik} \sim N(\mu_k, \sigma_k^2)$ $(i = 1, \ldots, n; k = 1, \ldots, K)$ are all independent.

Temporarily drop T and consider the model

$$L_i = \sum_{k=1}^{K} I_{ik}(W_k + E_{ik})$$

The log-likelihood of data generated from this model is difficult to compute, because the data are dependent. However, we can ameliorate the situation somewhat by writing

$$L_i = T + V_i + Z_i$$

where Z_i is the Gaussian mixture,

$$\begin{aligned} Z_i &= \sum_{k=1}^{K} I_{ik} E_{ik} \,, \\ T &= \sum_{k=1}^{K} \pi_k W_k \end{aligned}$$

and

$$V_i = \sum_{k=1}^{K} (I_{ik} - \pi_k) W_k \,.$$

Then T and Z_i are independent, T and V_i are uncorrelated, and V_i and V_j are uncorrelated for $i \neq j$. If we treat T and V_i as independent, then we can calculate the likelihood of the data. We leave this for future investigation.

Variable spawning times

The spawning period for a species can be quite broad; for southern bluefin tuna, spawning lasts for several months. Thus far, our modelling has not taken into

account variable spawning times. To explore this issue, consider fitting a generic growth model to a single sample. The growth model for a single fish of length L and age a is

$$L = L_\infty f(a - a_0; \theta) + \epsilon\,,$$

where L_∞ is asymptotic length, a_0 is the extrapolated age (usually negative) at which the fish has length 0, and f is a monotonic increasing function with parameter set θ that equals 0 when $a = a_0$ and approaches 1 as $a \to \infty$. For the familiar von Bertalanffy curve, $f = 1 - \exp(-\kappa(a - a_0))$ with $\theta = \{\kappa\}$. We normally assume that L_∞ is Gaussian with mean μ_∞ and variance σ^2_∞, and that ϵ is Gaussian with mean 0 and variance σ^2. Hence L is Gaussian with mean and variance

$$\mu_L(a) = \mu_\infty f(a - a_0; \theta) \tag{2a}$$

$$\sigma^2_L(a) = \sigma^2_\infty f^2(a - a_0; \theta) + \sigma^2. \tag{2b}$$

Recall that the majority of southern bluefin tuna spawn between about October and March, with the midpoint estimated to be January 1. The youngest fish present in South Australian waters in a given year (say 1970) will be the one-year olds spawned during the previous spawning season (between October 1968 and March 1969). We assign them the index $k = 1$, and denote the proportion of one-year-olds by π_1. In general, there are π_k fish of age k. For a k-year-old fish caught at fractional time t into the year, the age of the fish is $k + t + \Delta$, where Δ represents the variable spawning time. We assume that $\Delta \sim N(0, \sigma^2_\Delta)$. The mean is 0 because peak spawning is assumed to occur on January 1, and σ_Δ is about 6/52, so that about 70% of spawning takes place over a 12 week period centred around January 1. Note that $\Delta > 0$ for fish spawned early in the season (prior to January 1), and $\Delta < 0$ otherwise.

Let the random variables K and L denote the age group and length respectively of a randomly caught fish. Then

$$\Pr\{L = l\} = \sum_k \int_{-\infty}^{\infty} \Pr\{L = l | \Delta = \delta, K = k\} \Pr\{K = k, \Delta = \delta\}\, d\delta$$

$$= \sum_k \pi_k \int_{-\infty}^{\infty} \frac{\phi((l-\mu_\delta)/\sigma_\delta)}{\sigma_\delta} \frac{\phi(\delta/\sigma_\Delta)}{\sigma_\Delta} d\delta$$

where $\mu_\delta = \mu_L(a_\delta)$, $\sigma_\delta = \sigma_L(a_\delta)$ (see equations (2a) and (2b)), $a_\delta = k + t + \delta$ is the age of the fish and ϕ is the standard Gaussian density function. The integration must be carried out numerically. This is not difficult in principle, although we have not seen such an analysis in the fisheries' literature. If we make the assumption that $\sigma_\delta = \sigma_L(k+t)$ so that it does not depend on δ, and that μ_δ is (locally) linear in δ (so that $\mu_\delta \approx \mu_L(k+t)+\beta\delta$, where $\beta = \mu'_L(k+t)$), then we can carry out the integration explicitly. We end up with a Gaussian mixture model in which component k has mean $\mu_L(k+t)$ and a slightly inflated variance $\sigma_L^2(k+t) + \beta^2\sigma_\Delta^2$. This is effectively what we are doing in our data analysis, where we assign all fish in age group k the age $k + t$. For most commonly-used growth models, $\sigma_L(k + t)$ increases with age-group k, but β declines with k. These counter-balance to some extent, and as a compromise we fit constant group variances when fitting Gaussian mixtures to length-frequency data.

In practice, the proportions π_k will vary considerably between half-months because of the schooling nature of southern bluefin tuna, their highly patchy distribution and differential movement/migration with age. Additionally, there is probably considerable year-to-year variability in the porportion of an age-class that comes from a particular period in the spawning season

Conclusions

The results in this Appendix confirm the usefulness of length-frequency data for understanding growth processes, and that within-season growth can be detected and modelled. A number of previous publications have investigated how such growth information can be extracted. However, our study emphasises features that previous studies have not considered in detail.

1. Length-frequency growth patterns do not conform tightly to parametric growth curves. There appear to be significant additional sources of variation operat-

ing between seasons, between age-groups within seasons, between half-months within seasons and between age-groups and half-months within seasons (interactive effects). We are unable to offer explanations for all of these effects in terms of covariates, and suggest that initially they should be modelled as independent hierarchical and crossed random effects. Otherwise standard errors of growth parameters derived from length-frequency data are likely to be optimistically small.

2. Despite this complexity, each decade of southern bluefin tuna data consistently exhibits a seasonal pattern, in which growth is fastest over the summer, but flattens off in autumn. We propose that this seasonal growth can be modelled using a sine curve with amplitude and phase parameters estimated from the data.

3. Broad changes in growth from year to year can also be observed from the estimated between season random effects. For southern bluefin tuna these appear to be rather smooth, and suggest that they should be modelled as systematic effects rather than random effects. At a qualitative level, the mean length of one-year-old fish has changed only in minor ways between 1960 and 1990, but the age four fish in 1990 are considerably longer than those in 1960. Quantitative modelling of this trend is a large topic, which consider in Appendices 8 and 10.

Although length-frequency data provide unique and valuable information for modelling growth, they generally do not contain information on older individuals and thus are not adequate by themselves. The modelling approach used in this Appendix required us to assume a mean asymptotic length for southern bluefin tuna. We chose a value of 185 cm based on other studies, but the results over the age range represented by the length-frequency data are not sensitive to the value chosen. Tag-recapture data uniquely provide good information on individual fish variation, because there are two measurements per fish rather than one. The available otolith

data are biased towards older fish, and thus provide direct information on the mean asymptotic length. A comprehensive model for southern bluefin tuna growth requires an integrated analysis of length-frequency, tag-recapture and otolith data, each of which provides essential input into the final model.

References

FOURNIER, D.A., SIBERT, J.R., MAJKOWSKI, J. & HAMPTON, J. (1990) MULTIFAN: a likelihood based method for estimating growth and age composition from multiple length frequency data sets illustrated using data from southern bluefin tuna (*Thunnus maccoyii*). *Can. J. Fish. Aquat. Sci.* **47,** 301-313.

GRIFFITHS, D.A. & MILLER, A.J. (1973) Hyperbolic regression — a model based on two-phase piecewise linear regression with a smooth transition between regimes. *Comm. Statist.* **2,** 561-569.

HUNT, L. & JORGENSEN, M. (1999) Mixture model clustering using the MULTIMIX program. *Australian & New Zealand J. Stat.* **41,** 153-171.

LEIGH, G.M. & HEARN, W.S. (2000) Changes in growth of juvenile southern bluefin tuna (*Thunnus maccoyii*): an analysis of length-frequency data from the Australian fishery. *Mar. Freshwater Res.* **51,** (in press).

Figure 1. South Australian 1981/2 length-frequency data and fitted Gaussian mixtures. The scaled length-frequency data are plotted for the first half of December, January, February, March, April and June (half-months -1, 1, 3, 5, 7 and 11 respectively). For each period, a Gaussian mixture with 2, 3, 4, 3, 4 and 2 components respectively has been fitted. For the vast majority of half-months the number of components to fit was self-evident. Mostly the fits were excellent, but the 1981/2 season has been chosen deliberately to illustrate a case where the fit was problematic (half-month 7).

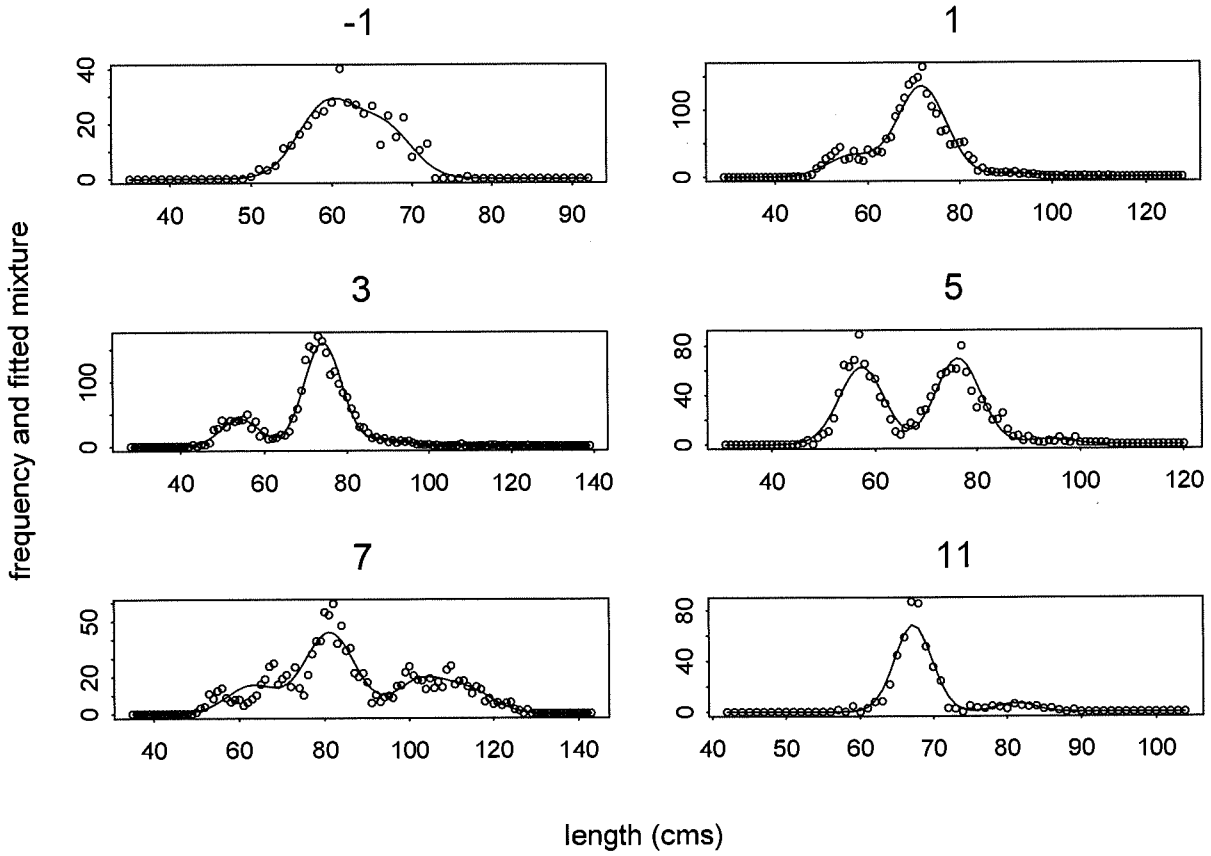

Figure 2. Fitted modes for age-groups 1, 2, 3, 4 and 5+ in the 1960s plotted against half-month. The estimated modes from the Gaussian mixture fitting program have been assigned to age-groups, with 1, 2, 3 and 4 year-olds plotted as circles, triangles, plusses and crosses respectively. (Diamonds correspond to 5+ year-olds, but we do not use this data in subsequent analyses.) The 2 and 3 year-olds are numerically dominant, and on average their modes tend to increase up to half-month 6 and then flatten off, reflecting faster summer growth.

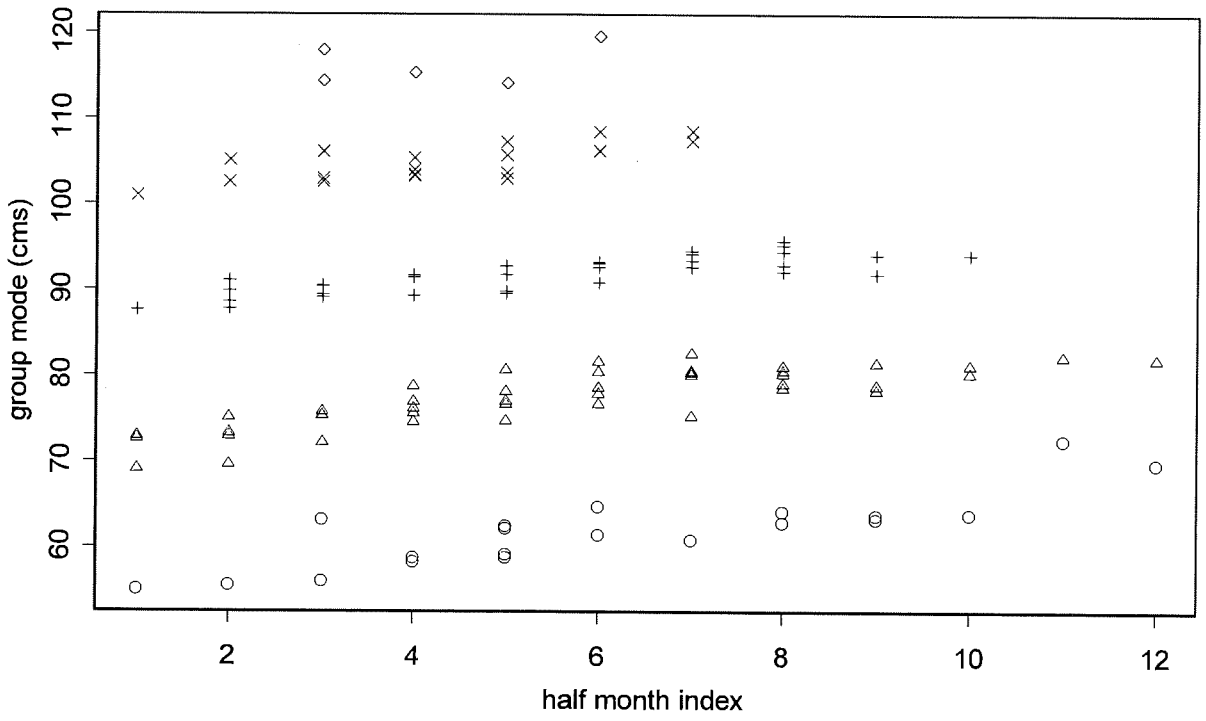

Figure 3. Fitted modes for age-groups 1, 2, 3, 4 and 5+ in the 1970s plotted against half-month. The symbols are the same as in Figure 2. Although the seasonal growth pattern is still evident, the plot is not as 'clean'.

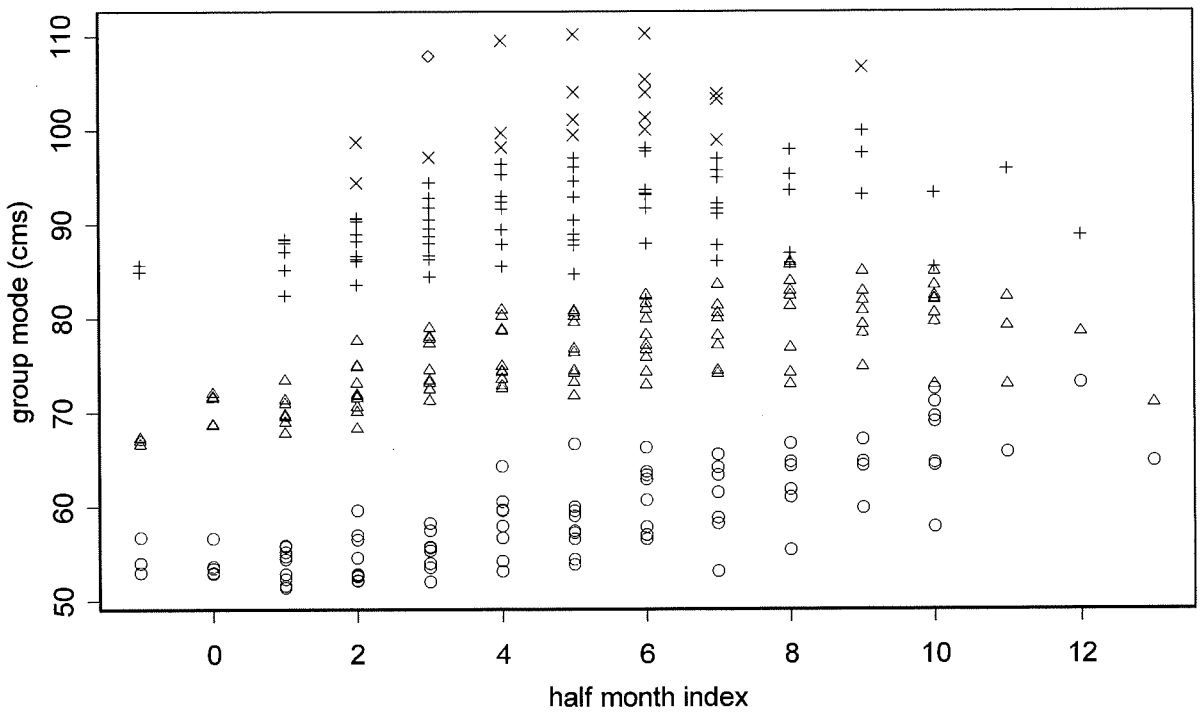

Figure 4. Fitted modes for age-groups 1, 2, 3, 4 and 5+ in the 1980s plotted against half-month. The symbols are the same as in Figure 2. There is good separation between age groups and a clear seasonal growth pattern.

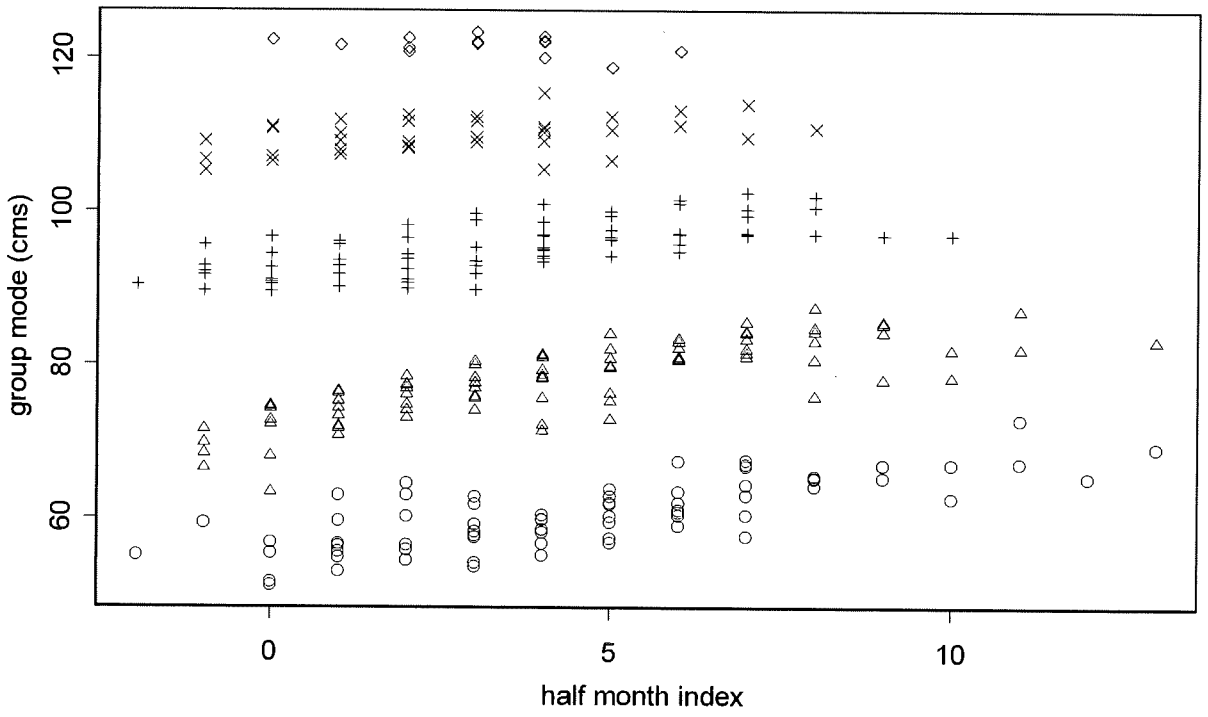

Figure 5. Overplot of the 1960s, 1970s and 1980s modes versus age. This suggests that growth in the 1960s and 1970s was similar, but that fish grew faster in the 1980s. The difference between the 1980s and the previous two decades is not very obvious for the 1 year-olds, but is very obvious for the 4 year-olds.

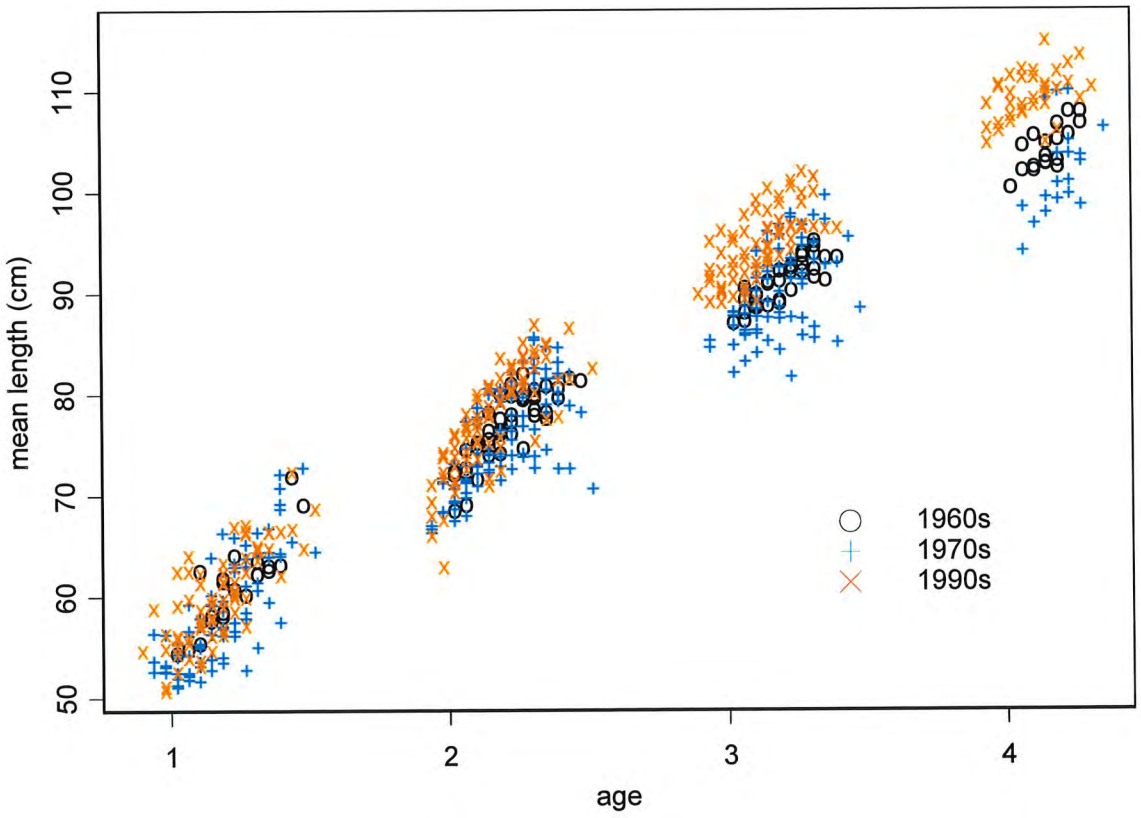

Figure 6. Estimated between-season effects plotted against season. These are supposed to be estimated realisations of independent random effects, but they follow a reasonably smooth trend. It seems likely that growth has been changing systematically over these three decades, and that this should be incorporated into a time-dependent growth model. The complex pattern in the 1970s may explain the poor separation between age groups in Figure 3.

Appendix 8:
The von Bertalanffy growth curve in a changing environment

Geoff M. Laslett, J. Paige Eveson and Tom Polacheck

FRDC Project 1999/104

Introduction

The von Bertalanffy curve is the dominant and primary model of fish growth. It states simply that a fish grows exponentially in length as it ages. More exactly, fish growth is proportional to $1 - \exp(-\kappa a)$, where κ is an unknown constant and a is the age of the fish. The proportionality factor is sometimes a constant, but in modern studies is more often a random variable representing the asymptotic length specific to a given fish quite. The von Bertalanffy curve adequately describes fish growth for many species, and, although many alternative models of fish growth have been proposed, its prevalence persists. Part of its popularity can be ascribed to its simplicity, and part to its derivation from a differential equation that is easily generalisable to more complex growth environments.

Modelling fish growth is important because it forms a direct input into stock assessments, from which sustainability of the fishery can be assessed, and quotas and other management measures can be determined. Southern bluefin tuna are of huge commercial importance to Australia, and have been intensively studied over many decades. A large spatio-time series of data has been accumulated, which, for our purposes, means that changes in growth might be estimated. Very few Australian fisheries enjoy such a sustained level of recording. With southern bluefin tuna levels falling to marginally sustainable levels, it has become more important than ever to understand the growth patterns of this species.

In this Appendix we generalise the von Bertalanffy growth curve by making κ a smooth function of time. We adopt a parametric modelling approach, but employ enough parameters to capture long-term changes in growth. Our parametric model is sufficiently flexible to imitate regression splines, but nevertheless is an explicit expression that can be stably evaluated without recourse to any recurrence relation. Our philosophy is to commence with a simple growth model with complex error structure. We estimate the error components, examine the estimates for non-random structure, and transfer such structure to the growth model. Our final model is a reasonably complex growth model with non-trivial error structure.

In this Appendix we introduce some alternative time-varying von Bertalanffy growth models, including a link to polynomial splines. We demonstrate how to incorporate seasonal growth rigorously and suggest how to generalise the time-varying von Bertalanffy growth model to a more complex growth curve. Finally we fit the time-varying von Bertalanffy growth model to some length-frequency data and some tag-recapture data.

The von Bertalanffy growth curve in a changing environment

Wang (1998) has proposed the following generalisation of the von Bertalanffy growth curve. Suppose a fish has length 0 at time t_0. Then the growth rate at time t is given by

$$l'(t) = (L_\infty - l(t))\, k(t)\,, \tag{1}$$

where $k(t)$, the function that controls the growth rate, may depend on time, but the asymptotic length L_∞, although random, does not change its distribution with time. The solution is

$$l(t) = L_\infty[1 - \exp(-K(t_0, t))]$$

where $K(t_0, t) = \int_{t_0}^{t} k(u)\, du$. The von Bertalanffy growth curve is recovered if $k(t) = \kappa$ for all t, but we wish to model the growth curve in an environment in which the growth curve is changing with time. An advantage of this approach is that covariates that explain the change in growth may easily be introduced into the model, as Wang (1998) has indicated. However, our thrust in this paper is to provide models when it has been observed that growth is changing, and we merely wish to describe the change in growth through modelling. We first propose various ways in which $k(t)$ may be modelled in a flexible but parsimonious manner.

It would be rather simpler to generalise the von Bertalanffy by substituting a time-dependent growth rate function $k(t)$ for κ in

$L_\infty(1 - \exp(-\kappa(t - t_0)))$. However, the derivative of this form does not have a simple interpretation.

Logistic time trends

We first suppose that the growth rate $k(t)$ varies according to a series of superimposed logistic curves. It is clear intuitively that such a model has the capacity to follow changes in growth. It is aimed at situations in which a von Bertalanffy growth curve applies, then a change in environment dictates that growth changes, until a new von Bertalanffy growth phase is achieved. The model allows for several such transitions, often in concert. Thus, set

$$k(t) \;=\; n\xi_0 + \sum_{i=1}^{n}(\xi_i - \xi_0)\frac{1}{1+\exp(-\beta(t-\alpha_i))}\,. \qquad (2)$$

where $\alpha_1 < \alpha_2 < \ldots < \alpha_n$ and $\beta > 0$. Note that t is time, and hence spans the whole real line. As $t \to -\infty$, $k(t) \to n\xi_0$, and as $t \to \infty$, $k(t) \to \sum_{i=1}^{n}\xi_i$. The ξ_i values can be any number, positive or negative subject to $k(t) > 0$. We could also make β depend on i, but that is likely to make the model over-parameterised. Although equation (2) encapsulates the reasoning for this model, it is not a suitable form for computation. In fact, we investigate two alternative parameterisations of the model. The first compares and contrasts our approach with that of polynomial splines. The second is computationally robust, and is particularly suitable for non-gradient optimisation methods.

First alternative parameterisation

There is an indirect link between (2) and quadratic B-splines, which we explore further in a later section. This provides some insight into the behaviour of the model. We set the scene here. Set

$$k(t) \;=\; \sum_{i=0}^{n}\kappa_i b_i(t)$$

where

$$b_0(t) \;=\; 1 - \frac{1}{1+\exp(-\beta(t-\alpha_1))}$$

$$
\begin{aligned}
b_i(t) &= \frac{1}{1+\exp(-\beta(t-\alpha_i))} - \frac{1}{1+\exp(-\beta(t-\alpha_{i+1}))} \quad \text{for } i = 1, \ldots, n-1 \\
b_n(t) &= \frac{1}{1+\exp(-\beta(t-\alpha_n))} .
\end{aligned}
$$

The ξs may be recovered from the κs by $\xi_0 = \kappa_0/n$ and $\xi_i = \kappa_i - \kappa_{i-1} + \kappa_0/n$. The $b_i(t)$ functions share some of the properties of natural polynomial B-splines, particularly quadratic B-splines (Schumaker, 1981, Section 8.2). They are non-negative, and for $1 \leq i \leq n-1$, $b_i(t)$ is unimodal with its peak at $(\alpha_i + \alpha_{i+1})/2$. In addition, $b_0(t)$ decreases from 1 to 0 and $b_n(t)$ increases from 0 to 1 as t increases, as with natural B-splines. Obviously $\sum_{i=0}^{n} b_i(t) = 1$ for any t. The $b_i(t)$s differ from B-splines in that they have infinite rather than finite support; that is, they are non-negative for all t, not just a finite range. Also, they depend on a parameter, β, unlike B-splines. They are more easily computed than B-splines, which is why we prefer them.

The B-spline properties of the $b_i(t)$ functions have important consequences for modelling. First, as $t \to -\infty$, $k(t) \to \kappa_0$ and as $t \to \infty$, $k(t) \to \kappa_n$, so that κ_0 and κ_n are easily interpreted. Also, it can be important when fitting the model to data to confine $k(t)$ to a sensible range of values. If $\kappa_l \leq \kappa_i \leq \kappa_u$ for all i, then $\kappa_l \leq k(t) \leq \kappa_u$ for all t. When fitting this model to data, one or more of the bounds may be reached during the fitting process. Such bounds need to be expanded and the fitting routine re-run. Even though it is much preferable to (2), convergence can still be quite slow with this parameterisation.

Suppose the fish is of length 0 at time t_0. An advantage of the logistic form is that it can be explicitly integrated. The key identity is

$$
\int \frac{dt}{1+\exp(-\beta(t-\alpha))} = t + \frac{\log(1+\exp(-\beta(t-\alpha)))}{\beta} .
$$

Thus

$$
\begin{aligned}
\int_{t_0}^{t} b_0(u)\,du &= \frac{-[\eta_1(t) - \eta_1(t_0)]}{\beta} \\
\int_{t_0}^{t} b_i(u)\,du &= \frac{[\eta_i(t) - \eta_i(t_0)] - [\eta_{i+1}(t) - \eta_{i+1}(t_0)]}{\beta} \quad \text{for } i = 1, \ldots, n-1 \\
\int_{t_0}^{t} b_n(u)\,du &= t - t_0 + \frac{\eta_n(t) - \eta_n(t_0)}{\beta}
\end{aligned}
$$

where $\eta_i(t) = \log(1 + \exp(-\beta(t - \alpha_i)))$. Hence the growth curve for a fish with length 0 at time t_0 is

$$l(t|t_0) = L_\infty \left(1 - e^{-\kappa_n(t-t_0)} \prod_{i=1}^{n} \left[\left\{ \frac{1 + e^{-\beta(t-\alpha_i)}}{1 + e^{-\beta(t_0-\alpha_i)}} \right\}^{-(\kappa_i - \kappa_{i-1})/\beta} \right] \right) \quad (3)$$

if $t \geq t_0$. Of course, $l(t|t_0) = 0$ if $t < t_0$. Note that the growth depends on all n component logistic growth rate curves, even if $t_0 > \alpha_i$ for some i.

Suppose we set $\kappa_i = \kappa$ for all i. Then (3) becomes the simple von Bertalanffy model with growth rate parameter κ.

For model building, we suggest two approaches:

(a) fixing the α_i values on a regular grid spanning the data, with a maximum density of one α per year, and then estimating the κ_i values with the other parameters associated with A and the error structure;

(b) fitting the α_i values, but making n as small as the data allows.

Capture-recapture data: Suppose that the time from t_0 to first capture is a random variable A, initially assumed to be identically distributed for all fish. Then, conditional on $A = a$, we can set $t_0 = t_1 - a$, so that (3) becomes

$$l(t|t_1, a) = L_\infty \left(1 - e^{-\kappa_n(t-t_1+a)} \prod_{i=1}^{n} \left[\left\{ \frac{1 + e^{-\beta(t-\alpha_i)}}{1 + e^{-\beta(t_1-a-\alpha_i)}} \right\}^{-(\kappa_i - \kappa_{i-1})/\beta} \right] \right) \quad (4)$$

Hence we can write down the joint likelihood of l_1, the capture length at time t_1, and l_2, the recapture length at time t_2. At time $t = t_1$, $t - t_1 + a = a$, the age at capture, and at time $t = t_2$, $t - t_1 + a = a_2$, the age at recapture.

A complication is that the distribution of A may depend on t, particularly if the tag-recapture data extend over three decades, as is the case with southern bluefin tuna. The modelling can still be done, but requires that $p(a|t)$, the density of A, must depend on time. If A was log-normal for example, we might assume that the mean of $\log A$ depends on time, but not the variance.

Length-frequency and otolith data: For length-frequency and otolith data, we know the age a and the time t of length measurement for each fish. We also know the time t. To model the data, we set $t_0 = t - a + a_0$, where a_0 is a parameter to be estimated. It is possible that we may need to allow $a_0 = a_0(t)$ to be a simple function of time. Note that $a > 0$ and usually $a_0 < 0$, so that $t_0 < t$. Thus when analysing otolith or length-frequency data we do not have to worry about forcing $l(t|t_0) = 0$ for $t < t_0$.

Second alternative parameterisation

Although B-splines are often recommended for computation, there is another way to parameterise the model that is more robust, in our experience. It can be used for all data types, although we illustrate it with length-frequency data. Choose $n+1$ times $\theta_0 < \theta_1 < \ldots < \theta_n$ and let $l_0, \ldots, l_n$ be the mean lengths of, say, two-year-old fish at these times. It is important to choose an age group a_θ heavily represented in the data, and two-year-olds dominate the tuna catch. The $\theta_0, \ldots, \theta_n$ may be fixed or variable. One possibility is to set $\theta_j = (\alpha_j + \alpha_{j+1})/2$ for $j = 1, \ldots, n-1$, and θ_0 and θ_n the start and end of the data collection period. We use $l_0, \ldots, l_n$ as parameters in place of $\kappa_0, \ldots, \kappa_n$. Given all the parameters, solve the following $n+1$ linear equations for κ_n and $\kappa_{jd} = \kappa_j - \kappa_{j-1}$:

$$\log(1 - l_i/\mu_\infty) \;=\; -\sum_{j=1}^{n} d_{ij}\,\kappa_{jd} - (a_\theta - a_0)\,\kappa_n$$

where

$$d_{ij} \;=\; [\log(1 + \exp(-\beta(\theta_i - \alpha_j))) - \log(1 + \exp(-\beta(\theta_i - a_\theta + a_0 - \alpha_j)))]/\beta\,.$$

for $i = 0, \ldots, n$. In d_{ij}, and elsewhere in this Appendix, we calculate $\log(1+\exp(x))$ in a stable way as $\log(1 + \exp(x_-)) + x_+ + \log(1 + \exp(-x_+)) - \log(2)$, where $x_+ = \max(x, 0)$ and $x_- = x - x_+$. This is suitable for scalars, vectors, matrices and arrays.

Solvers for such linear sets of equations are available in most mathematical computing packages. The κ_{jd} $(j = 1, \ldots, n)$ and κ_n are precisely the quantities required for calculating the mean lengths for all the data. The advantage of this

parameterisation is that the data bear directly on the l_j parameters, and it is very easy to constrain them to sensible values. Such stable parameterisations for non-linear models were promoted heavily by Ross (1975), and in more detail by Ross (1990). They are very useful when used in conjunction with gradient-free optimisation methods, but gradients and Hessians can be tedious to compute. Stable parameterisations of fish growth models have been promoted by Schnute (1981) and Francis (1988).

Polynomial spline trends

It is not compulsory to use logistic curves to model the trend, and we illustrate alternatives. Perhaps the most obvious is to use cubic splines, which can also be explicitly integrated. Thus, set

$$k(u) = \sum_{i=1}^{n} \eta_i B_i(u)$$

where $B_i(u)$ are the B-splines for a fixed set of knots. A cubic B-spline typically consists of a set of 4 smoothly linked cubics on 4 adjacent intervals: the B-spline has finite support and looks somewhat like a unimodal hill. To compute B-splines in a stable way, it is necessary to use a recursive algorithm. Mathematical packages will often have routines to calculate B-splines. However, we need the integrals of the B-splines, which are not generally available, so we move on to another type of spline.

It is important to clear up immediately the differences between the logistic b-splines $b_i(t)$ and the polynomial B-splines. For equally spaced knots, the logistic b-splines have their maximum half-way between the knots, as do the even order polynomial B-splines (quadratic, quartic and so on). We examine quadratic B-splines, which we differentiate from cubic B-splines by using the symbol Q. For

knots at 0, 1, 2, 3 the quadratic B-spline with maximum at 3/2 is

$$Q_1(x) = \begin{cases} x^2/2 & 0 \le x \le 1; \\ (-2x^2 + 6x - 3)/2 & 1 \le x \le 2; \\ (3-x)^2/2 & 2 \le x \le 3; \\ 0 & \text{otherwise.} \end{cases}$$

For knots at 0, 2, 4, 6 the quadratic B-spline is

$$Q_2(x) = \begin{cases} (x/2)^2/2 & 0 \le x \le 2; \\ (-2(x/2)^2 + 6(x/2) - 3)/2 & 2 \le x \le 4; \\ (3 - x/2)^2/2 & 4 \le x \le 6; \\ 0 & \text{otherwise.} \end{cases}$$

The relationship is clearly $Q_2(x) = Q_1(x/2)$. If the spacing is h, then $Q_h(x) = Q_1(x/h)$. This of course covers changes in scale.

We first compare $Q_1(x)$ with the logistic b-spline $b_1(x)$ with knots at 1 and 2 and maximum at 3/2. If we search for the β that minimises $\int (b_1(x) - Q_1(x))^2\, dx$, we find that $\beta = 3.988$. As an aid to memory, we adopt $\beta = 4$ as a good approximation. Visual inspection suggests that $b_1(x)$ and $Q_1(x)$ are very similar, with the maximum absolute difference being 0.021 at $x = 0.1$ and 2.9. The peak values are about 0.75.

It follows immediately that if the spacing between the knots is h, then $b_h(x)$ (with knots at h and $2h$) and $Q_h(x)$ (with knots at $0, h, 2h, 3h$) agree most closely when $\beta = 4/h$. If we choose n uniformly spaced knots to span data with range r, then $h = r/n$. Hence we recommend choosing $\beta = 4n/r$ when fitting the logistic model (3) to such growth data. This argument assumes evenly spaced knots, but we suggest that this choice of β is reasonable when fitting unequally spaced knots as well. We suggest that β should be fixed at this value at least until the final form of the model is established.

Hyperbolic splines

We can also use hyperbolic splines. Thus

$$k(t) = \mu_0 + \mu_1 t + \sum_{i=1}^{n} \eta_i \, h_i(t) \,, \tag{5}$$

where

$$h_i(t) = \frac{1}{2}\left(\sqrt{(t-\alpha_i)^2+\gamma^2} + t - \sqrt{\alpha_i^2+\gamma^2}\right) .$$

It transpires that $h_i(t)$ has an explicit integral. Let

$$h(x) = \sqrt{x^2+\gamma^2} + x \,.$$

Then

$$2\int h(x)dx = xh(x) + \gamma^2 \log h(x) + c \quad \equiv 4r(x) + c$$

where $c = \gamma^2 \log 2$ is a constant. Thus

$$2h_i(t) = h(t-\alpha_i) + c_i$$

where $c_i = \alpha_i - \sqrt{\alpha_i^2+\gamma^2}$. Hence

$$\begin{aligned}
4\int_{t_0}^{t} h_i(u)\,du &= 2\int_{t_0}^{t} (h(u-\alpha_i)+c_i)\,du \\
&= 2\int_{t_0-\alpha_i}^{t-\alpha_i} (h(u)+c_i)\,du \\
&= (t-\alpha_i)h(t-\alpha_i) - (t_0-\alpha_i)h(t_0-\alpha_i) \\
&\quad + \gamma^2 \log h(t-\alpha_i) - \gamma^2 \log h(t_0-\alpha_i) + 2(t-t_0)c_i \\
&\equiv 4(r(t-\alpha_i) - r(t_0-\alpha_i)) + 2(t-t_0)c_i \,.
\end{aligned}$$

Hence the growth curve for a fish with initial length time t_0 is

$$l(t|t_0) = L_\infty \left(1 - e^{-\mu_0(t-t_0) - \mu_1(t^2-t_0^2)/2 + \sum_{i=1}^{n} \eta_i [r(t-\alpha_i) - r(t_0-\alpha_i) + (t-t_0)c_i/2]}\right) .$$

The logistic trend curve model seems a bit neater. Of course, we could difference the hyperbolic functions to express the model in terms of hyperbolic B-splines.

Seasonal effects

Southern bluefin tuna, in common with many other fish species, grow much faster in summer than in winter. We would like to be able to incorporate such seasonal effects into our growth model. A common model for the seasonal von Bertalanffy curve is

$$l'(t) = (L_\infty - l(t))\,\kappa\,(1 + u_s \cos(2\pi(t - w_s)))\,,$$

where κ is a constant and u_s is the amplitude and w_s is the phase of the seasonal effect. The amplitude has bounds $-1 \leq u_s \leq 1$ so that $l'(t)$ is non-negative, and it is convenient to constrain the phase to $-0.5 < w_s \leq 0.5$ for southern bluefin tuna. When integrated we get the model

$$l(t) = L_\infty[1 - \exp(-\kappa\,(t - t_0 + (u_s/2\pi)\,\{\sin(2\pi(t - w_s)) - \sin(2\pi(t_0 - w_s)\})]$$

It is usual to just fit the model

$$l(t) = L_\infty[1 - \exp(-\kappa\,(t - t_0' + (u_s/2\pi)\,\sin(2\pi(t - w_s)))]$$

by combining the constants t_0 and $(u_s/2\pi)\sin(2\pi(t_0 - w_s))$ into t_0', but is must be borne in mind that t_0' is no longer the time of 0 length.

We now turn to the situation in which κ is a function of time, $k(t)$. For explicitness, focus on the logistic trend model for $k(t)$. There is a trick to including the seasonal effect in this type of model. Let $s(t) = (u_s/2\pi)\,\sin(2\pi(t - w_s))$ be the seasonal effect. Then we generalise (1) to

$$l'(t) = (L_\infty - l(t))\,k(t + s)(1 + s')\,, \tag{6}$$

where $s' = ds/dt$. Of course, this is the same general form as (1), because $k(t + s)(1 + s')$ is just a function of time. The trick is to include $k(t + s)$ in (6), rather than $k(t)$. Now note that

$$\int \frac{1 + s'}{1 + \exp(-\beta(t + s - \alpha))}\,dt = (t + s) + \frac{\log(1 + \exp(-\beta(t + s - \alpha)))}{\beta}\,.$$

Hence

$$l(t|t_0) = L_\infty \left(1 - e^{-\kappa_n(t+s-t_0-s_0)} \prod_{i=1}^{n} \left[\left\{ \frac{1+e^{-\beta(t+s-\alpha_i)}}{1+e^{-\beta(t_0+s_0-\alpha_i)}} \right\}^{-(\kappa_i-\kappa_{i-1})/\beta} \right] \right)$$

Thus we have an explicit rigorously derived equation including the seasonal effect. If desired, s_0 may be absorbed into t_0.

When analysing data, we use the following forms.

Capture-recapture data: Equation (4) generalises to

$$l(t|t_1,a) = L_\infty \left(1 - e^{-\kappa_n(t-t_1+a-s_0)} \prod_{i=1}^{n} \left[\left\{ \frac{1+e^{-\beta(t+s-\alpha_i)}}{1+e^{-\beta(t_1-a+s_0-\alpha_i)}} \right\}^{-(\kappa_i-\kappa_{i-1})/\beta} \right] \right)$$

where a is a realisation of A, the random time between length 0 and capture, and $s_0 = s(t_1 - a)$. When $t = t_1 - a$, $l(t|t_1, a) = 0$.

Length-frequency and otolith data: We know the age a of the fish at capture. Hence $t_0 = t - a + a_0$ and

$$l(t|a,a_0) = L_\infty \left(1 - e^{-\kappa_n(a-a_0+s-s_0)} \prod_{i=1}^{n} \left[\left\{ \frac{1+e^{-\beta(t+s-\alpha_i)}}{1+e^{-\beta(t-a+a_0+s_0-\alpha_i)}} \right\}^{-(\kappa_i-\kappa_{i-1})/\beta} \right] \right) \quad (7)$$

where $s_0 = s(t - a + a_0)$. When $t = t_0$, $a = a_0$ and $s = s_0$, so $l(t|a, a_0) = 0$. For length-frequency data, and sometimes for otolith data, southern bluefin tuna are assigned 1 January as a birth date, so that $t - a$ is an integer. Hence $s_0 = s(a_0)$.

When using optimisation routines to fit this model, it is helpful to have explicit expressions for the first derivatives. For the record, the formulae are given below. For a generic model of the type

$$l(t;\theta) = L_\infty \left(1 - e^{\rho(t;\theta)}\right)$$

where θ is a vector of parameters and $\rho(.)$ is a function, the partial derivative of $l(t;\theta)$ with respect to one of the parameters is

$$\frac{\partial l(t;\theta)}{\partial \theta_i} = -(L_\infty - l(t;\theta)) \frac{\partial \rho(t;\theta)}{\partial \theta_i}.$$

For the model (7)

$$\rho(t;\theta) \equiv = -\kappa_n(a - a_0 + s - s_0) - \sum_{i=1}^{n} \frac{(\kappa_i - \kappa_{i-1})}{\beta} P_i$$

where

$$P_i = \log(1 + e^{-\beta(t+s-\alpha_i)}) - \log(1 + e^{-\beta(t-a+a_0+s_0-\alpha_i)}) .$$

Hence the derivatives with respect to κ are

$$\begin{aligned}
\frac{\partial \rho}{\partial \kappa_0} &= P_1/\beta; \\
\frac{\partial \rho}{\partial \kappa_j} &= (P_j - P_{j+1})/\beta \quad \text{for } 1 \le j \le n-1; \\
\frac{\partial \rho}{\partial \kappa_n} &= P_n/\beta - (a - a_0 + s - s_0) .
\end{aligned}$$

The derivatives with respect to α are

$$\frac{\partial \rho}{\partial \alpha_j} = -(\kappa_j - \kappa_{j-1}) \left\{ \frac{1}{1 + e^{-\beta(t-a+a_0+s_0-\alpha_j)}} - \frac{1}{(1 + e^{-\beta(t+s-\alpha_j)})} \right\}$$

for $1 \le j \le n$. The derivative with respect to a_0 is

$$\frac{\partial \rho}{\partial a_0} = (1 + s_0') Q$$

where $s_0' = s'(t - a + a_0) = u_s \cos(2\pi(t - a + a_0 - w_s))$ and

$$Q = \kappa_0 + \sum_{i=1}^{n} (\kappa_i - \kappa_{i-1}) \frac{1}{1 + e^{-\beta(t-a+a_0+s_0-\alpha_i)}}) .$$

The derivatives with respect to u_s and w_s are

$$\begin{aligned}
\frac{\partial \rho}{\partial u_s} &= -\kappa_0 \left(\frac{\partial s}{\partial u_s} - \frac{\partial s_0}{\partial u_s} \right) - \frac{\partial s}{\partial u_s} \sum_{i=1}^{n} (\kappa_i - \kappa_{i-1}) R_i + \frac{\partial s_0}{\partial u_s} \sum_{i=1}^{n} (\kappa_i - \kappa_{i-1}) R_{0i} \\
\frac{\partial \rho}{\partial w_s} &= -\kappa_0 \left(\frac{\partial s}{\partial w_s} - \frac{\partial s_0}{\partial w_s} \right) - \frac{\partial s}{\partial w_s} \sum_{i=1}^{n} (\kappa_i - \kappa_{i-1}) R_i + \frac{\partial s_0}{\partial w_s} \sum_{i=1}^{n} (\kappa_i - \kappa_{i-1}) R_{0i}
\end{aligned}$$

where

$$\begin{aligned}
R_j &= \frac{1}{1 + e^{-\beta(t+s-\alpha_j)}} ; \\
R_{0j} &= \frac{1}{1 + e^{-\beta(t-a+a_0+s_0-\alpha_j)}} .
\end{aligned}$$

A time-varying VB $\log k$ model

So far we have only discussed the time-varying von Bertalanffy model. There are many other growth models that may be preferred. In Appendix 4, we introduced

the 'VB $\log k$' model, defined by

$$k(t) = k_1 + (k_2 - k_1)\frac{1}{1+\exp(-\beta_0(t-t_0-\alpha_0))}. \quad (8)$$

Here t represents time, but the model only depends on age $t - t_0$. For $t \ll t_0 + \alpha_0$, $k(t) \approx k_1$, and for $t \gg t_0 + \alpha_0$, $k(t) \approx k_2$. As t increases, $k(t)$ makes a smooth transition from k_1 to k_2. The rate of transition is governed by β_0, being sharper for larger β_0. We discovered that the model provided a significantly better fit to 1980s southern bluefin tag-recapture data than a simple von Bertalanffy model.

The obvious way to make this model depend on time is to make k_1 and k_2 functions of time:

$$k(t) = k_1(t) + (k_2(t) - k_1(t))\frac{1}{1+\exp(-\beta_0(t-t_0-\alpha_0))}. \quad (9)$$

In general this model is intractable, and probably over-parameterised, but there is one obvious tractable case, namely to set $k_1(t) = k(t)$, defined in equation (2), and $k_2(t) - k_1(t) = k_{21}$, a constant. This case assumes that $k_1(t)$ and $k_2(t)$ vary in parallel. If $k_1(t) = \kappa$ for all t, it becomes the VB $\log k$ model, and if $k_{21} = 0$, it reduces to the time-varying von Bertalanffy model.

For the tractable case,

$$\begin{aligned}\int_{t_0}^{t} k(u)\,du &= \int_{t_0}^{t} k_1(u)\,du + k_{21}(t-t_0) \\ &\quad + \frac{k_{21}}{\beta_0}\left(\log[1+\exp(-\beta_0(t-t_0-\alpha_0))] - \log[1+\exp(\alpha_0\beta_0)]\right).\end{aligned}$$

Hence the growth curve for a fish with initial length time t_0 is

$$l(t|t_0) = L_\infty\left(1 - e^{-\kappa(t-t_0)}\,g(t,t_0)\right) \quad (10)$$

where

$$g(t,t_0) = \prod_{i=1}^{n}\left[\left\{\frac{1+e^{-\beta(t-\alpha_i)}}{1+e^{-\beta(t_0-\alpha_i)}}\right\}^{-\kappa_{id}/\beta}\right]\left\{\frac{1+e^{-\beta_0(t-t_0-\alpha_0)}}{1+e^{\beta_0\,\alpha_0}}\right\}^{-k_{21}/\beta_0} \quad (11)$$

for $t \geq t_0$, $\kappa = \kappa_n + k_{21}$ and $\kappa_{id} = \kappa_i - \kappa_{i-1}$. Of course, $l(t|t_0) = 0$ if $t < t_0$. We shall not attempt to fit this model to any data in this chapter.

The seasonal version of (10) is

$$l(t|t_0) \;=\; L_\infty \left(1 - e^{-\kappa(t+s-t_0-s_0)}\, g(t+s, t_0+s_0)\right) .$$

Decade by decade analysis of both length-frequency data and tag-recapture data suggests that the traditional von Bertalanffy model is an adequate approximation for the 1960s, but that the VB $\log k$ model is needed for the 1980s. The time-varying VB $\log k$ model that we have described in (10) is not flexible enough to capture such a transition. A first modification would be to make $k_{21}(t) = k_2(t) - k_1(t)$ a linear function of t (as in $k_{21}(t) = a + bt$). Unfortunately, $k(t)$ does not have an explicit integral in terms of elementary functions. However, we can use the following trick. For a fish with starting time t_0, and for given α_0, write $k_{21}(t) = a + b(t_0 + \alpha_0) + b(t - t_0 - \alpha_0)$. Then the contribution of the linear component of $k_{21}(t)$ to the integral is

$$\begin{aligned}
\int_{t_0}^{t} \frac{u - t_0 - \alpha_0}{1 + \exp(-\beta_0(u - t_0 - \alpha_0))}\, du \;&=\; \frac{1}{\beta_0^2} \int_{t_0^*}^{t^*} \frac{y}{1 + \exp(-y)}\, dy \\
&=\; \frac{1}{\beta_0^2} \left[\int_{-300}^{t^*} \frac{y}{1 + \exp(-y)}\, dy - \int_{-300}^{t_0^*} \frac{y}{1 + \exp(-y)}\, dy \right] \\
&=\; \frac{1}{\beta_0^2} \{ I(t^*) - I(t_0^*) \}
\end{aligned}$$

where $t^* = \beta_0(t - t_0 - \alpha_0)$ and $t_0^* = -\beta_0\, \alpha_0$. The lower integration limit of -300 in $I(t)$ is imposed because α_0 and β_0 have upper bounds of 10 and 30 respectively in practice. The integrand $y/(1 + \exp(-y))$ does not depend on any parameters, so we can compute $I(t)$ on a fine grid $t = -300 + n\delta$ for $n = 1, 2, 3 \ldots$ using an accurate numerical integration algorithm prior to parameter estimation. During parameter estimation, $I(t)$ can be calculated by interpolation: $I(t) \approx (1 - f) I(-300 + n_t\delta) + f I(-300 + (n_t + 1)\delta)$, where $n_t = [(t + 300)/\delta]$ and $f = t - n_t\delta$.

Alternatively, we could take a pragmatic approach, and make k_{21} in (10) a suitable function of t. Given that the linear model for $k_{21}(t)$ is an approximation, this is probably the best compromise.

There is another exact approach that can bypass the need to integrate. Let

$z(t)$ be a monotone increasing function of time, and set

$$k(t) = k_1(t) + \frac{k_{21}(1 + z'(t))}{1 + \exp(-\beta_0(t - t_0 + z(t) - z(t_0) - \alpha_0))}.$$

Then the length model is given by (10), but with the factor

$$\left\{\frac{1 + e^{-\beta_0(t-t_0-\alpha_0)}}{1 + e^{\beta_0 \alpha_0}}\right\}^{-k_{21}/\beta_0}$$

in $g(t, t_0)$ (equation (11)) replaced by

$$\left\{\frac{1 + e^{-\beta_0(t-t_0+z(t)-z(t_0)-\alpha_0)}}{1 + e^{\beta_0 \alpha_0}}\right\}^{-\chi(t)/\beta_0}$$

where $\chi(t) = k_{21}(1 + z'(t))$. The seasonal model generalises in the obvious way, by replacing t by $t + s$ and t_0 by $t_0 + s_0$ everywhere.

The important point is that $\chi(t)$ can change with time. Judicious choice of $\chi(t)$ can allow for the transition from von Bertalanffy to VB $\log k$ model with time.

Fitting the time-varying von Bertalanffy model to southern bluefin tuna data

South Australian length-frequency data

We first fit the time-varying von Bertalanffy model to South Australian length-frequency data. The raw data are length measurements generated from commercial fishing operations. They represent samples of landed fish accumulated over each half-month of the fishing season. The analysed data are the estimated component means and standard errors for age-groups 1 to 4 from 1964/5 to 1988/89. We use the estimation procedure described in Appendix Length-Frequency: the model for season i of data is, in vector form,

$$y_i = \mu_i + 1\tau_i + X_\nu \nu_i + X_\omega \omega_i + e_i + \epsilon_i$$

where y_i is vector of data and μ_i is the vector of mean growths. Here τ_i, ν_i, ω_i, e_i and ϵ_i are independent random effects, representing a random seasonal effect, a

within-season random half-month effect, a within-season random age effect and a within-season half-month age interaction respectively. Finally, ϵ_i denotes sampling error, and is assumed known from previous data analysis. Also, X_ν and X_ω are design matrices: thus, $X_{\nu,mj} = 1$ if element m belongs to half-month j and is zero otherwise. We calculate μ from the relevant model, in this case equation (7). We tried fitting this model using the b-spline parameterisation with and without first derivatives of the likelihood, and the stable parameterisation of Ross (1990), Schnute (1981) and Francis (1988) without derivatives. We can only recommend the gradient method — it converged about 10 times faster than the derivative-free methods.

We fixed $\mu_\infty = 185$ cm. Extensive analysis of other data suggests that the asymptotic mean length has varied at most between about 183 cm and 187 cm between 1960 and 2000, and we use 185 cm as a representative figure. The length-frequency data do not bear on the asymptotic mean length. We tried fitting between 1 and 10 knots. The maximum log-likelihood $\log \lambda$ for each case is shown in Table 1.

Table 1: Optimal negative log-likelihood for time-varying von Bertalanffy growth model with K knots: complex error structure

K	$-\log \lambda$	K	$-\log \lambda$
1	893.23	6	873.23
2	889.97	7	872.25
3	889.77	8	871.47
4	884.65	9	870.47
5	873.94	10	869.87

It is clear that the data are adequately fitted using $K = 5$ knots, since there is no significant improvement in the log-likelihood with the addition of extra knots. The results for the 5 knot solution are

Table 2: Fitted parameters for the seasonal von Bertalanffy growth model with logistic growth rate: South Australian length-frequency data

μ_∞	185	$\hat{\sigma}_\tau$	0.010	$\hat{\kappa}_0$	0.155	$\hat{\alpha}_1$	1970.86
$\hat{a}_0$	-1.187	$\hat{\sigma}_\nu$	0.800	$\hat{\kappa}_1$	-0.850	$\hat{\alpha}_2$	1971.36
$\hat{u}_s$	0.743	$\hat{\sigma}_\omega$	1.817	$\hat{\kappa}_2$	1.185	$\hat{\alpha}_3$	1971.86
$\hat{w}_s$	0.128	$\hat{\sigma}_e$	1.741	$\hat{\kappa}_3$	0.141	$\hat{\alpha}_4$	1978.79
$\hat{\beta}$	0.833			$\hat{\kappa}_4$	0.169	$\hat{\alpha}_5$	1984.13
				$\hat{\kappa}_5$	0.164.		

Note that $\hat{\kappa}_0 = 0.155$ and $\hat{\kappa}_5 = 0.164$ may be compared to κ for a traditional von Bertalanffy growth model. It is interesting to compare these estimates with the corresponding values when fitting the model with constant κ to the same data, with $\mu_\infty = 185$ cm. Then $\hat{\kappa} = 0.154$, $\hat{a}_0 = -1.32$, $\hat{u}_s = 0.753$, $\hat{w}_s = 0.130$, $\hat{\sigma}_\tau = 2.454$, $\hat{\sigma}_\nu = 0.831$, $\hat{\sigma}_\omega = 2.152$ and $\hat{\sigma}_e = 1.738$. The estimates are all reasonably similar to those in Table 2, except that $\hat{\sigma}_\tau = 2.454$ in the constant κ model reduces to $\hat{\sigma}_u = 0.01$ (the lower bound) in the variable κ model. This suggests that the variable κ model has been successful in capturing the variation in κ with season.

We now illustrate some features of the model. Figure 1, top panel, shows how $\hat{k}(t)$, with the seasonal parameter u_s set to 0, varies with time. It broadly follows the shape of Figure 6 in Appendix 7. Rather surprisingly, there is a noticeable difference: the level of the peak at 1973 is about the same as that at 1985. It is of interest to compare $\hat{k}(t)$ with the estimates of k in a simple von Bertalanffy model fitted to the component decades: $\hat{\kappa} = 0.146$ for the 1960s, $\hat{\kappa} = 0.141$ for the 1970s and $\hat{\kappa} = 0.170$ for the 1980s. The average values of $\hat{k}(t)$ for these periods are 0.151, 0.153 and 0.165 respectively. Although similar, these are not identical to the decade by decade estimates — it would appear that the fitting of a single smooth curve $k(t)$ has a regression-to-the-mean effect.

The lower panel shows how the mean lengths for age groups 1 to 4 vary with

season. The pattern differs in an important way from that in the upper panel: the 1973 and 1985 peaks are the same height for the one-year-old fish, but the 1985 peak is clearly higher for the four-year-old fish. The two-year-old and three-year-old fish show intermediate effects. These results are consistent with the decade by decade results presented in Figure 5 in Appendix 7, which shows that the differences between the 1980s and previous decades was small for the one-year-olds, but progressively larger for older age groups. When comparing half-month Gaussian mixture fits to the 1970s length-frequency data, we experienced difficulty in following the age group changes. The fact that the growth curve appears to have been following a sine curve through that decade may explain the difficulty.

Figure 2 examines the fit of the model. The raw data are plotted as points, and the fitted values as smooth curves. The model captures the major variation with season. Some age-groups in some seasons do not fit very well. This is the reason for including the random effect w_{ik} in the model. It is not surprising that $\hat{\sigma}_w$ is the largest estimated random effect variance. Close inspection suggests that the four-year-old fits are too low in the 1980s. This may reflect the inadequacy of the von Bertalanffy growth model for this decade. The von Bertalanffy model is incapable of capturing the fast early growth of 1980s juveniles. This is yet another indicator that a more complex growth model may be required.

The fit can be examined further by plotting the estimated random effects in various ways. The traditional BLUP estimates of the random effects are

$$\begin{aligned}
\hat{\tau}_i &= \hat{\sigma}_\tau^2 \, 1' V^{-1} (y_i - \hat{\mu}_i) \\
\hat{\nu}_i &= \hat{\sigma}_\nu^2 \, X_\nu' V^{-1} (y_i - \hat{\mu}_i) \\
\hat{\omega}_i &= \hat{\sigma}_\omega^2 \, X_\omega' V^{-1} (y_i - \hat{\mu}_i) \\
\hat{e}_i &= \hat{\sigma}_e^2 \, V^{-1} (y_i - hat\mu_i)
\end{aligned}$$

where

$$V = \sigma_e^2 \, I + D_\epsilon + \sigma_\tau^2 11' + \sigma_\nu^2 X_\nu X_\nu' + \sigma_\omega^2 X_\omega X_\omega'$$

is the variance-covariance matrix of the data, and D_ϵ is the diagonal matrix of

sampling variances. In Figure 3 we plot $\hat{\omega}_i$, estimated for each season, against year for each age group. If the model is correct these plots should show no obvious structure, but there is a clear downward trend in the panels for one and two-year-olds, an upward trend with time for the three-year-olds and more complex structure for the four-year-olds. Studies in Appendices 4 and 9 indicate that this lack of fit can be ascribed to two causes: firstly, the lengths of one-year-olds in the length-frequency data set are bigger than those of corresponding fish in the tag-recapture and otolith data sets; and secondly, the von Bertalanffy growth curve does not describe 1980s tuna length data very well. The first problem must be resolved before more complex time-varying growth curves can be fitted. The objective of fitting more complex time-varying growth models is to remove such trends — the growth model becomes more complex, and removes the obvious non-random structure in the random effects.

Figure 4 shows some selected cohort growth curves, illustrating how they change with the season. The mean lengths for fish of ages 1 to 4 on January 1 are shown as broken lines. The model clearly includes an ameliorated cohort effect: the peaks and troughs in these mean length curves move to the right as age increases, but a given cohort does not follow this movement exactly. Cohort growth is strongly seasonal.

It is useful to know how much the solution changes if we fit the much simpler model

$$y_i = \mu + e_i + \epsilon_i \tag{12}$$

to the data in season i. In this case the log-likelihoods are

Table 3: Optimal negative log-likelihood for time-varying von Bertalanffy growth model with K knots: simple error structure

K	$-\log\lambda$	K	$-\log\lambda$
1	1090.44	6	985.69
2	1078.39	7	983.04

Table 3: continued

3	1062.41	8	980.25
4	994.51	9	976.25
5	990.65	10	975.36

The choice of K is no longer definitive. The simple error model forces some of the seasonal and within-season variation to be treated as trend, and this trend becomes more complex as K increases. The complex error model with hierarchical and crossed random effects allows deviations from a simple trend model to be treated as structured error rather than trend. We therefore prefer the complex error model.

Tag-recapture data

We now move on to fitting the time-varying von Bertalanffy growth curve to tag-recapture data. We have attempted to use the method of Appendix 4. The data file records the time t_1 and length l_1 at the time of tagging, and the time t_2 and length l_2 upon recapture for 6154 tuna. This is the total tag-recapture data base after quality control screening (see Appendix 3). The times t_1 range between 1959 and 1997. The model for fish i is

$$\begin{aligned} l_{1i} &= L_{\infty,i} f(t_{1i}; A_i, \theta) + \epsilon_{1i} \\ l_{2i} &= L_{\infty,i} f(t_{2i}; A_i, \theta) + \epsilon_{2i} \end{aligned}$$

where $L_{\infty,i}$ is the asymptotic mean length, $f(t; A, \theta)$ is the monotone increasing growth curve with asymptote 1 and parameter set θ, A_i is the time to first capture and ϵ_{1i} and ϵ_{2i} represent measurement error. All random variables are independent. We assume that $L_{\infty,i} \sim N(\mu_\infty, \sigma_\infty^2)$, $A_i \sim LogN(\mu_{\log A}, \sigma_{\log A})$ and $\epsilon_{ji} \sim N(0, \sigma^2)$ for $j = 1, 2$.

We have encountered a technical difficulty in analysing these data with a growth model with more than 4 parameters in θ: the optimisation method used to maximise the likelihood is very slow. We need to calculate the gradients of the

log-likelihood analytically, which should speed up the calculations by an order of magnitude. In the meantime we report some preliminary results from a sub-sample of size 1000 from this data set. We fit the model (4) with 4 knots and $\beta = 1$. We omit any seasonal parameters from θ to speed up the algorithm and again fix μ_∞ at 185 cm. The results are

Table 4: Fitted parameters for the von Bertalanffy growth model with logistic growth rate: tag-recapture data

μ_∞	185	$\hat{\kappa}_0$	0.173	$\hat{\alpha}_1$	1969.37
$\hat{\sigma}_\infty$	9.75	$\hat{\kappa}_1$	0.040	$\hat{\alpha}_2$	1972.80
$\hat{\mu}_{\log A}$	0.926	$\hat{\kappa}_2$	0.527	$\hat{\alpha}_3$	1973.30
$\hat{\sigma}_{\log A}$	0.246	$\hat{\kappa}_3$	0.141	$\hat{\alpha}_4$	1981.11
$\hat{\sigma}$	4.15	$\hat{\kappa}_4$	0.196		

The estimates of $k(t)$ and the mean lengths for age groups 1 to 4 are shown in Figure 5. Qualitatively $\hat{k}(t)$ is the same as that in Figure 1, even though this is an independent data set. There are obvious differences between Figures 1 and 5, but taking them together, we can safely conclude that the rate of growth of southern bluefin tuna is faster now than in 1960. The 1970s saw a period of change followed by a slow rise to its current level starting in the late 1970s. It must be stressed that the tag-recapture data set is deficient in the 1970s, so that estimation of $k(t)$ is likely to be relatively poor during this time. There were significant tagging voyages in the 1960s, 1980s and 1990s, but only about 200 taggings in the 1970s. In retrospect, the decision to scale down tagging in the 1970s was unfortunate, given the apparent change in growth in that decade.

Our first sample deliberately omitted data from the 1990s. We attempted to supplement the first analysis with a second analysis of a sample of 1000 data points from the 1980s and 1990s. The fitting program failed to converge. Inspection of the data reveals that there were no fish tagged between mid-February 1984 and late October 1990, a period of almost 7 years. We suspect that this caused the problem.

Much technical work remains to be done before we can fit dynamically changing growth curves with confidence.

Otolith data

We also attempted to fit the von Bertalanffy model with changing $k(t)$ to the otolith data. We confined our attention to 1980s and 1990s data with a maximum otolith age of 4 years. Older fish could have come from previous decades. There were only 420 points, and 25% of these came from one year (1993), with only 101 from the 1980s. In the end the data proved too sparse to model. The otolith data may be used to supplement other data sources, but fitting a model to these data alone is impractical. Currently we have not developed the changing $k(t)$ model to allow integrated fitting of growth curves to data of multiple types.

Concluding remarks

There is an extensive literature on parametric growth models, particularly applied to fish growth. Methods for fitting them have been developed for data generated from individual studies. However, models for changing growth over long time periods are virtually unknown. In this Appendix we have attempted to provide a new class of models for time-dependent von Bertalanffy growth. Fitting of this model to length-frequency and tag-recapture data sets of southern bluefin tuna revealed a common pattern, in which growth changed dramatically in the 1970s, with recent growth rates substantially higher than in the 1960s. The reason for these changes are unknown, although they undoubtedly reflect, in part, fishing pressure and changing stock levels.

Despite this success, there is more to be done. Time-variation needs to be incorporated into other growth models, and efficient methods of fitting such models to tag-recapture data in particular need to be developed. It may be desirable to move to non-parametric growth models. Once such models can be fitted successfully, the

ultimate challenge will be to fit them to length-frequency and tag-recapture data sets simultaneously.

References

ABRAMOWITZ, M. & STEGUN, I.A. (1964) *Handbook of mathematical functions with formulas, graphs and mathematical tables.* National Bureau of Standards: Applied Mathematics Series 55.

FRANCIS, R.I.C.C. (1988) Maximum likelihood estimation of growth and growth variability from tagging data. *NZ J. Mar. Freshw. Res.* **22,** 42-51.

ROSS, G.J.S. (1990) *Non-linear estimation.* Springer-Verlag: New York.

ROSS, G. J. S. (1970) The efficient use of function minimization in non-linear maximum-likelihood estimation. *Appl. Stat.* **19,** 205-221.

SCHNUTE, J. (1981) A versatile growth model with statistically stable parameters. *Can. J. Fish. Aquat. Sci.* **38,** 1128-1140.

SCHUMAKER, L.L. (1981) *Spline functions: basic theory.* Wiley: New York.

WANG, Y-G. (1998) Growth curves with explanatory variables and estimation of the effect of tagging. *Aust. N.Z. J. Stat.* **40,** 299-304.

Figure 1: Results from fitting a time-varying von Bertalanffy growth model to South Australian length-frequency data. a) The fitted von Bertalanffy growth rate $\hat{k}(t)$ versus time t. b) The mean lengths for age groups 1 to 4 versus time t. Note that the curves exhibit subtle differences, in that the early 1970s peak moves to the right as age increases, and the relative heights of the 1973 and 1985 peaks change with age group.

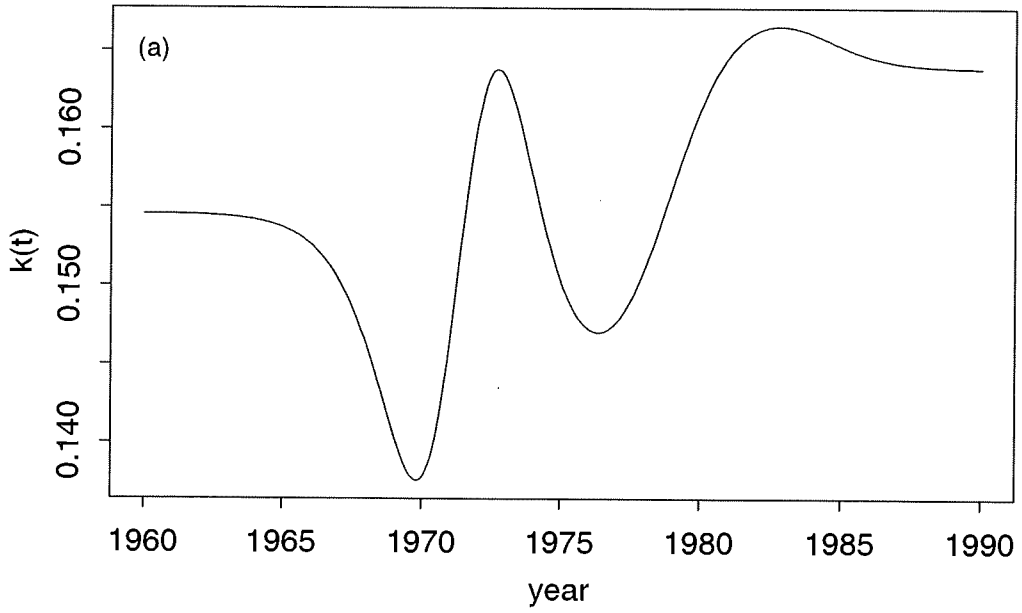

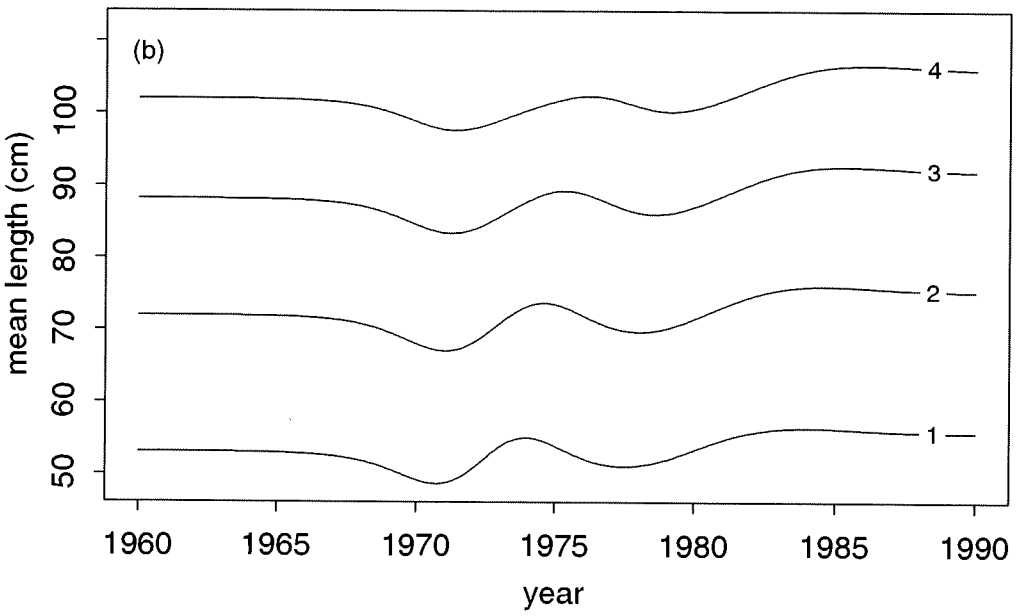

Figure 2: The fit of the time-varying von Bertalanffy growth model for South Australian length-frequency data. The raw data are plotted as points, and the fitted values as smooth curves. The fit is not perfect - for example, the 1980s four-year-old fitted values tend to fall below the data.

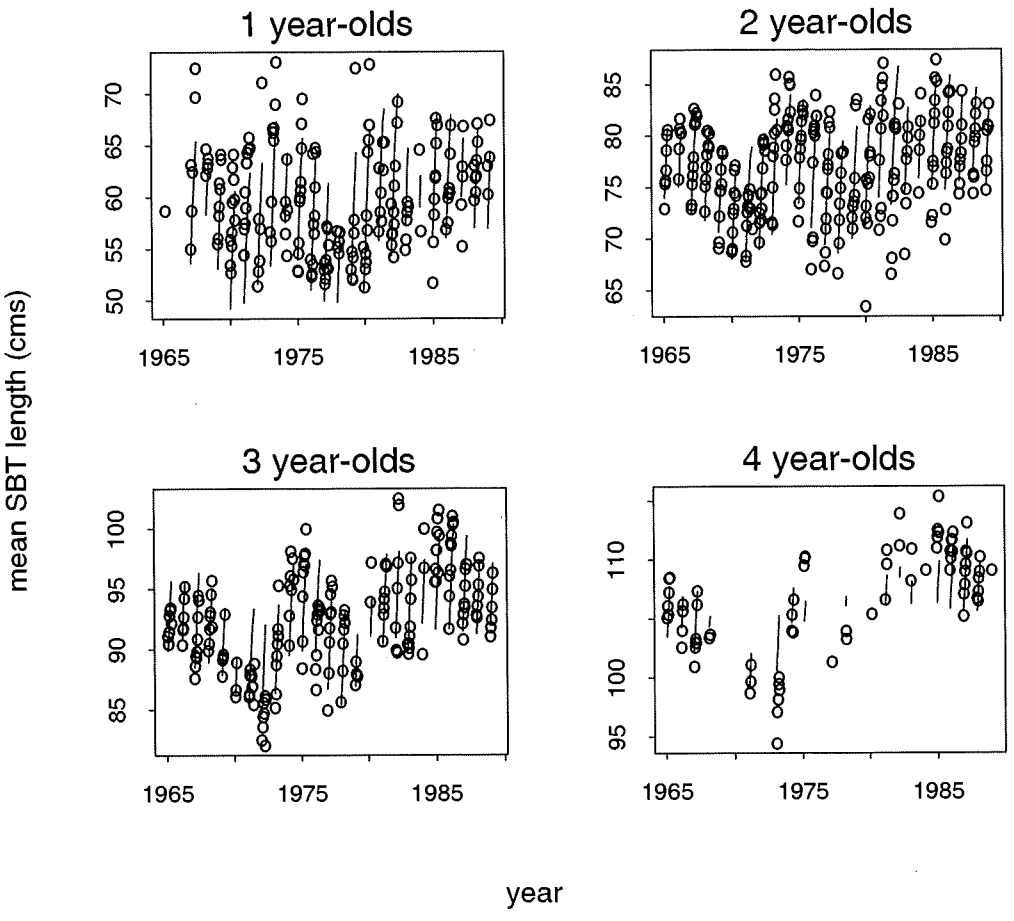

Figure 3: Estimated within-season age effects versus year. The plots exhibit trends and other structure inconsistent with a well-fitting model, confirming the problems with the model suspected from Figure 2.

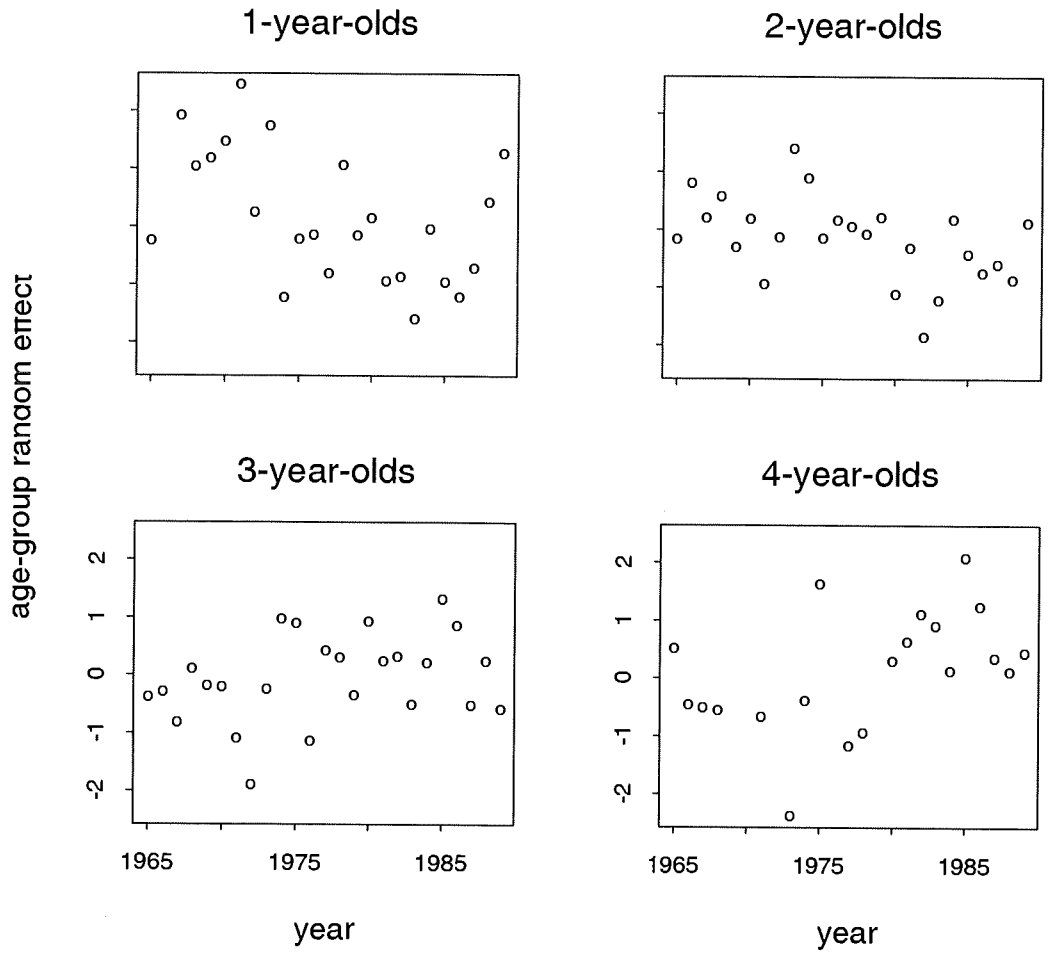

Figure 4: Selected cohort growth curves plotted against year. The subtle changes in cohort growth with time are illustrated.

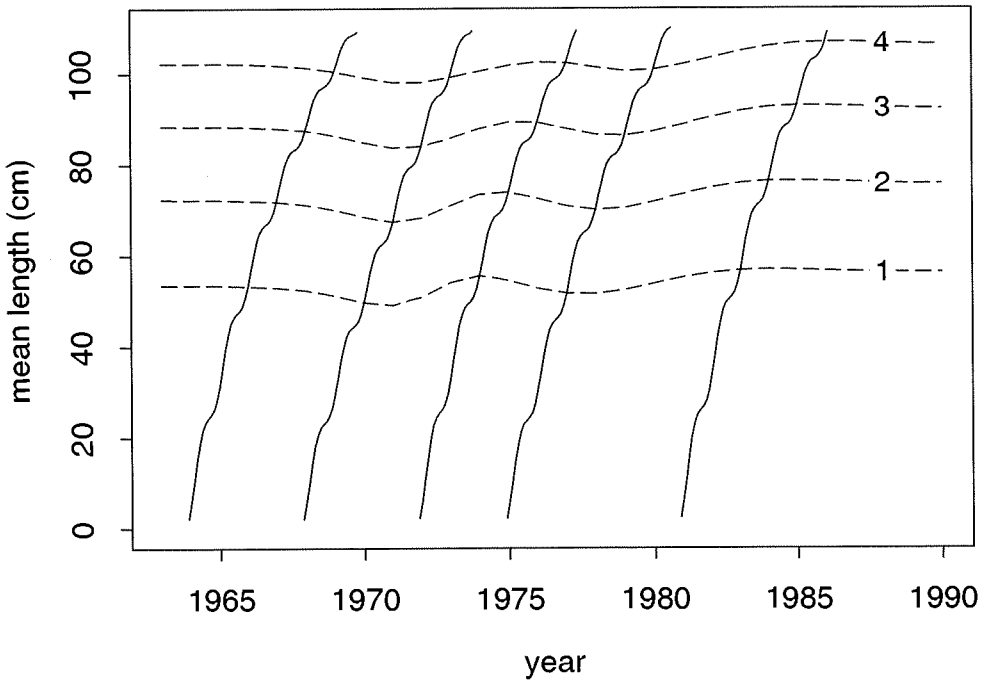

Figure 5: Results from fitting a time-varying von Bertalanffy growth model to tag-recapture data. a) The fitted von Bertalanffy growth rate $\hat{k}(t)$ versus time t. The trend is qualitatively similar to the upper panel of Figure 1 although there are obvious differences. For example, the peak in Figure 1 in the early 1970s is largely missing, possibly because of limited tagging in the 1970s. b) The mean lengths for age groups 1 to 4 versus time.

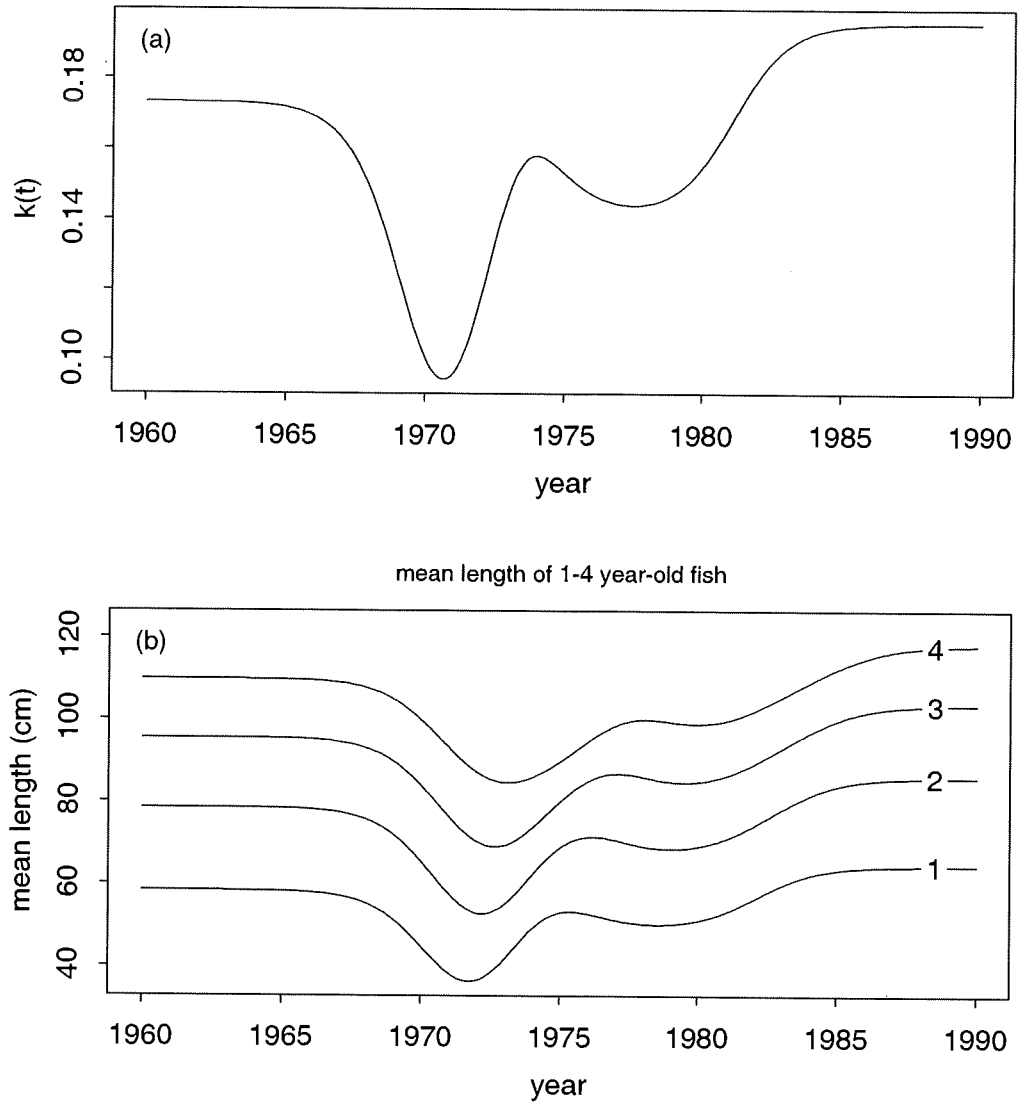

Appendix 9:

An integrated model for growth incorporating tag-recapture, length-frequency and direct aging data

J. Paige Eveson, Geoff M. Laslett and Tom Polacheck

FRDC Project 1999/104

Introduction

The growth of a fish is a fundamental component of fisheries research. Growth models are used either directly or indirectly in stock assessments to estimate the age composition of the catch, plus changes in growth have important implications about stock health and size. Information for studying fish growth can be obtained from a number of sources. Probably the three most common are: 1) release and recapture length data from tagging experiments; 2) length-frequency data from the commercial catches; and 3) direct age and length measurements, where age is estimated from annual deposits in hard tissue such as otoliths, scales, or vertebrae.

Various methods for fitting growth models to any one of these data sources individually have been developed. For tag-recapture data, the age of a fish at release is unknown so the traditional approach has been to model the incremental change in length of the fish over the time it was at liberty (Fabens 1965; Francis 1988b; James 1991). More recently, maximum likelihood approaches have been developed that model the joint density of the release and recapture lengths as opposed to the modelling the length increment (Palmer *et al.* 1991; Wang *et al.* 1995; Laslett *et al.* 2002). In these cases, the age at release is modelled as a random variable.

For a species that has a peak spawning period, the length-frequency distribution of the catch taken over a limited time interval will ordinarily exhibit modes that correspond to different age-classes, at least for younger ages. The progression of these modes over time can be tracked to give an estimate of growth. In particular, seasonal growth patterns can often be identified. Methods have been developed to analytically separate the modes by assuming the distribution is a finite mixture of normal or log-normal distributions (Hasselblad 1966; Macdonald and Pitcher 1979). Approaches that also incorporate the estimation of growth parameters into the length-frequency analysis have subsequently been developed (Schnute and Fournier 1980; Fournier *et al.* 1990; Leigh and Hearn 2000).

Direct age data is a useful source of growth information for species that deposit annual growth rings in their scales, otoliths, vertebrae or other hard tissue. The ability to determine age by counting the number of growth bands has been validated for many

species, including southern bluefin tuna (Clear *et al.* 2000). The best tissue and technique to use depends on the species and the specimen, and successful aging methods have not been found for many species. Direct age and length information has been used to estimate growth parameters in a number of studies (Yukinawa 1970; Thorogood 1987; Gunn and Farley 1998; Alves *et al.* 2002).

While many studies exist that estimate growth using one of the above data sources, analyses that integrate multiple data sources have been much rarer. Some papers have compared estimates of growth obtained from different data sources (Labelle *et al.* 1993). Others have used one data source to supplement another, such as Hearn and Polacheck (Submitted) who used the mean length of age one SBT from length-frequency data to convert the length-time relationship estimated from tag-recapture data to a length-age relationship. Although these studies make use of more than one data source, they do not attempt to model the data jointly. An exception is Kirkwood (1983), who performed a joint analysis of length-increment and age-length data (determined from length-frequency data) to estimate growth parameters for southern bluefin tuna.

We know of no analysis that integrates all three data sources into a unified growth model, and this provided the motivation for our current paper. These data sources will often be most informative about different portions of the life cycle. As such, the development of an integrated approach would allow for the different data sources to complement each other and provide a more robust and comprehensive basis for modelling growth. Questions have been raised about the validity of estimating mutual growth parameters using more than one data source (Francis 1988a). However, we believe that this is not an issue if an appropriate estimation method is used. We present a maximum likelihood approach for modelling growth that incorporates a likelihood component for each tag-recapture data, length-frequency data, and direct age-length data.

Our method was developed and will be illustrated in the context of southern bluefin tuna (SBT). However it should be broadly applicable to other species with perhaps small adjustments for the specific situation. SBT is an important species to both Australian and Japanese fisheries, and hence its growth has been intensely studied. Nevertheless, previous growth models are not fully satisfactory in that they have been

estimated using only one source of data, and the data from any one source does not provide complete information about growth over the lifespan of SBT.

We begin by discussing the three SBT data sets used in our analysis. We then describe the integrated model and estimation method that we have developed. The integrated model was developed in a piece-wise manner. We derived a statistical model in terms of a generic family of growth curves, and a likelihood function for fitting the model, for each data set separately. The likelihood components for the three data sources were then added together to obtain an overall objective function for the integrated model. Finally, we apply the integrated model with several variations to the SBT data, and discuss the results.

The Data

All of the tag-recapture, length-frequency, and direct aging data that are available for SBT are described in detail in Appendix 3, as are the screening processes applied in determining the data suitable for inclusion in a growth analysis. Some of the merits and limitations of each of the data types with respect to studying growth are also discussed there.

Although information on the growth of SBT exists from the 1950's until present, we chose to only include data for fish that experienced their early years of growth in the 1980's. Previous studies have found that the average growth rate of SBT increased from the 1960's to the 1980's (Hearn and Polacheck in press; Anon. 1994). This makes a combined analysis of all the data more complicated and is the topic of Appendices 8 and 10. We chose to analyse the 1980's data because extensive data sets exist in this decade for each of the data sources, with a large degree of overlap among data sets with respect to ages and lengths of SBT. Thus, the 1980's provided the best data for testing the integrated methods that we developed.

Following is a brief summary of the 1980's data that we used in the analysis presented in this Appendix.

Tag-Recapture Data

During the 1980's (in years 1980, 1983 and 1984), a total of 10741 fish aged 0 to 4 were tagged with conventional tags and released into the wild. Of these tagged fish, there have been 4341 reported recaptures to date (January 2002). Recaptures occurred throughout the geographical distribution of SBT, ranging in longitude from 0 to 180°E and in latitude from 30 to 50°S. After applying the screening criteria described in Appendix 3 to exclude data that were considered unsuitable for studying growth, 2181 recaptures from fish released in the 1980's remained for analysis. The release lengths ranged from 40 to 115 cm and the recapture lengths from 47 to 173 cm. The distribution of the times at liberty was highly skewed towards shorter times at liberty, and ranged from 30 to 4356 days (≈12 years) with a median value of 340 days. A plot of the change in length of the fish versus the time at liberty is shown in Figure 1.

Length-Frequency Data

For reasons discussed in Appendix 3, we only included length-frequency data from the Australian surface fishery operating in South Australia in our analysis. For the South Australian fishery, the sampling of fish for lengths occurred in a two-step procedure in which a sample of fish was taken from a sample of landings. In each half-monthly period, the length-frequency data were scaled up from the sample data using the weight of the total catch to represent a length-frequency distribution for the catch. Scale factors have been calculated which take into account the two-stage nature of the sampling, so that dividing the catch size in a period by the scale factor gives an estimate of the effective sample size if a simple random sample had been taken. The fishing season in South Australia generally spans from November to July. Length-frequency data exist for every year in the 1980's, but the half-monthly periods for which there are data depend on the year. Almost all years have data from mid-December to mid-April. Table 1 in Appendix 3 lists the years and periods for which data are available, as well as the corresponding catch sizes, scale factors, and effective sample sizes. For the 1980's, the effective sample size in a period ranged from a few fish to several thousand. The lengths of fish ranged from 31 to 229 cm. However, we only included data up to 130 cm in our analysis since modes cannot be distinguished beyond this length. Examples of the

length-frequency distributions for South Australia in 1981 and 1983 are shown in Figure 3 of Appendix 3.

Direct Aging Data

In our analysis, we included direct aging data from fish that were born in the 1980's, where birth year was estimated from the catch year and the number of bands in the otolith. Although otoliths from 1780 SBT born in the 1980's have been aged to date, not all of these were deemed suitable for inclusion in our growth analysis (see Appendix 3). In brief, SBT caught during the winter months of May to September were excluded since band formation occurs during these months and we cannot be sure whether or not a fish caught during this time has yet laid down a band. Fish up to and including age 14 that were caught on the spawning grounds were also excluded because for these ages maturity is associated with larger sizes within an age-class fish and thus there is a bias in the length-at-age of these fish (see Farley et al. 2001). Furthermore, fish with one band caught off the west coast of Western Australia were excluded since we believe they are less than 9 months old and we are not attempting to model such early growth in this analysis. The number of direct age-length observations in the 1980's remaining for analysis was 668, for which the number of bands ranged from 1 to 21 and the lengths of fish ranged from 45 to 200 cm. SBT from all geographical areas where fishing occurs are represented. However the majority of data is from older fish caught on the Indonesian spawning grounds.

Methods

We adopted a maximum likelihood approach in order to jointly analyse the three sources of growth information. For each data source, we developed a statistical model and a corresponding likelihood component. The likelihood components were then added together to obtain a final objective function that could be optimised to estimate the model parameters. The addition of likelihood components is an appropriate procedure provided that the data from the different sources are independent, which is a reasonable assumption in this situation.

An important feature of any growth model is the functional form for the relationship between fish length (l) and age (a). The most common in fisheries literature is the von Bertalanffy growth curve. However, there is evidence that SBT growth is better described by a function that allows for a transition in the growth rate (Laslett, Eveson, and Polacheck 2002; Hearn and Polacheck Submitted). In the derivation of our integrated model, we will leave the model very general by assuming a generic growth curve of the form

$$l(a) = L_\infty f(a - a_0; \theta),$$

where L_∞ is asymptotic length and f is a monotone increasing function with parameter set $\{a_0, \theta\}$ that approaches 1 as $a \to \infty$ and equals 0 when $a = a_0$. We can think of a_0 as the theoretical age at which a fish would have had length 0 if we were to project its growth curve backwards. For the familiar von Bertalanffy curve, $\theta = \{k\}$ and $f(a - a_0; k) = 1 - \exp(-k(a - a_0))$. As would be expected in an integrated growth model, we assumed a common growth function f throughout the model components for the different data sources.

Tag-Recapture Component

The method used to analyse the tag-recapture data is described in Appendix 4. It is based on estimating the joint density of tag and recapture lengths rather than modelling growth increments. In summary, a fish is tagged at time t_1 with release length l_1 and recaptured at time t_2 with length l_2, all of which are known. Let $A = t_1 - t_0$, where t_0 is the theoretical *time* at which a fish has length zero (analogous to the parameter a_0 on the age scale). Then A is a random variable, which we assume has density $p(\cdot)$ and whose parameters will be estimated in the model.

Although the age at release is unknown, if we denote it by a_1, then A is equivalent to $a_1 - a_0$. Similarly, $A + t_2 - t_1$ is equivalent to $a_2 - a_0$, where a_2 denotes the age at recapture. We introduce this notation to be consistent with the formulation of the growth function presented at the beginning of the section. Thus, we can specify the models for the release and recapture lengths respectively as

$$l_1 = L_\infty f(A;\theta) + \varepsilon_1$$
$$l_2 = L_\infty f(A + t_2 - t_1;\theta) + \varepsilon_2 .$$

We allow the asymptotic length to vary from fish to fish by modelling L_∞ as a random normal effect with mean μ_∞ and standard deviation σ_∞. The terms ε_1 and ε_2 represent measurement error. It is important to note that what we refer to as measurement error throughout this paper actually encompasses several sources of variation. Although measurement error is one principal source of variation in length, there may also be random variations due to environmental factors and genetic factors not captured by the random L_∞ parameter. Without further knowledge, we cannot separate this pooled source of error into its various components.

W assume ε_1 and ε_2 are independent from fish to fish, and also independent of L_∞ and A. Furthermore, we assume they are normally distributed with mean 0 and variance dependent on the length measurer (σ_s^2 if a scientist or trained staff measured the length and an additional component, σ_f^2, if a fisherman or factory staff measured the length). We expect measurements made by scientists to be more accurate than measurements made by fishermen. Note that scientists measured all release lengths. Explicitly, we can specify the variances by

$$V(\varepsilon_1) = \quad \sigma_s^2$$
$$V(\varepsilon_2) = \begin{cases} \sigma_s^2 & \text{if measured by a scientist} \\ \sigma_s^2 + \sigma_f^2 & \text{if measured by a fisherman.} \end{cases}$$

These error variances are specific to the SBT data, but the method is very flexible with regard to the choice of variance functions.

If we condition on A, then l_1 and l_2 are both the sum of random normal variables and their joint distribution, $h(l_1, l_2 \mid a)$, is bivariate normal. Their unconditional joint density can then by obtained by integrating over A. Namely,

$$h(l_1, l_2) = \int h(l_1, l_2 \mid a)\, p(a)\, da .$$

The product of the joint densities over all fish gives the likelihood function for the tag-recapture data. Thus, the negative log-likelihood function can be expressed as

$$-\ln(\lambda_1) = -\sum_i \ln h(l_{1i}, l_{2i}) \quad (1)$$

where i indexes the fish.

Length-Frequency Component

Analysis of the length-frequency data entailed a two-step procedure. First, we performed a mixture decomposition on each half-monthly sample independently to generate a mode and an accompanying standard error for each age-class represented in the sample. Second, we used the summary information from step one as input into the likelihood component for our length-frequency model.

The first step is described in detail in Appendix 7. Essentially, each length-frequency sample was assumed to be a mixture of Gaussian components, where the user specified the number of components and the age-classes to which they corresponded. Since we did not try to separate modes beyond age five, the modes were usually quite distinct and the corresponding age-classes were generally clear based on the length. There were several exceptions, of course, in which we simply had to use our best discretion. The estimation of the modes was unconstrained except for simple bound constraints. This differs from Leigh and Hearn (2000), who constrained mean growth over a season to be linear, and from Schnute and Fournier (1980), who constrained the means to follow a von Bertalanffy growth curve. The standard deviation of the components was assumed to be common within a sample, but was allowed to differ between samples. A standard error associated with each mode was calculated by inverting the observed information matrix. The estimation procedure took into account the fact that the data were scaled up from the actual sample size to the size of the catch (refer to Appendix 7). Figure 4 in Appendix 7 shows a plot of the summary modes versus the half-month index. The separation of modes into age-classes is evident in this figure, as is the seasonal pattern of growth (especially for age groups one and two).

In the second step, we modelled mean fish length using the estimated modes and standard errors from step one. We only included the data for age-classes one through four, even though a fifth mode was sometimes fitted. The fifth mode likely encompasses several age-classes since a maximum of five modes was fitted, and thus the fifth mode

acted as a catch-all for any data beyond age four. Furthermore, we only included data for modes where the estimated number of fish in the mode was greater than 50. The estimated number of fish in an age-class was obtained by multiplying the effective sample size for the period by the estimated proportion of fish in the age-class (which was obtained in step 1).

Let i index the year, j the half-month, and k the age group. We will denote the estimated mean length for a mode and its associated standard error by $\hat{\mu}_{ijk}$ and s_{ijk} respectively. Let a_{ijk} be the mean age assigned to a mode. To allocate a mean age to the fish from a given age group and half-month, we used the following procedure. Firstly, we assumed that fish are spawned on January 1 since this is the approximate mid-point of the spawning season for SBT (refer to Appendix 3). We then used the middle of the half-month to calculate a fractional age relative to January 1. Because the fishing season in South Australia generally runs from November to July, fish caught prior to January will not yet be as old as their assigned age-class. For example, the so-called age 2 mode in the first half of December will correspond to the age 2 mode in the first half of January, even though these fish are not yet age 2 according to their assumed birth date. Thus, we indexed the half-months by $j = -4,-3,\ldots,20$, where –4 corresponds to the first half of November, 0 corresponds to the first half of January, et cetera. Then, fish belonging to age group k and half-month j were allocated a final mean age of $k + (j - 0.5)/24$, since there are 24 half-months in total.

The model we used can be expressed as

$$\hat{\mu}_{ijk} = \mu_{\infty} f(a_{ikl} - a_0; \theta) + e_{ijk} + \varepsilon_{ijk} \qquad (2)$$

where e and ε are independent random effects representing sampling error and residual model error respectively. We assume $e_{ijk} \sim N(0, s_{ijk}^2)$, where the s_{ijk} are the known standard errors estimated in step one, and $\varepsilon_{ijk} \sim N(0, \sigma_{\varepsilon}^2)$. The parameter μ_{∞} represents the average asymptotic length for a group of fish, which we model as a fixed effect. We could model it as a random effect; however, in practice, there is almost no information from the length-frequency data on the mean asymptotic length of fish, let alone its variance. The negative log-likelihood for the model is given by

$$-\ln(\lambda_2) = \frac{1}{2}\sum_i\sum_j\sum_k\left[\ln\left(2\pi V(\hat{\mu}_{ijk})\right) + \frac{(\hat{\mu}_{ijk} - E(\hat{\mu}_{ijk}))^2}{V(\hat{\mu}_{ijk})}\right] \quad (3)$$

where

$$E(\hat{\mu}_{ijk}) = \mu_\infty f(a_{ijk} - a_0; \theta)$$

and

$$V(\hat{\mu}_{ijk}) = s_{ijk}^2 + \sigma_\varepsilon^2.$$

A more complex model could have been used that takes into account other structural aspects of the data. We explored models that incorporate a random fishing season effect, a within-season random half-month effect, and a within-season random age effect (refer to Appendix 7 for details). Although this might be desirable, the parameter estimates were unstable in practice, suggesting that there were insufficient data to fit a more complex model as well as possible confounding of parameters. The above model was found to provide an adequate fit without excessive unexplained variance.

Direct Age-Length Component

To model the direct aging data, we need to assign an age to a fish based on the number of bands in its otolith. The difficulties in doing so were discussed in Appendix 3. In this appendix, we assumed that the final otolith reads (i.e. the final band counts) were correct, and also that all fish were born on January 1 (the approximate mid-point of the spawning season). As such, a decimal age could be assigned to each fish as follows:

$$\text{age} = \begin{cases} n + r/365 & \text{if } r < d \\ n - 1 + r/365 & \text{if } r \geq d \end{cases} \quad (4)$$

where n is the final band count, r is the capture date, and d is the date of band formation. Both r and d are expressed in Julian days since January 1 of the year of capture.

The capture date is known accurately for almost all fish from which otoliths were collected. However, the time of band formation, d, is unknown and is variable among fish. An investigation into the time of band formation (see Appendix 11) could only conclude that bands can form any time during May through September. For fish caught during these months there is an uncertainty of one year in their age, so we omitted direct aging data from fish caught within this period from our analysis. This omission should

not induce biases into the growth parameter estimates, however it will result in them having higher variance.

For the remaining fish, there is still uncertainty in their assigned decimal age due to uncertainty in their birth date and possible errors in the band count. We adopted the simplest approach and used the decimal ages calculated using (4) as if they were exact in our analysis. Again, this should not induce biases in the growth parameter estimates since the age estimates should not be biased. However the precision of the estimates will be higher than if we had incorporated the uncertainty in ages.

We explored approaches for modelling these age uncertainties, including uncertainties in the time of band formation, the band count, and the birth date. These approaches are discussed in Appendix 12. They are still very much in the developmental stage and more work is required before we would be incorporating them into the integrated model.

Because we assume the age estimates to be accurate, the model for the direct aging data is relatively straightforward. Let l and a denote the length and age of a fish respectively, then the model can be expressed as

$$l = L_\infty f(a - a_0; \theta) + \gamma$$

where γ represents measurement error (and other unknown model error) and is assumed to be normally distributed with mean 0 and standard deviation σ_γ. As with the tag-recapture data, we model L_∞ as a random normal effect with mean μ_∞ and standard deviation σ_∞. We assume that L_∞ and γ are independent. Let i index a fish. Then the negative log-likelihood is given by

$$-\ln(\lambda_3) = \frac{1}{2}\sum_i \left[\ln\left(2\pi V(l_i)\right) + \frac{(l_i - E(l_i))^2}{V(l_i)} \right] \qquad (5)$$

where

$$E(l_i) = \mu_\infty f(a_i - a_0; \theta)$$

and

$$V(l_i) = \sigma_\infty^2 f(a_i - a_0; \theta)^2 + \sigma_\gamma^2 .$$

The integrated model

The overall objective function to be optimised, which we will denote by Λ, is simply the sum of the three negative log-likelihood functions given in equations (1), (3) and (5). That is,

$$\Lambda = -\left(\ln(\lambda_1) + \ln(\lambda_2) + \ln(\lambda_3)\right).$$

The parameters common to all three components are θ (the parameters of the growth function f) and μ_∞ (the mean asymptotic length). The asymptotic variance parameter σ_∞ is common to the tag-recapture and direct aging components. For the length-frequency component, we are not modelling lengths of individual fish but rather we are modelling mean lengths (see equation 2). As such, the asymptotic length parameter should have the same mean but not the same variance as the asymptotic length parameter in the tag-recapture and direct aging models. There is no information on fish older than age 4 in the length-frequency data alone to estimate the relevant asymptotic variance parameter, so we modelled the asymptotic length as a fixed effect for this component. Whether the asymptotic length is assumed to be random or fixed will have virtually no effect for fish aged 1 to 4. The parameter a_0 is common to the direct aging and length-frequency components; this parameter is not present in the tag-recapture model because it is encompassed in the random variable A. The parameters defining the lognormal distribution of A, $\mu_{\log A}$ and $\sigma_{\log A}$, are unique to the tag-recapture component. The various error parameters are unique to their corresponding components, namely σ_s and σ_f for the tag-recapture component, σ_ε for the length-frequency component, and σ_γ for the direct aging component.

Results

In order to apply the integrated growth model to the SBT data, a growth function, f, must be selected. Initially, we used the growth function corresponding to the traditional von Bertalanffy (VB) curve, namely

$$f(a - a_0; k) = 1 - e^{-k(a-a_0)}.$$

Previous analyses (Laslett, Eveson, and Polacheck 2002; Hearn and Polacheck Submitted) suggest there is a change in the growth process for SBT during the transition from juveniles to adults that cannot be adequately captured by a VB model. Hearn and Polacheck (Submitted) model SBT growth as a two-stage process in which the growth in each stage follows a different VB curve, such that there is a discontinuity in the growth rate at the transition between the two stages. In Appendix 4, we developed an alternate growth curve that can accommodate a change in the growth pattern at some point in the life cycle but allows for a gradual, smooth transition between stages. We call this new curve the von Bertalanffy growth curve with a logistic growth rate (abbreviated VB log k) to reflect the fact that the change in growth rate is modelled using a logistic function. The growth function for the VB log k model is given by

$$f(a-a_0;\{k_1,k_2,\alpha,\beta\}) = 1-e^{-k_2(a-a_0)}\left\{\frac{1+e^{-\beta(a-a_0-\alpha)}}{1+e^{\alpha\beta}}\right\}^{-(k_2-k_1)/\beta}.$$

As a increases, the function makes a smooth transition from a VB curve with growth rate parameter k_1 to a VB curve with growth rate parameter k_2. The parameter β governs the rate of the transition (being sharper for larger values), and α governs the age at which the midpoint of the transition occurs.

We obtained parameter estimates for both the VB and VB log k models by optimising the objective function, Λ, with the appropriate growth function (Table 1). Comparison of the results indicates that the asymptotic length is somewhat higher in the VB log k model. The initial rate of growth in the VB log k model is very similar to the growth rate in the VB model; however the VB log k model suggests that the growth rate slows considerably between ages two and three. Recall that α is the age of transition relative to a_0, so we estimate the midpoint of the transition to be at age $\alpha + a_0$. The fact that β converged to a preset upper bound of 30 suggests that the rate of transition between the two growth phases is very fast.

According to Akaike's information criterion (AIC) (Akaike 1974), the VB log k fit is significantly better than the VB fit (Table 2). To further evaluate how well the two models fit the data, we calculated residuals (fitted minus observed length) for each of the data sets. In order to calculate the fitted release and recapture lengths in the tag-recapture

data, we required a realised value of A and L_∞ for each fish. The approach outlined in Appendix 4 is to use the mean of the posterior distribution for A and L_∞, respectively, conditioned on the fish's release and recapture lengths. This approach yields unbiased estimates of L_∞, but, as discussed in Appendix 5, it leads to biased estimates of A. Instead, we used the approximately conditionally unbiased estimator $\tilde{A}_f$ that is described in Appendix 5.

The improvement in the fit of the VB log k model over the VB model is evident in the residual plots (compare Figures 2.1-2.3 with Figures 3.1-3.3). For the direct-aging component, the VB model overestimates the length of middle-aged fish (around ages 5 through 12); this is corrected by using the VB log k model. A local linear smooth of the recapture length residuals for the VB model shows a pattern in which the length of younger fish is underestimated and the length of older fish is overestimated; the transition occurs between recapture "ages" three and five (recall this is age relative to a_0). This pattern clearly supports a two-stage growth function, such as the VB log k curve. The recapture residuals for the VB log k model show no such pattern. The release residuals are also improved slightly in the VB log k model. The length-frequency residuals are more complicated. In both models, the predominant feature of the residuals is the overestimation of age-class one and the underestimation of age-classes two to four. However, overlooking this general lack of fit, which we discuss below, the fit to the four-year olds is better in the VB log k model.

In the introduction to Appendix 3, we discuss the fact that one-year old fish caught off of Western Australia (WA) are smaller on average than one-year old fish caught off of South Australia (SA) around the same time. Likely the WA fish were spawned later in the spawning period than the SA fish and are younger. Our method of assigning ages assumes all fish are spawned on the same day so this age difference cannot be captured. Because all of the length-frequency data is from SA, the length data for one-year olds will be biased towards bigger fish. This is evident in the model fits.

We assigned ages to both the length-frequency data and the direct aging data assuming a birth date of January 1. This introduces an uncertainty of several months into the age depending on the true time of spawning. This is primarily a problem for very

young fish whose growth is rapid enough that an age difference of a few months translates to a significant difference in length. The model for the tag-recapture data incorporates the estimation of the age-at-release, and hence has the ability to deal with variable spawning times by assigning suitable ages based on size. Ideally, we would like the model components for the length-frequency and direct aging data to incorporate this uncertainty as well; Appendix 7 and Appendix 12 discuss possible future approaches for doing so.

As an immediate and unbiased approach of dealing with the problem, we refit the integrated VB log k model leaving out the length-frequency data for age-class one and the direct aging data for fish with an estimated age of less than 1.5 years. Our justification for doing so is that the uncertainty in age has the most significant effect on the expected length of one-year old fish, with the effect diminishing exponentially with age. Moreover, by age two, the difference in lengths of fish from WA and SA appears to be negligible; perhaps the later-spawned fish catch up in size by age two, or perhaps the fish from the two areas mix during their second year of life so that the two-year old fish off WA and SA no longer correspond to late-spawned and early-spawned fish. Although the uncertainty in age is still present in fish older than age one, we expect only an increase in the variance of their length-at-age (which will diminish rapidly with age), and not a bias.

The largest impact of leaving out the one-year old length-frequency and direct aging data is that the initial stage of growth is steeper, as reflected by the increase in the parameters k_1 and a_0 (Table 1). The improvement in the fit to the length-frequency data is apparent in the residual plot (Figure 4.2). The fit to the other two data sets appears relatively unaffected (Figures 4.1 and 4.3).

SBT experience a period of fast growth during the southern summer (Hearn 1986); we see evidence of this in the length-frequency data and it is also the reason that SBT otoliths display annual growth bands. Neither of the above models captures this seasonality, and it is important to determine whether doing so could significantly improve the fits. A seasonal component can be incorporated into any growth function by adding an annually periodic function, $S(\cdot)$, to the independent age variable. Explicitly, $a - a_0$ can be replaced with $a - a_0 + S(t)$, where t is the fractional time of year since January 1.

In the tag-recapture data, we know the date of release and recapture so we can calculate t for both events. Similarly, we know the date of catch for the direct aging data. For each mode in the length-frequency data, we use the mid-point of the half-month as the catch date. Note that for the direct aging and length-frequency summary data, t simply corresponds to the decimal part of the fish's age, a, since we assumed a birth date of January 1 in assigning ages.

We considered a sinusoidal function for the seasonal effect, parameterised as

$$S(t) = \frac{u}{2\pi}\sin(2\pi(t - w))$$

where u is the amplitude and w is the phase. The amplitude is constrained to be between 0 and 1 to prevent negative growth, whereas we constrained the phase to be between –0.5 and 0.5. Any bounds with a span of one could have been chosen due to the periodicity of the function. The rate of growth is maximal at $t = w$ and diminishes symmetrically about w to a minimum at $t = w - 0.5$ and $t = w + 0.5$.

We refit the VB log k model with a seasonal component to the data including and excluding age one length-frequency and direct aging data. The estimates of the mean growth curves are almost identical to the mean curves estimated from fitting the non-seasonal VB log k model to the corresponding data (see the parameter estimates in Table 1). However, the estimates of the seasonality parameters, which are almost identical whether the age one data is included or not, suggest there is an appreciable seasonal pattern to growth. The estimate of the phase, w, suggests that SBT experience their fastest growth in mid-February, which is consistent with our prior expectation. A comparison of the AIC values between the seasonal and non-seasonal models fitted to the same data suggests that incorporating a seasonal component significantly improved the fits (Table 2). The improvement is visible in a plot of the fitted curve through the length-frequency data (Figure 5.2, top panel). Although the fits to the other two data sets do not look much different (Figures 5.1 and 5.3), the negative log-likelihood component for the tag-recapture data was reduced significantly for both the model with and without age one data. Note that these figures only show the results obtained without age one data; the same observations can be made for the equivalent figures for the model with age one data (see Figures 2a-2c in the Annex to Appendix 10).

Discussion

It is important to have a method for modelling growth that can incorporate all of the available data sources because any one data source does not usually contain complete information on growth over the entire lifespan of the species. Oftentimes, where one data set is deficient, another can provide valuable information. For example, in the case of SBT, the length-frequency and tag-recapture data lack the information on older fish that is available from the direct aging data. Conversely, the length-frequency data has information on seasonality not available from the other two data sources, whereas the tag-recapture data is the only source of information on the growth of individuals, which is important for understanding variability in the growth process. However, it only makes sense to combine data sets into a single analysis if the information between them is consistent; otherwise, the benefit gained from having multiple data sources becomes a weakness as the data sets work against each other. The SBT data sets show a very high level of consistency, with the exception of the one-year olds for reasons already discussed. We can infer this from the fact that the integrated model fitted all of the data sets well. However a plot with the data sets overlaying one another shows the consistency clearly (Figure 6). We have omitted the age one length-frequency and direct aging data from the plot. The ages of release and recapture for the tag-recapture data are the estimated values from the seasonal VB log k model fit to the reduced (without age one) data sets. Recall that when we obtain these age estimates, they are actually relative to a_0. Thus, we have added to them the a_0 value estimated from the model for the length-frequency and direct aging data in order to make the age-axis comparable between all data sets.

Data from all of the sources discussed will not always be available. An advantage of developing an integrated model of growth under a likelihood framework is the ease with which data sources can be excluded from (or included in) the model. If one of the data sources is not available for a species, then the likelihood component corresponding to the missing data set can be removed from the overall objective function. On the other hand, if a data set other than the three we discussed exists, then it is possible to add on a

likelihood component for this data set. Of course, the development of an appropriate model for these new data may not be trivial.

We modelled the seasonal growth pattern of SBT using a sinusoidal function. There is some suggestion in the length-frequency summary data (see Figures 1 to 3 in Appendix 7) that the growth of SBT is fast over the summer season before levelling off sometime around May and remaining almost flat for the winter. Lack of data over the entire year makes the pattern difficult to confirm. If this were the case, an alternative seasonality function may be more appropriate. Even so, the sinusoidal function appears to have performed adequately.

With regard to the direct aging data, research scientists and trained staff collect the otoliths and also measure the lengths of the fish; therefore, it seems reasonable to assume that the measurement error should be the same as that for length measurements made by scientists in the tag-recapture data (i.e. $\sigma_\gamma = \sigma_s$). In our results, σ_γ is actually much greater than σ_s. The tag-recapture model estimates the age-at-release intrinsically, so the data points can be adjusted along the age axis to put them closer to the mean curve. For the direct aging data, we assign an age assuming a common birth date for all fish and take this age as precise. Therefore, it is not surprising that the residual variability in length-at-age (above and beyond the variation due to a random L_∞) is greater for the direct aging data than the tag-recapture data.

The questions raised by Francis (1988a) about the validity of estimating common growth parameters using tagging and age-length data are only relevant when growth increments are being modelled for the tagging data. When the release and recapture lengths are modelled directly as opposed to the change in length, these issues are no longer relevant. In this appendix, we have successfully demonstrated that data from three sources can be integrated to obtain consistent estimates of growth.

References

Anon. 1994. Report of the southern bluefin tuna trilateral workshop. Hobart, Australia, January/February 1994. 161 pp.

Akaike, H. 1974. A new look at the statistical model identification. Institute of Electrical and Electronic Engineers Transactions on Automated Control **AC-19**: 265-289.

Alves, A., de Barros, P., and Pinho, M.R. 2002. Age and growth studies of bigeye tuna *Thunnus obesus* from Madeira using vertebrae. Fisheries Research **54**: 389-393.

Anon. 1994. Report of the southern bluefin tuna trilateral workshop. Hobart, Australia, January/February 1994. 161 pp.

Clear, N.P., Gunn, J.S., and Rees, A.J. 2000. Direct validation of annual increments in the otoliths of juvenile southern bluefin tuna, *Thunnus maccoyii*, by means of a large-scale mark-recapture experiment with strontium chloride. Fish. Bull. **98**: 25-40.

Fabens, A.J. 1965. Properties and fitting of the von Bertalanffy growth curve. Growth **29**: 265-289.

Fournier, D.A., Sibert, J.R., Majkowski, J., and Hampton, J. 1990. MULTIFAN a likelihood-based method for estimating growth parameters and age composition from multiple length frequency data sets illustrated using data for southern bluefin tuna (*Thunnus maccoyii*). Can. J. Fish. Aquat. Sci. **47**: 301-317.

Francis, R.I.C.C. 1988a. Are growth parameters estimated from tagging and age-length data comparable? Can. J. Fish. Aquat. Sci. **45**: 936-942.

Francis, R.I.C.C. 1988b. Maximum likelihood estimation of growth and growth variability from tagging data. N.Z. J. of Mar. Freshwater Res. **22**: 42-51.

Gunn, J.S. and Farley, J.H. 1998. Otolith analyses suggest that the growth rate of juvenile SBT began to increase in the late 1970's and that growth rates have continued to increase

through the 1980's and 1990's. CCSBT-SC/9807/9.

Hasselblad, V. 1966. Estimation of parameters for a mixture of normal distributions. Technometrics **8**: 431-444.

Hearn, W.S. 1986. Mathematical methods for evaluating marine fisheries. Ph.D. thesis, University of New South Wales, Kensington, NSW, Australia.

Hearn, W.S. and Polacheck, T. In press. Estimating long-term growth rate changes of southern bluefin tuna from tag-return data. Fish. Bull.

James, I.R. 1991. Estimation of von Bertalanffy growth curve parameters from recapture data. Biometrics **47**: 1519-1530.

Kirkwood, G.P. 1983. Estimation of von Bertalanffy growth curve parameters using both length increment and age-length data. Can. J. Fish. Aquat. Sci. **40**: 1405-1411.

Labelle, M., Hampton, J., Bailey, K., Murray, T., Fournier, D.A., and Sibert, J.R. 1993. Determination of age and growth of South Pacific albacore (*Thunnus alalunga*) using three methodologies. Fish. Bull. **91**: 649-663.

Laslett, G.M., Eveson, J.P., and Polacheck, T. 2002. A flexible maximum likelihood approach for fitting growth curves to tag-recapture data. Can. J. Fish. Aquat. Sci. **59**: 976-986.

Leigh, G.M. and Hearn, W.S. 2000. Changes in growth of juvenile southern bluefin tuna (*Thunnus maccoyii*): an analysis of length-frequency data from the Australian fishery. Mar. Freshwater Res. **51**: 143-154.

Macdonald, P.D.M. and Pitcher, T.J. 1979. Age-groups from size-frequency data: a versatile and efficient method of analyzing distribution mixtures. J. Fish. Res. Board Canada **36**: 987-1001.

Palmer, M.J., Phillips, B.F., and Smith, G.T. 1991. Application of nonlinear models with random coefficients to growth data. Biometrics **47**: 623-635.

Sainsbury, K.J. 1980. Effect of individual variability on the von Bertalanffy growth equation. Can. J. Fish. Aquat. Sci. **37**: 241-247.

Schnute, J. and Fournier, D.A. 1980. A new approach to length-frequency analysis: growth structure. Can. J. Fish. Aquat. Sci. **37**: 1337-1351.

Thorogood, J. 1987. Age and growth rate determination of southern bluefin tuna, *Thunnus maccoyii*, using otolith banding. J. Fish Biol. **30**: 7-14.

Wang, Y.-G., Thomas, M.R., and Somers, I.F. 1995. A maximum likelihood approach for estimating growth from tag-recapture data. Can. J. Fish. Aquat. Sci. **52**: 252-259.

Yukinawa, M. 1970. Age and growth of southern bluefin tuna *Thunnus maccoyii* (Castelnau) by use of scale. Bull. Far Seas Fish. Res. Lab. **3**: 229-257.

Table 1: Parameter estimates from applying the integrated growth model to 1980's southern bluefin tuna data. Results are for various growth curves and data subsets, as specified.

Growth curve	Exclude Age 1?	Parameter estimates														
		μ_∞	σ_∞	k_1	k_2	α	β[1]	u	w	$\mu_{\log A}$	$\sigma_{\log A}$	a_0	σ_s	σ_f	σ_ε	σ_γ
VB	No	179.7	6.1	0.21	–	–	–	–	–	0.66	0.17	-0.57	2.7	4.5	4.2	5.5
VB log k	No	184.9	7.8	0.22	0.17	2.9	30.0	–	–	0.58	0.17	-0.44	2.3	4.3	4.4	4.5
VB log k	Yes	183.9	8.4	0.24	0.18	2.5	30.0	–	–	0.52	0.17	-0.18	2.3	4.1	2.6	4.1
Seasonal VB log k	No	184.7	8.1	0.22	0.17	2.8	18.3	0.34	0.13	0.58	0.17	-0.43	2.1	4.2	4.6	4.3
Seasonal VB log k	Yes	183.8	8.7	0.24	0.18	2.5	30.0	0.35	0.12	0.52	0.17	-0.18	2.1	4.0	2.5	4.1

[1] β constrained to be ≤ 30

Table 2: Negative log likelihood values and Akaike's information criterion (AIC) for the various model fits.

Growth curve	Exclude Age 1?	# parameters	-log likelihood	AIC
VB	No	10	17752.1	35524.1
VB log k	No	13	17649.5	35325.1
VB log k	Yes	13	17259.1	34544.2
Seasonal VB log k	No	15	17607.1	35244.3
Seasonal VB log k	Yes	15	17209.1	34448.2

Figure 1: Southern bluefin tag-recapture data for fish released in the 1980's (only data remaining for analysis after screening is shown).

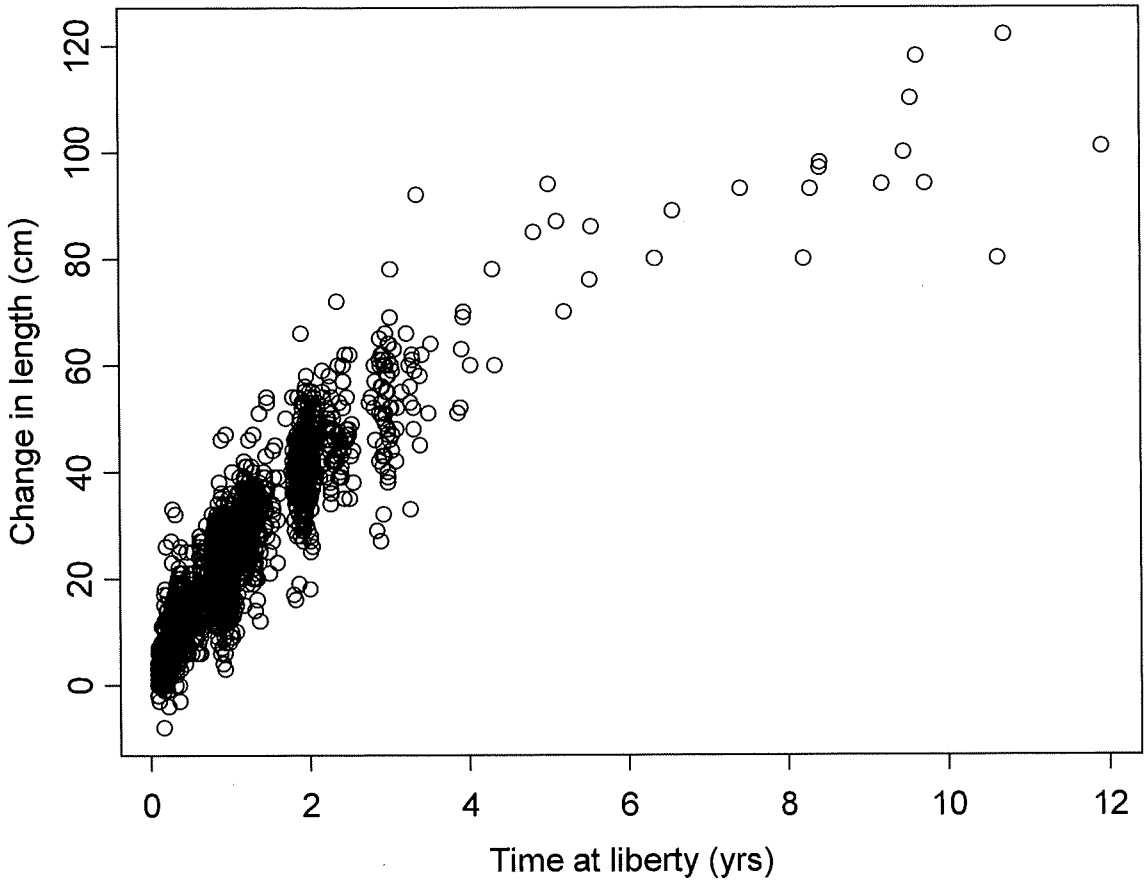

Figure 2.1: Diagnostic plots for the optimal integrated VB model fitted to the 1980's southern bluefin tuna growth data. Panel (i) shows the direct aging data along with the mean fitted curve. Panel (ii) shows the corresponding residuals (observed – fitted).

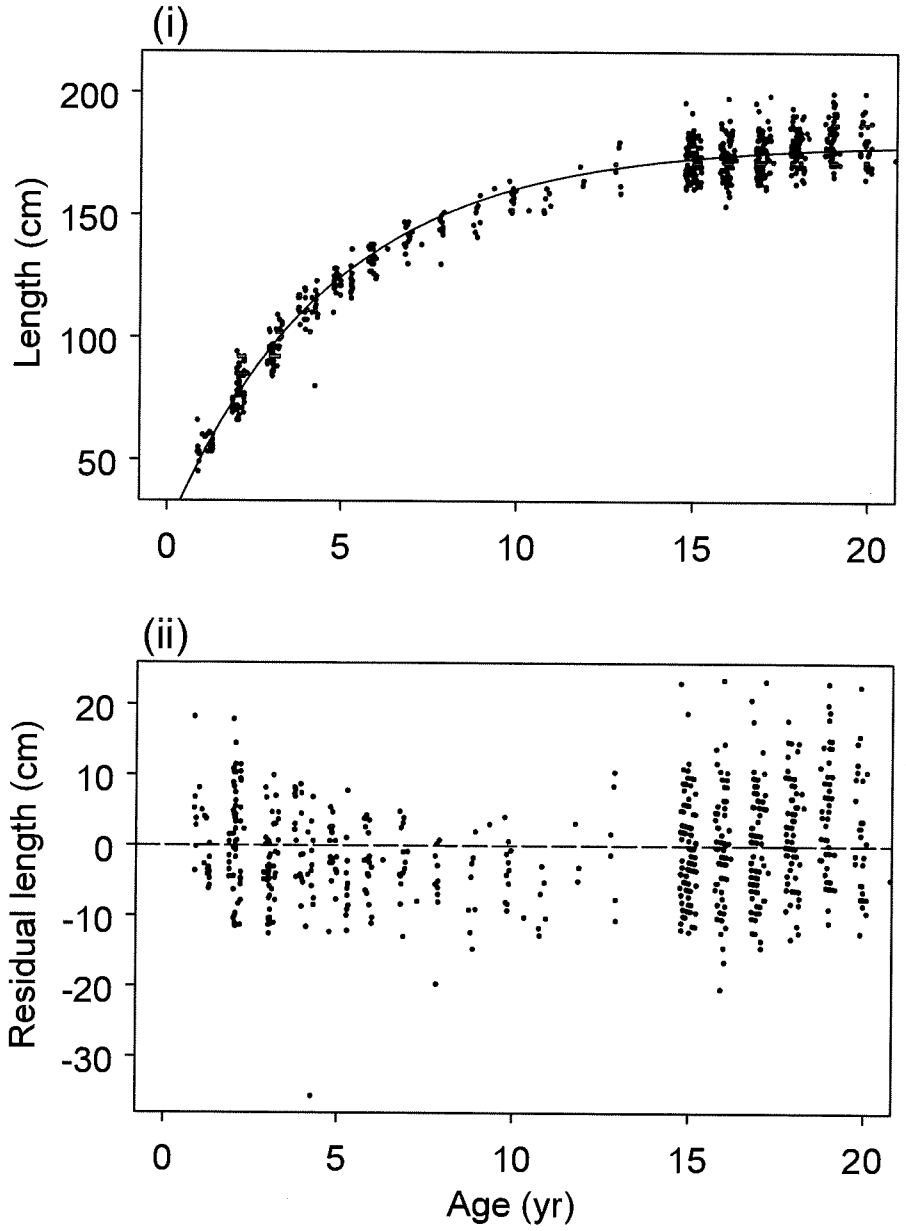

Figure 2.2: Diagnostic plots for the optimal integrated VB model fitted to the 1980's southern bluefin tuna growth data. Panel (i) shows the summary modes and ages obtained from the length-frequency data along with the mean fitted curve. Panel (ii) shows the corresponding residuals (observed – fitted).

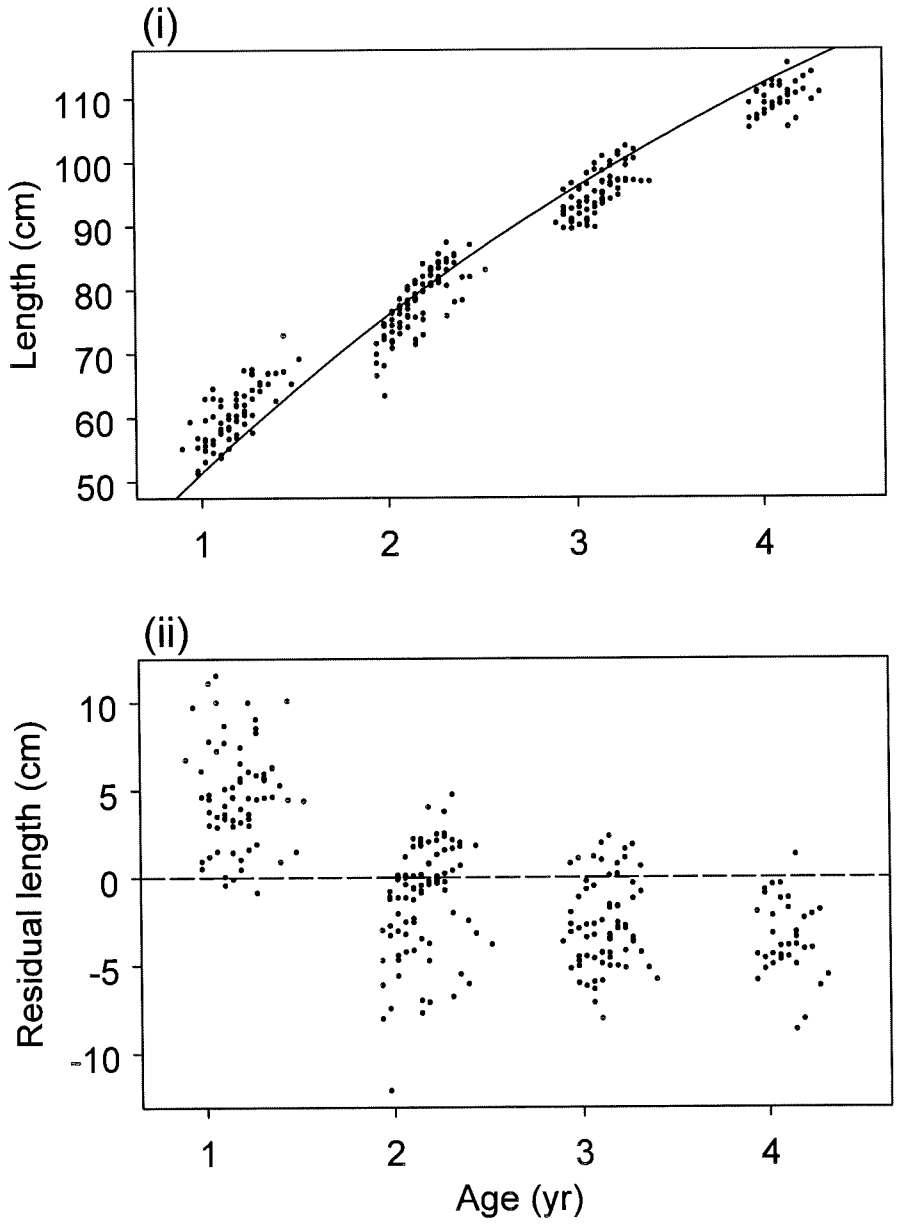

Figure 2.3: Diagnostic plots for the optimal integrated VB model fitted to the 1980's southern bluefin tuna growth data. Panel (i) shows the residual release lengths for the tag-recapture data plotted against the estimated ages at release relative to a_0 (i.e. $\tilde{A}_f$). Panel (ii) shows the residual recapture lengths plotted against the estimated ages of recapture relative to a_0 (i.e. $\tilde{A}_f + t_2 - t_1$). For legibility, we have left the words "relative to a_0" off the age axis labels. In both panels, a local linear smooth of the residuals is shown to reveal any patterns.

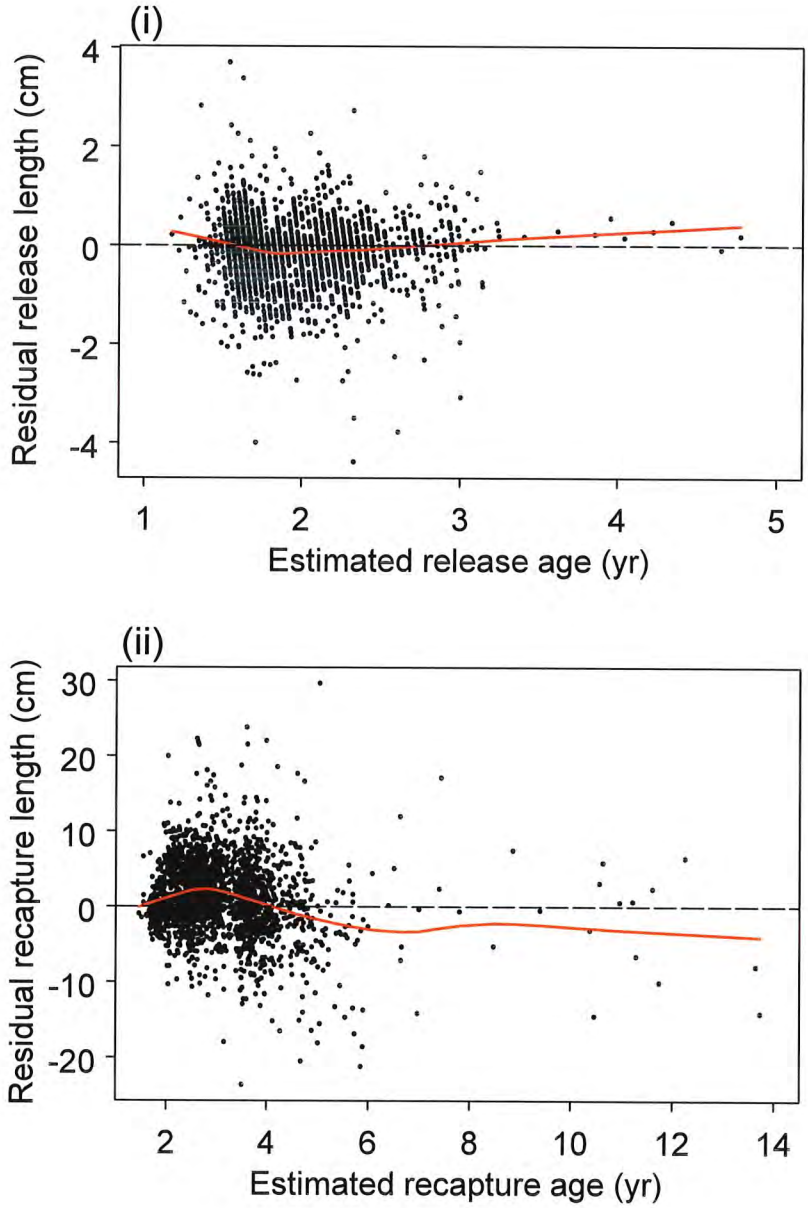

Figure 3.1: Diagnostic plots for the optimal integrated VB log k model fitted to the 1980's southern bluefin tuna growth data. Panel (i) shows the direct aging data along with the mean fitted curve. Panel (ii) shows the corresponding residuals (observed – fitted).

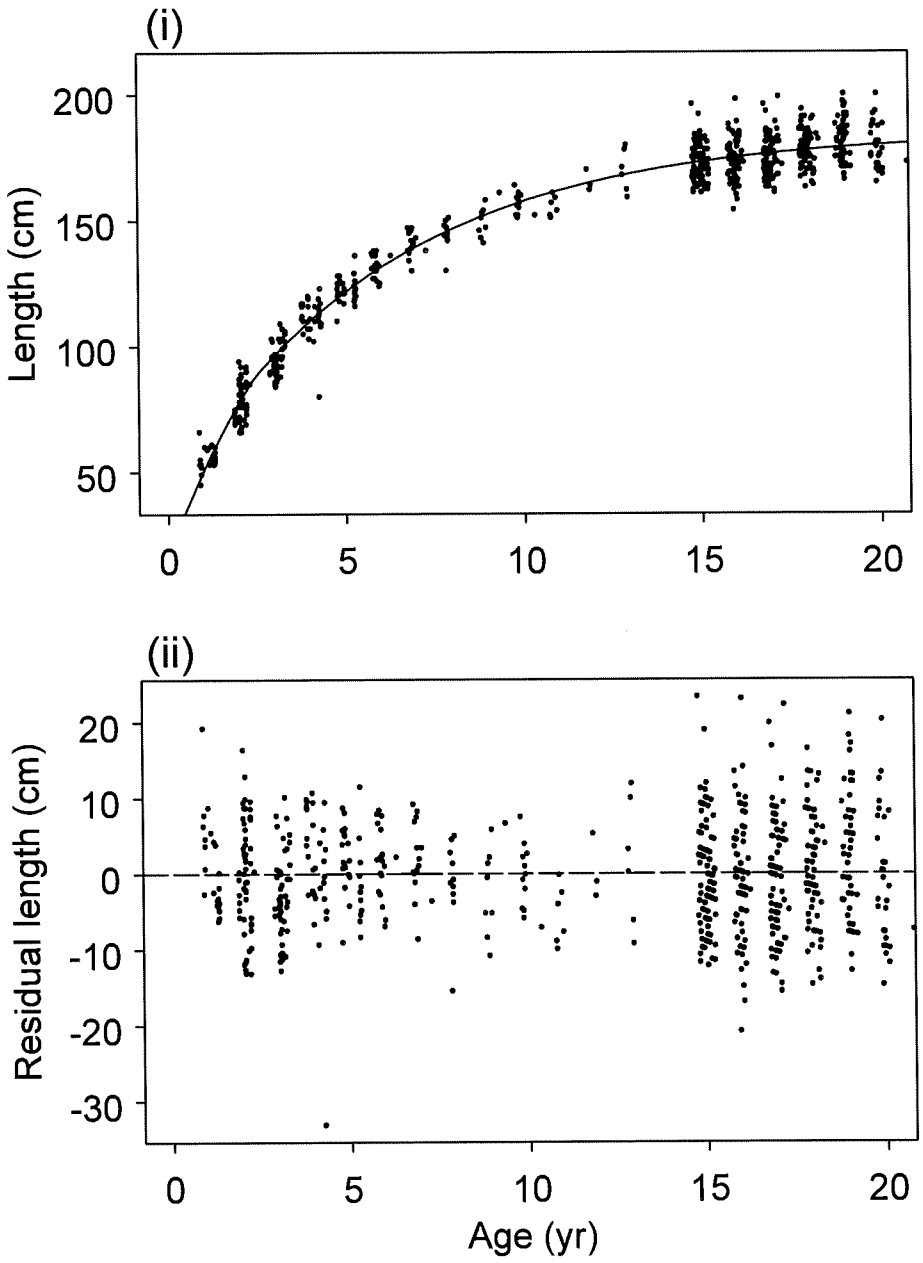

Figure 3.2: Diagnostic plots for the optimal integrated VB log k model fitted to the 1980's southern bluefin tuna growth data. Panel (i) shows the summary modes and ages obtained from the length-frequency data along with the mean fitted curve. Panel (ii) shows the corresponding residuals (observed – fitted).

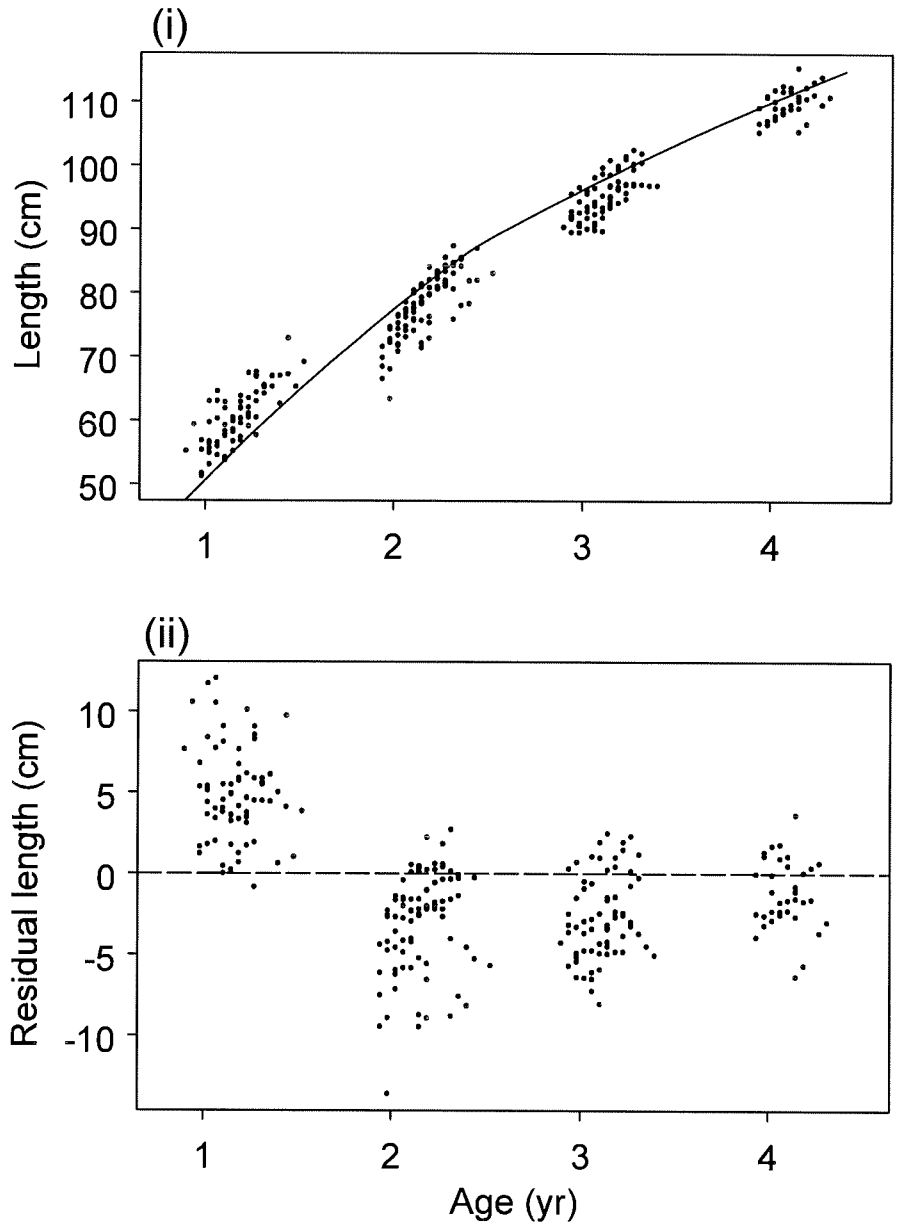

Figure 3.3: Diagnostic plots for the optimal integrated VB log k model fitted to the 1980's southern bluefin tuna growth data. Panel (i) shows the residual release lengths for the tag-recapture data plotted against the estimated ages at release relative to a_0 (i.e. $\tilde{A}_f$). Panel (ii) shows the residual recapture lengths plotted against the estimated ages of recapture relative to a_0 (i.e. $\tilde{A}_f + t_2 - t_1$). For legibility, we have left the words "relative to a_0" off the age axis labels. In both panels, a local linear smooth of the residuals is shown to reveal any patterns.

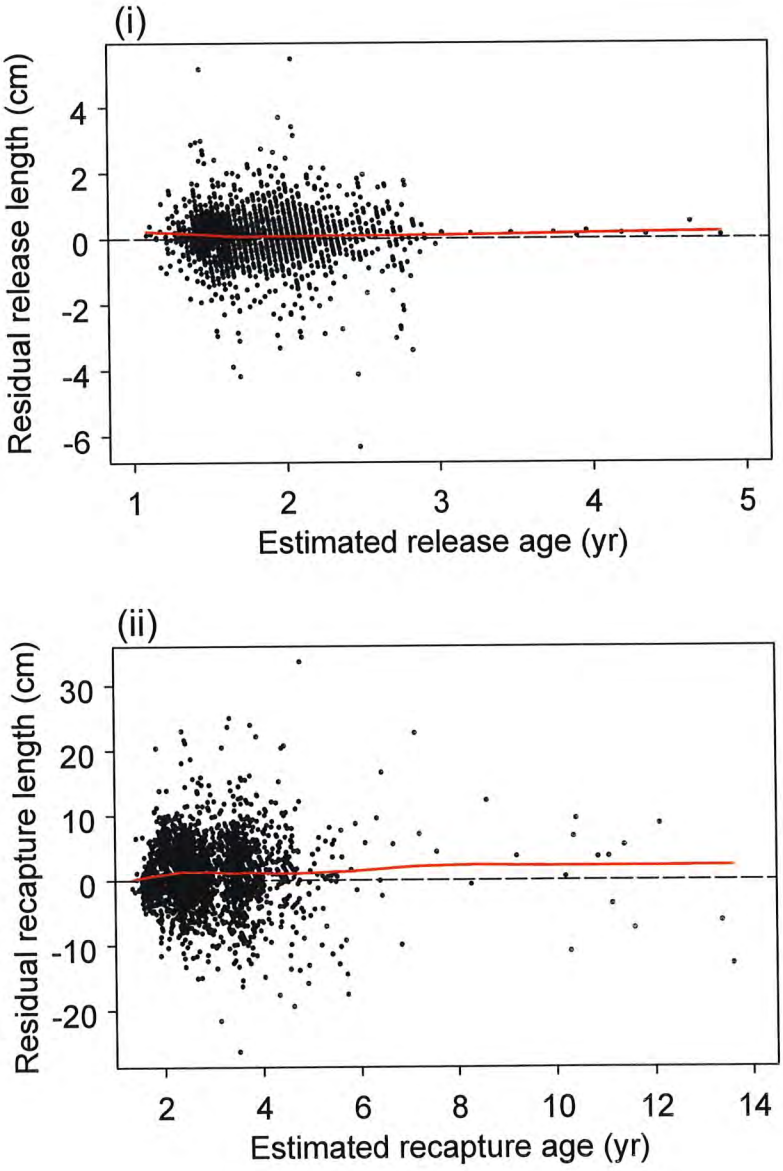

Figure 4.1: Diagnostic plots for the optimal integrated VB log k model fitted to the 1980's southern bluefin tuna growth data excluding the age one direct aging and length-frequency data. Panel (i) shows the direct aging data along with the mean fitted curve. Panel (ii) shows the corresponding residuals (observed – fitted).

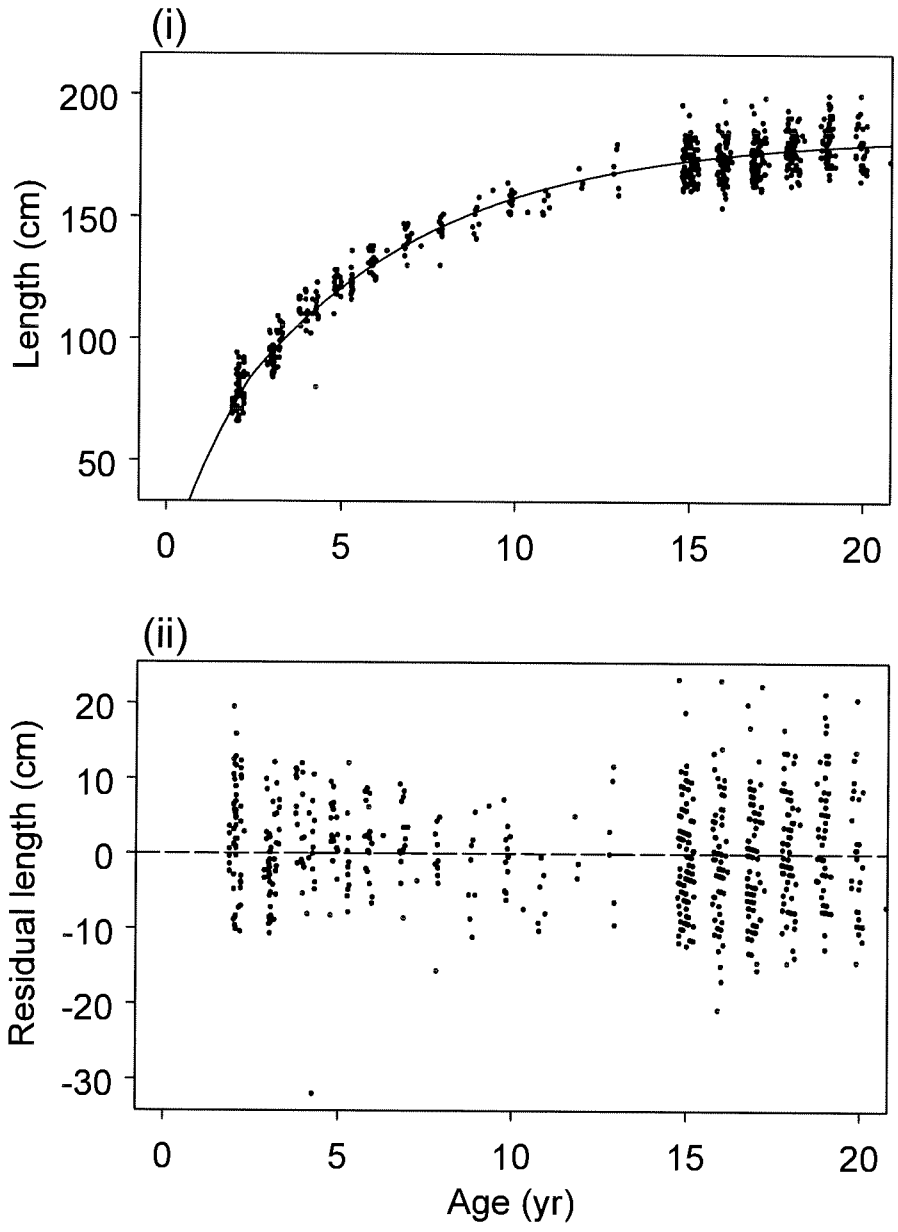

Figure 4.2: Diagnostic plots for the optimal integrated VB log k model fitted to the 1980's southern bluefin tuna growth data excluding the age one direct aging and length-frequency data. Panel (i) shows the summary modes and ages obtained from the length-frequency data along with the mean fitted curve. Panel (ii) shows the corresponding residuals (observed – fitted).

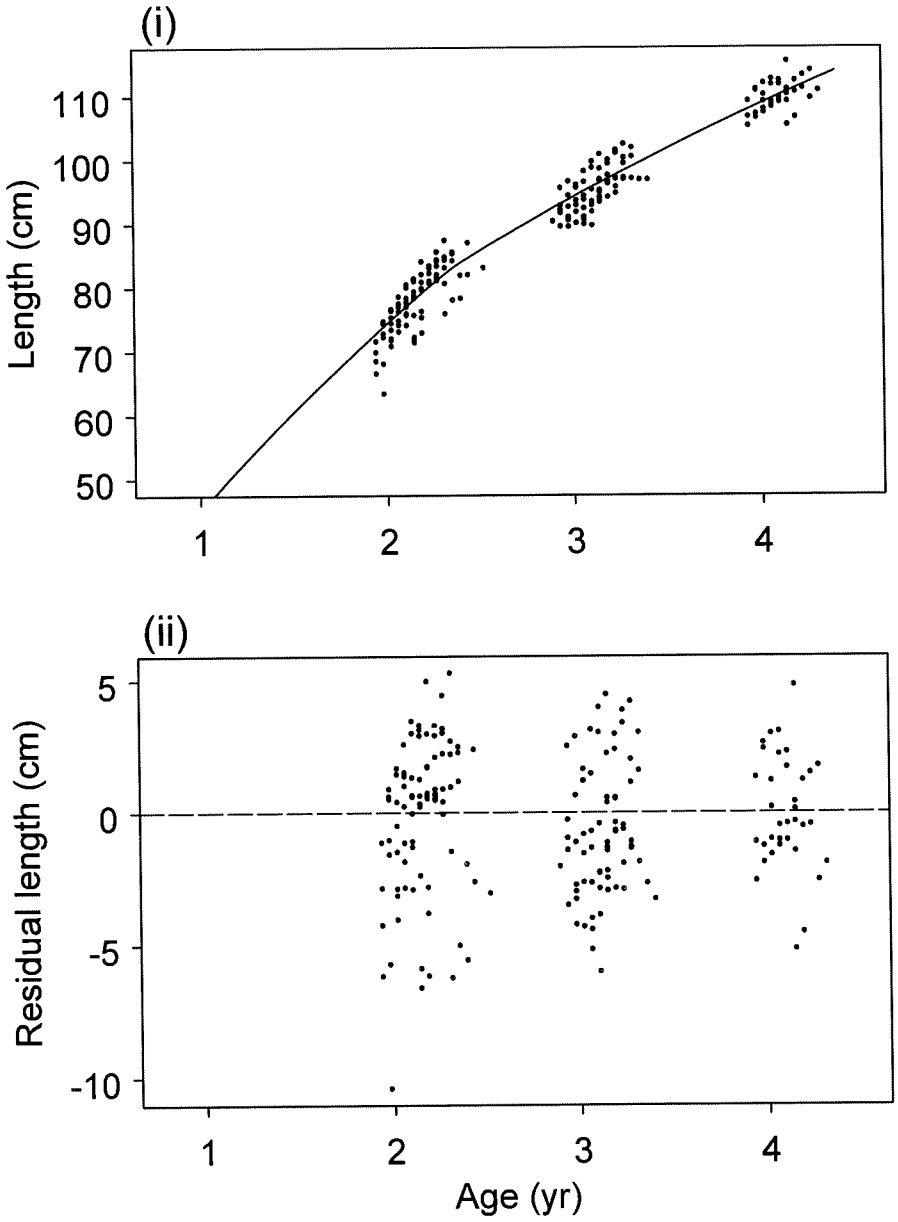

Figure 4.3: Diagnostic plots for the optimal integrated VB log k model fitted to the 1980's southern bluefin tuna growth data excluding age one direct aging and length-frequency data. Panel (i) shows the residual release lengths for the tag-recapture data plotted against the estimated ages at release relative to a_0 (i.e. $\tilde{A}_f$). Panel (ii) shows the residual recapture lengths plotted against the estimated ages of recapture relative to a_0 (i.e. $\tilde{A}_f + t_2 - t_1$). For legibility, we have left the words "relative to a_0" off the age axis labels. In both panels, a local linear smooth of the residuals is shown to reveal any patterns.

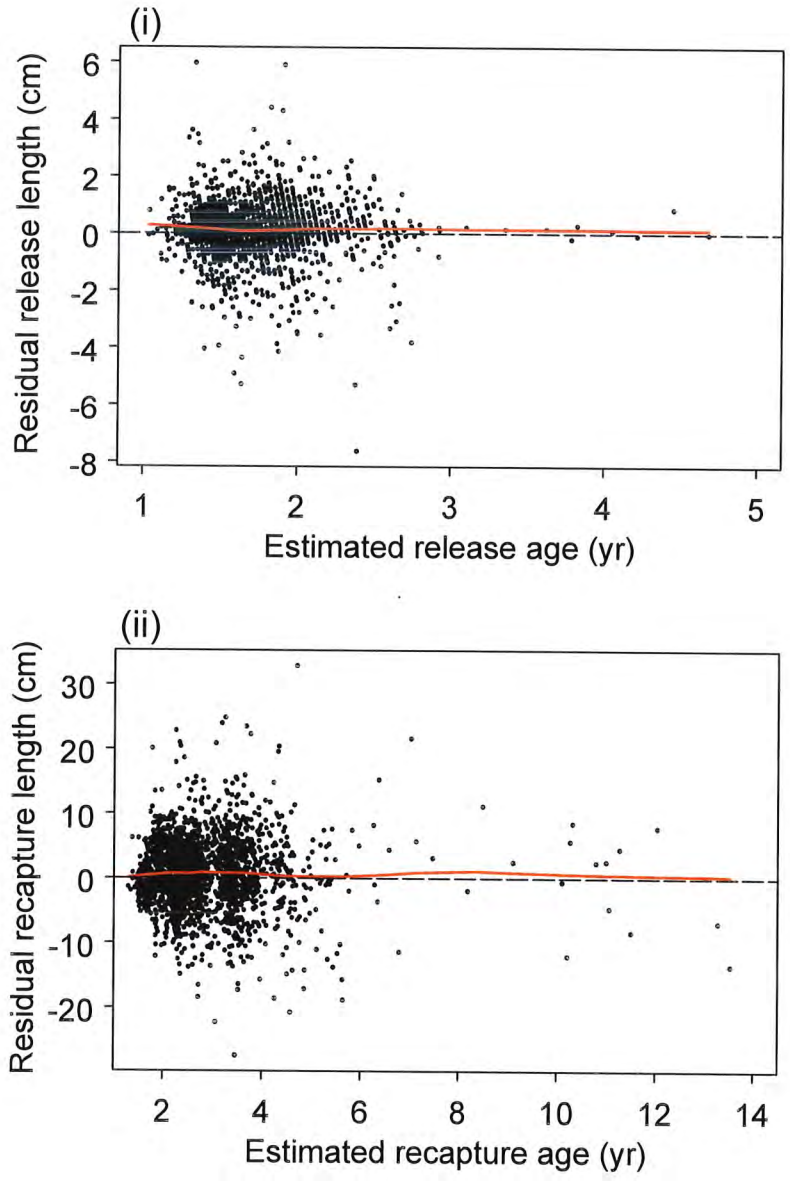

Figure 5.1: Diagnostic plots for the optimal integrated VB log k model with seasonality fitted to the 1980's southern bluefin tuna growth data excluding the age one direct aging and length-frequency data. Panel (i) shows the direct aging data along with the mean fitted curve. Panel (ii) shows the corresponding residuals (observed – fitted).

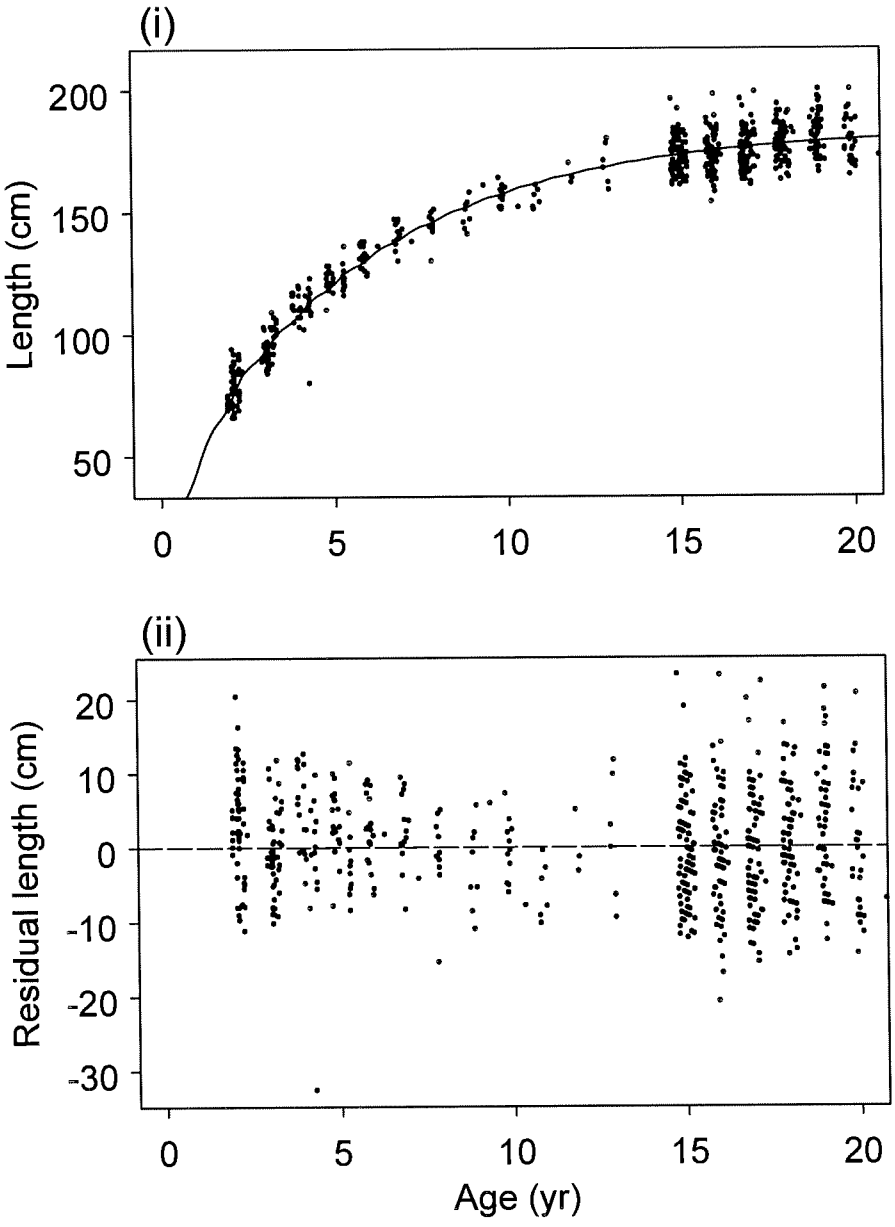

Figure 5.2: Diagnostic plots for the optimal integrated VB log k model with seasonality fitted to the 1980's southern bluefin tuna growth data excluding the age one direct aging and length-frequency data. Panel (i) shows the summary modes and ages obtained from the length-frequency data along with the mean fitted curve. Panel (ii) shows the corresponding residuals (observed – fitted).

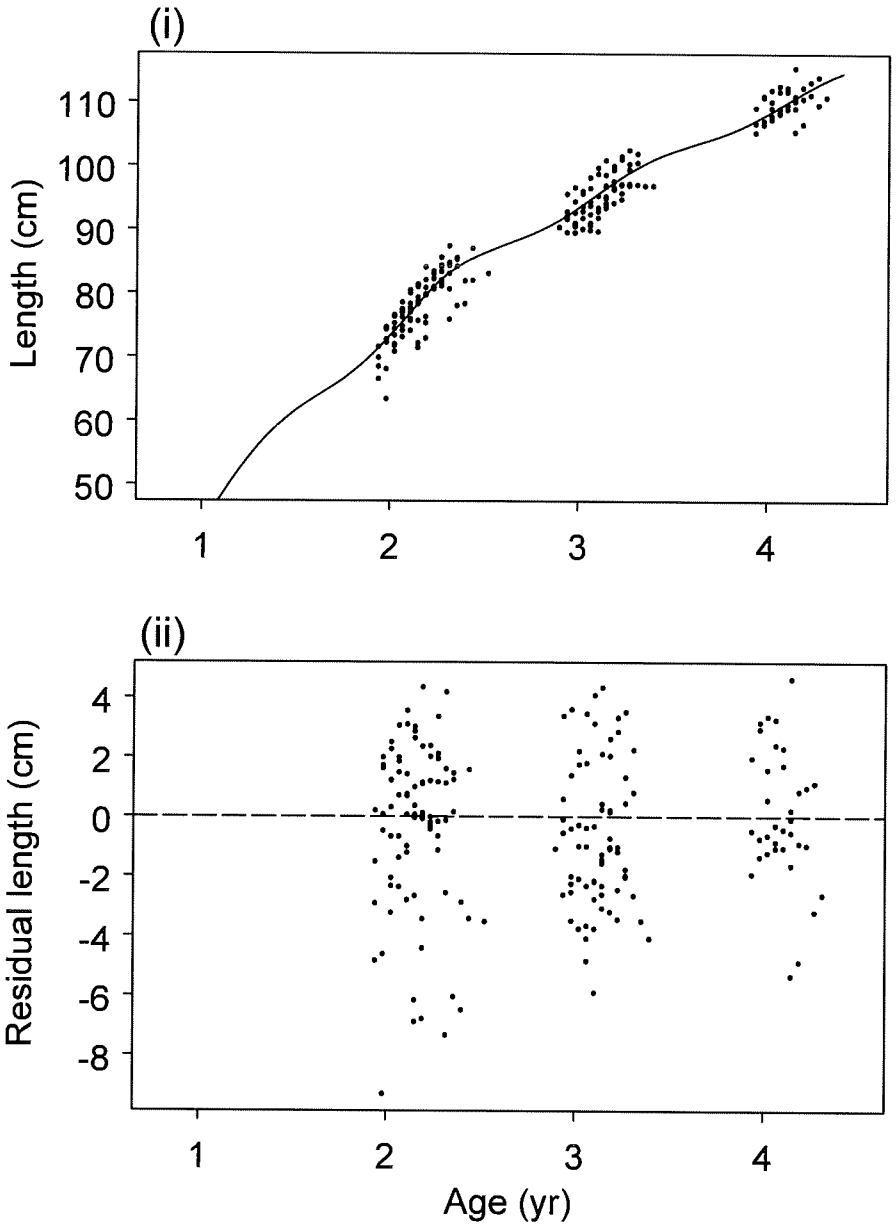

Figure 5.3: Diagnostic plots for the optimal integrated VB log k model with seasonality fitted to the 1980's southern bluefin tuna growth data excluding age one direct aging and length-frequency data. Panel (i) shows the residual release lengths for the tag-recapture data plotted against the estimated ages at release relative to a_0 (i.e. $\tilde{A}_f$). Panel (ii) shows the residual recapture lengths plotted against the estimated ages of recapture relative to a_0 (i.e. $\tilde{A}_f + t_2 - t_1$). For legibility, we have left the words "relative to a_0" off the age axis labels. In both panels, a local linear smooth of the residuals is shown to reveal any patterns.

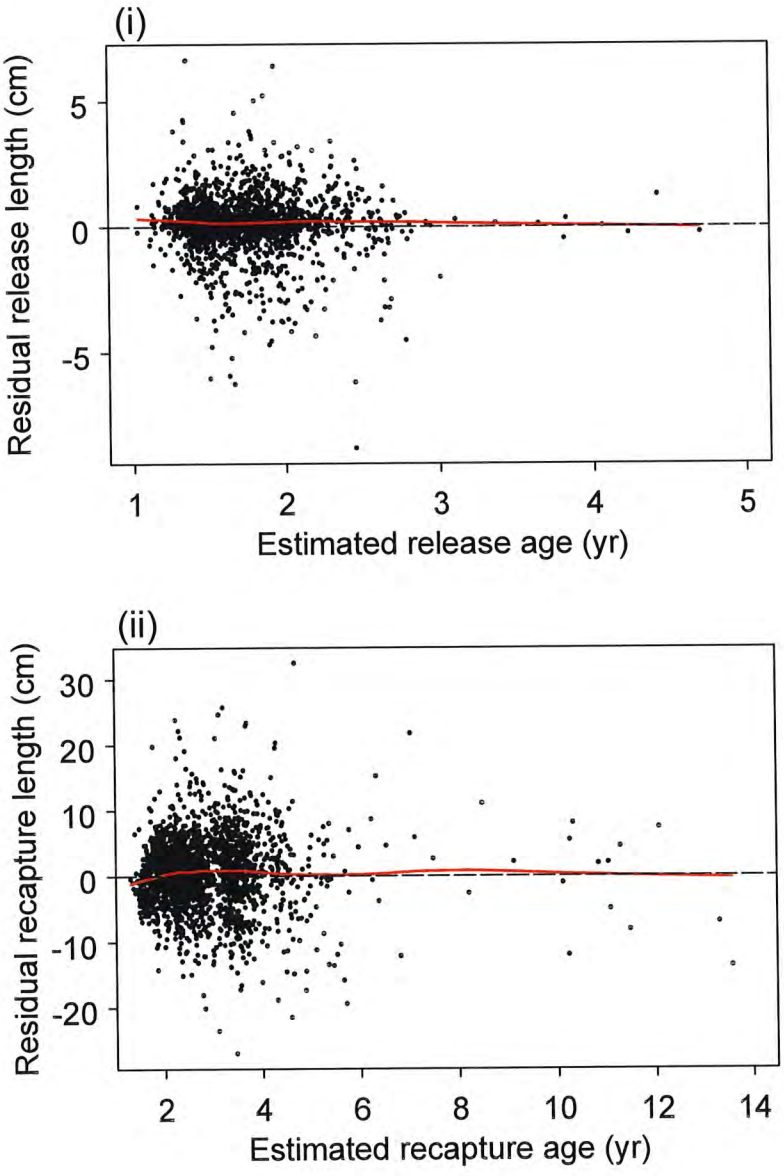

Figure 6: The 1980's southern bluefin tuna length and age data, excluding age one direct aging and length-frequency data. The data comes from three sources of growth information: 1) direct aging data (+); 2) modes estimated from length-frequency data (o); and 3) tag-recapture data (•). The ages of release and recapture for the tag-recapture data are the values plotted in Figure 5.3 plus the a_0 value estimated from the corresponding model (i.e. the integrated VB log k model with seasonality fitted to the data shown). The bottom panel is simply a close-up of the younger age classes.

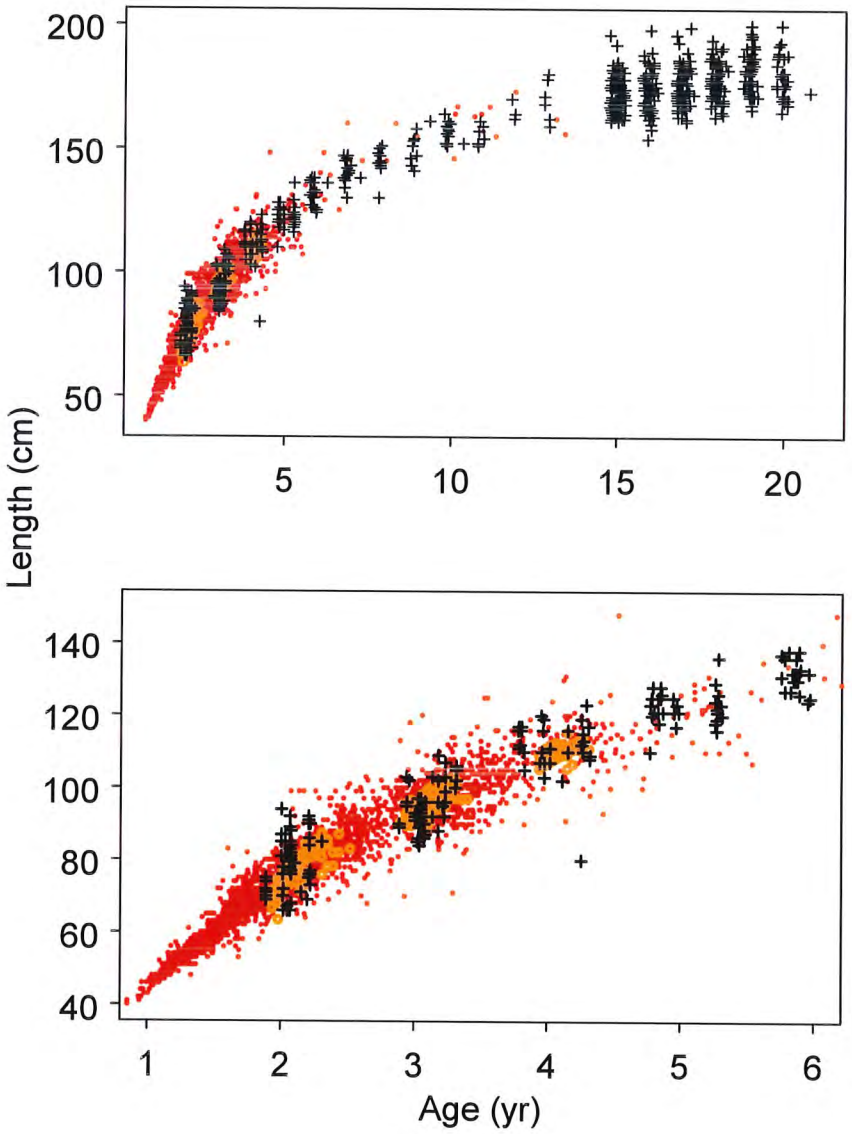

Appendix 10:

Comparison of growth rates of southern bluefin tuna over four decades – 1960 to 2000

Tom Polacheck, J. Paige Eveson and Geoff M. Laslett

FRDC Project 1999/104

Introduction

Understanding how growth changes over time can provide important insights into the processes underlying population and ecosystem dynamics (e.g. density dependent growth and regime shifts in the environment). In addition, estimates of growth rates are fundamental to most stock assessments and the provision of scientific advice on the consequences of future management actions. In the absence of any direct information, growth rates are generally assumed to remain static over time in stock assessments. However, if growth rates are changing and these changes are not accounted for, they can result in substantial biases in estimates of stock productivity, sustainable catch levels and recovery in the case of a depleted stock.

In spite of the importance of knowing how growth may have changed, estimates of long-term temporal trends and variability in growth are seldom available for most commercially exploited fish stocks. Often this is due to the absence of long-term data series. In other cases a variety of different sources of growth information (e.g. tagging, length-frequency and direct aging data) may be available, but the data collection processes have resulted in fragmented time series for any single source. When such fragmented data exist, a statistical framework is required that can integrate information from the different sources and can also cope with temporal changes in growth. Even the simpler problem of integrating several data sources from a period of static growth is not straightforward. Eveson et al. (submitted) have developed an estimation framework that integrates growth data from tagging studies, from direct aging of hard parts, and from modal length analyses of length-frequency data. In the current paper, we apply this framework to southern bluefin tuna data collected in each of the four decades from 1960 to 2000, assuming that growth remained relatively stable within each decade. The results are used to quantify changes in SBT growth over this 40-year period.

A large amount of data relevant to the estimation of growth for SBT has been collected since the early 1960's. Several previous studies have used subsets of data from a single source to address the question of changes in SBT growth. Comparisons of growth increment data from tag experiments conducted in the 1960's and 1980's have demonstrated that there was a substantial increase in SBT growth rates between these two periods (Hearn and Polacheck 1993, 2003, Anon. 1994). Concurrently, there was a substantial decline in the SBT stock, suggesting the change in growth may

have been density dependent. Analyses of length-frequency data for juvenile fish caught in the Australian domestic fishery also demonstrated a substantial increase in the growth of juveniles between these two periods (Leigh and Hearn 2000). Previous studies have been unable to provide estimates of growth rates in the 1970's and 1990's because of the limited data available for these decades at the time of analyses.

Direct aging techniques were developed and verified in the 1990's for aging SBT using their otoliths (Clear et al. 2000). The direct aging data that have accumulated since then provide important growth information on fish born in the 1970's, and they also have the potential to clarify uncertainties that previous studies had in comparing asymptotic lengths (Hearn and Polacheck 2003). Moreover, substantial information on growth of fish spawned in the 1990's is now available. With all of the data currently available and with an integrated analysis method, we were able to obtain rigorous estimates of growth in each of the past four decades and to identify significant changes in growth over this time.

Recent SBT stock assessments suggest that the stock continued to decline from the 1980's until the mid 1990's, after which the trend is uncertain (Polacheck and Preece 2001, Kolody and Polacheck 2001). Given the previously documented changes in SBT growth, the depleted status of the SBT stock and uncertainty about the most recent stock trends (Anon. 1998a, 1998b, 2001, Polacheck et al. 1999), knowing how SBT growth rates in the 1990's compare with previous periods has been seen as an important indicator of the current stock status (Gunn et al. 1998), and may provide insight into possible mechanisms underlying growth changes.

Material and Methods

Data

Data from three sources were used in the analyses considered here:

1) release and recapture length and time data from tag-recapture experiments;
2) modal progression within a year from length-frequency data from commercial catches; and
3) direct age estimates from otolith readings combined with the length of a fish at the time of capture.

For each of these data sources, extensive documentation exists (see Appendix 3 and references cited therein). Table 1 summarizes the extent of available data for each source by decade.

All of the tag-recapture data come from fish tagged as juveniles (primarily ages 1-4). Only tagging data from fish tagged and measured at release by trained tagging personnel are used here. Recapture information (particularly recapture lengths) was obtained from commercial fishermen, factory personnel and scientifically trained staff. Data from the trained staff had lower measurement errors and hence were assigned a different factor level in the analyses. The maximum time at liberty for which release and recapture data are available is approximately 14 years. However, the majority of recapture times are less than 4 years. As such the tagging data are most informative about growth rates for juvenile and sub-adult SBT. (SBT can live past 40 years of age and the mean age of maturity appears to be on the order of 10-12 years; Kalish et al. 1996, Davis et al. 2001). Tagging experiments were conducted during each of the four decades considered, but the number of releases and release years varied substantially. Consequently the extent of growth data differs considerably. In particular, tagging data from the 1970's are limited, and all of the tagging data from the 1980's comes from the first half of the decade (Table 1).

Length-frequency distributions of the commercial catches landed in South Australia each half-month exhibit modes corresponding to age classes. The progression in length of these modes over the year provides information on growth rates. The catch was sampled either in canning processing plants or at the time of landing. The data consisted of length measurements from a sample of the landings within a half-month period. Caudal fork lengths were measured and recorded to the nearest centimetre and pooled into one-centimetre groups. Trained technicians made all measurements. The sample length frequencies from an individual landing were scaled up by the total weight of the landing relative to the weight of the sample to provide an estimate of the length-frequency distribution for an individual landing. The length-frequencies from individual landings were then pooled across half-months to provide an estimate of the length-frequency of the catch for that half-month period. Not all landings in a half-month were sampled, so the length-frequency distributions from the sampled landings were raised by the total weight of the catch from all landings in that period and area.

For South Australia, length-frequency data are available since the 1964/65 fishing season (Table 1). Data after 1989 are not used in the current paper because the nature of the surface fishery changed dramatically to one dominated by small landings aimed at the sashimi market and later to farming. In both cases, there are indications of a high level of size selectivity. In addition, the level of sampling in the farms has been quite low.

Verified methods for directly aging SBT from their otoliths were developed in the 1990's (Clear et al. 2002) and extensive collection of otoliths was undertaken during this period. Otoliths were collected from juvenile fish landed in the surface fishery and from fish caught during tagging programs. Otoliths were also collected by observers aboard Japanese longline vessels operating in the Australian EEZ as well as on the high seas. In addition, a large number of otoliths were collected at the time of landing in Indonesia from longline vessels operating on the spawning grounds. The age range of fish sampled covers 40 age classes. Thus, these data provide information on growth for fish born in each of the four decades considered in this paper. However, the degree of overlap in ages among the decades is low because almost all the otoliths were collected in the 1990's (Table 1). In order to avoid aging errors due to uncertainty in the time of band formation, direct aging data were only used for fish collected from October through April (see Appendix 12). Also, there is evidence of size selectivity in spawning within an age-class below age 14 (Farley et al. 2001). Therefore, only the direct aging data for fish 14 and older from fish caught on the spawning grounds were used to avoid biasing the results for younger ages.

Growth Model

The basic growth function used in this paper for describing SBT growth is the VB log k model, which is described in Appendix 4. There is evidence in SBT of a significant departure from the commonly used von Bertalanffy (VB) model (Anon. 1994, Hearn and Polacheck 2003, Laslett et al. 2002, Appendix 9). All of these analyses suggest that there is a discernible change in the growth process during the transitional period from juveniles to sub-adults. The VB log k model was developed by Laslett et al. (2002) to accommodate such a transition in growth. It provides a more flexible framework with better statistical properties using the same number of parameters than the two-stage VB growth model used for SBT and similar species

(Bayliff 1991, Hearn and Polacheck 2003). The VB log k model uses six parameters to describe length, l, as a function of age, a:

$$l(a) = L_\infty \left[1 - e^{-k_2(a-a_0)} \left\{ \frac{1+e^{-\beta(a-a_0-\alpha)}}{1+e^{\alpha\beta}} \right\}^{-(k_2-k_1)/\beta} \right] \quad (1)$$

where

a_0 is the theoretical age when a fish would have length zero;

L_∞ is the asymptotic length;

k_1 is the growth rate parameter for the first stage of growth;

k_2 is the growth rate parameter for the second stage of growth;

β is a parameter governing the rate of transition between k_1 and k_2;

α is a parameter determining the central age of transition.

As age increases, this function makes a smooth transition (according to a logistic function) from a VB curve with growth rate parameter k_1 to a VB curve with growth rate parameter k_2. If k_1 equals k_2, the model reduces to the standard VB curve.

In addition to this basic model, a seasonal component was included in the model to reflect the fact that SBT growth, particularly as juveniles, appears to be substantially greater during the austral summer months than during the winter. Seasonality in growth was modelled by replacing $a - a_0$ with $a - a_0 + S(t)$ in equation 1, where t is the fractional time of year since January 1. Within-year growth was modelled as a sinusoidal function:

$$S(t) = \frac{u}{2\pi} \sin(2\pi(t - w)) \quad (2)$$

where u is the amplitude and w controls the phase shift. Both parameters were estimated in the growth model, with u constrained to be between 0 and 1 to prevent negative growth and w constrained to be between –0.5 and 0.5 (any bounds with a span of one could have been chosen due to the periodicity of the function). In this formulation, the rate of growth is maximal at $t = w$ and diminishes symmetrically

about w to a minimum at $t = w - 0.5$ and $t = w + 0.5$. Other formulations for $S(t)$ could have been considered, but a sinusoidal function provided an adequate fit and data limitations did not allow for further resolution of the within-season growth pattern.

Parameter Estimation

The model was fit to the data from each of the four decades separately. For the otolith data, we separated the data into decades according to cohorts (i.e. year of birth), as determined from the year of capture and the estimated age. For the tag-recapture data, we separated the data into decades according to the year of release because the age of the fish at release (and hence its cohort) is not known. Similarly, the length-frequency data were separated into decades according to the year of capture. To separate based on cohorts would have required the data collected within the same year to be split up in some years. We did not do so because the initial step of the analysis involves fitting a mixture decomposition to the length-frequency data from each year, and also because we explored estimating year effects in the subsequent stage of the analysis. As such, in both the tag-recapture and length-frequency decadal data sets, there may be a small proportion of fish that were actually born in the last few years of the previous decade. This does not have any substantive effects on the results.

In fitting the model to the data, several sources of variation were taken into account. It is well known that if allowance is not made for individual variability in growth, the resulting estimates can be substantially biased depending upon the estimation method. Individual variability in growth was modelled by allowing the asymptotic length to vary from fish to fish. Thus, L_∞ was assumed to be a random normal variable with mean μ_∞ and standard deviation σ_∞. Other formulations for individual variability in growth were considered, but treating L_∞ as a random normal variate appears to provide both an adequate representation of the error and leads to similar predictions as other possible formulations (e.g. random growth rate parameters). In addition to individual variability in growth we allowed for additional measurement and model error. This was achieved by assuming that for any given observed length at age there was an additional normal random variability associated with the observation. The source and magnitude of the variation would be expected to

be different among the different data sources and this was taken into account in the estimation model (see Appendix 9 for details). In total, four different model/measurement variance parameters were estimated. These were:

σ_s^2 = the variance of the model and measurement error components for the tagging data when the (either release or recapture) lengths were measured by scientists

σ_f^2 = the additional variance components for the tagging data when the tag recapture lengths were measured by fishermen

σ_γ^2 = the variance of the model and measurement error component for the direct aging otolith data

σ_ε^2 = the variance of the model and measurement error component for length-frequency data

A maximum likelihood approach was used to obtain the parameter estimates. For each of the data sources a separate likelihood function was defined. The likelihood functions that are used here were developed and described in detail in Appendices 4 and 9. As such, the details are not repeated here and the reader is referred to these appendices for a complete description. Since each of the data sources were independent, the integrated log-likelihood across all of the data sources is simply the sum of the log-likelihood components. The integrated likelihood incorporated common parameters across components for the parameters defining the mean growth function (i.e. μ_∞, k_1, k_2, a_0, β, α, u and w) and for the asymptotic variance parameter (σ_∞), but had component-specific parameters for the measurement/model variance terms for each data source. Two additional parameters, $\mu_{\log A}$ and $\sigma_{\log A}$, were estimated in the fitting of the tag-recapture data; they define the lognormal distribution that was used to model the unknown ages at release. These parameters are not of primary interest and the estimates of the growth rate parameters are generally insensitive to how the distribution of initial ages is modelled, as long as a reasonably appropriate distribution is used (see Laslett et al. 2002). Overall, the integrated VB log k model has 15 parameters to be estimated.

We also compared the fit of the VB log k model to that of a standard VB growth curve:

$$l(a) = L_\infty\left(1 - e^{-k(a-a_0)}\right) \tag{3}$$

where the parameters have the same definition as in equation 1 above. In this case, we used the same basic likelihood functions and still retained the seasonal component. The number of parameters is reduced by three (i.e. β, α and one of the k parameters are eliminated).

To evaluate how well a model fit the data, we calculated residuals (fitted minus observed length) for each of the data sets. In order to calculate the fitted release and recapture lengths in the tag-recapture data, we required a realised value of A and L_∞ for each fish. The approach outlined in Appendix 4 is to use the mean of the posterior distribution for A and L_∞, respectively, conditioned on the fish's release and recapture lengths. This approach yields unbiased estimates of L_∞, but, as discussed in Appendix 5, it leads to biased estimates of A. Instead, we used the approximately conditionally unbiased estimator $\tilde{A}_f$ that is described in Appendix 5.

We computed approximate variances and co-variances of the parameter estimates by evaluating the inverted Hessian matrix at the minimum of the negative log-likelihood function. In some cases this matrix was not positive definite. We were forced to treat the estimates of some of the less "well-behaved" parameters as known quantities. As such, no variance or co-variance estimates were calculated for these parameters.

Results and Discussion

Table 2 provides the parameter estimates for the individual decadal maximum likelihood fits to the overall growth model. Comparison of the parameter values suggests that there has been little or no change in the asymptotic length (μ_∞), at least since 1970, but that there has been an increasing trend in growth rates at younger ages as reflected in estimates of the k_1 parameters. Comparison of the estimated average growth curves from the maximum likelihood fits indicates that the predicted length of juvenile fish increased between the 1960's and 1970's, continued to increase between

the 1970's and 1980's, and changed little between the 1980's and 1990's (Figure 1). The overall increase between the 1960's and 1980's is quite substantial; the estimated average size of a two year old in the 1980's is nearly equal to that of a three year old in the 1960's. Although Figure 1 suggests that there may not be much difference in growth between the 1980's and 1990's, a closer examination of the two curves suggest that a difference of about 4 cm existed at age 2 and of about 2 cm existed at age 3 (Figure 2). After this age, the estimated differences were generally less than 1 cm (see below for more discussion of this).

In order to test formally whether the growth curves estimated for each decade were different, the fit when the data for two adjacent decades were combined was compared to the fits to each decade separately (Table 3). In all cases, there was a very substantial and statistically significant decrease in the negative log-likelihood when separate curves were fitted to the data from each decade.

Common μ_∞?

Comparison of the parameter estimates for μ_∞ in Table 1 raises the question of whether μ_∞ has varied over time – in particular whether the apparently lower value for μ_∞ of around 3 cm for fish born after 1970 is associated with the higher growth rates in these later years. Fitting all four decades unconstrained with a common μ_∞ parameter resulted in a significant increase in the negative log-likelihood (Table 4). It is clear from Table 4 that the difference is driven primarily by the higher estimate of μ_∞ for the 1960's, with little difference in the other three decades. However, it should be noted that the likelihood profile for μ_∞ for the 1990's data is quite flat (Figure 3) and there is little basis for distinguishing whether μ_∞ is different in this decade from any of the other decades including the 1960's. This is not surprising as the oldest fish in the data sets for the 1990's is around age 10 (by necessity) and fish are still exhibiting substantial growth (i.e. they are only ~80% of their asymptotic length). For the 1980's, the likelihood profile with respect to μ_∞ is substantially steeper than for the 1990's and the estimate of μ_∞ is significantly different from that for the 1960's (Figure 3). Nevertheless, there are no fish older than age 20 in the 1980's data sets and some indeterminacy might be expected in the estimate of μ_∞ since SBT still appear to exhibit appreciable growth after this age.

Thus, the main basis for assessing whether there has been a change in μ_∞ comes from the comparison of the estimates for 1970's with that of the 1960's. For both decades there are a substantial number of length observations for animals estimated to be over 25 years of age. For these two decades, the estimates of μ_∞ are significantly different based on differences in the log-likelihoods (Table 5, Figure 3). Moreover, a non-model based comparison of the mean length of fish estimated to be older than 25 also suggests a significant difference in the asymptotic length (Table 6). In spite of a significant difference existing in the estimates of μ_∞, the estimates of length at age for the 1960's are relatively insensitive to the value used for μ_∞ (Figure 4). Thus, for the range of ages for prediction of the age structure likely to be important within a stock assessment context, there is at most 1.5 centimetres difference (e.g. below age 20) and the differences in μ_∞ have little effect on the residual patterns (Annex 1). The parameter estimates for the other decades are similar whether μ_∞ is estimated separately or a common value is estimated for all four decades (Tables 2 and 7).

VB log k or Standard VB model?

Comparison of the k_1 and k_2 parameters suggests that, for the 1960's and perhaps for the 1970's, they may be equal (Table 2), in which case the VB log k model is equivalent to the standard VB growth model. In order to see if this was the case, the data from each decade were fitted separately to a standard VB model, and the resulting likelihoods compared (Table 8). The results indicate that there is no significant difference between the standard VB and VB log k model for the 1960's. A comparison of the residuals for the 1960's data sets suggests the same conclusion (Figures 1a-c in Annex 1 versus Figures 1a-c in Annex 2). The VB log k model provides a significantly better fit to the 1970's data, as well as to the 1980's and 1990's data. Table 9 provides the parameter estimates for the fit to the VB model for the 1960's.

The lack of difference between the VB log k and VB models for the 1960's is not consistent with results in Hearn and Polacheck (2003) and Anon. (1994). Using only tagging data, these previous studies found a significant difference for the 1960's between the standard VB model and the two-stage VB model, which they were using

to model a change in growth rates between juvenile and adult phases[1]. (This model is similar to the VB log k except the transition is abrupt.) The reason for the difference appears due, at least in part, to the inclusion of the direct aging data in the current study. The direct aging data are highly informative with respect to μ_∞. In contrast, as discussed in Hearn and Polacheck (2003), the tagging data provide only minimal information for estimating μ_∞. The direct aging data clearly indicate that μ_∞ is around 185-190 cm (Table 6 and Figure 1a(i) in Annex 1) compared to the estimate of 211 cm in Hearn and Polacheck (2003). Reducing the estimate of μ_∞ will increase the estimate of k_2 in order to achieve a relatively similar fit to the growth information on intermediate ages since k_2 and μ_∞ are highly negatively correlated. There are other possible reasons for the difference, such as L_∞ was modelled as a random variable in the current paper and the estimation methods used are different.

In any case, it is not clear whether the available data would have sufficient statistical power to distinguish between the VB and VB log k models. Most of the data on growth rates for the cohorts born prior to 1970 provides information on growth either below around age 5 or greater than age 25. These latter data provide informative data for estimating μ_∞ but would be equally compatible with a wide range of growth rate models for the intervening ages. The only data in the intermediate age ranges from 5 to 20 comes from tag return data in which the return lengths were measured by fishermen. The amount of data is small, and there is clearly large measurement error associated with these return lengths as indicated by the large residuals for these data (see Annex 1) and the large estimate of the additional variance component for fishermen-measured return lengths, σ_f^2 (Table 1).

For the 1970's data, it is worth noting that the estimate of k_1 is in fact less than the estimate of k_2. This is the reverse of the situation for the 1980's and 1990's cohorts and contrary to what was expected given previous discussions and suggestions for why a transition may occur in SBT (e.g. Hearn and Polacheck 2003). This issue is discussed further below.

[1] Hearn and Polacheck (in press) found that the first stage of the two-stage VB model could be equivalently represented as a linear function.

Examination of Residuals

Examination of the residuals for each data set in each decade indicates that in general the growth model provides a reasonable and consistent fit (Annex 1). There is no indication of any substantive inconsistency among the different data sources. This provides additional confidence in the overall estimates since each of the data sources was collected independently and suggests that substantial selection biases did not occur. This is particularly true for the 1980's and 1990's where the data are extensive and there is a large overlap in the age ranges for which these sources are providing information on growth.

The only substantive systematic pattern in the residuals that would suggest a serious lack of fit to the model occurs in the modal length-frequency data for age 1 in the 1980's. In this case the modal data suggest that the length of an age 1 fish was larger than that predicted by the model. As discussed in Appendix 3, there is substantial spatial segregation in size for age 1 between fish found in Western Australia and South Australia. On average, one-year-old fish are larger in South Australia than Western Australia. This appears to reflect a combination of effects. The actual range of biological ages within the one-year-old age class is large relative to their true age due to the protracted six-month spawning season of SBT. Thus, fish that are classified as age 1 based on a January 1 birthday may differ by as much as six months in their actual age. For an age 1 fish this would induce large differences in their expected size. There also appears to be a tendency for the older/larger fish to migrate farther east and into the Great Australian Bight (i.e. South Australia), which is consistent with the current understanding of the general migration of young fish from the spawning grounds off Indonesia, along the west Australian coast and then into the waters south of Australia. As such, estimates of the size and growth for age 1 fish will be sensitive to the relative proportion that came from early and late spawners in a given year and also sensitive to relative sampling intensity in South Australia and Western Australia.

A consequence of this is that modelling the growth of SBT below age 2 will contain some ambiguity and uncertainty. In theory, by using daily rings in the otolith (Rees et al. 1996, Itoh and Tsuji 1996), it might be possible to resolve some of the problems by estimating the actual birth date of individual fish and thus correct for differences in age among age 1 fish. Besides the practical difficulty in doing this

(counting daily rings is both expensive and time intensive), the results would likely be confounded by compensation in growth during these early ages (i.e. faster growth during the first year by late spawners). In terms of the objectives of this project and the overall use of estimates of growth within the assessment context (i.e. assigning cohort to the catch at length data and estimating the weight of the spawning biomass), this uncertainty and ambiguity about the best estimate of the growth and length of fish below age 2 is of little consequence. In terms of the assignment of cohorts, the growth at these earliest ages is very rapid. As such, the difference in the length at age for ages 1 and 2 provides a reasonably robust basis for assigning cohorts as long as a reasonable value is used for the size of an age 1 fish (i.e. the modes in the length-frequency distributions tend to be quite distinct). Moreover, in terms of the current SBT fishery, the amount of fish being caught below age 2 is quite small (Preece et al. 2001). Finally, since SBT appear to mature around age 10-14 with no indication of maturity before age 8 (Davis et al. 2001), estimates of the size of an age 1 fish have no relevance to the estimation of the spawning stock biomass.

Variances/Covariances for the Parameter Estimates

Estimates of the standard errors indicate that most of the non-variance related parameters are estimated with a high degree of precision. All of the parameters that are used in the estimation of the expected or average length at age have a coefficient of variation (CV) less than 7% except for u and w (Table 10). These latter two parameters determine the seasonal pattern of growth. It is not surprising that u and w are less precisely estimated as the amount of information within the data on the seasonal component is substantially less (e.g. only from the shorter term tag returns and the within-year pattern of the means in the length-frequency distributions over a limited portion of the year). Moreover, there appears to be some year-to-year variation in the period of peak growth within the austral summer months (Appendix 7). This would be expected given annual variation in environmental conditions. Nevertheless, even for u and w, the estimates of the CV's are less than 35%.

It should be noted that there was one parameter related to the expected value of the growth curve for which we were not able to estimate its standard error. This was the parameter β, which governs the rate of transition between the two growth rate parameters k_1 and k_2. In all cases, the estimates of β were large and frequently

equal to the upper bound of 30 that we set for this parameter. For values of β over 10 the rate of transition is very rapid and any difference in the predicted length at age for larger values would be restricted to a very narrow age range within a year. As such the likelihood function for higher values of β is very flat. Thus, the model is predicting with a high degree of certainty that the rate of transition between k_1 and k_2 is very rapid. The fact that we are not able to estimate a variance for β reflects the fact that there is basically no predictive or practical difference in the value chosen for β once β is estimated to be large (e.g. >10).

Many of the variance related parameters are estimated with reasonably high precision. In most cases their estimated CV is less than 12%. One exception is the variance for the parameter σ_γ (the residual measurement standard deviation in the model for the direct aging data). In the two cases where we were able to estimate the standard error of this variance parameter it had a CV of over 100%. However, in most instances, we had to assume that this parameter was known in order to be able to achieve a positive definite Hessian. The reason for this is not obvious. Nevertheless, the estimates of this parameter appear to have little correlation with the other parameters. As such, the fact that we had to assume that it was fixed in estimating the variance and co-variance matrix should have little effect on the results for the other parameters.

The correlation matrix of the parameter estimates has some high entries, mostly negative (Annex 3). Most of these are expected given the structural form of the model. Thus, high negative correlations between μ_∞ and the growth rate parameters (k's) are a well known feature of VB type growth models. Similarly, the variance related parameters are often frequently highly negatively correlated. This is not surprising as they are providing alternative ways of explaining the residuals around the mean growth curve (e.g. increasing the value of one results in less variance that needs to be explained by the others).

The estimates of the variance-covariance matrix can be used to produce estimates of the confidence intervals around the predicted growth curves based on normality assumptions. We calculated these confidence intervals and found that they are very narrow. The upper and lower 95% confidence intervals are almost indistinguishable from the predicted curves when plotted on the same scale as Figure 1. The small CV's for the growth parameter estimates and the narrowness of the

confidence intervals indicate that the growth model is estimating the mean length at age with a very high level of precision. Such high precision reflects the large amount of data going into each of the estimated curves and the high degree of consistency across the different data sources.[1]

Nevertheless, these estimates of the variances, covariances and confidence intervals are too precise. We would not recommend that these be used to represent the actual uncertainty in the mean growth of SBT during these decades. There are at least five reasons why the uncertainty is being under-represented: (1) model uncertainty (e.g. the choice of modelling L_∞ as a random effect); (2) lack of normality in the parameter estimates; (3) non-independence in the data (e.g. non-independence among fish tagged in the same school; over-estimation of the effective sample size in the length-frequency data; reader biases in the otolith data, etc); (4) non-representative sampling from the SBT population (e.g. all tagging was done in near-shore surface fisheries close to Australia; potential size selectivity in the catch; etc); and (5) the tag-recapture model fitting procedure is very flexible and may overfit the data with respect to the age at release, A, as explained in Appendix 6 (this is a quite recent discovery). Alternative methods for estimating the variances (e.g. Bayesian) would likely result in somewhat larger variance estimates because we would not have to regard any of the unknown parameters as fixed. However, application of these approaches was not feasible given the size of the data sets and the time required to achieve a single solution. Moreover, there is little information for incorporating many of the unaccounted sources of uncertainty in the estimation of the variances. The estimation of the variances for the parameters is an area requiring further research.

Model Simplification?

In addition to considering whether the VB log k model could be simplified to the standard VB model, consideration was also given to whether inclusion of the seasonal component with the two additional parameters provided a significantly better fit. In all cases, it did. As would be expected, addition of this seasonal component had almost no effect on the estimates of the parameters describing the overall longer term growth patterns (for more detail see Appendix 9).

[1] Note that while the variability in the estimated mean growth curve is very small, there is clearly a large amount of individual variability around the mean curve.

The estimates for a number of the variance related parameters are similar among some or all of the decades. This is particularly encouraging as it suggests consistency in the growth processes and measurement processes and that the model is capturing these reasonably well. In particular, it was somewhat surprising that the estimates of σ_∞ across the four decades were as similar as they were (ranging fro 7.0 to 8.7) as there are no observations for the 1980's and 1990's for ages that have essentially reached their asymptotic lengths. We have not attempted to fit models in which any of these variance related parameters were assumed to be common across decades. This was due in part to practical considerations. Attempting to fit models with common parameters proved to be highly computer intensive, requiring extensive amounts of time because of the magnitude of the data sets, the number of parameters that needed to be estimated, and the large number of different parameter combinations that needed to be tested. More importantly, the results of such an exercise would not provide any substantial improvement for modelling the growth within a decade or for predicting the expected distribution of lengths at age for these different decades.

General Discussion

The results from applying the integrated model to the data from the 1960's and 1980's confirm previous results that the latter cohorts grew substantially faster at younger ages. They also demonstrate that this difference was consistently seen in three independently derived data sources, indicating that the observed difference was not an artefact of differences in the data collection or processing procedures over time. The estimated difference in the growth curves between these two decades is somewhat less than that estimated in either Hearn and Polacheck (1993, 2003) or Anon. (1994). These previous studies were based only on tag-recapture data and used Fabens' estimation method (Fabens 1966) without any allowance for individual variability in growth. Fabens' approach has been shown to be biased if there is individual variability in L_∞ (Maller and deBoer 1988). The results in this and previous appendices strongly suggest such variability exists, and taking into account this variability is probably the primary source of the difference.

The results in this appendix also indicate that growth of young fish in the 1990's was faster than in the 1980's up to about age 4. The estimated growth curve suggests that after this age growth slowed down so that fish from the 1990's are

predicted to be the same size on average as those born in the 1980's (Figure 2). However, the limitations in the 1990's data need to be recognized. Only half of the cohorts born in the 1990's can possibly contribute data on growth for fish older than age 5 because 2000 was the last year for which data were available for inclusion in this study (cohorts born after 1995 would be younger than age 5 in 2000). In addition, the last tag releases of SBT were of age 1 and 2 fish in 1997. The most recent cohort for which an otolith was read was from the 1995 cohort and only 7 otoliths were read from fish collected after 1995. As such, the estimated growth curve for the 1990's, particularly for ages past 5, is based almost exclusively on the growth experienced in the first part of the decade. Thus, if growth rates have on average been increasing in the 1990's, the estimates for the older ages may be biased downward relative to what may be observed when more complete and representative data are available. In this regard, it is worth noting that in the tag-recapture data there is a tendency for the residuals for the oldest fish from the 1990's to be negative (Figure 4-6, Annex 1). These fish were born in the first few years of the 1990's or in some cases in the late 1980's.

The 1970's results suggest that this decade saw a period of transition with quite variable growth. The results from the integrated analyses for the combined data from this decade suggest that growth rates at younger ages were slightly greater than those in the 1960's. Examination of residual plots for the length-frequency data either by year or cohort (Figures 5 and 6) strongly suggests that growth in the early part of the decade was substantially slower than in the latter years (see also Appendix 7). Thus, when the data are pooled for this decade they will provide intermediate values. Attempts to further resolve the growth in the 1970's using this integrated framework were not successful. The data for the 1970's are relatively sparse and would not, for example, support half-decadal estimates. The limitations in the 1970's data are important to recognize in any interpretation of the results. In particular, there is little information on growth for intermediate ages (i.e. between 6 and 15 years of age).

The estimates of μ_∞ suggest that there may have been a small decrease in the average asymptotic length between the 1960's and 1970's. As discussed above, it is difficult to evaluate whether this represents a real change in the underlying growth dynamics or is the result of other factors (e.g. sexual dimorphism in growth or sampling/age-reading effects). More significant in this regard is the fact that the

estimates of μ_∞ appear to be larger than the size distribution of adult fish that were caught historically. In the first 20 or so years of the SBT fishery (prior to 1970) less than 0.05% of all fish caught on the spawning ground by Japanese longliners were estimated to be greater than 184 cm and the proportion never exceeded 0.4% in any year (Figure 7). The proportion of fish greater than 184 cm in the spawning stock would have been expected to have been in excess of 9% for a stable age distribution if μ_∞ was at post-1960 levels, given current estimates of age of maturity (10-14) and adult survival rates (0.08-0.10)[1]. The observed proportion in the catch is about 200 times less than what would be expected in an unexploited population. Fish greater than 184 cm were similarly rare in the longline catches off the spawning grounds in the years of the fishery (Figure 8). Interestingly, in the spawning ground catches, fish over 184 cm began to make a non-negligible contribution to the catches around 1970 and in the feeding ground catches around 1980 (Figure 9). Their contribution after 1980 has generally been increasing. In addition, the contribution of larger fish to the catch showed a rather steady increase (Figures 8 and 9, see also Anon 1994 for further details). Under constant growth conditions, such an increase is contrary to what is expected in the initial period of exploitation of a fishery, namely that the age and size distributions shift towards younger and smaller fish (i.e. the increase in mortality reduces average life expectancy).

The spawning ground fisheries operating prior to 1970 would have been catching adult SBT born prior to 1950 for fish older than age 20. The contrast between the estimates of μ_∞ from all fish born after 1960 and the absence of fish in the corresponding size range in the pre-1970 spawning ground fisheries raises the question of whether μ_∞ was substantially less prior to the commencement of the fishery. The hypothesis that μ_∞ was substantially smaller would be consistent with a density dependent response in the post-juvenile phase of the SBT life cycle. Under this hypothesis, the large catches of adult fish in the late 1950's and early 1960's and the corresponding large reduction in the adult SBT biomass would have permitted

[1] This 9% figure is derived from calculating the proportion of the SBT stock aged 10 and above that would be over age 25 years based on a stable age distribution and assuming that half of these would be greater then 184 cm. This provides a conservative estimate since a substantial number of fish appear to reach lengths of 184 cm prior to attaining 25 years of age.

SBT, particularly those born after around 1950 (i.e. less than age 10), to have developed a positive response to the reduction in the adult and sub-adult biomass (possibly as the result of reduced competition for food). This would be consistent with fish larger than 184 cm appearing in non-negligible proportions in the spawning ground and feeding ground catches in the 1970's and 1980's and would suggest that there is a large element of indeterminate growth in SBT.

The above hypothesis is clearly speculative. Unfortunately there are no available data or biological material from which to estimate growth rates for cohorts born prior to 1960 or for determining the age of larger fish that were caught in the 1950's and 1960's. However in the SBT stock assessment, values for the growth rates or alternatively the distribution of the lengths at age are required. As such, developing plausible hypotheses for the growth prior to and during the early years of exploitation is an essential component of the stock assessment. The estimates that are used can potentially have a large effect on current levels of depletion and the productivity of the stock. While the above hypothesis is speculative, it does provide a consistent and plausible explanation for the lack of larger fish in the early catches. It needs to be considered in relationship to other plausible hypotheses.

In the current stock assessments, the underlying hypothesis is that growth rates for cohorts born prior to 1960 were similar to those observed for the cohorts born in the 1960's. While this is the simplest parsimonious hypothesis in terms of the direct information on growth, it raises the question of why only negligible amounts of fish around the hypothesized asymptotic length were captured in the early years of the fishery, and why they began to be caught in increasing proportions beginning in the 1970's and continuing until present. There are at least three potential alternative hypotheses:

1. A period of sustained very low recruitment existed such that very few adults greater than 20 years of age were alive at the beginning of the fishery and for the next 15-20 years (e.g. a major "regime shift").
2. High natural mortality existed prior to the fishery such that fish did not generally live to age 20 and older, and thus did not attain their potential asymptotic length.

3. Strong negative size selectivity for very large fish existed in the Japanese longline fishery (particularly on the spawning ground), but this diminished overtime.
4. Large sampling or measurement biases exist in the earlier size data collected from the Japanese longline fishery.

The first two hypotheses would seem equally as speculative as a changing asymptotic length with no direct data to support them. In addition, with respect to the first hypothesis, a period of low recruitment is not consistent with the estimates of recruitment trends in the assessments (e.g. an extended period of low recruitments prior and during the early years of exploitation would be inconsistent with the large catches and estimated spawning biomass in the late 1950's and early 1960's).

The third of these alternative hypotheses seems rather less plausible. It is difficult to imagine a mechanism in terms of the longline gear that would generate such strong negative selectivity only for very large fish. Originally, there was very intensive fishing effort for SBT on the spawning grounds. As such, it is hard to conceive of a temporal/spatial refuge only for very large fish. Finer scale analyses of the shift in size towards larger fish on the spawning grounds suggest that this was not a consequence of temporal or spatial shifts in the distribution of effort (Anon. 1994). Moreover, there appears to have been a shift towards targeting bigeye tuna during the 1960's and the residual fishing on the spawning ground after 1970 has been reported to generally be fishing deep. This should have resulted in an increasing selectivity towards smaller fish (Davis et al. 2001) and is the opposite of what has been observed. Finally, the current Indonesian fishery operating in the same general area and period catches substantial numbers of large SBT (i.e. they are a primary source of the otolith samples for large fish — see Appendix 3).

Measurement bias seems an unlikely source for the lack of large fish being reported in the Japanese catch considering all of the early size measurements of the Japanese catches were made in port by trained scientific samplers. It also seems unlikely that there were large selection biases against large fish in the choice of fish that were sampled. There have been hearsay suggestions that in the earliest years of the fishery (during the 1950's) there may have been some selection bias due to large SBT being cut in half to fit into available storage space. Even if this practice was

extensive (which it would have had to have been to explain the lack of large fish in the samples), it would not explain the persistent lack of large fish up to 1970.

The hypothesis that μ_∞ was substantially less prior to the commencement of the fishery could also provide a possible explanation for why there is no significant difference between the VB and the VB log k models in the data from the 1960's. If the underlying growth process of SBT involves a substantial transition between the juvenile and sub-adult stages as suggested by the post 1960's data, the lack of a transition in the 1960's could have stemmed from the fact that during the 1960's there was a substantial increase in the growth rate associated with the post-juvenile stage in conjunction with the increase in μ_∞. The resulting change in growth rates could have been such that k_1 and k_2 became essentially equivalent. Such a hypothesis would be consistent with a density dependent response in the post-juvenile phase to the large declines that occurred in the spawning stock during the 1960's.

A hypothesis for the subsequent increase in the juvenile growth rate (k_1) in the 1980's and 1990's would also be that it was a density dependent response. In this case, the response would have been primarily to the declining recruitment combined with even larger proportional declines in juveniles as a result of the large increases in juvenile catches in the surface fishery (Caton 1991, Polacheck and Preece 2001, Kolody and Polacheck 2001). The small but continued increase in the juvenile growth rate estimated to have occurred in the 1990's is consistent with the estimated continuing, but slowed, declines in recruitment. These two hypotheses are speculative, but they are at least broadly consistent and plausible given the set of estimated growth rate parameters from this integrated analysis, the history of the fishery and the general trends in the SBT stock. Under these hypotheses, juvenile SBT growth rates would be expected to decline if substantive increases in recruitment occur, while adult growth rates and μ_∞ would be expected to decline only if quite substantial rebuilding of the spawning stock occurs.

References

Anon. 1994. Report of the southern bluefin tuna trilateral workshop. Hobart, Australia, January/February 1994. 161 pp.

Anon. 1998a. CCSBT. Report of the 1998 Scientific Committee meeting. 3-6 August 1998. Tokyo, Japan.

Anon. 1998b. CCSBT. Report of the 1998 Stock Assessment Group Meeting. 23-31 July 1998. Shimizu, Japan.

Anon. 2001. CCSBT. Report of the sixth meeting of the Scientific Committee. Tokyo, Japan, 28 - 31 August 2001

Bayliff, W.H., Ishizuka, I., and Deriso, R.B. 1991. Growth, movement, and attrition of northern bluefin tuna, *Thunnus thynnus*, in the Pacific Ocean, as determined by tagging. Inter-Amer. Trop. Tuna Comm. Bull. **20**(1): 1-94.

Caton, A.E. 1991. Review of aspects of southern bluefin tuna: biology, population and fisheries. Inter-Amer. Trop. Tuna Comm., Spec. Rep. **7**: 181-357.

Clear, N.P., Gunn, J.S., and Rees, A.J. 2000. Direct validation of annual increments in the otoliths of juvenile southern bluefin tuna, *Thunnus maccoyii*, by means of a large-scale mark-recapture experiment with strontium chloride. Fish. Bull. **98**: 25-40.

Davis, T.L.O., Farley, J.H., and Gunn, J.S. 2001. Size and Age at 50% Maturity in SBT: An integrated view from published information and new data from the spawning ground. CCSBT-SC/0108/16.

Eveson, J.P., Laslett, G.M., and Polacheck, T. Submitted. An integrated model for growth incorporating tag-recapture, length-frequency and direct aging data. Can. J. Fish. Aquat. Sci.

Fabens, A.J. 1965. Properties and fitting of the von Bertalanffy growth curve. Growth **29**: 265-289.

Francis, R.I.C.C. 1988. Maximum likelihood estimation of growth and growth variability from tagging data. N.Z. J. of Mar. Freshwater Res. **22**: 42-51.

Farley, J.H., Davis, T.L.O, and Eveson, J.P. 2001. Length at age distribution of southern bluefin tuna in the Indonesian longline catch on the spawning ground. CCSBT-SC/0108/12.

Gunn, J.S., Polacheck, T., Davis, T.L.O., Klaer, N., Cowling, A., Farley, J.H., Caton, A., Williams, K., Hearn, W.S., Preece, A., and Clear, N.P. 1998. Fishery indicators for the SBT stock: An update of 12 indicators first used in 1988 plus additional indicators from the 1990's. CCSBT-SC/98/40.

Hearn, W.S. and Polacheck, T. 2003. Estimating long-term growth-rate changes of southern bluefin tuna (*Thunnus maccoyii*) from two periods of tag-return data. Fish. Bull. **101**: 58-74.

Hearn, W.S. and Polacheck, T.W. 1993. Estimating age-at-length relations for the 1960's and 1980/90's. SBFWS/93/4.

Itoh, T. and Tsuji, S. 1996. Age and growth of juvenile southern bluefin tuna *Thunnus maccoyii* based on otolith microstructure. Fisheries Science **62**: 892-896.

Kalish, J.M., Johnston, J.M., Gunn, J.S., and Clear, N.P. 1996. Use of bomb radiocarbon chronometer to determine age of southern bluefin tuna (*Thunnus maccoyii*). Mar. Ecol. Prog. Ser. **143**: 1-8.

Kolody, D. and Polacheck, T.W. 2001. Application of a statistical catch-at-age and length integrated analysis model for the assessment of southern bluefin tuna stock dynamics. 1951-2000. CCSBT-SC/0108/13.

Laslett, G.M., Eveson, J.P., and Polacheck, T.W. 2002. A flexible maximum likelihood approach for fitting growth curves to tag-recapture data. Can. J. Fish. Aquat. Sci. **59**: 976-986.

Leigh, G.M. and Hearn, W.S. 2000. Changes in growth of juvenile southern bluefin tuna (*Thunnus maccoyii*): An analysis of length-frequency data from the Australian fishery. Mar. Freshwater Res. **51**: 143-154.

Maller, R.A. and deBoer, E.S. 1988. An analysis of two methods of fitting the von Bertalanffy curve to capture-recapture data. Aust. J. Freshwater Res. **39**: 459-466.

Polacheck, T.W., Preece, A., Klaer, N., and Betlehem, A. 1999. Treatment of data and model uncertainties in the assessment of southern bluefin tuna stocks. In: F. Funk, T.J. Quinn II, J. Heifetz, J.N. Ianelli, J.E. Powers, J.F. Schweigert, P.J. Sullivan, and C.-I. Zhang (eds.) Fishery stock assessment models. University of Alaska Sea Grant, AK-SG-98-01.

Polacheck, T.W. and Preece, A. 2001. An integrated statistical time series assessment of the southern bluefin tuna stock based on catch at age data. CCSBT-SC/0108/13.

Preece, A., Polacheck, T.W., Kolody, D., Eveson, J.P., Ricard, D., Jumppanen, P., Farley, J.H., and Davis, T.L.O. 2001. Summary of the primary data inputs to CSIRO's 2001 stock assessment models. CCSBT-SC/0108/21.

Rees, A.J., Gunn, J.S., and Clear N.P. 1996. Age determination of juvenile southern bluefin tuna, *Thunnus maccoyii*, based on scanning electron microscopy of otolith microincrements. CCSBT/SC/96/8 (Appendix). Second Meeting of the Commission for the Conservation of Southern Bluefin Tuna (CCSBT), 26 Aug-5 Sep 1996, CSIRO Marine Laboratories, Hobart, Tasmania. 122 pp.

Table 1: Summary of data used in estimation of decadal growth curves.

	Otolith Readings		Tag-Recapture Data		Length-Frequency Data		
Decade	No. born in decade	Age range[a]	Release years[b]	No. recaptures	Sampled years	Mean no. length samples per year (sd)[c]	No. estimated modes
1960's	277	22-38	1961-66	791	1965-1969	24 019 (6 937)	119
1970's	1298	12-30	1973-74,1977-78	202	1970-1979	21 788 (8 903)	288
1980's	668	1-21	1983-84	2181	1980-1989	17 865 (10 875)	269
1990's	281	1-6	1991-95	2980	-	-	-

[a] All otoliths were collected in the 1990's so fish born in progressively earlier decades were progressively older by the time of catch.

[b] Years with at least 5% of the total releases for that decade.

[c] Length samples were taken using a two-stage procedure; the sample sizes shown are estimates of the equivalent sample size had a simple random sample been taken (refer to Leigh and Hearn 2000 for details).

Table 2: Parameter estimates for the VB log k model with a seasonal growth component based on the integrated best fit to the data from each decade.

Decade	μ_∞	σ_∞	k_1	k_2	α	β	a_0	u	w	$\mu_{\log A}$	$\sigma_{\log A}$	σ_s	σ_f	σ_γ	σ_ε
1960's	187.8	7.0	0.14	0.15	5.5	30.0*	-1.6	0.53	-0.07	1.2	0.16	2.4	3.1	5.9	2.0
1970's	184.3	7.9	0.15	0.19	5.7	30.0*	-1.3	0.92	0.06	0.8	0.12	2.1	4.7	0.0*	3.5
1980's	184.7	8.1	0.22	0.17	2.8	18.3	-0.4	0.34	0.13	0.6	0.17	2.1	4.2	4.6	4.3
1990's	184.9	8.7	0.25	0.16	2.5	12.4	-0.3	0.41	0.26	0.7	0.32	1.8	4.9	5.6	–

* Estimate is equal to the upper or lower bound set for this parameter.

Table 3: Comparison of the negative log-likelihood values when a single growth curve is fitted to the pooled data from two consecutive decades compared to when individual growth curves are fitted to data from each decade separately.

	Negative Log-Likelihood		Number of Additional	Difference in
Decades Compared	Separate	Combined	Parameters	Log-Likelihood
1960's & 1970's	12973.8	13319.5	15	345.7
1970's &1980's	24169.0	24560.8	15	391.7
1980's & 1990's	40482.6	41272.9	14	790.3

Table 4: Comparison of the negative log-likelihood values when μ_∞ is estimated separately for each decade (values in Table 2) versus when a common μ_∞ is estimated across all decades (in which case the best fit estimate of μ_∞ is 185.6 cm)

Decade	Separate μ_∞	Common μ_∞
1960's	6411.9	6417.3
1970's	6561.9	6564.1
1980's	17607.1	17607.6
1990's	22875.4	22875.5
Sub-total 70's-90's	47044.5	47047.2
Total	53456.3	53464.5

Table 5: Comparison of the negative log-likelihood values when μ_∞ is estimated separately for the 1960's and 1970's and when a common value is estimated for the two decades. (The estimated common value for μ_∞ is 186 cm.)

Decade	Separate μ_∞	Common μ_∞
1960's	6411.9	6415.5
1970's	6561.9	6565.6
Total	12973.8	12981.1

Table 6: Mean length and standard error (SE) for fish over 25 years of age based on direct age estimates from otolith readings. (Note that sufficient time has not elapsed for otoliths of this age to exist in the 1980's and 1990's.)

Decade	N	Mean Length	SE
1960's	263	186.0	0.53
1970's	225	184.0	0.57

Table 7: Parameter estimates for the VB log k model with a seasonal growth component based on the integrated best fit to the data for each decade, but with a common μ_∞ value for all decades.

Decade	μ_∞	σ_∞	k_1	k_2	α	β	u	w	$\mu_{\log A}$	$\sigma_{\log A}$	σ_s	σ_f	a_0	σ_γ	σ_ε
1960's	185.6	6.59	0.14	0.16	5.59	30.00	0.54	-0.07	1.19	0.16	2.41	3.09	-1.56	6.60	2.01
1970's	185.6	7.98	0.15	0.17	5.66	30.00	0.91	0.06	0.77	0.12	1.97	4.74	-1.28	0.00	3.54
1980's	185.6	8.12	0.22	0.17	2.86	15.75	0.34	0.13	0.58	0.17	2.08	4.20	-0.43	4.56	4.29
1990's	185.6	8.71	0.25	0.16	2.46	12.40	0.41	0.26	0.72	0.31	1.81	4.85	-0.31	5.58	-

Table 8: Comparison of the differences in the negative log-likelihood values for the best fit to the standard VB model and the VB log k model.

Decade	VB	VB log k	Number of additional parameters	Difference in log-likelihood
1960's	6414.9	6411.9	3	3.0
1970's	6575.3	6561.9	3	13.4
1980's	17708.7	17607.1	3	101.6
1990's	23040.9	2275.4	3	65.5

Table 9: Parameter estimates for the standard VB model with a seasonal growth component based on the integrated best fit to the 1960's data.

Decade	μ_∞	σ_∞	k_1	u	w	$\mu_{\log A}$	$\sigma_{\log A}$	σ_s	σ_f	a_0	σ_γ	σ_ε
1960's	188.8	7.86	0.14	0.49	-0.06	1.18	0.16	2.35	3.01	-1.53	4.75	1.99

Table 7: Estimates of the coefficient of variation (100*SE/mean) for the best fit to the VB log k model for each decade. Also shown are the estimated coefficients of variation for the best fit to the VB model for the 1960's data (in which case k_1 denotes the single growth rate parameter k). A dash indicates that the parameter needed to be treated as fixed.

	VB log k				VB
	1960's	1970's	1980's	1990's	1960's
μ_∞	0.3	0.3	0.4	0.3	0.3
σ_∞	3.6	3.2	3.3	-	3.8
k_1	1.2	1.6	1.6	0.9	1.1
k_2	4.0	5.3	2.4	1.2	n/a
α	4.5	3.4	4.2	2.0	n/a
β	-	-	-	-	n/a
a_0	2.7	4.0	6.6	-	2.5
u	16.5	13.9	12.1	15.3	17.2
w	30.7	30.8	12.2	19.3	35.7
$\mu_{\log A}$	1.1	2.4	2.6	1.3	1.0
$\sigma_{\log A}$	3.1	8.0	1.8	1.5	3.1
σ_s	4.9	35.0	6.0	5.7	5.4
σ_f	11.2	22.2	5.4	4.0	11.5
σ_γ	-	-	159.3	-	318.4
σ_ε	7.1	4.4	4.7	n/a	7.0

Figure 1. (*top*) The optimal integrated seasonal VB log *k* growth curve for each decade. (*bottom*) The same curves plotted relative to the 1960's curve for better comparison.

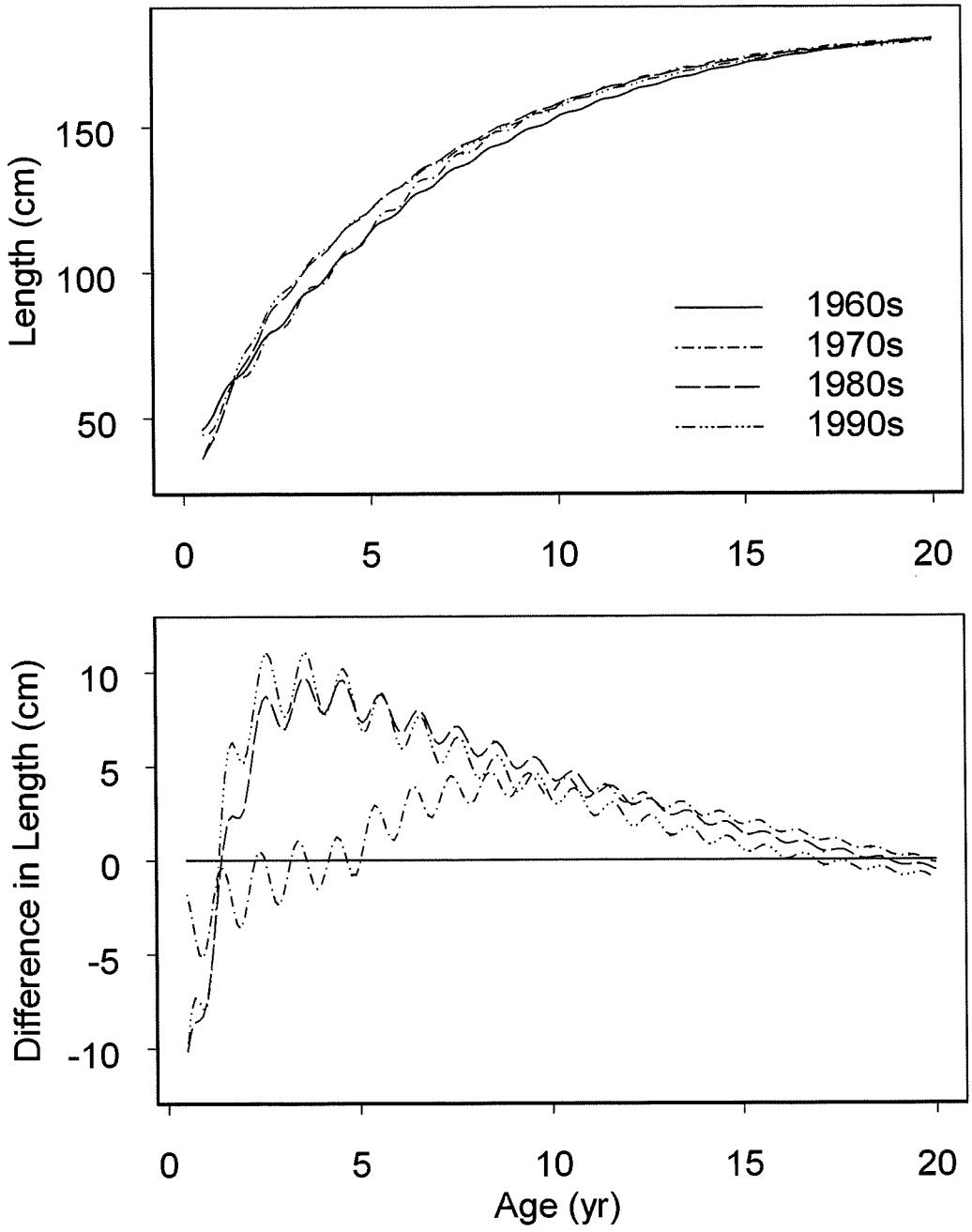

Figure 2. The optimal integrated seasonal VB log k growth curve for the 1990's decade plotted relative to the 1980's curve.

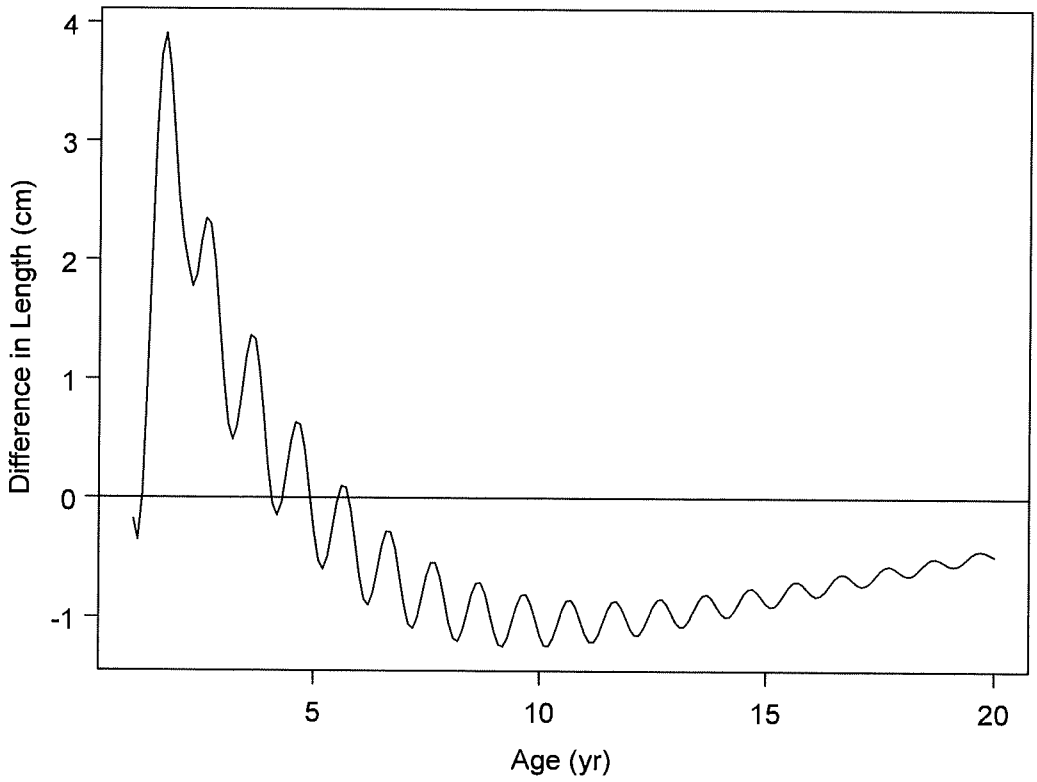

Figure 3. Change in the negative log-likelihood relative to its minimum value as a function of μ_∞.

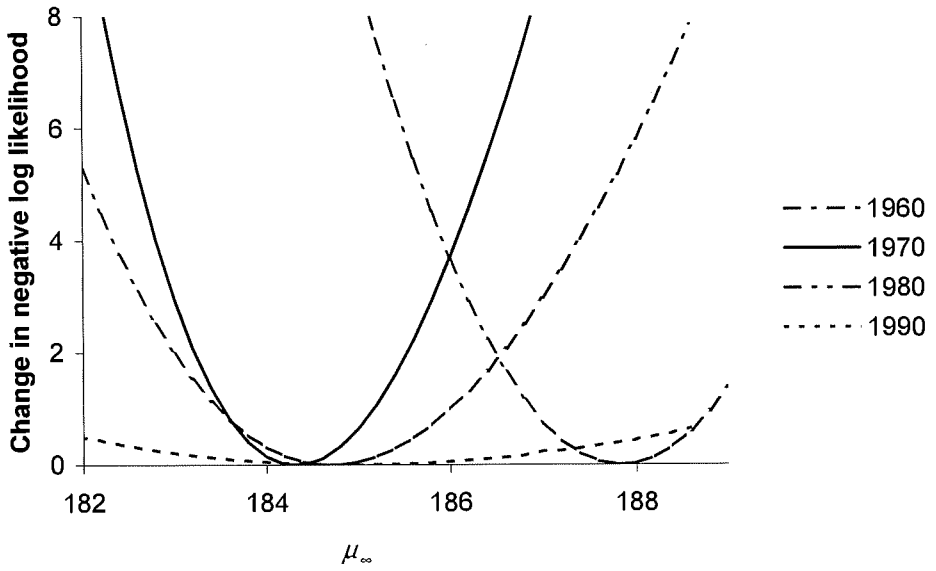

Figure 4. (*top*) Integrated seasonal VB log k growth curves for the 1960's with μ_∞ fixed at: 1) the optimal value for the 1960's data alone (187.8); 2) the optimal value when μ_∞ is constrained to be the same in all decades (185.6); 3) the optimal value when μ_∞ is constrained to be the same in the 1970's, 1980's, and 1990's (184.4). (*bottom*) The same curves plotted relative to the optimal 1960's curve (with μ_∞ = 187.8) for better comparison.

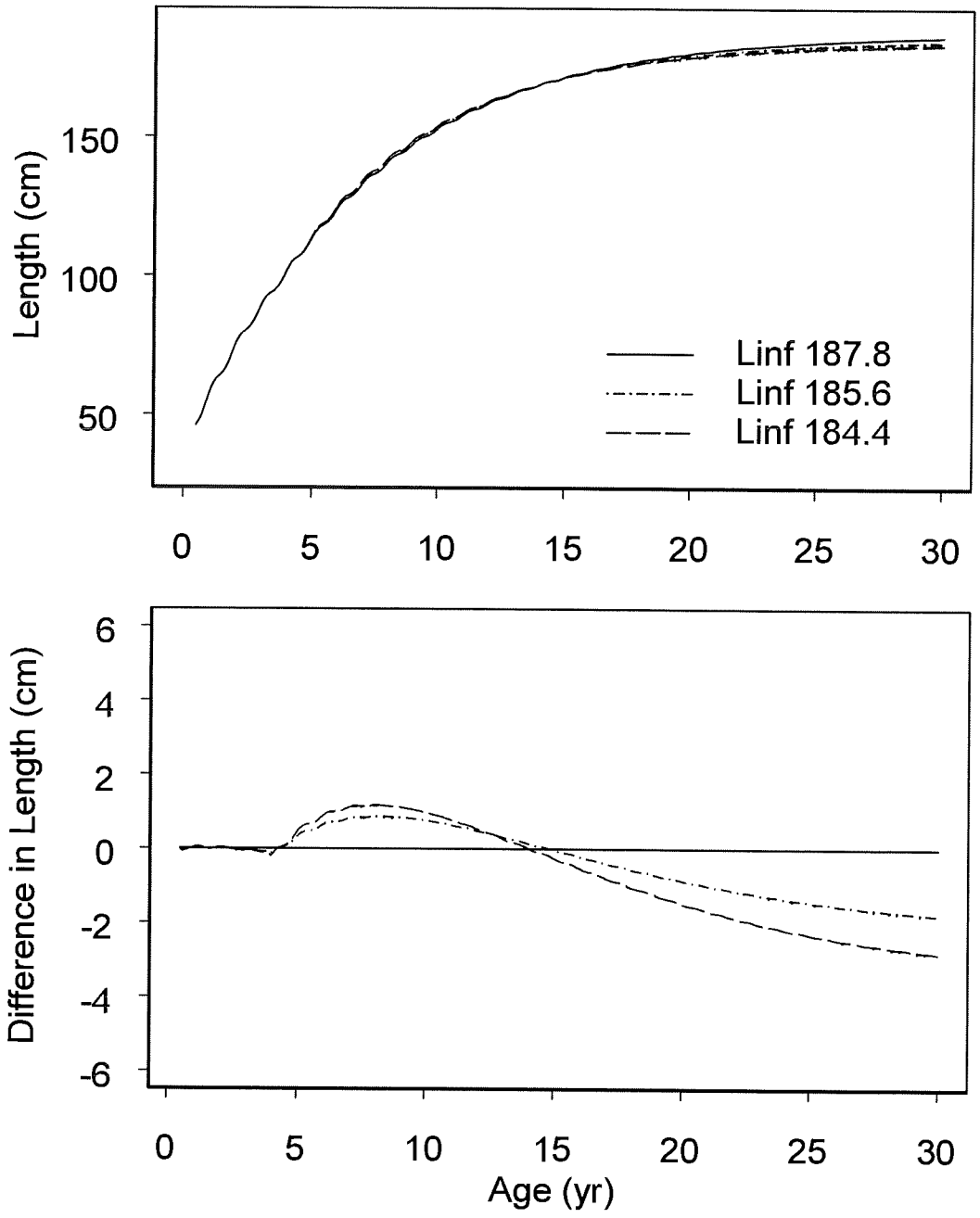

Figure 5. The residual (observed minus fitted) for the length-frequency data as a function of year for the best fit to the VB log k model for each decade.

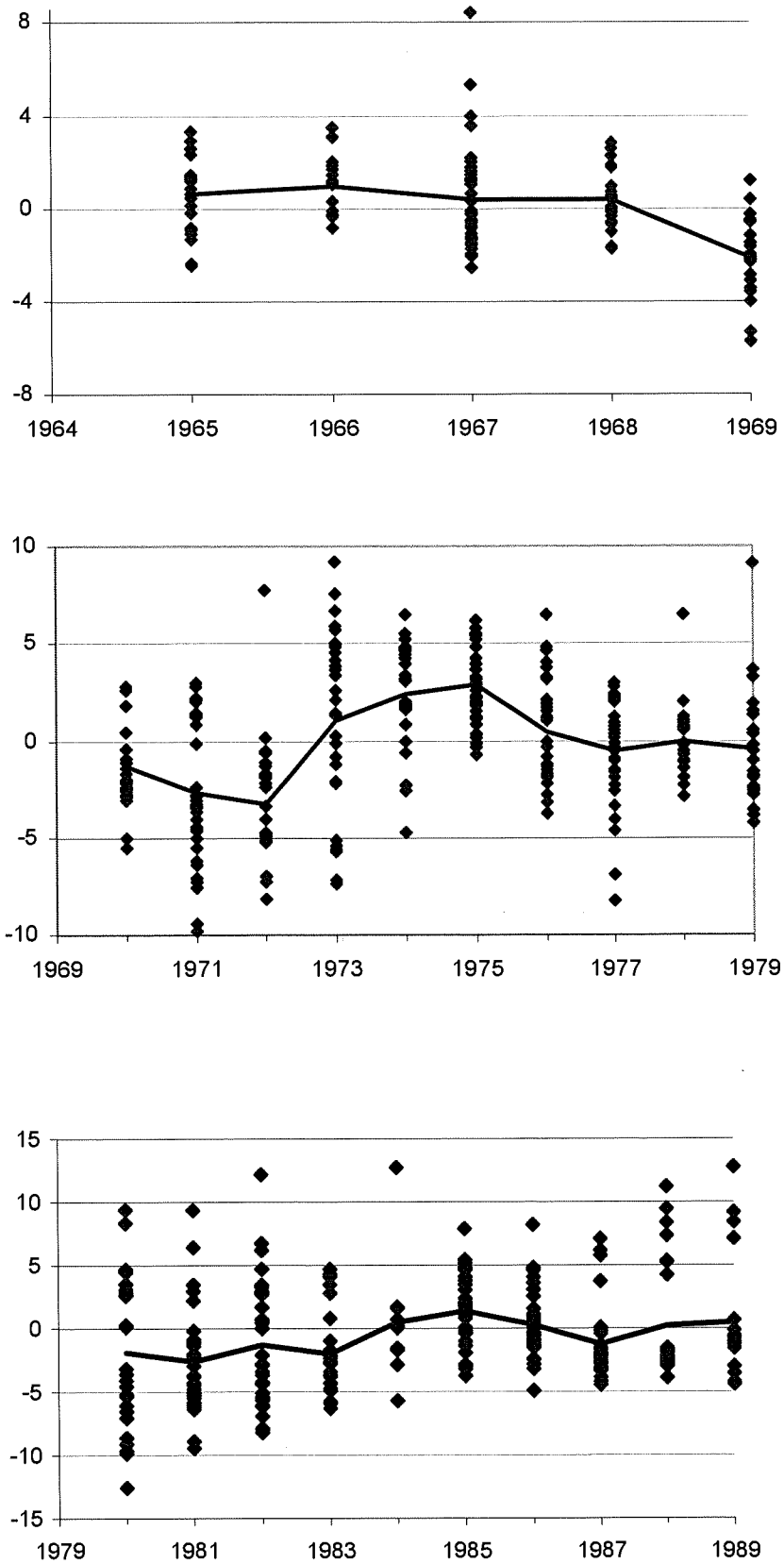

Figure 6. The residual (observed minus fitted) for the length-frequency data as a function of cohort for the best fit to the VB log k model for each decade.

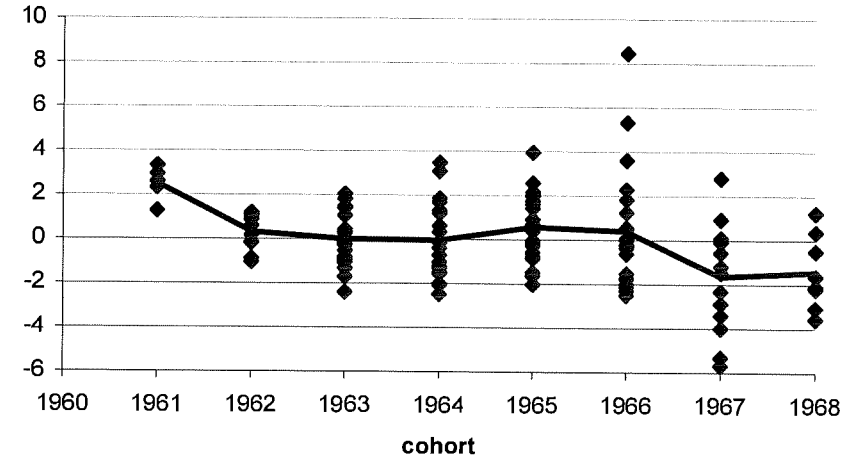

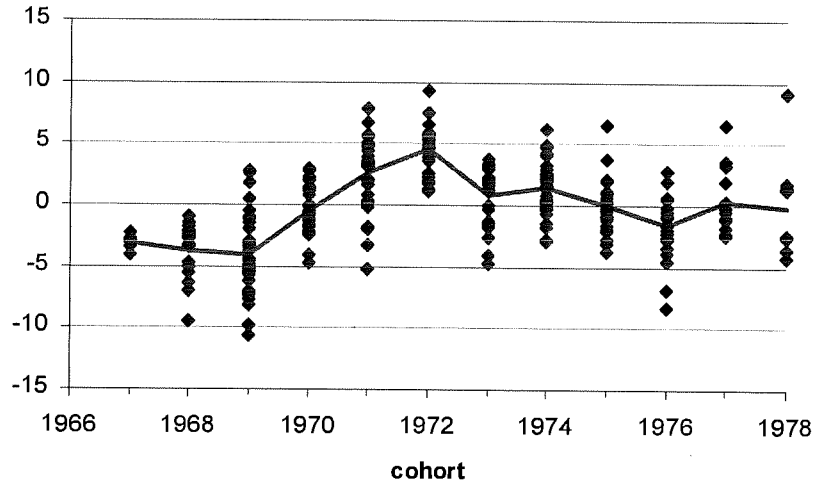

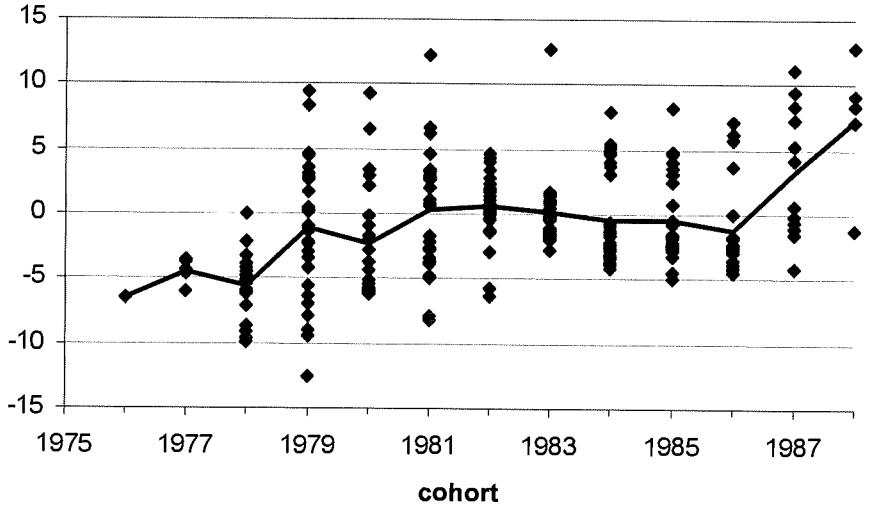

Figure 7. The proportion of the catch by spawning season by Japanese longliners from the SBT spawning ground (Statistical Area 1) estimated to be over 184 cm. (See Caton, 1991, for definitions of the statistical areas.)

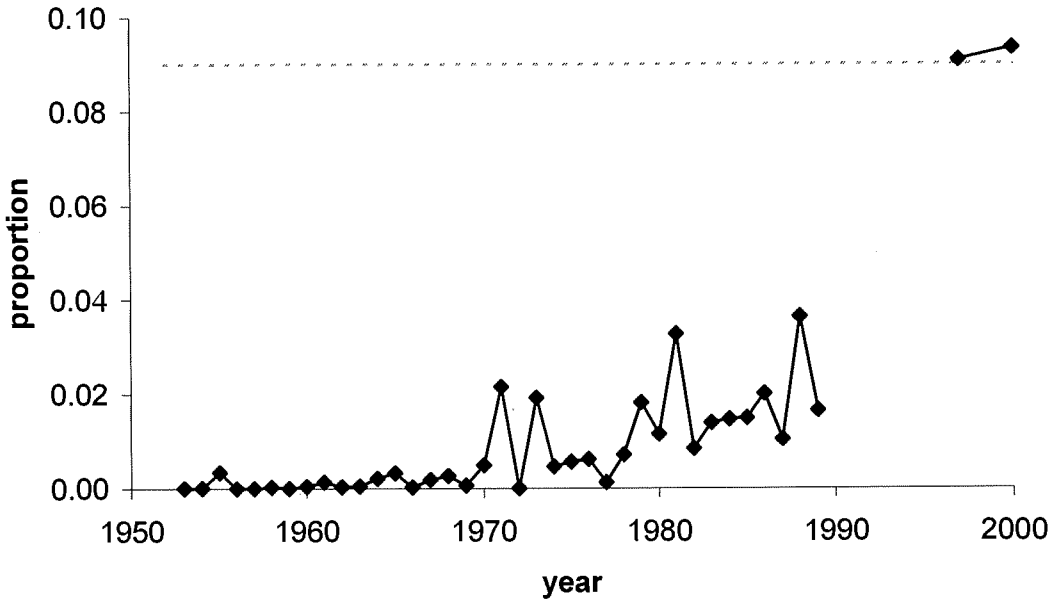

Figure 8. The proportion of the annual catch by Japanese longliners from the SBT feeding grounds (Statistical Areas 4–9) estimated to be over 184 cm. The lower dotted line is for the proportion of the total catch and the upper solid line is the proportion of the catch for fish larger than 130 cm. (See Caton, 1991, for definitions of the statistical areas.)

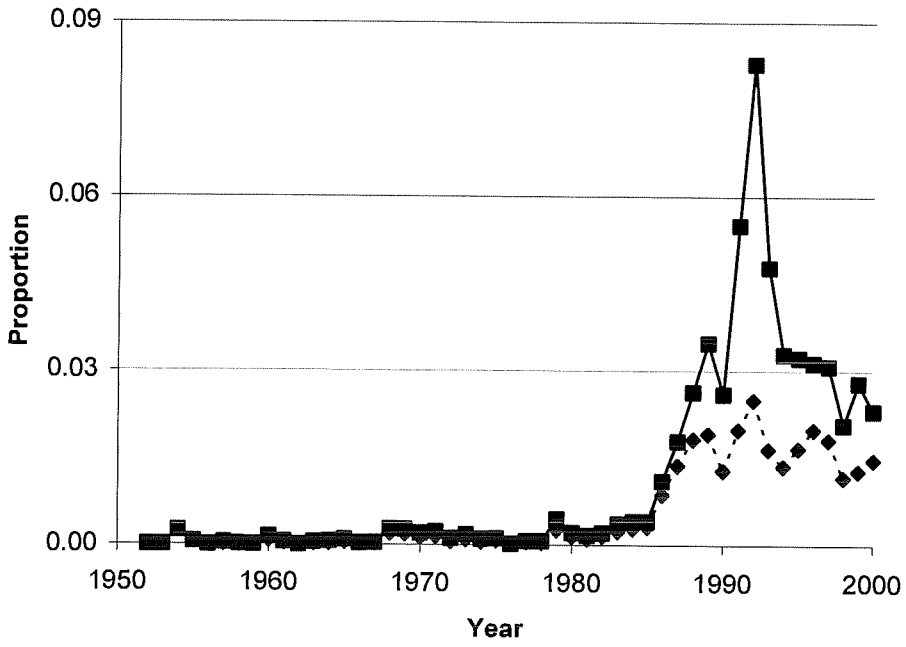

Figure 9. The cumulative proportion of the catch by spawning season by Japanese longliners from the SBT spawning ground (Statistical Area 1) estimated to be over a given length. (See Caton, 1991, for definitions of the statistical areas.)

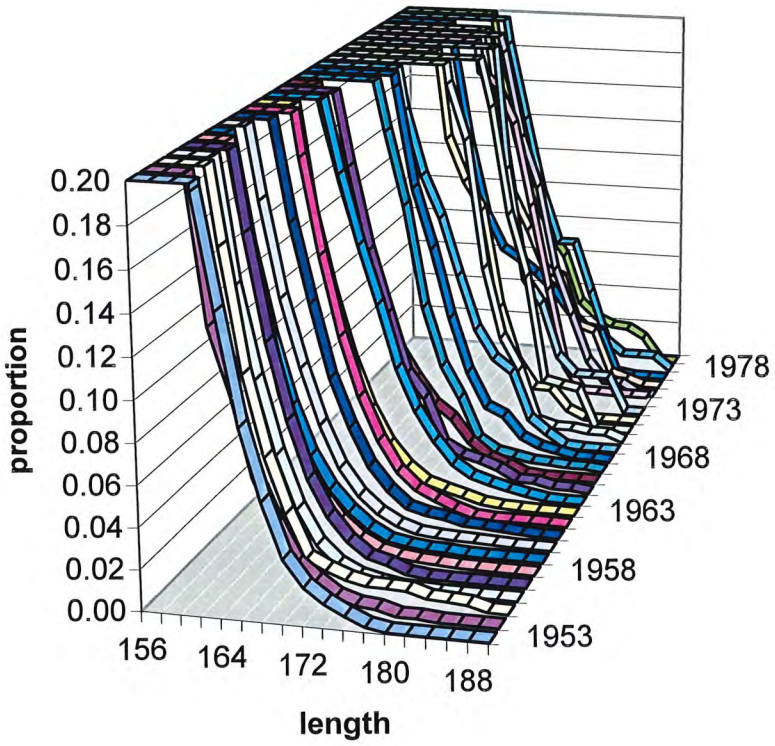

ANNEX 1: Residual Plots of the Best Fit to the VB log *k* Model for Each Decade

Figure 1a. Diagnostic plots for the optimal integrated seasonal VB log *k* model fitted to the 1960's growth data. Panel (i) shows the 1960's direct aging data along with the mean fitted curve. Panel (ii) shows the corresponding residuals (observed – fitted). A local linear smooth has been put through the residuals to reveal any patterns.

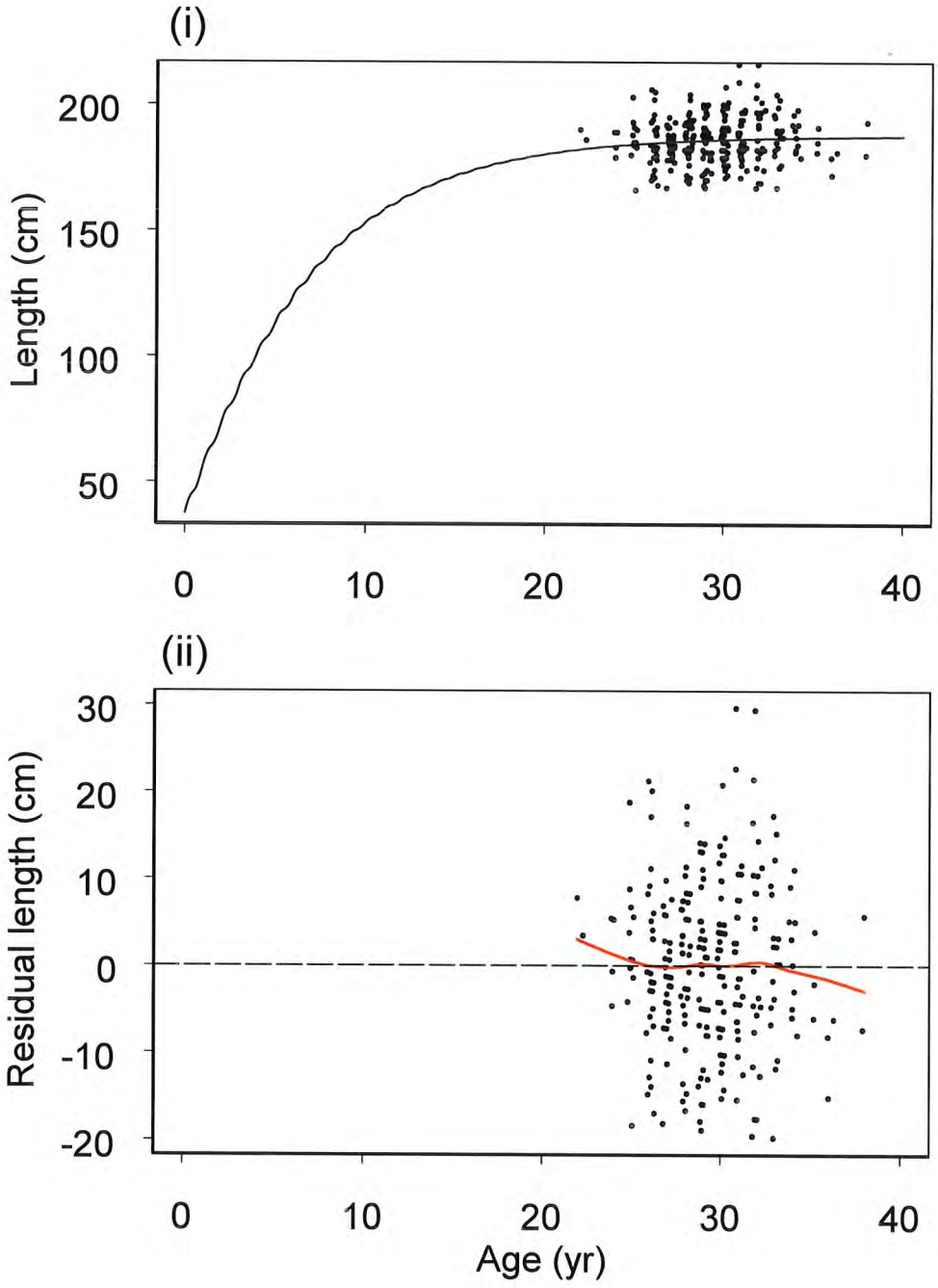

Figure 1b. Diagnostic plots for the optimal integrated seasonal VB log k model fitted to the 1960's growth data. Panel (i) shows the summary modes and ages obtained from the 1960's length-frequency data along with the mean fitted curve. Panel (ii) shows the corresponding residuals (observed – fitted). A local linear smooth has been put through the residuals to reveal any patterns.

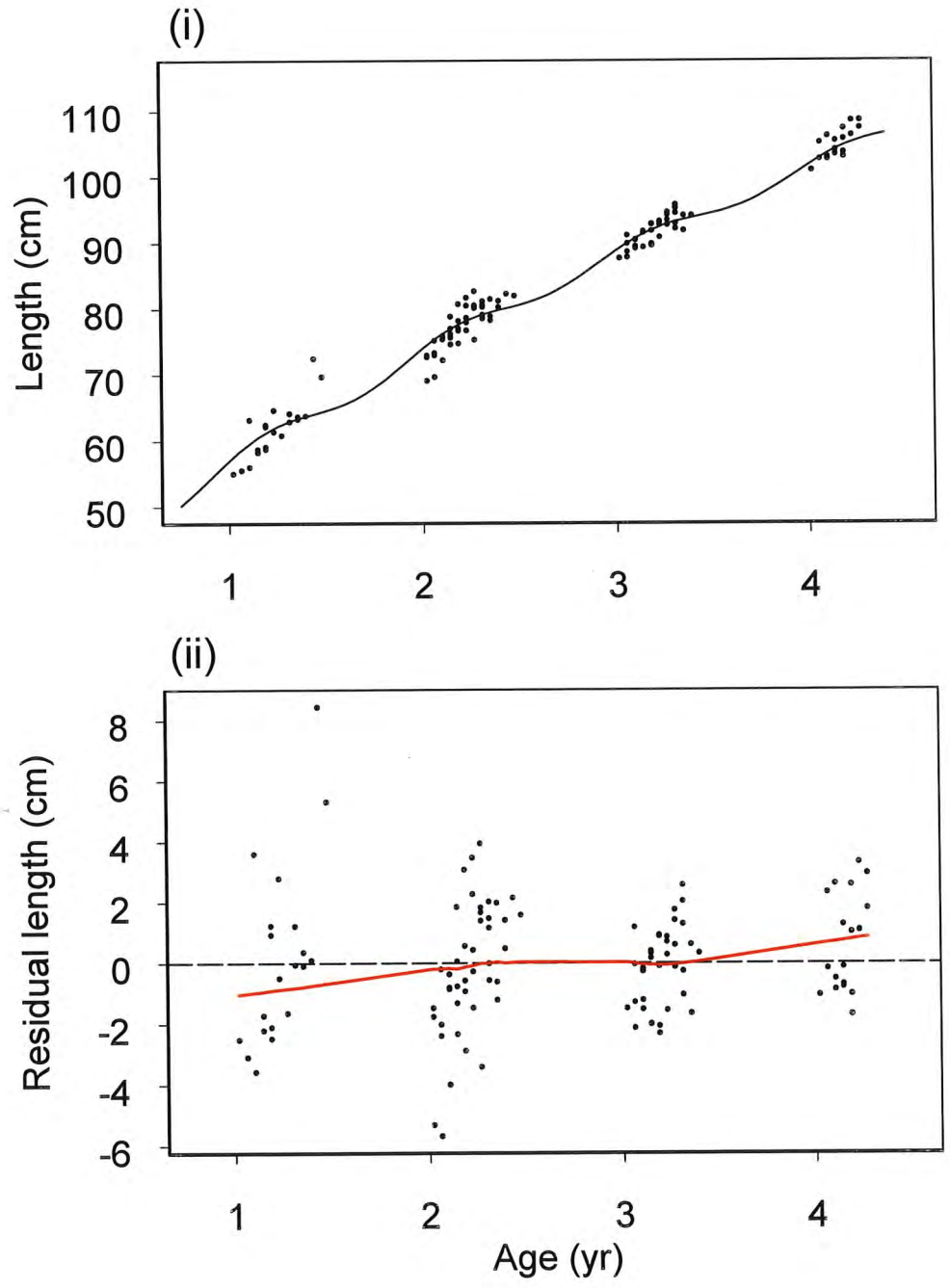

Figure 1c. Diagnostic plots for the optimal integrated seasonal VB log k model fitted to the 1960's growth data. Panel (i) shows the residual release lengths for the 1960's tag-recapture data plotted against the estimated ages at release relative to a_0 (i.e. $\tilde{A}_f$, as described in Appendix 5). Panel (ii) shows the residual recapture lengths plotted against the estimated ages of recapture relative to a_0 (i.e. $\tilde{A}_f + t_2 - t_1$). A local linear smooth has been put through the residuals to reveal any patterns.

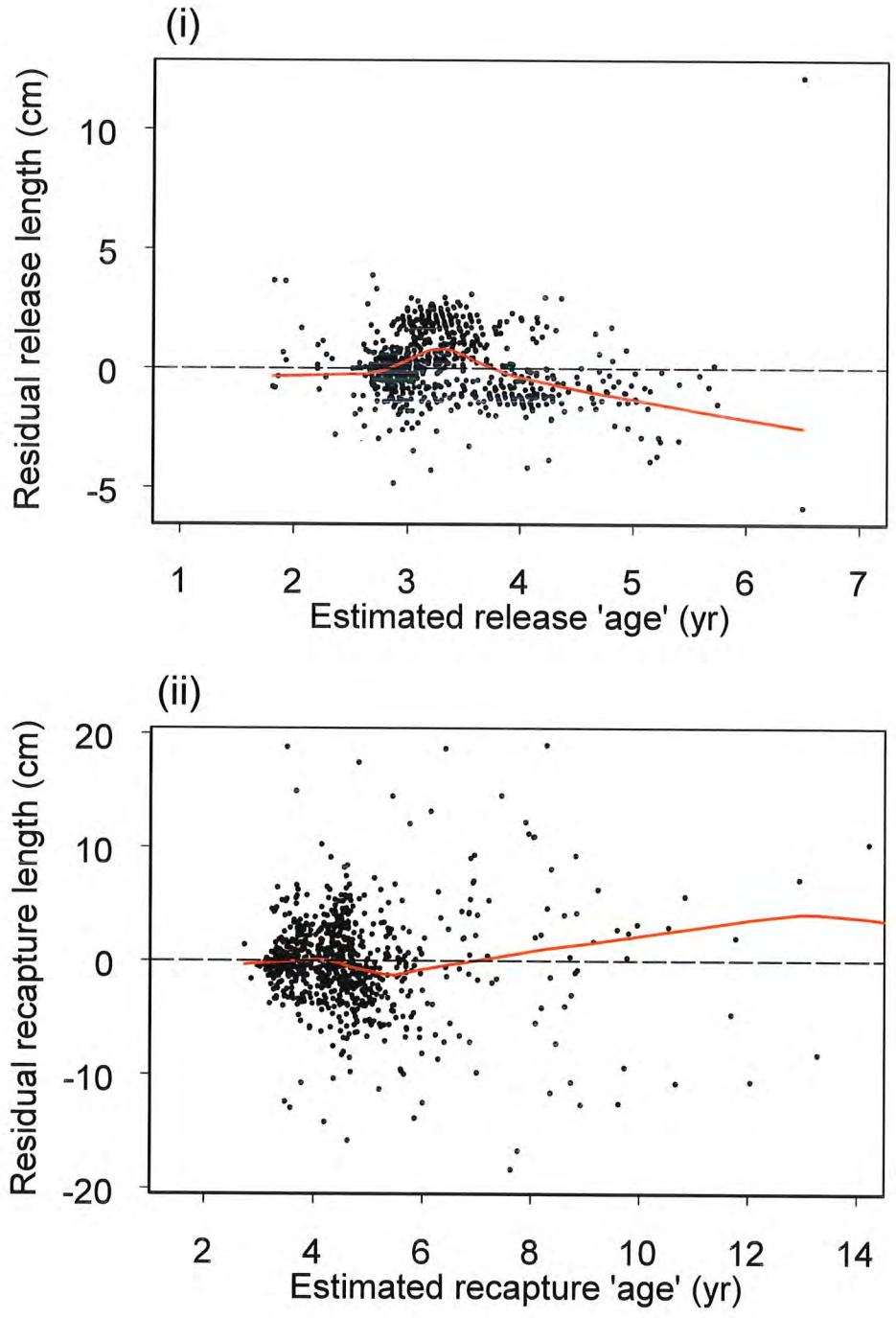

Figure 2a. Diagnostic plots for the optimal integrated seasonal VB log *k* model fitted to the 1970's growth data. Panel (i) shows the 1970's direct aging data along with the mean fitted curve. Panel (ii) shows the corresponding residuals (observed – fitted). A local linear smooth has been put through the residuals to reveal any patterns.

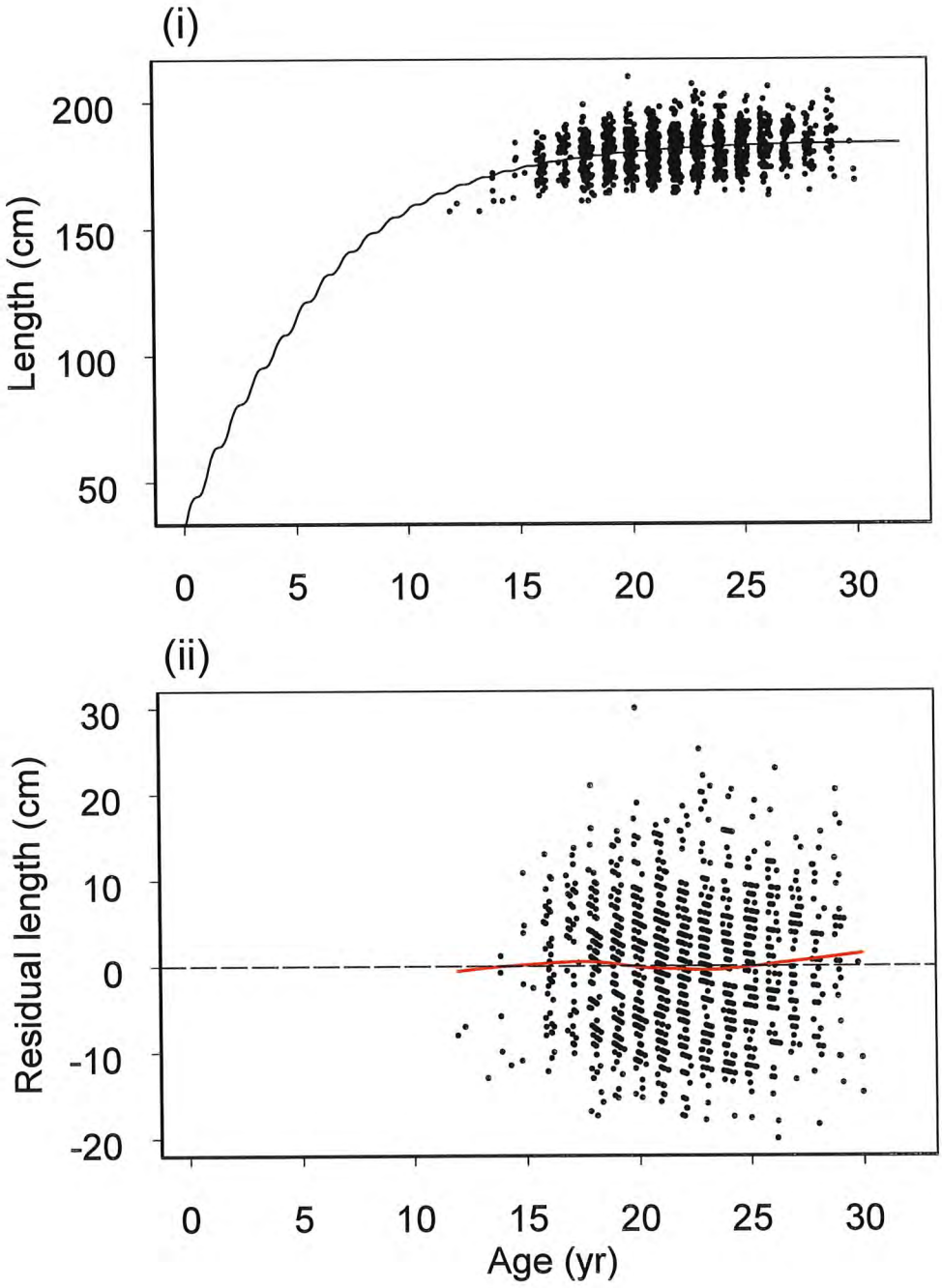

Figure 2b. Diagnostic plots for the optimal integrated seasonal VB log k model fitted to the 1970's growth data. Panel (i) shows the summary modes and ages obtained from the 1970's length-frequency data along with the best fitting curve. Panel (ii) shows the corresponding residuals (observed – fitted). A local linear smooth has been put through the residuals to reveal any patterns.

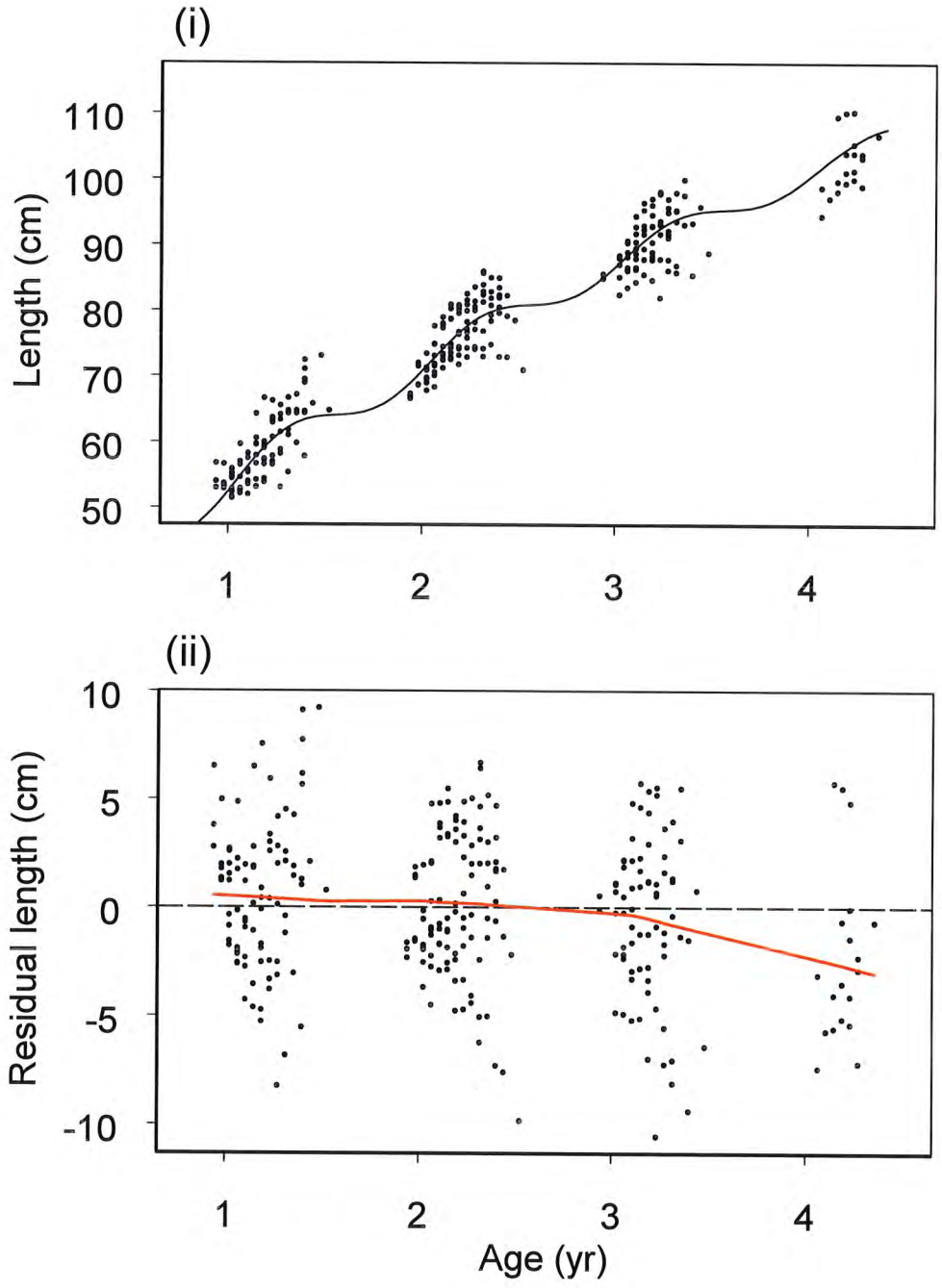

Figure 2c. Diagnostic plots for the optimal integrated seasonal VB log k model fitted to the 1970's growth data. Panel (i) shows the residual release lengths for the 1970's tag-recapture data plotted against the estimated ages at release relative to a_0 (i.e. $\tilde{A}_f$, as described in Appendix 5). Panel (ii) shows the residual recapture lengths plotted against the estimated ages of recapture relative to a_0 (i.e. $\tilde{A}_f + t_2 - t_1$). A local linear smooth has been put through the residuals to reveal any patterns.

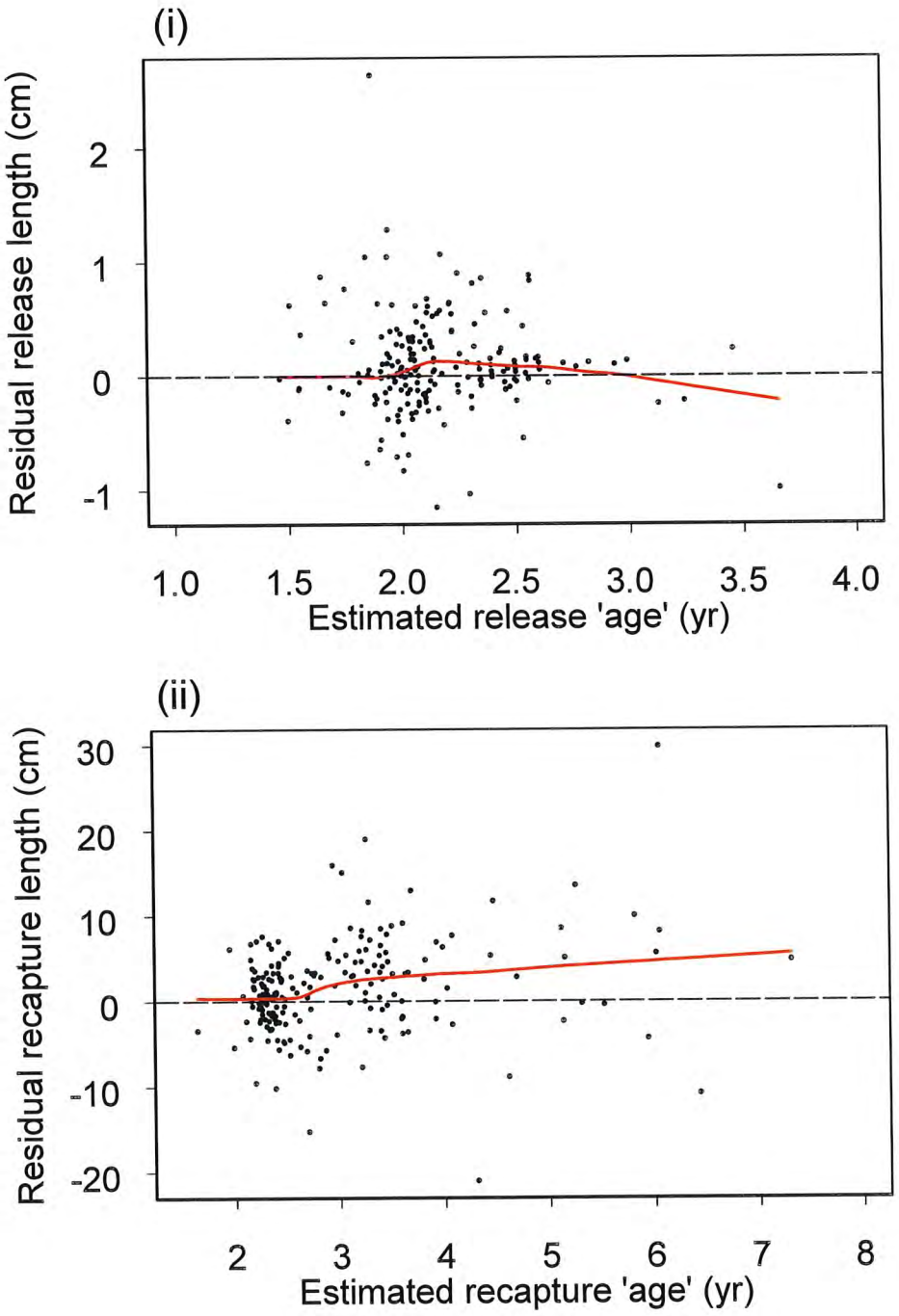

Figure 3a. Diagnostic plots for the optimal integrated seasonal VB log k model fitted to the 1980's growth data. Panel (i) shows the 1980's direct aging data along with the mean fitted curve. Panel (ii) shows the corresponding residuals (observed – fitted). A local linear smooth has been put through the residuals to reveal any patterns.

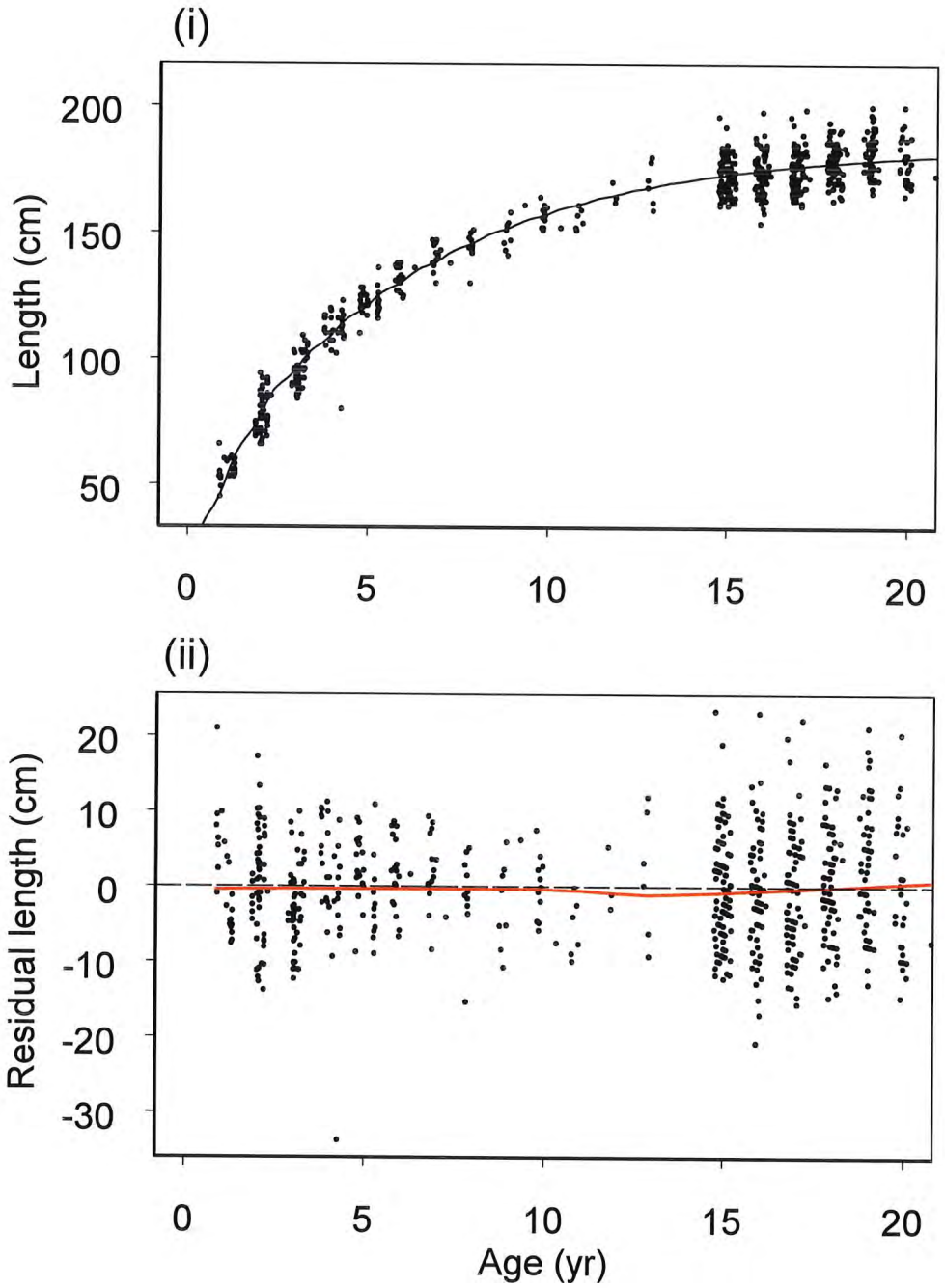

Figure 3b. Diagnostic plots for the optimal integrated seasonal VB log k model fitted to the 1980's growth data. Panel (i) shows the summary modes and ages obtained from the 1980's length-frequency data along with the best fitting curve. Panel (ii) shows the corresponding residuals (observed – fitted). A local linear smooth has been put through the residuals to reveal any patterns.

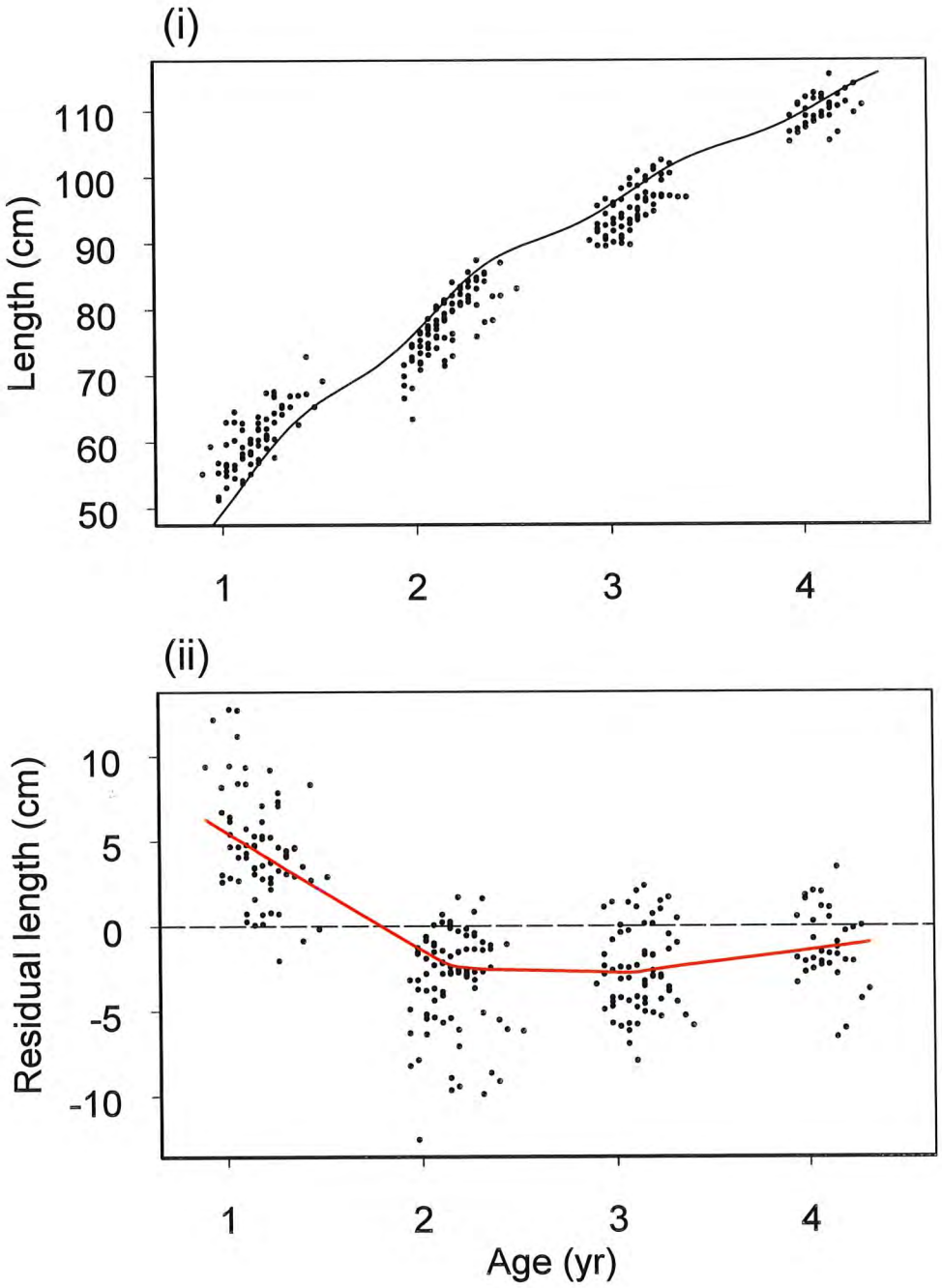

Figure 3c. Diagnostic plots for the optimal integrated seasonal VB log k model fitted to the 1980's growth data. Panel (i) shows the residual release lengths for the 1980's tag-recapture data plotted against the estimated ages at release relative to a_0 (i.e. $\tilde{A}_f$, as described in Appendix 5). Panel (ii) shows the residual recapture lengths plotted against the estimated ages of recapture relative to a_0 (i.e. $\tilde{A}_f + t_2 - t_1$). A local linear smooth has been put through the residuals to reveal any patterns.

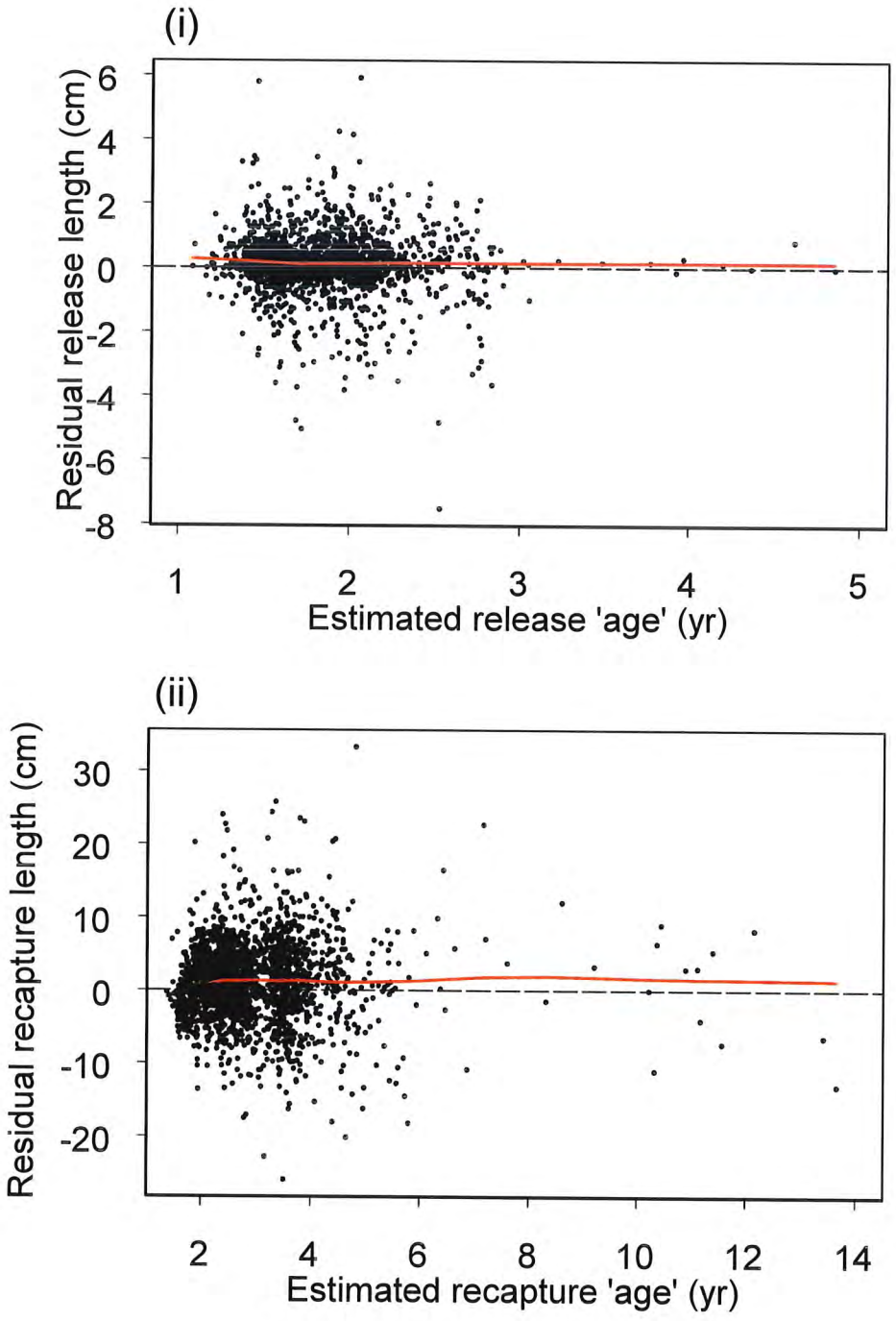

Figure 4a. Diagnostic plots for the optimal integrated seasonal VB log k model fitted to the 1990's growth data. Panel (i) shows the 1990's direct aging data along with the mean fitted curve. Panel (ii) shows the corresponding residuals (observed – fitted). A local linear smooth has been put through the residuals to reveal any patterns.

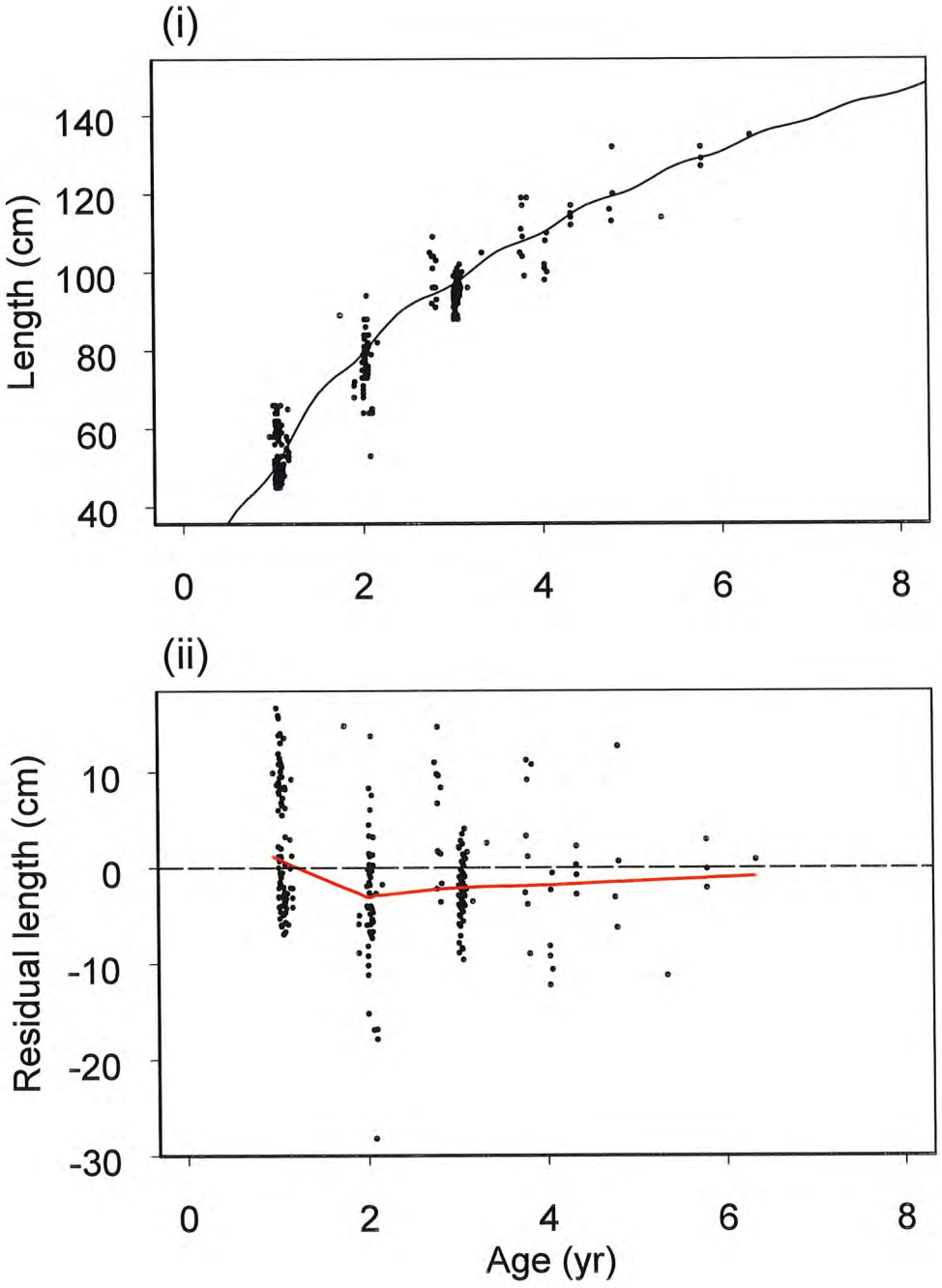

Figure 4b. Diagnostic plots for the optimal integrated seasonal VB log k model fitted to the 1990's growth data. Panel (i) shows the residual release lengths for the 1990's tag-recapture data plotted against the estimated ages at release relative to a_0 (i.e. $\tilde{A}_f$, as described in Appendix 5). Panel (ii) shows the residual recapture lengths plotted against the estimated ages of recapture relative to a_0 (i.e. $\tilde{A}_f + t_2 - t_1$). A local linear smooth has been put through the residuals to reveal any patterns.

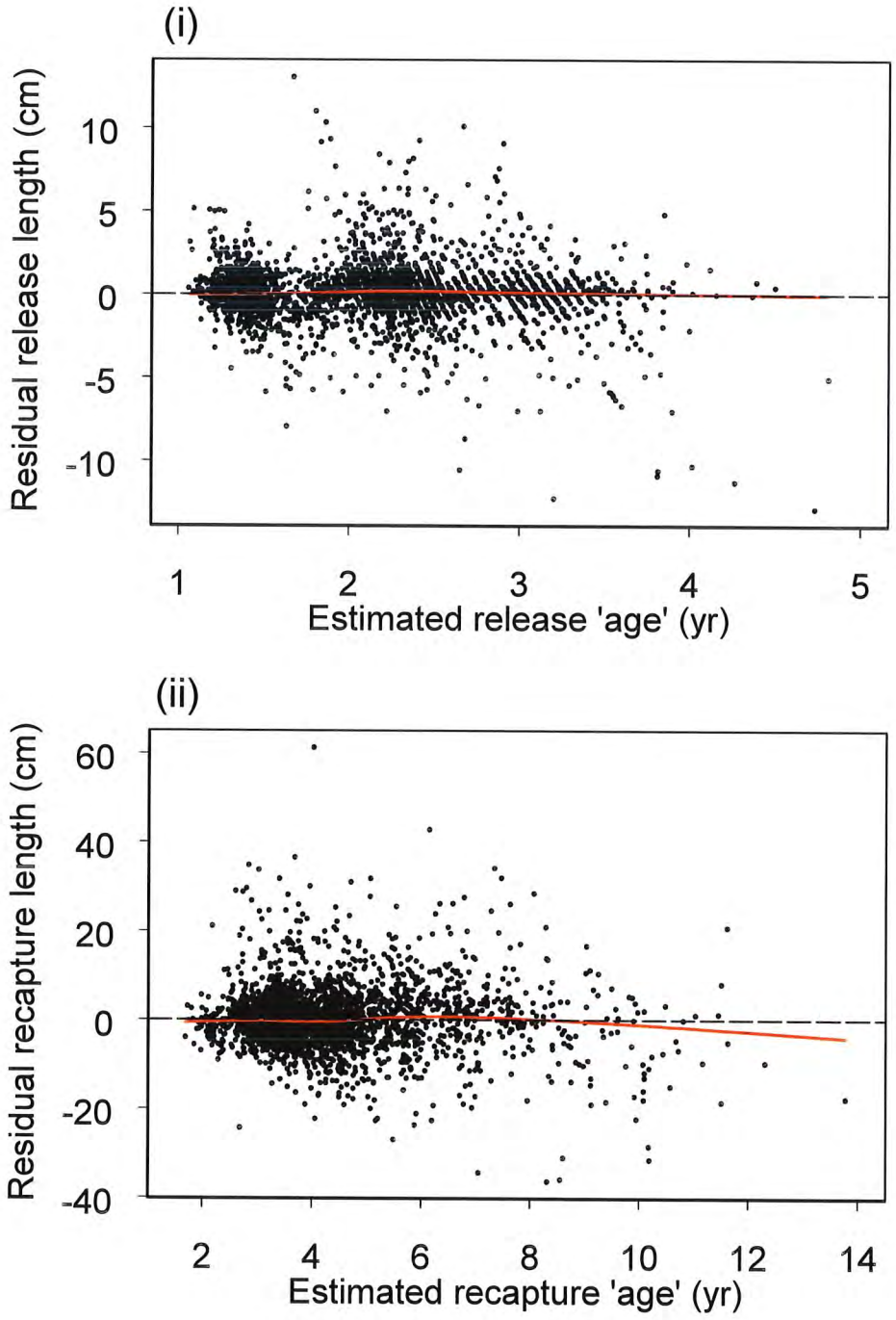

Figure 5a. Diagnostic plots for the integrated seasonal VB log k model fitted to the 1960's growth data with μ_∞ fixed at 184.4. Panel (i) shows the 1960's direct aging data along with the mean fitted curve. Panel (ii) shows the corresponding residuals (observed – fitted). A local linear smooth has been put through the residuals to reveal any patterns.

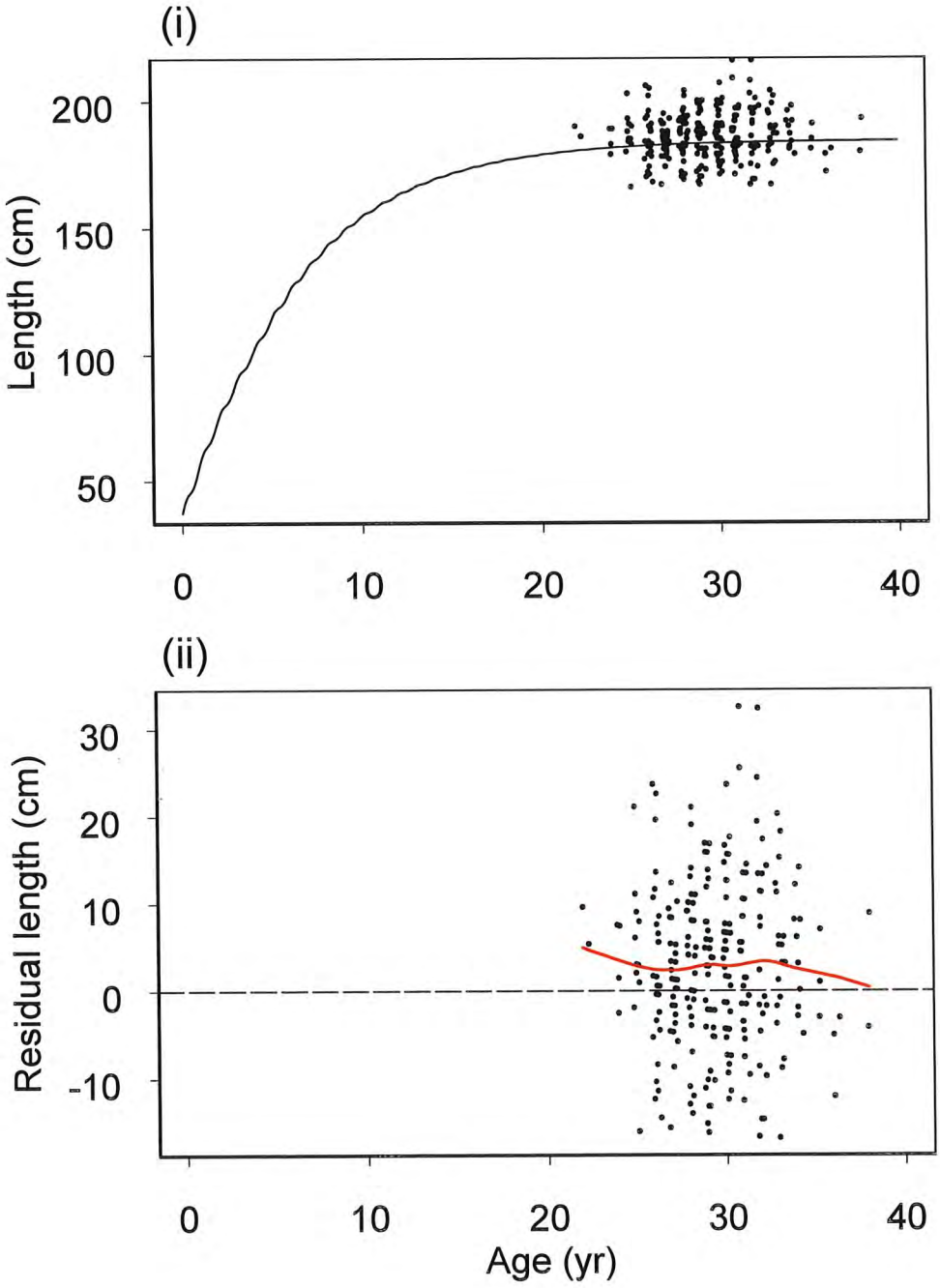

Figure 5b. Diagnostic plots for the integrated seasonal VB log k model fitted to the 1960's growth data with μ_∞ fixed at 184.4. Panel (i) shows the summary modes and ages obtained from the 1960's length-frequency data along with the mean fitted curve. Panel (ii) shows the corresponding residuals (observed – fitted). A local linear smooth has been put through the residuals to reveal any patterns.

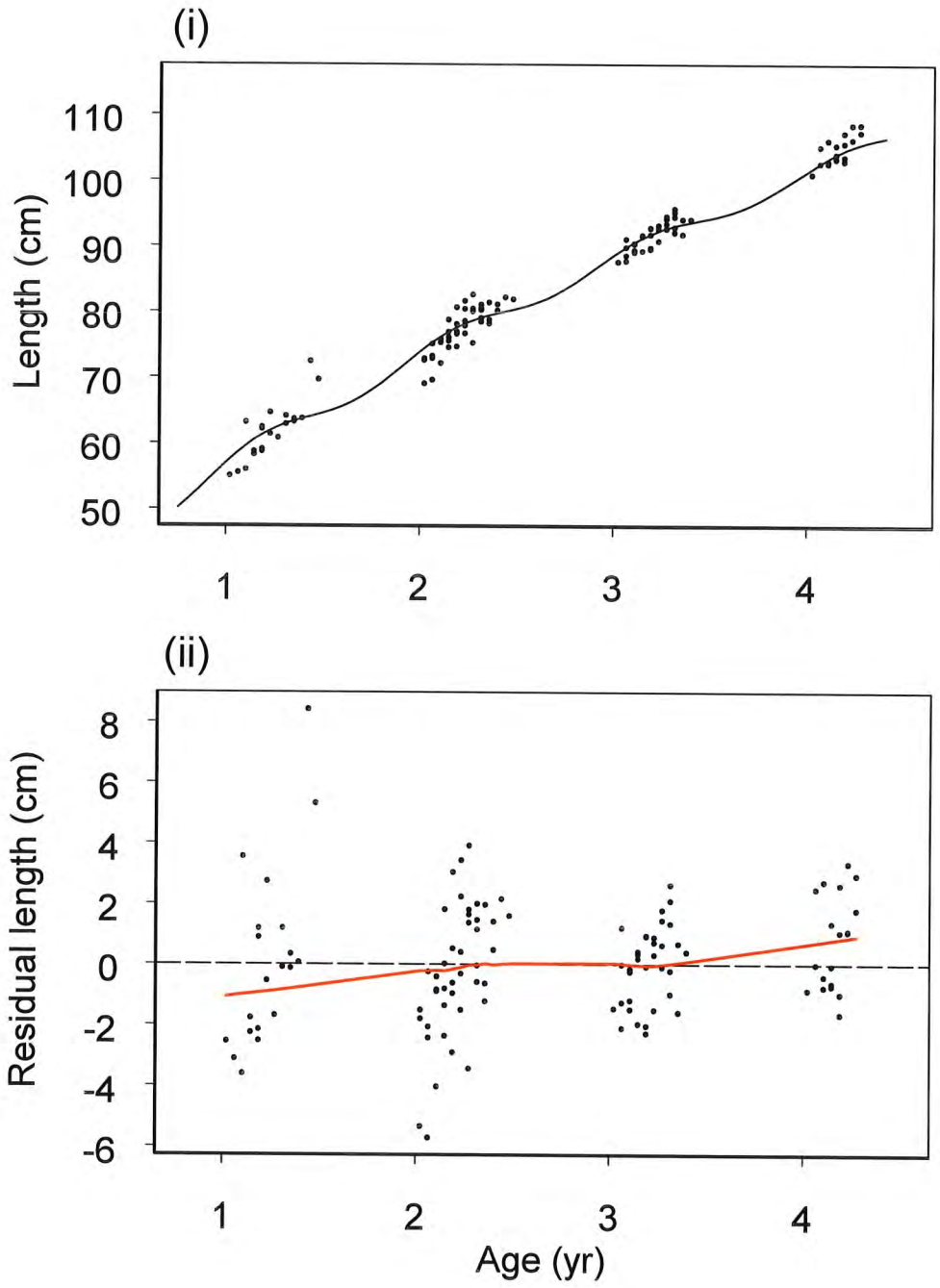

Figure 5c. Diagnostic plots for the integrated seasonal VB log k model fitted to the 1960's growth data with μ_∞ fixed at 184.4. Panel (i) shows the residual release lengths for the 1960's tag-recapture data plotted against the estimated ages at release relative to a_0 (i.e. $\tilde{A}_f$, as described in Appendix 5). Panel (ii) shows the residual recapture lengths plotted against the estimated ages of recapture relative to a_0 (i.e. $\tilde{A}_f + t_2 - t_1$). A local linear smooth has been put through the residuals to reveal any patterns.

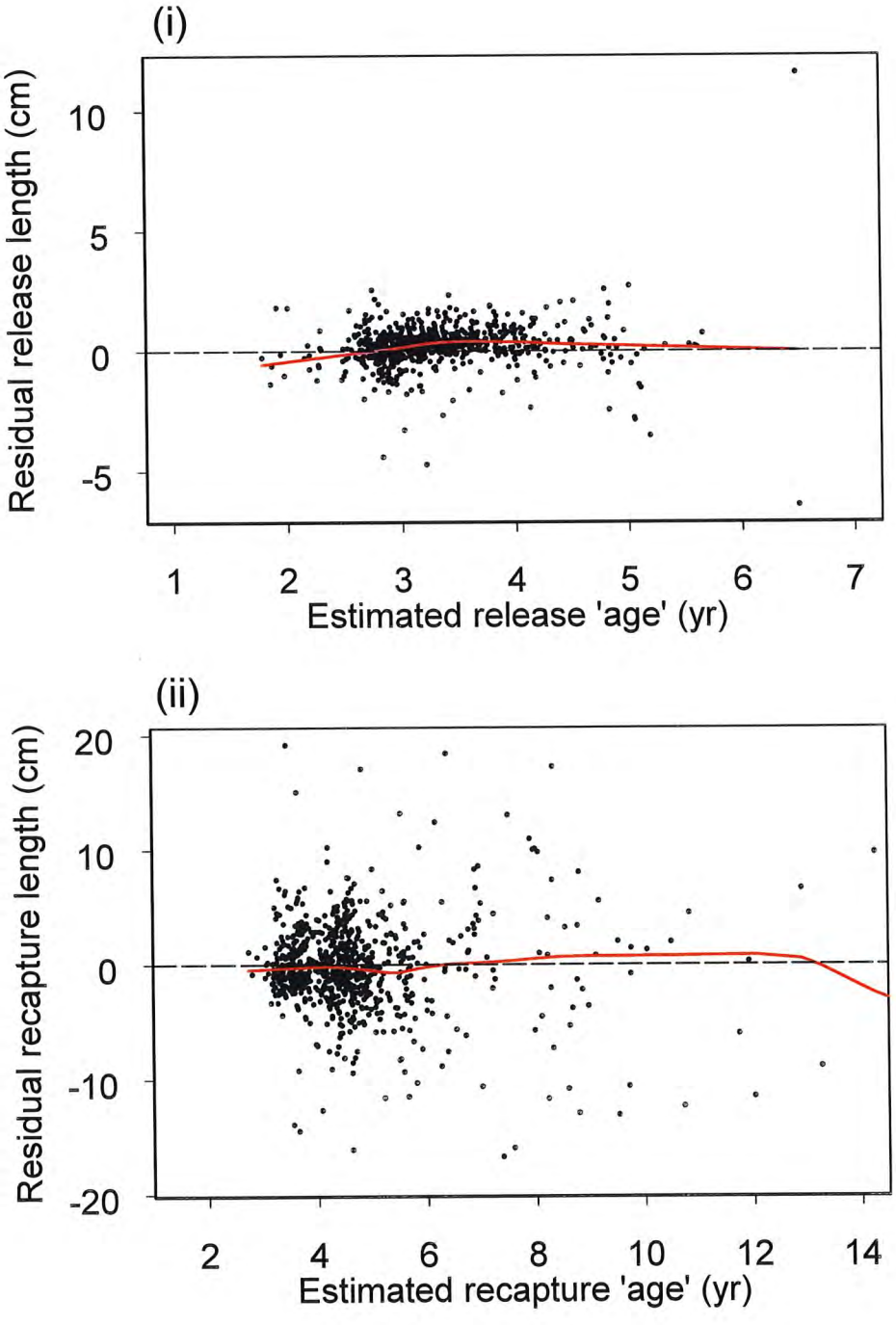

Figure 6a. Diagnostic plots for the integrated seasonal VB log k model fitted to the 1970's growth data with μ_∞ fixed at 187.8 (the optimal value for the 1960's). Panel (i) shows the 1970's direct aging data along with the mean fitted curve. Panel (ii) shows the corresponding residuals (observed – fitted). A local linear smooth has been put through the residuals to reveal any patterns.

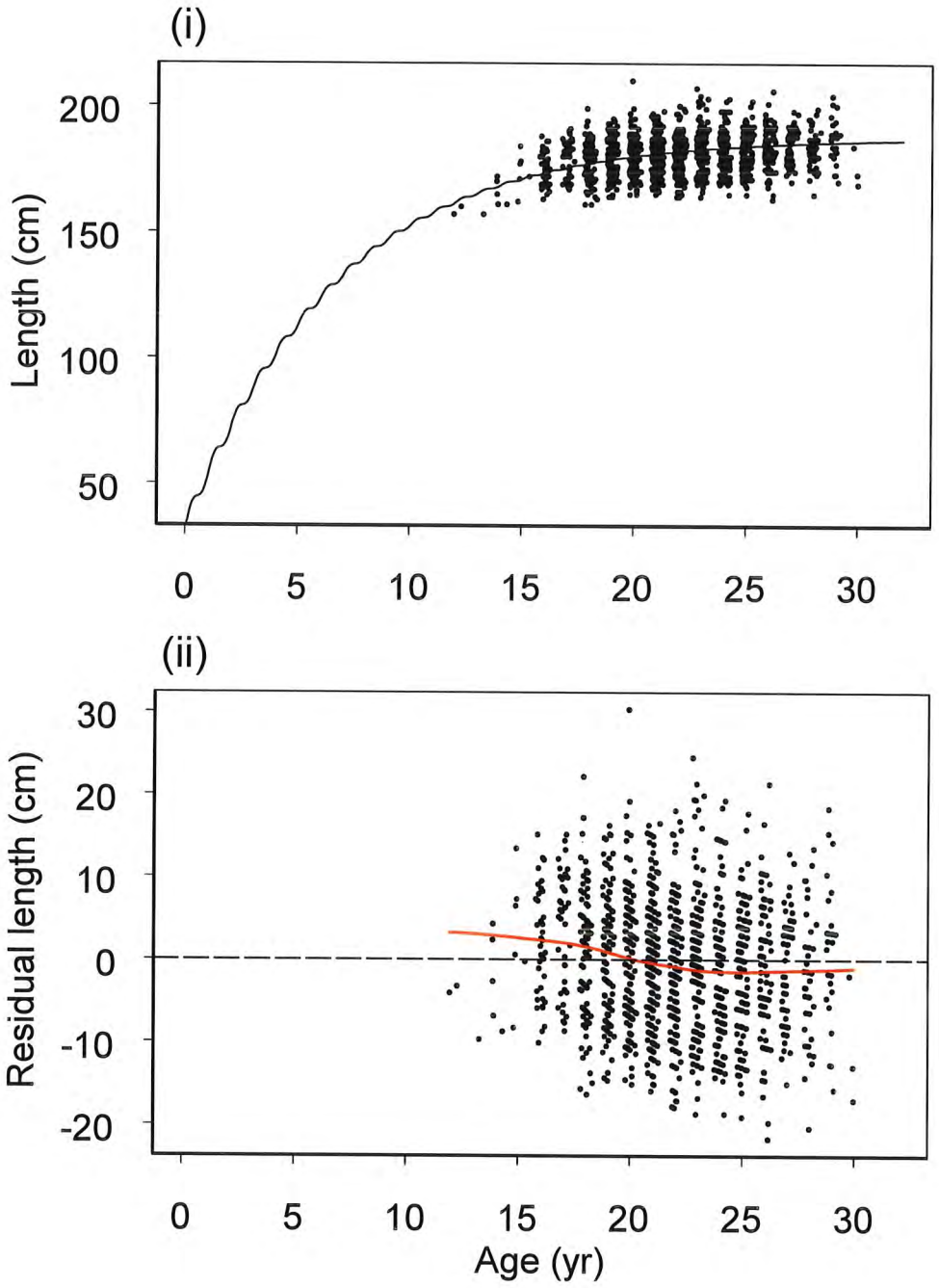

Figure 6b. Diagnostic plots for the integrated seasonal VB log k model fitted to the 1970's growth data with μ_∞ fixed at 187.8 (the optimal value for the 1960's). Panel (i) shows the summary modes and ages obtained from the 1970's length-frequency data along with the mean fitted curve. Panel (ii) shows the corresponding residuals (observed – fitted). A local linear smooth has been put through the residuals to reveal any patterns.

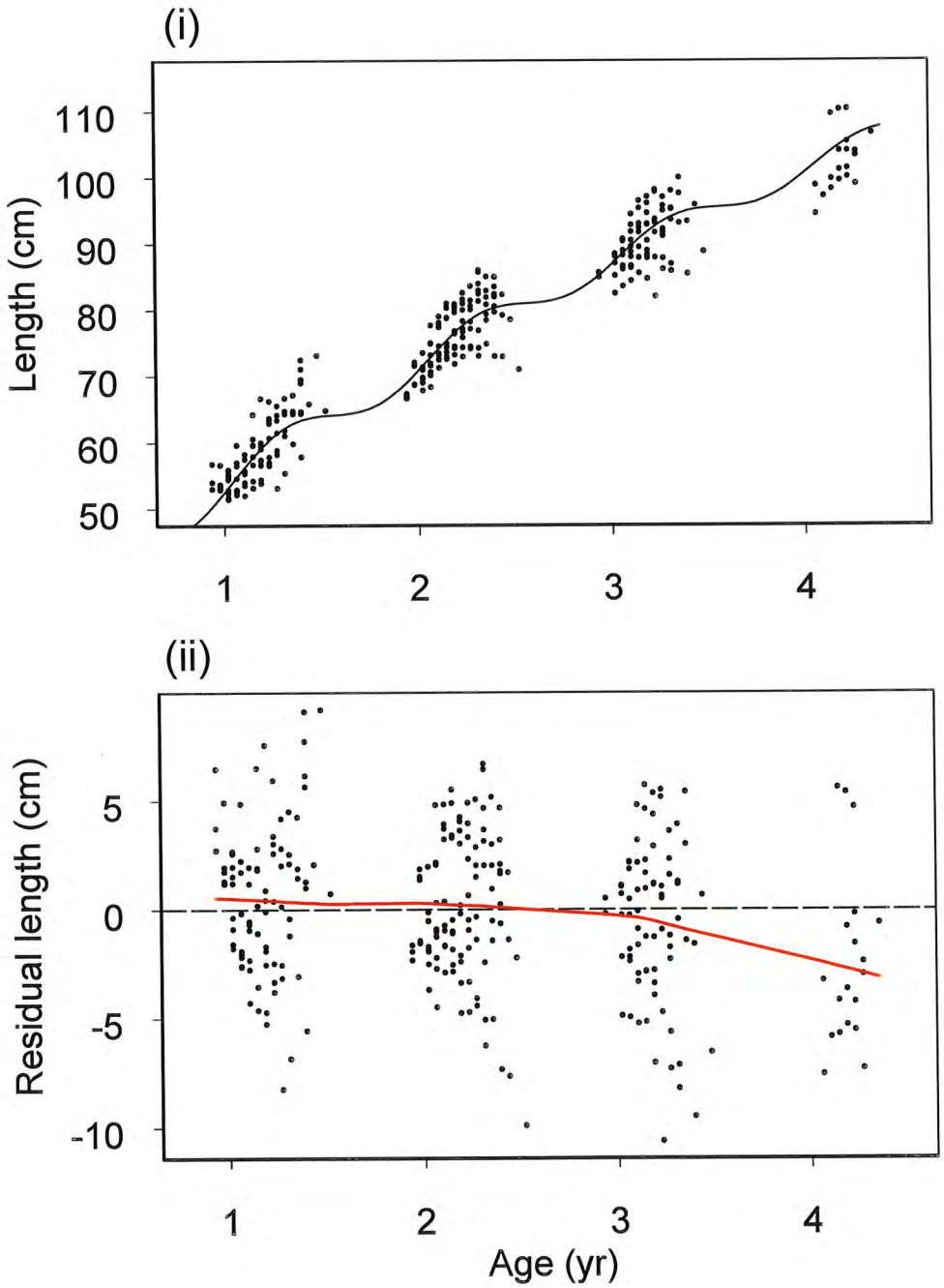

Figure 6c. Diagnostic plots for the integrated seasonal VB log k model fitted to the 1970's growth data with μ_∞ fixed at 187.8 (the optimal value for the 1960's). Panel (i) shows the residual release lengths for the 1970's tag-recapture data plotted against the estimated ages at release relative to a_0 (i.e. $\tilde{A}_f$, as described in Appendix 5). Panel (ii) shows the residual recapture lengths plotted against the estimated ages of recapture relative to a_0 (i.e. $\tilde{A}_f + t_2 - t_1$). A local linear smooth has been put through the residuals to reveal any patterns.

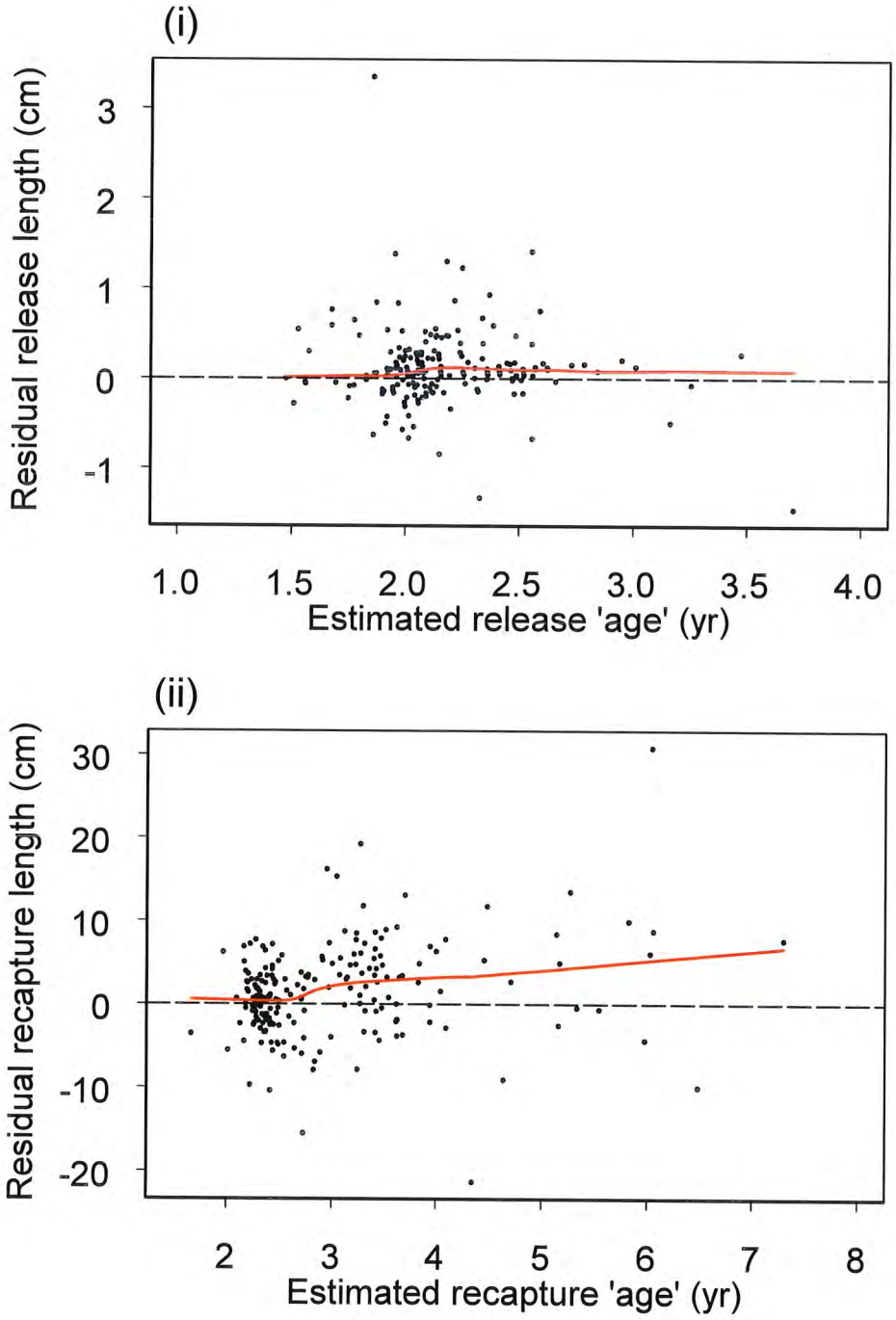

ANNEX 2: Residual Plots of the Best Fit to the Standard VB Model for the Data from the 1960's

Figure 1a. Diagnostic plots for the optimal integrated seasonal VB model fitted to the 1960's growth data. Panel (i) shows the 1960's direct aging data along with the mean fitted curve. Panel (ii) shows the corresponding residuals (observed – fitted). A local linear smooth has been put through the residuals to reveal any patterns.

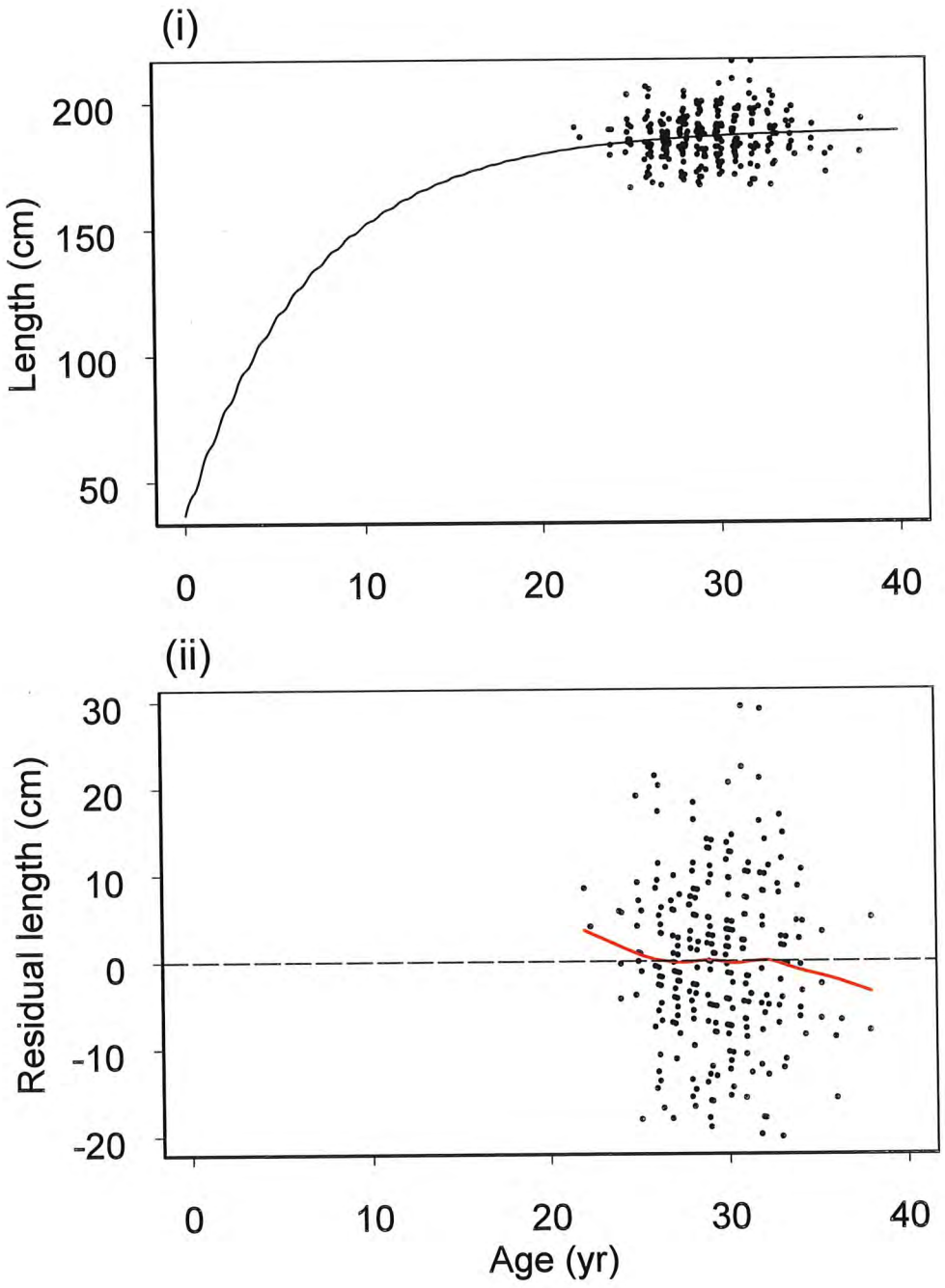

Figure 1b. Diagnostic plots for the optimal integrated seasonal VB model fitted to the 1960's growth data. Panel (i) shows the summary modes and ages obtained from the 1960's length-frequency data along with the mean fitted curve. Panel (ii) shows the corresponding residuals (observed – fitted). A local linear smooth has been put through the residuals to reveal any patterns.

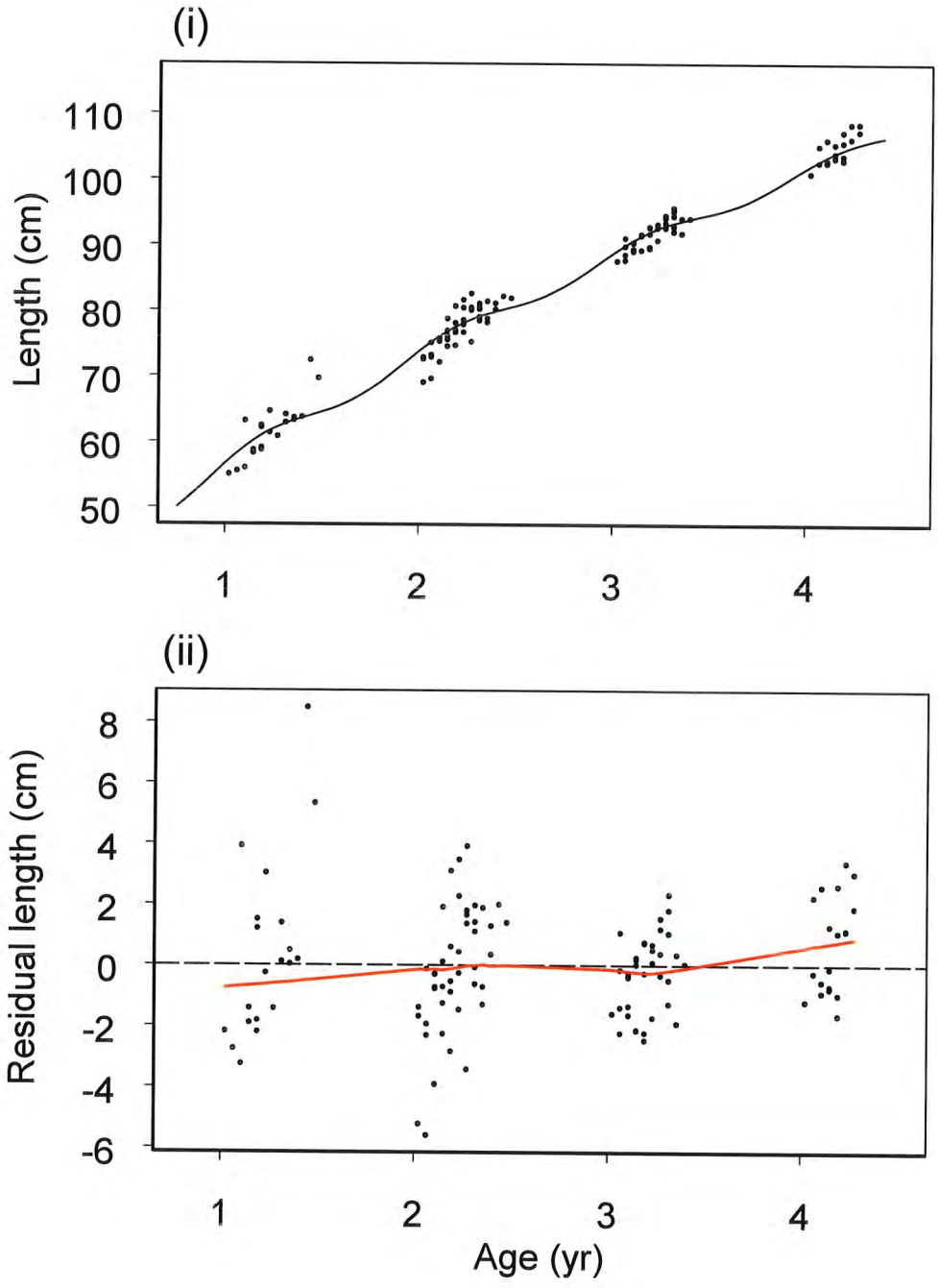

Figure 1c. Diagnostic plots for the optimal integrated seasonal VB model fitted to the 1960's growth data. Panel (i) shows the residual release lengths for the 1960's tag-recapture data plotted against the estimated ages at release relative to a_0 (i.e. $\tilde{A}_f$, as described in Appendix 5). Panel (ii) shows the residual recapture lengths plotted against the estimated ages of recapture relative to a_0 (i.e. $\tilde{A}_f + t_2 - t_1$). A local linear smooth has been put through the residuals to reveal any patterns.

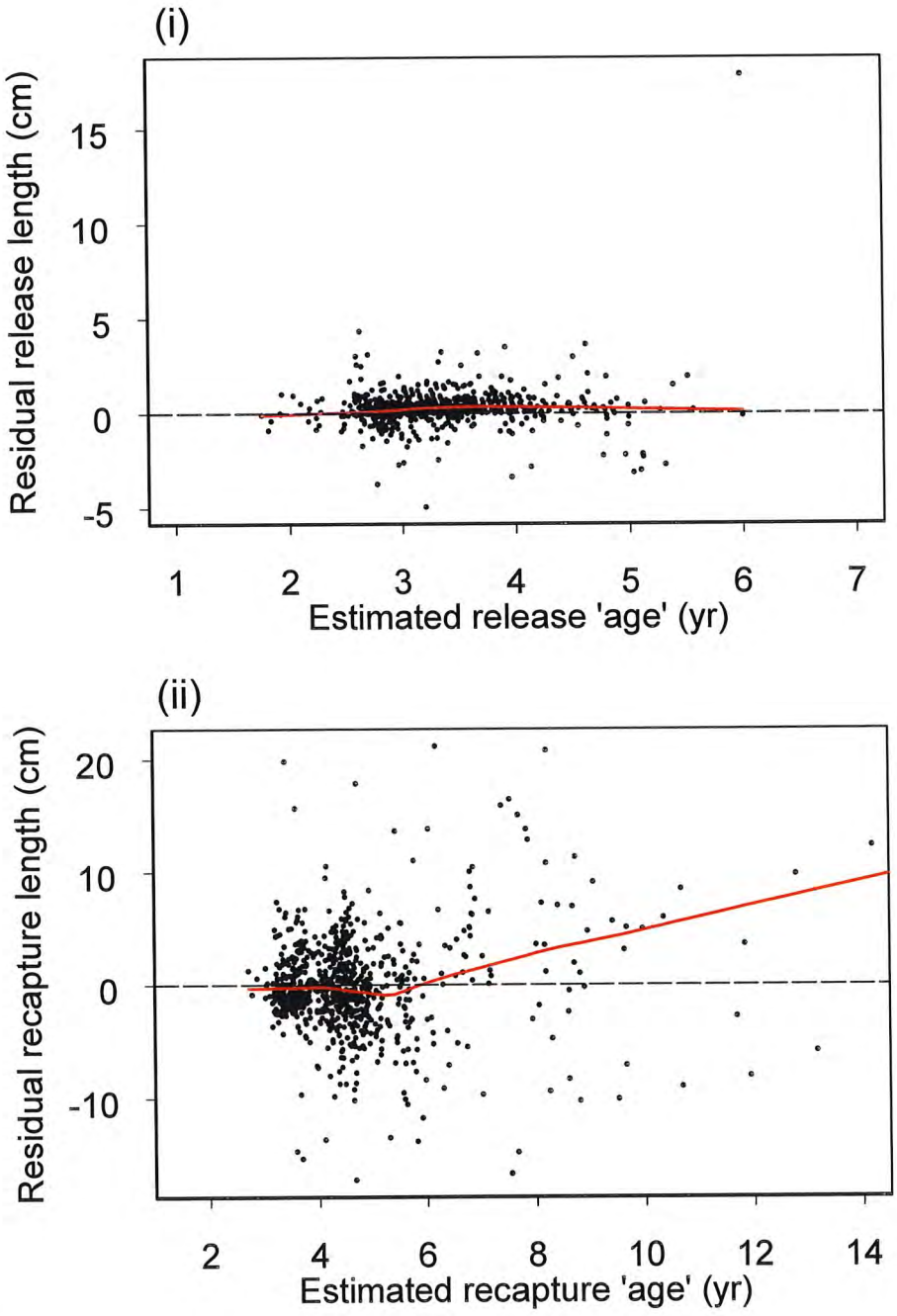

ANNEX 3: Estimates of the Correlation Matrix for the Parameter Estimates from the Best Fit to the VB log *k* Model for Each Decade and to the Standard VB Model for the 1960's

Table 1: Correlation matrix for the parameter estimates from the VB log *k* model fit to the 1960's data.

	μ_∞	σ_∞	k_1	k_2	α	a_0	u	w	$\mu_{\log A}$	$\sigma_{\log A}$	σ_s	σ_f	σ_ε
μ_∞	1.00	0.04	-0.36	-0.65	-0.15	0.00	-0.06	0.03	0.00	-0.02	-0.03	0.01	-0.01
σ_∞		1.00	0.01	-0.11	0.00	0.03	-0.01	-0.01	-0.02	-0.01	-0.23	0.06	0.00
k_1			1.00	0.12	0.11	0.86	-0.32	0.38	-0.81	0.16	-0.03	-0.04	-0.22
k_2				1.00	0.34	-0.10	0.11	-0.04	0.11	0.00	0.07	-0.01	0.02
α					1.00	0.01	0.03	-0.04	-0.04	0.03	-0.09	0.05	0.10
a_0						1.00	-0.11	0.48	-0.81	0.13	-0.02	-0.03	-0.23
u							1.00	0.12	0.30	-0.14	0.06	0.05	0.10
w								1.00	-0.43	0.20	-0.03	0.02	-0.34
$\mu_{\log A}$									1.00	-0.16	0.03	0.04	0.22
$\sigma_{\log A}$										1.00	-0.18	0.06	-0.09
σ_s											1.00	-0.41	0.01
σ_f												1.00	0.01
σ_ε													1.00

Table 2: Correlation matrix for the parameter estimates from the VB model fit to the 1960's data.

	μ_∞	σ_∞	k	σ_γ	a_0	u	w	$\mu_{\log A}$	$\sigma_{\log A}$	σ_s	σ_f	σ_ε
μ_∞	1.00	0.00	-0.58	-0.01	-0.30	0.08	-0.09	0.30	-0.06	0.01	0.02	0.04
σ_∞		1.00	-0.03	-0.01	-0.04	0.02	-0.05	0.05	-0.04	-0.20	0.03	0.02
k			1.00	0.01	0.80	-0.25	0.35	-0.73	0.11	0.04	-0.08	-0.17
σ_γ				1.00	-0.01	-0.06	-0.02	-0.01	-0.01	-0.01	-0.04	-0.02
a_0					1.00	-0.02	0.47	-0.77	0.11	0.06	-0.07	-0.20
u						1.00	0.13	0.23	-0.12	0.01	0.08	0.06
w							1.00	-0.42	0.20	0.00	0.00	-0.32
$\mu_{\log A}$								1.00	-0.13	-0.06	0.09	0.20
$\sigma_{\log A}$									1.00	-0.18	0.06	-0.08
σ_s										1.00	-0.44	0.00
σ_f											1.00	0.01
σ_ε												1.00

Table 3: Correlation matrix for the parameter estimates from the VB log k model fit to the 1970's data.

	μ_∞	σ_∞	k_1	k_2	α	a_0	u	w	$\mu_{\log A}$	$\sigma_{\log A}$	σ_s	σ_f	σ_ε
μ_∞	1.00	0.06	-0.35	-0.92	-0.04	-0.08	0.00	0.02	0.09	-0.02	0.03	-0.01	0.01
σ_∞		1.00	-0.18	-0.05	0.09	-0.07	0.52	-0.05	0.05	0.38	-0.72	0.60	-0.04
k_1			1.00	0.29	-0.19	0.89	-0.29	-0.07	-0.77	-0.10	0.20	-0.30	0.22
k_2				1.00	0.10	0.04	0.04	-0.02	-0.06	0.03	-0.05	0.04	-0.02
α					1.00	-0.21	0.15	0.02	0.16	0.07	-0.12	0.15	-0.09
a_0						1.00	-0.09	-0.28	-0.81	-0.05	0.08	-0.19	0.23
u							1.00	-0.19	0.12	0.34	-0.69	0.62	-0.06
w								1.00	0.31	0.03	0.06	-0.07	-0.07
$\mu_{\log A}$									1.00	0.03	-0.05	0.15	-0.20
$\sigma_{\log A}$										1.00	-0.56	0.46	-0.03
σ_s											1.00	-0.83	0.05
σ_f												1.00	-0.07
σ_ε													1.00

Table 4: Correlation matrix for the parameter estimates from the VB log k model fit to the 1980's data.

	μ_∞	σ_∞	k_1	k_2	α	σ_γ	a_0	u	w	$\mu_{\log A}$	$\sigma_{\log A}$	σ_s	σ_f	σ_ε
μ_∞	1.00	0.08	-0.54	-0.84	0.32	-0.01	-0.23	-0.04	0.03	0.22	-0.09	0.03	0.03	-0.05
σ_∞		1.00	0.15	-0.08	-0.18	0.01	0.14	0.06	-0.01	-0.18	-0.05	-0.62	0.24	0.04
k_1			1.00	0.54	-0.89	0.01	0.89	-0.05	-0.12	-0.91	0.09	-0.12	-0.16	0.29
k_2				1.00	-0.50	0.01	0.32	0.05	-0.06	-0.29	0.08	-0.01	-0.04	0.07
α					1.00	-0.01	-0.81	0.03	0.15	0.86	-0.09	0.19	0.05	-0.20
σ_γ						1.00	0.00	-0.04	-0.03	-0.01	0.00	-0.04	0.00	-0.03
a_0							1.00	-0.12	-0.24	-0.90	0.08	-0.04	-0.22	0.32
u								1.00	0.22	0.14	0.00	-0.05	0.00	-0.04
w									1.00	0.23	-0.20	0.00	0.12	-0.03
$\mu_{\log A}$										1.00	-0.08	0.12	0.16	-0.30
$\sigma_{\log A}$											1.00	-0.08	0.02	0.01
σ_s												1.00	-0.51	0.02
σ_f													1.00	-0.12
σ_ε														1.00

Table 5: Correlation matrix for the parameter estimates from the VB log k model fit to the 1990's data.

	μ_∞	k_1	k_2	α	u	w	$\mu_{\log A}$	$\sigma_{\log A}$	σ_s	σ_f
μ_∞	1.00	0.11	-0.65	-0.69	0.50	0.37	0.14	0.00	0.20	0.00
k_1		1.00	-0.44	-0.66	0.61	0.49	-0.58	-0.13	-0.08	0.09
k_2			1.00	0.50	-0.68	-0.48	0.01	0.17	-0.10	-0.04
α				1.00	-0.65	-0.49	0.30	-0.03	-0.09	-0.06
u					1.00	0.38	-0.07	-0.17	0.28	-0.10
w						1.00	0.04	-0.31	-0.05	0.13
$\mu_{\log A}$							1.00	-0.07	0.17	-0.09
$\sigma_{\log A}$								1.00	-0.06	0.02
σ_s									1.00	-0.54
σ_f										1.00

Appendix 11:

Investigating the timing of annual growth zones in otoliths of southern bluefin tuna (*Thunnus maccoyii*)

Naomi P. Clear, J. Paige Eveson and Tom Polacheck

FRDC Project 1999/104

Introduction

Otoliths are calcified 'ear-stones' in teleost fishes used for balance and/or hearing. They are metabolically inert and, unlike other hard parts of fish such as scales and vertebrae, are not subject to resorption (Campana 1999). In addition, otoliths continue to grow throughout the life of a fish and hence contain a permanent chronological record.

Otolith growth is not constant. During periods of fast growth the accreted otolith material is opaque whereas it is translucent during slow growth periods. An opaque zone and subsequent translucent zone is referred to as an 'increment' and they appear as a light and a dark band, respectively, when placed on a black background and viewed under a dissecting microscope with reflected light.

Increments in the otoliths of southern bluefin tuna, *Thunnus maccoyii*, (SBT) are formed annually (Clear et al. 2000), with fast growth occurring during the southern summer and slow growth during the southern winter. Thus, the number of increments can be counted to give an age estimate of SBT in years. We refer to this procedure as making a "reading" from an otolith.

There are three pairs of otoliths; in most fishes, including tunas, the sagittae are the largest pair. Because of their size, sagittae are the easiest to handle and prepare so they are most often the otoliths chosen for research, as they were for this study. Previous studies involving direct age estimates of SBT have included two methods of preparing sagittal otoliths for "reading", one in which the otolith was left whole and the other in which the otolith was sectioned (Gunn et al. In press). The whole otolith method has been used successfully for fish less than about 6 years old (~ 135 cm fork length); after this age subsequent increments are deposited too closely to differentiate them. Sectioned otoliths have been used for all ages, however the first 4 or 5 increments are particularly difficult to decipher. With both methods, if the start of a new translucent zone (or band) is detected on the otolith margin an additional increment (known as the marginal increment) is counted as a year.

Using the number of increments as an estimate of fish's (integer) age is not straightforward because variation occurs in the time of year when individual fish form their translucent band. Consider two fish from the same cohort. One fish is caught in

April and has not yet started to form the translucent band within the marginal increment. There are N increments visible on its otolith, so the fish is assigned age N. The other fish is caught two months later. By this time it has started to form a translucent band, so it is estimated to be age $N + 1$, despite the fact that the two fish came from the same cohort.

If we know the date, d, when the translucent band becomes detectable, then we can estimate the cohort to which a fish belongs. For example, if we assume that all fish are born on January 1st (the approximate mid-point in the SBT spawning season), then we can correct the ages such that all fish from the same cohort are assigned the same age as follows:

$$\text{age} = \begin{cases} N & \text{if capture date} < d \\ N-1 & \text{if capture date} \geq d \end{cases},$$

where N is the number of bands counted, and both d and the capture date are expressed in Julian days since January 1 of the year of capture.

As part of this Appendix, we carried out an investigation to determine d, the time when the translucent band is formed, using data from a previous age-validation study (Clear et al. 2000). In the Clear et al. (2000) study, a number of SBT that were caught as part of a large-scale tagging program were injected with strontium chloride at the time of tagging. Strontium chloride ($SrCl_2$) is a harmless salt that deposits in the otolith and provides a "time-stamp" of the date of tagging. When the fish are recaptured and the otoliths are removed, the number of increments formed subsequent to marking is determined by counting the number of translucent zones ('bands') deposited after the strontium mark; the translucent zones are narrower and more defined than the opaque zones and hence easier to count. Because the amount of time the fish has been at liberty is known, we can determine whether or not the translucent zone for the recapture year has yet been formed (or is yet detectable).

The results of this investigation did not provide as fine a resolution for determining when during the winter period the translucent band was formed as we had anticipated. This was considered a significant issue for the current growth project because a substantial number of otoliths had been aged from fish captured during these winter

months. Results of fitting growth curves to the otolith age and length data were found to be sensitive to assumptions about the time of band formation. As a consequence, additional work was undertaken to see if a more precise and accurate estimate of the time of band formation could be determined.

A pilot study was conducted in which a small number of unread strontium-marked otoliths from fish caught during the winter months were selected from the CSIRO archives. In addition to counting the number of bands formed subsequent to the strontium mark, several additional observations were also made. In particular, the samples were chosen from fish that had had both otoliths extracted so that one otolith could be read using the whole method and the other could be read using the sectioned method. Some preliminary exploration of existing otolith data suggested that the ability to detect a translucent zone forming on the margin may differ between the two methods. The results from the pilot study further indicated that this was a possibility. Consequently, a larger study was conducted in which otolith pairs were read both sectioned and whole and the readings compared.

Methods

Time of band formation study based on strontium chloride marked otoliths

As part of the Clear et al. (2000) age-validation study, 59 otoliths were read from fish that had been strontium injected and recaptured. Details on the strontium chloride tagging experiment can be found in Clear et al. (2000).

Using the release date of the fish (at which point the strontium mark was deposited in the otolith), the recapture date, and the number of increments subsequent to the strontium mark, we can determine if a translucent band had yet been formed in the year of recapture. For example, if a fish released in January 1990 and recaptured in July 1994 has four translucent bands in its otolith after the strontium mark, we can assume that its translucent band for 1994 has not yet been formed, or at least cannot yet be seen. In doing so, we are assuming that the count of increments subsequent to the strontium mark is accurate. We are also assuming that the only uncertainty in the number of translucent bands that should have formed comes from the year of recapture, and not the year of

release. The majority of fish were tagged and released during the summer months of December to March; months during which a translucent band would not be forming. However, two of the 59 fish were released in June and one in May, and we cannot be sure whether the band corresponding to the year of release would have been formed prior or subsequent to the strontium mark. Thus, we excluded these three fish from our analyses.

For each month of recapture, we tabulated how many fish had already formed a band in the year of recapture. We could then estimate the range of months during which band formation can occur, and also an average date by which SBT otoliths exhibit a translucent band.

Pilot study

A pilot study was conducted in which 24 unread strontium-marked otoliths from fish caught during the winter months (May-September) were extracted from the CSIRO archives. The number of bands formed subsequent to the strontium mark were counted and checked against the time at liberty to determine if a band had yet been formed by the recapture date. Several additional observations were also made.

Two methods have been developed for reading otoliths – one in which the otolith is left whole and one in which it is sectioned (Gunn et al. In press). Preliminary exploration of existing otolith data suggested that the ability to detect a translucent zone forming on the margin may differ between the two methods. In particular, a plot of fork length versus estimated age showed obvious disparities in the lengths-at-age of young fish that had been caught in the winter months. Further investigation revealed that these disparities were consistent with fish aged using the sectioned method being one year too young, which would occur if a band forming on the otolith margin was not being detected in the sectioned otoliths. However several confounding factors also existed which could explain the differences, one being that the same fish that were aged using the sectioned method were also caught in a very different area of the ocean than the fish that had been aged using the whole method. We used the pilot study to investigate this issue further. The 24 otoliths that were selected for the pilot study came from fish for which both otoliths had been collected (called sister otoliths). One otolith was read whole and the

other otolith was read sectioned. In addition, for both methods the reader recorded whether or not a translucent band was counted on the margin of the otolith.

Whole versus sectioned otoliths study

Exploratory data analyses in conjunction with results from the pilot study suggested that there may be a consistent difference in the time at which the translucent band being formed on the margin of an otolith becomes detectable between otoliths read whole and otoliths read sectioned. For fish caught during the winter months while a marginal band is forming, it is important to know whether in fact a difference does exist. If it does, then the age assigned to these fish could be one year different depending on the method used. A difference in age of one year for small fish can have a significant impact on the estimation of growth rates. Furthermore, it was realized that if a significant difference did exist, it could be exploited to refine the time when bands become detectable with both methods by comparing otolith readings using both methods from the same fish. For example, the first month in which a difference in the number of bands was found between the two methods would indicate the month when bands first became detectable with the method yielding the higher number of bands. This month would mark the beginning of the potential period of band formation. The subsequent month in which both methods yielded the same number of bands would indicate the month when bands were consistently detectable by both methods, and would mark the end limit of the period of band formation.

In order to address the problem of whether a consistent difference did exist and whether it could be used to refine the estimates of the time of detectable band formation, we conducted a study using pairs of sagittal otoliths from the same fish. One otolith was read whole and the other was read sectioned to see if there was a consistent difference in the readings around the time of band formation, and if so, for what months the difference was present.

Pairs of sagittal otoliths (paired otoliths from the same fish are referred to as 'sister otoliths') were chosen from the CSIRO Hard Parts Archives. Samples were selected from fish with lengths less than 135 cm since whole otoliths from fish larger than this are usually very difficult to read. Furthermore, otoliths were selected from fish

caught during the months of March to November since the translucent zone would almost surely have been deposited sometime within this period. In three of these months (April, August and November), fewer than 20 intact pairs of otoliths were available from the Archives. The small sample sizes could possibly obscure a pattern in the development of the translucent band through the year. However, the numbers of fish in the adjacent months are high, which should still allow for a general pattern to be detected if it exists. Furthermore, the length distribution is fairly similar across months, especially in the potential months of band formation (Figure 1). This would be important if the ability to detect the marginal band using a particular method is related to the size of the otolith, and hence the size of the fish.

Sister sagittal otoliths were prepared using two techniques: one otolith for reading whole and one for reading sectioned. The otolith to be read whole was burned on a 400°C hot plate until it turned golden brown. This accentuates the opaque-translucent banding pattern since the colour change in the translucent zones is greater, making them more visible (Figure 2). The other sagitta of the pair was sectioned along the transverse axis (Figure 3a), producing a 0.35 mm thick cross-section containing the primordium (Figure 3b).

Age estimates were successfully made using both the whole and sectioned method for 227 pairs of sister otoliths. Regardless of the method, two counts were made 'blindly' from each otolith (without knowledge of the size of fish or any previous estimates). A third reading was made to determine a final age estimate (FAE); this reading was made with the knowledge of the previous two readings. Two readers, both with extensive experience in age and growth studies of SBT, made all of the readings. The average percentage error (APE) of Beamish and Fournier (1981) was calculated to compare age estimates between the FAEs from each method. This index provides a measure of the precision or reproducibility of age estimates.

Results

Time of band formation based on strontium chloride marked otoliths

None of the fish recaptured in the months of January to May (inclusive) had a detectable band on the otolith margin, i.e. the band had not yet begun to form during the year of recapture (Table 1). Of the 11 fish caught in June, two had formed a band in that year, while three of the four fish caught in July had formed a band. All fish recaptured after July had already deposited a band in their otolith by the time of recapture. This data implies that band formation can occur during June and July, with July being most common. Unfortunately, we have no data for August so we cannot say anything about band formation during this month. Likewise, the sample sizes in all months surrounding the identified period of band formation are so small that we cannot be sure about the boundaries of the period, or reliably estimate the probability of a band being formed and becoming detectable during these transition periods. From the available information, we infer that band formation can occur any time during the months of May to September, with July 1 as the approximate average time.

It is important to note that all of the otoliths used in this strontium chloride marking study had been read using the whole otolith method. Thus, the results only apply to the time when bands become detectable with this method, but this also means that there is no potential confounding based on the method of reading. In addition, all of the otoliths came from fish recaptured in years 1992 to 1995 in waters south of Australia between 110°E and 170°E and 32°S and 44°S, with the majority caught in the Great Australian Bight or off Tasmania.

It is conceivable that the year or the spatial environment of the fish may affect the timing of band formation. The formation of otoliths is thought to be determined in part by the environmental conditions experienced by the fish (temperature, salinity, etc.) and in part by other factors such as ontogeny, growth rates and physiological processes, although their relative contributions remain uncertain (Campana 1999). To add to this complex picture, the ability of SBT to maintain body temperature above ambient temperature may possibly obscure the water temperature signal to some unknown degree. However, if fast and slow growth periods are related in part to hot and cold water

temperatures respectively, then either a year with an unusually warm autumn, or else a warm place of residence during autumn, might prolong the fast growth period and hence delay the formation of the translucent zone. For this reason we stratified the data in Table 1 by recapture year and by recapture area respectively (Table 2 shows the results stratified by year). We found the pattern in the number of bands formed by each month to be similar across years and across areas.

The recapture ages of the fish (as determined by the number of increments in the otolith) ranged from one to six, with the majority of fish aged three or four. The detection of the marginal band may be affected by the age of the fish. In juvenile SBT the width of the new translucent zone decreases with each subsequent increment formed, so for older fish the marginal band might be more difficult to detect until it has been more fully formed. Thus, we stratified the data in Table 1 by recapture age. Again, we found the pattern in the number of marginal translucent bands formed by each month to be similar across ages.

Caution must be used in interpreting these results because the sample sizes in each month after stratification are so small that the data are not very informative. The results certainly cannot be taken as conclusive, and they cannot be generalized outside the range of the data. The fish included in the study came from a fairly narrow range of the population with respect to years, areas, and ages. It is possible that one or more of these factors play a role in the formation or detection of bands that we were unable to identify.

Pilot study

Of the 24 pairs of sister otoliths selected for the pilot study there were 3 pairs that had to be omitted completely from the study due to both otoliths being unreadable or the release and recapture information being unbelievable. Of the remaining otolith pairs, the whole otolith was unreadable in 3 cases and the sectioned otolith was unreadable in 2 cases. For investigating the time of the band formation, this left 18 whole otoliths and 19 sectioned otoliths; for comparing the two reading methods, this left only 16 pairs with both readings available.

The results from the investigation on the time of band formation (Table 3) were not very informative for clarifying the period of band formation. This was due largely to

the small sample sizes. The results from both the sectioned readings and whole readings indicate that bands can form in May, June and July. Only one sample from each of August and September was included in the study. In both cases, the whole otolith was unreadable and the sectioned otolith exhibited a band on the margin, but clearly nothing can be concluded about these months with a sample size of one. The small sample sizes are unfortunate but were due to several reasons: a) this was only intended as pilot study and resources were limited (the process of preparing an otolith and obtaining a final reading is expensive and time-consuming), b) there are limited numbers of strontium-marked otoliths available (only 2 remain in August, which is a critical month for defining the period), and c) strontium-marked otolith samples for which both sister otoliths are available are even more limited.

Recall that for each sectioned otolith, the number of bands deposited after the strontium mark was counted, and it was also recorded whether a band was detected on the margin of the otolith. For 100% of the sectioned otoliths, if a band was detected on the margin of the otolith, then the post-strontium count indicated the presence of a band in the year of recapture; if a band was not detected on the margin, then the post-strontium count indicated a band was not present in the year of recapture. Because both sets of results are equivalent, we will only refer to the detection of a marginal band results for sectioned otoliths.

Despite the small amount of data, some interesting results were obtained. The proportion of fish with a marginal band in May was high, whereas the proportion of fish with a marginal band in July was small, and these observations were consistent whether using the whole otolith or sectioned otolith. These results are somewhat contradictory to those from the previous study (see Table 1), but the difference is not startling since the sample sizes for May and July are so small in both studies. A more interesting result is that the proportion of fish with a marginal band in June was high based on whole otoliths and low based on sectioned otoliths.[1]

[1] In the previous study, which used only whole otoliths, June had a low proportion of otoliths with a band detected in the year of catch. However, the results from the two studies are not completely comparable – (continued on next page)

In comparing the whole and sectioned readings on sister otoliths, the whole reading was generally one greater than the sectioned reading for fish caught in June (Table 4). The two readings tended to agree in the other months, although June is the only month with a reasonable sample size for comparison. This finding supported our hypothesis that the ability to detect a marginal band may differ between the two methods, with a band becoming detectable sooner with whole otoliths than with sectioned otoliths. This led to a more comprehensive study comparing whole and sectioned readings on sister otoliths, the results of which are presented below.

Whole versus sectioned otoliths study

Using the final age estimates (FAEs) from 227 pairs of sister otoliths, where one sister was read using the whole otolith method and the other using the sectioned otolith method, we calculated the average percent error (APE) between the methods to be 5.8%. This is well within the acceptable level of 10%. For each pair we also calculated the difference between the whole and the sectioned read. Of the 227 pairs included in the study, the whole and sectioned readings agreed in 146 cases (64.3%). The whole reading was one greater than the sectioned reading in 17 cases (7.5%) and two greater in 4 cases (1.8%); it was one less in 55 cases (24.2%) and two less in 5 cases (2.2%). This trend is consistent across months (Figure 4). This would suggest that there is a tendency to count an extra band using the sectioned method versus the whole method. If the difference was due to new bands being detectable earlier in the year in sectioned otoliths than whole otoliths, then we would expect the sectioned readings to be one greater during the early months of band formation and equal later in the year. Instead, all months show the same pattern, which implies that the difference is not due to the timing of band formation.

The main purpose of this study was to see if the method used to read the otolith affects the perceived time of band formation. However, out of interest, we plotted the

---

the results from the previous study are based on counts of the number of bands after the strontium mark in whole otoliths, whereas the results obtained from whole otoliths in the pilot study are based on whether or not a band was detected on the margin of the otolith. Post-strontium counts were only made on sectioned otoliths in the pilot study.

fork length of the fish versus the whole and sectioned readings (Figure 5). The sectioned readings show greater variability in length at age than the whole readings, especially at younger ages. From our knowledge about the length-at-age distribution of young SBT, the sectioned readings show a greater range than expected. For example, it is unlikely that a fish of age two is over 100 cm in length. This suggests that the whole readings may be more precise, at least at young ages. This result may not be overly surprising since it has been documented that the first four or five increments are difficult to interpret in sectioned otoliths (Gunn et al. In press).

Discussion

From the data available, we found that the time of year at which SBT deposit a translucent zone in their otoliths can vary from May to September, with July 1 being an approximate average date. Although some of the variability may be due to errors in the increment counts, most of the variability is likely due to the fact that the time of translucent band formation differs considerably from fish to fish. Growth in SBT, and hence the formation of otolith increments, is believed to be related in part (and indirectly) to water temperature, with slow growth occurring when the water is cooler. SBT are found throughout a large area of the ocean with very different environmental conditions. As such, it is not surprising that the time at which the band forms can vary greatly between fish. The annual formation of increments in otoliths may also be, at least in part, physiologically controlled; this too could cause the timing of band formation to differ between fish.

In our comparison of sister otoliths read whole and sectioned, we found no relationship between the difference in the readings and the time of year. This means that comparison of number of bands from the same fish using the same method cannot be used to provide further information on the timing of band formation. However, it also means that the fact that all the otoliths read in the Clear et al. (2000) strontium-chloride experiment were read whole should not affect our findings about the period of band formation, and that the conclusions from this study can be applied to otoliths read with either method.

Although the main purpose of comparing whole and sectioned otolith readings was to see if the methods differed in their detection of the marginal increment, some other interesting results came from the study. For example, although the methods show quite good agreement (64%), there appears to be a tendency for the sectioned count to have one more band than the whole count. The discrepancy between the whole reading and the sectioned reading does not appear to be related to the size of the fish (Figure 6), although the sample sizes in the smaller length-classes are too small to be certain. Based on Figure 5 and our prior knowledge of the length-at-age distribution of young fish, we believe the whole count is more reliable for young (small) fish. However, the whole method cannot be used for larger fish (fork length >135 cm). Thus, with respect to using direct aging data to model growth, it might be preferable to use only data from otoliths read whole up to a given size, and then use data from the sectioned method subsequently. Of course, one would need to decide (probably somewhat arbitrarily) an exact figure to use for the transition size.

There are still some unread otoliths in the CSIRO Hard Parts Archives that were collected from strontium-injected SBT. These otoliths could perhaps be used to better define the period of band formation, but preparation and reading of them was beyond the scope of this study. There are at least 20 unread strontium-marked otoliths collected in each month from January to June (with the exception of 16 in May) that could help to define the start of the period. Unfortunately, there are only 7 unread otoliths from fish caught in July, 2 from August, and 5 from both September and October. This means that there are insufficient samples to reliably estimate the end of this period with any confidence.

All of the strontium-mark otoliths included in our investigation of the time of band formation came from fish aged six or less that were caught in southern Australian waters in years 1992 to 1995. The time of band formation may differ for fish outside these ranges since the physical environment in other regions may differ and there may be differences in habitat use with age. By proposing a fairly broad range of months in which band formation can occur (May to September), we hope to have enveloped the time of band formation for the vast majority of fish.

Without more information, uncertainty of one year exists about the age of a fish caught during the period of band formation. In turn, this uncertainty could induce substantial uncertainty into the estimation of growth curves if fish caught during this transition period are included. While statistical approaches can be developed to deal with this problem (see Appendix 12), their application is complex, requires substantial amounts of data and was outside the scope of the current project. It is important to note that the exclusion of direct aging data from fish captured during the months when bands are being formed would not bias the estimation of growth, but their inclusion with some assumption about the time of band formation could. Thus, only direct aging data from fish caught outside the proposed months of band formation (i.e. from October through April) were included in growth analyses for the current project. In doing this, we believe that we should have excluded almost all, if not all, fish for which the time of band formation could potentially confound the estimation of its age.

References

Beamish, R.J. and Fournier, D.A. 1981. A method for comparing the precision of a set of age determinations . Can. J. Fish. Aquat. Sci. **38**: 982-983.

Campana, S.E. 1999. Chemistry and composition of fish otoliths: pathways, mechanisms and applications. Mar. Ecol. Prog. Ser. **188**: 263-297.

Clear, N.P., Gunn, J.S., and Rees, A.J. 2000. Direct validation of annual increments in the otoliths of juvenile southern bluefin tuna, *Thunnus maccoyii*, by means of a large-scale mark-recapture experiment with strontium chloride. Fish. Bull. **98**: 25-40.

Gunn, J.S., Clear, N.P., Carter, T.I., Rees, A.J., Stanley, C.J., and Farley, J.H. In press. The direct estimation of age and growth in southern bluefin tuna, *Thunnus maccoyii* (Castelnau), using otoliths, scales and vertebrae. Fish. Bull.

Table 1. Direct aging data from 56 southern bluefin tuna that were part of a tag-recapture experiment with strontium chloride. The table shows how many of the fish recaptured in each month had yet deposited a detectable band in their otolith for that year.

Recapture Month	Band deposited yet?		Total
	No	Yes	
January	3		3
February	9		9
March	14		14
April	3		3
May	2		2
June	9	2	11
July	1	3	4
August			
September		2	2
October		4	4
November		1	1
December		3	3
Total	41	15	56

Table 2. The data from Table 1 stratified by year of recapture. The time when bands are formed does not appear to be affected by year; however, the sample sizes in each month are much too small to be conclusive.

Recapture Year	Recapture Month	Band deposited yet?		Total
		No	Yes	
1992	3	1		1
	4	1		1
	6		1	1
	7		2	2
	10		1	1
1992 Total		2	4	6
1993	1	1		1
	2	4		4
	3	8		8
	4	1		1
	5	2		2
	6	1		1
	7		1	1
	10		2	2
	11		1	1
	12		3	3
1993 Total		17	7	24
1994	1	1		1
	2	1		1
	3	3		3
	6	4		4
	7	1		1
	9		2	2
	10		1	1
1994 Total		10	3	13
1995	1	1		1
	2	4		4
	3	2		2
	4	1		1
	6	4	1	5
1995 Total		12	1	13
Grand Total		41	15	56

Table 3. Summary results from the pilot study. The table shows how many of the fish captured in each month had a detectable band forming on the margin of their otolith according to a) the whole method and b) the sectioned method.

Recapture Month	Whole Method		Sectioned Method	
	No	Yes	No	Yes
May	1	3	2	3
June	2	8	7	1
July	3	1	3	1
August	0	0	0	1
September	0	0	0	1

Table 4. Difference between whole reading and sectioned reading for otoliths read as part of the pilot study. Only 16 of the otolith pairs could be included in the comparison due to one or both of the otoliths being unreadable using the method for which it was prepared.

Recapture Month	Whole – Sectioned			Total
	-1	0	+1	
May	0	4	0	4
June	0	2	6	8
July	1	2	1	4
August	0	0	0	0
September	0	0	0	0

Figure 1. Fork length versus month caught for the 227 fish selected for the study comparing whole and sectioned readings from sister otoliths. The length distributions are reasonably similar across months, especially in the most probable months of band formation, so length should not be a confounding factor in whether or not a method can detect a band in a particular month.

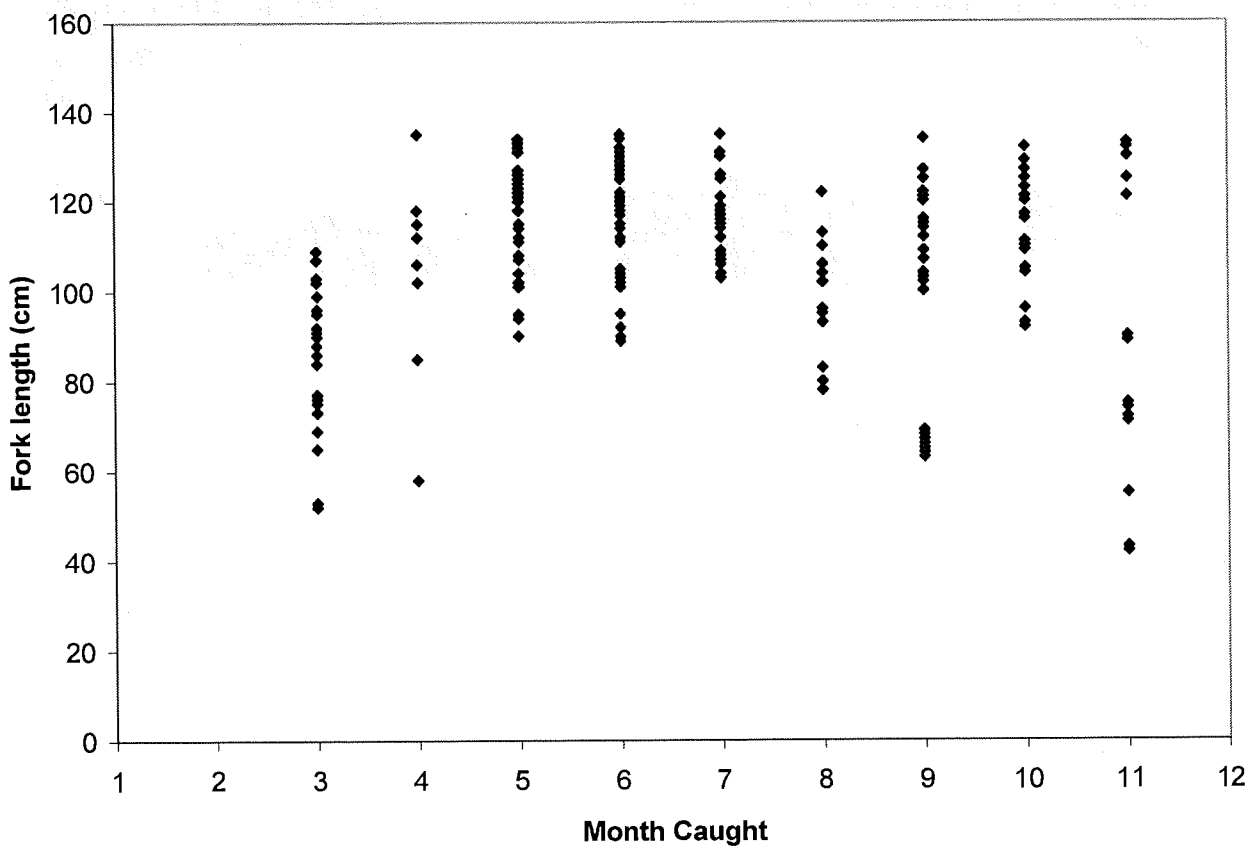

Figure 2. In preparation for being read whole, the sagittal otoliths were burnt on a hot plate accentuating the translucent zones (bands). Scale bar: 1 mm.

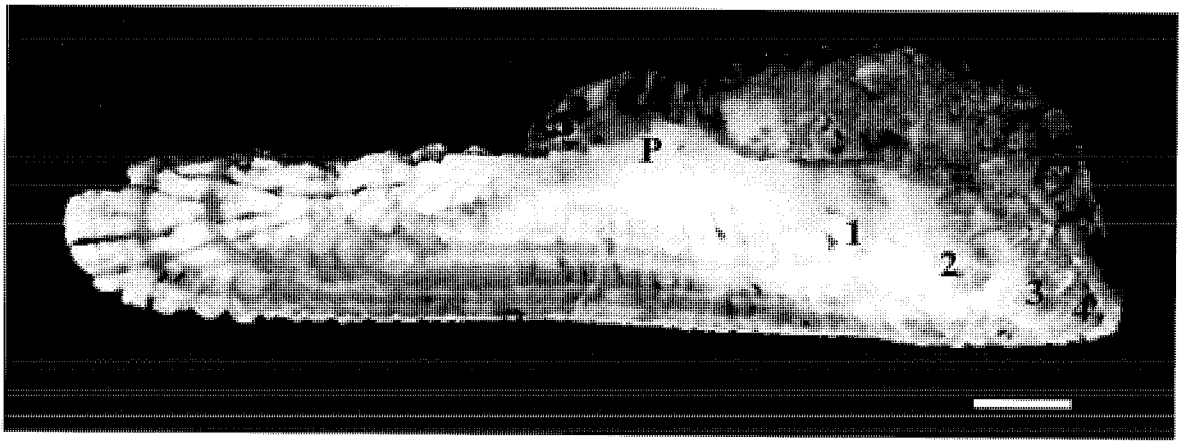

Figure 3. a) Sagittal otoliths were sectioned along the transverse axis, producing a 3.5-mm thick cross-section that contained the primordium. b) Age estimates were made by counting increments along the longer arm of the cross-section, from primordium to margin. Scale bar: 1mm.

a)

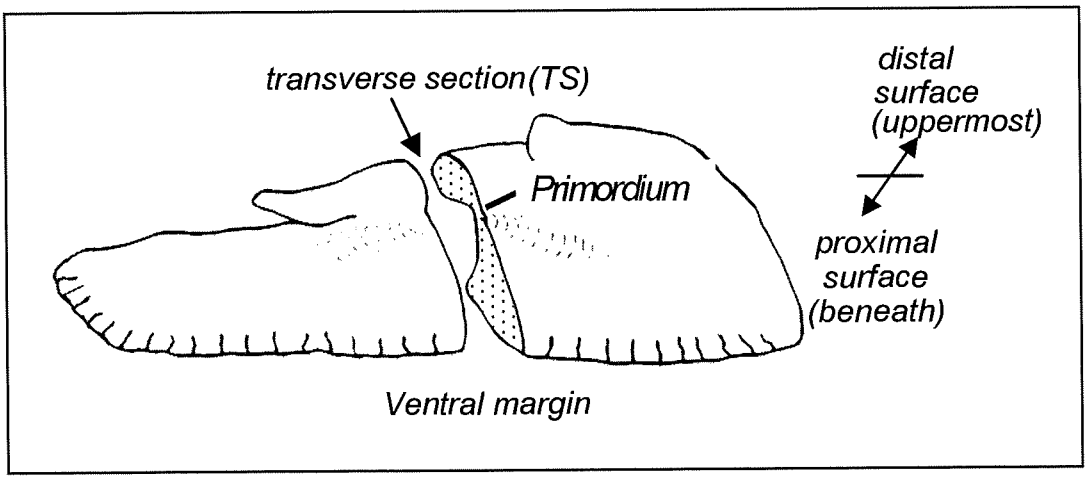

b)

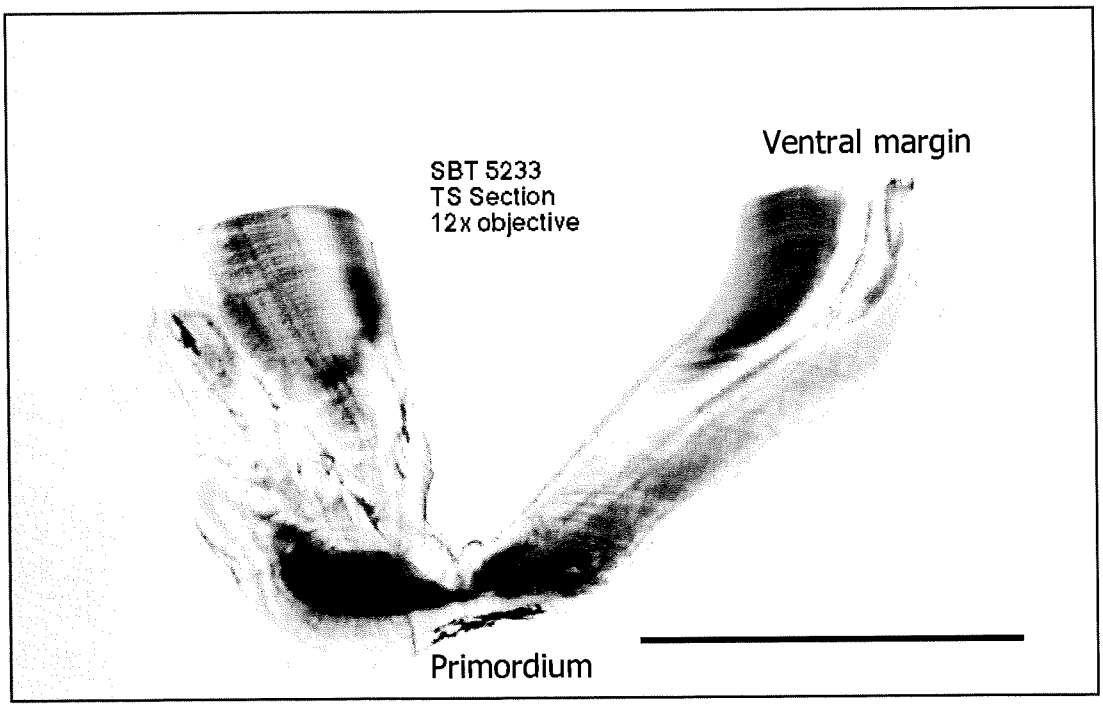

Figure 4. Barplots of the difference in whole versus sectioned readings made from sister otoliths broken down by month. a) Each bar shows the number of otolith pairs from that month for which the whole reading minus the sectioned reading was 2, 1, 0, –1, and –2 respectively. b) Same as a) but showing percents instead of absolute numbers.

a)

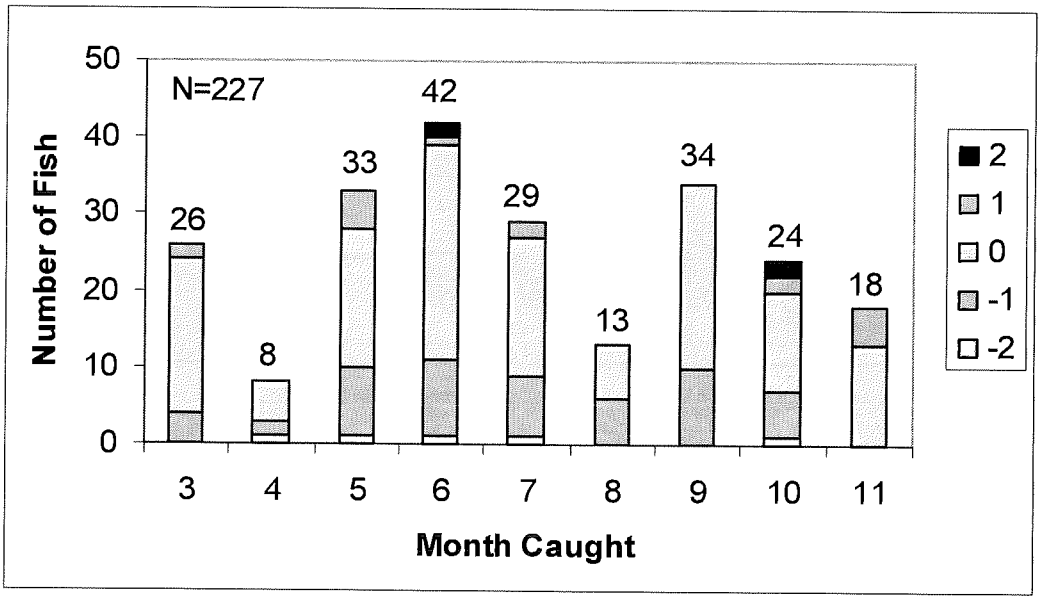

b)

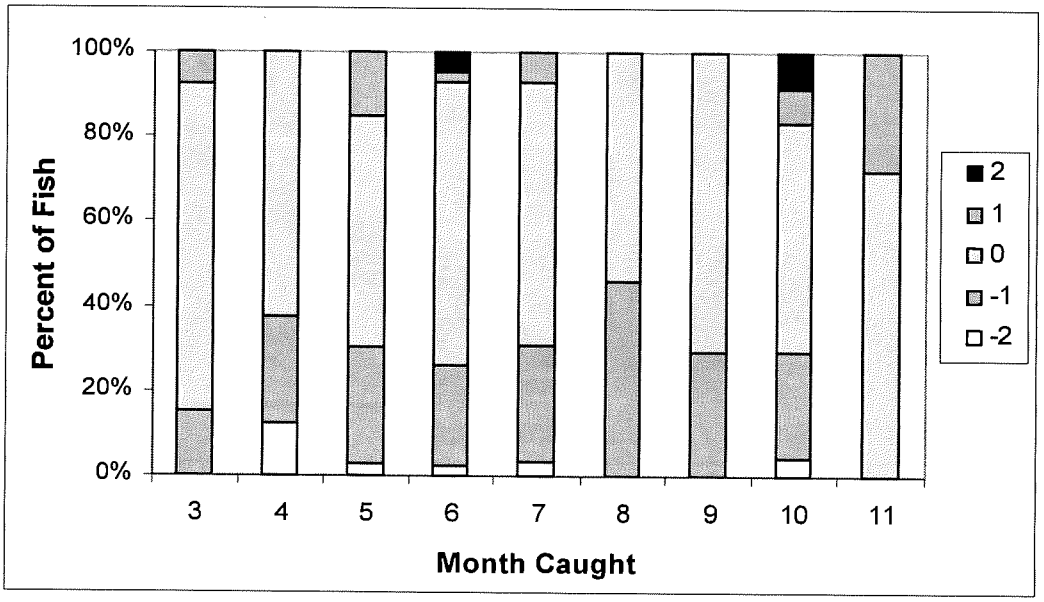

Figure 5. Fork length of fish versus final otolith reading, for both sectioned and whole otoliths.

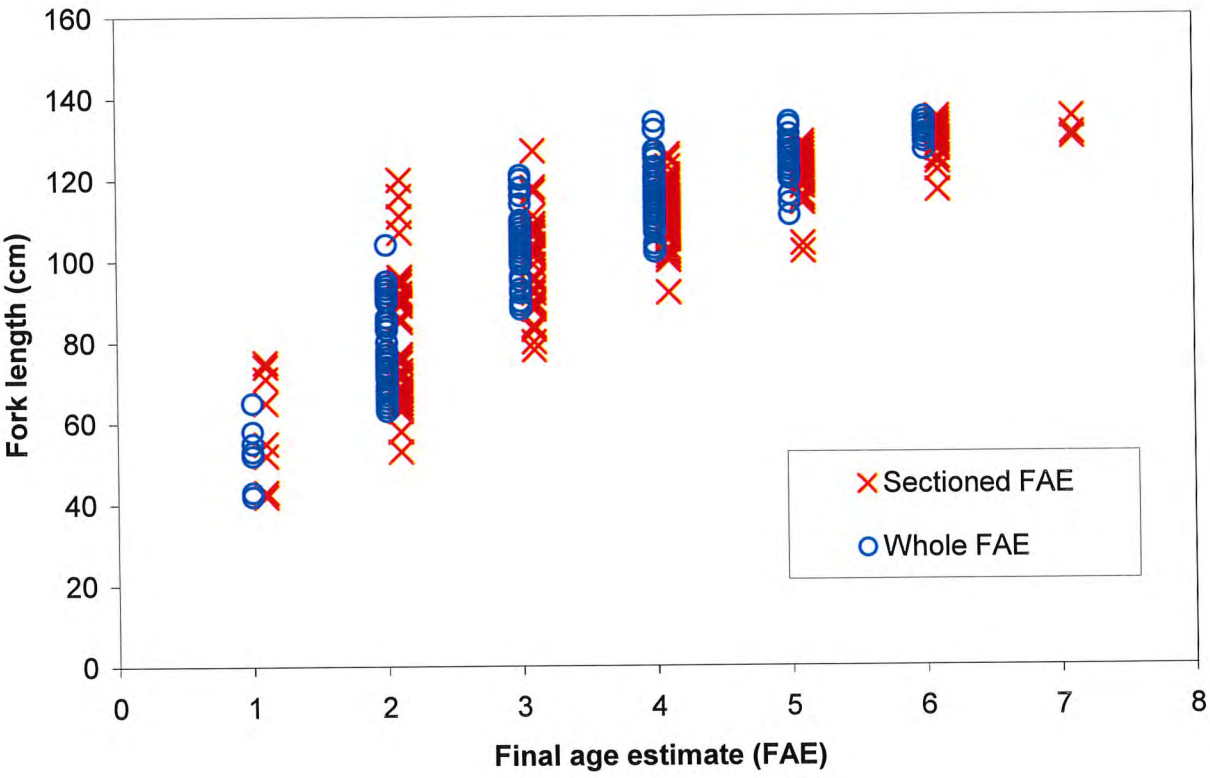

Figure 6. Barplot of the difference in whole versus sectioned readings made from sister otoliths broken down by 10-cm length classes. The x-axis label gives the start of the length class. Each bar shows the number of otolith pairs coming from fish in that length-class for which the whole reading minus the sectioned reading was 2, 1, 0, –1, and –2 respectively.

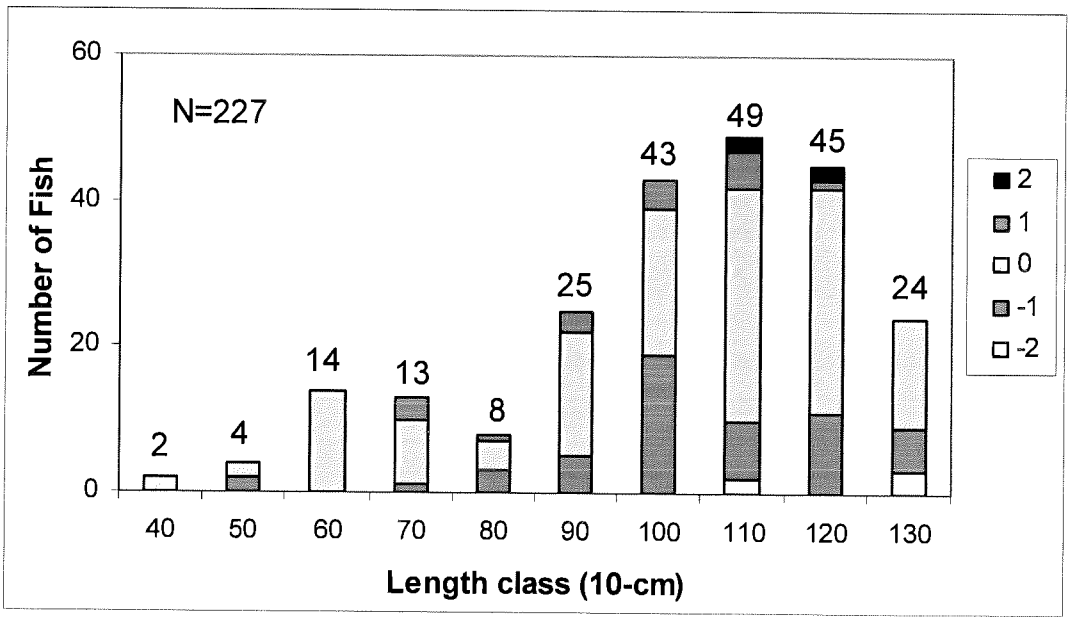

Appendix 12:
Statistical models for growth curve estimation using otolith data

Geoff M. Laslett, J. Paige Eveson and Tom Polacheck

FRDC Project 1999/104

Introduction

The growth of southern bluefin tuna is much faster in summer than in winter. This seasonal growth pattern is reflected in the tuna's otolith (ear-bone), which exhibits bands corresponding to slower winter growth. These bands can be counted, yielding a measure of the age of the fish (Clear *et al.* 2000). When a fish is caught and its otoliths are extracted, its length l is also measured. The number of bands in one or both of the otoliths is counted under an optical microscope. This is called reading an otolith. An otolith can be read by two methods, either whole or sectioned. It has been common to use the whole otolith on young fish, partly for cost considerations. As a fish ages, its growth slows and the otolith bands crowd together. On older fish (over age six), the otolith must be sectioned so that adjacent bands can be distinguished better.

The analysis of otolith data represents a considerable statistical challenge. Even if counting is correct, the age of the fish is known only to within a year because of uncertainty in the birth date. Moreover, the time when bands are formed varies among fish so errors of plus or minus a year can be induced in the age estimates of fish caught during this time. In addition to age uncertainties, there are other sources of variation that may need to be accounted for, such as possible reader effects, method effects and regional differences. In the current growth project, we avoided the worst of these complications by excluding otolith data from fish captured during the period of band formation (see Appendices 3 and 11) as well as otolith data from the spawning grounds that was known to have size biases (see Appendix 3). However, this resulted in potentially useful data being omitted. We also made simplifying assumptions with respect to birth dates, measurement error, et cetera. While these assumptions should not induce biases into the parameter estimates of the growth model, they will result in them having higher variances. It was beyond the scope of this project to develop rigorous statistical theory to deal with all these issues. However, we have developed some initial ideas and approaches which we present in this Appendix. These are preliminary ideas that need further development

and testing, but we present them as a basis for stimulating further work.

A first approach

There are two response variables measured on an aged fish: the length l and the number of bands z. We also know the time t at which the fish was caught. We require a statistical model of the data. The length l is assumed to follow a growth curve

$$l = L_\infty f(a;\theta) + \epsilon$$

where L_∞ (the asymptotic length) is random from fish to fish with mean μ_∞ and variance σ^2_∞, a is age, θ is a vector of fixed unknown parameters and $\epsilon \sim N(0,\sigma^2)$ represents measurement error. For example, for the von Bertalanffy growth curve

$$f(a;\theta) = \begin{cases} 1-\exp(-k(a-a_0)) & \text{if } a > a_0; \\ 0 & \text{otherwise,} \end{cases}$$

so that $\theta' = \{k, a_0\}$.

The age a of the fish is not measured directly, but we can assume that the age and the number of bands z are related by

$$a = z + \tau - m - \delta$$

where $0 \leq \tau = t - [t] < 1$ is the time of the year at which the fish was caught, $m = 1$ if the fish has laid down a band during the current calendar year and is 0 otherwise and $\delta \sim N(0,\sigma^2_\delta)$ reflects the variable spawning time of southern bluefin tuna. The distribution for δ implicitly assumes that the mean time of spawning is January 1. The band is laid down in the winter, so that $m = 0$ at the beginning of the year when τ is close to 0, and $m = 1$ at the end of the year when τ is close to 1. Imagine a given fish passing through the stroke of midnight at the end of a calendar year: then m switches from 1 to 0 and τ simultaneously switches from 1 to 0. For the purposes of this Appendix, we assume that the time of laying down the

band is symmetric about July 1 with a standard deviation of about 1 month, but we recognize that further work on this is needed (see Appendix 11). A reasonable model for m is therefore

$$\text{logit}\,\Pr[m = 1|\tau] = 30\,(\tau - 0.5)\,.$$

We assume that the standard deviation σ_δ of δ is about 0.1, and that δ and m are independent. This may not be true for fish in their first year of life, but we suspect that it is true in later years. However, we have very few fish less than one year old, so we ignore this point, and note that the growth rates of fish below this age are not important in terms of their use in the stock assessment.

Note, in passing, that we could model dependence between m and δ quite easily by setting, for example,

$$\text{logit}\,\Pr[m = 1|\delta, \tau] = 30\,(\tau - \alpha\delta|\delta|^z - 0.5)\,.$$

The function $|\delta|^z$ ensures that the correlation between m and δ declines as the age of the fish increases. Other functions could be used. If $\delta > 0$, the fish was spawned after January 1, and we suspect that the first band would tend to be laid down after July 1 the next year, so that $\alpha > 0$. However, we leave this for future work.

For a fish caught at time τ let

$$g(l|z, \delta, m, \tau) = \frac{1}{\sqrt{2\pi}\sqrt{\sigma_\infty^2 f^2 + \sigma^2}} \exp\left(-\frac{1}{2}\frac{(l - \mu_\infty f)^2}{\sigma_\infty^2 f^2 + \sigma^2}\right)\,.$$

where $f = f(z + \tau - m - \delta; \theta)$. We can therefore write down the likelihood of the length l given z as

$$g(l|z, \tau) = \int_{-\infty}^{\infty} \sum_{m=0}^{1} g(l|z, \delta, m, \tau)\ \Pr[m|\tau]\, h(\delta)\, d\delta$$

where

$$h(\delta) = \frac{1}{\sigma_\delta}\phi\left(\frac{\delta}{\sigma_\delta}\right)$$

and $\phi(.)$ is the standard normal density. If m and δ are correlated, we simply replace $\Pr[m|\tau]$ by $\Pr[m|\delta, \tau]$.

The unknown parameters could be estimated by maximising the log-likelihood

$$\sum_{i=1}^{n} \log g(l_i|z_i, \tau_i) .$$

This involves either one integral per fish, or, if the summation is moved before the integral, two integrals for each fish, one for $m = 0$ and one for $m = 1$. If we do one integration, the integrand might be quite complicated, so we might need to use Simpson's rule, but if we do two, the integrals could be handled by Gauss-Hermite quadrature. However, it is probably adequate to approximate the integral by a sum, particularly as there are no unknown parameters in the distribution of δ. Thus we could make the distribution of δ discrete, with probabilities of say 0.01, 0.10, 0.39, 0.39, 0.10, 0.01 of being spawned in October, November, December, January, February and March respectively, which would correspond to $\delta = -0.21, -0.13, -0.04, 0.04, 0.13, 0.21$. An advantage of this approach is that a non-Gaussian (e.g. bimodal) distribution for δ could be handled easily. Also, the cell sizes do not need to be equal, so we could divide December and January into two, say.

In practice there are complications. First, the observed number of bands z might be the true number of bands z^* measured with error, and this error may depend on the reader, the method used, and the age of the fish. One possibility is to condition on the number of bands reported, and to work out a distribution for the number of true bands given the number of reported bands. This is called a Berkson error model. An obvious first candidate is

$$\Pr[z^*|z] = \Phi((z^* + 0.5 - z - \beta)/\sigma_z) - \Phi((z^* - 0.5 - z - \beta)/\sigma_z)$$

where the second term on the right is omitted if $z^* = 0$. The probabilities then sum to 1. We should probably make σ_z depend on z too. For example, if counting errors are expected to have a 10% coefficient of variation, set $\sigma_z = 0.1(z+0.5)$. The bias β would change with the reader/method combination — for one such combination, say Reader 1 with sectioned otoliths, set $\beta = 0$, and estimate a different β for the other

reader/method combinations. This of course adds an extra sum into the likelihood:

$$g(l|z,\tau) = \sum_{z^*} \sum_{\delta} \sum_{m} g(l|z^*,\delta,m,\tau)\ \Pr[m|\tau]\ \Pr[\delta]\ \Pr[z^*|z]\,.$$

Note that β and σ_z could be made to depend on covariates. For example, we might expect a greater bias or error around the time of band formation, in which case β could be made a suitable function of τ.

The second complication is that fish in different areas might exhibit slightly different growth rates or times of band formation. There are several possible ways to model this. We might make some of the growth parameters, k or a_0, depend on the area.

A more pragmatic approach

In this Appendix we shall take a more pragmatic approach. Let i index the region and j the fish within that region. We let the age be

$$a = z + \tau - M$$

where $M = 1$ if $\tau > 0.5$ and $M = 0$ otherwise. We are ignoring the randomness in a, because we believe that other sources of variation may be more important, and we wish to concentrate on them initially. Our first model is

$$l_{ij} = L_{\infty,ij} f(a_{ij};\theta) + u_i + \sum_{r=1}^{R_o} \delta_{ij,r}\alpha_r + \epsilon_{ij}\,,$$

where

$$L_{\infty,ij} = \mu_\infty + v_{ij}$$

and R_o is the number of reader/method combinations. Here u, v and ϵ are all independent random effects. We assume that $u \sim N(0,\sigma_u^2)$, $v \sim N(0,\sigma_\infty^2)$ and $\epsilon \sim N(0,\sigma^2)$. Thus u represents a random regional effect and v the natural variability of fish lengths. In addition, ϵ represents sampling error, and its variance is assumed known — although in practice it will be estimated from other data.

The final component of the model is the reader/method combination α_r, which we treat as a fixed effect. Thus

$$\delta_{ij,r} = \begin{cases} 1 & \text{if fish otolith } ij \text{ is read with method } r; \\ 0 & \text{otherwise.} \end{cases}$$

We need to avoid redundancy in the α_r parameters by setting $\sum_r \alpha_r = 0$. Once again, it is possible to make this effect depend on covariates such as τ. For example, we could replace α_r by $\gamma_{ij,r} = \alpha_r \sin^2(\pi\tau_{ij})$. This implies that there is virtually no reader effect if the fish is caught in December or January, but the reader effect becomes very pronounced if the fish is caught in June or July. It should be noted that the reader effect is likely to vary randomly from fish to fish, and will not just be a fixed amount captured by the parameter α_r. This could be modelled by adding in a term w_{ij}, so the model becomes

$$l_{ij} = L_{\infty,ij} f(a_{ij};\theta) + u_i + \sum_{r=1}^{R_o} \delta_{ij,r}\alpha_r + w_{ij} + \epsilon_{ij}\,,$$

where $w_{ij} \sim N(0, \sigma_w^2)$. Analysis of independent replicate measurements suggests that $\sigma_w \approx 0.1(z + 0.5)$. In practice, $v_{ij}\, f(a_{ij};\theta)$ and w_{ij} are likely to be highly confounded, and therefore we omit w_{ij} from the model. However, it might be necessary to include w_{ij} explicitly if the tag-recapture data are being analysed at the same time. Alternatively, we could assume that σ_w is known.

We assume that we estimate the parameters by maximising the likelihood of the data. It would be normal to write the model in vector form as

$$l = T\beta + Uu + d$$

where l is the vector of length data, $T = (f\ \Delta)$, f is the vector of growth function values, Δ is a fixed effects design matrix such that $\Delta_{ij,r} = 1$ if fish ij is measured using reader/method r and is 0 otherwise, U is a random effects design matrix such that $U_{ij,i} = 1$ if fish ij is caught in region i and is zero otherwise and $d = f\,v + \epsilon$ where v and ϵ are the vectors of v_{ij} and ϵ_{ij} values respectively. All of the linear parameters are placed into a single vector β; that is, $\beta' = (\mu_\infty, \alpha)'$. However, we

need to be aware that some parameters will be common to other data sets in an integrated analysis, and hence we shall write the model as

$$l = \mu + \Delta\alpha + Uu + d$$

where $\mu = \mu_\infty f$. We emphasise that when analysing data we need to take into account the constraint that $\sum_r \alpha_r = 0$, or, equivalently, that the rows of Δ sum to 1, so that the columns are not independent vectors. It is simplest to omit the final column of Δ to overcome this problem, so that we estimate $\alpha_1, \ldots, \alpha_{r-1}$, and then calculate $\alpha_r = -\sum_{r=1}^{R_o-1} \alpha_r$. In what follows, it shall be be implicitly assumed that the final column of Δ has been omitted.

We need to compute the likelihood. There are two approaches. The first is to calculate the log-likelihood of the full data in one operation. The second is to recognise that regions are independent, and to compute the log-likelihood separately for each region.

The full log-likelihood

The log-likelihood is

$$\log \lambda = -0.5 \log |V| - 0.5(y - \Delta\alpha)' V^{-1} (y - \Delta\alpha)\,,$$

where $y = l - \mu$ and V is the variance-covariance matrix of the data. Now

$$V = D + \sigma_u^2 UU'$$

where $D = \sigma^2 I + \sigma_\infty^2 D_w$ and D_w is the diagonal matrix with diagonal elements f^2. There are multitudinous papers on how to solve the likelihood equations in the most efficient manner, but we want to use a vector-based statistical language, in which we maximise the likelihood from first principles with an efficient optimisation routine. We assume that we are in an iteration trial of the routine, so that the parameters μ_∞, σ_u^2 and σ^2 are known, that U and Δ have been computed and we need to calculate α and compute the likelihood.

There are three steps to perform when computing the log-likelihood.

1. $|\mathbf{V}|$**:** When calculating the likelihood we need to compute $|D+X\,X'|$, where $X = \sigma_u U$ is an $n \times p$ matrix, where n is the number of data values in the season, and p is the number of design levels. Generally, $n \gg p$. Computations involving matrices of order n are generally proportional to n^3, so if we can make the computations of order p rather than n, we should increase speed substantially. We can use the following result to reduce the amount of computation in this way.

$$|I + XX'| = |I + X'X|\,.$$

Now $|I + XX'|$ is the determinant of an $n \times n$ matrix and $|I + X'X|$ is that of a $p \times p$, so the latter requires much less computer time to calculate.

In fact, we need $|D + XX'|$. Set $Y = D^{-1/2}X$, and note that

$$D + XX' = D^{1/2}(I + YY')D^{1/2}\,.$$

Thus $|D + XX'| = |D||I + YY'| = |D||I + Y'Y|$.

2. $\hat{\alpha}$**:** We need to calculate $\hat{\alpha} = (\Delta' V^{-1}\Delta)^{-1}\Delta' V^{-1}y$. Note first that

$$(I + XX')^{-1} = I - X(I + X'X)^{-1}X'\,.$$

This result is easily checked. In fact, we need $(D + XX')^{-1}$. Note again that

$$D + XX' = D^{1/2}(I + YY')D^{1/2}\,.$$

Hence

$$(D + XX')^{-1} = D^{-1/2}(I + YY')^{-1}D^{-1/2}\,.$$

First let $P = D^{-1/2}\Delta$ and $Q = Y'P$. Then

$$\begin{aligned}
\Delta' V^{-1}\Delta &= \Delta' D^{-1/2}(I - Y(I + Y'Y)^{-1}Y')D^{-1/2}\Delta \\
&= P'P - Q'(I + Y'Y)^{-1}Q \\
&= P'P - R'Q\,,
\end{aligned}$$

where R is the solution of $(I + Y'Y)R = Q$.

Similarly let $\eta = D^{-1/2}y$ and $\xi = Y'\eta$. Then

$$\begin{aligned}\Delta' V^{-1} y &= \Delta' D^{-1/2}(I - Y(I + Y'Y)^{-1}Y')D^{-1/2}y \\ &= P'\eta - Q'(I + Y'Y)^{-1}Q \\ &= P'\eta - R'\xi\,.\end{aligned}$$

Finally, $\hat{\alpha}$ is obtained by solving $(P'P - R'Q)\,\alpha = P'\eta - R'\xi$.

3. $(\mathbf{y} - \boldsymbol{\Delta}\hat{\alpha})'\mathbf{V}^{-1}(\mathbf{y} - \boldsymbol{\Delta}\hat{\alpha})$**:** We need to compute, as part of the log likelihood, the residual sum of squares $(y-\Delta\hat{\alpha})'(D+XX')^{-1}(y-\Delta\hat{\alpha})$. Set $\nu = D^{-1/2}(y-\Delta\hat{\alpha})$ and $\omega = Y'\nu$. Then

$$\begin{aligned}(y - \Delta\hat{\alpha})'(D + XX')^{-1}(y - \Delta\hat{\alpha}) &= \nu'(I + YY')^{-1}\nu \\ &= \nu'(I - Y(I + Y'Y)^{-1}Y')\nu \\ &= \nu'\nu - \omega'(I + Y'Y)^{-1}\omega \\ &= \nu'\nu - \omega'\gamma\end{aligned}$$

where γ is the solution of the equations $(I + Y'Y)\gamma = \omega$.

Finally, we compute the log-likelihood as

$$\lambda = -0.5d_t - 0.5r\,.$$

Once the likelihood has been maximised, we need to calculate the random effects. It is usual to use the BLUPs:

$$\hat{u}_i = \hat{\sigma}_u^2 U'V^{-1}(l - \hat{\mu} - \Delta\hat{\alpha})$$

Using our usual notation,

$$V^{-1}(l - \hat{\mu} - \Delta\hat{\alpha}) = D^{-1/2}(\nu - Y\gamma)\,.$$

The standardised BLUPs are obtained by dividing through by the relevant standard deviation:

$$\begin{aligned} \hat{u}_i/\hat{\sigma}_u &= \hat{\sigma}_u U' V^{-1}(l - \hat{\mu} - \Delta\hat{\alpha}) \\ &= Y'(\nu - Y\gamma)\,. \end{aligned}$$

These are scale invariant. The corresponding true standardised random effects (e.g. u_i/σ_u) have mean 0 and variance 1. If $\hat{\sigma}_r = 0$ for any random effect r, then the BLUPs and standardised BLUPs are obviously 0.

We apply this method to southern bluefin tuna otolith data, as described in Appendix 3, using the full suite of data prior to screening. Briefly, each otolith has been read whole, sectioned or both, and assigned a final read by one of two readers. We assume that growth followed the VB $\log k$ growth curve introduced in Appendix 4. For a fish with zero length at time t_0, the length at time t is

$$l(t) = L_\infty \left[1 - e^{-k_2(t-t_0+s-s_0)} \left\{ \frac{1 + e^{-\beta(t-t_0+s-s_0-\alpha_0)}}{1 + e^{\beta_0 \alpha_0}} \right\}^{-(k_2-k_1)/\beta_0} \right]$$

where $s(t) = u_s \sin(2\pi(t - w_s))/(2\pi)$ is the seasonal effect. We can write $t - t_0$ as $a - a_0$, where a is the age of the fish at time t and a_0 is the extrapolated age at which the fish has length 0. The results are set out in Table 1.

Table 1: Fitted parameters for the VB $\log k$ growth model fitted to otolith data

μ_∞	186.79	$\hat{k}_1$	0.179	$\hat{a}_0$	-1.489
$\hat{\sigma}_\infty$	7.28	$\hat{k}_2$	0.144	$\hat{\sigma}_u$	5.944
$\hat{u}_s$	0.930	$\hat{\alpha}_0$	3.780	σ	3.5
$\hat{w}_s$	0.456	β_0	10		

The parameters β_0 and σ are held fixed. It is very difficult to estimate β_0

unless there is a huge amount of data, and σ_u cannot be estimated well because there are only 8 regions. The estimates of σ_u and σ are likely to be heavily confounded. We therefore fix σ at 3.5, derived from the analysis of tag-recapture data.

The regions in which the fish were caught were treated as random effects. The estimated *standardised* random effects are

Table 2: Estimated random effects of regions

Region	estimate	# tuna
Farm	0.024	9
Indonesia	0.157	1548
New Zealand	-0.257	299
South Australia	-1.057	250
South Africa	0.227	297
South East Indian Ocean	0.213	311
Tasmania	-0.271	559
Western Australia	-2.553	181

The fitted growth model and the data from the 8 regions are plotted in Figure 1. The fits seem adequate to the eye. Of most concern is the non-trivial negative estimates for the South Australian and Western Australian regions. These are the two areas from which substantial numbers of relatively small fish are caught. The estimates need to be multiplied by $\hat{\sigma}_u = 5.9$ cm, and suggest that for these two regions the model misses by 5 to 10 cm. These failures suggest that more work needs to be done.

We also estimated the reader/method combinations as fixed effects.

Table 3: Estimated fixed effects of readers and otolith methods

Reader	Method	estimate	# tuna
1	Whole	-0.233	474

Table 3: continued

1	Both	0.974	126
1	Sectioned	-0.500	369
2	Sectioned	-0.241	2485

Reader 2 in fact read two otoliths both whole and sectioned, but this was too small to estimate a separate effect, so these two data points were pooled with the 2483 measured using sections only. The interesting feature is that the measurements using only one method tend to agree. However, when Reader 1 used both methods, one to two more rings seem to be counted. These estimates could easily change with different growth models, so we caution that these estimates should not be over-interpreted.

We note that the analysis has not proved convincing, and take a closer look at the data. A table of reader/method combination by region yields

Table 4: Confounding between reader/method combinations and regions

Reader/method	Farm	Indonesia	NZ	SA	SAfrica	SEIO	TAS	WA
1/whole	9	0	0	227	6	9	44	179
1/both	0	0	0	21	10	8	86	1
1/sectioned	0	53	0	2	6	72	236	0
2/both	0	0	0	0	1	0	1	0
2/sectioned	0	1495	299	0	274	222	192	1

This table suggests that comparisons between reader/method combinations should best be done on Tasmanian data, where all four combinations are reasonably well represented. Further comparisons between Readers 1 and 2 on sectioned data could emerge from Indonesian and South-East Indian Ocean data, and some comparison between Reader 1 whole and both could be derived from the South Aus-

tralian data. Other comparisons are likely to be highly confounded with regional differences.

Independent regions

The log-likelihood for a given region is

$$\log \lambda_r = -0.5 \log |V_r| - 0.5(y_r - \Delta_r \alpha_r)' V_r^{-1} (y_r - \Delta_r \alpha_r) ,$$

where $y_r = l_r - \mu_r$ and V_r is the variance-covariance matrix of the data. Now

$$V_r = D_r + \sigma_u^2 1_r 1_r'$$

where D_r, Δ_r, y_r and α_r refer only to the submatrices and subvectors of D, Δ, y and α for the region in question, and 1_r is a vector of ones with the same length as y_r. The computation proceeds as for the full-likelihood case. The log-likelihood to be maximised is

$$\sum_r \log \lambda_r .$$

Concluding remarks

We have presented some preliminary approaches for rigorously analysing otolith data. These approaches are still in the developmental stage, but there is a need for models of this type in order to fully utilize direct aging data, including data collected during the period of band formation. We have reported some preliminary analyses of the pooled otolith data set, which suggests that Western Australian and South Australian data still exhibit some deviation from a common model. There are at least two possible explanations for this. First, there appears to be a size segregation in one-year-old fish caught off Western Australia and South Australia and in the general eastward movement of young fish within a fishing season. The Western Australian fish may have been spawned late in the season, and hence their assigned age is too high (Appendix 3). Second, other work suggests a

bias in the Indonesian data. Fish caught in Indonesian waters are usually spawners. Tuna in the age range 8 to 14 years exhibit size-dependent maturity, and those seen in the spawning grounds tend to be longer at a given age than the population average. Since there are a large number of otoliths from fish caught in Indonesian waters in the 8 to 14 age range, these data may be dominating the analysis and causing a misfit in the young fish from Western Australia and South Australia. A more sophisticated model would take this into account. We have also assessed reader effects, but the results must be treated with great caution.

We have not reported analyses of the otolith data using the first approach, taking into account uncertainty in the time of spawning and the time of band formation. We have developed both classical and Bayesian methods to fit this model, but we were unable to implement these methods within the extent of this project.

References

CLEAR, N.P., GUNN, J.S. & REES, A.J. (2000) Direct validation of annual increments in the otoliths of juvenile southern bluefin tuna, *Thunnus maccoyii,* by means of a large-scale mark-recapture experiment with strontium chloride. *Fish. Bull.* **98,** 25-40.